UNIVERSITY OF CALIFORNIA,
IRVINE

Hydrogen-Atom-Transfer Initiated Radical Bicyclizations: Concise Syntheses of Highly Oxidized Abietane Diterpenoids

DISSERTATION

submitted in partial satisfaction of the requirements for the degree of

DOCTOR OF PHILOSOPHY

in Chemistry

by

Darius Vrubliauskas

Dissertation Committee:
Professor Christopher D. Vanderwal
Professor Scott D. Rychnovsky
Professor Sergey V. Pronin

2021

DEDICATION

“Žmogus atranda save kovodamas su pačiu savimi.”

-Juozas Erlickas

TABLE OF CONTENTS

DEDICATION ii

TABLE OF CONTENTS iii

LIST OF TABLES v

LIST OF FIGURES vi

LIST OF SCHEMES viii

LIST OF ABBREVIATIONS xii

ACKNOWLEDGEMENTS xv

CURRICULUM VITAE xvi

CHAPTER 1: OVERVIEW OF RADICAL-INITIATED POLYENE CYCLIZATIONS AND MHAT-MEDIATED C-C BOND FORMING REACTIONS 1

1.1 Radical-Initiated Polyene Cyclizations 1

1.1.1 PET-Initiated Cyclizations of Farnesol-Derived Polyprenes 3

1.1.2 Use of Acyl Selenides as Initiators in Tin-Based Polycyclizations 5

1.1.3 Mn(III)-Mediated Oxidative Radical Cyclizations of Polyenes 6

1.1.4 Ti(III)-Mediated Reductive Radical Cyclizations of Epoxypolyprenes 9

1.1.5 Organo-SOMO Catalyzed Oxidative Radical Polyene Cyzlization 13

1.1.6 MHAT-Initiated Radical Polycyclization in Liu's Synthesis of Hispidanin A 14

1.2 MHAT Initiated Carbon-Carbon Bond Formation 16

1.2.1 Reductive Aldol-Type Reactions 17

1.2.2 Alkene Isomerizations, Cycloisomerizations, and Giese Reactions 18

1.2.3 MHAT-Initiated Polycyclizations in Terpenoid Synthesis 21

1.2.4 MHAT-Initiated Oxidative Radical-Polar Crossover Reactions 23

1.2.5 Dual-Catalyzed Hydroarylations of Alkenes 25

1.3 Notes and References 28

CHAPTER 2: COBALT-CATALYZED HYDROGEN-ATOM TRANSFER INDUCES BICYCLIZATIONS THAT TOLERATE ELECTRON-RICH AND ELECTRON-DEFICIENT INTERMEDIATE ALKENES 33

2.1 Abstract 33

2.2 Introduction 33

2.2.1 Prevalence of C-20 Oxidized Decalin Motifs in Natural Terpenoids 34

2.3 Results and Discussion 35

2.3.1 Optimization of Reaction Conditions 35

2.3.2 Bicyclizations of Substrates Bearing Nitrile Substituted Internal Alkenes 38

2.3.3 Bicyclizations of Substrates Bearing Methyl Substituted Internal Alkenes 39
2.4 Preliminary Mechanistic Experiments 41
2.4.1 Plausible Mechanistic Pathways 41
2.4.2 Cyclizations of Substrates Bearing E-Internal Alkenes 42
2.4.3 Bicyclizations Initiated By HAT to Monosubstituted Alkenes 43
2.4.4 Experiments Probing Intermediacy of Cationic Intermediates 45
2.4.5 Deuterium Labeling Experiments 47
2.4.6 The Role of 1,1,1,3,3,3-Hexafluoro-2-propanol (HFIP) 49
2.5 Conclusions 50
2.6 Experimental Procedures 52
2.7 Notes and References 102
CHAPTER 3: STEREOCONTROLLED RADICAL BICYCLIZATIONS OF OXYGENATED PRECURSORS ENABLE SHORT SYNTHESES OF OXIDIZED ABIETANE DITERPENOIDS 108
3.1 Abstract 108
3.2 Introduction 108
3.3 Stereochemical Control by Pendent Oxygen Functions 112
3.3.1 C3 Oxygenation 113
3.3.2 C2 Oxygenation 113
3.3.3 C1 Oxygenation 114
3.3.4 C18 Oxygenation 117
3.3.5 B-Ring Oxygenation 118
3.3.6 C6 Oxygenation 119
3.3.7 C7 Oxygenation 120
3.4 Doubly Oxygenated Precursors 121
3.5 Total Synthesis of Abietane Diterpenoids 123
3.5.1 (+)-2-O-Deacetyl Plebedipenes A and C 124
3.5.2 (±)-Plebedipene B 126
3.6 Outlook 127
3.7 Conclusions 130
3.8 Experimental Procedures 131
3.9 Notes and References 207
APPENDIX A: ^{1}H, ^{13}C, 2D NMR & ISOTOPE MASS RATIO SPECTRA 214
APPENDIX B: X-RAY CRYSTALLOGRAPHIC DATA 537

LIST OF TABLES

Table 2. 1: Optimization of bicyclization reaction conditions. 37

Table 2. 2: Comparison table of ^{1}H NMR data [δ_H (J, Hz)] for natural[22] and synthetic carnosaldehyde:..... 100

Table 3. 1: Reaction conditions screened for the dearomative oxidative cyclization of 3.73. The presence of acid was critical (DDQ likely contained trace amounts of HCN), whereas inclusion of bases led to decomposition. [a]Under these conditions, 2-*O*-deacetyl plebedipene C (3.17) was also observed (~20%). 191

Table 3. 2: Comparison of ^{1}H NMR chemical shifts 192

Table 3. 3: Comparison of ^{13}C NMR chemical shifts 193

Table 3. 4: Comparison of ^{1}H NMR chemical shifts 194

Table 3. 5: Comparison of ^{13}C NMR chemical shifts 195

Table 3. 6: Comparison of ^{1}H NMR chemical shifts of natural..... 203

Table 3. 7: Comparison of ^{13}C NMR chemical shifts of natural..... 204

LIST OF FIGURES

Figure 1. 1: Structures of representative natural terpenoids that were synthesized using biomimetic polyene cyclizations as key carbon-carbon bond forming reactions. 1

Figure 2. 1: Atisane alkaloids and neotripterifordin inspired our efforts to develop bicyclization reactions with electron-withdrawing groups at C20. 34

Figure 2. 2: Scope of the bicyclization of nitrile-substituted substrates (yields shown are for isolated and purified compounds). Boc=*tert*-butoxycarbonyl, Ts=*para*-toluenesulfonyl. 39

Figure 2. 3: The reactivity of methyl-substituted substrates mirrors that of the corresponding nitrile-bearing compounds (yields shown are for isolated and purified compounds). 40

Figure 2. 4: Stereochemical outcomes of bicyclizations initiated by HAT to monosubstituted alkenes (product ratios and yields determined using ^{1}H NMR spectroscopy with an internal standard). 45

Figure 3. 1: a) Breslow's pioneering radical bicyclization of farnesyl acetate. b) Our previous report of MHAT-initiated radical bicyclizations that tolerated an oxidized C20 (as the nitrile). c) Liu's use of the C2 silyloxy group to control diastereoselectivity in an MHAT-initiated bicyclization. 110

Figure 3. 2: a) The possibility of using preoxidized bicyclization precursors to access highly oxidized abietane-type scaffolds. b) Representative oxidized aromatic diterpenoids. 112

Figure 3. 3: Stereochemical outcomes of bicyclization reactions using substrates with C1-C3 oxygen functional groups. 114

Figure 3. 4: Hydrogen-bonding directed regiocontrol in substrates bearing unsymmetrical methoxy arenes. 116

Figure 3. 5: Outcomes of bicyclization reactions using substrates with C1 oxygenation and *p*-methoxyphenyl terminating groups. 117

Figure 3. 6: Surprisingly high diastereoselectivity for equatorial (C18) disposition of oxygenation in bicyclizations of allylic alcohol derivatives. 118

Figure 3. 7: Proto-B-ring oxygenation has little impact on overall reaction diastereoselectivity. 120

Figure 3. 8: Radical bicyclizations of doubly oxygenated substrates. 121

LIST OF SCHEMES

Scheme 1. 1: Breslow's radical-initiated polyene cyclization of farnesyl acetate. 2

Scheme 1. 2: Demuth's first-generation approach to PET-initiated cyclizations of polyprenes. .. 3

Scheme 1. 3: PET-initiated radical polyene cyclizations of farnesol-derived polyprenes. 4

Scheme 1. 4: A visible-light mediated cyclization approach reported by Guo and co-workers. ... 5

Scheme 1. 5: Pattenden's radical polycyclization utilizing acyl selenides as initiating moieties. . 6

Scheme 1. 6: Mechanism of Mn(III)-mediated single electron oxidation of β-ketoesters. 7

Scheme 1. 7: Snider's Mn(III)-mediated bicyclization approach to (+/-)podocarpic acid (**1.34**).. 7

Scheme 1. 8: Mn(III)-mediated tetracyclization reactions to access polycyclic diterpenoid frameworks by Snider and Zoretic. 8

Scheme 1. 9: A catalytic variant of Mn(III)-mediated free-radical cyclizations by the Baran lab. 9

Scheme 1. 10: a) The mechanism of Ti(III)-mediated reductive heterolysis of epoxides. b) Early examples of radical-initated epoxypolyene cyclizations by Cuerva and co-workers. 10

Scheme 1. 11: Cyclization of epoxypolyene 1.50 via cationic or radical intermediates. 10

Scheme 1. 12: The Ti(III)-mediated radical cyclization of ketoepoxypolyprene 1.54. 11

Scheme 1. 13: The Ti(III)-mediated polycyclization used by Li and co-workers en route to xiamycin A. 12

Scheme 1. 14: a) The key polycyclization in Kobayashi's total synthesis of fomitellic acid B. b) Synthesis of valparane reported by Barrero and co-workers. 13

Scheme 1. 15: The mechanism of McMillan and Rendler's organo-SOMO catalyzed cyclization. 14

Scheme 1. 16: The proposed mechanism for MHAT-initiated polycyclization in Liu's synthesis of hispidanin A. 15

Scheme 1. 17: a) Mukaiyama's MHAT-initiated aldol-type reaction between electron-deficient alkenes and aldehydes. b) Intramolecular variant of the above reaction reported by Krische and co-workers. 17

Scheme 1. 18: a) MHAT-initiated radical cyclizations of aryl alkenes reported by Van der Donk and co-workers. b) The first report of an MHAT-initiated polyene cyclization by Norton and co-workers. 18

Scheme 1. 19: a) MHAT-initiated coupling of olefins via a Giese-type reaction reported by Baran and co-workers. b) Heteroatom-functionalized alkene coupling with α,β-unsaturated carbonyl derivatives. 19

Scheme 1. 20: Co(III)-catalyzed isomerization, cycloisomerization, and retrocycloisomerization of alkenes reported by Shenvi and co-workers. 21

Scheme 1. 21: Catalyst-controlled cycloisomerization and cyclohydrogenation of diene **1.107** reported by Norton and co-workers. 21

Scheme 1. 22: MHAT-initiated polycyclization towards emindole SB reported by Pronin and co-workers. 22

Scheme 1. 23: Pronin's reductive MHAT polycyclization and annulation approaches used in the syntheses of nodulisporic and C and forskolin respectively. 23

Scheme 1. 24: a) The proposed mechanism for Shigehisa's Co(II)-catalyzed intramolecular hydroarylation of olefins. b) Selected examples from the substrate scope. 24

Scheme 1. 25: Catalyst-controlled bifurcation of radical-polar crossover pathways reported by Pronin and co-workers. 25

Scheme 1. 26: Dual-catalyzed intramolecular hydroarylations of unactivated alkenes reported by Shenvi and co-workers. a) Redox-neutral strategy using a Co(II)-precatalyst; b) Reductive-MHAT approach using Fe(III)/Ni(II) precatalysts. 27

Scheme 2. 1: Plausible mechanistic options for bicyclization reactions. 41

Scheme 2. 2: Attempted bicyclizations with acrylate esters as the internal alkene. 43

Scheme 2. 3: An attempt to probe the intermediacy of cationic intermediates instead supports radical-based reactivity (yields shown are for isolated and purified compounds). 46

Scheme 2. 4: Deuteration experiments suggest oxidation followed by proton transfer, rather than back MHAT, as the final stages of the reactions. 48

Scheme 2. 5: Aerobic oxidation of Co(II) complex C1 in HFIP and isomerization of diene **2.24** using catalyst C1* in benzene. 50

Scheme 3. 1: a) Typical trans-Decalin Formation by Cationic Bicyclizations of Oligoisoprenes. b) Overview of the Biosynthesis of Oxidized Aromatic Abietane Diterpenoids. 109

Scheme 3. 2: Stereoselective Syntheses of (+)-2-O-Deacetyl Plebedipenes A and C. 125

Scheme 3. 3: Synthesis of (±)-Plebedipene B. 127

Scheme 3. 4: a) Proposed termination using various alkenes and nucleophilic trapping of the intermediate cationic species. b) A hypothetical convergent approach to complex terpenoid frameworks. 128

Scheme 3. 5: a) Dearomative cyclization of a furan bearing substrate. b) Oxidative cleavage of carnosic acid in a semisynthetic approach to (–)-antrocin reported by Yang and co-workers. .. 129

Scheme 3. 6: Proposed HAT-initiated carbocyclizations of novel dialkenyl arene substrates (a) and an intermolecular variant enabling tandem fragment coupling-hydroarylation reactions (b). 130

Scheme 3. 7: Synthesis of C1 Oxygenated Substrates. 132

Scheme 3. 8: Synthesis of C2 Oxygenated Substrates. 133

Scheme 3. 9: Synthesis of C3 Oxygenated Substrates. 133

Scheme 3. 10: Synthesis of C18/19 Oxygenated Substrates. 133

Scheme 3. 11: Synthesis of C6 Oxygenated Substrates. 134

Scheme 3. 12: Synthesis of C7 Oxygenated Substrates. 134

LIST OF ABBREVIATIONS

Å	Ångstroms
Ac	Acetyl
Atm	Atmosphere
Bn	Benzyl
Boc	tert-butoxycarbonyl
Bp	Boiling point
Bu	Butyl
BuLi	Butyllithium
Bz	Benzoyl
C	Carbon
°C	Degree Celsius
cat.	Catalytic
CI	Chemical ionization
COSY	Correlation spectroscopy
CSA	Camphorsulfonic acid
d	doublet
DBU	1,8-Diazabicyclo[5.4.0]undec-7-ene
δ	Chemical shift
DEPT	Distortionless enhancement polarization transfer
DIBAL-H	Diisobutylaluminum hydride
DMAP	4-Dimethylaminopyridine
DMF	*N*,*N*-Dimethylformamide
DMP	Dess-Martin periodinane
DMSO	Dimethyl sulfoxide
d.r.	Diastereomeric ratio
E	Ester
ee	Enantiomeric excess
EI	Electron-impact ionization
e.r.	Enantiomeric ratio

eq.	Equation
equiv.	Equivalents
ESI	Electrospray ionization
Et	Ethyl
GC	Gas chromatography
h	Hour(s)
HAT	Hydrogen-atom-transfer
HFIP	1,1,1,3,3,3-hexafluoro-2-propanol
HRMS	High Resolution Mass Spectrometry
Hz	Hertz
i	iso
IBX	2-iodoxybenzoic acid
J	Coupling constant
KHMDS	Potassium hexamethyldisilazide
LAH	Lithium aluminium hydride
LDA	Lithium diisopropylamide
LiHMDS	Lithium hexamethyldisilazide
LLS	Longest linear sequence
μ	Micro
m	Multiplet, milli
M	Molar
m-CPBA	3-Chloroperoxybenzoic acid
min	Minute(s)
Me	Methyl
MHz	Megahertz
MS	Mass spectrometer
NMR	Nuclear magnetic resonance
NOE	Nuclear Overhauser Effect
Ph	Phenyl
ppm	Parts per million
rt	Room temperature

sec	Second(s)
t	tert
TBAC	Tetra-*n*-butylammonium chloride
TBAF	Tetra-*n*-butylammonium fluoride
TBS	*t*-butyldimethylsilyl
Tf	Trifluoromethanesulfonyl
TFA	Trifluoroacetic acid
THF	Tetrahydrofuran
THP	Tetrahydropyran
TLC	Thin layer chromatography
TMDSO	1,1,3,3-Tetramethyldisiloxane
TMS	Trimethylsilyl
Ts	4-Toluenesulfonyl
TsOH	4-Toluenesulfonic acid

ACKNOWLEDGEMENTS

First and foremost, I would like to thank Prof. Vanderwal for taking me on as a graduate student. His unwavering support over the past five years has been crucial to my success as a synthetic organic chemist. I also wish to extend a big thanks to Zef Könst, David George, Shun Kitahata, Benjamin Groβ, and Lucas Johnson with whom I had the pleasure of working. Past and present members of the Vanderwal, Rychnovsky, Overman and Pronin groups have played an important role in my life and I feel incredibly fortunate to have had the opportunity to interact with so many intelligent and all-around good people. Matthias Göhl, Sunshine Burns, Alexander Burtea, Danielle Perrota, Natalie Dwulet, Bryant Lim, Chuck Dooley and Chao Gao deserve a special thanks for their continuous kindness and friendship. The pandemic night shift crew, Johnathan Chung, Ramakrishna Kankanala, Jane Supantanapong, Griffin Barnes, Lucas and Fabian Hörmann have been like family over the past year and a half.

I feel incredibly fortunate to have parents and siblings who have always been supportive of my endeavors. Last but not least, I would like to thank Buddha Khatri, Michal Glogowski and Professors Scott McNeill Sieburth and Steven Fleming without whom, I would have never been exposed the wonders of synthetic organic chemistry.

CURRICULUM VITAE

Darius Vrubliauskas
6407 Adobe Circle Rd S
Irvine, CA 19116
(215)-964-0500
dvrublia@uci.edu

Education

- Ph. D., Chemistry, University of California, Irvine (2016-2021)
- Advisor: Professor Christopher D. Vanderwal
- Thesis: Hydrogen-Atom-Transfer Initiated Radical Bicyclizations: Concise Syntheses of Highly Oxidized Abietane Diterpenoids

- B. S., Chemistry, Temple University, Philadelphia, PA (2011-2015)
- Advisor: Professor Scott McNeil Sieburth

Publications

1. "Stereocontrolled Radical Bicyclizations of Oxygenated Precursors Enables Short Syntheses of Oxidized Abietane Diterpenoids" D. Vrubliauskas, B. M. Gross, C. D. Vanderwal, *J. Am. Chem. Soc.* **2021**, 2021, *143*, 2944–2952.

2. "Bioinspired Polyene Cyclizations of Highly Functionalized Substrates", D. Vrubliauskas, C. D. Vanderwal, (review) *manuscript in preparation.*

3. "Cobalt-Catalyzed Hydrogen-Atom Transfer Induces Bicyclizations that Tolerate Electron-Rich and Electron-Deficient Intermediate Alkenes." D. Vrubliauskas, C. D. Vanderwal, *Angew. Chem. Int. Ed.* **2020**, *59*, 6115–6121.

4. "Catalyst-Controlled Stereoselective Synthesis Secures the Structure of the Antimalarial Isocyanoterpene Pustulosaisonitrile-1" A. M. White, K. Dao, D. Vrubliauskas, Z. A. Könst, G. K. Pierens, A. Mándi, K. T. Andrews, T. S. Skinner-Adams, M. E. Clarke, P. T. Narbutas, D. C. M. Sim, K. L. Cheney, T. Kurtán, M. J. Garson, C. D. Vanderwal, *J. Org. Chem.* **2017**, *82*, 13313–13323.

5. "Photo-[4+4]-cycloaddition (para) of meta substituted benzenes with 2-pyridones." B.B. Khatri, D. Vrubliauskas, S. M. Sieburth, *Tet. Lett.* **2015**, *56*, 4520–4522.

Poster/ Oral Presentations

- D. Vrubliauskas, and C. D. Vanderwal, *Cobalt-Catalyzed Hydrogen-Atom-Transfer Bicyclizations,* **2020 Vertex Day at UCI**, 2020, University of California, Irvine.

- D. Vrubliauskas, and C. D. Vanderwal. *MHAT Initiated Bicyclizations Enabled by Co(II) Catalysis*, **46TH National Organic Symposium**, 2019, Indiana University, Bloomington.

- D. Vrubliauskas, M. Glogowski, B. Bloomer, and S.M. Sieburth. *2-Pyridone-Benzene Photo-[4+4]-Cycloadditions and Applications Thereof*, **2015 Temple University URP Symposium**, 2015, 1801 North Broad Street, Philadelphia, PA.
- D. Vrubliauskas, M. Glogowski, and S.M. Sieburth. *Photo-[4+4]-cycloaddition (para) of Substituted Benzenes*, **22nd TURF-CreWS: Temple Undergraduate Research Forum-Creative Works Symposium**, 2015, 1801 North Broad Street, Philadelphia, PA.

Awards and Fellowships

- NSF Graduate Research Fellowship Program, 2017

- Sloviter Research Award for the 2015 Academic year, Temple University, Department of Chemistry, Philadelphia, PA, USA. June 2015.

- Edward and Frances Fineman Memorial Scholarship for the 2012 Academic year, Temple University, Department of Chemistry, Philadelphia, PA, USA. August 2013.

ABSTRACT OF THE DISERTATION

Hydrogen-Atom-Transfer Initiated Radical Bicyclizations: Concise Syntheses of Highly Oxidized Abietane Diterpenoids

By

Darius Vrubliauskas

Doctor of Philosophy in Chemistry

University of California, Irvine, 2021

Professor Christopher D. Vanderwal, Chair

This dissertation describes the development and applications of a radical bicyclization reaction that is initiated via hydrogen-atom-transfer (HAT) to 1,1-disubstituted alkenes. In the first chapter, biomimetic radical polyene cyclizations and HAT-mediated C-C bond forming reactions are reviewed. Mechanistic and strategic aspects pertaining to radical-polar crossover are emphasized throughout, highlighting unique possibilities offered by oxidative or reductive termination.

The second chapter details the development of a novel cobalt(II)-catalyzed bicyclization. The process is presumably initiated by metal-catalyzed hydrogen-atom transfer (MHAT) to 1,1-disubstituted or monosubstituted alkenes. Notably, electron-rich methyl or electron-deficient nitrile substituted internal alkenes are tolerated. Electron-rich aromatic terminators are required in both cases. Terpenoid scaffolds with different substitution patterns are obtained with excellent diastereoselectivities, and the bioactive C20-oxidized abietane diterpenoid carnosaldehyde was

made to showcase the utility of the nitrile-bearing products. Also provided are the results of several mechanistic experiments that suggest the process features an MHAT-induced radical bicyclization with late-stage oxidation to regenerate the aromatic terminator.

The third chapter details our studies in applying cobalt(II)-catalyzed bicyclizations to the synthesis of oxygenated terpenoid scaffolds. A systematic evaluation of substrates bearing different oxygenation patterns was conducted to assess the practicality of using preoxidized bicyclization precursors. The degree of stereoselectivity was often high, but varied with oxygenation locus, with free hydroxy groups performing well in most contexts. The stereochemical outcomes of cyclizations of dioxygenated polyenes were dictated by aliphatic chain oxygenation closest to the initiating 1,1-disubstituted alkene. Simple analyses of non-bonding interactions in the putative cyclization transition states were sufficient to rationalize stereochemical outcomes in most cases. Intramolecular hydrogen bonding directed regioselectivity was observed in one substrate class. To further validate the use of preoxidized polycyclization precursors in bioactive diterpenoid synthesis, we completed the first total syntheses of (+)-2-O-deacteyl plebedipene A, (±)-plebedipene B, and (+)-2-O-deacetyl plebedipene C. Lastly, experiments aimed at expanding the scope of cobalt(II)-catalyzed polycyclizations are proposed.

CHAPTER 1: OVERVIEW OF RADICAL-INITIATED POLYENE CYCLIZATIONS AND MHAT-MEDIATED C-C BOND FORMING REACTIONS

1.1 Radical-Initiated Polyene Cyclizations

The polycyclic products of biosynthetic polyene-type cyclizations are endowed with a wealth of structural diversity and biological activity. Inspired by these compelling secondary metabolites and their fascinating biogeneses, chemists have engaged in decades of work emulating nature's polyene cyclizations[1] starting with the seminal studies of the groups of Stork[2], Eschenmoser[3], Johnson[4], van Tamelen[5], and others. As a result, chemists have accrued an excellent understanding of the reactivity and stereochemical outcomes of cation-initiated polycyclizations of polyenes as applied to bioinspired terpenoid synthesis. Many new polycyclization methods have been developed and subsequently tested in the total syntheses of these natural products (**Figure 1.1**). These advances include methods underpinned by either radical or organometallic intermediates.[6]

Figure 1. 1: Structures of representative natural terpenoids that were synthesized using biomimetic polyene cyclizations as key carbon-carbon bond forming reactions[7].

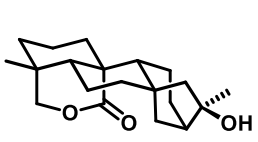

1.1: ***neotripterifordin***

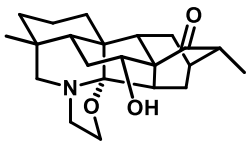

1.2: ***septedine***

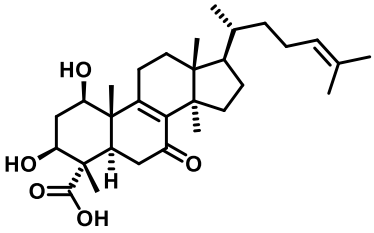

1.3: ***fomitelic acid B***

Unlike their cationic counterparts, radical polycyclization reactions are thought to proceed in a stepwise manner via distinct open-shell intermediates.[8] This might suggest that a highly-stereoselective radical polyene cyclization would be challenging to execute. To this end, Breslow and co-workers were the first to propose and later dismiss the idea that biosynthetic polyene

cyclizations could proceed via radical pathways.[6e] Their seminal studies showed that a polycyclization of farnesyl acetate (**1.4**) can be effected via radical addition to the alkene terminus, giving *trans*-decalin **1.5** as a single stereoisomer (**Scheme 1.1**). It is worthwhile to note that the analogous cation-initiated polyene cyclizations afford the tricyclic scaffold as a thermodynamic mixture of endocyclic olefin isomers.[9]

Scheme 1. 1: Breslow's radical-initiated polyene cyclization of farnesyl acetate.

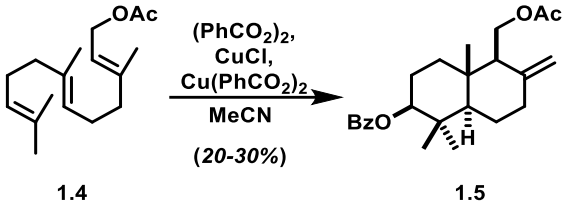

The use of cationic polyene cyclizations in biomimetic approaches towards terpenoids containing *trans*-decalin frameworks is widely regarded as the most straightforward approach. However, difficulties in mimicking the action of cyclase enzymes are exacerbated in cases where the targets of interest are highly oxidized. The highly reactive nature of cationic intermediates often limits the degree to which polyprene precursors can be functionalized and still undergo efficient cyclizations. This is to be expected of course, since in nature oxidation of the carbon skeleton typically occurs post-cyclization.[10] To address these and other issues plaguing non-enzymatic polyene cyclizations, a variety of radical polycyclization approaches have been developed.[11] All of the strategies outlined below offer distinct opportunities in the context of polycyclic terpenoid synthesis. However, gaps in this general area remain, including in the cyclization of systems that electronically deviate significantly from natural terpenoid precursors.

1.1.1 PET-Initiated Cyclizations of Farnesol-Derived Polyprenes

In 1993, Demuth reported a photoinduced electron transfer (PET) mediated radical polycyclization of farnesyl acetate in a micellar medium (**Scheme 1.2**).[12] This process is initiated by regioselective single-electron oxidation of the least sterically hindered alkene in the substrate to give a radical-cation species **1.6**. Nucleophilic trapping of the nascent carbocation occurs in anti-Markovnikov fashion, while a radical cascade furnishes the *trans*-decalin scaffold **1.8**. Termination via hydrogen atom abstraction was deemed most likely. Single-electron reduction was ruled out because deuteration at C-8 was not observed when D_2O was used as solvent.

Scheme 1. 2: Demuth's first-generation approach to PET-initiated cyclizations of polyprenes.

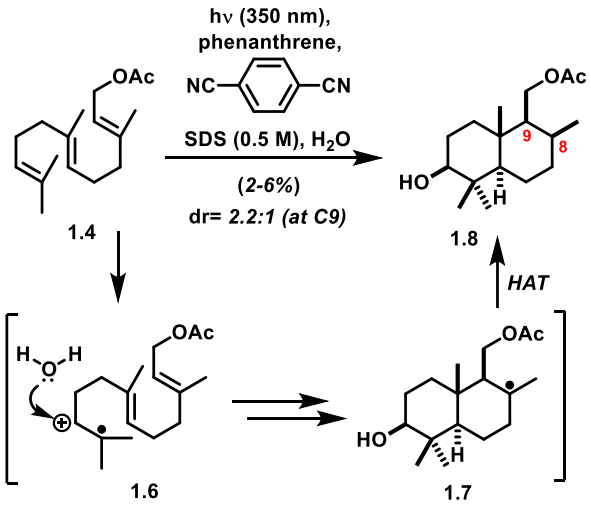

In subsequent investigations, Demuth and co-workers discovered that employing DCTMB (1,4-Diacyano-2,3,5,6-tetramethylbenzene) as an acceptor and biphenyl as a co-sensitizer led to modestly improved yields (**Scheme 1.3**, **a**).[13] Moreover, the authors demonstrated that electron-deficient olefins, such as the ones found in **1.11** and **1.13,** can serve as suitable terminating groups and kinetic preference for 6-*endo* cyclizations can be overridden by electronic bias (**Scheme 1.3, c**).[14] The penalty due to construction of vicinal quaternary carbon centers in **1.14** is likely

outweighed by stabilization of the penultimate radical species by the malononitrile moiety. Using deuterated solvents led to formation of monodeuterated products (at C-14 in **1.13**), indicating that termination involving electron-deficient acceptors proceeds most likely proceeds via single-electron reduction. The mode of termination for arene-terminated cyclizations (**Scheme 1.3, d**) remains nebulous since both HAT and single-electron oxidation/deprotonation pathways seem possible under the reaction conditions.[15] Despite the poor isolated yields, Demuth's studies using the PET approach convincingly demonstrated that simple farnesol and geranylgeranyl derivatives can undergo radical polycyclizations with excellent stereochemical fidelity.

Scheme 1. 3: PET-initiated radical polyene cyclizations of farnesol-derived polyprenes.

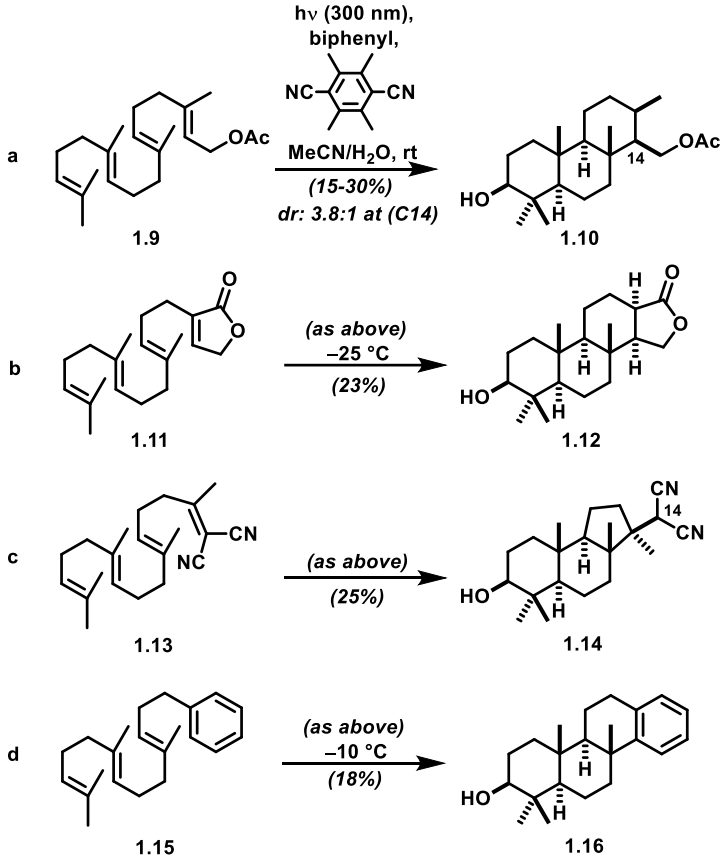

In 2015, Luo and co-workers reported a much more efficient, visible-light mediated approach to polyprene cyclizations (**Scheme 1.4**).[16] As in Demuth's reports, it was proposed that

the radical cascade is initiated via PET to generate a cation-radical species **1.18**. The authors postulate that this intermediate undergoes cyclization accompanied by a hydrogen shift to give radical cation **1.19**. Reduction of this species by the radical anion of Eosin Y gave tetracyclic scaffold **1.20**. Although the exact details of the hydrogen-shifting remain speculative, it was proposed that hexafluoroisopropanol aids in stabilization of high-energy intermediates throughout this process.[17] This methodology is limited to use of heteroatom nucleophiles as terminating groups but nevertheless serves as a highly attractive alternative to the analogous protonative polycyclizations where unprotected phenol would likely interfere with desired reactivity.

Scheme 1. 4: A visible-light mediated cyclization approach reported by Guo and co-workers.

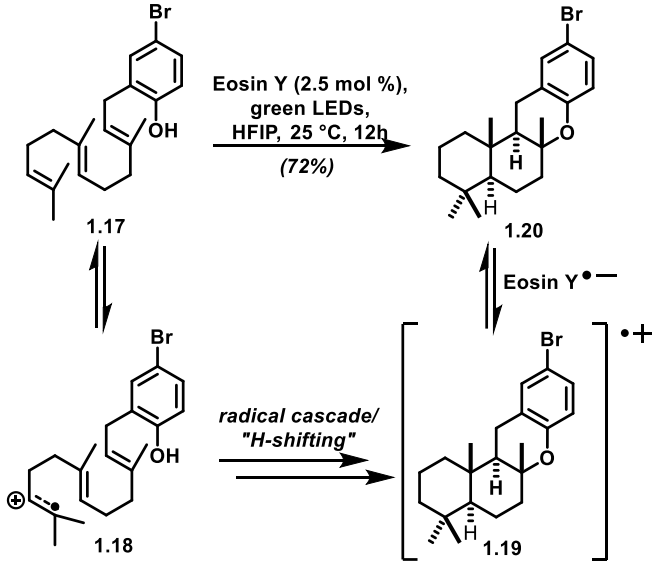

1.1.2 Use of Acyl Selenides as Initiators in Tin-Based Polycyclizations

The advent of new synthetic methods to initiate radical processes spurred the deviation from canonical geraniol-derived polycyclization precursors. Building on early reports from the Boger group,[18] Pattenden and co-workers found that acyl selenides can serve as initiating functional groups for radical cyclizations to afford complex terpenoid-like scaffolds shown as shown in **Scheme 1.15**.[19] The stereochemical outcome of these cyclizations was found to be dependent on

the electronic nature of the intermediary alkenes which could be leveraged to access both *cis*- and *trans*-decalin motifs. For instance, cyclization of substrate **1.21** led formation of *cis*-*trans*-*cis* fusions at the first three ring junctions in the major product **1.22** (**Scheme 1.15, a**).[20] In another striking example Pattenden and co-workers incorporated a cyclopropane fragmentation-transannular cyclization sequence into the radical cascade to give tetracyclic scaffold **1.26** (**Scheme 1.15, b**). Nevertheless, this approach to radical polycyclizations is limited to termination via hydrogen atom abstraction and the acyl selenide precursors are cumbersome to prepare.

Scheme 1. 5: Pattenden's radical polycyclization utilizing acyl selenides as initiating moieties.

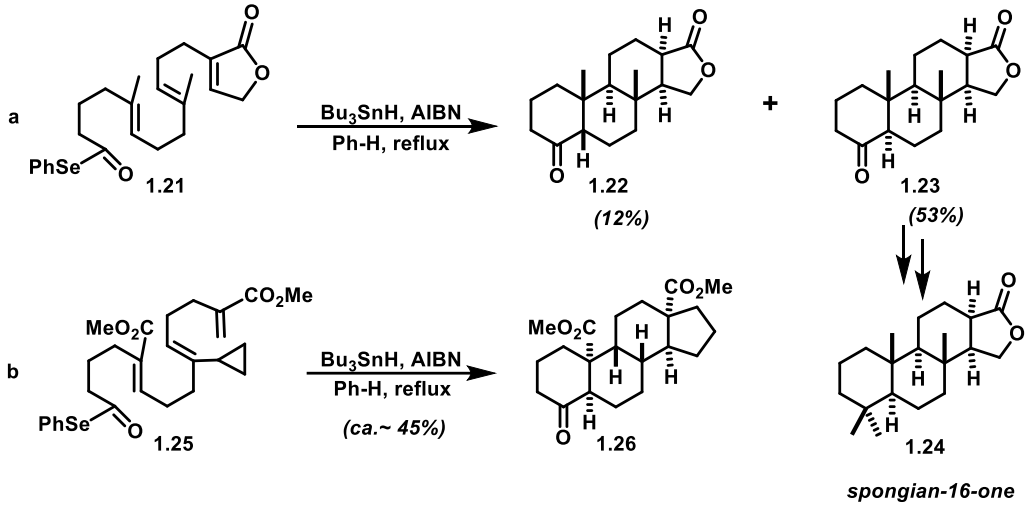

1.1.3 Mn(III)-Mediated Oxidative Radical Cyclizations of Polyenes

Breslow's seminal report (**Scheme 1.1**) described a net-oxidative radical cyclization but its poor efficiency when compared to cationic epoxypolyene approaches deterred further investigations.[6e] A more chemoselective strategy to generate carbon-centered radicals under oxidative conditions was clearly necessary. Manganese-mediated oxidation of enols proved to be effective in this context.[21] In the presence of Mn(III) salts, readily enolizable carbonyl derivatives such as β-ketoesters can undergo single-electron oxidation to generate electron-deficient α-acyl

radicals (**Scheme 1.6**).[22] These species can then engage pendent unactivated alkenes in cyclization processes that are terminated *via* oxidation of the penultimate carbon-centered radical.

Scheme 1. 6: Mechanism of Mn(III)-mediated single electron oxidation of β-ketoesters.

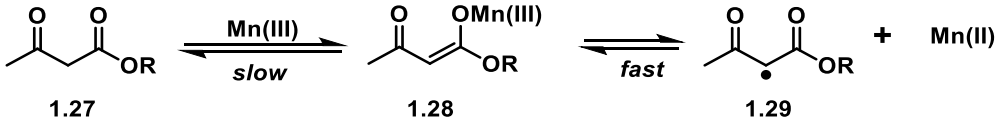

Snider and co-workers extended this methodology to access diterpenoid-like decalin motifs as described in their formal synthesis of (+/-) podocarpic acid (**scheme 1.7, 1.34**).[6d, 23] One should note the stereoselectivity of the first ring-closure as it secures C-19 oxidation which is present in many natural diterpenoids. Subsequent studies suggested that radical additions to unactivated arenes proceed sluggishly and Mn(III)-mediated oxidation of the corresponding tertiary alkyl radical is faster.[24] Upon radical-polar crossover, the resulting tertiary carbocation can be intercepted by arenes via a Friedel-Crafts type alkylation.

Scheme 1. 7: Snider's Mn(III)-mediated bicyclization approach to (+/-)podocarpic acid (**1.34**).

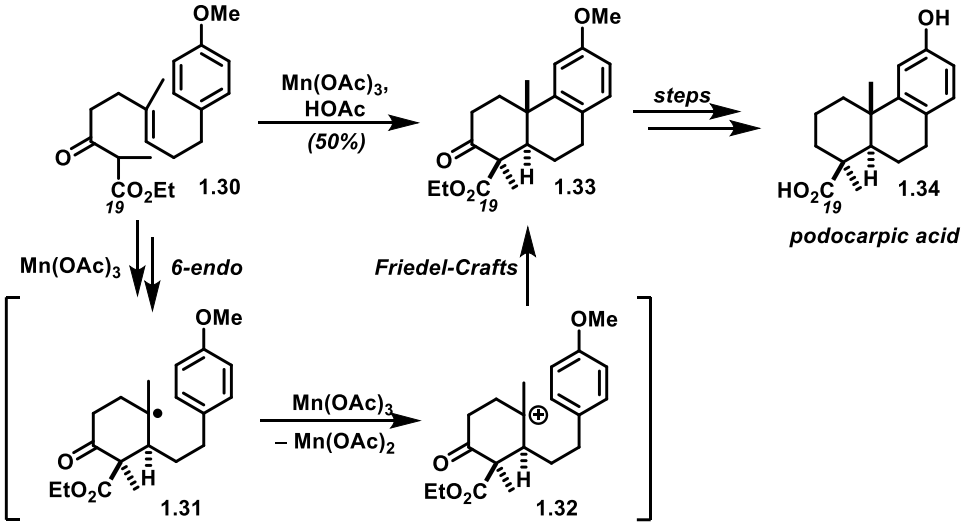

Termination with unactivated alkenes necessitates the use of stronger single electron oxidants such as Cu(II) salts. When the penultimate alkyl-radical species is primary or secondary,

the corresponding alkylcopper(III) intermediates typically undergo oxidative-elimination yielding alkene bearing products.[25] In an elegant display, Snider utilized this chemistry to access a bayerane framework in one step from a linear polyalkene (**Scheme 1.8**).[26] In this remarkable transformation, three consecutive 6-*endo* radical cyclizations followed by a 5-*endo* cyclization assemble a bridged framework **1.38** containing four quaternary carbon centers. It should be noted that the first cyclization is polarity matched, whereas the rest are driven by exothermicity of trading π-bonds for sp^3 C-C bonds. Another striking example from Zoretic and co-workers (**Scheme 1.8**, **b**) suggests that judicious intermediate polarity matching can be used to introduce useful functional handles for subsequent operations while maintaining modest efficiency.[27]

Scheme 1. 8: Mn(III)-mediated tetracyclization reactions to access polycyclic diterpenoid frameworks by Snider and Zoretic.

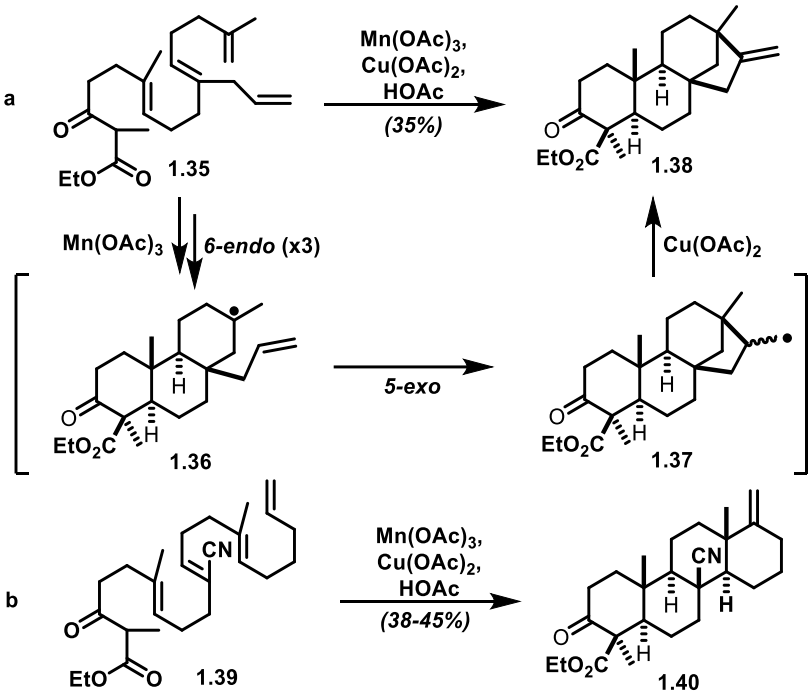

The examples described above involve the use of multiple equivalents of metal-based oxidants which is scale-limiting, not economical, and complicates reaction work-up protocols. Baran reported a catalytic variant of this reaction, wherein electrochemical oxidation of Mn(II)

salts facilitated catalyst turnover (**Scheme 1.9**).[28] Although efficiency of this process was slightly worse than that of the super-stoichiometric variant (48%), it serves as a model for rendering these reactions viable for large-scale synthesis.

Scheme 1. 9: A catalytic variant of Mn(III)-mediated free-radical cyclizations by the Baran lab.

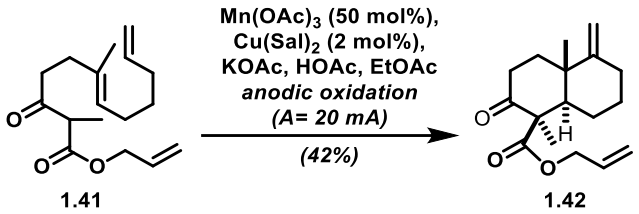

1.1.4 Ti(III)-Mediated Reductive Radical Cyclizations of Epoxypolyprenes

In recent years, Cp_2TiCl has emerged as a versatile single electron reductant capable of facilitating many useful transformations such as homolytic opening of epoxides.[29] Termination of these processes is reductive, but careful control of reaction conditions can yield olefinic products via mixed disproportionation pathways (**Scheme 1.10, a**).[30] Application of this methodology to bioinspired terpenoid synthesis was first reported by Cuerva and co-workers.[6a] Their extensive studies in this area also led to the development of protocols employing catalytic amounts of Cp_2TiCl_2 (**Scheme 1.10, b**).[31] It is worth noting that compound **1.47** is similar to that synthesized by Breslow and co-workers in their seminal studies (**Scheme 1.1**). Clearly, the Ti(IV) catalyzed approach is more efficient; high chemoselectivity in radical initiation is evident in successful cyclization of triterpene **1.48** (**Scheme 1.10, b**). Moreover, this method offers an opportunity to relay the epoxide stereochemistry to stereogenic centers formed via the polycyclization.

Scheme 1. 10: a) The mechanism of Ti(III)-mediated reductive heterolysis of epoxides. **b)** Early examples of radical-initated epoxypolyene cyclizations by Cuerva and co-workers.

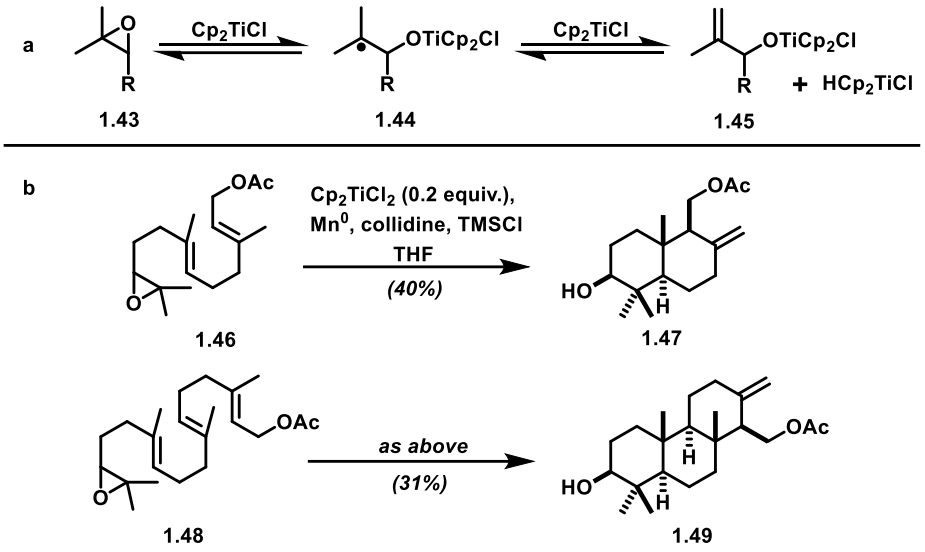

In 2009, Barerro and co-workers developed a Ti(III)-mediated polycyclization strategy for the synthesis of *seco*-C-oleanane.[32] Interestingly, the same precursor was previously shown to produce amyrins under cationic conditions (**Scheme 1.11**).[33] Computational studies suggested that the radical pathway to form the pentacyclic amyrin core is thermodynamically unfavorable and has a high activation barrier thus favoring premature termination.

Scheme 1. 11: Cyclization of epoxypolyene **1.50** via cationic or radical intermediates.

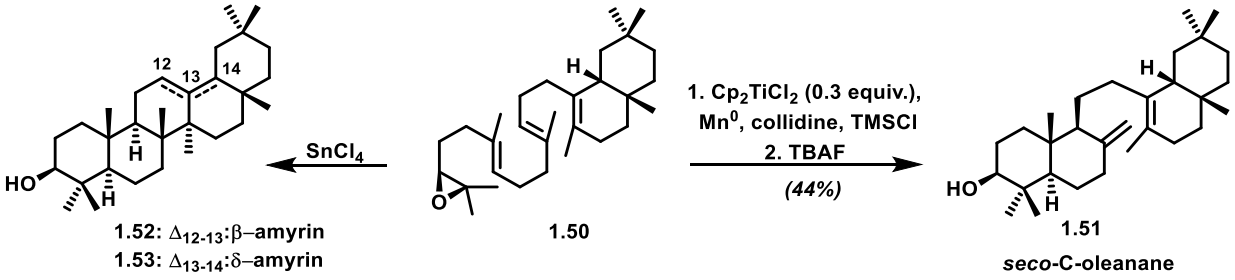

Changing the electronics of the internal alkenes by introducing ketones can lead to unexpected stereochemical outcomes. For instance, Cuerva and co-workers showed that cyclizations of ketoepoxypolyprenes can give *cis*-fused decalins from substrates bearing only *E*-

alkenes (**Scheme 1.12**).[34] Although the origin of stereocontrol in these reactions was unclear, DFT calculations suggested that oxygenated groups can chelate the Ti-catalyst thus restricting the reactive intermediates to a particular conformation. Additionally, enones can serve as terminating groups in these radical cascades because reduction of the intermediary α-acyl radicals to the corresponding titanium enolates is kinetically favored over further cyclization events.

Scheme 1. 12: The Ti(III)-mediated radical cyclization of ketoepoxypolyprene **1.54**.

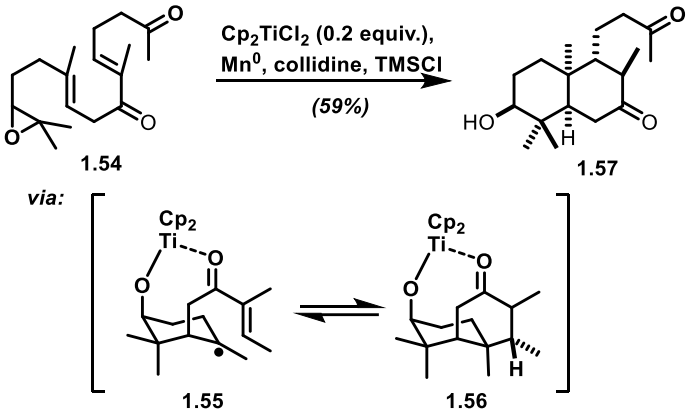

Li and coworkers showed that electron deficient radicals can be tolerated at the outset of Ti(III)-mediated polycyclizations. In their asymmetric synthesis of xiamycin A, undesired reduction of the α-acyl radical was suppressed by using Hünig's base instead of collidine (**Scheme 1.13**).[35] The synthetic utility of this approach is highlighted by the fact that analogous substrates fail to cyclize under Lewis acid-catalyzed conditions.[36] It is likely that Lewis-acid coordination to the carbonyl functionality in such α-functionalized epoxides inhibits heterolysis of the carbon-oxygen bond by destabilizing the resulting cation. Conversely, the corresponding radical species is stabilized via delocalization and well-poised to react with π-rich acceptors.

Scheme 1. 13: The Ti(III)-mediated polycyclization used by Li and co-workers en route to xiamycin A.

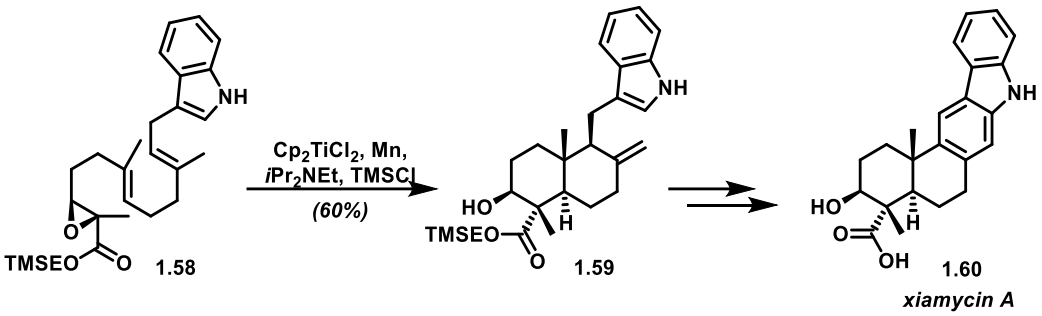

Termination via *endo*-trig cyclizations with pendant allylic acetates is another useful tactic that can be employed when using the Ti(IV)-catalyzed radical polyene cyclization. A striking example of this can be drawn from Kobayashi's total synthesis of fomitellic acid B (**Scheme 1.14, a**).[7c] Two quaternary carbon centers are forged in a single step, delivering a C3 and C18 oxygenated decalin framework **1.62** as the major product along with a small amount of monocyclized by-products. Lewis acid catalyzed approaches would likely fare poorly in scenarios like this, due to highly congested nature of the substrate and presence of multiple lewis basic sites. More recently, Barrero and co-workers reported an allylic acetate terminated cyclization to access the seven-membered C ring containing (–)-valparane (**Scheme 1.14, b**).[37]

Scheme 1. 14: a) The key polycyclization in Kobayashi's total synthesis of fomitellic acid B. **b)** Synthesis of valparane reported by Barrero and co-workers.

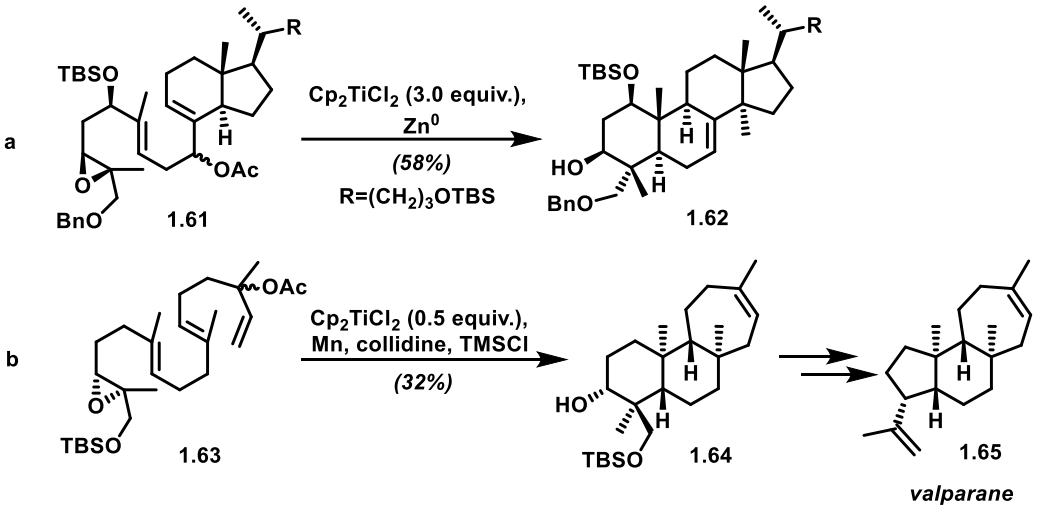

1.1.5 Organo-SOMO Catalyzed Oxidative Radical Polyene Cyzlization

In 2010, MacMillan and Rendler reported an enantioselective, organo-SOMO catalyzed approach to the polyene cyclization.[38] This process is initiated by condensation of a chiral amine catalyst **1.67** with the aldehyde in the substrate (**Scheme 1.15**). The resulting enamine **1.68** is oxidized by $Cu(OTf)_2$ to give an α-imino radical cation **1.69**, which engages the polyalkene chain in a face-selective manner. It should be noted that for tri- and higher order cyclizations, the alkene acceptors were alternated in polarity to favor 6-*endo* cyclization pathways. Lastly, radical addition to the arene and Cu(II)-mediated oxidation of the corresponding cyclohexadienyl radical furnished terpenoid-like polycycles (**Scheme 1.14, b**). Substrates bearing arenes with meta substitution gave regioisomeric mixtures where "ortho" products were major (**Scheme 1.14, 1.73**). Antecedent computational studies suggested that "ortho" regioisomers were formed more readily due to greater stabilization of the cyclohexadienyl radical by the methoxy substituent. This is sharp contrast with cationic processes were the "para" regioisomer is always preferred. Despite the lack

of application to total synthesis, this approach offers an attractive radical-polar crossover strategy to access functionalized terpenoid scaffolds.

Scheme 1. 15: The mechanism of McMillan and Rendler's organo-SOMO catalyzed cyclization.

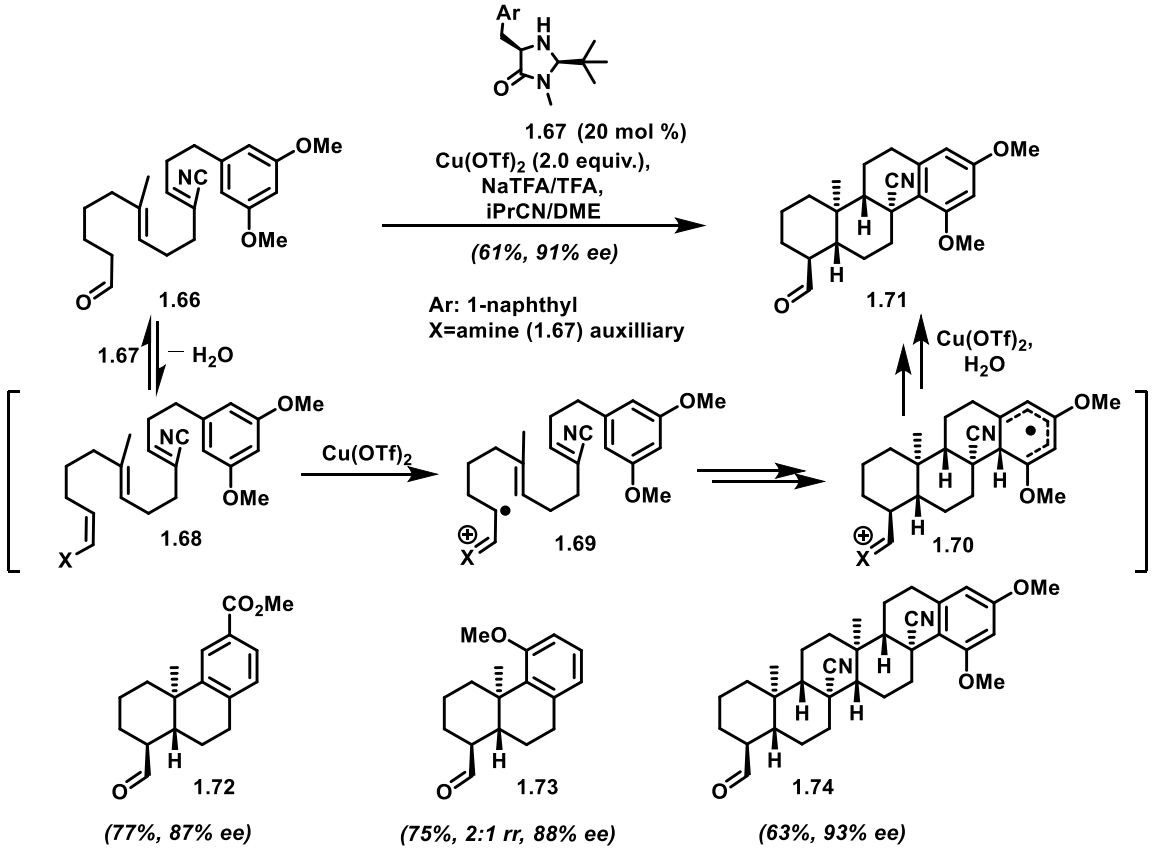

1.1.6 MHAT-Initiated Radical Polycyclization in Liu's Synthesis of Hispidanin A

It is well-known that certain metal-hydrides can undergo hydrogen-atom-transfer (HAT) to alkenes to generate carbon centered radicals. The initiation of these processes is highly chemo- and Markovnikov-selective, thus providing reliable means for hydrofunctionalization of unactivated olefins.[39] In 2017, Liu and coworkers reported the synthesis of a dimeric diterpenoid hispidanin A.[40] To access the monomer bearing oxidation at C-20, the authors devised a HAT initiated radical polycyclization approach (**Scheme 1.16**). Submitting polyene **1.75** to Fe(III)-catalyzed conditions reported by Baran[41] gave a mixture of stereoisomers which was resolved after

desilylation to furnish tricyclic scaffold **1.76** in 45% yield. Since this process is net-reductive, it was not immediately obvious whether the second cyclization event proceeded via radical or polar intermediates. When this reaction was carried out using ethanol-d_1 as solvent, deuteration at C-8 (of **1.76**) was observed. However, this does not rule out the possibility of premature reduction of intermediate **1.78**, in which case the second cyclization could proceed via an iron-enolate Michael addition.

Scheme 1. 16: The proposed mechanism for MHAT-initiated polycyclization in Liu's synthesis of hispidanin A.

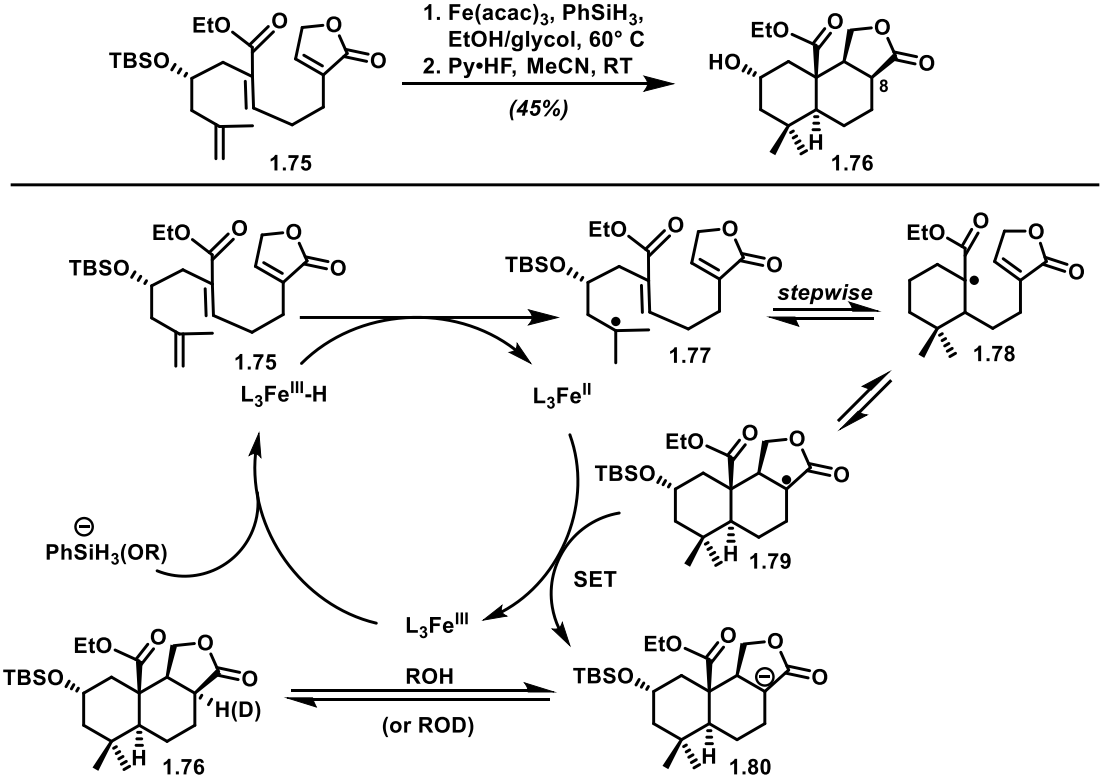

Liu's hispidanin A synthesis and a short study from the Norton group[42] (discussed in section **1.22**, see **Scheme 1.18**), serve as excellent proofs of concept for the development of polyene cyclizations initiated by HAT. The main drawbacks of these approaches are that they both proceed via net reductive processes, limiting the terminating moieties that can be engaged. For

instance, arenes would most likely fail to cyclize due to difficulties associated with regenerating aromaticity in a reductive environment.[43] We surmised that employing a redox-neutral or oxidative catalytic system would circumvent this issue and greatly expand the synthetic utility of this approach. The remainder of this chapter is aimed at introducing the reader to a selection of reports where MHAT was used to initiate C-C bond-forming processes.

1.2 MHAT Initiated Carbon-Carbon Bond Formation

The advent of mild and selective MHAT to alkenes has greatly enriched the field of alkene hydrofunctionalizations. Alkyl radicals generated in this manner can be trapped with good Markovnikov selectivity using a variety of radical acceptors including alkenes.[39a] In cases where cage-escape is operative, the reactivity of the nascent radical species often parallels that of open-shell species generated by other means.[44] This is a considerable advantage since alkenes can be accessed in a straightforward manner via many different approaches. Likewise, by sidestepping tedious installation of sensitive radical precursors, radical cascade strategies can become more viable in complicated settings.

A variety of approaches have been developed to effect MHAT using reductive or oxidative catalytic cycles. Systems utilizing Fe, Mn, and Co catalysts with weak-field ligands have received the most attention thus far.[39b] This can be attributed to weaker M-H bonds in the corresponding metal hydrides, permitting rapid MHAT to unactivated alkenes. Weak-field complexes typically have intermediate or high spin electronic configurations, where unpaired electrons can reside in antibonding orbitals. Such metal-hydrides are often paramagnetic and not isolable making thorough reaction interrogation challenging.[45] Despite this, continued interest from the synthetic community fuels research in this area.

1.2.1 Reductive Aldol-Type Reactions

During their seminal studies of alkene hydrations, Mukaiyama and co-workers reported a Co-catalyzed reductive coupling of α,β-unsaturated carbonyl derivatives and aldehydes (**Scheme 1.17, a**).[46] This transformation most likely involves HAT to the electron-deficient alkene followed by formation of the corresponding cobalt enolate which undergoes an aldol-type addition with the aldehyde. The Krische group developed this methodology further to effect intramolecular aldol cyclizations (**Scheme 1.16, b**).[47] This approach offers excellent *syn*-diastereoselectivity which can be difficult to achieve in base or acid catalyzed systems. Nonetheless, a variety of other hydrides can effect similar transformations thus rendering these reactions not particularly groundbreaking for synthesis.

Scheme 1. 17: a) Mukaiyama's MHAT-initiated aldol-type reaction between electron-deficient alkenes and aldehydes. **b)** Intramolecular variant of the above reaction reported by Krische and co-workers.

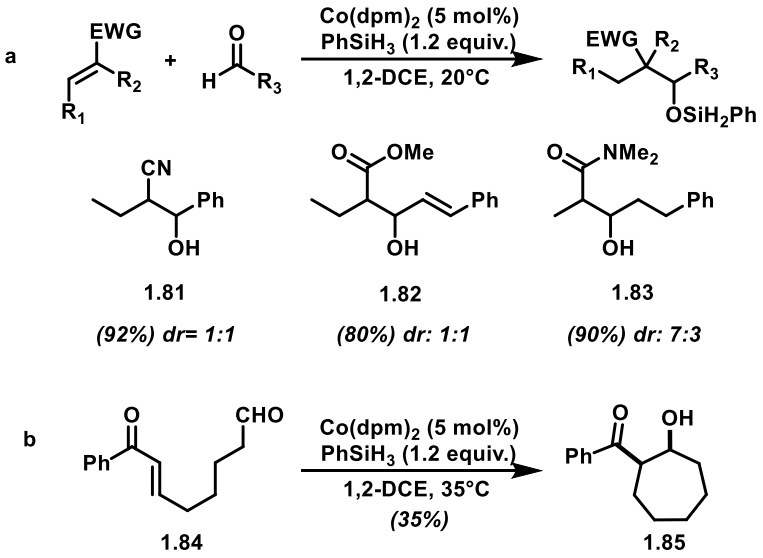

1.2.2 Alkene Isomerizations, Cycloisomerizations, and Giese Reactions

In 2002, van der Donk group described a vitamin B12 catalyzed dimerization of arylalkenes.[48] In a subsequent report, the authors also disclosed reductive and net neutral cyclizations involving pendant unactivated alkenes (**Scheme 1.7, a**).[49] Mechanistic studies suggested a radical mechanism; however, involvement of MHAT was not discussed likely due to a dearth of knowledge in this field at the time. Strong-field complexes were investigated in this context by the Norton group, who demonstrated that $CpCr(CO)_3H$ can initiate radical cyclizations of electron deficient dienes. Norton and co-workers have also reported the first radical polyene cyclization initiated by HAT (**Scheme 1.7, b**). The relatively poor efficiency of these reactions can be attributed to the fact that the M-H bond in complexes bearing strong field ligands is stronger, rendering the MHAT event endothermic.[50]

Scheme 1. 18: a) MHAT-initiated radical cyclizations of aryl alkenes reported by Van der Donk and co-workers. **b)** The first report of an MHAT-initiated polyene cyclization by Norton and co-workers.

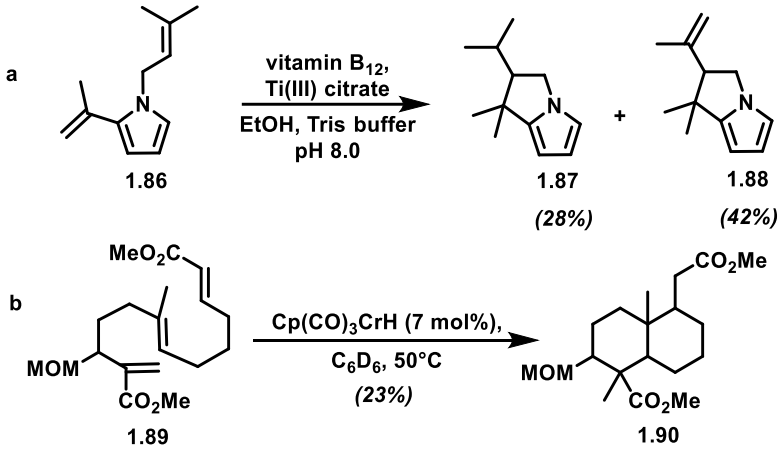

Led by the work of their predecessors, in 2014 Baran and co-workers reported a hydrogen-atom transfer mediated reductive alkene cross-coupling.[41] After regioselective MHAT to an electron rich alkene, the resulting radical undergoes a Giese-type addition reaction with the

electron deficient coupling partner (**Scheme 1.18, a**). Most remarkably, the native reactivity of heteroatom-functionalized alkenes can be reversed when using this approach (**Scheme 1.18, b**).[51] Optimization studies indicated that inexpensive Fe(III) catalysts bearing weak-field acetylacetonate or di-isobutyrylmethane ligands could catalyze this process efficiently. Although these studies utilized phenylsilane as the hydride donor, Shenvi later demonstrated that isopropoxy(phenyl)silane is a superior hydride source in this context.[52] Excellent chemoselectivity for hydrogen atom transfer was observed in most cases, unravelling a general reactivity trend: electron rich alkenes reacted with metal hydrides in preference to α,β-unsaturated systems. Nebulous aspects of the catalytic cycle involved, such as the fate of the Fe(II) species upon HAT and the role of the solvent, were investigated in 2019 by Holland and co-workers.[53]

Scheme 1. 19: a) MHAT-initiated coupling of olefins via a Giese-type reaction reported by Baran and co-workers. **b)** Heteroatom-functionalized alkene coupling with α,β-unsaturated carbonyl derivatives.

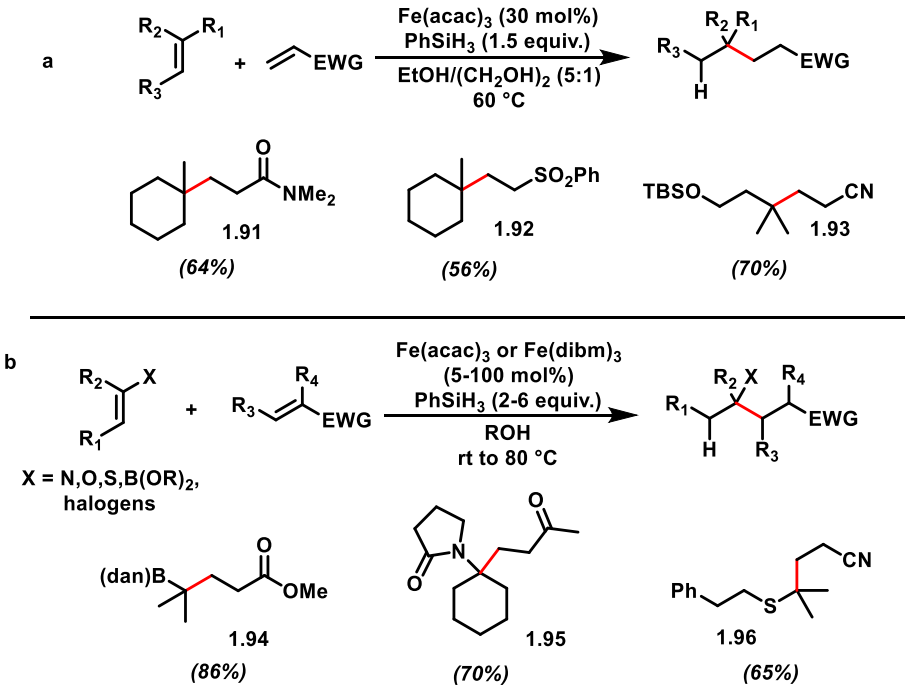

In 2014, the Shenvi group reported an operationally simple Co(III)(salen)-catalyzed approach to alkene isomerizations, cycloisomerizations and retrocycloisomerizations.[54] Experimental observations and literature precedent suggested a radical mechanism initiated by reversible MHAT from cobalt-hydride **1.98** (**Scheme 1.19**). The resulting carbon-centered radical **1.99** could undergo back-HAT to the Co(II) species regenerating the metal-hydride species, and forming the thermodynamically more stable alkene product **1.100**. The authors argued that success of these reactions depended on the persistence of the carbon-centered radical, which is tied to the stability of a metal-ligand "counterradical". Substrates bearing pendant alkenes or arenes underwent cycloisomerization, suggesting that this methodology could be applied in radical cascade cyclizations. Around the same time period, Norton and co-workers reported that other catalysts can effect such reactions under hydrogen gas (**Scheme 1.20**).[55] For instance, $Co(dmgBF_2)(THF)_2$ proved to be an effective catalyst for isomerizations and cycloisomerizations. Interestingly, the authors previous work demonstrated that cyclohydrogenation prevails when superstoichiometric amounts of strong-field complexes such as $CpCr(CO)_3H$ are used.[56]

Scheme 1. 20: Co(III)-catalyzed isomerization, cycloisomerization, and retrocycloisomerization of alkenes reported by Shenvi and co-workers.

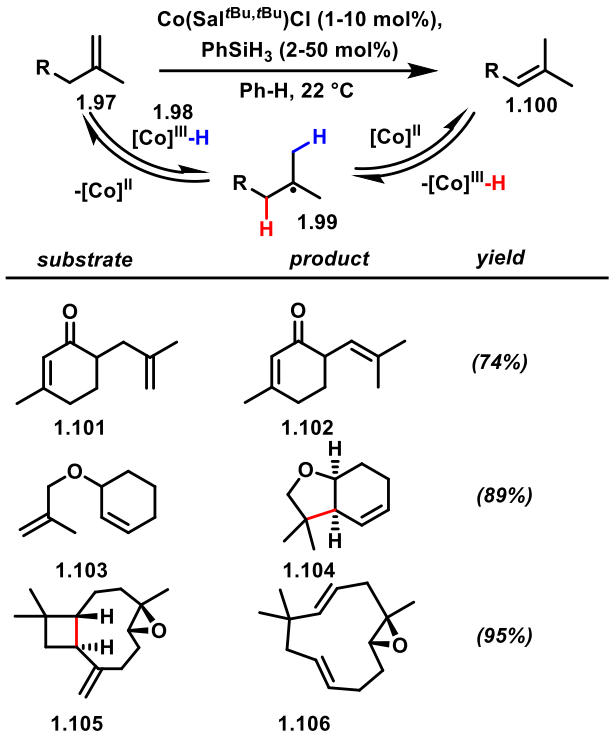

Scheme 1. 21: Catalyst-controlled cycloisomerization and cyclohydrogenation of diene **1.107** reported by Norton and co-workers.

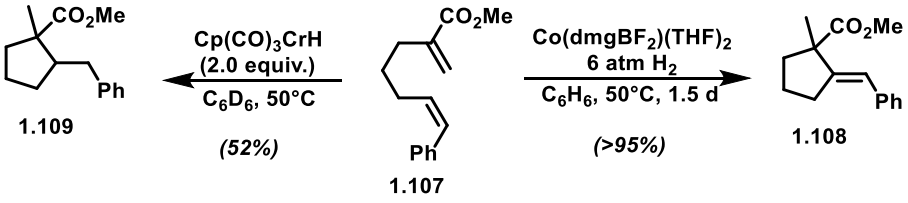

1.2.3 MHAT-Initiated Polycyclizations in Terpenoid Synthesis

Formation of C-C bonds via reductive MHAT catalysis has found application in the context of complex terpenoid synthesis. Several total syntheses have been reported by Pronin and co-workers, where MHAT initiated radical-polar crossover cascades were featured as key steps. In their first report, the authors constructed the tricyclic core of emindole SB via a radical cyclization-

reductive aldol cascade (**Scheme 1.21**).[57] Chemoselective hydrogen atom transfer to the 1,1-disubstituted alkene in substrate **1.109** resulted in formation of a tertiary alkyl radical **1.110** which engaged the pendant enal to close the first six-membered ring. Reduction of the resulting α-acyl radical generated enolate **1.111** which underwent an intramolecular aldol reaction with the pendant aliphatic aldehyde to give **1.112**. The authors used a similar approach to assemble a tricyclic fragment in the convergent synthesis of nodulisporic acid (**1.118**).[58] More recently, the Pronin group reported an intermolecular annulation variant of this strategy which was utilized to access an early bicyclic intermediate in the synthesis of forskolin (**Scheme 1.22, b**).[59]

Scheme 1. 22: MHAT-initiated polycyclization towards emindole SB reported by Pronin and co-workers.

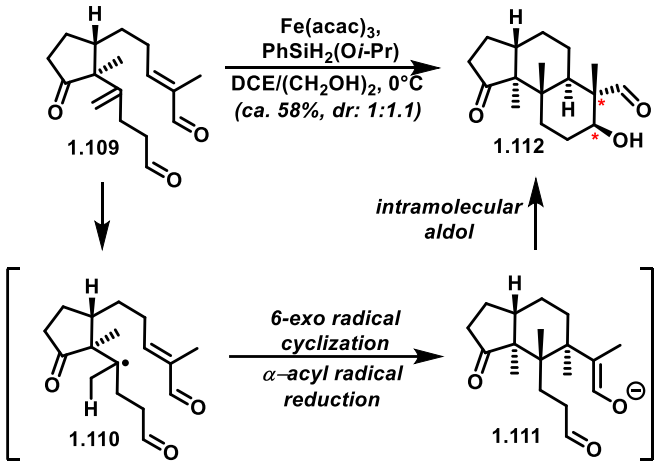

Scheme 1. 23: Pronin's reductive MHAT polycyclization and annulation approaches used in the syntheses of nodulisporic and C and forskolin respectively.

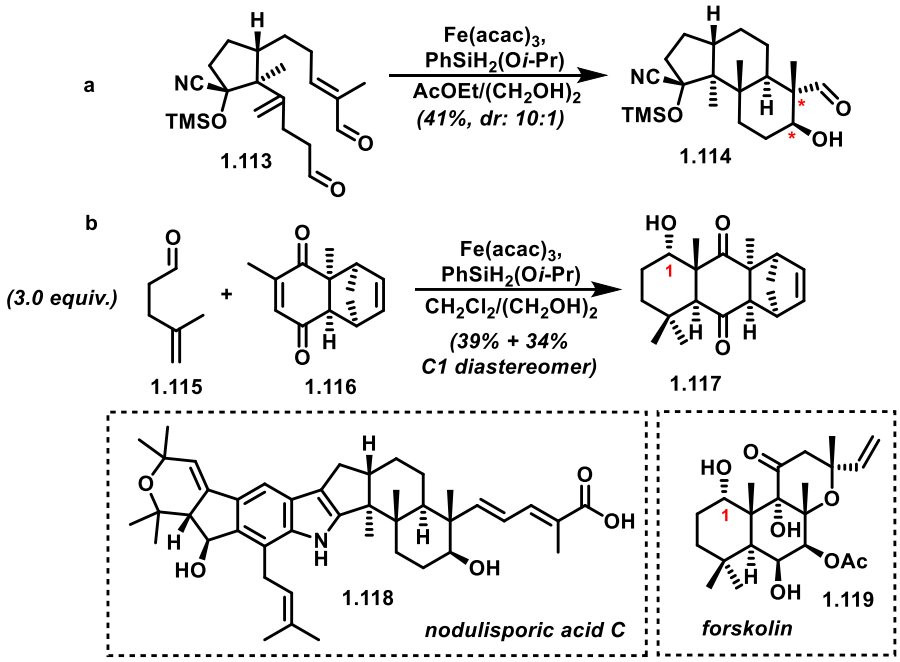

1.2.4 MHAT-Initiated Oxidative Radical-Polar Crossover Reactions

Oxidative approaches to construct C-C bonds via MHAT catalysis have received considerably less attention. The possibility of carbon-centered radical species undergoing radical-polar crossover to form carbocations directly was postulated in several reports on MHAT hydrofunctionalizations by Shigehisa and co-workers.[60] For instance, a hydroarylation requiring at least two equivalents of an external oxidant was proposed to proceed via a cationic pathway (**Scheme 1.23, a**).[61] Interestingly, oxidation of tertiary alkyl radicals using *N*-fluoropyridinium salts[62] alone is unprecedented in the literature. This suggests that the metal catalyst might be facilitating the oxidation process; however, formation of tertiary alkylcobalt species is also poorly precedented.

Seminal reports from Halpern and co-workers demonstrated that secondary alkylcobalt(IV) species generated by oxidation of the corresponding Co(III) complexes can undergo invertive

displacement.[63] However, the authors also noted that use of certain Schiff base complexes led to S_N1 or S_Ni type reactivity.[64] In a recent report on catalytic radical-polar crossover reactions with allylic alcohols, Pronin and co-workers observed catalyst-controlled bifurcation of the of the radical-polar crossover pathways (**Scheme 1.24**).[65] In agreement with Halpern's studies, an intramolecular displacement of a secondary Co(IV) species **1.131** was invoked to rationalize epoxide (**1.127**) formation. Ring expansion via a semipinacol rearrangement (**1.128**) was proposed to occur via cation-like intermediate formation, but alkylcobalt intermediacy could not be ruled out.

Scheme 1. 24: a) The proposed mechanism for Shigehisa's Co(II)-catalyzed intramolecular hydroarylation of olefins. **b)** Selected examples from the substrate scope.

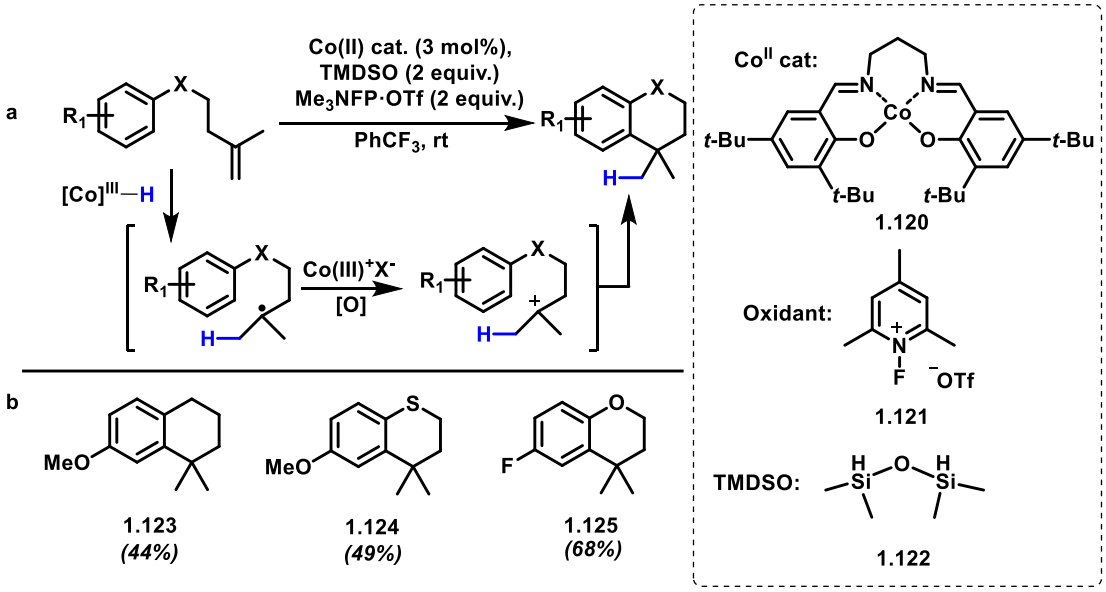

Scheme 1. 25: Catalyst-controlled bifurcation of radical-polar crossover pathways reported by Pronin and co-workers.

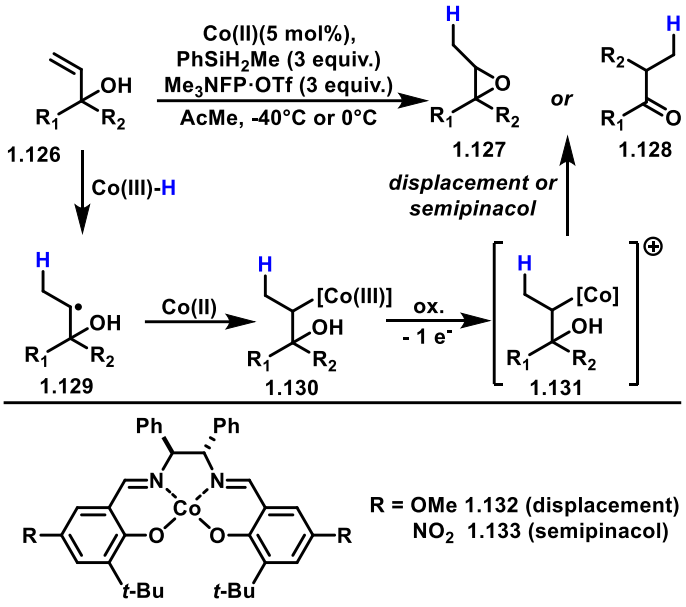

1.2.5 Dual-Catalyzed Hydroarylations of Alkenes

In 2016, Shenvi and co-workers reported a Co/Ni-catalyzed cross-coupling of iodoarenes with unactivated alkenes. This dual-catalytic approach advanced interception of radicals generated via MHAT with other metal centers. Subsequent mechanistic studies allowed differentiation between cage-escape/nickel-capture and direct transmetalation pathways, favoring the latter (**Scheme 1.25, a**). This unprecedented process was described to occur in a cage-rebound manner, implying direct electron/alkyl transfer to the Ni center (**1.135** to **1.137**). The resulting cationic Co(III) species is then reduced by the silane to regenerate the metal hydride and turn over the catalytic cycle. It should be noted that direct transmetalation permits use of substoichiometric amounts of oxidant, rendering the overall transformation redox neutral.

In 2018, Shenvi group reported another highly Markovnikov-selective hydroarylation of alkenes using an iron-nickel dual-catalytic approach (**scheme 1.25, b**).[66] This reaction likely proceeds in an analogous manner to the Co/Ni catalyzed approach but without direct

transmetalation. Since the intermediacy of tertiary alkyl-iron complexes is highly unlikely, it was proposed that the corresponding tert-alkyl radicals reacted directly with the Ni(I)/Ni(III) complexes and Mn(0) reduced the Ni(I) species after reductive elimination. Notably, this approach was effective at forging quaternary carbon centers (**1.143-1.146**) where Friedel-Crafts or cationic strategies would be expected to fare poorly.[67]

The literature precedents described in the previous sections and other studies suggest that MHAT catalysis could be utilized in the development of oxidative radical cascade processes to form multiple C-C bonds. Reductive and net-neutral approaches have already been met with considerable success in this context. It stands to reason that an oxidative approach could permit cascade termination using electron rich moieties rather than being limited to electron deficient alkenes and carbonyl derivatives. Inspired by this, we undertook the challenge of developing a general MHAT-initiated radical polyolefin cyclization. The development and applications of an MHAT-initiated bicyclization is discussed in the next two chapters.

Scheme 1. 26: Dual-catalyzed intramolecular hydroarylations of unactivated alkenes reported by Shenvi and co-workers. **a)** Redox-neutral strategy using a Co(II)-precatalyst; **b)** Reductive-MHAT approach using Fe(III)/Ni(II) precatalysts.

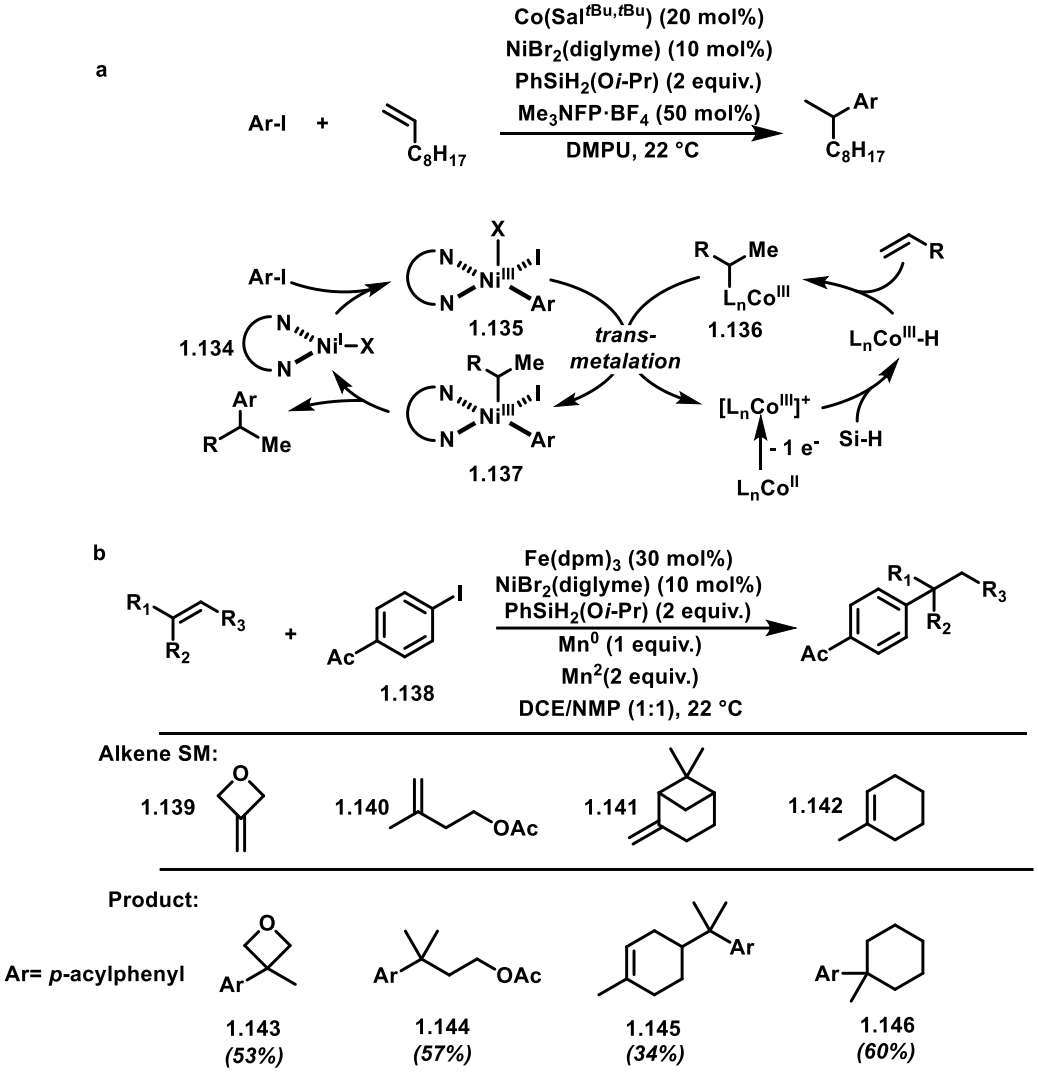

1.3 Notes and References

(1) Yoder, R. A.; Johnston, J. N. *Chem. Rev.* **2005**, *105*, 4730–4756.

(2) Stork, G.; Burgstahler, A. W. *J. Am. Chem. Soc.* **1955**, *77*, 5068–5077.

(3) Eschenmoser, A.; Ruzicka, L.; Jeger, O.; Arigoni, D. *Helv. Chim. Acta* **1955**, *38*, 1890–1904.

(4) Johnson, W. S. *Acc. Chem. Res.* **1968**, *1*, 1–8.

(5) van Tamelen, E. E.; Willet, J.; Schwartz, M.; Nadeau, R. *J. Am. Chem. Soc.* **1966**, *88*, 5937–5938.

(6) a) Barrero, A. F.; Cuerva, J. M.; Herrador, M. M.; Valdivia, M. V. *J. Org. Chem.* **2001**, *66*, 4074–4078; b) Chen, L.; Gill, G. B.; Pattenden, G.; Simonian, H. *J. Chem. Soc., Perkin Trans. 1* **1996**, 31–43; c) Zoretic, P. A.; Fang, H.; Ribeiro, A. A. *J. Org. Chem.* **1998**, *63*, 7213–7217; d) Snider, B. B.; Mohan, R.; Kates, S. A. *J. Org. Chem.* **1985**, *50*, 3659–3661; eBreslow, R.; Olin, S. S.; Groves, J. T. *Tetrahedron Lett.* **1968**, *9*, 1837–1840.

(7) a) Corey, E. J.; Liu, K. *J. Am. Chem. Soc.* **1997**, *119*, 9929–9930; b) Zhou, S.; Guo, R.; Yang, P.; Li, A. *J. Am. Chem. Soc.* **2018**, *140*, 9025–9029; c) Yamaoka, M.; Nakazaki, A.; Kobayashi, S. *Tetrahedron Lett.* **2009**, *50*, 6764–6768.

(8) Romero, K. J.; Galliher, M. S.; Pratt, D. A.; Stephenson, C. R. J. *Chem. Soc. Rev.* **2018**, *47*, 7851–7866.

(9) Stadler, P. A.; Eschenmoser, A.; Schinz, H.; Stork, G. *Helv. Chim. Acta* **1957**, *40*, 2191–2198.

(10) Bathe, U.; Tissier, A. *Phytochemistry* **2019**, *161*, 149–162.

(11) Justicia, J.; Álvarez de Cienfuegos, L.; Campaña, A. G.; Miguel, D.; Jakoby, V.; Gansäuer, A.; Cuerva, J. M. *Chem. Soc. Rev.* **2011**, *40*, 3525–3537.

(12) Hoffmann, U.; Gao, Y.; Pandey, B.; Klinge, S.; Warzecha, K. D.; Krueger, C.; Roth, H. D.; Demuth, M. *J. Am. Chem. Soc.* **1993**, *115*, 10358–10359.

(13) Heinemann, C.; Xing, X.; Warzecha, K. D.; Ritterskamp, P.; Görner, H.; Demuth, M. *Pure Appl. Chem.* **1998**, *70*, 2167–2176.

(14) a) Goeller, F.; Heinemann, C.; Demuth, M. *Synthesis* **2001**, *112*, 1114–1116; b) Warzecha, K.-D.; Xing, X.; Demuth, M. *Pure Appl. Chem.* **1997**, *69*, 109–112.

(15) Rosales, V.; Zambrano, J.; Demuth, M. *Eur. J. Org. Chem.* **2004**, *2004*, 1798–1802.

(16) Yang, Z.; Li, H.; Zhang, L.; Zhang, M.-T.; Cheng, J.-P.; Luo, S. *Chem. Eur. J.* **2015**, *21*, 14723–14727.

(17) Colomer, I.; Chamberlain, A. E. R.; Haughey, M. B.; Donohoe, T. J. *Nat. Rev. Chem.* **2017**, *1*, 0088.

(18) Boger, D. L.; Mathvink, R. J. *J. Am. Chem. Soc.* **1990**, *112*, 4003–4008.

(19) a) Chen, L.; Gill, G. B.; Pattenden, G. *Tetrahedron Lett.* **1994**, *35*, 2593–2596; b) Batsanov, A.; Chen, L.; Gill, G. B.; Pattenden, G. *J. Chem. Soc., Perkin Trans. 1* **1996**, 45–55; c) Double, P.; Pattenden, G. *J. Chem. Soc., Perkin Trans. 1* **1998**, 2005–2008; d) Handa, S.; Pattenden, G. *J. Chem. Soc., Perkin Trans. 1* **1999**, 843–846; e) Pattenden, G.; Roberts, L.; J. Blake, A. *J. Chem. Soc., Perkin Trans. 1* **1998**, 863–868.

(20) Handa, S.; Pattenden, G. *Chem. Commun.* **1998**, 311–312.

(21) Snider, B. B. *Chem. Rev.* **1996**, *96*, 339–364.

(22) Snider, B. B. *Tetrahedron* **2009**, *65*, 10738–10744.

(23) Zhang, Q.; Mohan, R. M.; Cook, L.; Kazanis, S.; Peisach, D.; Foxman, B. M.; Snider, B. B. *J. Org. Chem.* **1993**, *58*, 7640–7651.

(24) Snider, B. B.; Mohan, R.; Kates, S. A. *Tetrahedron Lett.* **1987**, *28*, 841–844.

(25) Kochi, J. K. *Acc. Chem. Res.* **1974**, *7*, 351–360.

(26) Snider, B. B.; Kiselgof, J. Y.; Foxman, B. M. *J. Org. Chem.* **1998**, *63*, 7945–7952.

(27) Zoretic, P. A.; Chen, Z.; Zhang, Y.; Ribeiro, A. A. *Tetrahedron Lett.* **1996**, *37*, 7909–7912.

(28) Merchant, R. R.; Oberg, K. M.; Lin, Y.; Novak, A. J. E.; Felding, J.; Baran, P. S. *J. Am. Chem. Soc.* **2018**, *140*, 7462–7465.

(29) RajanBabu, T. V.; Nugent, W. A. *J. Am. Chem. Soc.* **1994**, *116*, 986–997.

(30) Justicia, J.; Jiménez, T.; Morcillo, S. P.; Cuerva, J. M.; Oltra, J. E. *Tetrahedron* **2009**, *65*, 10837–10841.

(31) Gansäuer, A.; Bluhm, H.; Pierobon, M. *J. Am. Chem. Soc.* **1998**, *120*, 12849–12859.

(32) Domingo, V.; Arteaga, J. F.; López Pérez, J. L.; Peláez, R.; Quílez del Moral, J. F.; Barrero, A. F. *J. Org. Chem.* **2012**, *77*, 341–350.

(33) Corey, E. J.; Lee, J. *J. Am. Chem. Soc.* **1993**, *115*, 8873–8874.

(34) Morcillo, S. P.; Miguel, D.; Resa, S.; Martín-Lasanta, A.; Millán, A.; Choquesillo-Lazarte, D.; García-Ruiz, J. M.; Mota, A. J.; Justicia, J.; Cuerva, J. M. *J. Am. Chem. Soc.* **2014**, *136*, 6943–6951.

(35) Meng, Z.; Yu, H.; Li, L.; Tao, W.; Chen, H.; Wan, M.; Yang, P.; Edmonds, D. J.; Zhong, J.; Li, A. *Nat. Commun.* **2015**, *6*, 6096.

(36) Rajendar, G.; Corey, E. J. *J. Am. Chem. Soc.* **2015**, *137*, 5837–5844.

(37) Quílez del Moral, J. F.; Pérez, Á.; Herrador, M. d. M.; Barrero, A. F. *J. Nat. Prod.* **2019**, *82*, 9–15.

(38) Rendler, S.; MacMillan, D. W. C. *J. Am. Chem. Soc.* **2010**, *132*, 5027–5029.

(39) a) Crossley, S. W. M.; Obradors, C.; Martinez, R. M.; Shenvi, R. A. *Chem. Rev.* **2016**, *116*, 8912–9000; b) Shevick, S. L.; Wilson, C. V.; Kotesova, S.; Kim, D.; Holland, P. L.; Shenvi, R. A. *Chem. Sci.* **2020**, *11*, 12401–12422.

(40) a) Deng, H.; Cao, W.; Liu, R.; Zhang, Y.; Liu, B. *Angew. Chem. Int. Ed.* **2017**, *56*, 5849–5852; b) Cao, W.; Deng, H.; Sun, Y.; Liu, B.; Qin, S. *Chem. Eur. J.* **2018**, *24*, 9120–9129.

(41) Lo, J. C.; Yabe, Y.; Baran, P. S. *J. Am. Chem. Soc.* **2014**, *136*, 1304–1307.

(42) Hartung, J.; Pulling, M. E.; Smith, D. M.; Yang, D. X.; Norton, J. R. *Tetrahedron* **2008**, *64*, 11822–11830.

(43) Castillo, A.; del Moral, J. F. Q.; Barrero, A. F. *Nat. Prod. Commun.* **2017**, *12*, 1934578X1701200503.

(44) Koenig, T. W.; Hay, B. P.; Finke, R. G. *Polyhedron* **1988**, *7*, 1499–1516.

(45) Shevick, S. L.; Obradors, C.; Shenvi, R. A. *J. Am. Chem. Soc.* **2018**, *140*, 12056–12068.

(46) Shigeru, I.; Teruaki, M. *Chem. Lett.* **1989**, *18*, 2005–2008.

(47) Baik, T.-G.; Luis, A. L.; Wang, L.-C.; Krische, M. J. *J. Am. Chem. Soc.* **2001**, *123*, 5112–5113.

(48) Shey, J.; McGinley, C. M.; McCauley, K. M.; Dearth, A. S.; Young, B. T.; van der Donk, W. A. *J. Org. Chem.* **2002**, *67*, 837–846.

(49) McGinley, C. M.; Relyea, H. A.; van der Donk, W. A. *Synlett* **2006**, *2006*, 211–214.

(50) Eisenberg, D. C.; Norton, J. R. *Isr. J. Chem.* **1991**, *31*, 55–66.

(51) Lo, J. C.; Gui, J.; Yabe, Y.; Pan, C.-M.; Baran, P. S. *Nature* **2014**, *516*, 343–348.

(52) Obradors, C.; Martinez, R. M.; Shenvi, R. A. *J. Am. Chem. Soc.* **2016**, *138*, 4962–4971.

(53) Kim, D.; Rahaman, S. M. W.; Mercado, B. Q.; Poli, R.; Holland, P. L. *J. Am. Chem. Soc.* **2019**, *141*, 7473–7485.

(54) Crossley, S. W. M.; Barabé, F.; Shenvi, R. A. *J. Am. Chem. Soc.* **2014**, *136*, 16788–16791.

(55) Li, G.; Kuo, J. L.; Han, A.; Abuyuan, J. M.; Young, L. C.; Norton, J. R.; Palmer, J. H. *J. Am. Chem. Soc.* **2016**, *138*, 7698–7704.

(56) Smith, D. M.; Pulling, M. E.; Norton, J. R. *J. Am. Chem. Soc.* **2007**, *129*, 770–771.

(57) George, D. T.; Kuenstner, E. J.; Pronin, S. V. *J. Am. Chem. Soc.* **2015**, *137*, 15410–15413.

(58) Godfrey, N. A.; Schatz, D. J.; Pronin, S. V. *J. Am. Chem. Soc.* **2018**, *140*, 12770–12774.

(59) Thomas, W. P.; Schatz, D. J.; George, D. T.; Pronin, S. V. *J. Am. Chem. Soc.* **2019**, *141*, 12246–12250.

(60) Shigehisa, H. *Chem. Pharm. Bull.* **2018**, *66*, 339–346.

(61) Shigehisa, H.; Ano, T.; Honma, H.; Ebisawa, K.; Hiroya, K. *Org. Lett.* **2016**, *18*, 3622–3625.

(62) Umemoto, T.; El-Awa, A., in *Encyclopedia of Reagents for Organic Synthesis*.

(63) Magnuson, R. H.; Halpern, J.; Levitin, I. Y.; Vol'pin, M. E. *J. Chem. Soc., Chem. Commun.* **1978**, 44–46.

(64) Vol'pin, M. E.; Levitin, I. Y.; Sigan, A. L.; Halpern, J.; Tom, G. M. *Inorg. Chim. Acta* **1980**, *41*, 271–277.

(65) Touney, E. E.; Foy, N. J.; Pronin, S. V. *J. Am. Chem. Soc.* **2018**, *140*, 16982–16987.

(66) Green, S. A.; Vásquez-Céspedes, S.; Shenvi, R. A. *J. Am. Chem. Soc.* **2018**, *140*, 11317–11324.

(67) Naredla, R. R.; Klumpp, D. A. *Chem. Rev.* **2013**, *113*, 6905–6948.

CHAPTER 2: COBALT-CATALYZED HYDROGEN-ATOM TRANSFER INDUCES BICYCLIZATIONS THAT TOLERATE ELECTRON-RICH AND ELECTRON-DEFICIENT INTERMEDIATE ALKENES

2.1 Abstract

A novel Co^{II}-catalyzed polyene cyclization was developed that is uniquely effective when performed in hexafluoroisopropanol as the solvent. The process is presumably initiated by metal-catalyzed hydrogen-atom transfer (MHAT) to 1,1-disubstituted or monosubstituted alkenes, and the reaction is remarkable for its tolerance of internal alkenes bearing either electron-rich methyl or electron-deficient nitrile substituents. Electron-rich aromatic terminators are required in both cases. Terpenoid scaffolds with different substitution patterns are obtained with excellent diastereoselectivities, and the bioactive C20-oxidized abietane diterpenoid carnosaldehyde was made to showcase the utility of the nitrile-bearing products. Also provided are the results of several mechanistic experiments that suggest the process features an MHAT-induced radical bicyclization with late-stage oxidation to regenerate the aromatic terminator.

2.2 Introduction

The polycyclic products of biosynthetic polyene-type cyclizations are endowed with a wealth of structural diversity and biological activity. Inspired by these compelling secondary metabolites and their fascinating biogeneses, chemists have engaged in decades of work emulating nature's polyene cyclizations, starting with the seminal studies of the groups of Stork, Eschenmoser, Johnson, van Tamelen, and others.[1,2] As a result, chemists have accrued an excellent understanding of the reactivity and stereochemical outcomes of cation-initiated polycyclizations of polyenes as applied to bioinspired terpenoid synthesis. Many new polycyclization methods have been developed that have been tested in the total syntheses of these natural products. These advances include methods under-pinned by either radical or organometallic intermediates.[3,4] However, gaps

in this general area remain, including in the cyclization of systems that electronically deviate significantly from the natural terpenoid precursors.

Figure 2. 1: Atisane alkaloids and neotripterifordin inspired our efforts to develop bicyclization reactions with electron-withdrawing groups at C20.

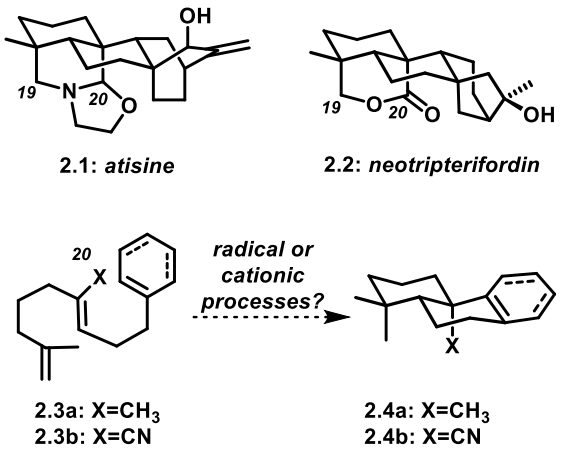

2.2.1 Prevalence of C-20 Oxidized Decalin Motifs in Natural Terpenoids

Inspired in part by the structures of the atisane alkaloids (**Figure 2.1**) and their more complex hetisine and hetidine congeners,[5] as well as the C19–C20 lactone-containing diterpenoids such as neotripterifordin (**2.2**),[6] we aimed to develop bicyclization reactions that would tolerate an electron-withdrawing group (ester or nitrile) in place of the ubiquitous, geraniol-derived C20 methyl group (see **2.3** to **2.4**).Although biosynthetically the oxidation of this carbon center surely occurs post-cyclization, it would be strategically valuable to incorporate these functional groups prior to cyclization in the laboratory setting. This idea is in line with our broader program to extend the range of functionalized substrates in stereocontrolled polycyclizations.[7] We presumed that this C20 "handle" would prove advantageous in subsequent applications to molecules such as **2.1**, **2.2**, and the many other diterpenoids with an oxidized C20 that is also frequently part of a ring structure. These synthesis endeavors themselves were largely discouraged by recent attractive, closely

related successes by Li and co-workers,[8] who included a secondary allylic ether function at this position in a Carreira-type enantioselective polycyclization,[4b] and Ma and co-workers,[9] who used a different scaffold-building strategy to make nitrile compounds related to **2.4b**. However, as our studies unfolded, we were surprised to discover conditions for Co-catalyzed HAT-initiated dialkenylarene bicyclizations with a rather broad scope, including the intriguing tolerance of either a C20 electron-donating methyl group (**2.3a**) or an electron-withdrawing nitrile (**2.3b**). These results and some preliminary mechanistic investigations are the subject of this chapter.

2.3 Results and Discussion

2.3.1 Optimization of Reaction Conditions

Building upon extensive recent reports in the area of metal-catalyzed hydrogen-atom transfer reactions to alkenes (MHAT),[10] we surmised that a tertiary radical could be easily generated from the 1,1-disubstituted alkenes of type **2.3**, and that under appropriate oxidative conditions, such as those from the group of Shigehisa,[11,12] cation generation could result by radical oxidation. Depending upon relative rates of oxidation and cyclization, either radical or cationic C−C bond-forming events would take place. Because we were most interested in developing cyclizations with C20 electron-withdrawing groups, we initiated our studies with the diene **2.5a** (**Table 1**), which was easily assembled by virtue of the oxygenation at C2.[13] We first evaluated a catalytic system similar to the one reported by Shigehisa for the hydroarylation of alkenes.[11d] Treatment of **2.5a** in acetone with phenylsilane, N-fluoropyridinium oxidant (**O**), and the cobalt complex **C1** yielded the tricyclic framework **2.6a** in moderate yield (entry 1). The use of substoichiometric quantities of oxidant was not tolerated (entry 2), and different silanes, including the "Ruben-silane"[14] (entries 3 and 4), did not significantly improve the outcome. For its convenience and low price, TMDSO

was chosen as the preferred silane. Other single-electron oxidants, including $Cu(OTf)_2$ and CAN, led to decomposition. Fortuitously, a small solvent screen revealed that carrying out the reaction in HFIP led to significantly improved yields (entries 4–8). A screen of a few different catalysts (entries 8–10) revealed that only **C1** gave good yields of **2.6a** in 3 hours. Decreasing the quantity of silane resulted in lower conversion and increased formation of unidentified side products (not shown). For practical purposes, using three equivalents of both silane and oxidant was found to be optimal as the reaction time was drastically reduced, and the reactivity was cleaner. Traces of the desired product were observed without any added oxidant (entry 11). Although we considered that this result might be due to adventitious oxygen, replacing the N-fluoropyridinium oxidant with an atmosphere of molecular oxygen led to a complex mixture, containing only traces of **2.6a** (entry 12). In the context of the optimal solvent for this transformation, it is noteworthy that Shigehisa has reported a method for hydrofunctionalization of alkenes employing fluorinated alcohols as nucleophiles using the same catalytic system.[11a] Other conditions evaluated (not shown) but found to be ineffective included: a) Shenvi's Co-catalyzed conditions for alkene isomerization, which can also lead to cyclization and hydroarylation;[15] b) Shenvi's Mn-mediated conditions for intramolecular radical hydroarylation;[16] and c) Baran's Fe-catalyzed system,[17] which is excellent at promoting Giese-type reactions[18] that strongly resemble the first ring formation in the transformation of **2.5a** into **2.6a**.

Table 2. 1: Optimization of bicyclization reaction conditions.

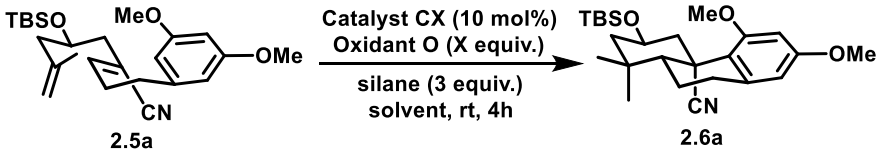

Entry[a]	Catalyst	Silane	X	Solvent[b]	Yield [%][c]
1	C1	$PhSiH_3$	3.0	Me_2CO	40
2	C1	$PhSiH_3$	0.5	Me_2CO	<5[d]
3	C1	$Ph(i\text{-}PrO)SiH_2$	3.0	Me_2CO	45
4	C1	TMDSO	3.0	Me_2CO	42
5	C1	$PhSiH_3$	3.0	*i*-PrOH	0
6	C1	TMDSO	2.0	$PhCF_3$	0
7	C1	TMDSO	3.0	CH_2Cl_2	<5
8	C1	TMDSO	3.0	*i*-PrOH	<5
9	C1	TMDSO	3.0	HFIP	87
10	C2	TMDSO	3.0	HFIP	31[d]
11	C3	TMDSO	3.0	HFIP	<5
12	C1	TMDSO	0	HFIP	<5[d]
13[e]	C1	TMDSO	O_2	HFIP	<5
14	*none*	TMDSO	3.0	HFIP	0

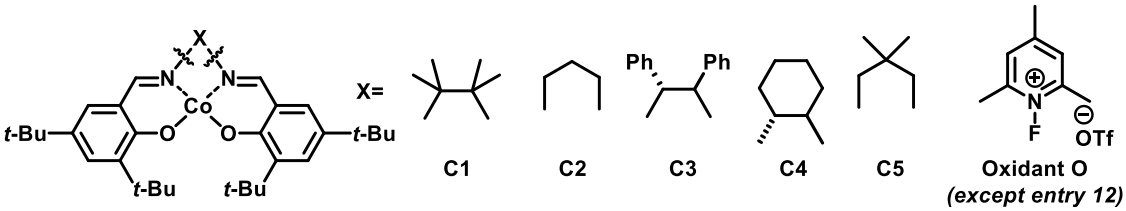

[a] All reactions were carried out using 5 a (0.02 mmol), oxidant, catalyst (0.002 mmol), silane (0.07 mmol), in solvent (0.5 m) at ambient temperature (RT) for 4 h under Ar. [b] Reaction mixtures were purged with Ar for 10 min. before the addition of silane. [c] For entries 1, 3, 4, 8, and 9 yields reported are those for the isolated products; for other entries yields were estimated by ^{1}H NMR spectroscopic analysis. [d] Incomplete conversion was observed. [e] Reaction was run for 12 h. HFIP=1,1,1,3,3,3-hexafluoroisopropanol, TBS=tert-butyldimethylsilyl, TMDSO=tetramethyldisiloxane.

2.3.2 Bicyclizations of Substrates Bearing Nitrile Substituted Internal Alkenes

With the optimized reaction conditions in hand, we investigated the scope of this process (**Figure 2.2**). Substrates with alkoxy-substituted aromatic terminators underwent bicyclization yielding the products **2.6a**–**c** in good yields and with excellent diastereoselectivities. Products bearing TBS-protected alcohols at C2 were each isolated as single stereoisomers, presumably owing to the preference for the bulky silyloxy substituent to assume a pseudoequatorial orientation in the transition structure for the first ring closure. A related system was used by Liu and co-workers in an elegant synthesis of hispidanin A. In this case the key iron-catalyzed, HAT-initiated bicyclization terminated onto an electron-poor alkene and was not fully stereoselective.[19] The *meta*-substituted anisole substrate gave a 1.7:1 *para*/*ortho* mixture of regioisomers (**2.6b**). The aryl bromide functionality in **2.6c** was tolerated under the reaction conditions. Naphthyl and toluyl substrates underwent cyclization in moderate yields (products **2.6d** and **2.6e**), suggesting that electron-rich arenes are the best terminators for this process. A Boc-protected indole substrate cyclized to give an indoline product **2.6f** along with a small quantity of the anticipated indole product; the same was observed for the corresponding *N*-tosyl substrate yielding **2.6g**. The indoline product might be produced by a competitive silane reduction of a post-cyclization cationic intermediate (see section **2.4**). Cyclization to generate the tricyclic scaffold **2.6h** was performed on a 1 mmol scale and constitutes a formal total synthesis of pisiferin (not shown).[20] Further, we converted **2.6h** into the recently described bioactive aromatic abietane diterpenoid[21] carnosaldehyde in three steps,[13,22] demonstrating the utility of the C20-oxidized products. Ester- and trifluoromethyl-bearing arenes did not yield any of the desired cyclization products (**2.6i** and **2.6j**, respectively), suggesting that electron-poor arenes are not suitable terminating groups for these reactions.

Figure 2. 2: Scope of the bicyclization of nitrile-substituted substrates (yields shown are for isolated and purified compounds). Boc=*tert*-butoxycarbonyl, Ts=*para*-toluenesulfonyl.

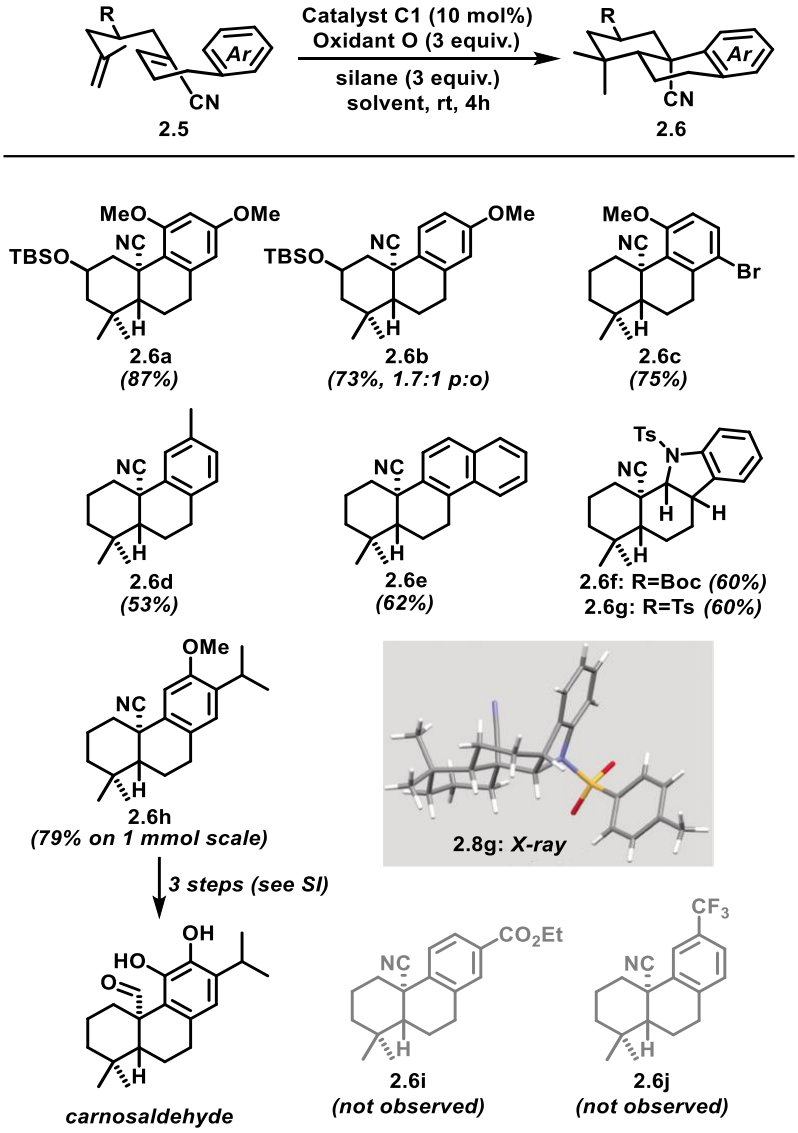

2.3.3 Bicyclizations of Substrates Bearing Methyl Substituted Internal Alkenes

In light of Shigehisa's report on hydroarylation of unactivated alkenes,[11d] we changed the substrate to include the trisubstituted, methyl-bearing internal alkene that is more typical of bioinspired polyene cyclizations. Several of these substrates reacted productively, generating the tricyclic compounds **2.8a**–**d** with reasonable efficiency[23] under nearly identical reaction

conditions used for the nitrile substrates (**Figure 2.3**); in these cases the less sterically crowded catalyst **C2** proved slightly superior to **C1**. Product **2.8c**, a known compound,[24] was formed along with products of terminal to internal alkene isomerization of the substrate; owing to the formation of multiple products of similar polarity, it could only be obtained in about 90 % purity. The product of furan termination (**2.8e**) was not observed, which was unexpected; however, Co-catalyzed MHAT to furans is known.[25] The failure to produce **2.8f** and **2.8g** by termination with electron-poor arenes mirrors our results with similar acrylonitrile substrates shown in **Figure 2.3**.

Figure 2. 3: The reactivity of methyl-substituted substrates mirrors that of the corresponding nitrile-bearing compounds (yields shown are for isolated and purified compounds).

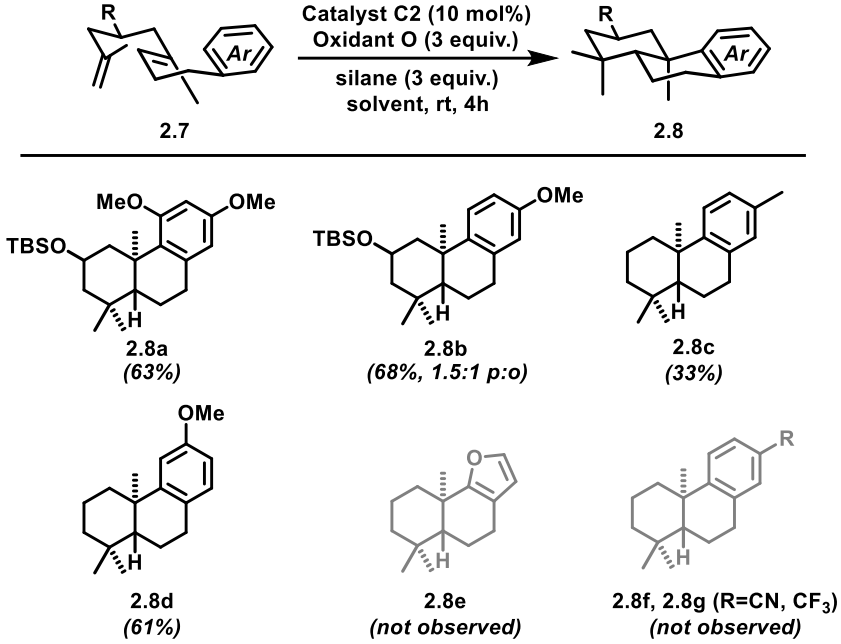

2.4 Preliminary Mechanistic Experiments

2.4.1 Plausible Mechanistic Pathways

We realized our initial goal to develop bicyclization reactions that tolerated both electron-deficient and electron-rich internal alkenes. With the exception of the reactions of indole substrates that gave the indoline products **2.6f** and **2.6g**, these reactions are redox neutral with a presumed initial alkene reduction by MHAT, which therefore necessitates an oxidation at some point further along in the overall reaction mechanism. The three plausible mechanisms that follow from this assumption are shown in **Scheme 2.1**. We had considered the possibility that the first cyclizations in the acrylonitrile cases are 6-*endo* Giese-type,[18] but that the much slower radical cyclization in the substrates lacking the activating nitrile could allow radical oxidation to compete, with the cyclizations proceeding by carbocationic manifolds. However, as discussed below, most of our results, along with some of our preliminary mechanistic experiments that we will describe, suggest the likelihood that the bicyclization reactions of both substrate types are radical in nature.

Scheme 2. 1: Plausible mechanistic options for bicyclization reactions.

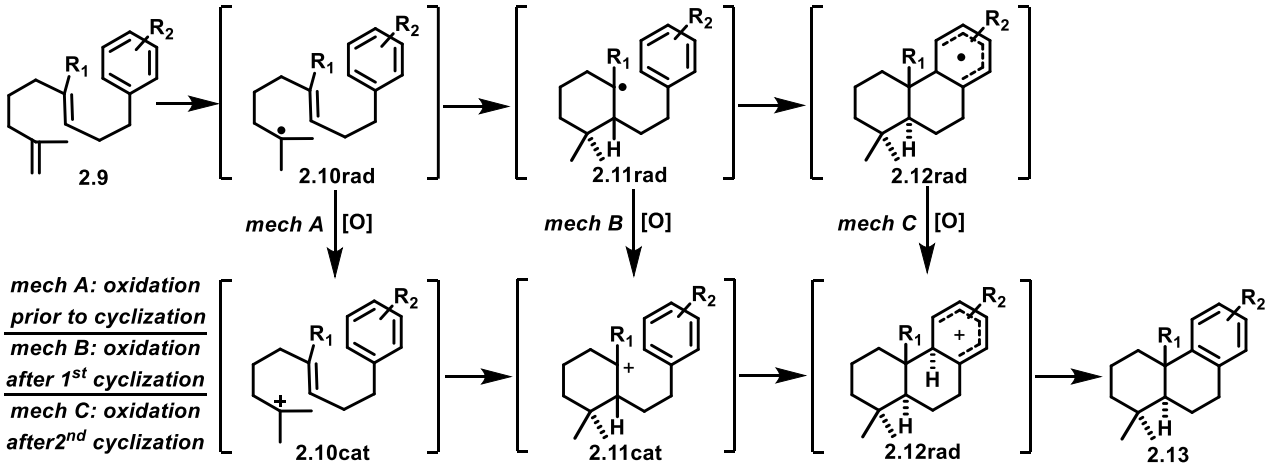

2.4.2 Cyclizations of Substrates Bearing E-Internal Alkenes

Initially designed to expand the scope with respect to electron-withdrawing group, the substitution of the nitrile group with an ester instead yielded surprising results (**Scheme 2.2**). Submitting **2.14-*Z*** to standard reaction conditions yielded a complex mixture in which the expected product **2.15** was not observed (**Scheme 2**). Coincidentally, we found that the geometrical isomer **2.14-*E*** underwent a 5-*exo* cyclization process to give **2.16**. Products containing the expected decalin framework were not detected in this case, either. For this transformation, substoichiometric amounts of oxidant were sufficient for full conversion (conditions as shown, plausibly just enough oxidant to generate Co^{III}), suggesting that the mechanism could be akin to that in the Co^{III}-catalyzed HAT-induced cycloisomerizations reported by Shenvi et al.[15] We currently have no explanation for the lack of productive reactivity of **2.14-*Z***. The desired bicyclization of the *E* isomer likely suffers from severe nonbonded interactions in the transition structure;[26] we see the same reactivity with the *E*-unsaturated nitrile substrates, but have never been able to isolate the product corresponding to **2.16** in pure form. Another unexplained result is the lack of formation of a cyclopentane product analogous to **2.16** from **2.14-*Z***, in spite of the very similar steric demand on these two cyclizations. Finally, it is noteworthy that we have never seen *cis*-decalin structures resulting from the *E* isomers of the nitrile substrates (in cases where 1,1-disubstituted initiating alkenes were used).[26]

Scheme 2. 2: Attempted bicyclizations with acrylate esters as the internal alkene.

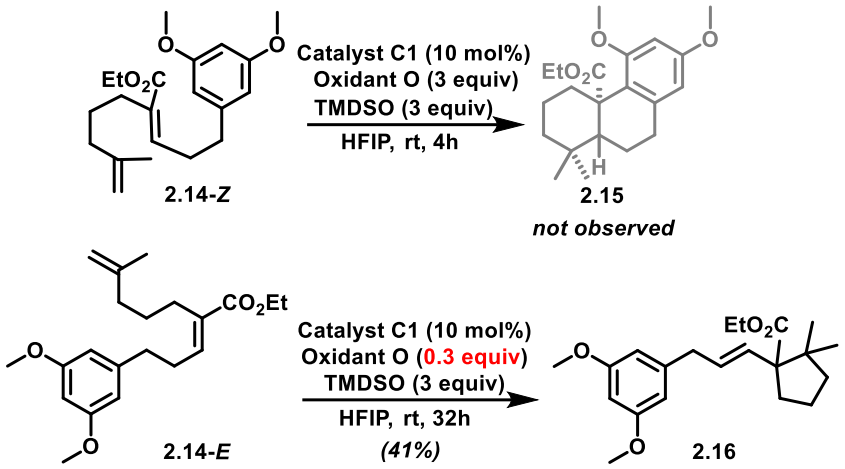

2.4.3 Bicyclizations Initiated By HAT to Monosubstituted Alkenes

Given the high energy of secondary carbocations, we assumed that secondary radicals resulting from HAT to monosubstituted alkenes, such as **2.17** (**Figure 2.4**) could not be oxidized prior to cyclization; if the reaction worked it was expected to involve a Giese-type first cyclization. HAT to monosubstituted alkenes is normally slower than to 1,1-disubstituted alkenes of types **2.5** and **2.7** that we had been investigating up to this point;[10,27] nonetheless, the reaction of **2.17** under our standard reaction conditions yielded a separable mixture of three stereoisomeric products. Surprisingly, the product ratios were found to be dependent on the structure of the cobalt complex. Secondary alkylcobalt(III) intermediates are thought to be in equilibrium with secondary radicals formed by MHAT[12, 28] and it is therefore plausible that (some of) the catalysts might be associated with the activated substrate after the MHAT event to **2.17**, thus providing a possible explanation for the catalyst-dependent difference in product ratios. We found that the less sterically encumbered cobalt complexes **C2**, **C4**, and **C5** gave better stereoselectivity (ratio **2.18**:**2.20**) for the formation of the first C−C bond, which could be consistent with the bulky catalyst **C1** being more dissociated from the organic radical. Conversely, closure of the final ring proceeded with

similarly modest selectivity regardless of the catalyst structure (ratio **2.18** + **2.20** : **2.19**). It is likely that *cis*-decalin formation (**2.19**) is only kinetically feasible without an axial methyl group on C4, which is consistent with the sole formation of *trans*-decalins with the disubstituted alkene substrates used in **Figure 2.2** and in many other related systems.[26] Collectively, these results suggest that the reaction of **2.17** is stereoselective but not stereospecific with respect to the trisubstituted alkene and is thus likely to involve radical intermediates. However, this tentative conclusion cannot be directly transferred to the reactions described in **Figure 2.1**, because in that case oxidation of the initially formed radical to a tertiary carbocation could reasonably occur. The same terminal alkene initiation site was used with the methyl-substituted internal alkene **2.21**, and no characterizable products were observed. Although a bicyclization reaction via radical intermediates might be expected to occur on the basis of our other results, the success of the reaction of **2.21** requires a competitive HAT to the terminal alkene over the plausibly more reactive electron-rich internal trisubstituted alkene.[10, 27]

Figure 2. 4: Stereochemical outcomes of bicyclizations initiated by HAT to monosubstituted alkenes (product ratios and yields determined using ^{1}H NMR spectroscopy with an internal standard).

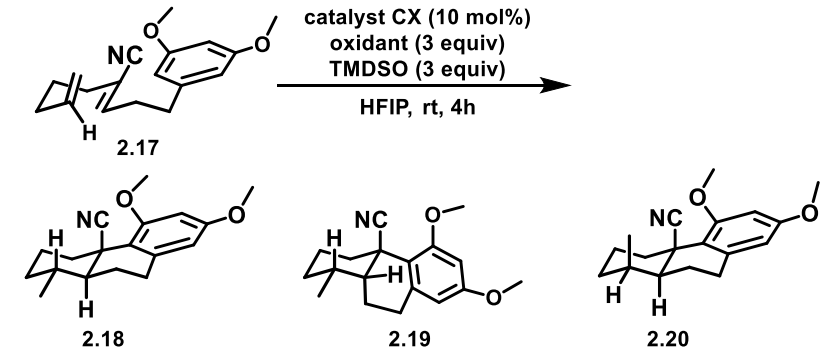

catalyst	yield	2.20 : 2.21 : 2.22
C1	78	1.0 : 0.4 : 0.4
C2	72	1.0 : 0.6 : 0.1
C4	60	1.0 : 0.6 : 0.2
C5	50	1.0 : 0.6 : 0.1

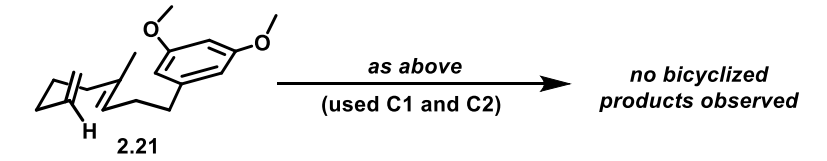

2.4.4 Experiments Probing Intermediacy of Cationic Intermediates

In a further attempt to probe whether or not carbocationic intermediates were involved in these reactions, we submitted carbonate **2.22** to standard reaction conditions (**Scheme 2.3**). No cyclic carbonate products of type **2.23** were detected. Instead, the alkyl fluoride **2.25** was identified as the major product when **C2** was used. The use of **C1** gave a mixture of alkene isomers where **2.24** was the major isolated product. These results provide circumstantial evidence against carbocation intermediates; each outcome corresponds to radical-based transformations previously reported by the Shigehisa/Hiroya group[11a] and the Shenvi group.[15] Interestingly, we note that the catalysts used in our hydrofluorination and alkene isomerization results are in fact interchanged

with those used in the original reports. We also investigated the cyclization of **2.26**, the success of which should require the intermediacy of an α-nitrilo-cation for nucleophilic capture by the pendant hydroxy group.[29] This reaction yielded a complex mixture of unidentifiable products from which **2.27** was not observed.

Scheme 2. 3: An attempt to probe the intermediacy of cationic intermediates instead supports radical-based reactivity (yields shown are for isolated and purified compounds).

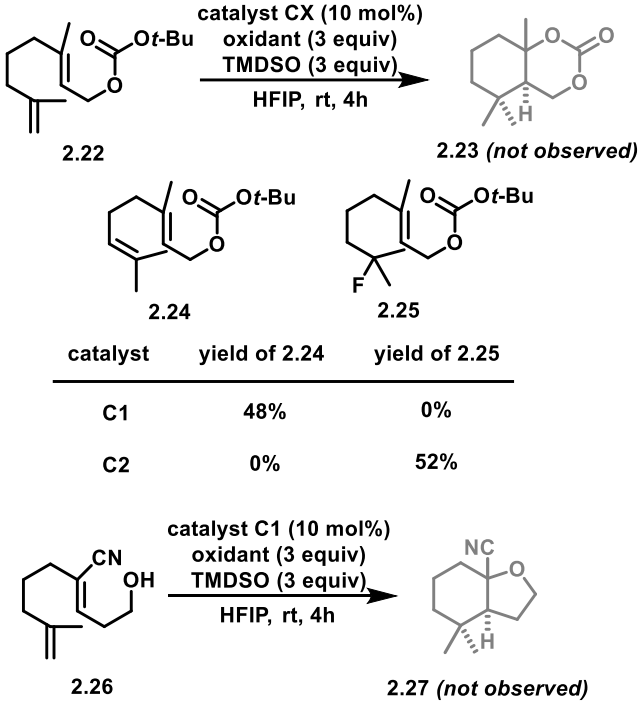

The bicyclizations with the *meta*-anisole substrates **2.5b** (nitrile) and **2.7b** (methyl) provided products **2.6b** and **2.8b**, respectively, with a remarkably similar, albeit slight preference for second ring closures at the *para* positions (1.7:1 *para*/*ortho* for **2.6b** and 1.5:1 for **2.8b**). While Rendler and MacMillan's polycyclizations afforded predominantly the *ortho* regioisomer (2:1 *ortho*/*para*) and a radical process is strongly implicated,[3a] and cationic processes normally feature a moderate precedent for cyclization at the *para* position[30] (consistent with our results), we have trouble rationalizing how our two results could be so similar without the final bond

construction proceeding by a radical mechanism in both cases. Simply put, with different mechanisms in the two cases, we would anticipate a different regiochemical outcome. Moreover, a cationic mechanism for both would likely also provide different regioselectivities owing to the very different energies of the tertiary alkyl versus tertiary α-nitrilo cations.

The reaction of a homologue of substrate **2.7a** (extra isoprene unit, see **S2.34** in the **Experimental Procedures** section) under our standard, optimized conditions failed in a tricyclization attempt, affording alkene isomerization and decomposition. This failure is not easy to explain if the process features cationic intermediates, given that **2.7a** itself cyclizes well. Such a result is easier to support with a radical cyclization mechanism, wherein polarity alternation is often required for high-yielding multibond-forming processes. For example, Rendler and MacMillan's study showed that organocatalyzed radical polycyclizations benefit from the alternation of electron-rich and electron-deficient alkenes, leveraging unsaturated nitriles as key components of their substrates.[3a]

2.4.5 Deuterium Labeling Experiments

At this stage, the majority of our experiments provide support for mechanism C (**Scheme 1**), in which both C−C bond-forming reactions are radical in nature. We remained interested in further understanding the final stages of the reaction, in which an oxidation must occur. From the postulated cyclohexadienyl radical intermediate **2.12rad**, both oxidation to the corresponding cation **2.12cat**, by either the Co catalyst or the chemical oxidant, or back MHAT from **2.12rad** to a Co^{II} intermediate, appear reasonable. To investigate, we synthesized the pentadeuterated substrate **2.28** (**Scheme 2.4**) from [D_6]benzene.[13] If back-MHAT from **2.12rad** were involved, we would expect significant deuterium incorporation at the C18 or C19 methyl groups (or possibly at

C3, if some alkene isomerization takes place) because of subsequent MDAT from Co−D. If oxidation to **2.12cat** occurred, then the deuteron should be lost to base in solution, and there would be little expectation of reincorporation. The results of this key experiment showed the conversion of pentadeuterated **2.28** into **2.29** with more than 95 % d_4, strongly supporting an oxidation event followed by proton (deuteron) removal. The isolation of the overall reduction products **2.6f** and **2.6g** are the only outlying data, but a slower deprotonation of the more stable cationic intermediate might allow competitive ionic reduction by excess silane reagent. Interestingly, deuterated **2.14-*E*** (**2.14-*E*-d_2**) underwent cyclization in poor yield, but with substantial reincorporation of deuterium. This Shenvi-type cycloisomerization would be expected to generate intermediate cobalt deuterides for MDAT to the subsequently engaged substrate. Unexpectedly, in this particular case, we found most of the label appeared to be at the methylene rather than the methyl groups, which suggests alkene isomerization prior to cyclization.[13, 23]

Scheme 2. 4: Deuteration experiments suggest oxidation followed by proton transfer, rather than back MHAT, as the final stages of the reactions.

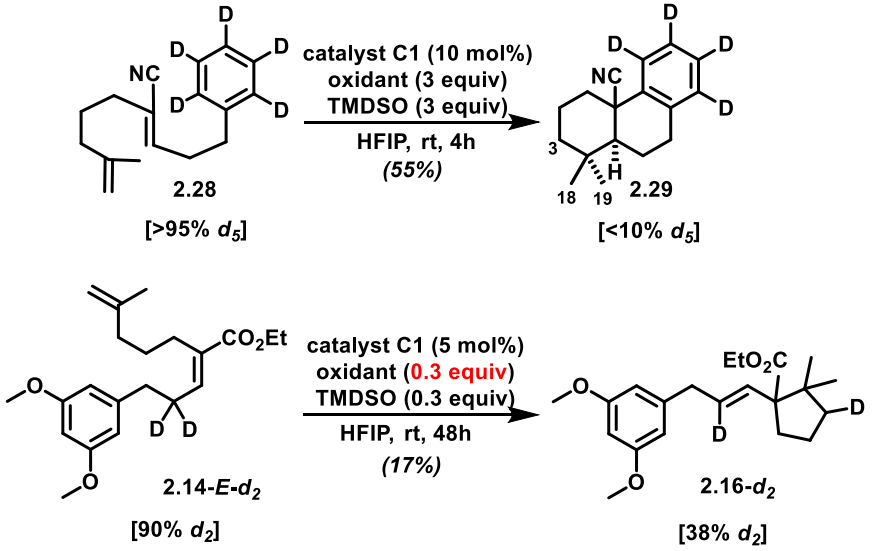

2.4.6 The Role of 1,1,1,3,3,3-Hexafluoro-2-propanol (HFIP)

Finally, the importance of HFIP as the solvent in these reactions is worth reiterating. Other common solvents, with the exception of acetone, did not lead to productive reactivity. In acetone, many side products were observed, and the overall reaction efficiency was lower. HFIP is known have powerful effects on cationic processes, but little is known about its ability to alter or improve the course of radical reactions.[31] It is well known that cobalt(II) salen complexes reversibly uptake oxygen in strongly coordinating solvents.[32] The resulting cobalt(III)-superoxide complexes are thought to be in equilibrium with μ-peroxocobalt(III) dimers.[33] To test whether these species can serve as precursors to cobalt(III) hydrides, we attempted to isomerize the 1,1-disubstituted alkene in **2.22** without any exogenous oxidant (**Scheme 2.5**). First, catalyst C1 was dissolved in aerated HFIP and immediately concentrated in vacuo to give a black residue (presumably a Co(III) superoxide species, **C1***). Then, following Shenvi's isomerization protocol we observed clean but incomplete conversion of diene **2.22** to **2.24** in degassed benzene. This result and our previous observations (**Table 2.1**, entries 12 & 13) suggest that dioxygen can fulfil the role of oxidant in generation of the cobalt(III) hydride necessary for the initial MHAT event in HFIP, but a stronger oxidant is needed for termination of the second cyclization. It is important to note that in most of our experiments, the solvent was degassed after dissolution of the cobalt(II) pre-catalyst, the oxidant, and the substrate (see experimental information). Therefore, it is likely that in all of the bicyclization experiments, the initial oxidation of the cobalt(II) complexes is actually facilitated by dioxygen and HFIP. From a practical point of view, rigorous deoxygenation of HFIP is cumbersome and would certainly complicate our otherwise operationally simple protocols for performing these reactions.

Scheme 2. 5: Aerobic oxidation of Co(II) complex C1 in HFIP and isomerization of diene **2.24** using catalyst **C1*** in benzene.

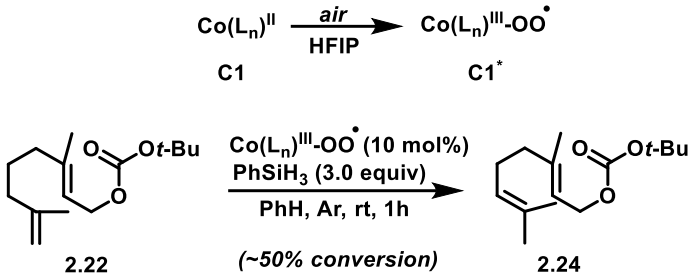

On the basis of our data, we tentatively propose that the two rings are forged by radical processes, followed by a final oxidation of the cyclohexadienyl radical (or equivalent) to the corresponding cation and subsequent proton removal. Overall, the similarity in behavior of nitrile- and alkyl-substituted systems under nearly identical reaction conditions remains the most interesting aspect of this bicyclization method.

2.5 Conclusions

In summary, we have developed an oftentimes highly efficient HAT-inititated polyene cyclization for the stereocontrolled construction of terpenoid scaffolds. Although the method in its current form is limited to electron-rich terminating arenes, the intermediate alkene substituents can be either electron-withdrawing or electron-donating, which is highly unusual. The reaction conditions are mild and tolerate a variety of functionalities, offering an attractive alternative to the few methods for protonative polyene cyclizations.[1] The experiments that we have performed to date suggest that the cyclization events proceed via radical intermediates, with a late-stage oxidation; however, some questions remain, underscoring the need for more refined experiments to improve our understanding of HAT-initiated reactions that proceed under oxidative conditions. Finally, the ability to effect bicyclization reactions that directly deliver terpenoid-like scaffolds

with C20 preoxidized opens many opportunities for natural product synthesis;[34] these applications are currently ongoing in our laboratory.

2.6 Experimental Procedures

General Experimental Information

All reactions were performed in oven-dried (120 °C) or flame-dried glassware under an atmosphere of dry argon unless otherwise noted. Reaction solvents including dichloromethane (CH_2Cl_2, Fisher, HPLC Grade), hexanes (Fisher, HPLC Grade), diethyl ether (Et_2O, Fisher, BHT stabilized, HPLC Grade), benzene (C_6H_6, Fisher, HPLC Grade), tetrahydrofuran (THF, Fisher, HPLC Grade), and toluene ($PhCH_3$, Fisher, HPLC Grade) were dried by percolation through a column packed with neutral alumina and a column packed with Q5 reactant, a supported copper catalyst for scavenging oxygen, under a positive pressure of argon. Solvents for workup and chromatography were: hexanes (Fisher or EMD, ACS Grade), EtOAc (Fisher, ACS Grade), dichloromethane (CH_2Cl_2, Fisher, ACS Grade), and diethyl ether (Fisher, ACS Grade). Column chromatography was performed using EMD Millipore 60 Å (0.040–0.063 mm) mesh silica gel (SiO_2). Analytical and preparatory thin-layer chromatography was performed on Merck silica gel 60 F254 TLC plates. Visualization was accomplished with UV (254 or 210 nm), and *p*-anisaldehyde, vanillin, potassium permanganate, 2,4-dinitrophenylhydrazine, or ceric ammonium molybdate and heat as developing agents. Chloroform-d ($CDCl_3$, D 99.8%, DLM-7) was purchased from Cambridge Isotope Laboratories. K_2CO_3 (anhydrous, 99%, Alfa Aesar), $NaHCO_3$ (ACS grade, Fisher), NaOH (ACS grade, Macron or Fisher), $Na_2S_2O_3$ (ACS grade, Fisher), triethylamine (Et_3N, EMD, CaH_2) and pyridine (Alfa Aesar, CaH_2),were distilled from the indicated drying agents prior to use. Proton and carbon magnetic resonance spectra (^{1}H NMR and ^{13}C NMR) were recorded at 298K on a Bruker CRYO500 (500 MHz, ^{1}H; 125 MHz, ^{13}C) or a Bruker AVANCE600 (600 MHz, ^{1}H; 151 MHz, ^{13}C) spectrometer with solvent resonance as the internal standard (^{1}H NMR: $CHCl_3$ at 7.26 ppm, ^{13}C NMR: $CDCl_3$ at 77.16 ppm). ^{1}H NMR data

are reported as follows: chemical shift, multiplicity (s = singlet, d = doublet, t = triplet, q = quartet, dd = doublet of doublets, ddd = doublet of doublet of doublets, td = triplet of doublets, tdd = triplet of doublet of doublets, qd = quartet of doublets, m = multiplet, br. s. = broad singlet), coupling constants (Hz), and integration. High resolution mass spectra (HRMS) were recorded on a Waters LCT Premier spectrometer using ESI-TOF (electrospray ionization-time of flight) and data are reported in the form of (m/z). To quantify the extent of deuterium incorporation, the purified samples were analyzed by isotope ratio mass spectrometry modeling (flow injection analysis). Catalysts **C1**[35], **C2**[36], **C3**[37], **C4**[38] and **C5**[39] were prepared as described in the literature and used without further purification.

α,β-Unsaturated Nitrile Substrate Synthesis and Characterization

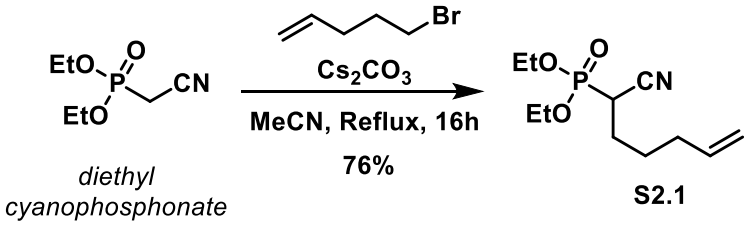

To a solution of diethyl cyanophosphonate (1.77 g, 10.0 mmol, 1.0 equiv.) in MeCN (36 mL) was added Cs_2CO_3 (3.26 g, 10 mmol, 1.0 equiv.) followed by 5-bromo-1-pentene (1.80 g, 12.1 mmol, 1.2 equiv.). The resulting suspension was heated to reflux for 16 h, cooled to ambient temperature and the volatiles were removed *in vacuo*. The resulting residue was partitioned between H_2O (20 mL) and EtOAc (40 mL) and the aqueous phase was extracted with EtOAc (3 x 20 mL). The combined organic extracts were washed with brine, dried over Na_2SO_4, filtered and concentrated *in vacuo.* The resulting crude residue was purified via flash column chromatography using a mixture of MeOH/ DCM (2:98) as eluent to give **S2.1** as a colorless oil (1.86 g, 7.60 mmol, 76% yield). **^{1}H NMR** (500 MHz, $CDCl_3$) δ 5.76 (ddt, *J* = 16.9, 10.1, 6.7 Hz, 1H), 5.03 (dd, *J* = 17.1,

1.6 Hz, 1H), 4.99 (d, *J* = 10.2 Hz, 1H), 4.28 – 4.15 (m, 4H), 2.89 (ddd, *J* = 23.7, 10.3, 4.7 Hz, 1H), 2.17 – 2.04 (m, 2H), 1.96 – 1.82 (m, 2H), 1.81 – 1.73 (m, 1H), 1.63 – 1.52 (m, 1H), 1.37 (t, *J* = 7.1 Hz, 6H); **^{13}C NMR** (126 MHz, $CDCl_3$) δ 137.3, 116.3 (d, *J* = 9.3 Hz), 115.8, 64.2 (d, *J* = 7.0 Hz), 63.8 (d, *J* = 6.8 Hz), 32.8, 30.0 (d, *J* = 143.8 Hz), 27.1 (d, *J* = 12.2 Hz), 26.5 (d, *J* = 4.3 Hz), 16.50 (d, *J* = 2.5 Hz), 16.46 (d, *J* = 2.5 Hz); **HRMS** (ES+) *m/z* calc'd for $C_{11}H_{20}NO_3PH$ $[M+H]^+$: 246.1259, found 246.1259.

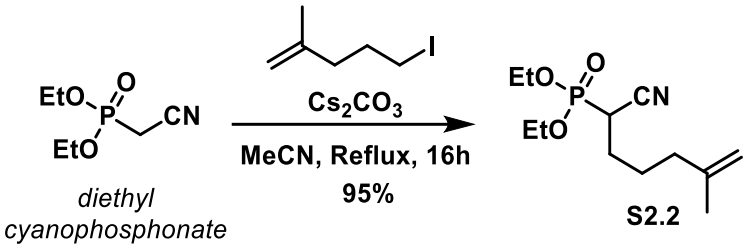

To a solution of diethyl cyanophosphonate (1.32 g, 7.48 mmol, 1.0 equiv.) in MeCN (30 mL) was added Cs_2CO_3 (2.44 g, 7.48 mmol, 1.0 equiv.) followed by 5-iodo-2-methylpent-1-ene[40] (1.90 g, 9.05 mmol, 1.2 equiv.). The resulting suspension was heated to reflux for 16 h, then the volatiles were removed *in vacuo*. The resulting residue was partitioned between H_2O (20 mL) and EtOAc (40 mL) and the aqueous phase was extracted with EtOAc (3 x 20 mL). The combined organic extracts were washed with brine, dried over Na_2SO_4, filtered and concentrated *in vacuo.* The resulting crude residue was purified via flash column chromatography using a mixture of EtOAc/ hexanes (35:65) as eluent to give **S2.2** as a colorless oil (1.84 g, 7.09 mmol, 95% yield). **^{1}H NMR** (600 MHz, $CDCl_3$) δ 4.74 (s, 1H), 4.69 (s, 1H), 4.28 – 4.18 (m, 4H), 2.91 (ddd, *J* = 23.7, 10.1, 4.6 Hz, 1H), 2.14 – 2.02 (m, 2H), 1.93 – 1.79 (m, 3H), 1.71 (s, 3H), 1.65 – 1.58 (m, 1H), 1.38 (t, *J* = 7.1 Hz, 6H); **^{13}C NMR** (151 MHz, $CDCl_3$) δ 144.4, 116.4 (d, *J* = 9.3 Hz), 111.1, 64.2 (d, *J* = 7.0 Hz), 63.8 (d, *J* = 6.8 Hz), 36.9, 30.1 (d, *J* = 143.7 Hz), 26.6 (d, *J* = 4.3 Hz), 25.7 (d, *J* = 12.2 Hz),

22.3, 16.53 (d, J = 3.3 Hz), 16.50 (d, J = 3.3 Hz); **HRMS** (ES+) *m/z* calc'd for $C_{12}H_{22}NO_3PNa$ [M +Na]$^+$: 282.1235, found 282.1233.

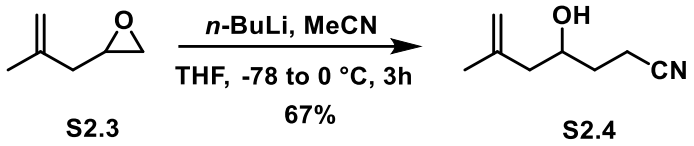

To a solution of acetonitrile (2.24 mL, 41.1 mmol, 2.0 equiv.) in THF (70 mL) was added a 1.6 M solution of *n*-butyllithium (18.7 mL, 30.0 mmol, 1.4 equiv.) in hexanes at –78 °C. The resulting solution was stirred for 1 h, then a solution of epoxide **S2.3**[13] (2.1 g, 21.4 mmol, 1.0 equiv.) in THF (10 mL) was added over a period of 3 minutes. The mixture was warmed to 0 °C, stirred for 3 hours and then quenched with satd. $NH_4Cl_{(aq)}$ (30 mL). The aqueous phase was extracted with EtOAc (3 x 20 mL), the combined organic extracts were washed with brine, dried over Na_2SO_4, filtered and concentrated *in vacuo.* The resulting crude residue was purified via flash column chromatography using a mixture of EtOAc/ hexanes (30:70) as eluent to give **S2.4** as a colorless oil (2.00 g, 14.3 mmol, 67% yield). **^{1}H NMR** (600 MHz, $CDCl_3$) δ 4.93 (s, 1H), 4.82 (s, 1H), 3.84 (tt, J = 9.2, 3.4 Hz, 1H), 2.54 (td, J = 7.1, 3.9 Hz, 2H), 2.21 (dd, J = 13.6, 3.6 Hz, 1H), 2.14 (dd, J = 13.6, 9.3 Hz, 1H), 1.89 – 1.82 (m, 2H), 1.77 (s, 3H), 1.75 – 1.68 (m, 1H); **^{13}C NMR** (151 MHz, $CDCl_3$) δ 141.8, 120.0, 114.5, 66.6, 46.2, 32.5, 22.5, 13.9; **HRMS** (ES+) *m/z* calc'd for $C_{16}H_{26}N_2O_2Na$ [2M +Na]$^+$: 301.1892, found 301.1892.

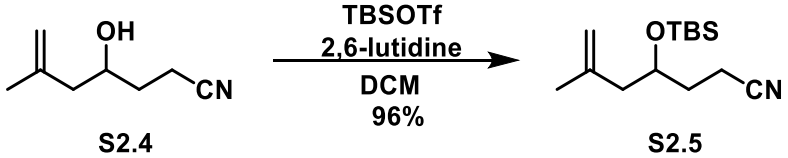

To a solution of alcohol **S2.4** (2.00 g, 14.3 mmol, 1.0 equiv.) and 2,6-lutidine (5.00 mL, 43.2 mmol, 3.0 equiv.) in DCM (20 mL) was added TBSOTf (4.96 mL, 21.6 mmol, 1.5 equiv.). The mixture

stirred for 1 hour at ambient temperature, then methanol (5.0 mL) was added. The volatiles were removed *in vacuo*, and the resulting crude residue was directly purified via flash chromatography using a mixture of EtOAc/hexanes (10:90) as eluent to give silyl ether **S2.5** as a colorless oil (3.52 g, 90%). **^{1}H NMR** (600 MHz, $CDCl_3$) δ 4.80 (s, 1H), 4.72 (s, 1H), 4.01 – 3.82 (m, 1H), 2.46 – 2.34 (m, 2H), 2.28 (dd, *J* = 13.6, 4.9 Hz, 1H), 2.12 (dd, *J* = 13.6, 8.3 Hz, 1H), 1.91 – 1.82 (m, 1H), 1.73 (s, 3H), 1.66 (td, *J* = 14.1, 6.9 Hz, 1H), 0.89 (s, 9H), 0.09 (s, 3H), 0.09 (s, 3H); **^{13}C NMR** (126 MHz, $CDCl_3$) δ 141.8, 120.1, 113.9, 68.8, 46.0, 32.0, 25.9, 23.0, 18.1, 13.2, –4.2, –4.7; **HRMS** (ES+) *m/z* calc'd for $C_{14}H_{27}NOSiNa$ $[M+Na]^+$: 276.1760, found 276.1764.

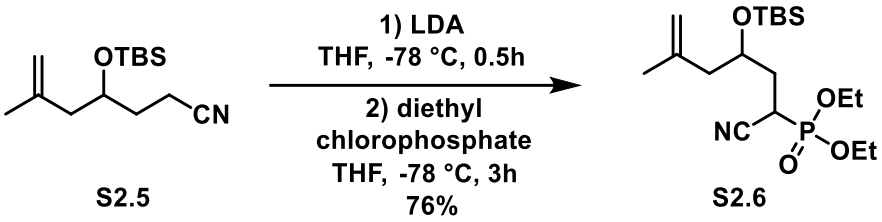

To a solution of diisopropylamine (2.08 mL, 14.7 mmol, 2.2 equiv.) in THF (25 mL) was added a 1.6 M solution of *n*-butyllithium (8.79 mL, 14.1 mmol, 2.1 equiv.) at –78 °C. The mixture was allowed to warm to 0 °C, stirred for 30 minutes and cooled back down to –78 °C. A solution of nitrile **S2.5** (1.7 g, 6.7 mmol, 1.0 equiv.) in THF (5 mL) was added dropwise and the mixture was stirred for 30 minutes at –78 °C. Diethyl chlorophosphate (1.07 mL, 7.37 mmol, 1.1 equiv.) was added dropwise (neat). After stirring for 3 hours at –78 °C, satd. $NH_4Cl_{(aq)}$ (30 mL) was added to the reaction mixture. The aqueous phase was extracted with EtOAc (3 x 20 mL), the combined organic extracts were washed with brine, dried over Na_2SO_4, filtered and concentrated *in vacuo*. The resulting crude residue was purified via flash column chromatography, using a mixture of EtOAc/hexanes (30:70) as eluent to give an inconsequential mixture (2:1) of cyanophosphonate

S2.6 diastereomers as a colorless oil (1.98 g, 5.1 mmol, 76% yield). *Note: signals are reported for the major diastereomer only*. **^{1}H NMR** (600 MHz, $CDCl_3$) δ4.81 (*major*-s, 1H), 4.74 (*major*-s, 1H), 4.29 – 4.18 (*overlapping* m, 4H), 4.05 – 3.99 (*major*-m, 1H), 3.17 (*overlapping* -ddd, *J* = 23.2, 12.4, 3.3 Hz, 1H), 2.38 (*major*-dd, *J* = 13.6, 4.0 Hz, 1H), 2.27 (*major*-qd, *J* = 13.7, 6.5 Hz, 1H), 2.15 (*overlapping*- dd, *J* = 13.6, 9.0 Hz, 1H), 2.03 – 1.92 (*overlapping* m, 1H), 1.83 – 1.76 (*major*-m, 1H), 1.74 (*major*- s, 3H), 1.37 (*overlapping*- t, *J* = 7.1 Hz, 6H), 0.89 (*overlapping*- s, 9H), 0.14 (*major*-s, 3H), 0.12 (*major*-s, 3H); **^{13}C NMR** (126 MHz, $CDCl_3$) δ141.19 (*major*), 116.24 (*major*-d, *J* = 9.3 Hz), 114.07 (*major*), 67.93 (d, *J* = 13.8 Hz), 64.04 (*major*-d, *J* = 6.9 Hz), 63.72 (*major*-d, *J* = 6.8 Hz), 46.48 (*major*), 33.78 (*major*-d, *J* = 4.0 Hz), 26.96 (*major*-d, *J* = 145.5 Hz), 25.85 (*overlapping*), 22.85 (*major*), 18.01 (*major*), 16.41 (*overlapping*-d, *J* = 3.2 Hz), 16.37 (*overlapping*-d, *J* = 3.2 Hz), –4.05 (*major*), –4.77 (*major*); **HRMS** (ES+) *m/z* calc'd for $C_{18}H_{36}NO_4PSiNa$ $[M+Na]^+$: 412.2044, found 412.2036.

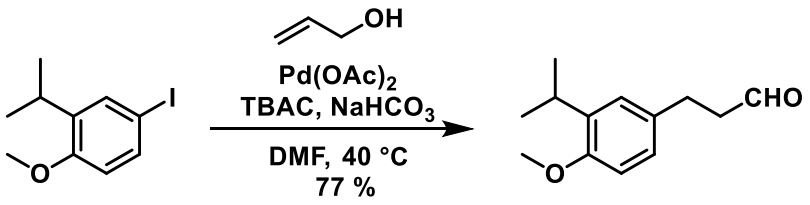

S2.7 **S2.8**

To a solution of iodoanisole **S2.7**[41] (3.50 g, 12.7 mmol, 1.0 equiv.) in degassed DMF (50 mL) was added tetrabutylammonium chloride (3.53 g, 12.7 mmol, 1.0 equiv.), allyl alcohol (1.72 mL, 25.4 mmol, 2.0 equiv.), sodium bicarbonate (2.67 g, 31.8 mmol, 2.5 equiv.), and finally $Pd(OAc)_2$ (144 mg, 0.64 mmol, 0.05 equiv.). The resulting mixture was stirred at 40 °C for 6 hours, then Et_2O (80 mL) was added and the organic phases were washed with DI H_2O (3x 30 mL). The combined organic extracts were washed with brine (30 mL), dried over Na_2SO_4, filtered and concentrated *in vacuo.* The crude residue was purified via flash column chromatography (EtOAc/hexanes 4:96) to

give aldehyde **S2.8** as a clear yellow oil (2.02 g, 9.78 mmol, 77% yield).**^{1}H NMR** (600 MHz, $CDCl_3$) δ 9.83 (s, 1H), 7.03 (s, 1H), 6.98 (d, *J* = 8.3 Hz, 1H), 6.78 (d, *J* = 8.3 Hz, 1H), 3.81 (s, 3H), 3.30 (septet, *J* = 6.9 Hz, 1H), 2.91 (t, *J* = 7.6 Hz, 2H), 2.76 (t, *J* = 7.6 Hz, 2H), 1.21 (d, *J* = 7.0 Hz, 6H); **^{13}C NMR** (151 MHz, $CDCl_3$) δ 202.1, 155.5, 137.3, 132.2, 126.2, 126.1, 110.6, 55.6, 45.8, 27.7, 26.9, 22.8 (2C); **HRMS** (ES+) *m/z* calc'd for $C_{13}H_{18}O_2Na$ $[M + Na]^+$: 229.1205, found 229.1209.

General Procedure A (HWE reaction for the synthesis of α,β-unsaturated nitrile substrates):

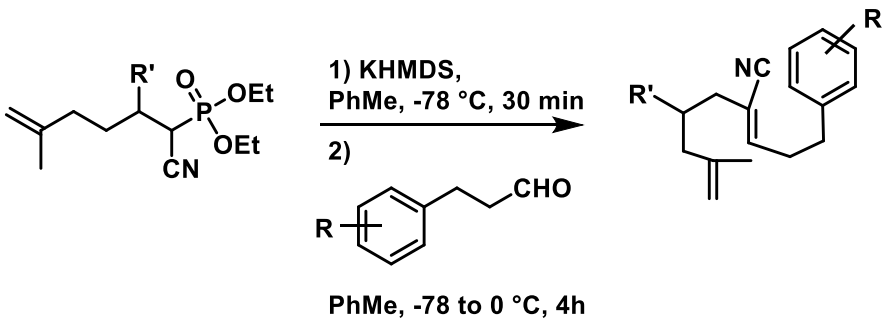

To a cooled (−78 °C) solution of cyanophosphonate **S2.1**, **S2.2** or **S2.6** (1.5 mmol, 1.0 equiv.) in dry toluene (15 mL) was added dropwise a solution of KHMDS (3.0 mL, 1.0 equiv., 0.5 M in toluene). After stirring for at least 30 min at −78 °C, a solution of aldehyde (1.5 mmol, 1.0 equiv.) was added dropwise in dry toluene (15 mL). The resulting solution was stirred at −78 °C for 1 h then allowed to warm to 0 °C and stirred for 3 h. Then, satd. $NH_4Cl_{(aq)}$ (10 mL) was added and the aqueous layer was extracted with Et_2O (3 x 20 mL). The combined organic extracts were washed with brine, dried over Na_2SO_4, filtered and concentrated *in vacuo.* The resulting crude residue was purified via flash column chromatography on SiO_2, using a mixture of Et_2O/hexanes or EtOAc/hexanes as eluent.

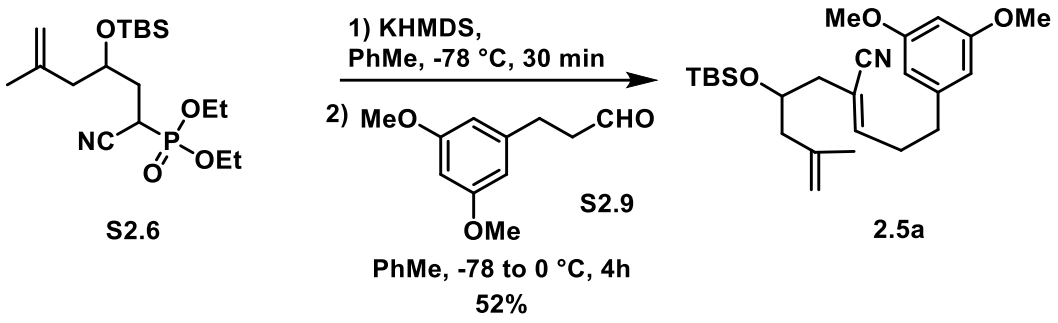

Prepared according to general procedure A, using cyanophosphonate **S2.6** *(2.62 mmol) and aldehyde* **S2.9**[42] *(2.75 mmol) to give a 1:4 (E:Z) mixture of α,β-unsaturated nitriles*. Yield of **2.5a**: 52% (586 mg, 1.36 mmol, colorless oil) of Z ; R_f= 0.15 (3:97 EtOAc/hexanes); **^{1}H NMR** (500 MHz, $CDCl_3$) δ 6.34 (d, *J* = 2.1 Hz, 2H), 6.32 (t, *J* = 2.2 Hz, 1H), 6.16 (t, *J* = 6.0 Hz, 1H), 4.79 (s, 1H), 4.69 (s, 1H), 3.98 (tt, *J* = 7.4, 5.3 Hz, 1H), 3.78 (s, 6H), 2.75 – 2.62 (m, 4H), 2.37 (dd, *J* = 14.0, 4.0 Hz, 1H), 2.20 (dd, *J* = 13.9, 5.0 Hz, 1H), 2.17 (dd, *J* = 14.1, 7.6 Hz, 1H), 2.10 (dd, *J* = 13.6, 7.4 Hz, 1H), 1.73 (s, 3H), 0.87 (s, 9H), 0.06 (s, 3H), 0.05 (s, 3H); **^{13}C NMR** (126 MHz, $CDCl_3$) δ 161.1, 149.1, 142.7, 142.1, 117.8, 113.9, 112.8, 106.6, 98.4, 69.0, 55.4, 46.0, 41.7, 35.0, 33.0, 26.0, 23.1, 18.2, –4.4, –4.5; **HRMS** (ES+) *m/z* calc'd for $C_{25}H_{39}NO_3SiNa$ $[M + Na]^+$: 452.2597, found 452.2599.

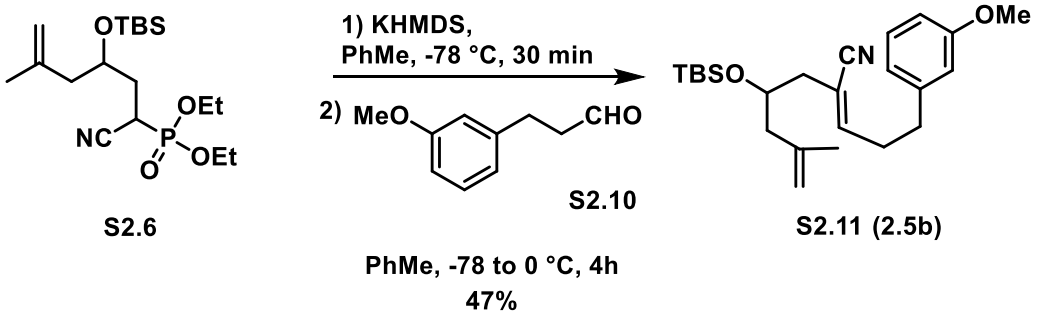

Prepared according to general procedure A, using cyanophosphonate **S2.6** *(1.16 mmol) and aldehyde* **S2.10**[43] *(1.22 mmol) to give a 1:4 (E:Z) mixture of α,β-unsaturated nitriles*. Yield of **S2.11**: 47% (218 mg, 0.545 mmol, colorless oil) of Z ; R_f=0.15 (2:98 EtOAc/hexanes); **^{1}H NMR**

(500 MHz, $CDCl_3$) δ 7.21 (t, *J* = 7.8 Hz, 1H), 6.80 – 6.72 (m, 3H), 6.16 (t, *J* = 7.0 Hz, 1H), 4.80 (s, 1H), 4.69 (s, 1H), 3.98 (tt, *J* = 7.5, 4.9 Hz, 1H), 3.80 (s, 3H), 2.77 – 2.65 (m, 4H), 2.37 (dd, *J* = 14.0, 4.1 Hz, 1H), 2.21 (dd, *J* = 13.9, 5.6 Hz, 1H), 2.17 (dd, *J* = 14.2, 7.8 Hz, 1H), 2.11 (dd, *J* = 13.6, 7.4 Hz, 1H), 1.73 (s, 3H), 0.87 (s, 9H), 0.06 (s, 3H), 0.05 (s, 3H); **^{13}C NMR** (126 MHz, $CDCl_3$) δ 159.9, 149.1, 142.1, 142.0, 129.7, 120.9, 117.8, 114.3, 113.9, 112.8, 111.8, 69.0, 55.3, 46.0, 41.7, 34.8, 33.1, 26.0, 23.1, 18.2, –4.4, –4.5; **HRMS** (ES+) *m/z* calc'd for $C_{24}H_{37}NO_2SiNa$ $[M + Na]^+$: 422.2491, found 422.2484.

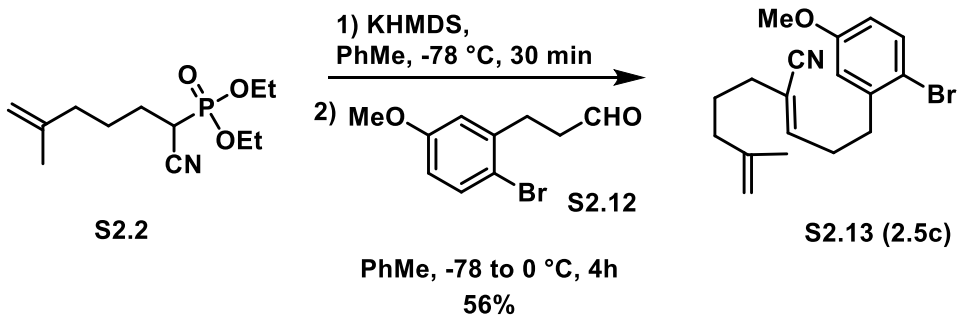

Prepared according to general procedure A, using cyanophosphonate **S2.2***(2.06 mmol) and aldehyde* **S2.12**[44]*(2.06 mmol) to give a 1:4 (E:Z) mixture of α,β-unsaturated nitriles*. Yield of **S2.13**: 56% (401 mg, 1.15 mmol, colorless oil) of Z ; R_f=0.15 (3:97 EtOAc/hexanes); **^{1}H NMR** (500 MHz, $CDCl_3$) δ 7.41 (d, *J* = 8.8 Hz, 1H), 6.77 (d, *J* = 2.8 Hz, 1H), 6.65 (dd, *J* = 8.7, 2.9 Hz, 1H), 6.17 (t, *J* = 7.6 Hz, 1H), 4.73 (s, 1H), 4.66 (s, 1H), 3.78 (s, 3H), 2.84 (t, *J* = 7.5 Hz, 2H), 2.72 – 2.66 (m, 2H), 2.18 (t, *J* = 7.6 Hz, 2H), 1.99 (t, *J* = 7.5 Hz, 2H), 1.71 (s, 3H), 1.68 – 1.61 (m, 2H); **^{13}C NMR** (126 MHz, $CDCl_3$) δ 159.2, 146.1, 144.8, 140.6, 133.6, 117.5, 116.2, 115.7, 114.9, 113.9, 110.8, 55.6, 36.7, 35.2, 33.8, 31.7, 25.9, 22.3; **HRMS** (ES+) *m/z* calc'd for $C_{18}H_{22}BrNONa$ $[M + Na]^+$: 370.0782, found 370.0775.

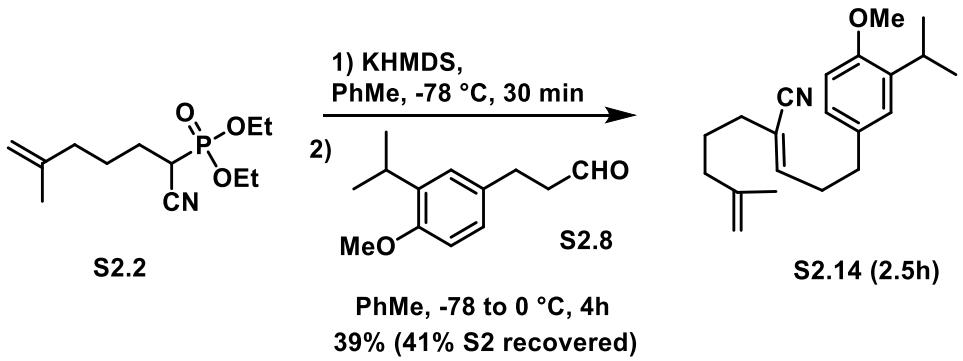

Prepared according to general procedure A, using cyanophosphonate **S2.2***(4.12 mmol) and aldehyde* **S2.8***(4.12 mmol) to give a 1:4 (E: Z) mixture of α, β-unsaturated nitriles*. Yield of **S2.14**: 39% (41% recovered SM) of Z (500 mg, 1.61 mmol, colorless oil); R_f= 0.15 (2:98 EtOAc/hexanes); **^{1}H NMR** (600 MHz, $CDCl_3$) δ 7.01 (s, 1H), 6.97 (d, *J* = 8.2 Hz, 1H), 6.78 (d, *J* = 8.2 Hz, 1H), 6.14 (t, *J* = 7.2 Hz, 1H), 4.73 (s, 1H), 4.65 (s, 1H), 3.81 (s, 3H), 3.31 (septet, *J* = 6.9 Hz, 1H), 2.73 – 2.63 (m, 4H), 2.17 (t, *J* = 7.5 Hz, 2H), 1.97 (t, *J* = 7.5 Hz, 2H), 1.70 (s, 3H), 1.67 – 1.61 (m, 2H), 1.21 (d, *J* = 6.9 Hz, 6H); **^{13}C NMR** (151 MHz, $CDCl_3$) δ 155.4, 147.1, 144.8, 137.2, 132.2, 126.3, 126.2, 117.7, 115.1, 110.8, 110.5, 55.6, 36.6, 34.3, 33.7, 33.4, 26.9, 25.9, 22.8, 22.3; **HRMS** (ES+) *m/z* calc'd for $C_{21}H_{29}NONa$ $[M + Na]^+$: 334.2147, found 334.2153.

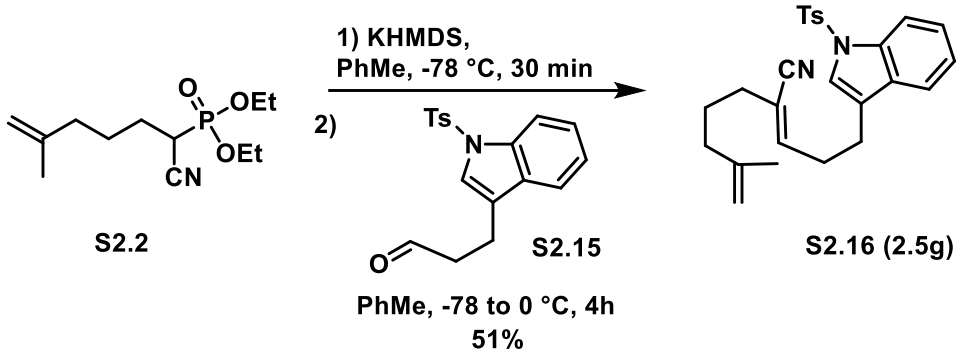

Prepared according to general procedure A, using cyanophosphonate **S2.2***(0.77 mmol) and aldehyde* **S2.15**[45]*(0.77 mmol) to give a 1:4 (E:Z) mixture of α,β-unsaturated nitriles*. Yield: 51% of **S2.16** (170 mg, 0.39 mmol, off-white solid); R_f=0.15 (8:92 EtOAc/hexanes) **^{1}H NMR** (600

MHz, $CDCl_3$) δ 7.89 (d, *J* = 8.3 Hz, 1H), 7.65 (d, *J* = 7.8 Hz, 2H), 7.38 (d, *J* = 7.8 Hz, 1H), 7.26 (s, 1H), 7.22 (t, *J* = 7.7 Hz, 1H), 7.14 (t, *J* = 8.0 Hz, 1H), 7.11 (d, *J* = 8.0 Hz, 2H), 6.05 (t, *J* = 7.4 Hz, 1H), 4.63 (s, 1H), 4.55 (s, 1H), 2.71 (t, *J* = 7.3 Hz, 2H), 2.66 – 2.61 (m, 2H), 2.23 (s, 3H), 2.06 (t, *J* = 7.6 Hz, 2H), 1.89 (t, *J* = 7.4 Hz, 2H), 1.60 (s, 3H), 1.53 – 1.50 (m, 2H); **^{13}C NMR** (151 MHz, $CDCl_3$) δ 146.2, 145.0, 144.7, 135.4, 130.7, 130.0, 126.9, 125.0, 123.3, 123.0, 121.4, 119.4, 117.5, 115.8, 113.9, 110.9, 36.7, 33.7, 31.0, 25.9, 24.2, 22.3, 21.7; **HRMS** (ES+) *m/z* calc'd for $C_{26}H_{28}N_2O_2SNa$ $[M + Na]^+$: 455.1769, found 455.1774.

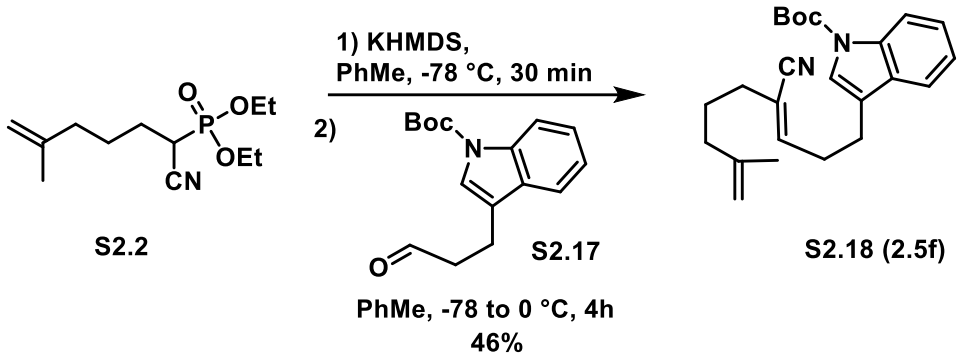

Prepared according to <u>general procedure A</u>, using cyanophosphonate **S2.2** *(1.16 mmol) and aldehyde* **S2.17**[46] *(1.16 mmol) to give a 1:4 (E:Z) mixture of α,β-unsaturated nitriles*. Yield: 46% of **S2.18** (200 mg, 0.53 mmol, off-white solid); R_f=0.15 (5:95 EtOAc/hexanes) **^{1}H NMR** (500 MHz, $CDCl_3$) δ 8.14 (br s, 1H), 7.52 (d, *J* = 7.7 Hz, 1H), 7.39 (s, 1H), 7.32 (ddd, , *J* = 7.2, 7.2, 1.1 Hz, 1H), 7.25 (ddd, 7.2, 7.2, 1.1, 1H), 6.20 (t, *J* = 7.3 Hz, 1H), 4.72 (s, 1H), 4.65 (s, 1H), 2.85 (dd, *J* = 7.8, 6.8 Hz, 2H), 2.78 (dd, *J* = 14.5, 7.0 Hz, 2H), 2.18 (t, *J* = 7.6 Hz, 2H), 1.99 (t, *J* = 7.5 Hz, 2H), 1.70 (s, 3H), 1.67 (s, 9H), 1.69-1.62 (m, 2H); **^{13}C NMR** (126 MHz, $CDCl_3$) (Note: *mixture of rotamers*) δ 149.8 (broad), 146.8 (broad), 144.7, 135.7 (broad), 130.4, 124.6, 122.8, 122.6, 119.3, 118.9, 117.6, 115.53, 115.45, 110.9, 83.7, 36.7, 33.7, 31.1, 28.4, 25.9, 24.2, 22.3; **HRMS** (ES+) m/z calc'd for $C_{24}H_{31}N_2O_2$ $[M + H]^+$: 379.2386, found 379.2373.

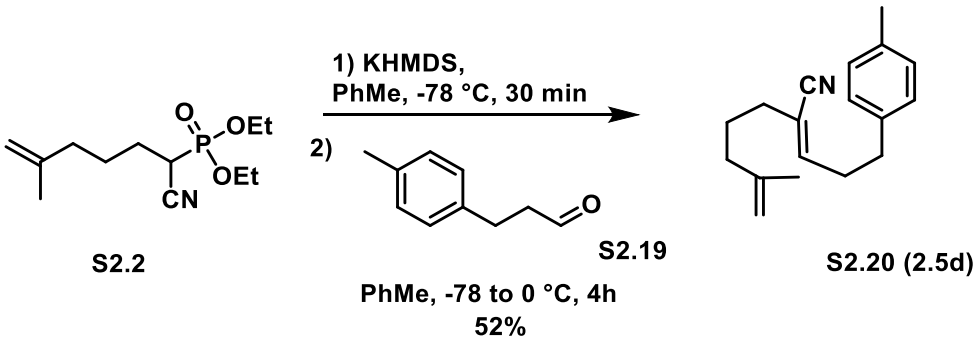

Prepared according to general procedure A, using cyanophosphonate **S2.2***(1.54 mmol) and aldehyde* **S2.19**[47]*(1.54 mmol) to give a 1:4 (E:Z) mixture of α,β-unsaturated nitriles*. Yield: 52% of **S2.20** (203 mg, 0.80 mmol, colorless oil); R_f=0.15 (2:97 Et_2O/hexanes); **^{1}H NMR** (500 MHz, $CDCl_3$) δ 7.11 (d, *J* = 8.0 Hz, 2H), 7.08 (d, *J* = 8.1 Hz, 2H), 6.13 (t, *J* = 7.3 Hz, 1H), 4.74 (s, 1H), 4.66 (s, 1H), 2.73 (dd, *J* = 11.0, 4.3 Hz, 2H), 2.67 (dd, *J* = 14.4, 7.1 Hz, 2H), 2.33 (s, 3H), 2.17 (t, *J* = 7.5 Hz, 2H), 1.98 (t, *J* = 7.5 Hz, 2H), 1.71 (s, 3H), 1.68 – 1.60 (m, 2H); **^{13}C NMR** (126 MHz, $CDCl_3$) δ 146.9, 144.8, 137.2, 135.9, 129.3, 128.4, 117.7, 115.3, 110.8, 36.6, 34.5, 33.7, 33.2, 25.9, 22.3, 21.1; **HRMS** (ES+) m/z calc'd for $C_{18}H_{23}NNa$ [M + Na]+: 276.1728, found 276.1731.

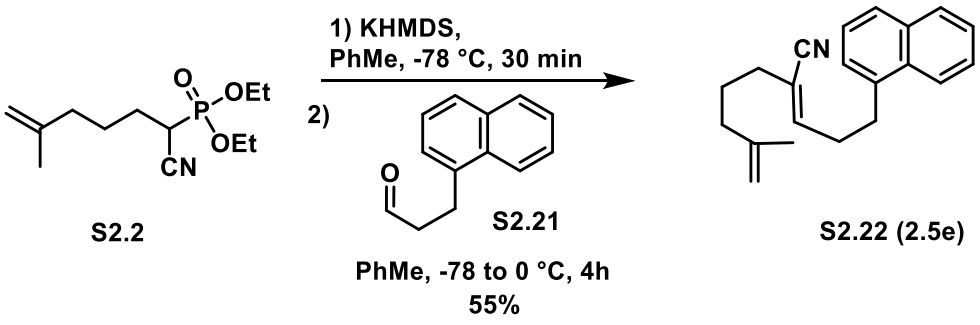

Prepared according to general procedure A, using cyanophosphonate **S2.2***(1.16 mmol) and aldehyde* **S2.21**[48]*(1.05 mmol) to give a 1:4 (E:Z) mixture of α,β-unsaturated nitriles*. Yield: 55% of **S2.22** (183 mg, 0.63 mmol, colorless oil); R_f=0.15 (2:98 Et_2O/Hexanes); **^{1}H NMR** (600 MHz,

$CDCl_3$) δ 8.04 (d, *J* = 8.4 Hz, 1H), 7.88 (d, *J* = 8.1 Hz, 1H), 7.76 (d, *J* = 8.2 Hz, 1H), 7.55 (t, *J* = 7.2 Hz, 1H), 7.50 (t, *J* = 7.4 Hz, 1H), 7.42 (t, *J* = 7.6 Hz, 1H), 7.34 (d, *J* = 6.9 Hz, 1H), 6.21 (t, *J* = 7.6 Hz, 1H), 4.75 (s, 1H), 4.67 (s, 1H), 3.23 (t, *J* = 7.6 Hz, 2H), 2.84 (dd, *J* = 15.2, 7.6 Hz, 2H), 2.18 (t, *J* = 7.6 Hz, 2H), 1.99 (t, *J* = 7.5 Hz, 2H), 1.72 (s, 3H), 1.68 – 1.61 (m, 2H); **^{13}C NMR** (151 MHz, $CDCl_3$) δ 146.7, 144.8, 136.4, 134.0, 131.8, 129.0, 127.3, 126.3, 126.2, 125.8, 125.6, 123.6, 117.6, 115.4, 110.8, 36.7, 33.8, 32.4, 32.0, 25.9, 22.3; **HRMS** (ES+) m/z calc'd for $C_{21}H_{23}NNa$ [M + Na]+: 312.1728, found 312.1729.

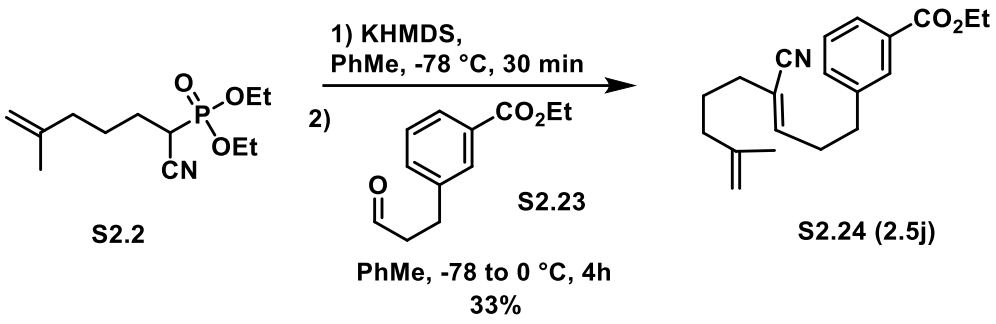

Prepared according to general procedure A, using cyanophosphonate **S2.2***(1.54 mmol) and aldehyde* **S2.23**[49]*(1.54 mmol) to give a 1:4 (E:Z) mixture of α,β-unsaturated nitriles*. Yield: 33% of **S2.24** (157 mg, 0.50 mmol, colorless oil); R_f=0.15 (15:85 Et_2O/hexanes); **^{1}H NMR** (500 MHz, $CDCl_3$) δ 7.93 – 7.88 (m, 1H), 7.86 (s, 1H), 7.41 – 7.36 (m, 2H), 6.12 (t, *J* = 7.5 Hz, 1H), 4.72 (s, 1H), 4.64 (s, 1H), 4.38 (q, *J* = 7.1 Hz, 2H), 2.82 (t, *J* = 7.5 Hz, 2H), 2.73 – 2.68 (m, 2H), 2.16 (t, *J* = 7.6 Hz, 2H), 1.96 (t, *J* = 7.5 Hz, 2H), 1.69 (s, 3H), 1.67 – 1.59 (m, 2H), 1.40 (t, *J* = 7.1 Hz, 3H); **^{13}C NMR** (126 MHz, $CDCl_3$) δ 166.7, 146.1, 144.7, 140.6, 133.0, 130.9, 129.6, 128.7, 127.8, 117.5, 115.9, 110.9, 61.1, 36.6, 34.7, 33.7, 32.9, 25.9, 22.3, 14.5; **HRMS** (ES+) m/z calc'd for $C_{20}H_{25}NO_2H$ [M + H]+: 312.1964, found 312.1961.

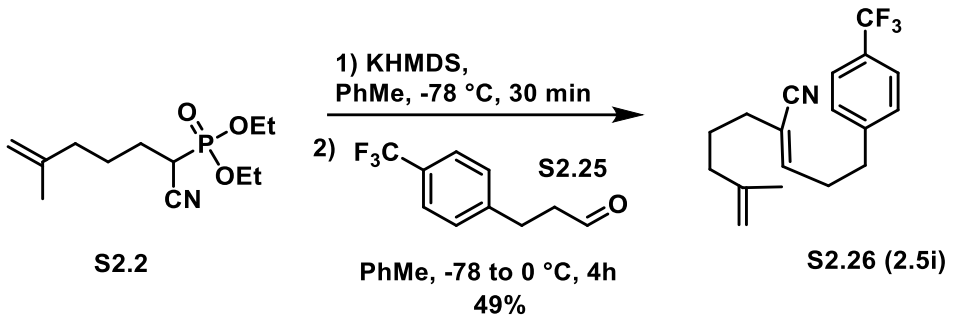

Prepared according to general procedure A, using cyanophosphonate **S2.2***(1.16 mmol) and aldehyde* **S2.25**[50]*(1.05 mmol) to give a 1:4 (E:Z) mixture of α,β-unsaturated nitriles*. Yield: 49% of **S2.26** (174 mg, 0.57 mmol, colorless oil) ; R_f=0.15 (4:96 Et_2O/hexanes); **^{1}H NMR** (600 MHz, $CDCl_3$) δ 7.56 (d, *J* = 8.0 Hz, 2H), 7.30 (d, *J* = 7.9 Hz, 2H), 6.11 (t, *J* = 7.5 Hz, 1H), 4.73 (s, 1H), 4.64 (s, 1H), 2.83 (t, *J* = 7.5 Hz, 2H), 2.72 – 2.69 (m, 2H), 2.17 (t, *J* = 7.5 Hz, 2H), 1.97 (t, *J* = 7.5 Hz, 2H), 1.69 (s, 3H), 1.66 – 1.60 (m, 2H); **^{13}C NMR** (151 MHz, $CDCl_3$) δ 145.8, 144.7, 144.4, 128.9 (q, *J* = 32.4 Hz), 128.9 (2C), 125.6 (q, *J* = 3.7 Hz, 2C), 124.4 (q, *J* = 271.8 Hz), 117.5, 116.1, 110.9, 36.6, 34.7, 33.7, 32.7, 25.8, 22.3; **HRMS** (ES+) m/z calc'd for $C_{18}H_{20}F_3NNa$ [M + Na]+: 330.1446, found 330.1442.

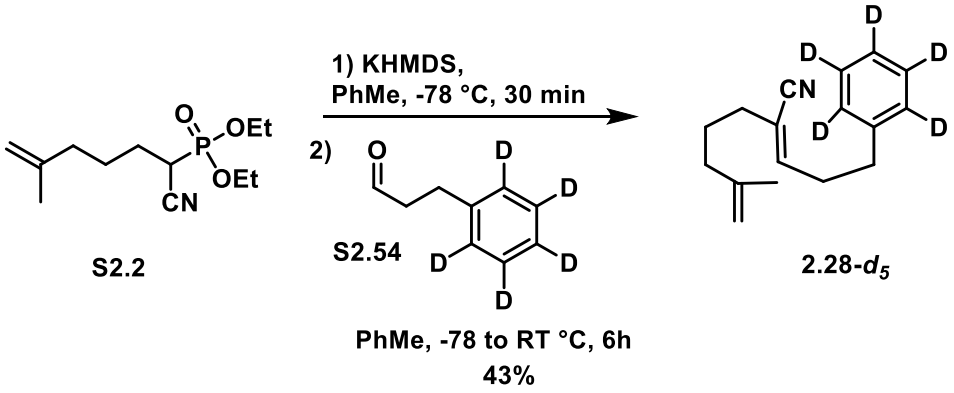

Prepared according to general procedure A, using cyanophosphonate **S2.2** *(1.44 mmol) and aldehyde* **S2.54**[51] *(1.44 mmol) to give a 1:8 (E:Z) mixture of α,β-unsaturated nitriles*. Yield: 43% of **2.28** (151 mg, 0.62 mmol, colorless oil); R_f=0.15 (1.5:98.5 EtOAc/Hexanes); **^{1}H NMR** (600

MHz, $CDCl_3$) δ 6.13 (t, *J* = 7.5 Hz, 1H), 4.73 (s, 1H), 4.65 (s, 1H), 2.77 (t, *J* = 7.5 Hz, 2H), 2.69 (dd, *J* = 14.9, 7.4 Hz, 2H), 2.17 (t, *J* = 7.5 Hz, 2H), 1.98 (t, *J* = 7.5 Hz, 2H), 1.70 (s, 3H), 1.67 – 1.61 (m, 2H); **^{13}C DEPTQ NMR** (151 MHz, $CDCl_3$) δ 146.7, 144.8, 140.1, 128.1(t, *J* = 24.3 Hz, 2C), 128.1(t, *J* = 24.3 Hz, 2C), 125.9 (t, *J* = 24.3 Hz), 117.6, 115.4, 110.8, 36.6, 34.8, 33.7, 33.1, 25.9, 22.3; **HRMS** (ES+) *m/z* calc'd for $C_{17}H_{16}D_5NNa$ $[M + Na]^+$: 267.1885, found 267.1884.

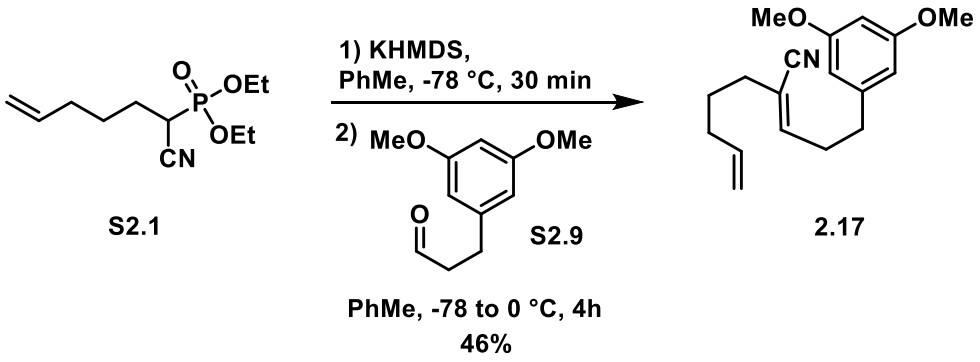

Prepared according to general procedure A, using cyanophosphonate **S2.1** *(1.63 mmol) and aldehyde* **S2.9**[9] *(1.48 mmol) to give a 1:4 (E: Z) mixture of α,β-unsaturated nitriles*. Yield: 46% of **2.17** (215 mg, 0.75 mmol, colorless oil); R_f=0.15 (3:97 EtOAc/hexanes); **^{1}H NMR** (500 MHz, $CDCl_3$) δ 6.35 – 6.31 (m, 3H), 6.11 (t, *J* = 6.8 Hz, 1H), 5.75 (ddt, *J* = 17.0, 10.2, 6.7 Hz, 1H), 5.03 – 4.95 (m, 2H), 3.78 (s, 6H), 2.75 – 2.64 (m, 4H), 2.18 (t, *J* = 7.5 Hz, 2H), 2.01 (q, *J* = 7.1 Hz, 2H), 1.65 – 1.54 (m, 2H); **^{13}C NMR** (126 MHz, $CDCl_3$) δ 161.0, 146.7, 142.7, 137.8, 117.7, 115.5, 115.3, 106.6, 98.4, 55.4, 35.1, 33.6, 32.7, 32.6, 27.2; **HRMS** (ES+) *m/z* calc'd for $C_{18}H_{23}NO_2H$ $[M + H]^+$: 286.1807, found 286.1805. Yield: 14% of *E*-isomer (64 mg, 0.22 mmol, colorless oil); R_f=0.15 (4:96 EtOAc/hexanes); **^{1}H NMR** (600 MHz, $CDCl_3$) δ 6.35 (t, *J* = 7.6 Hz, 1H), 6.33 (s, 1H), 6.30 (s, 2H), 5.75 (td, *J* = 16.7, 6.9 Hz, 1H), 5.04– 4.96 (m, 2H), 3.78 (s, 6H), 2.66 (t, *J* = 7.5 Hz, 2H), 2.48 (q, *J* = 7.5 Hz, 2H), 2.14 (t, *J* = 7.6 Hz, 2H), 2.04 (q, *J* = 6.9 Hz, 2H), 1.59 – 1.52 (m, 2H); **^{13}C NMR** (151 MHz, $CDCl_3$) δ 161.1, 146.9, 142.7, 137.7, 120.0, 115.5, 115.3, 106.7,

98.3, 55.4, 34.9, 32.9, 30.2, 28.0, 27.1; **HRMS** (ES+) *m/z* calc'd for $C_{18}H_{23}NO_2Na$ [M + Na]$^+$: 308.1627, found 308.1631.

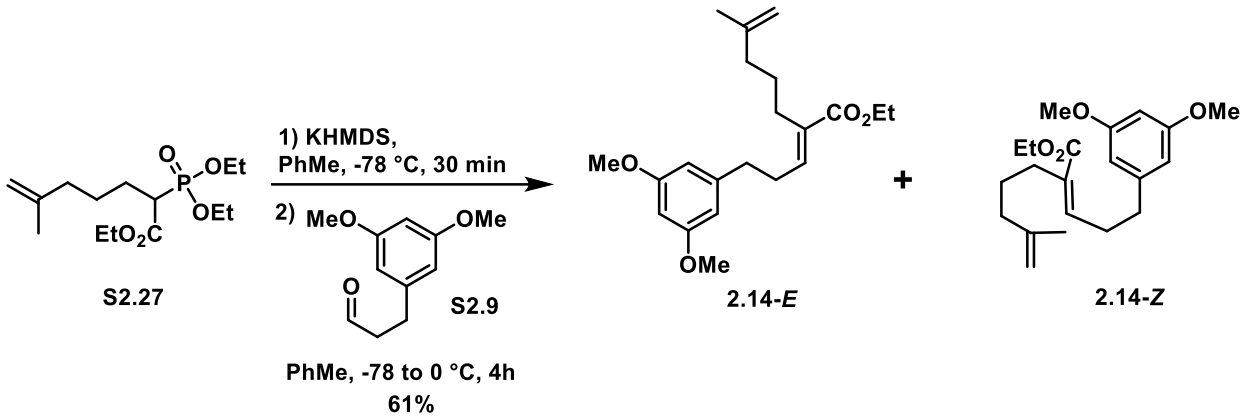

Prepared according to general procedure A, using phosphonoacetate **S2.27**[19b] *(0.849 mmol) and aldehyde* **S2.9**[9] *(1.02 mmol) to give a 1:4 (E:Z) mixture of α,β-unsaturated nitriles*. Yield: 48% of **2.14-*E*** (140 mg, 0.40 mmol, colorless oil) of E; R_f=0.15 (2:98 EtOAc/hexanes); **^{1}H NMR** (500 MHz, $CDCl_3$) δ 6.78 (t, *J* = 7.4 Hz, 1H), 6.35 (d, *J* = 2.1 Hz, 2H), 6.32 (t, *J* = 2.2 Hz, 1H), 4.70 (s, 1H), 4.67 (s, 1H), 4.19 (q, *J* = 7.1 Hz, 2H), 3.78 (s, 6H), 2.69 (t, *J* = 7.8 Hz, 2H), 2.50 – 2.48 (m, 2H), 2.28 – 2.23 (m, 2H), 2.00 (t, *J* = 7.6 Hz, 2H), 1.70 (s, 3H), 1.51 – 1.44 (m, 2H), 1.29 (t, *J* = 7.1 Hz, 3H); **^{13}C NMR** (126 MHz, $CDCl_3$) δ 168.0, 161.0, 145.7, 143.8, 141.3, 133.2, 110.1, 106.6, 98.2, 60.5, 55.4, 37.8, 35.5, 30.5, 27.2, 26.6, 22.5, 14.4; **HRMS** (ES+) *m/z* calc'd for $C_{21}H_{31}O_4$ [M + H]$^+$: 347.2222, found 347.2217.

Yield: 13% of **2.14-*Z*** (38 mg, 0.11 mmol, colorless oil); R_f=0.16 (2:98 EtOAc/hexanes); **^{1}H NMR** (500 MHz, $CDCl_3$) δ 6.36 (d, *J* = 2.2 Hz, 2H), 6.30 (t, *J* = 2.2 Hz, 1H), 5.87 (t, *J* = 7.1 Hz, 1H), 4.70 (s, 1H), 4.65 (s, 1H), 4.20 (q, *J* = 7.1 Hz, 2H), 3.77 (s, 6H), 2.76 – 2.70 (m, 2H), 2.70 – 2.64 (m, 2H), 2.25 – 2.19 (m, 2H), 1.99 (t, *J* = 7.6 Hz, 2H), 1.70 (s, 3H), 1.58 – 1.50 (m, 2H), 1.30 (t, *J* = 7.1 Hz, 3H); **^{13}C NMR** (126 MHz, $CDCl_3$) δ 168.2, 160.9, 145.7, 144.1, 140.3, 132.9, 110.2,

106.7, 98.1, 60.2, 55.4, 37.3, 36.0, 34.3, 31.0, 27.1, 22.5, 14.5; **HRMS** (ES+) *m/z* calc'd for $C_{21}H_{30}O_4Na$ $[M + Na]^+$: 369.2042, found 369.2029.

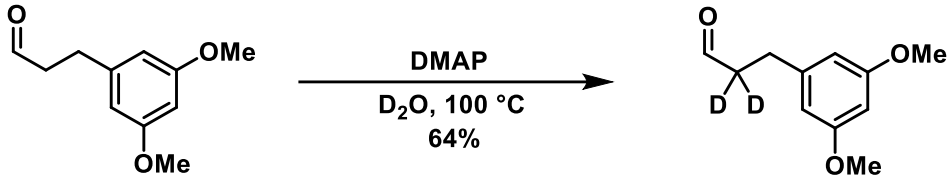

S2.9 **S2.9-*d*$_2$**

A sealed tube charged with a magnetic stirring bar, aldehyde **S2.9** (250 mg, 1.29 mmol), DMAP (16 mg, 0. 13 mmol), and heavy water (0.50 ml) was heated to 100 °C for 2h. After cooling to room temperature, the suspension was extracted with diethyl ether (3 x 2 mL), the combined organic extracts were washed with brine (2 mL), dried over Na_2SO_4, filtered and concentrated *in vacuo*. The resulting crude residue was purified via flash column chromatography on SiO_2, using a mixture of EtOAc/ hexanes (2:8) as eluent to give α-d_2 aldehyde **S2.9– *d*$_2$** as a colorless oil (161 mg, 0.82 mmol, 64% yield – *ca. ~90% deuteration at the α-position estimated by ^{1}H NMR*); **^{1}H NMR** (500 MHz, $CDCl_3$) δ 9.82 (s, 1H), 6.34 (d, *J* = 2.2 Hz, 2H), 6.32 (t, *J* = 2.2 Hz, 1H), 3.77 (s, 6H), 2.88 (s, 2H); **^{13}C NMR** (151 MHz, $CDCl_3$) δ 201.8, 161.1, 142.8, 106.5, 98.2, 55.4, 44.6 (pent, *J* = 19.5 Hz), 28.4; **HRMS** (ES+) *m/z* calc'd for $C_{11}H_{13}D_2O_3$ $[M + H]^+$: 197.1147, found 197.1149.

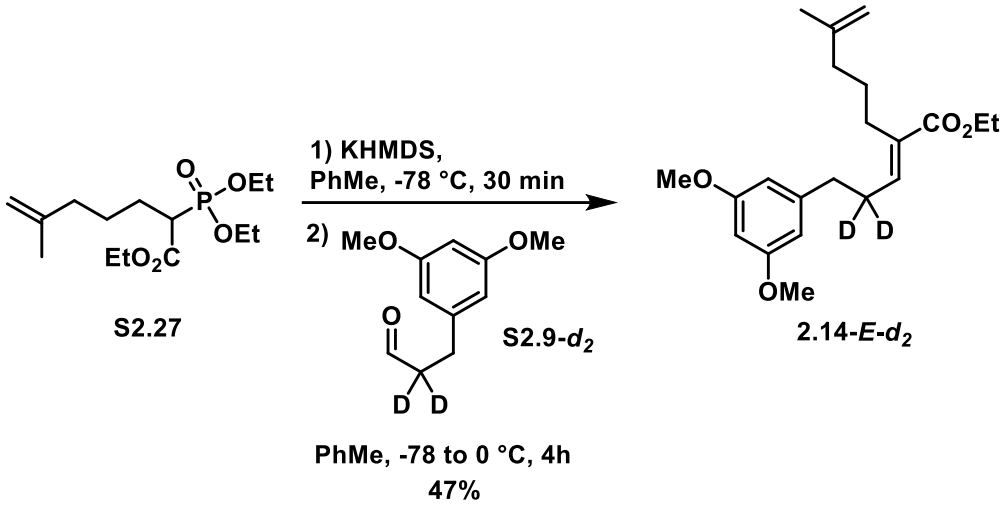

Prepared according to general procedure A, using phosphonoacetate **S2.27**[19b] *(0. 97 mmol) and aldehyde* **S2.9–*d*$_2$** *(0.97 mmol) to give a 5:1 (E:Z) mixture of α,β-unsaturated nitriles*. Yield: 47% of **2.14–*E*–*d*$_2$** (160 mg, 0.46 mmol, colorless oil) of E; R_f=0.15 (2:98 EtOAc/hexanes - *ca. ~90% deuteration at the α-position estimated by ^{1}H NMR*); **^{1}H NMR** (600 MHz, $CDCl_3$) δ 6.84 (s, 1H), 6.40 (s, 2H), 6.37 (s, 1H), 4.76 (s, 1H), 4.73 (s, 1H), 4.24 (q, *J* = 7.1 Hz, 2H), 3.83 (s, 6H), 2.73 (s, 2H), 2.34 – 2.29 (m, 2H), 2.06 (t, *J* = 7.6 Hz, 2H), 1.76 (s, 3H), 1.54 (dd, *J* = 15.4, 7.7 Hz, 2H), 1.35 (t, *J* = 7.1 Hz, 3H); **^{13}C NMR** (151 MHz, $CDCl_3$) δ 167.9, 160.9, 145.6, 143.7, 141.1, 133.2, 110.1, 106.5, 98.1, 60.4, 55.3, 37.7, 35.3, 29.7 (pent, *J* = 19.5 Hz) 27.1, 26.5, 22.4, 14.4; **HRMS** (ES+) *m/z* calc'd for $C_{21}H_{28}D_2O_4Na$ $[M + Na]^+$: 371.2167, found 371.2171.

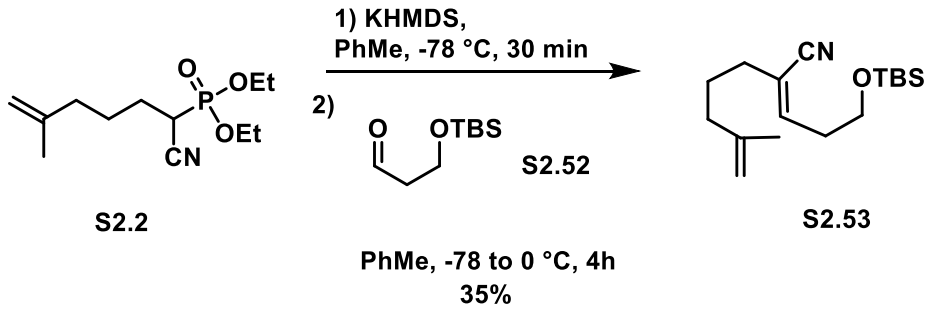

Prepared according to general procedure A, using cyanophosphonate **S2.2***(0.77 mmol) and aldehyde* **S2.52**[52] *(0.77 mmol) to give a 1:8 (E:Z) mixture of α,β-unsaturated nitriles*. Yield: 35% of **S2.53** (80 mg, 0.27 mmol, colorless oil); R_f=0.15 (1:99 EtOAc/hexanes);**^{1}H NMR** (500 MHz, $CDCl_3$) δ 6.23 (t, *J* = 7.5 Hz, 1H), 4.73 (s, 1H), 4.67 (s, 1H), 3.70 (t, *J* = 6.1 Hz, 2H), 2.55 (dd, *J* = 13.3, 6.3 Hz, 2H), 2.20 (t, *J* = 7.6 Hz, 2H), 2.03 (t, *J* = 7.5 Hz, 2H), 1.71 (s, 3H), 1.71 – 1.64 (m, 2H), 0.89 (s, 9H), 0.05 (s, 6H); **^{13}C DEPTQ NMR** (151 MHz, $CDCl_3$) δ 145.0, 144.8, 117.7, 116.0, 110.8, 61.6, 36.7, 35.1, 33.8, 26.1, 26.0, 25.9, 22.3, -5.3; **HRMS** (GG-CI) *m/z* calc'd for $C_{17}H_{32}NOSiH$ $[M + H]^+$: 294.2253, found 294.2263.

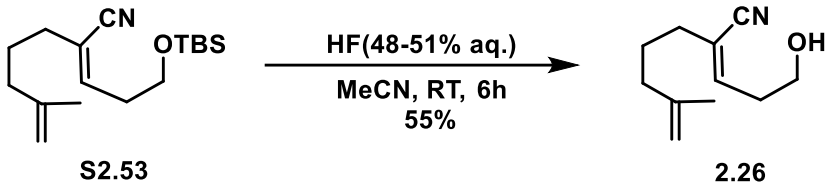

To a solution of silyl ether **S53** (80 mg, 0.27 mmol) in acetonitrile (1.0 mL) was added a solution of HF in water (48-51%, 0.10 mL). After stirring for 6 hours at room temperature, the mixture was diluted with water (3 mL) and extracted with EtOAc (3 x 5 mL). The combined organic extracts were washed with brine (2 mL), dried over Na_2SO_4, filtered and carefully concentrated *in vacuo (caution: the product is volatile).* The resulting crude residue was purified via flash column chromatography on SiO_2, using a mixture of EtOAc/ hexanes (3:7) as eluent to give alcohol **26** as a colorless oil (27 mg, 0.15 mmol, 55% yield); **^{1}H NMR** (600 MHz, $CDCl_3$) δ 6.25 (t, *J* = 7.5 Hz,

1H), 4.73 (s, 1H), 4.67 (s, 1H), 3.74 (t, *J* = 6.1 Hz, 1H), 2.60 (q, *J* = 6.6 Hz, 1H), 2.22 (t, *J* = 7.6 Hz, 1H), 2.02 (t, *J* = 7.5 Hz, 1H), 1.78 (s, 1H), 1.70 (s, 1H), 1.71 – 1.65 (m, 1H); **^{13}C DEPTQ NMR** (151 MHz, $CDCl_3$) δ 144.7, 144.3, 117.7, 116.8, 110.9, 61.3, 36.7, 34.9, 33.8, 25.8, 22.3; **HRMS** (ES+) *m/z* calc'd for $C_{11}H_{17}NONa$ $[M + Na]^+$: 202.1208, found 202.1208.

C-20 Methyl Substrate Synthesis and Characterization

General Procedure B (copper catalyzed allylic substitution):

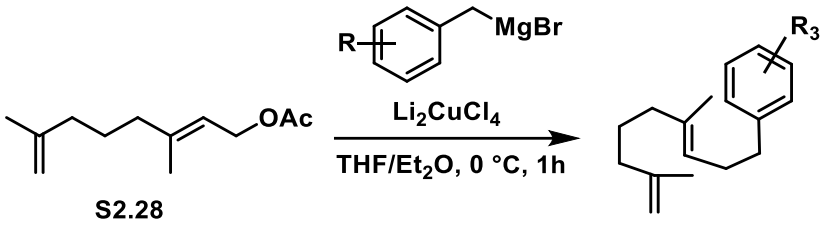

Grignard reagents were prepared from corresponding benzylic chlorides (or bromides) as follows: A suspension of activated Mg^0 turnings (2.0 equiv.) in Et_2O was cooled to 0 °C, and the benzyl halide (1.0 equiv., ~1.0M) was added slowly enough to maintain the reaction temperature under 20 °C. The resulting suspension was stirred vigorously at ambient temperature for 1 hour prior to use. Concentrations were determined using salicylaldehyde phenylhydrazone as titrant, and generally gave 1.0–1.2M solutions.

To an ice-cold solution of allylic acetate **S2.28**[53] (1.00 mmol, 1 equiv.) in THF (0.5 mL) was added a 1.0 M solution of Li_2CuCl_4 (0.10 mmol, 0.1 equiv.). The resulting mixture was stirred for 10 minutes and a solution of freshly prepared benzylic Grignard reagent (2.0 mmol, 2.0 equiv., ~ 1.0M in Et_2O) was added dropwise. After stirring for 2 hours at 0 °C, the reaction mixture was quenched with satd. $NH_4Cl_{(aq)}$ (10 mL) and stirred for 1 hour while warming to ambient temperature. The aqueous phase was extracted with Et_2O (3 x 20 mL), then the combined organic extracts were washed with brine, dried over Na_2SO_4, filtered and concentrated *in vacuo.* The

resulting crude residue was purified via flash column chromatography on SiO_2, using a mixture of Et_2O/ hexanes as eluent (NOTE: *the products contained ~11% of the inseparable trisubstituted alkene isomer, since* **S2.28** *contained ~11% of geraniol acetate*).

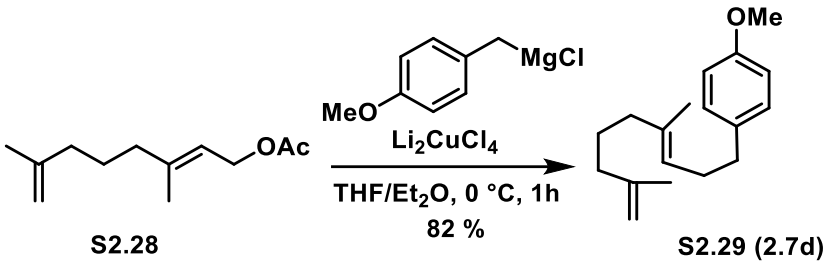

Prepared according to general procedure B, using allylic acetate **S2.28** *(2.36 mmol) and p-methoxybenzyl chloride (4.71 mmol) to give a 89:11 mixture of alkene isomers*. Yield: 82% of **S2.29** (501 mg, 1.94 mmol, colorless oil); R_f=0.30 (2:98 EtOAc/hexanes); **^{1}H NMR** (500 MHz, $CDCl_3$) δ 7.10 (d, *J* = 8.6 Hz, 2H), 6.82 (d, *J* = 8.6 Hz, 2H), 5.17 (td, *J* = 7.0, 1.2 Hz, 1H), 4.70 (s, 1H), 4.66 (s, 1H), 3.79 (s, 3H), 2.60 – 2.56 (m, 2H), 2.27 (dd, *J* = 15.2, 7.4 Hz, 2H), 1.98-1.93 (m, 4H), 1.71 (s, 3H), 1.54 (s, 3H), 1.53 – 1.49 (m, 2H); **^{13}C NMR** (126 MHz, $CDCl_3$) δ 157.8, 146.3, 135.8, 134.7, 129.5, 124.0, 113.8, 109.8, 55.4, 39.4, 37.5, 35.4, 30.3, 26.1, 22.6, 16.0; ; **HRMS** (ES+) *m/z* calc'd for $C_{18}H_{26}O$ $[M]^+$: 258.1984, found 258.1991.

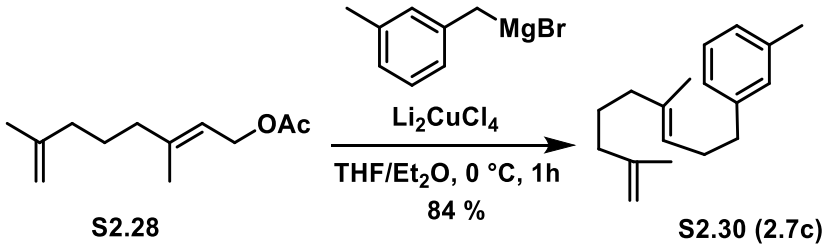

Prepared according to general procedure B, using allylic acetate **S2.28** *(1.18 mmol) and 3-methylbenzyl bromide (2.36 mmol) to give a 89:11 mixture of alkene isomers*. Yield: 84% of **S2.30** (241 mg, 0.99 mmol, colorless oil); R_f=0.73 (hexanes); **^{1}H NMR** (600 MHz, $CDCl_3$) δ 7.17 (t, *J* =

7.4 Hz, 1H), 7.02 – 6.98 (m, 3H), 5.19 (t, *J* = 6.5 Hz, 1H), 4.70 (s, 1H), 4.66 (s, 1H), 2.60 (t, *J* = 7.8 Hz, 2H), 2.33 (s, 3H), 2.31 – 2.26 (m, 2H), 2.01 – 1.91 (m, 4H), 1.71 (s, 3H), 1.56 (s, 3H), 1.54 – 1.48 (m, 2H); **^{13}C NMR** (151 MHz, $CDCl_3$) δ 146.2, 142.5, 137.8, 135.8, 129.4, 128.3, 126.5, 125.6, 124.0, 109.9, 39.4, 37.5, 36.2, 30.1, 26.1, 22.6, 21.6, 16.0; ; **HRMS** (ES+) *m/z* calc'd for $C_{18}H_{26}$ $[M]^+$: 242.2034, found 242.2045.

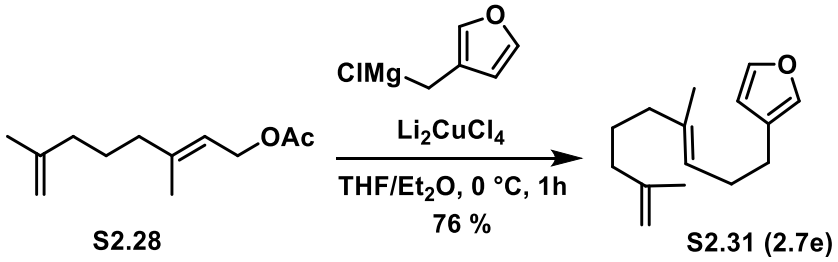

Prepared according to general procedure B, using allylic acetate **S2.28** *(1.00 mmol) and 3-chloromethylfuran (2.00 mmol) to give a 89:11 mixture of alkene isomers*. Yield: 76% of **S2.31** (165 mg, 0.76 mmol, colorless oil); R_f=0.40 (hexanes); **^{1}H NMR** (500 MHz, $CDCl_3$) δ 7.34 (t, *J* = 1.6 Hz, 1H), 7.21 (d, *J* = 0.9 Hz, 1H), 6.28 (s, 1H), 5.19 – 5.15 (m, 1H), 4.70 (d, *J* = 0.7 Hz, 1H), 4.66 (d, *J* = 0.8 Hz, 1H), 2.45 (t, *J* = 7.6 Hz, 2H), 2.25 (q, *J* = 7.4 Hz, 2H), 2.01 – 1.94 (m, 4H), 1.71 (s, 3H), 1.59 (s, 3H), 1.56 – 1.48 (m, 2H); **^{13}C NMR** (126 MHz, $CDCl_3$) δ 146.2, 142.7, 139.0, 135.9, 125.1, 124.0, 111.2, 109.9, 39.4, 37.5, 28.6, 26.0, 25.2, 22.6, 16.1; **HRMS** (ES+) *m/z* calc'd for $C_{15}H_{22}OH$ $[M + H]^+$: 219.1749, found 219.1656.

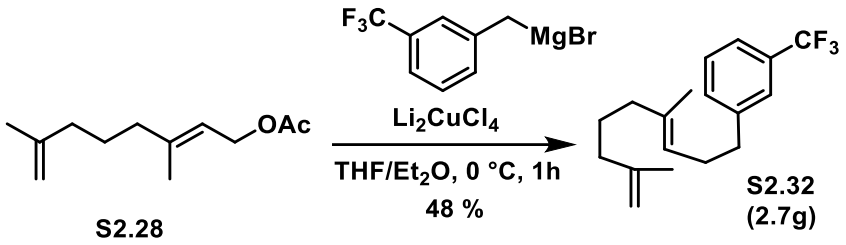

Prepared according to general procedure B, using allylic acetate **S2.28** *(1.18 mmol) and 3-(trifluoromethyl)benzyl bromide (2.95 mmol) to give a 89:11 mixture of alkene isomers*. Yield: 48% of **S2.32** (168 mg, 0.57 mmol, colorless oil); R_f=0.65 (hexanes); **^{1}H NMR** (600 MHz, $CDCl_3$) δ 7.45 – 7.43 (m, 2H), 7.40 – 7.35 (m, 2H), 5.15 (td, *J* = 7.1, 1.1 Hz, 1H), 4.70 (s, 1H), 4.66 (s, 1H), 2.71 (t, *J* = 7.6 Hz, 2H), 2.33 (q, *J* = 7.4 Hz, 2H), 2.00 – 1.91 (m, 4H), 1.71 (s, 3H), 1.52 (s, 3H), 1.53 – 1.49 (m, 2H); **^{13}C NMR** (151 MHz, $CDCl_3$) δ 146.1, 143.2, 136.5, 132.0, 130.5 (q, *J* = 31.9 Hz), 128.6, 125.3 (q, *J* = 3.7 Hz), 124.4 (q, *J* = 271.8 Hz), 123.0, 122.6 (q, *J* = 3.8 Hz), 109.8, 39.3, 37.4, 35.9, 29.6, 25.9, 22.4, 15.9; **HRMS** (ES+) *m/z* calc'd for $C_{18}H_{23}F_3NH_4$ [M + NH_4]$^+$: 314.2096, found 314.2093.

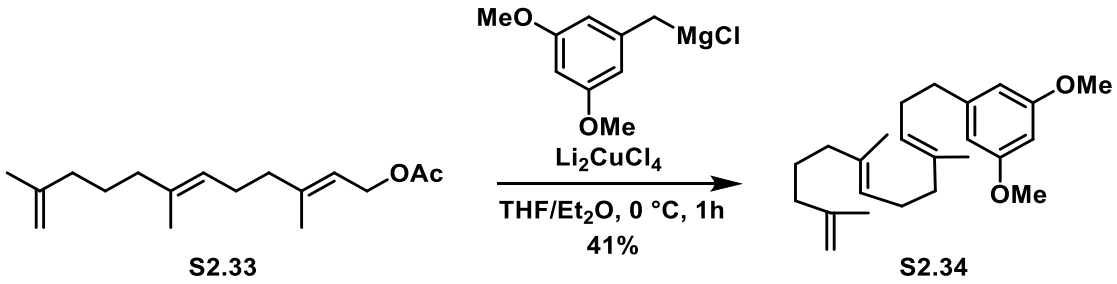

Prepared according to general procedure B, using allylic acetate **S2.33**[54] *(0.340 mmol, 1.0 equiv.) and 3,5-dimethoxybenzyl chloride (0.6.80 mmol, 2.0 equiv) to give a 89:11 mixture of alkene isomers*. Yield: 41% of **S2.34** (55 mg, 0.15 mmol, colorless oil); R_f=0.21 (2:98 Et_2O/hexanes); **^{1}H NMR** (500 MHz, $CDCl_3$) δ 6.37 (d, *J* = 2.0 Hz, 2H), 6.32 (d, *J* = 1.9 Hz, 1H), 5.20 (t, *J* = 7.0 Hz, 1H), 5.12 (t, *J* = 6.7 Hz, 1H), 4.71 (s, 1H), 4.68 (s, 1H), 3.79 (s, 6H), 2.62 – 2.56 (m, 2H), 2.33 –

2.30 (m, 2H), 2.13 – 2.04 (m, 4H), 2.03 – 1.95 (m, 4H), 1.73 (s, 3H), 1.60 (s, 3H), 1.60 (s, 3H), 1.53 (dt, *J* = 15.2, 7.7 Hz, 2H); **^{13}C NMR** (126 MHz, $CDCl_3$) δ 160.8, 146.2, 145.0, 135.9, 135.1, 124.5, 123.7, 109.9, 106.7, 97.8, 55.4, 39.9, 39.4, 37.5, 36.6, 29.9, 26.9, 26.8, 26.1, 22.6, 16.2, 16.0; **HRMS** (ES+) *m/z* calc'd for $C_{24}H_{37}O_2$ $[M + H]^+$: 357.2794, found 357.2787.

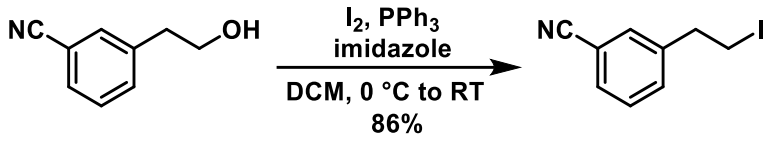

S2.35 **S2.36**

To an ice-cold solution of triphenylphosphine (5.88 g, 22.4 mmol, 1.5 equiv.) in CH_2Cl_2 (35 mL) was added iodine (5.69 g, 22.4 mmol, 1.5 equiv.). After 10 min., imidazole (2.54 g, 37.4 mmol, 2.5 equiv.) was added and the mixture was stirred for 10 min. A solution of alcohol **S2.35** (2.20 g, 15.0 mmol, 1.0 equiv.) in CH_2Cl_2 (15 mL) was added dropwise over approximately 5 min. After 90 min., satd. $Na_2SO_{3(aq)}$ (40 mL) was added in one portion and the aqueous phase was extracted with CH_2Cl_2 (2 x 20 mL). The combined organic extracts were washed with brine (20 mL), dried over Na_2SO_4, filtered and concentrated *in vacuo.* The crude residue was purified via flash column chromatography (EtOAc/hexanes 5:95) to give iodide **S2.36** as a crystalline white solid (3.32 g, 12.9 mmol, 86% yield). **^{1}H NMR** (500 MHz, $CDCl_3$) δ 7.58 – 7.55 (m, 1H), 7.50 (s, 1H), 7.46 – 7.43 (m, 2H), 3.35 (t, *J* = 7.4 Hz, 2H), 3.21 (t, *J* = 7.4 Hz, 2H); **^{13}C NMR** (126 MHz, $CDCl_3$) δ 141.8, 133.1, 132.1, 130.8, 129.6, 118.8, 112.9, 39.4, 4.4. **HRMS** (ES+) *m/z* calc'd for C_9H_8IN $[M]^+$: 256.9702, found 256.9713.

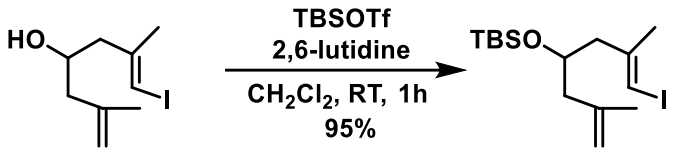

S2.37 **S2.38**

To a solution of alcohol **S2.37**[7] (100 mg, 0.376 mmol, 1.0 equiv.) and 2,6-lutidine (200 μL, 1.73 mmol, 4.6 equiv.) in CH_2Cl_2 (1 mL) was added TBSOTf (130 μL, 0.564 mmol, 1.5 equiv.). The mixture was stirred for 1 h at ambient temperature, then methanol (5.0 mL) was added. Volatiles were removed *in vacuo*, and the resulting crude residue was directly purified via flash chromatography using a mixture of EtOAc/hexanes (1:99) as eluent to give silyl ether **S2.38** as a colorless oil (3.52 g, 95%).**^{1}H NMR** (500 MHz, $CDCl_3$) δ 5.90 (d, *J* = 0.8 Hz, 1H), 4.79 (s, 1H), 4.70 (s, 1H), 3.90 (tdd, *J* = 7.4, 5.6, 4.5 Hz, 1H), 2.35 (dd, *J* = 13.5, 4.0 Hz, 1H), 2.27 (dd, *J* = 13.5, 7.6 Hz, 1H), 2.19 (dd, *J* = 13.6, 5.5 Hz, 1H), 2.12 (dd, *J* = 13.6, 7.2 Hz, 1H), 1.83 (d, *J* = 0.9 Hz, 3H), 1.73 (s, 3H), 0.87 (s, 9H), 0.03 (s, 3H), 0.01 (s, 3H): **^{13}C NMR** (126 MHz, $CDCl_3$) δ 145.1, 142.5, 113.5, 77.6, 69.0, 47.0, 46.4, 26.0, 24.6, 23.2, 18.2, –4.4(2C); **HRMS** (ES+) *m/z* calc'd for $C_{15}H_{29}IOSiH$ $[M+H]^+$: 381.1111, found 381.1109.

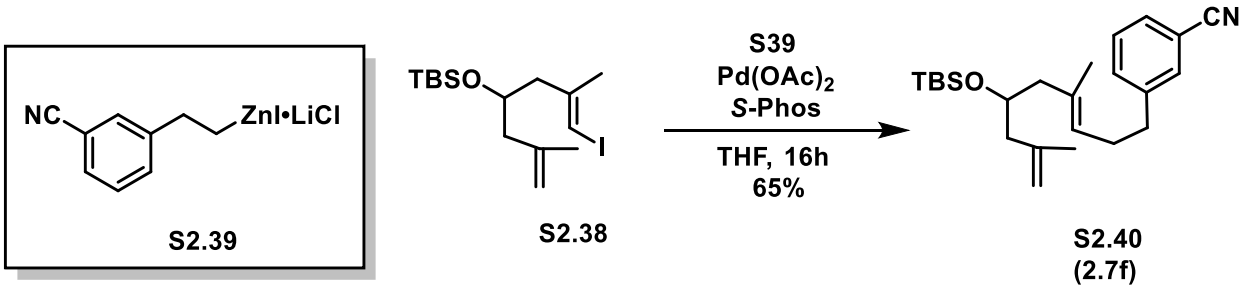

Preparation of the homobenzylic zinc reagent **S2.39**: LiCl (53 mg, 1.25 mmol, 1.9 equiv.) was dried under high-vacuum for 2 h at 170 °C, then Zn^0 dust (82 mg, 1.25 mmol, 1.9 equiv.) was added and the mixture was dried for another 2 h. The flask was cooled to ambient temperature, the

contents were suspended in THF (0.5 mL). The zinc dust was activated by adding 5 drops of a saturated I_2 solution in THF and sonicating the suspension until the brown color faded. A THF (4 mL) solution of homobenzylic iodide **S2.36** (169 mg, 0.66 mmol, 1.25 equiv.) was added and the mixture was stirred at 50 °C for 4 h.

Negishi Cross-Coupling: To a solution of $Pd(OAc)_2$ (15 mg, 65.8 μmol, 0.1 equiv.) and S-Phos (59 mg, 0.132 mmol, 0.2 equiv.) in THF (1 mL) was added a solution of vinyl iodide **S2.38** (200 mg, 0.526 mmol, 1.0 equiv.) in THF (0.5 mL). The aforementioned solution of homobenzylic zinc reagent **S2.39** was quickly added and the resulting suspension was stirred at room temperature for 16 h. Then, satd. $NH_4Cl_{(aq)}$ (10 mL) was added and the reaction mixture was extracted with Et_2O (3 x 20 mL). The combined organic extracts were washed with brine, dried over Na_2SO_4, filtered and concentrated *in vacuo*. The resulting crude residue was purified via flash column chromatography using a mixture of Et_2O/ hexanes (2:98) as eluent to give **S2.40** as a colorless oil (131 mg, 0.341 mmol, 65% yield); **^{1}H NMR** (600 MHz, $CDCl_3$) δ 7.51 – 7.45 (m, 2H), 7.41 (d, *J* = 7.8 Hz, 1H), 7.37 (t, *J* = 7.9 Hz, 1H), 5.15 (t, *J* = 6.6 Hz, 1H), 4.76 (d, *J* = 1.4 Hz, 1H), 4.67 (s, 1H), 3.86 (p, *J* = 6.3 Hz, 1H), 2.73 – 2.62 (m, 2H), 2.36 – 2.25 (m, 2H), 2.13 – 2.03 (m, 4H), 1.71 (s, 3H), 1.55 (s, 3H), 0.86 (s, 9H), 0.01 (s, 3H), -0.00 (s, 3H); **^{13}C NMR** (151 MHz, $CDCl_3$) δ 143.7, 143.0, 133.9, 133.3, 132.1, 129.7, 129.1, 125.8, 119.3, 113.2, 112.3, 69.5, 47.7, 46.0, 35.6, 29.7, 26.0, 23.1, 18.2, 16.7, –4.4, –4.5; **HRMS** (ES+) *m/z* calc'd for $C_{24}H_{37}NOSiNa$ $[M + Na]^+$: 406.2542, found 406.2540.

General Procedure C (B-alkyl Suzuki coupling):

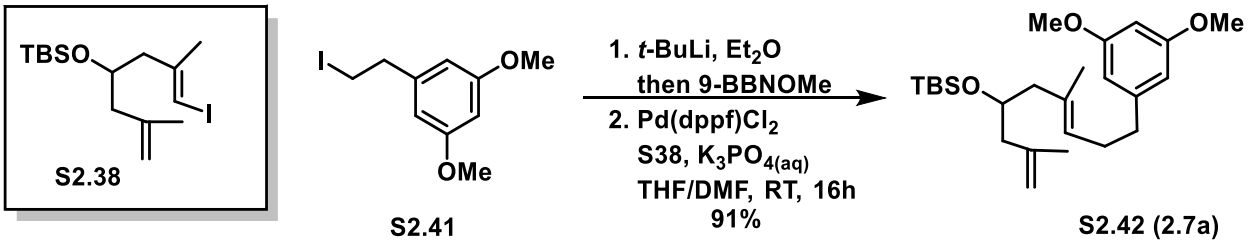

To a solution of homobenzylic iodide **S2.41**[55] (200 mg, 0.684 mmol, 1.3 equiv.) in Et_2O (2 mL) was added a 1.7 M solution of *tert*-butylithium (1.24 mL, 2.1 mmol, 4.0 equiv.) in pentane at –78 °C. The resulting mixture was stirred for 10 minutes and a 1.0 M solution of 9-BBN-OMe (2.4 mL, 4.5 equiv.) was added dropwise and the reaction flask was allowed to warm to ambient temperature over 30 min. THF (2 mL) followed by 3.0 M $K_3PO_{4(aq)}$ (0.44 mL, 1.3 mmol, 2.5 equiv.) were added, then the mixture was stirred for 1 h at room temperature. A solution of vinyl iodide **S2.38** (200 mg, 0.526 mmol, 1.0 equiv.) in DMF (2.0 mL), followed by $Pd(dppf)Cl_2$ (43 mg, 0.053 mmol, 0.1 equiv.) were finally added and the resulting suspension was stirred overnight under Ar. Next, the mixture was diluted with Et_2O (30 mL) and the organic phases were washed with DI H_2O (3 x 10 mL). The combined organic extracts were washed with brine (10 mL), dried over Na_2SO_4, filtered and concentrated *in vacuo.* The crude residue was purified via flash column chromatography (Et_2O/ hexanes 4:96) to give **S2.42** as a colorless oil (200 mg, 0.479 mmol, 91 % yield); **^{1}H NMR** (500 MHz, $CDCl_3$) δ 6.35 (d, *J* = 2.2 Hz, 2H), 6.30 (t, *J* = 2.1 Hz, 1H), 5.20 (t, *J* = 6.9 Hz, 1H), 4.76 (s, 1H), 4.68 (s, 1H), 3.91 – 3.85 (m, 1H), 3.78 (s, 6H), 2.62 – 2.55 (m, 2H), 2.34 – 2.24 (m, 2H), 2.12 – 2.06 (m, 4H), 1.71 (s, 3H), 1.60 (s, 3H), 0.87 (s, 9H), 0.02 (s, 3H), 0.01 (s, 3H); **^{13}C NMR** (151 MHz, $CDCl_3$) δ 160.7, 144.8, 143.1, 132.9, 126.7, 112.9, 106.5, 97.7, 69.7, 55.3, 47.8, 45.9, 36.3, 29.9, 29.3, 25.9, 23.05, 18.17, 16.69, –4.49; **HRMS** (ES+) *m/z* calc'd for $C_{25}H_{42}O_3SiNa$ $[M + Na]^+$: 441.2801, found 441.2818.

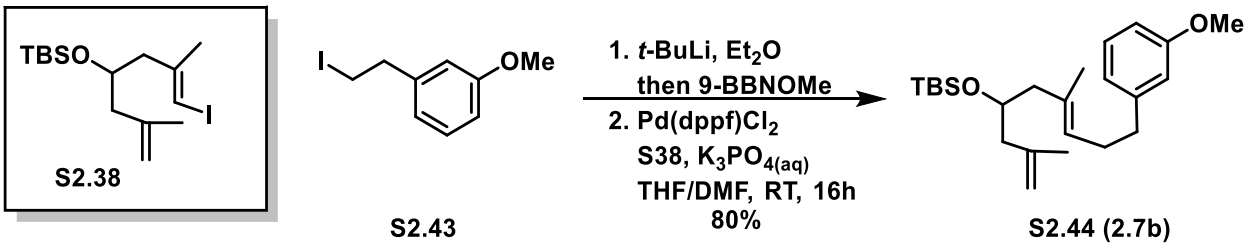

Prepared according to general procedure C, using vinyl iodide **S2.38** *(0.71 mmol) and homobenzylic iodide* **S2.43**[56] *(0.92 mmol)*. Yield: 80% of **S2.44** (220 mg, 0.57 mmol, colorless oil); R_f=0.38 (3:97 Et_2O/hexanes); **^{1}H NMR** (600 MHz, $CDCl_3$) δ 7.19 (t, *J* = 7.8 Hz, 1H), 6.79 (d, *J* = 7.4 Hz, 1H), 6.76 – 6.71 (m, 2H), 5.22 (t, *J* = 6.8 Hz, 1H), 4.77 (s, 1H), 4.69 (s, 1H), 3.88 (p, *J* = 6.2 Hz, 1H), 3.80 (s, 3H), 2.68 – 2.58 (m, 2H), 2.31 (dt, *J* = 14.7, 7.2 Hz, 2H), 2.16 – 2.06 (m, 4H), 1.72 (s, 3H), 1.59 (s, 3H), 0.87 (s, 9H), 0.03 (s, 3H), 0.02 (s, 3H); **^{13}C NMR** (151 MHz, $CDCl_3$) δ 159.7, 144.2, 143.2, 133.0, 129.3, 126.9, 121.0, 114.4, 113.0, 111.1, 69.8, 55.3, 47.9, 46.0, 36.1, 30.1, 26.0(3C), 23.2, 18.3, 16.8, –4.4(2C); **HRMS** (ES+) *m/z* calc'd for $C_{24}H_{40}O_2SiNa$ $[M + Na]^+$: 411.2695, found 411.2702.

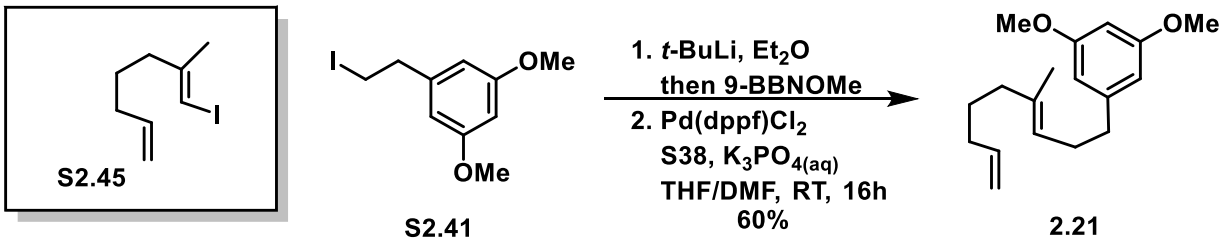

Prepared according to general procedure C, using vinyl iodide **S2.45**[57] *(0.53 mmol) and homobenzylic iodide* **S2.41**[21] *(0.68 mmol)*. Yield: 60% of **2.21** (86 mg, 0.31 mmol, colorless oil); R_f=0.28 (2:98 Et_2O/hexanes); **^{1}H NMR** (600 MHz, $CDCl_3$) δ 6.36 (d, *J* = 2.0 Hz, 2H), 6.31 (d, *J* = 2.0 Hz, 1H), 5.81 (ddt, *J* = 16.9, 10.2, 6.6 Hz, 1H), 5.18 (t, *J* = 7.0 Hz, 1H), 5.00 (d, *J* = 17.1 Hz, 1H), 4.94 (d, *J* = 10.2 Hz, 1H), 3.78 (s, 6H), 2.63 – 2.55 (m, 2H), 2.30 (dd, *J* = 15.3, 7.5 Hz, 2H), 2.03 – 1.96 (m, 4H), 1.57 (s, 3H), 1.52 – 1.44 (m, 2H); **^{13}C DEPTQ NMR** (151 MHz, $CDCl_3$) δ

160.8, 145.0, 139.1, 135.8, 123.9, 114.5 (2C), 106.7 (2C), 97.8, 55.4 (2C), 39.2, 36.6, 33.5, 29.8, 27.3, 16.0; **HRMS** (ES+) *m/z* calc'd for $C_{18}H_{27}O_2$ $[M + H]^+$: 275.2011, found 275.2010.

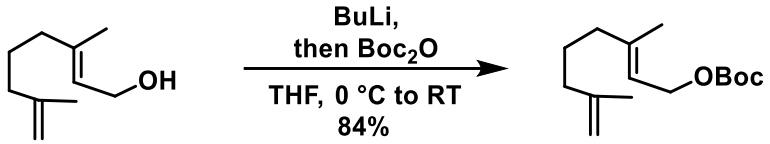

S2.47 **2.22**

To an ice-cold solution of alcohol **S2.47**[58] (700 mg, 4.54 mmol, 1.0 equiv.) in THF (12 mL) was added a 2.4M solution of *n*-butyllithium (1.9 mL, 4.54 mmol, 1.0 equiv.) in hexanes. The resulting solution was stirred for 15 minutes, and a solution of Boc_2O (990 mg, 4.54 mmol, 1.0 equiv.) in THF (6 mL) added dropwise. After stirring for 1 hour, satd. $NH_4Cl_{(aq)}$ (10 mL) was added. The aqueous phase was extracted with EtOAc (3 x 10 mL), the combined organic extracts were washed with brine (10 mL), dried over Na_2SO_4, filtered and concentrated *in vacuo.* The resulting crude residue was purified via flash column chromatography, using a mixture of EtOAc/ hexanes (5:95) as eluent to give carbonate **2.22** as a colorless oil (969 mg, 3.81 mmol, 84% yield). **^{1}H NMR** (500 MHz, $CDCl_3$) δ 5.37 (t, *J* = 7.1 Hz, 1H), 4.70 (s, 1H), 4.66 (s, 1H), 4.58 (d, *J* = 7.2 Hz, 2H), 2.04 – 2.00 (m, 2H), 2.00 – 1.95 (m, 2H), 1.70 (s, 6H), 1.57 – 1.52 (m, 2H), 1.48 (s, 9H); **^{13}C NMR** (126 MHz, $CDCl_3$) δ 153.8, 145.8, 142.7, 118.3, 110.1, 82.0, 63.9, 39.2, 37.4, 28.0, 25.6, 22.5, 16.5; ; **HRMS** (ES+) *m/z* calc'd for $C_{15}H_{26}O_3Na$ $[M + Na]^+$: 277.1780, found 277.1782.

Cobalt Catalyzed Bicyclizations and Product Characterization

General Procedure D (Cobalt catalyzed bicyclization):

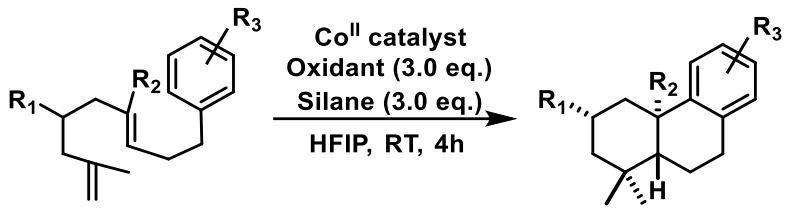

A dry round-bottom flask was charged with a magnetic stirring bar, bicyclization substrate (0.20 mmol, 1.0 equiv.) cobalt catalyst (0.02 mmol, 0.1 equiv.) and 1-fluoro-2,4,6-trimethylpyridinium triflate (0.60 mmol, 3.0 equiv.). The reagents were dissolved in HFIP (1.0 mL, 0.2 M based on substrate), and the flask was capped with a rubber septum. A balloon equipped with a syringe needle was used to bubble Ar through the solution for 10 minutes (a syringe needle was used as an outlet). Then, the flask was sealed from the atmosphere and TMDSO (0.60 mmol, 3 equiv.) was added dropwise at a rate of 1 drop per 3 seconds. The resulting solution gradually turned dark red or tan from its initial, dark green color. After 4-9 hours, TLC indicated complete starting material consumption and the volatiles were removed *in vacuo*. The resulting residue was directly purified via flash column chromatography. *Note: if ^{1}H NMR spectrum of the crude reaction mixture is desired, the crude residue should be passed through a short silica plug (using EtOAc as eluent) to remove paramagnetic cobalt complexes*.

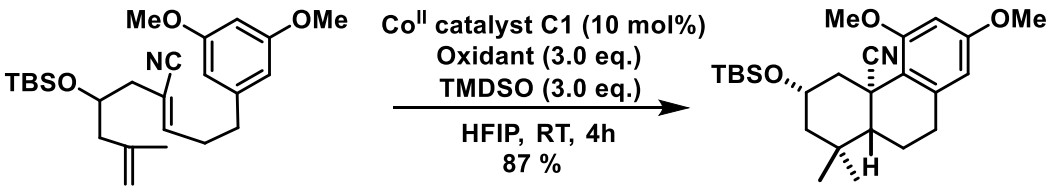

2.5a **2.6a**

Prepared according to general procedure D, using α,β-unsaturated nitrile **2.5a** *(0.12 mmol), cobalt catalyst* **C1** *(0.012 mmol), 1-fluoro-2,4,6-trimethylpyridinium triflate (0.36 mmol), and 1,1,3,3-tetramethyldisiloxane (0.36 mmol).* Yield: 87% of **2.6a** (44 mg, 0.10 mmol, white crystalline solid); R_f=0.15 (5:95 Et_2O/hexanes); **^{1}H NMR** (500 MHz, $CDCl_3$) δ 6.32 (d, *J* = 2.1 Hz, 1H), 6.23 (d, *J* = 1.8 Hz, 1H), 4.22 (tt, *J* = 11.3, 4.0 Hz, 1H), 3.85 (s, 3H), 3.77 (s, 3H), 3.68 (d, *J* = 12.6 Hz, 1H), 2.90 – 2.82 (m, 2H), 1.98 (d, *J* = 13.2 Hz, 1H), 1.80 (d, *J* = 11.3 Hz, 1H), 1.70 – 1.59 (m, 2H), 1.34 – 1.28 (m, 2H), 1.20 (s, 3H), 1.20 – 1.14 (m, 4H), 0.94 (s, 10H), 0.15 (s, 6H); **^{13}C NMR** (151 MHz, $CDCl_3$) δ 160.0, 159.9, 139.8, 122.8, 118.6, 105.4, 97.8, 66.2, 55.6, 55.4, 52.5, 50.5, 43.3, 39.4, 34.9, 33.0, 32.8, 26.1, 21.6, 21.0, 18.5, –4.5; **HRMS** (ES+) *m/z* calc'd for $C_{25}H_{39}NO_3SiNa$ $[M + Na]^+$: 452.2597, found 452.2600.

S2.11 (2.5b) **2.6b(*p*)** **2.6b(*o*)**

Prepared according to general procedure D, using α,β-unsaturated nitrile **S2.11** *(0.38 mmol), cobalt catalyst* **C1***(0.038 mmol), 1-fluoro-2,4,6-trimethylpyridinium triflate (1.13 mmol), and 1,1,3,3-tetramethyldisiloxane (1.13 mmol).* Combined yield: 73%; *p*-regioisomer **2.6b(*p*)**: Yield: 46% (69 mg, 0.17 mmol, white solid); R_f=0.15 (2:2:96 benzene/EtOAc/hexanes); **^{1}H NMR** (600 MHz, $CDCl_3$) δ 7.33 (d, *J* = 8.8 Hz, 1H), 6.77 (dd, *J* = 8.8, 2.7 Hz, 1H), 6.64 (d, *J* = 2.6 Hz, 1H), 4.24 (tt, *J* = 11.3, 4.0 Hz, 1H), 3.78 (s, 3H), 3.01 (dd, *J* = 17.3, 5.2 Hz, 1H), 2.92 – 2.82 (m, 2H),

2.05 (dd, *J* = 13.1, 7.3 Hz, 1H), 1.90 – 1.86 (m, 1H), 1.79 (ddd, *J* = 12.9, 3.9, 2.1 Hz, 1H), 1.51 – 1.45 (m, 1H), 1.32 – 1.25 (m, 2H), 1.17 (s, 3H), 1.03 (s, 3H), 0.93 (s, 9H), 0.16 (s, 3H), 0.15 (s, 3H); **^{13}C NMR** (151 MHz, $CDCl_3$) δ 159.2, 137.6, 129.8, 126.7, 123.5, 114.2, 113.0, 65.9, 55.4, 50.5, 50.0, 45.2, 39.8, 35.0, 32.2, 30.4, 26.1, 21.3, 21.1, 18.3, –4.4(2C); ; **HRMS** (ES+) *m/z* calc'd for $C_{24}H_{37}NO_2SiNa$ $[M + Na]^+$: 422.2491, found 422.2490.

o-regioisomer **2.6b(o)**: Yield: 27% (41 mg, 0.10 mmol, white solid); R_f=0.20 (2:2:96 benzene/EtOAc/hexanes); **^{1}H NMR** (600 MHz, $CDCl_3$) δ 7.17 (t, *J* = 7.9 Hz, 1H), 6.76 – 6.70 (m, 2H), 4.24 (ddd, *J* = 15.3, 7.7, 4.0 Hz, 1H), 3.88 (s, 3H), 3.73 (d, *J* = 12.6 Hz, 1H), 2.94 – 2.83 (m, 2H), 2.03 – 1.97 (m, 1H), 1.82 (ddd, *J* = 12.8, 3.9, 2.1 Hz, 1H), 1.70 – 1.63 (m, 1H), 1.38 – 1.29 (m, 2H), 1.21 (s, 3H), 1.20 – 1.16 (m, 1H), 1.05 (s, 3H), 0.94 (s, 9H), 0.15 (s, 6H); **^{13}C NMR** (151 MHz, $CDCl_3$) δ 158.9, 139.0, 128.8, 125.7, 122.6, 122.4, 109.5, 66.3, 55.6, 52.5, 50.6, 43.0, 39.7, 35.0, 33.0, 32.4, 26.1, 21.6, 20.9, 18.5, –4.48, –4.50; **HRMS** (ES+) *m/z* calc'd for $C_{24}H_{37}NO_2SiNa$ $[M + Na]^+$: 422.2491, found 422.2489.

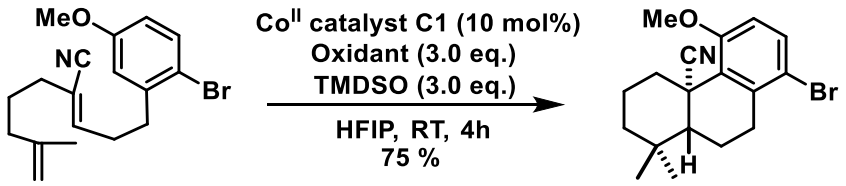

S2.13 (2.5c) **2.6c**

Prepared according to general procedure D, using α,β-unsaturated nitrile **S2.13** *(0.11 mmol), cobalt catalyst* **C1** *(0.011 mmol), 1-fluoro-2,4,6-trimethylpyridinium triflate (0.33 mmol), and 1,1,3,3-tetramethyldisiloxane (0.33 mmol)*. Yield of **2.6c**: 75% (30 mg, 0.57 mmol, white solid); R_f=0.15 (3:97 EtOAc/hexanes); **^{1}H NMR** (600 MHz, $CDCl_3$) δ 7.44 (d, *J* = 8.8 Hz, 1H), 6.67 (d, *J* = 8.8 Hz, 1H), 3.87 (s, 3H), 3.48 (d, *J* = 13.1 Hz, 1H), 2.93 (dd, *J* = 17.7, 3.6 Hz, 1H), 2.74 – 2.56 (m, 1H), 2.08 (dd, *J* = 13.4, 6.1 Hz, 1H), 1.99 (qt, *J* = 13.7, 3.3 Hz, 1H), 1.71 – 1.58 (m, 3H),

1.31 (d, *J* = 11.8 Hz, 1H), 1.26 (td, *J* = 13.4, 3.8 Hz, 1H), 1.18 (s, 3H), 1.13 (td, *J* = 13.3, 3.3 Hz, 1H), 1.02 (s, 3H); **^{13}C NMR** (151 MHz, $CDCl_3$) δ 158.4, 138.3, 132.5, 129.1, 122.6, 117.0, 111.2, 55.9, 52.3, 40.9, 40.2, 35.0, 34.2, 34.2, 32.7, 21.2, 20.6, 20.5; **HRMS** (ES+) *m/z* calc'd for $C_{18}H_{22}BrNONa$ $[M + Na]^+$: 370.0782, found 370.0783.

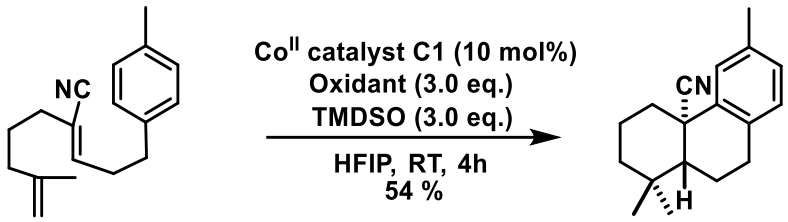

S2.20 (2.5d) **2.6d**

Prepared according to general procedure D, using α,β-unsaturated nitrile **S2.20** *(0.20 mmol), cobalt catalyst* **C1** *(0.020 mmol), 1-fluoro-2,4,6-trimethylpyridinium triflate (0.59 mmol), and 1,1,3,3-tetramethyldisiloxane (0.59 mmol).* Yield: 54% of **2.6d** (27 mg, 0.57 mmol, white solid); R_f=0.15 (2:98 Et_2O/hexanes); **^{1}H NMR** (600 MHz, $CDCl_3$) δ 7.23 (s, 1H), 7.05 – 7.01 (m, 2H), 2.98 (dd, *J* = 16.9, 5.0 Hz, 1H), 2.87 – 2.81 (m, 2H), 2.32 (s, 3H), 2.09 – 1.99 (m, 2H), 1.92 – 1.83 (m, 1H), 1.82 – 1.77 (m, 1H), 1.60 (ddd, *J* = 13.5, 4.6, 3.2 Hz, 1H), 1.49 (td, *J* = 13.4, 3.5 Hz, 1H), 1.35 (dd, *J* = 12.1, 1.9 Hz, 1H), 1.26 (td, *J* = 13.7, 3.8 Hz, 1H), 1.16 (s, 3H), 1.01 (s, 3H); **^{13}C NMR** (151 MHz, $CDCl_3$) δ 137.9, 136.1, 133.1, 129.8, 128.8, 126.2, 123.9, 50.6, 40.8, 40.1, 36.8, 33.8, 32.1, 30.0, 21.7, 21.3, 20.11, 20.08; **HRMS** (ES+) m/z calc'd for $C_{18}H_{23}NNa$ [M + Na]+: 276.1728, found 276.1739.

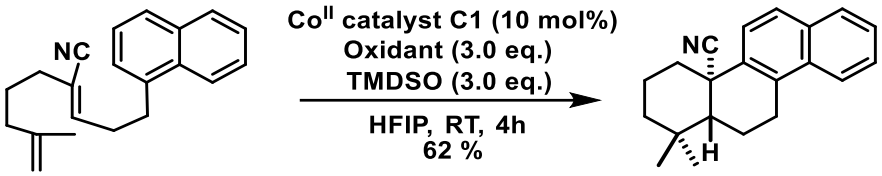

S2.22 (2.5e) **2.6e**

Prepared according to general procedure D, using α,β-unsaturated nitrile **S2.22** *(0.17 mmol), cobalt catalyst* **C1** *(0.017 mmol), 1-fluoro-2,4,6-trimethylpyridinium triflate (0.52 mmol), and 1,1,3,3-tetramethyldisiloxane (0.52 mmol)*. Yield: 62% of **2.6e** (31 mg, 0.11 mmol, white crystalline solid); R_f=0.15 (2:98 Et_2O/hexanes); **^{1}H NMR** (600 MHz, $CDCl_3$) δ 8.00 (d, *J* = 8.3 Hz, 1H), 7.82 (d, *J* = 7.9 Hz, 1H), 7.74 (d, *J* = 8.8 Hz, 1H), 7.57 (d, *J* = 8.8 Hz, 1H), 7.56 – 7.53 (m, 1H), 7.51 (t, *J* = 7.3 Hz, 1H), 3.46 (dd, *J* = 17.3, 5.6 Hz, 1H), 3.22 – 3.13 (m, 1H), 2.93 (d, *J* = 13.0 Hz, 1H), 2.30 (dd, *J* = 13.5, 6.7 Hz, 1H), 2.15 – 2.05 (m, 1H), 2.03 – 1.96 (m, 1H), 1.86 – 1.82 (m, 1H), 1.63 (d, *J* = 13.5 Hz, 1H), 1.53 – 1.46 (m, 2H), 1.33 – 1.25 (m, 1H), 1.22 (s, 3H), 1.07 (s, 3H); **^{13}C NMR** (151 MHz, $CDCl_3$) δ 135.1, 132.7, 132.4, 132.1, 128.5, 127.5, 126.7, 126.3, 123.7, 123.6, 123.2, 50.5, 40.8, 40.7, 37.2, 33.7, 32.1, 27.7, 21.5, 20.3, 20.1; **HRMS** (ES+) *m/z* calc'd for $C_{21}H_{23}NNa$ $[M + Na]^+$: 312.1728, found 312.1724.

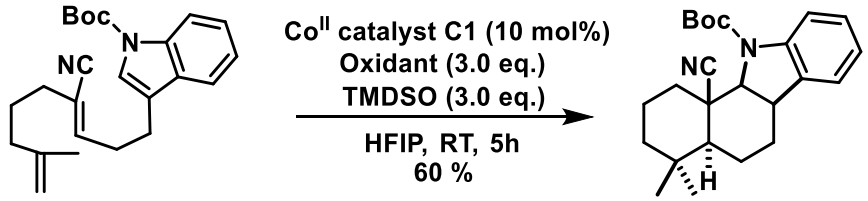

S2.18 (2.5f) **2.6f**

Prepared according to general procedure D, using α,β-unsaturated nitrile **S2.18** *(0.13 mmol), cobalt catalyst* **C1** *(0.013 mmol), 1-fluoro-2,4,6-trimethylpyridinium triflate (0.40 mmol), and 1,1,3,3-tetramethyldisiloxane (0.40 mmol)*. Yield: 60% of **2.6f** (30 mg, 0.08 mmol, white

crystalline solid); R_f=0.18 (2.5:97.5 EtOAc/hexanes); **^{1}H NMR** (600 MHz, $CDCl_3$) (Note: *mixture of rotamers, integrations are relative*) δ 7.48 – 7.30 (m (br), 1H), 7.24 (t (br), *J* = 7.3 Hz, 1H), 7.16 – 7.11 (m(br), 1H), 7.07 (t, *J* = 7.4 Hz, 1H), 4.63 – 4.18 (m(br), 2H), 3.63 (t (br), *J* = 7.0 Hz, 2H), 2.51 (d, *J* = 14.1 Hz, 1H), 2.45 – 2.29 (m (br), 2H), 1.95 – 1.80 (m , 2H), 1.78 – 1.64 (m(br), 5H), 1.60 (s(br), 3H), 1.57 (s(br), 15H), 1.29 – 1.16 (m(br), 4H), 1.03 – 0.98 (m, 3H), 0.95 (s(br), 6H).**^{13}C NMR** (151 MHz, $CDCl_3$) δ 171.3, 153.4(br), 143.4(br), 133.9(br), 131.6(br), 128.0(br), 123.8, 123.8, 121.62br), 118.7(br), 117.7, 82.0(br), 69.1(br), 60.6(br), 49.4(br), 45.5, 44.0(br), 41.0, 40.8, 39.7(br), 38.1, 37.9, 33.4, 32.4, 28.5, 28.5, 24.3, 21.2, 21.1, 20.6, 20.6(br), 20.36, 19.2(br), 19.0(br), 14.34. **HRMS** (ES+) *m/z* calc'd for $C_{24}H_{32}N_2O_2Na$ $[M + Na]^+$: 403.2361, found 403.2367.

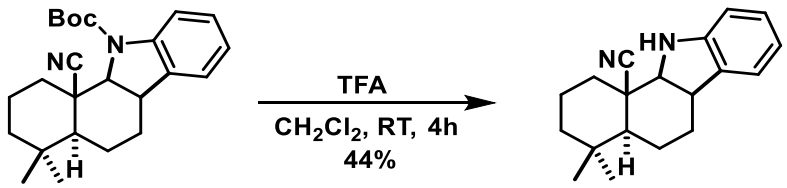

To a solution of indoline **2.6f** (30 mg, 0.079 mmol) in CH_2Cl_2 (1 mL) was added trifluoroacetic acid (100 μL, 1.3 mmol, ~16 equiv.). The mixture was stirred for 4 h at ambient temperature, then a satd. $NaHCO_{3(aq)}$ solution (2.0 mL) was added. The resulting biphasic mixture was vigorously stirred for 1h then the aqueous phase was extracted with CH_2Cl_2 (3 x 2 mL). The combined organic phases were washed with brine (3 mL), dried over Na_2SO_4, filtered and concentrated *in vacuo*. The resulting crude residue was directly purified via flash chromatography using a mixture of EtOAc/ hexanes (15:85) as eluent to give N-H indoline **S2.49** as a crystalline white solid (13 mg, 44%); **^{1}H NMR** (600 MHz, $CDCl_3$) δ 7.10 – 7.05 (m, 2H), 6.80 (t, *J* = 7.4 Hz, 1H), 6.69 (d, *J* = 7.7 Hz, 1H), 4.34 (s, 1H), 3.47 – 3.44 (m, 2H), 2.49 – 2.42 (m, 1H), 2.27 (d, *J* = 13.0 Hz, 1H), 1.90 (ddd,

J = 16.2, 11.3, 5.6 Hz, 1H), 1.84 – 1.72 (m, 2H), 1.64 – 1.49 (m, 3H), 1.27 (td, *J* = 13.2, 3.5 Hz, 1H), 1.20 (td, *J* = 13.5, 3.5 Hz, 1H), 1.00 (s, 3H), 1.00 – 0.97 (m, 1H), 0.95 (s, 3H); **^{13}C NMR** (151 MHz, $CDCl_3$) δ 150.7, 130.0, 128.0, 122.4, 122.3, 119.4, 109.6, 69.3, 48.2, 42.7, 41.2, 40.6, 38.0, 33.4, 32.2, 24.7, 20.7, 20.6, 19.0. **HRMS** (ES+) *m/z* calc'd for $C_{19}H_{24}N_2Na$ $[M + Na]^+$: 303.1936, found 303.1939.

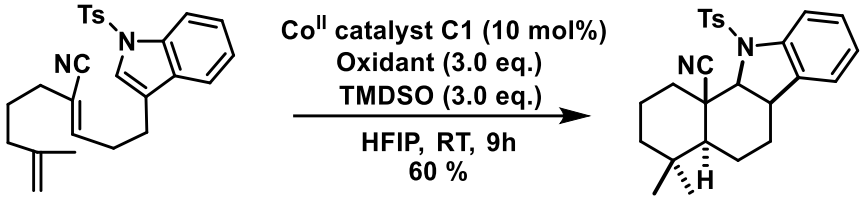

S2.16 (2.5g) **2.6g**

Prepared according to general procedure D, using α,β-unsaturated nitrile **S2.16** *(0.23 mmol), cobalt catalyst* **C1** *(0.023 mmol), 1-fluoro-2,4,6-trimethylpyridinium triflate (0.69 mmol), and 1,1,3,3-tetramethyldisiloxane (0.69 mmol)*. Yield: 60% of **2.6g** (60 mg, 0.14 mmol, white crystalline solid); R_f=0.15 (1:9 EtOAc/hexanes); **^{1}H NMR** (600 MHz, $CDCl_3$) δ 7.68 (d, *J* = 8.0 Hz, 1H), 7.48 (d, *J* = 7.7 Hz, 2H), 7.30 (t, *J* = 7.7 Hz, 1H), 7.16 (t, *J* = 7.5 Hz, 1H), 7.13 (d, *J* = 7.9 Hz, 2H), 6.97 (d, *J* = 7.4 Hz, 1H), 3.99 (d, *J* = 7.5 Hz, 1H), 2.78 (d, *J* = 13.8 Hz, 1H), 2.71 (t, *J* = 6.8 Hz, 1H), 2.35 (s, 3H), 2.26 (d, *J* = 15.1 Hz, 1H), 1.75 (q, *J* = 13.6 Hz, 1H), 1.70 – 1.61 (m, 3H), 1.50 (d, *J* = 13.4 Hz, 1H), 1.43 (td, *J* = 13.5, 3.0 Hz, 1H), 1.37 (q, *J* = 12.2 Hz, 1H), 1.22 (td, *J* = 13.3, 2.7 Hz, 1H), 0.97 (d, *J* = 11.8 Hz, 1H), 0.93 (s, 3H), 0.92 (s, 3H); **^{13}C NMR** (151 MHz, $CDCl_3$) δ 144.2, 142.9, 135.9, 135.8, 129.8, 128.5, 127.1, 126.3, 122.0, 121.2, 120.3, 72.2, 49.7, 43.1, 41.2, 39.5, 37.1, 33.5, 32.3, 24.4, 21.7, 20.6, 20.1, 18.9; **HRMS** (ES+) *m/z* calc'd for $C_{26}H_{30}N_2O_2SNa$ $[M + Na]^+$: 457.1926, found 457.1926.

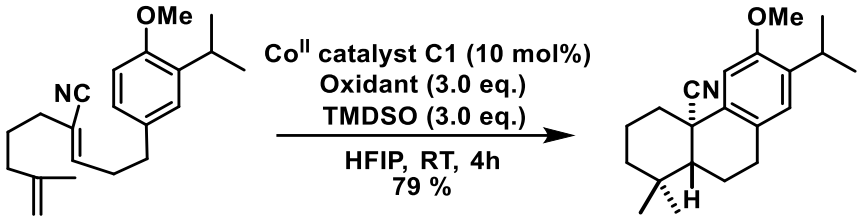

S2.14 (2.5h) **2.6h**

Prepared according to general procedure D, using α,β-unsaturated nitrile **S2.14** *(1.00 mmol), cobalt catalyst* **C1** *(0.10 mmol), 1-fluoro-2,4,6-trimethylpyridinium triflate (3.00 mmol), and 1,1,3,3-tetramethyldisiloxane (3.00 mmol).* Yield: 79% of **2.6h** (245 mg, 0.79 mmol, white crystalline solid, *spectral data were in accordance with that reported in the literature* [20]); R_f=0.20 (2:2.5:95.5 benzene/EtOAc/hexanes); **^{1}H NMR** (600 MHz, $CDCl_3$) δ 6.92 (s, 1H), 6.83 (s, 1H), 3.81 (s, 3H), 3.25 (sept, *J* = 6.9 Hz, 1H), 3.00 – 2.88 (m, 1H), 2.85 – 2.75 (m, 2H), 2.10 – 1.98 (m, 2H), 1.89 – 1.83 (m, 1H), 1.82 – 1.77 (m, 1H), 1.59 (dd, *J* = 13.5, 1.3 Hz, 1H), 1.52 (td, *J* = 13.3, 3.5 Hz, 1H), 1.37 (dd, *J* = 12.1, 1.7 Hz, 1H), 1.26 (td, *J* = 13.7, 3.7 Hz, 1H), 1.19 (t, *J* = 7.1 Hz, 6H), 1.16 (s, 3H), 1.01 (s, 3H); **^{13}C NMR** (151 MHz, $CDCl_3$) δ 155.63, 137.31, 135.70, 127.98, 127.35, 123.97, 107.22, 55.63, 50.65, 40.83, 40.26, 36.85, 33.76, 32.14, 29.77, 26.65, 22.73, 21.89, 20.121, 20.116; **HRMS** (ES+) *m/z* calc'd for $C_{21}H_{29}NONa$ $[M + Na]^+$: 334.2147, found 334.2153.

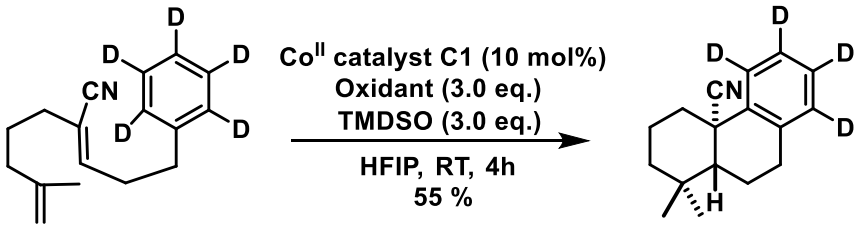

2.28 **2.29**

Prepared according to general procedure D, using α,β-unsaturated nitrile **2.28** *(0.53 mmol), cobalt catalyst* **C1** *(0.053 mmol), 1-fluoro-2,4,6-trimethylpyridinium triflate (1.60 mmol), and 1,1,3,3-tetramethyldisiloxane (1.60 mmol).* Yield: 55% of **2.29** (72 mg, 0.29 mmol, white crystalline solid); R_f=0.15 (1.5:98.5 EtOAc/hexanes- recrystallized from a mixture of

methanol/hexanes); **^{1}H NMR** (600 MHz, $CDCl_3$) δ 3.09 (ddd, *J* = 17.1, 6.0, 1.7 Hz, 1H), 2.95 (ddd, *J* = 18.6,12.0, 6.7 Hz, 1H), 2.89 (d, *J* = 13.1 Hz, 1H), 2.14 (dd, *J* = 13.4, 6.5 Hz, 1H), 2.08 (tt, *J* = 13.9, 3.3 Hz, 1H), 1.95 (ddd, *J* = 25.6, 12.2, 6.0 Hz, 1H), 1.89 – 1.82 (m, 1H), 1.66 (d, *J* = 13.5 Hz, 1H), 1.56 (td, *J* = 13.4, 3.5 Hz, 1H), 1.43 (dd, *J* = 12.1, 1.7 Hz, 1H), 1.32 (td, *J* = 13.6, 3.7 Hz, 1H), 1.22 (s, 3H), 1.07 (s, 3H); **^{13}C DEPTQ NMR** (151 MHz, $CDCl_3$) δ 137.9, 136.1, 129.4 (t, *J* = 24.0 Hz), 127.3 (t, *J* = 24.4 Hz), 126.1 (t, *J* = 24.8 Hz), 125.2 (t, *J* = 24.0 Hz), 123.6, 50.4, 40.7, 40.1, 36.7, 33.7, 32.0, 30.1, 21.5, 20.0, 20.0; **HRMS** (ES+) *m/z* calc'd for $C_{17}H_{17}D_4NNa$ $[M + Na]^+$: 266.1823, found 266.1826. *To quantify the extent of deuterium incorporation (~5% D_2), the purified samples were analyzed by isotope ratio mass spectrometry modeling (flow injection analysis)- see the attached spectra*.

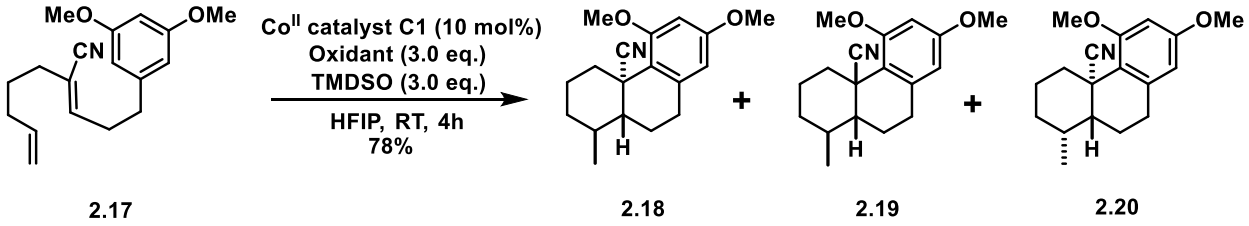

Prepared according to general procedure D, using α,β-unsaturated nitrile **2.17** *(0.31 mmol), cobalt catalyst* **C1** *(0.031 mmol), 1-fluoro-2,4,6-trimethylpyridinium triflate (0.92 mmol), and 1,1,3,3-tetramethyldisiloxane (0.92 mmol)*. Combined yield: 78% (69 mg, 0.24 mmol) - individual yields were determined from crude ^{1}H NMR spectra, using an internal standard (CH_2Br_2). Pure samples of each stereoisomer were obtained via extensive preparatory TLC (multiple developments using 5:1:4 benzene /chloroform /hexanes mixture as eluent).

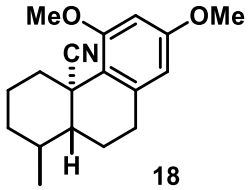

18

Stereoisomer **2.18**: white crystalline solid; R_f=0.15 (5:1:4 benzene/chloroform/hexanes); **^{1}H NMR** (600 MHz, $CDCl_3$) δ 6.33 (d, *J* = 2.5 Hz, 1H), 6.23 (d, *J* = 2.4 Hz, 1H), 3.85 (s, 3H), 3.78 (s, 3H), 3.32 (d, *J* = 13.1 Hz, 1H), 2.87 – 2.75 (m, 2H), 2.08 – 2.03 (m, 1H), 1.99 – 1.87 (m, 2H), 1.86 – 1.82 (m, 1H), 1.80 – 1.74 (m, 1H), 1.49 (ddd, *J* = 18.2, 12.7, 6.2 Hz, 1H), 1.26 – 1.22 (m, 1H), 1.21 – 1.17 (m, 1H), 1.07 (ddd, *J* = 24.9, 13.2, 4.4 Hz, 1H), 1.01 (d, *J* = 6.5 Hz, 3H); **^{13}C NMR** (151 MHz, $CDCl_3$) δ 160.2, 159.9, 140.3, 122.2, 117.6, 105.3, 97.8, 55.6, 55.4, 51.8, 42.3, 35.7, 34.7, 33.1, 32.1, 23.5, 22.7, 20.1; **HRMS** (ES+) *m/z* calc'd for $C_{18}H_{23}NO_2Na$ $[M + Na]^+$: 308.1627, found 308.1637.

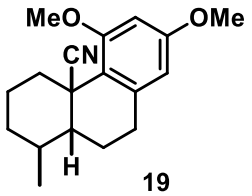

19

Stereoisomer **2.19**: white crystalline solid; R_f=0.13 (5:1:4 benzene/chloroform/hexanes); **^{1}H NMR** (600 MHz, $CDCl_3$) δ 6.35 (d, *J* = 2.4 Hz, 1H), 6.24 (d, *J* = 2.4 Hz, 1H), 3.88 (s, 3H), 3.78 (s, 3H), 2.85 – 2.74 (m, 2H), 2.43 (d, *J* = 13.9 Hz, 1H), 2.40 – 2.32 (m, 1H), 2.03 (d, *J* = 13.1 Hz, 1H), 1.85 – 1.75 (m, 2H), 1.72 – 1.66 (m, 1H), 1.60 – 1.54 (m, 1H), 1.52 – 1.49 (m, 1H), 1.46 (td, *J* = 13.8, 3.9 Hz, 1H), 1.13 (qd, *J* = 13.1, 3.9 Hz, 1H), 1.01 (d, *J* = 6.9 Hz, 3H); **^{13}C NMR** (151 MHz, $CDCl_3$) δ 159.8, 158.8, 138.4, 124.3, 118.3, 105.3, 97.9, 55.8, 55.4, 45.3, 40.1, 31.9, 30.9, 30.3, 28.5, 23.6, 19.8, 16.9; **HRMS** (ES+) *m/z* calc'd for $C_{18}H_{23}NO_2Na$ $[M + Na]^+$: 308.1627, found 308.1620.

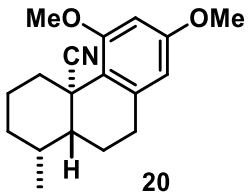

20

Stereoisomer **2.20**: white crystalline solid; R_f=0.14 (5:1:4 benzene/chloroform/hexanes); **^{1}H NMR** (600 MHz, $CDCl_3$) δ 6.31 (d, *J* = 2.5 Hz, 1H), 6.22 (d, *J* = 2.5 Hz, 1H), 3.84 (s, 3H), 3.77 (s, 3H), 3.44 (d, *J* = 13.3 Hz, 1H), 2.92 (ddd, *J* = 18.2, 12.6, 5.9 Hz, 1H), 2.82 (dd, *J* = 16.5, 4.3 Hz, 1H), 2.14 – 2.07 (m, 1H), 2.07 – 2.00 (m, 2H), 1.98 – 1.95 (m, 1H), 1.72 (ddd, *J* = 12.3, 4.5, 1.4 Hz, 1H), 1.69 – 1.61 (m, 3H), 1.25 ([*overlapping with silicone grease signal*] d, *J* = 6.5 Hz, 3H), 1.18 (td, *J* = 13.4, 3.0 Hz, 1H); **^{13}C NMR** (151 MHz, $CDCl_3$) δ 160.2, 159.8, 139.9, 123.7, 118.9, 105.4, 97.7, 55.5, 55.3, 47.1, 38.3, 35.3, 34.4, 32.6, 32.2, 26.3, 19.3, 13.7. **HRMS** (ES+) *m/z* calc'd for $C_{18}H_{23}NO_2Na$ $[M + Na]^+$: 308.1627, found 308.1628.

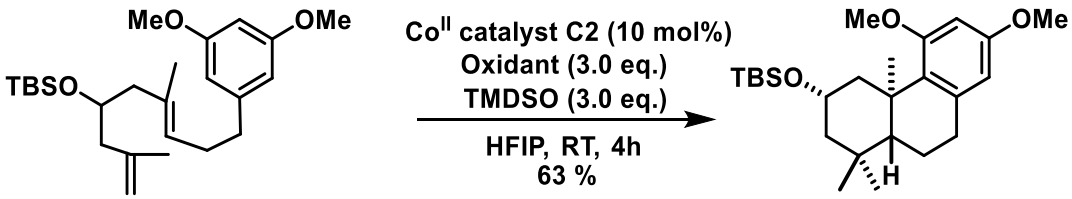

S2.42 2.8a

Prepared according to general procedure D, using terminal alkene **S2.42** *(0.12 mmol), cobalt catalyst* **C2** *(0.012 mmol), 1-fluoro-2,4,6-trimethylpyridinium triflate (0.36 mmol), and 1,1,3,3-tetramethyldisiloxane (0.36 mmol)*. Yield: 63% of **2.8a** (32 mg, 0.08 mmol, white solid); R_f=0.20 (2:98 EtOAc/hexanes); **^{1}H NMR** (500 MHz, $CDCl_3$) δ 6.28 (d, *J* = 2.5 Hz, 1H), 6.19 (d, *J* = 2.4 Hz, 1H), 4.01 (tt, *J* = 11.3, 4.1 Hz, 1H), 3.77 (s, 3H), 3.76 (s, 3H), 3.45 – 3.34 (m, 1H), 2.89 – 2.80 (m, 2H), 1.83 – 1.76 (m, 1H), 1.75 – 1.68 (m, 1H), 1.55 – 1.49 (m, 1H), 1.29 (s, 3H), 1.27 – 1.21 (m, 2H), 1.15 – 1.08 (m, 1H), 0.99 (s, 3H), 0.95 (s, 3H), 0.94 (s, 9H), 0.12 (s, 6H); **^{13}C NMR** (126

MHz, $CDCl_3$) δ 159.6, 158.0, 138.6, 129.8, 105.1, 97.7, 66.5, 55.2, 55.1, 52.9, 51.1, 46.1, 40.4, 34.8, 34.2, 33.6, 26.3(3C), 23.1, 20.9, 18.8, 18.6, –4.3(2C); **HRMS** (ES+) *m/z* calc'd for $C_{25}H_{42}O_3SiNa$ $[M + Na]^+$: 441.2801, found 441.2818.

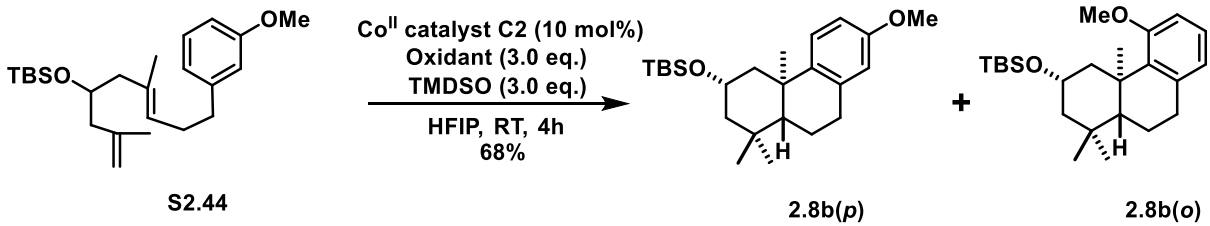

S2.44 2.8b(*p*) 2.8b(*o*)

Prepared according to general procedure D, using terminal alkene **S2.44** *(0.13 mmol), cobalt catalyst* **C2** *(0.013 mmol), 1-fluoro-2,4,6-trimethylpyridinium triflate (0.39 mmol), and 1,1,3,3-tetramethyldisiloxane (0.39 mmol)*. Combined yield: 68%; *p*-regioisomer **2.8b(*p*)** : Yield: 41% (21 mg, 0.053 mmol, white solid); R_f=0.14 (5:1:94 benzene/EtOAc/hexanes); **^{1}H NMR** (600 MHz, $CDCl_3$) δ 7.17 (d, *J* = 8.7 Hz, 1H), 6.70 (dd, *J* = 8.7, 2.8 Hz, 1H), 6.58 (d, *J* = 2.7 Hz, 1H), 4.03 (tt, *J* = 11.3, 4.0 Hz, 1H), 3.76 (s, 3H), 2.93 (dd, *J* = 17.2, 6.6 Hz, 1H), 2.89 – 2.81 (m, 1H), 2.44 (ddd, *J* = 12.2, 3.6, 2.2 Hz, 1H), 1.87 (dd, *J* = 13.3, 7.7 Hz, 1H), 1.75 – 1.70 (m, 1H), 1.70 – 1.64 (m, 1H), 1.38 (t, *J* = 11.7 Hz, 1H), 1.30 (dd, *J* = 12.6, 2.3 Hz, 1H), 1.26 (t, *J* = 12.1 Hz, 1H), 1.18 (s, 3H), 0.99 (s, 3H), 0.96 (s, 3H), 0.94 (s, 9H), 0.13 (s, 3H), 0.12 (s, 3H); **^{13}C NMR** (151 MHz, $CDCl_3$) δ 157.3, 142.1, 136.4, 125.4, 113.4, 112.0, 66.4, 55.3, 51.3, 49.9, 48.4, 39.0, 34.8, 33.5, 30.6, 26.2, 26.0, 22.7, 18.9, 18.5, –4.30, –4.33; **HRMS** (ES+) *m/z* calc'd for $C_{24}H_{40}O_2SiNa$ $[M + Na]^+$: 411.2695, found 411.2693.

o-regioisomer **2.8b(*o*)**: Yield: 27% (14 mg, 0.035 mmol, white solid); R_f=0.15 (5:1:94 benzene/EtOAc/hexanes); **^{1}H NMR** (600 MHz, $CDCl_3$) δ 7.05 (t, *J* = 7.8 Hz, 1H), 6.70 – 6.65 (m, 2H), 4.02 (tt, *J* = 11.3, 4.2 Hz, 1H), 3.79 (s, 3H), 3.45 (ddd, *J* = 12.6, 3.7, 2.2 Hz, 1H), 2.88-2.66

(m, 2H), 1.83 – 1.77 (m, 1H), 1.72 (ddd, *J* = 12.5, 4.2, 2.2 Hz, 1H), 1.32 (s, 3H), 1.27 – 1.22 (m, 3H), 1.15 (t, *J* = 12.0 Hz, 1H), 1.00 (s, 3H), 0.96 (s, 3H), 0.94 (s, 9H), 0.12 (s, 6H); **^{13}C NMR** (151 MHz, $CDCl_3$) δ 158.6, 138.0, 136.9, 126.3, 122.4, 109.3, 66.5, 55.1, 52.7, 51.0, 45.8, 40.9, 34.8, 34.2, 33.1, 26.3(3C), 23.2, 20.7, 18.8, 18.7, –4.3(2C); **HRMS** (ES+) *m/z* calc'd for $C_{24}H_{40}O_2SiNa$ $[M + Na]^+$: 411.2695, found 411.2697.

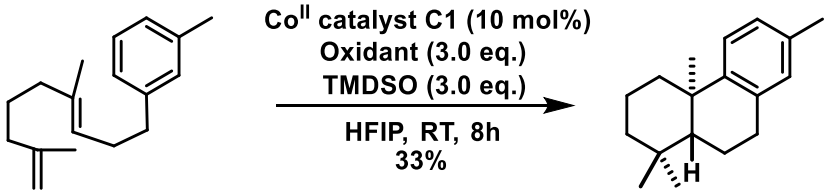

S2.30 (2.7c) **2.8c**

Prepared according to general procedure D, using terminal alkene **S2.30** *(0.21 mmol), cobalt catalyst* **C1***(0.021 mmol), 1-fluoro-2,4,6-trimethylpyridinium triflate (0.62 mmol), and 1,1,3,3-tetramethyldisiloxane (0.62 mmol)*. Yield: 33% of **2.8c**(17 mg, 0.07 mmol, white solid, ~80% purity by ^{1}H NMR); R_f=0.64 (hexanes); *spectral data were in accordance with that reported in the literature*[59]: **^{1}H NMR** (500 MHz, $CDCl_3$) δ 7.15 (d, *J* = 8.0 Hz, 1H), 6.94 (d, *J* = 8.3 Hz, 1H), 6.86 (s, 1H), 2.90 (dd, *J* = 16.4, 6.5 Hz, 1H), 2.86 – 2.78 (m, 1H), 2.27 (s, 4H), 1.90 – 1.83 (m, 1H), 1.77 – 1.72 (m, 1H), 1.71 – 1.66 (m, 1H), 1.63 – 1.57 (m, 2H), 1.48 (d, *J* = 13.3 Hz, 1H), 1.38 (td, *J* = 13.3, 3.7 Hz, 1H), 1.32 (dd, *J* = 12.5, 2.3 Hz, 1H), 1.23 (dd, *J* = 13.7, 3.8 Hz, 1H), 1.18 (s, 3H), 0.94 (s, 3H), 0.93 (s, 3H); **^{13}C NMR** (151 MHz, $CDCl_3$) δ 147.5, 135.3, 134.7, 129.7, 126.6, 124.5, 77.4, 77.2, 77.0, 50.7, 41.9, 39.1, 37.6, 33.6, 33.5, 30.5, 25.0, 21.8, 20.9, 19.5, 19.2.

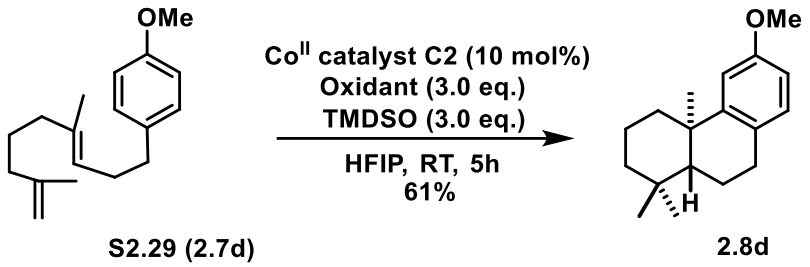

S2.29 (2.7d) 2.8d

Prepared according to general procedure D, using terminal alkene **S2.29** *(0.39 mmol), cobalt catalyst* **C2** *(0.039 mmol), 1-fluoro-2,4,6-trimethylpyridinium triflate (1.16 mmol), and 1,1,3,3-tetramethyldisiloxane (1.16 mmol).* Yield: 61% of **2.8d** (61 mg, 0.24 mmol, white crystalline solid, *spectral data were in accordance with that reported in the literature*[60]); R_f=0.15 (1:99 EtOAc/hexanes); **^{1}H NMR** (600 MHz, $CDCl_3$) δ 6.96 (d, *J* = 8.4 Hz, 1H), 6.82 (d, *J* = 2.6 Hz, 1H), 6.66 (dd, *J* = 8.3, 2.7 Hz, 1H), 3.78 (s, 3H), 2.89 (dd, *J* = 16.4, 6.4 Hz, 1H), 2.84 – 2.73 (m, 1H), 2.25 (d, *J* = 12.7 Hz, 1H), 1.87 (dd, *J* = 13.2, 7.6 Hz, 1H), 1.80 – 1.71 (m, 1H), 1.70 – 1.65 (m, 1H), 1.64 – 1.59 (m, 1H), 1.48 (dd, *J* = 13.2, 1.2 Hz, 1H), 1.41 (td, *J* = 12.9, 3.5 Hz, 1H), 1.33 (dd, *J* = 12.5, 2.3 Hz, 1H), 1.22 (td, *J* = 13.5, 4.0 Hz, 1H), 1.19 (s, 3H), 0.95 (s, 3H), 0.93 (s, 3H); **^{13}C NMR** (151 MHz, $CDCl_3$) δ 157.8, 151.6, 129.9, 127.6, 110.8, 110.3, 55.4, 50.5, 41.8, 39.0, 38.2, 33.6, 33.5, 29.7, 24.9, 21.8, 19.5, 19.3; **HRMS** (ES+) *m/z* calc'd for $C_{18}H_{26}O_3$ $[M]^+$: 258.19484, found 258.1978.

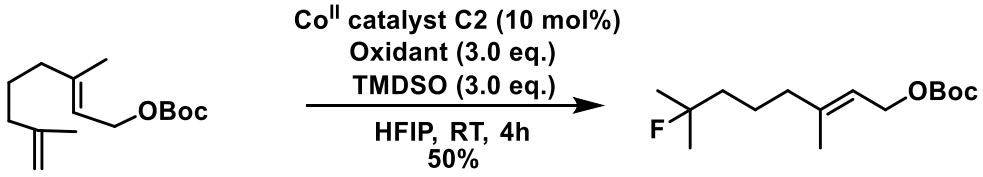

2.22 2.24

Prepared according to general procedure D, using terminal alkene **2.22** *(0.20 mmol), cobalt catalyst* **C2** *(0.020 mmol), 1-fluoro-2,4,6-trimethylpyridinium triflate (0.60 mmol), and 1,1,3,3-tetramethyldisiloxane (0.60 mmol).* Yield: 50% of **2.24** (25 mg, 0.10 mmol, clear colorless oil);

R_f=0.40 (1:9 EtOAc/hexanes); *Note: The sample contained other regio- and sterioisomers, which could not be separated (~70% purity).* **^{1}H NMR** (600 MHz, $CDCl_3$) δ 5.37 (t, *J* = 7.1 Hz, 1H), 4.58 (d, *J* = 7.1 Hz, 2H), 2.04 (t, *J* = 7.0 Hz, 2H), 1.70 (s, 3H), 1.59 – 1.55 (m, 2H), 1.55 – 1.50 (m, 2H), 1.48 (s, 9H), 1.33 (d, *J* = 21.4 Hz, 6H); **^{13}C NMR** (151 MHz, $CDCl_3$) δ 153.8, 142.4, 118.6, 95.7 (d, *J* = 164.6 Hz), 82.0, 63.8, 41.0 (d, *J* = 23.0 Hz), 39.7, 27.9, 26.8 (d, *J* = 24.9 Hz), 21.93, 21.91(d, *J* = 5.1 Hz), 16.4; **HRMS** (ES+) *m/z* calc'd for $C_{15}H_{27}FO_3Na$ $[M + Na]^+$: 297.1841, found 297.1836.

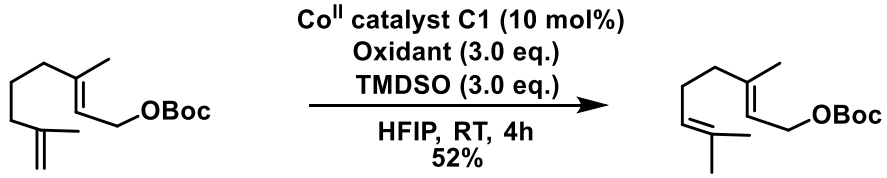

2.22 **2.25**

Prepared according to general procedure D, using terminal alkene **2.22** *(0.20 mmol), cobalt catalyst* **C1** *(0.020 mmol), 1-fluoro-2,4,6-trimethylpyridinium triflate (0.60 mmol), and 1,1,3,3-tetramethyldisiloxane (0.60 mmol).* Yield: 52% of **2.25** (26 mg, 0.10 mmol, clear colorless oil); R_f=0.40 (1:9 EtOAc/hexanes); *spectral data were in accordance with that reported in the literature*[61] ; **^{1}H NMR** (600 MHz, $CDCl_3$) δ 5.37 (td, *J* = 7.1, 1.1 Hz, 1H), 5.08 (t, *J* = 6.8 Hz, 1H), 4.59 (d, *J* = 7.1 Hz, 2H), 2.13 – 2.06 (m, 2H), 2.06 – 2.01 (m, 2H), 1.70 (s, 3H), 1.68 (s, 3H), 1.59 (s, 3H), 1.48 (s, 9H); **^{13}C NMR** (151 MHz, $CDCl_3$) δ 153.8, 142.7, 132.0, 123.9, 118.2, 82.0, 63.9, 39.7, 28.0, 26.4, 25.8, 17.8, 16.7; **HRMS** (ES+) *m/z* calc'd for $C_{15}H_{26}O_3Na$ $[M + Na]^+$: 277.1780, found 277.1784.

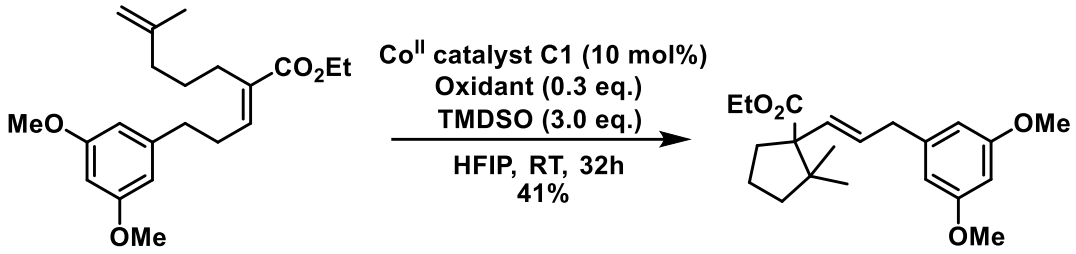

2.14-*E* **2.16**

Prepared according to general procedure D, using α,β-unsaturated ethyl ester **2.14**–***E*** *(0.14 mmol), cobalt catalyst* **C1** *(0.014 mmol), 1-fluoro-2,4,6-trimethylpyridinium triflate (0.05 mmol), and 1,1,3,3-tetramethyldisiloxane (0.42 mmol)*. Yield: 41% of **2.16** (21 mg, 0.06 mmol, clear colorless oil); R_f=0.15 (2:98 EtOAc/hexanes); **^{1}H NMR** (500 MHz, $CDCl_3$) δ 6.33 (d, *J* = 1.9 Hz, 2H), 6.31 (t, *J* = 2.1 Hz, 1H), 5.90 (d, *J* = 15.7 Hz, 1H), 5.62 – 5.50 (m, 1H), 4.19 – 4.09 (m, 2H), 3.76 (s, 6H), 3.34 (d, *J* = 6.9 Hz, 2H), 2.44 – 2.35 (m, 1H), 1.98 – 1.91 (m, 1H), 1.82 – 1.71 (m, 1H), 1.67 – 1.57 (m, 2H), 1.54 – 1.48 (m, 1H), 1.27 (t, *J* = 7.1 Hz, 3H), 1.06 (s, 3H), 0.94 (s, 3H); **^{13}C NMR** (126 MHz, $CDCl_3$) δ 175.0, 160.9, 143.3, 133.1, 127.8, 106.6, 98.3, 60.9, 60.4, 55.4, 46.1, 39.7, 39.5, 30.7, 25.3, 24.6, 19.9, 14.4; **HRMS** (ES+) *m/z* calc'd for $C_{21}H_{30}O_4Na$ $[M + Na]^+$: 369.2042, found 369.2045.

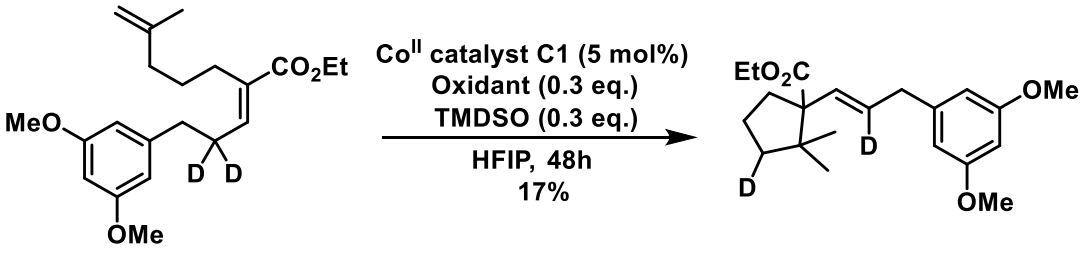

2.14-*E*-d_2 **2.16-d_2**

Prepared according to general procedure D, using α,β-unsaturated ethyl ester **2.14–*E*–d_2** *(0.066 mmol), cobalt catalyst* **C1** *(0.0033 mmol), 1-fluoro-2,4,6-trimethylpyridinium triflate (0.02 mmol), and 1,1,3,3-tetramethyldisiloxane (0.020 mmol). Note: the reaction time was 48h. The crude reaction mixture contained a considerable amount of isomerized starting material*. Yield: 17% of

2.16–*d*$_2$ (4 mg, 0.011 mmol, clear colorless oil); R_f=0.15 (2:98 EtOAc/hexanes – purified via PTLC); **^{1}H NMR** (600 MHz, $CDCl_3$) δ 6.33 (d, *J* = 2.0 Hz, 2H), 6.31 (t, *J* = 2.0 Hz, 1H), 5.90 (s, 1H), 4.17 – 4.09 (m, 2H), 3.76 (s, 6H), 3.34 (s, 2H), 2.47 – 2.32 (m, 1H), 1.98 – 1.90 (m, 1H), 1.80 – 1.72 (m, 1H), 1.65 – 1.58 (m, 2H), 1.53 – 1.47 (m, 1H), 1.27 (t, *J* = 7.1 Hz, 3H), 1.06 (s, 3H), 0.94 (s, 3H); **^{13}C NMR** (151 MHz, $CDCl_3$) δ 175.0, 160.9 (2C), 143.3, 132.9, 127.5 (t, *J* = 23.0 Hz), 106.6 (2C), 98.3, 60.9, 60.4, 55.4 (2C), 46.1, 39.6, 39.4, 30.6, 25.3, 24.6, 19.9, 14.4; **HRMS** (ES+) *m/z* calc'd for $C_{21}H_{28}D_2O_4Na$ $[M + Na]^+$: 371.2167, found 371.2175. *To quantify the extent of deuterium incorporation (~38% D_2), the purified samples were analyzed by isotope ratio mass spectrometry modeling (flow injection analysis)- see the attached spectra*.

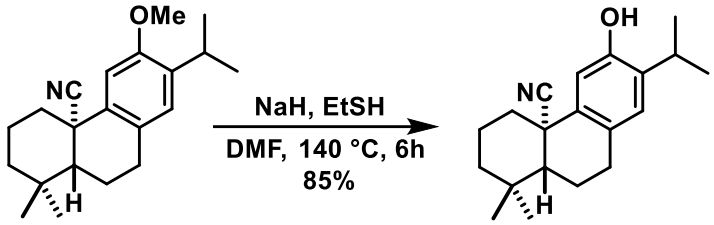

2.6h **S2.50**

To a cooled (4 °C) suspension of sodium hydride (60% in mineral oil, 167 mg, 4.18 mmol, 10 equiv.) in DMF (2.0 mL), ethanethiol (0.6 mL, 8.36 mmol, 20 equiv.) was added dropwise. The resulting mixture was stirred for 30 min. while warming to ambient temperature, then a solution of **2.6h (**130 mg, 0.42 mmol, 1.0 equiv.) in DMF (1.0 mL) was added and the mixture was heated to 140 °C. After stirring for 6 hours, the mixture was cooled to ambient temperature, diluted with Et_2O (20 mL) and a solution of 2N $HCl_{(aq.)}$ (5 mL) was added. After stirring vigorously for 15 min., the organic phase was washed with DI H_2O (3 x 10 mL), then brine (10 mL), dried over Na_2SO_4, filtered and concentrated *in vacuo.* The crude residue was purified via flash column chromatography (EtOAc/ hexanes 15:85, R_f= 0.34) to give **S2.50** as a white solid (106 mg, 0.355 mmol, 85 % yield); **^{1}H NMR** (600 MHz, $CDCl_3$) δ 6.90 (s, 1H), 6.80 (s, 1H), 5.15 (s (broad), 1H),

3.15 (hept, *J* = 6.9 Hz, 1H), 2.93 (dd, *J* = 16.7, 4.9 Hz, 1H), 2.84 – 2.75 (m, 1H), 2.69 (d, *J* = 13.1 Hz, 1H), 2.06 (dd, *J* = 13.4, 6.4 Hz, 1H), 2.00 (qt, *J* = 13.9, 3.2 Hz, 1H), 1.83 (qd, *J* = 12.3, 5.9 Hz, 1H), 1.79 – 1.74 (m, 1H), 1.58 (d, *J* = 13.4 Hz, 1H), 1.48 (td, *J* = 13.4, 3.5 Hz, 1H), 1.35 (dd, *J* = 12.1, 1.5 Hz, 1H), 1.23 (d, *J* = 6.9 Hz, 3H), 1.21 (d, *J* = 6.9 Hz, 3H), 1.15 (s, 3H), 1.00 (s, 3H); **^{13}C DEPTQ NMR** (151 MHz, $CDCl_3$) δ 151.7, 135.8, 135.0, 128.1, 127.6, 123.9, 112.1, 50.5, 40.8, 40.0, 36.8, 33.7, 32.1, 29.7, 27.0, 22.7, 22.6, 21.9, 20.08, 20.07; **HRMS** (ES+) *m/z* calc'd for $C_{20}H_{27}NONa$ $[M + Na]^+$: 320.1990, found 320.1992.

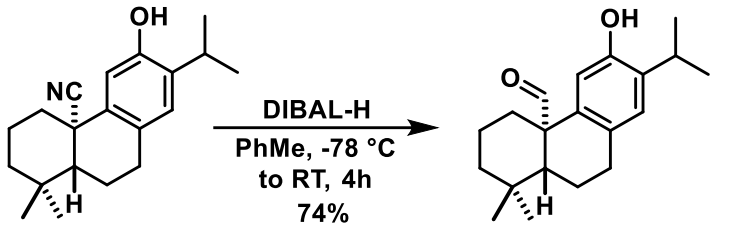

S2.50 **S2.51** ***pisiferal***

To a cooled (–78 °C) solution of nitrile **S2.50** (8 mg, 0.027 mmol, 1 equiv.) in toluene (0.5 mL), a 1.0 M solution of diisobutylaluminum hydride (0.8 mL, 0.80 mmol, 30 equiv.) was added dropwise. The resulting mixture was stirred at –78 °C for 2 hours, warmed to ambient temperature, quenched with a saturated aqueous solution of sodium potassium tartrate (2.0 mL) and stirred vigorously for 1 h. The aqueous phase was extracted with EtOAc (3 x 3 mL), then the combined organic extracts were washed with brine (5 mL), dried over Na_2SO_4, filtered and concentrated *in vacuo.* The resulting crude residue was purified via flash column chromatography on SiO_2, using a mixture of EtOAc/ hexanes (6:94) as eluent to give **S2.51** (+/– ***pisiferal***) as a white solid (6 mg, 0.020 mmol, 74% yield, *spectral data are in agreement with that reported in the literature*[62]); **^{1}H NMR** (600 MHz, $CDCl_3$) δ 9.90 (s, 1H), 6.92 (s, 1H), 6.60 (s, 1H), 5.40 (s (broad), 1H), 3.16 (hept, *J* = 6.8 Hz, 1H), 2.99 – 2.85 (m, 3H), 2.14 – 2.01 (m, 2H), 1.76 – 1.57 (m, 3H), 1.46 (d, *J* = 13.2 Hz, 1H), 1.27 (td, *J* = 13.5, 4.3 Hz, 1H), 1.22 (d, *J* = 6.9 Hz, 3H), 1.22 (d, *J* = 6.8 Hz, 3H), 1.20 –

1.16 (m, 1H), 1.00 (s, 3H), 0.83 (s, 3H); **^{13}C DEPTQ NMR** (151 MHz, $CDCl_3$) δ 201.5, 152.0, 134.5, 133.2, 130.4, 127.4, 113.9, 53.4, 51.9, 41.4, 34.0, 32.7, 31.7, 30.2, 27.0, 22.7, 22.5, 20.7, 19.7, 18.5; **HRMS** (ES+) *m/z* calc'd for $C_{20}H_{27}O_2$ $[M - H]^-$: 299.2011, found 299.2023.

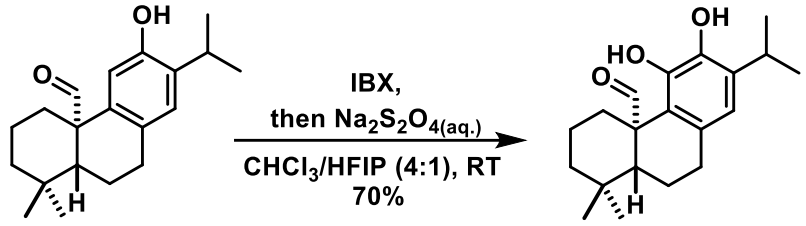

S2.51 ***carnosaldehyde***

To a solution of **S2.51** (8 mg, 0.027 mmol, 1 equiv.) in a mixture of $CHCl_3$ and HFIP (4:1, 0.5 mL) was added 2-Iodoxybenzoic acid (14 mg, 0.049 mmol, 1.5 equiv.). The resulting suspension was stirred in the dark for 3 hours or until **S2.51** was consumed as determined via TLC. Then, a saturated solution of $Na_2S_2O_4$(aq.) (2.0 mL) was added and the biphasic mixture was stirred vigorously for 3 hours. The aqueous phase was extracted with $CHCl_3$ (3 x 3.0 mL), then the combined organic extracts were washed with satd. $NaHCO_{3(aq)}$ (5.0 mL), brine (5.0 mL), dried over Na_2SO_4, filtered and concentrated *in vacuo.* The resulting crude residue was purified via flash column chromatography on SiO_2, using a mixture of EtOAc/ hexanes (7:93) as eluent to give +/- ***carnosaldehyde*** as a white solid (6 mg, 0.019 mmol, 70% yield, *spectral data are in agreement with that reported in the literature- only ^{1}H NMR data[22]is known*); **^{1}H NMR** (600 MHz, $CDCl_3$) δ 9.90 (s, 1H), 7.13 (s, 1H), 6.60 (s, 1H), 5.78 (s, 1H), 3.28 – 3.19 (m, 2H), 2.87 (dd, *J* = 8.5, 3.5 Hz, 2H), 2.03 (d, *J* = 13.3 Hz, 1H), 1.86 (tt, *J* = 13.2, 8.9 Hz, 1H), 1.62 (d, *J* = 12.1 Hz, 1H), 1.60 – 1.52 (m, 2H), 1.48 (d, *J* = 13.4 Hz, 1H), 1.33 (td, *J* = 13.1, 4.9 Hz, 1H), 1.21 (d, *J* = 6.9 Hz, 6H), 1.14 (td, *J* = 13.0, 3.1 Hz, 1H), 1.04 (s, 3H), 0.90 (s, 3H); **^{13}C DEPTQ NMR** (151 MHz, $CDCl_3$) δ 203.7, 143.4, 142.5, 134.7, 130.1, 119.5, 116.4, 116.3, 54.1, 53.1, 41.5, 34.4, 32.0, 31.7, 30.6,

27.3, 22.5, 22.3, 21.7, 19.8, 19.0; **HRMS** (ES+) *m/z* calc'd for $C_{20}H_{28}O_3$ $[M - H]^-$: 315.1960, found 315.1950.

Table 2. 2: Comparison table of ^1H NMR data [δ_H (J, Hz)] for natural[22] and synthetic carnosaldehyde:

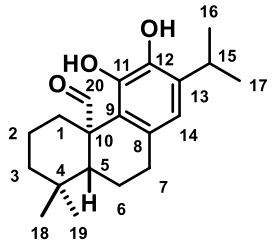

Note: some signals have been reassigned based on 2D NMR data (highlighted in green). Aside from minor impurities in the natural sample, the spectra are identical. *Overlapping signals.

^1H Signal	natural carnosaldehyde	synthetic carnosaldehyde
1α	1.13 m	1.14 td (13.0, 3.1)
1β	3.22 m*	3.28 – 3.19 m*
2α	1.48 – 1.59 m*	1.60 – 1.52 m*
2β	1.48 – 1.59 m*	1.60 – 1.52 m*
3α	1.15 – 1.36 m*	1.33 td (13.1, 4.9)
3β	1.15 – 1.36 m*	1.48 d, (13.4)
5	1.62 dd (12.7, 1.7)	1.62 d (12.1)
6α	2.03 m	1.86 tt, (13.2, 8.9)
6β	1.86 tt (13.2, 8.7)	2.03 d (13.3)
7α	2.87 dd (8.5, 3.6)	2.87 dd (8.5, 3.5)
7β	2.87 dd (8.5, 3.6)	2.87 dd (8.5, 3.5)
14	6.60 s	6.60 s
15	3.23 m*	3.28 – 3.19 m*
16	1.21 d (6.9)	1.21 d (6.9)
17	1.21 d (6.9)	1.21 d (6.9)
18	1.04 s	1.04 s
19	0.9 s	0.90 s

20	9.9 d (1.5)	9.90 s
11-OH	7.13 s	7.13 s
12-OH	5.78 s	5.78 s

2.7 Notes and References

(1) For an excellent review, see: Yoder, R. A.; Johnston, J. N. *Chem. Rev.* **2005**, *105*, 4730–4756.

(2) For representative pioneering achievements, see: a) Stork, G.; Burgstahler, A. W. *J. Am. Chem. Soc.* **1955**, *77*, 5068–5077; b) Eschenmoser, A.; Ruzicka, L.; Jeger, O.; Arigoni, D. *Helv. Chim. Acta* **1955**, *38*, 1890–1904; c) Johnson, W. S. *Acc. Chem. Res.* **1968**, *1*, 1–8; d) van Tamelen, E. E.; Willet, J.; Schwartz, M.; Nadeau, R. *J. Am. Chem. Soc.* **1966**, *88*, 5937–5938.

(3) For selected examples of radical polycyclizations that mirror the biomimetic cationic reactions of the type described in this chapter, see: a) Rendler, S.; MacMillan, D. W. C. *J. Am. Chem. Soc.* **2010**, *132*, 5027–5029; b) Barrero, A. F.; Cuerva, J. M.; Herrador, M. M.; Valdivia, M. V. *J. Org. Chem.* **2001**, *66*, 4074–4078; c) Chen, L.; Gill, G. B.; Pattenden, G.; Simonian, H. *J. Chem. Soc., Perkin Trans. 1* **1996**, 31–43; d) Zoretic, P. A.; Fang, H.; Ribeiro, A. A. *J. Org. Chem.* **1998**, *63*, 7213–7217; e) Snider, B. B.; Mohan, R.; Kates, S. A. *J. Org. Chem.* **1985**, *50*, 3659–3661; f) Breslow, R.; Olin, S. S.; Groves, J. T. *Tetrahedron Lett.* **1968**, *9*, 1837–1840.

(4) For selected examples of organometallic polycyclizations that mirror biomimetic cationic reactions described in this chapter, see: a) Mullen, C. A.; Gagné, M. R. *J. Am. Chem. Soc.* **2007**, *129*, 11880–11881; b) Schafroth, M. A.; Sarlah, D.; Krautwald, S.; Carreira, E. M. *J. Am. Chem. Soc.* **2012**, *134*, 20276–20278.

(5) a) Atta-ur-Rahman; Iqbal Choudhary, M. *Nat. Prod. Rep.* **1999**, *16*, 619–635; b) Wang, F.-P.; Chen, Q.-H.; Liu, X.-Y. *Nat. Prod. Rep.* **2010**, *27*, 529–570.

(6) a) Chen, K.; Shi, Q.; Fujioka, T.; Zhang, D.-C.; Hu, C.-Q.; Jin, J.-Q.; Kilkuskie, R. E.; Lee, K.-H. *J. Nat. Prod.* **1992**, *55*, 88–92; b) Chen, K.; Shi, Q.; Fujioka, T.; Nakano, T.; Hu, C.-Q.; Jin, J.-Q.; Kilkuskie, R. E.; Lee, K.-H. *Biorg. Med. Chem.* **1995**, *3*, 1345–1348.

(7) Michalak, S. E.; Nam, S.; Kwon, D. M.; Horne, D. A.; Vanderwal, C. D. *J. Am. Chem. Soc.* **2019**, *141*, 9202–9206.

(8) Zhou, S.; Guo, R.; Yang, P.; Li, A. *J. Am. Chem. Soc.* **2018**, *140*, 9025–9029.

(9) Liu, J.; Ma, D. *Angew. Chem. Int. Ed.* **2018**, *57*, 6676–6680.

(10) Crossley, S. W. M.; Obradors, C.; Martinez, R. M.; Shenvi, R. A. *Chem. Rev.* **2016**, *116*, 8912–9000.

(11) a) Shigehisa, H.; Nishi, E.; Fujisawa, M.; Hiroya, K. *Org. Lett.* **2013**, *15*, 5158–5161; b) Shigehisa, H.; Koseki, N.; Shimizu, N.; Fujisawa, M.; Niitsu, M.; Hiroya, K. *J. Am. Chem. Soc.* **2014**, *136*, 13534–13537; c) Shigehisa, H.; Hayashi, M.; Ohkawa, H.; Suzuki, T.; Okayasu, H.; Mukai, M.; Yamazaki, A.; Kawai, R.; Kikuchi, H.; Satoh, Y.; Fukuyama, A.; Hiroya, K. *J. Am. Chem. Soc.* **2016**, *138*, 10597–10604; d) Shigehisa, H.; Ano, T.; Honma, H.; Ebisawa, K.; Hiroya, K. *Org. Lett.* **2016**, *18*, 3622–3625; e) Shigehisa, H. *Chem. Pharm. Bull.* **2018**, *66*, 339–346.

(12) Pronin and colleagues have recently used this catalytic system to convert allylic alcohols into either semi-pinacol or epoxide products, the latter with control of enantioselectivity. See: a) Touney, E. E.; Foy, N. J.; Pronin, S. V. *J. Am. Chem. Soc.* **2018**, *140*, 16982–16987; b) Discolo, C. A.; Touney, E. E.; Pronin, S. V. *J. Am. Chem. Soc.* **2019**, *141*, 17527–17532.

(13) Dai, M.; Krauss, I. J.; Danishefsky, S. J. *J. Org. Chem.* **2008**, *73*, 9576–9583.

(14) Obradors, C.; Martinez, R. M.; Shenvi, R. A. *J. Am. Chem. Soc.* **2016**, *138*, 4962–4971.

(15) Crossley, S. W. M.; Barabé, F.; Shenvi, R. A. *J. Am. Chem. Soc.* **2014**, *136*, 16788–16791.

(16) Crossley, S. W. M.; Martinez, R. M.; Guevara-Zuluaga, S.; Shenvi, R. A. *Org. Lett.* **2016**, *18*, 2620–2623.

(17) a) Lo, J. C.; Yabe, Y.; Baran, P. S. *J. Am. Chem. Soc.* **2014**, *136*, 1304–1307; b) Lo, J. C.; Gui, J.; Yabe, Y.; Pan, C.-M.; Baran, P. S. *Nature* **2014**, *516*, 343–348.

(18) Giese, B. *Angew. Chem. Int. Ed. Eng.* **1983**, *22*, 753–764.

(19) a) Deng, H.; Cao, W.; Liu, R.; Zhang, Y.; Liu, B. *Angew. Chem. Int. Ed.* **2017**, *56*, 5849–5852; b) Cao, W.; Deng, H.; Sun, Y.; Liu, B.; Qin, S. *Chem. Eur. J.* **2018**, *24*, 9120–9129.

(20) Kametani, T.; Kondoh, H.; Tsubuki, M.; Honda, T. *J. Chem. Soc., Perkin Trans. 1* **1990**, 5–10.

(21) González, M. A. *Nat. Prod. Rep.* **2015**, *32*, 684–704.

(22) Fischedick, J. T.; Standiford, M.; Johnson, D. A.; Johnson, J. A. *Biorg. Med. Chem.* **2013**, *21*, 2618–2622.

(23) Substrates **2.7c–g** were used as an 89:11 mixture of the terminal alkene to the internal trisubstituted (geranyl-type) alkene. In control experiments, we found this alkene type to undergo bicyclization reactions under our standard conditions, but significantly more slowly and in depressed yield. Therefore, we would expect the yields of **2.8c** and **2.8d** to be higher than reported if isomerically pure substrates were obtained and used in these reactions. For a relevant example, see: Chou, T.-H.; Yu, B.-H.; Chein, R.-J. *Chem. Commun.* **2019**, *55*, 13522–13525.

(24) Rosales, V.; Zambrano, J.; Demuth, M. *Eur. J. Org. Chem.* **2004**, *2004*, 1798–1802.

(25) Oswald, J. P.; Woerpel, K. A. *J. Org. Chem.* **2018**, *83*, 9067–9075.

(26) Julia, M. *Acc. Chem. Res.* **1971**, *4*, 386–392.

(27) Ma, X.; Herzon, S. B. *Chem. Sci.* **2015**, *6*, 6250–6255.

(28) a) Stolzenberg, A. M.; Cao, Y. *J. Am. Chem. Soc.* **2001**, *123*, 9078–9090; b) Shevick, S. L.; Obradors, C.; Shenvi, R. A. *J. Am. Chem. Soc.* **2018**, *140*, 12056–12068.

(29) Although unlikely, we note that mesomeric stabilization of α-nitrilo cations is expected to partially offset the inductively destabilizing effect of this functional group. See: Creary, X. *Chem. Rev.* **1991**, *91*, 1625–1678.

(30) For a relevant example of an epoxide-intiated cationic polycyclization, also carried out in HFIP, see: Tian, Y.; Xu, X.; Zhang, L.; Qu, J. *Org. Lett.* **2016**, *18*, 268–271.

(31) Colomer, I.; Chamberlain, A. E. R.; Haughey, M. B.; Donohoe, T. J. *Nat. Rev. Chem.* **2017**, *1*, 0088.

(32) Floriani, C.; Calderazzo, F. *J. Chem. Soc. A* **1969**, 946–953.

(33) a) Tovrog, B. S.; Kitko, D. J.; Drago, R. S. *J. Am. Chem. Soc.* **1976**, *98*, 5144–5153; b) Reiss, H.; Shalit, H.; Vershinin, V.; More, N. Y.; Forckosh, H.; Pappo, D. *J. Org. Chem.* **2019**, *84*, 7950–7960.

(34) For recent examples of MHAT-induced cyclization reactions in the synthesis of complex natural products, see: a) Ji, Y.; Xin, Z.; He, H.; Gao, S. *J. Am. Chem. Soc.* **2019**, *141*, 16208–16212; b) Zhang, B.; Zheng, W.; Wang, X.; Sun, D.; Li, C. *Angew. Chem. Int. Ed.* **2016**, *55*, 10435–10438.

(35) Girijavallabhan, V.; Arasappan, A.; Bennett, F.; Chen, K.; Dang, Q.; Huang, Y.; Kerekes, A.; Nair, L.; Pissarnitski, D.; Verma, V.; Alvarez, C.; Chen, P.; Cole, D.; Esposite, S.; Huang, Y.; Hong, Q.; Liu, Z.; Pan, W.; Pu, H.; Rossman, R.; Truong, Q.; Vibulbhan, B.; Wang, J.; Zhao, Z.; Olsen, D.; Stamford, A.; Bogen, S.; Njoroge, F. G. *Nucleosides, Nucleotides and Nucleic Acids* **2016**, *35*, 277–294.

(36) Doğan, F.; Ulusoy, M.; Öztürk, Ö. F.; Kaya, İ.; Salih, B. *J. Therm. Anal. Calorim.* **2009**, *98*, 785.

(37) Chawner, S. J.; Cases-Thomas, M. J.; Bull, J. A. *Eur. J. Org. Chem.* **2017**, *2017*, 5015–5024.

(38) Schaus, S. E.; Brandes, B. D.; Larrow, J. F.; Tokunaga, M.; Hansen, K. B.; Gould, A. E.; Furrow, M. E.; Jacobsen, E. N. *J. Am. Chem. Soc.* **2002**, *124*, 1307–1315.

(39) Zendehdel, M.; Khanmohamadi, H.; Mokhtari, M. *J. Chin. Chem. Soc.* **2010**, *57*, 205–212.

(40) Larock, R. C.; Yang, H.; Weinreb, S. M.; Herr, R. J. *J. Org. Chem.* **1994**, *59*, 4172–4178.

(41) Hickey, D. M. B.; Leeson, P. D.; Novelli, R.; Shah, V. P.; Burpitt, B. E.; Crawford, L. P.; Davies, B. J.; Mitchell, M. B.; Pancholi, K. D.; Tuddenham, D.; Lewis, N. J.; O'Farrell, C. *J. Chem. Soc., Perkin Trans. 1* **1988**, 3103–3111.

(42) Nikas, S. P.; Thakur, G. A.; Makriyannis, A. *Synth. Commun.* **2002**, *32*, 1751–1756.

(43) Satyanarayana, G.; Maier, M. E. *Tetrahedron* **2012**, *68*, 1745–1749.

(44) Satyanarayana, G.; Maier, M. E. *Org. Lett.* **2008**, *10*, 2361–2364.

(45) Fridén-Saxin, M.; Pemberton, N.; da Silva Andersson, K.; Dyrager, C.; Friberg, A.; Grøtli, M.; Luthman, K. *J. Org. Chem.* **2009**, *74*, 2755–2759.

(46) Panther, J.; Röhrich, A.; Müller, T. J. J. *ARKIVOC* **2012**, 297–311.

(47) Zhao, H.; Cai, M.-Z.; Hu, R.-H.; Song, C.-S. *Synth. Commun.* **2001**, *31*, 3665–3669.

(48) van Gemmeren, M.; Börjesson, M.; Tortajada, A.; Sun, S.-Z.; Okura, K.; Martin, R. *Angew. Chem. Int. Ed.* **2017**, *56*, 6558–6562.

(49) Gesinski, M. R.; Tadpetch, K.; Rychnovsky, S. D. *Org. Lett.* **2009**, *11*, 5342–5345.

(50) Chen, X.; Zhang, Y.; Wan, H.; Wang, W.; Zhang, S. *Chem. Commun.* **2016**, *52*, 3532–3535.

(51) Botting, N. P.; Robertson, A. A. B.; Morrison, J. J. *J. Labelled Compd. Radiopharm.* **2007**, *50*, 260–263.

(52) Kim, Y.; Fuchs, P. L. *Org. Lett.* **2007**, *9*, 2445–2448.

(53) Demertzidou, V. P.; Pappa, S.; Sarli, V.; Zografos, A. L. *J. Org. Chem.* **2017**, *82*, 8710–8715.

(54) Ungur, N. D.; Popa, N. P.; Van Tuen, N.; Vlad, P. F. *Chem. Nat. Compd.* **1993**, *29*, 473–478.

(55) Lanni, T. B.; Greene, K. L.; Kolz, C. N.; Para, K. S.; Visnick, M.; Mobley, J. L.; Dudley, D. T.; Baginski, T. J.; Liimatta, M. B. *Bioorg. Med. Chem. Lett.* **2007**, *17*, 756–760.

(56) Kopach, M. E.; Fray, A. H.; Meyers, A. I. *J. Am. Chem. Soc.* **1996**, *118*, 9876–9883.

(57) Negishi, E.-i.; Maye, J. P.; Choueiry, D. *Tetrahedron* **1995**, *51*, 4447–4462.

(58) Novák, L.; Poppe, L.; Szántay, C.; Szabó, É. *Synthesis* **1985**, *1985*, 939–941.

(59) Ishihara, K.; Ishibashi, H.; Yamamoto, H. *J. Am. Chem. Soc.* **2002**, *124*, 3647–3655.

(60) Crusco, A.; Bordoni, C.; Chakroborty, A.; Whatley, K. C. L.; Whiteland, H.; Westwell, A. D.; Hoffmann, K. F. *Eur. J. Med. Chem.* **2018**, *152*, 87–100.

(61) Trost, B. M.; Malhotra, S.; Chan, W. H. *J. Am. Chem. Soc.* **2011**, *133*, 7328–7331.

(62) Pati, L. C.; Mukherjee, D. *Tetrahedron Lett.* **2004**, *45*, 9451–9453.

CHAPTER 3: STEREOCONTROLLED RADICAL BICYCLIZATIONS OF OXYGENATED PRECURSORS ENABLE SHORT SYNTHESES OF OXIDIZED ABIETANE DITERPENOIDS

3.1 Abstract

The power of cation-initiated cyclizations of polyenes for the synthesis of polycyclic terpenoids cannot be overstated. However, a major limitation is the intolerance of many relevant reaction conditions toward the inclusion in the substrate of polar functionality, particularly in unprotected form. Radical polycyclizations are important alternatives to bioinspired cationic variants, in part owing to the range of possible initiation strategies, and in part for the functional group tolerance of radical reactions. In this article, we demonstrate that Co-catalyzed MHAT-initiated radical bicyclizations are not only tolerant of oxidation at virtually every position in the substrate, oftentimes in unprotected form, but these functional groups can also contribute to high levels of stereochemical control in these complexity-generating transformations. Specifically, we show the effects of protected or unprotected hydroxy groups at six different positions and their impact on stereoselectivity. Further, we show how multiply oxidized substrates perform in these reactions, and finally, we document the utility of these reactions in the synthesis of three aromatic abietane diterpenoids.

3.2 Introduction

In nature, polyene cyclizations are mediated by terpene cyclase enzymes and proceed via cationic pathways[1] (**Scheme 3.1a**), as shown in low resolution for the aromatic abietane diterpenoids in **Scheme 3.1b**.[2] The resultant polycyclic frameworks are frequently decorated with oxygen functionality by cytochrome P450 oxygenases,[3] which in the cases of the abietanes leads to dozens of congeners that sample oxidation and/or dehydrogenation at every single carbon atom.

Different combinations of oxidations result in vast structural diversity.[4] Some synthetic efforts to mimic this two-phase (cyclase/oxidase) strategy toward other classes of terpenoids have been met with significant success, particularly by the Baran group,[5] but chemoselective late-stage oxidation remains a challenging task.[6,7] Reversing the order of operations by oxidizing the carbon skeleton prior to cyclization can be strategically risky, since polar cationic cascades tend to be sensitive to electronic effects and the presence of Lewis basic functional groups can interfere with many of the catalysts employed in these reactions.[8] Employing radical polycyclizations in highly oxidized contexts could be a viable alternative because they are generally more functional group tolerant and might be expected to perform better in sterically demanding situations.[9,10]

Scheme 3. 1: a) Typical trans-Decalin Formation by Cationic Bicyclizations of Oligoisoprenes. **b)** Overview of the Biosynthesis of Oxidized Aromatic Abietane Diterpenoids.

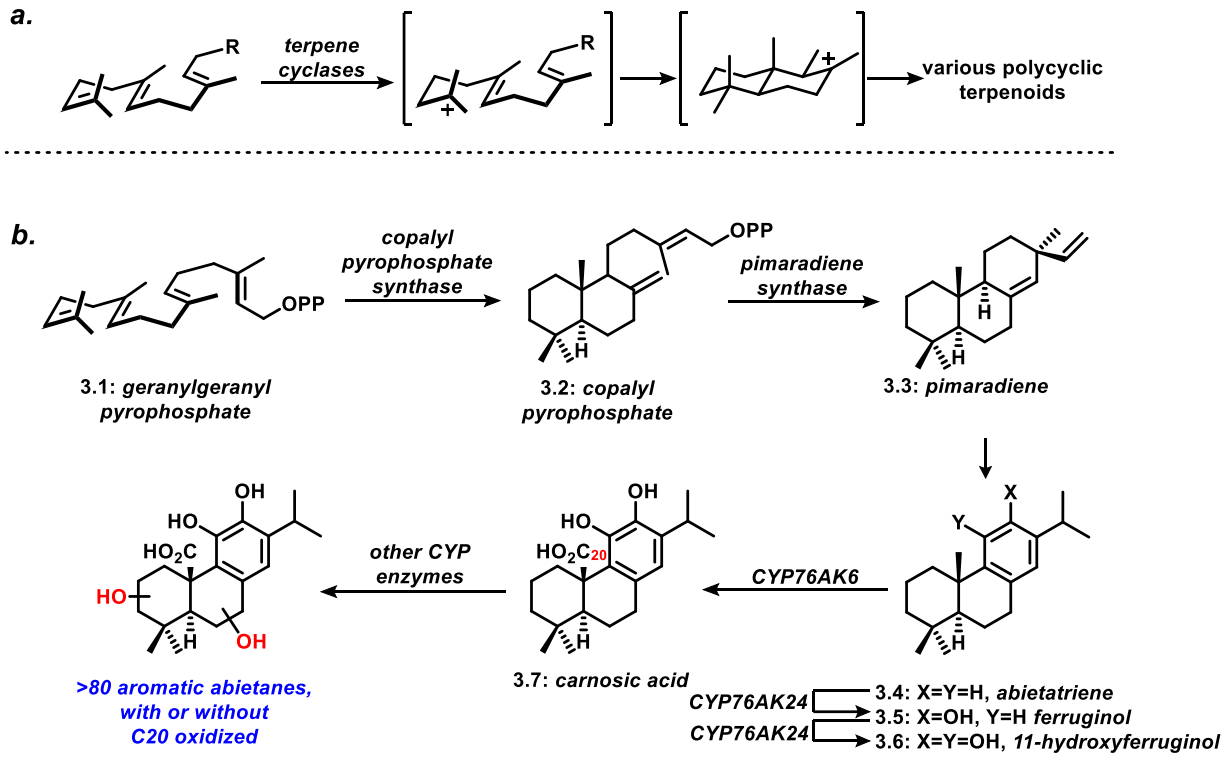

Since Breslow's seminal investigations of benzoyl radical addition to farnesyl acetate (**Figure 3.1a**),[11] a range of unique radical polyene cyclization methods have been described, in

some cases offering new opportunities to deviate from canonical geraniol/farnesol/geranylgeraniol-derived starting materials.[12] Representative noteworthy advances include (1) acyl-radical-initiated polycyclizations[13] by the Boger and Pattenden laboratories, (2) Mn(III)-induced reactions of β-ketoesters[14] as described by the Snider and Zoretic groups, (3) photoinduced-electron-transfer-triggered polycyclizations from Demuth and co-workers,[15] (4) the use of Nugent/Rajanbabu-type single-electron epoxide reduction[16] to initiate ring closures[17] by the groups of Gansauer, Barrero, and Cuerva, and (5) the MacMillan lab's single electron oxidation of catalytically generated chiral enamines.[18] A few years ago, Liu and co-workers used metal-catalyzed hydrogen atom transfer (MHAT)[19] to an alkene to initiate bicyclization in the context of their hispidanin A synthesis;[20] iron catalysis related to the previous work of Baran was key to this achievement.[21,22,23] Very recently, in efforts to effect polyene cyclizations in which electron-deficient alkenes were competent reactants, we found that cobalt catalysis of MHAT[24,25,26] was uniquely effective in generating products with strategic oxidation at C20, in the form of the nitrile (see **3.10** to **3.11**, **Figure 3.1b**).[27]

Figure 3. 1: a) Breslow's pioneering radical bicyclization of farnesyl acetate. **b)** Our previous report of MHAT-initiated radical bicyclizations that tolerated an oxidized C20 (as the nitrile). **c)** Liu's use of the C2 silyloxy group to control diastereoselectivity in an MHAT-initiated bicyclization.

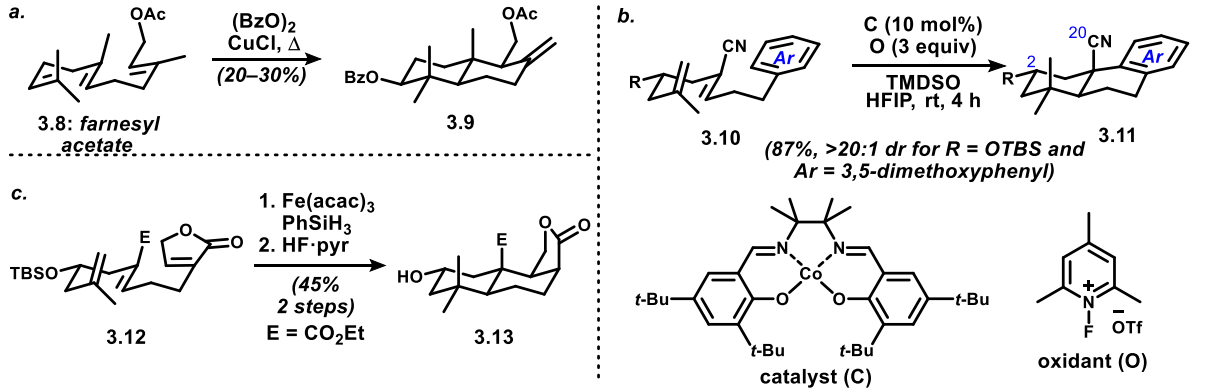

Although stereocontrolled radical cyclizations have been utilized as key steps in many total syntheses, the stereochemical influence of pendent functionalities has not been investigated systematically in reactants leading to diterpenoid scaffolds. As already mentioned, Liu and co-workers reported an MHAT-initiated triene cyclization where high stereoselectivity was observed with respect to a C2 substituent that was later excised (**3.12** to **3.13**, **Figure 3.1c**).[20] In our investigations of Co(II)-catalyzed radical bicyclizations, we also observed excellent stereocontrol induced by a *tert*-butyldimethylsilyloxy group at C2.[27] These results prompted us to further investigate the compatibility with and the stereodirecting role of oxygenated substituents at other positions in these reactants.

As part of our program to make use of prefunctionalized π-cyclization precursors to generate complex terpenoids,[27,28] we sought to systematically investigate the stereodirecting ability of pendant alkoxy substituents on cyclization substrates (**Figure 3.2a**). For this study, we focused on substrates with C20 in nitrile form, because many abietane and related diterpenoids are oxidized at this position, and the method is particularly adept at addressing this challenge. Prior work documented the unique suitability of the nitrile as electron-withdrawing group at this position, with no productive cyclizations observed with the corresponding esters.[27] Furthermore, examples are known with C20 oxidized and with further oxygenation at every position on the *trans*-decalin substructure (some examples shown in **Figure 3.2b**).[4,29,30] In this report, we describe the excellent functional group tolerance and often high stereoselectivity of these radical bicyclizations and establish the utility of these reactions with the total syntheses of three bioactive abietane diterpenoids bearing different oxidation patterns, as well as access to the complex oxygenation pattern found in a cassane diterpenoid.

Figure 3. 2: a) The possibility of using preoxidized bicyclization precursors to access highly oxidized abietane-type scaffolds. **b)** Representative oxidized aromatic diterpenoids.

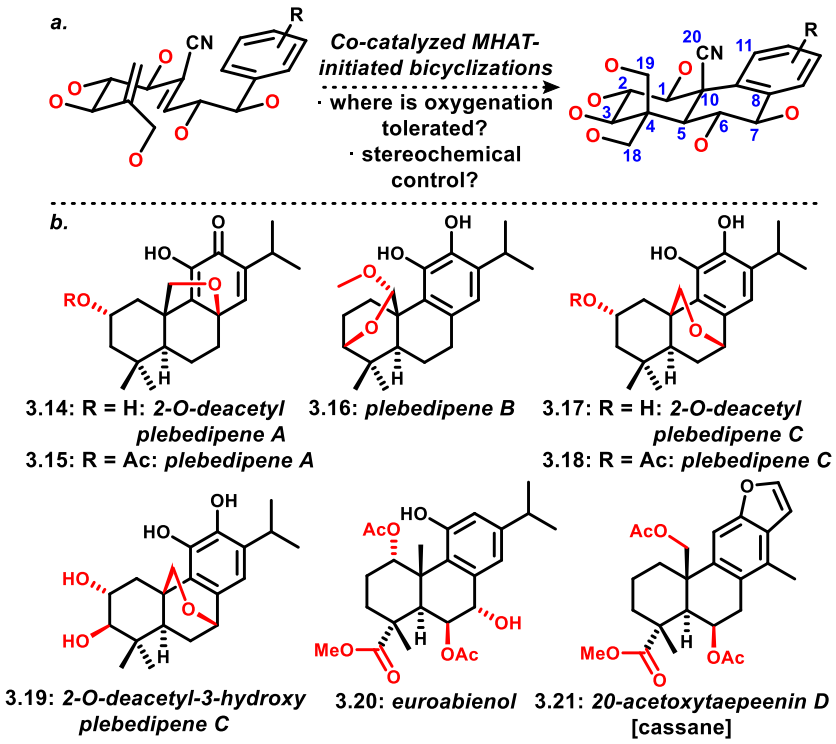

3.3 Stereochemical Control by Pendent Oxygen Functions

For the purpose of consistency and ease of synthesis, the 3,5-dimethoxyphenyl group was used as the terminator in investigations of stereochemical control by pendent oxygen-based functional groups. On the basis of our prior work, these results were expected to translate to substrates with a broad range of electron-rich arenes.[27] Further, the use of different terminators in the natural product syntheses are described in the latter half of this report. Systems with only one backbone oxygenated substituent at a time were examined initially, and it could be anticipated that these effects might be positively or negatively reinforcing in multiply substituted contexts depending upon the stereochemical arrangement. Interesting examples of this phenomenon are provided both in this section and in the natural product syntheses that follow.

3.3.1 C3 Oxygenation

Substrates bearing oxygenation at C3 (**3.22a**–**d**, **Figure 3.3**) were expected to cyclize with high diastereoselectivity via chairlike conformations from which the oxygenated substituent would emerge in an equatorial position. In this case, however, we found a significant protecting-group-dependence on stereochemical outcome. The stereoselectivity in the case of the free hydroxy group (**3.22a**) was moderate in favor of the equatorial isomer **3.23** (dr: 3:1), whereas TBS-protected alcohol **3.22d** showed a surprisingly strong preference for the axial product **3.24** (dr: 1:8). This outcome could prove quite useful since both polar and radical epoxypolyene cyclizations tend to be highly selective for equatorial orientation of the C3 hydroxy group. Ti(III)-catalyzed radical cyclizations of epoxypolyprenes only produce scaffolds with equatorial C3 hydroxyl groups, presumably due to intermediacy of bulky titanoalkoxides.[31] The only direct way to access the axial C3 hydroxyl moiety was described by Corey et al. in their report on In(III)-catalyzed alkyne-initiated cationic cascades.[32] The incorporation of less bulky protecting groups like acetate (**3.22b**) and methoxymethyl (**3.22c**) resulted in negligible selectivity.

3.3.2 C2 Oxygenation

Oxygen substitution at C2 was associated with efficient bicyclization and exclusive selectivity for the equatorial group with both the free hydroxy group and the corresponding silyl ether (**3.25a** and **3.25b**). While both our previous work[27] and that of Liu[20] documented the use of C2 *t*-butyldimethylsilyloxy groups in these radical cyclizations, the efficiency of reactions with the free alcohol is a key point in this and many of the reactions that are described here. In this case, even though the OH/OTBDMS groups are not “large” (A values <1.2), the penalty for their axial

disposition would be significant because of the axial methyl group that comprises C18, and the axial nitrile (despite an A value of only 0.17).

Figure 3. 3: Stereochemical outcomes of bicyclization reactions using substrates with C1-C3 oxygen functional groups.

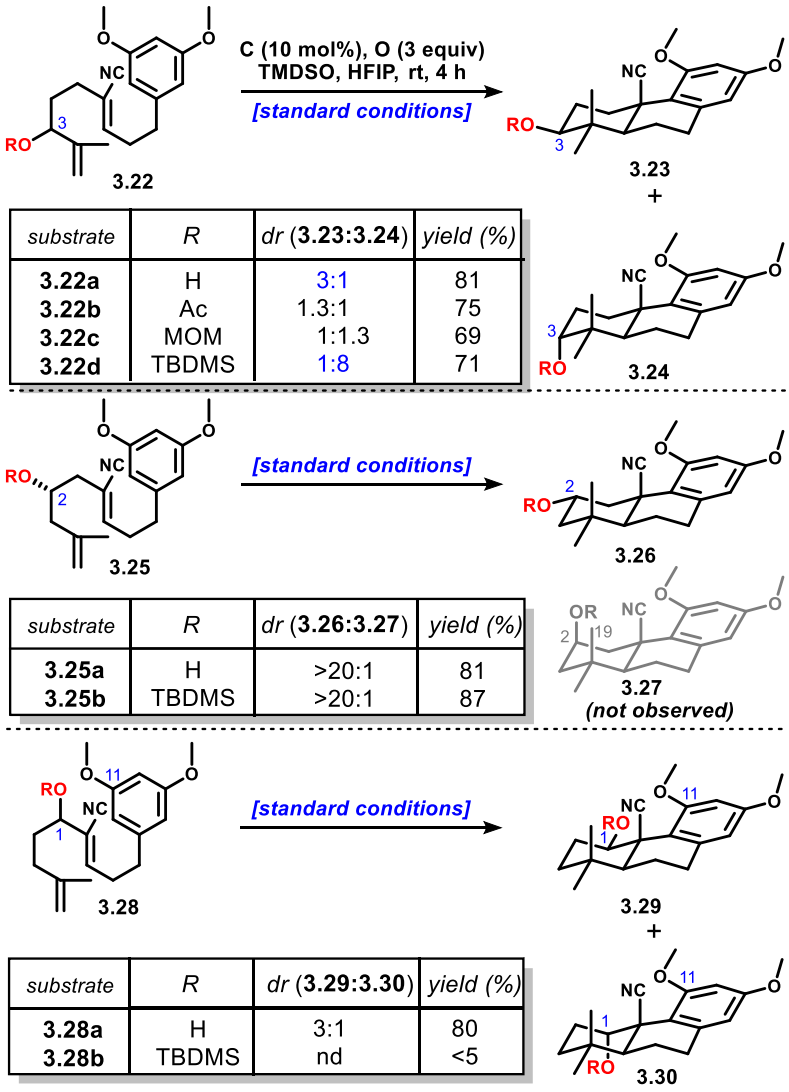

substrate	R	dr (**3.23**:**3.24**)	yield (%)
3.22a	H	3:1	81
3.22b	Ac	1.3:1	75
3.22c	MOM	1:1.3	69
3.22d	TBDMS	1:8	71

substrate	R	dr (**3.26**:**3.27**)	yield (%)
3.25a	H	>20:1	81
3.25b	TBDMS	>20:1	87

substrate	R	dr (**3.29**:**3.30**)	yield (%)
3.28a	H	3:1	80
3.28b	TBDMS	nd	<5

3.3.3 C1 Oxygenation

The substrate with a C1 hydroxy group (**3.28a**) cyclized efficiently in a 3:1 ratio favoring diastereomer **3.29a** with the alcohol equatorial. Interestingly, that is the same ratio as was observed with the C3 hydroxy group, perhaps simply reflecting the moderate steric bias against an axial OH

group on the α-face in the transition structure for the first cyclization (no other axial substituents on that face). However, we expected significant impacts of steric interactions between the C1 substituent and the C11 methoxy group: (1) the two groups are in very close proximity in equatorial product **3.29**, and (2) we anticipated that these interactions of the hydroxy group in the axial configuration would hinder the B-ring cyclization, although postcyclization these groups in **3.30** are not mutually encumbering. It is conceivable that hydrogen-bonding between the C1-OH and the C11-methoxy group facilitates the reaction leading to **3.30**. While we were somewhat surprised to observe any axial product **3.30** on kinetic grounds, this functional group arrangement (C1 axial acetoxy and C11 phenol) is found in the natural product euroabienol (**3.20**, **Figure 3.2b**).[30b] On the other hand, the stereochemical arrangement that places the C1 equatorial hydroxy group in very close proximity to the arene methoxy group (as in **3.29a**) is not known in the literature. We have obtained an X-ray crystallographic structure of **3.29a** that indicates hydrogen-bonding between the C1-OH and the C11 ether oxygen and an A-ring twist-boat conformation (see **Appendix B**).

We suspected that this intramolecular hydrogen-bonding could be leveraged to direct the regiochemical outcome of the polycyclizations when unsymmetrical arenes are used. To test this, we synthesized and evaluated substrate **3.31** bearing a carbinol and a methoxy group at C1 and C11 respectively. Chromatographic purification of the crude post-cyclization material yielded a 2.6:1 diastereomeric mixture of 'ortho' regioisomers (**3.32** and **3.33**), which was resolved after selective oxidation of the minor isomer bearing an axial hydroxy group using PCC. The stereoselectivity of the first ring closure closely mirrors that observed for **3.28a**, but the strong preference for the 'ortho' isomer in the final cyclization is remarkable. As described in our previous report, an analogous substrate bearing an OTBS group at C2 gave a 1.7:1 mixture of

regioisomers favoring the 'meta' isomer (see **Figure 2.2** in **Chapter 2**).[27] To the best of our knowledge, this is the first example where intramolecular hydrogen-bonding is utilized to control the regiochemical outcome of such polycyclizations.

Figure 3. 4: Hydrogen-bonding directed regiocontrol in substrates bearing unsymmetrical methoxy arenes.

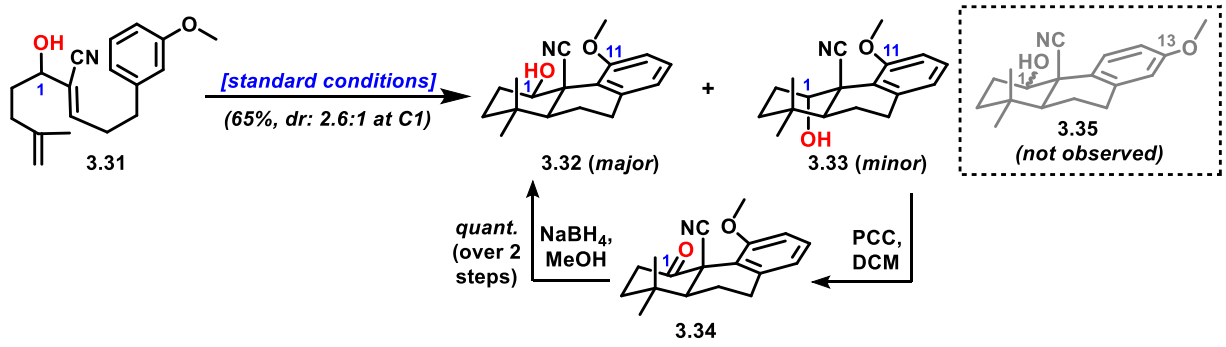

Perhaps unsurprisingly, the silyl protected substrate **3.28b** did not react productively. To further ascertain the potential importance of the steric and/or hydrogen bonding effects in **28a/b**, we evaluated *p*-methoxyphenyl substrates **3.36a**–**c**; this terminating group also worked well in our previous studies.[27] In this case, substrate **3.36a** with the free hydroxy group did not proceed to tricyclic products, but the silyl-protected version **3.36b** was converted with low efficiency to **3.37** with apparent complete selectivity for the axial silyloxy group. The mass balance could not be characterized. It is difficult to ascertain the inherent stereoselectivity in the first ring closure in this case, because the equatorial stereoisomer might form selectively in the first cyclization but fail to undergo the second ring formation. Finally, we evaluated the corresponding C1-acetoxy substrate, and found only cyclohexene nitrile **3.39** (32% + 35% recovered starting material), presumably resulting from elimination of acetoxy radical.

Figure 3. 5: Outcomes of bicyclization reactions using substrates with C1 oxygenation and *p*-methoxyphenyl terminating groups.

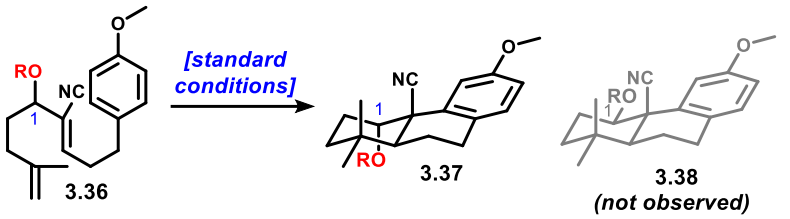

substrate	*R*	*dr (**3.37**:**3.38**)*	*yield (%)*
3.36a	H	nd	<5
3.36b	TBDMS	>20:1	25
3.36c	Ac	na	32% of **3.39**

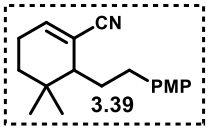

3.3.4 C18 Oxygenation

While oxidation on the terminal carbon of the substrate clearly cannot control the facial selectivity of π-cyclization, we wondered whether or not there would be an intrinsic preference for disposition of the resulting oxygenated carbon in the equatorial (C18) or axial (C19) position (**Figure 3.6**). We expected at best a modest preference for the slightly larger group to assume the equatorial position. However, we were surprised to observe complete selectivity (>20:1) for the equatorial diastereomer with both the TBS-protected and unprotected substrates (**3.40** and **3.45** respectively). In the case of silyl ether **3.40**, an efficient reaction resulted in the formation of **3.41** along with small and variable quantities of what we believe to be enoxysilane **3.42** (could not be purified to homogeneity for unambiguous structural determination). It is likely formed as a result of back-HAT to the Co(II) catalyst from the α-alkoxy methylene adjacent to the intermediary tertiary alkyl radical. Deprotection of **3.41** yielded neopentylic alcohol **3.43**, for which NOE experiments supported the stereochemical assignment. Interestingly, the desilylated substrate **3.45** cyclized to give a ~2:1 mixture of carbinol **3.43** and aldehyde **3.46**, both with the same relative configurations (**3.46** was reduced to **3.43** in aid of structural proof). The oxidation event likely occurs prior to the first cyclization since resubmitting

carbinol **3.43** to reaction conditions did not give the oxidized product, and the ratio of **3.43**:**4.46** did not change appreciably with conversion. At this stage, we do not have a good explanation for the oxidation chemistry or the unanticipatedly high stereoselectivity. It is noteworthy that cationic epoxypolyene cyclizations involving terminal, 2,2-disubstituted epoxides lead to the same stereochemical preference but with moderate (4–5:1 selectivity), in the absence of other pendant stereodirecting groups.[28]

Figure 3. 6: Surprisingly high diastereoselectivity for equatorial (C18) disposition of oxygenation in bicyclizations of allylic alcohol derivatives.

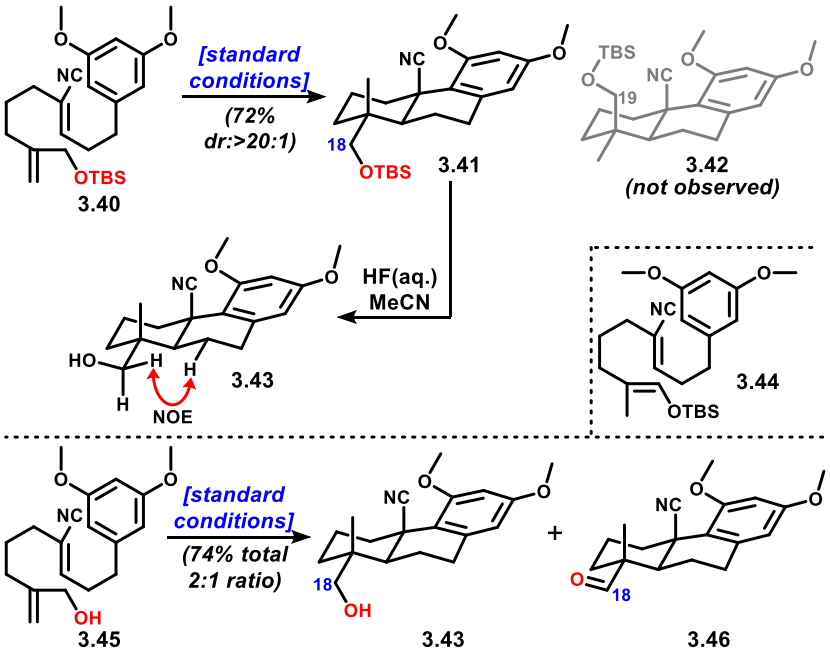

3.3.5 B-Ring Oxygenation

While oxygenation on the proto-A-ring portion of the bicyclization substrates often resulted in useful levels of stereoselectivity upon cyclization, we posited that substitutions at C6 or C7 (corresponding to the B-ring) would be less impactful. This hypothesis was based solely on the supposition that these cyclizations proceed stepwise, and that the impact of substitution at these positions on the conformational preferences for the first cyclization would be minimal.

Nonetheless, we needed experimental validation of this hypothesis, which would simultaneously permit us to assess the efficiency of these cyclizations. Assuming that oxygenation was tolerated at these positions, then the possibility of stereochemical control in polyoxygenated systems could still be powerful (see below). Moreover, just the simple ability to use prefunctionalized substrates, even in the absence of stereochemical control, might offer strategic advantages in complex molecule synthesis.

3.3.6 C6 Oxygenation

We first evaluated substrate **3.47a/b** with C6 oxygenation (**Figure 3.7**), and found that only the acetoxy derivative **3.47a** cyclized efficiently. As anticipated, this reaction occurred with essentially no stereochemical control, because the C6-configuration is unlikely to exert any control on facial selectivity in the first cyclization event. That the two diastereomeric intermediates cyclize with apparently similar efficiency to give axial and equatorial acetoxy products (**3.48** and **3.49**, respectively) might be understood by the fact that each reaction builds in a new *syn*-pentane-like interaction between the acetoxy group and either the C18 or C19 methyl groups. We were surprised that the silyloxy-substituted substrate did not lead to detectable quantities of bicyclized products, but rather underwent slower conversion to a range of unidentified decomposition products. The unprotected C6-hydroxy substrate could not be evaluated because it proved unstable under the conditions for its formation by deprotection of either the acetate- or silicon-masked precursor. The C6-acetoxy-substituted reactant will become relevant in the context of multiply oxidized substrates (see below).

Figure 3. 7: Proto-B-ring oxygenation has little impact on overall reaction diastereoselectivity.

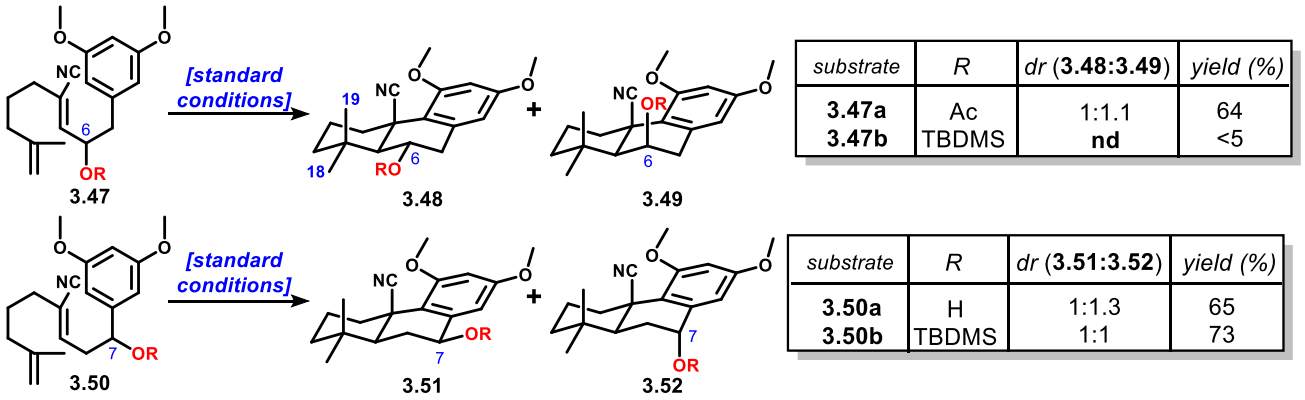

substrate	R	dr (**3.48:3.49**)	yield (%)
3.47a	Ac	1:1.1	64
3.47b	TBDMS	**nd**	<5

substrate	R	dr (**3.51:3.52**)	yield (%)
3.50a	H	1:1.3	65
3.50b	TBDMS	1:1	73

3.3.7 C7 Oxygenation

Both silyloxy and hydroxy substituents at C7 (see **3.50a/b**) were tolerated, and relatively efficient cyclization was observed in both cases, again with negligible stereochemical control from the preexisting stereogenic center. Showcasing the differences between cationic and radical polyene cyclizations, Chiba et al. reported that the presence of pendent ester groups (*C*-linked) in this benzylic position caused excellent stereocontrol in a protonative polyene cyclization.[33] There, the presumed concerted reaction with the substituent adopting the pseudoaxial orientation leads to high selectivity; in the case at hand, the stepwise radical bicyclization process ensures little impact of the distal stereogenic center on the first cyclization.

An interesting aspect of this work is that the formation of c*is*-decalin products is never observed. The second ring closure always favors the formation of the *trans*-decalin, irrespective of the necessary axial orientation of the C6/C7 oxygen-based group in roughly 50% of the material. Therefore, the configuration of the A-ring might generally control the stereochemical disposition of B-ring substituents, assuming that a diastereomerically pure precursor can be accessed (see below).

3.4 Doubly Oxygenated Precursors

We examined a select set of doubly oxygenated substrates (**Figure 3.8**). Terminally oxidized substrates with C7 and C6 oxygen groups (**3.53** and **3.56**, respectively) each cyclized with reasonable efficiency. We were unsurprised to find low levels of stereochemical control with **3.53**. However, because the C7 benzylic hydroxyl group is easily manipulated to make ether or lactone bridges (see **Figure 3.2b** for examples), or can be converted into either C7-epimer via either Mitsunobu inversion or oxidation/reduction,[34] this reaction still represents a powerful construction of compounds with this oxidation pattern, and further documents the reliability of the radical bicyclization in complex contexts.

Figure 3. 8: Radical bicyclizations of doubly oxygenated substrates.

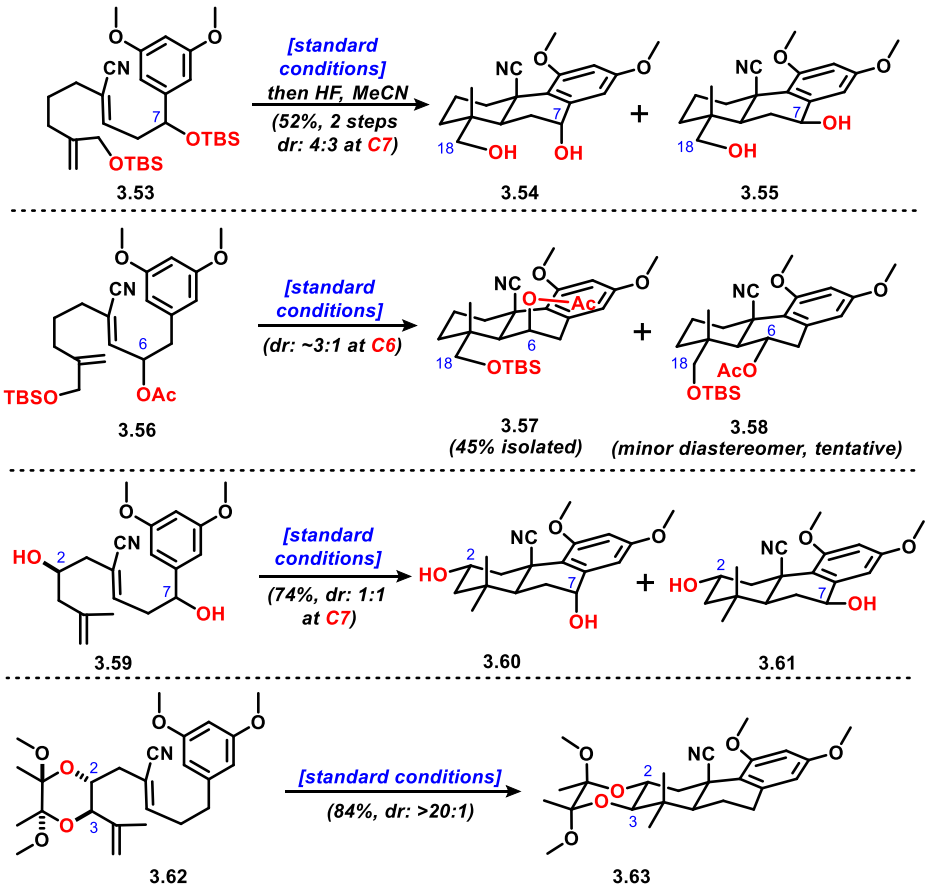

Of more interest, substrate **3.56**, with the C6-acetoxy group, preferentially provided C6-axial diastereomer **3.57** (3:1 dr observed in the crude reaction mixture but purified to a 14:1 mixture favoring **3.57**). We were unable to fully purify and characterize the minor product that we tentatively assign as stereoisomer **3.58**. The stereoselectivity of this reaction might arise from the avoidance of steric strain between the acetoxy group and the silyloxymethyl group in the transition structure. However, we note the change relative to the reaction of **3.47a** (**Figure 3.7**), lacking C18 oxygenation, and that the size difference of silyloxymethyl and methyl groups might not be solely accountable for this change. It might be argued that the presence of an electronegative silyl ether proximal to the tertiary radical intermediate leads to a later transition state owing to diminished nucleophilicity of the radical species. As a result, this could lead to a preference for the C6-acetoxy group to assume the pseudoaxial orientation necessary for hyperconjugative σ*-donation to the adjacent p-orbital of the electrophilic olefin. While the isolated yield of **3.57** is only 45%, this outcome is noteworthy for expedient access to the stereochemical and functional arrangement of the complex cassane diterpenoid 20-acetoxytaepeenin D[30c] (**3.21**, **Figure 3.2b**).

Next, we wished to show that a resident stereogenic center in the A-ring area of the substrate could control the outcome with respect to B-ring stereogenic centers. We made diol **3.59** as an equimolar mixture of diastereomers in enantiopure form, starting from epichlorohydrin. Under standard conditions, this substrate generated an equimolar mixture of **3.60** and **3.61** in good yield, thus demonstrating that the C2 stereogenic center controls the outcome of the bicyclization reaction and indicating that if a single diastereomer of substrate were made, a single diastereomer of product would result. The synthesis of a diastereomerically pure substrate should be accessible by catalyst-controlled diastereoselective reduction of the C7-ketone. However, we also note again that postcyclization manipulation of the benzylic carbon should be

facile. Of course, this reaction is also noteworthy for its efficiency in the presence of an unprotected diol. Further, this is a demonstrable case of A-ring substituents exerting influence over the equatorial/axial disposition of B-ring substituents. It is expected that the same type of control would arise from different combinations of substituents in a predictable way (A-ring C1, C2, or C3 oxygenation with B-ring C6 or C7 oxygenation).

Lastly, we wanted to test whether systems with vicinal oxygenation on the A-ring would be tolerated. Substrate **3.62** bearing a butanedione 2,3-bis acetal (BBA)[35] protected trans-diol at C2 and C3 underwent the desired cyclization in excellent yield, giving tetracyclic scaffold **3.63** as a single diastereomer. It is conceivable that the BBA protected diol moiety aids the first cyclization by restricting the isopropenyl substituent to an equatorial disposition. This A-ring oxygenation pattern is found in many diterpenoids[36] (see **3.19** in **Figure 3.2b**), setting the stage for applications to highly oxidized terpenoid syntheses that are ongoing in our lab.

3.5 Total Synthesis of Abietane Diterpenoids

Inspired by the results described above and to showcase the utility of the Co(II)-catalyzed radical bicyclizations, we targeted several C20 oxidized abietane diterpenoids bearing different oxygenation patterns. Close to 100 aromatic abietane diterpenoids have been reported, and they include members that are oxidized at every carbon of their aliphatic architecture. Moreover, many are endowed with intriguing bioactivities.[4] Guo and co-workers recently reported the isolation of plebedipenes A, B, and C,[29] C20 oxidized abietanes with further oxygenation at either C2 or C3 (**3.15**, **3.16**, and **3.18** in **Figure 3.2b**). The 2-*O*-deacetyl version of plebedipene A (**3.14**) was also reported, and the deacetyl analogue of plebedipene C (**3.17**) was previously reported by Fu and colleagues.[37] On the basis of the results in **Figure 3.3**, we posited that stereocontrolled radical

bicyclizations could grant quick access to the cores of these targets with appropriate oxygenation patterns and configurations.

3.5.1 (+)-2-O-Deacetyl Plebedipenes A and C

The synthesis of 2-*O*-deacetyl plebedipenes A (**3.14**) and C (**3.17**) began with known epoxide **3.64**,[38] which was opened with lithiated acetonitrile, the product of which was protected as silyl ether **3.65** (**Scheme 3.2**). Conversion to the phosphonate **3.66** was straightforward. To generate the electrophile for the convergent Horner–Wadsworth–Emmons (HWE) reaction, we began with regioselective oxidation of known iodophenol **3.67**.[39] The crude catechol was protected as orthoformate **3.68**, because of the need for a readily removable group in the late stages of the synthesis. Heck coupling with allyl alcohol gave aldehyde **3.69**, which was reacted with phosphonate **3.66** in a Z-selective (9:1) HWE alkenylation to give bicyclization precursor **3.70** as an inconsequential mixture of diastereomers with respect to the orthoformate carbon (*). Co(II)-catalyzed bicyclization in the presence of 1 equiv of 2,6-di-*tert*-butylpyridine (DTBP, needed because of the sensitive orthoformate) delivered **3.71** with excellent stereochemical control in 75% yield on gram scale. The unusual catechol protective group was chosen after the dimethylated catechol analogue of **3.70** failed to undergo radical bicyclization. This failure was explained by a likely gearing effect of the three contiguous substituents

Scheme 3. 2: Stereoselective Syntheses of (+)-2-O-Deacetyl Plebedipenes A and C.

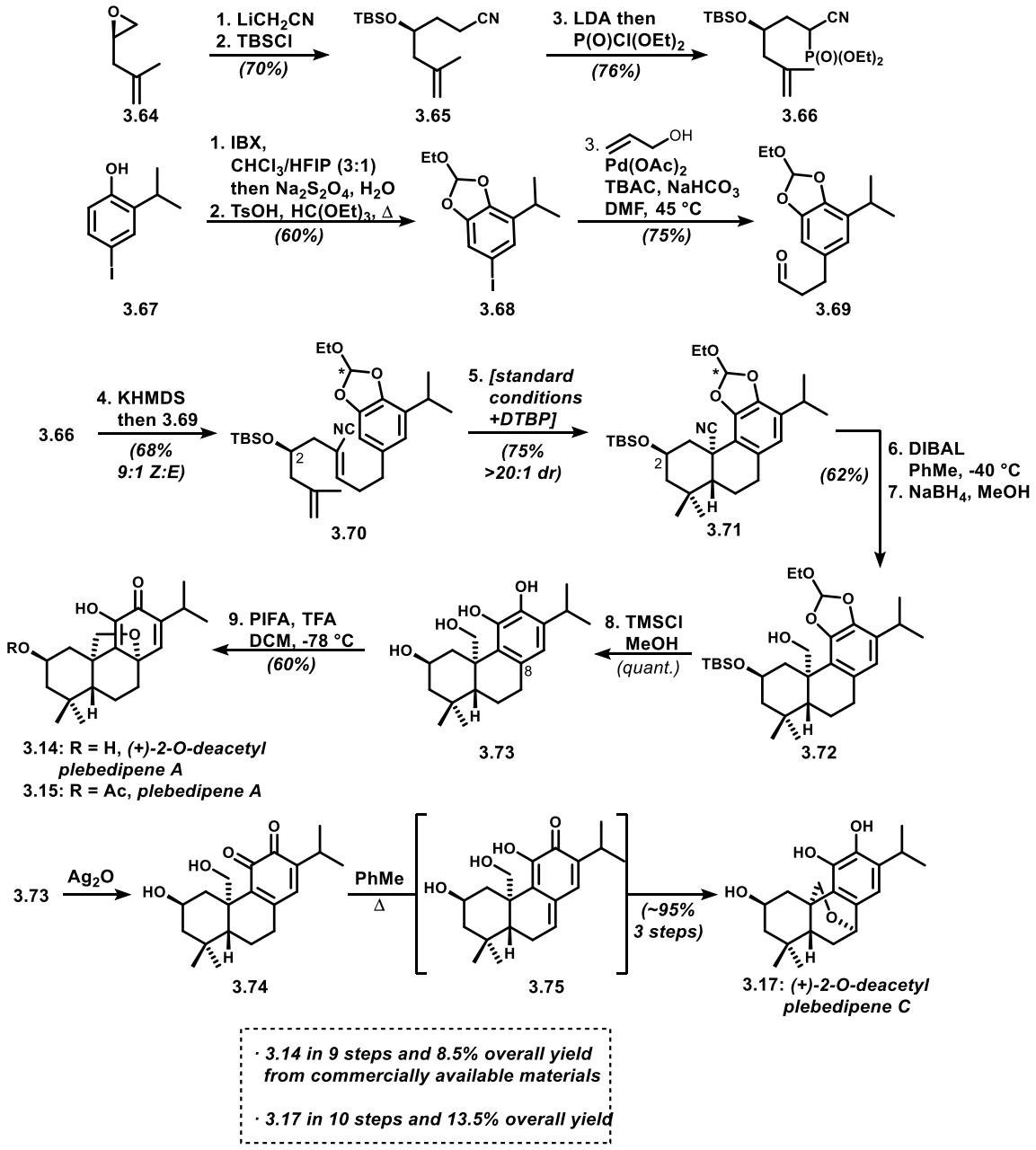

causing the C11 methoxy group to orient itself in a way that sterically shielded the desired reaction site. Surprisingly, NMR data indicated that **3.71** was isolated as a single diastereomer, suggesting that the orthoformate is equilibrated to its more stable diastereomer (unassigned) under the reaction conditions. Reduction of the hindered nitrile using DIBAL-H in toluene delivered the

corresponding imine, which was hydrolyzed on silica gel and further reduced using $NaBH_4$ in MeOH to give carbinol **3.72**. Removal of the silyl and orthoformate protecting groups with TMSCl in MeOH gave tetraol **3.73**, which was concentrated and directly used in the next steps without purification. We envisioned that the tetrahydrofuran ring could be constructed via oxidative cyclization of the pendent primary alcohol to C8 of the catechol. Screening a variety of conditions revealed that the inclusion of an acid source in the optimal hypervalent-iodine-mediated oxidation is critical[40] (see **Experimental Procedures** section). This observation suggests that the intermediary orthoquinone needs to be protonated for the hydroxyl group to attack C8. The result of this oxidative THF formation is the synthesis of (+)-2-*O*-deacetyl plebedipene A (**3.14**).[39] Subjection of tetraol **3.73** to an alternate oxidation protocol using silver oxide, as reported in a related context by Majetich and co-workers,[40] delivered (+)-2-*O*-deacetyl plebedipene C (**3.17**)[37] after heating the intermediate *o*-quinone in toluene overnight.[39]

3.5.2 (±)-Plebedipene B

An analogous convergent approach to the one described above was utilized for synthesis of plebedipene B. Cyclization precursor **3.76** (**Scheme 3.3**) was generated by HWE alkenylation of the same aldehyde **3.69** with a different cyanophosphonate reagent (see **Experimental Procedures**). The results from studies above (**Figure 3**) suggested that to access scaffolds bearing equatorial oxygenation at C3 in reasonable yield, the stereodirecting moiety should be a free hydroxyl group. With this in mind, **3.76** was treated with TBAF and submitted to bicyclization conditions in the presence of DTBP to furnish the desired scaffold **3.78** (3:1 dr at C3, as anticipated, purified to C3 stereochemical homogeneity in 45% yield). Interestingly, and in contrast to **64** (**Scheme 2**), **73** was isolated as an inconsequential 2:1 mixture of orthoformate diastereomers. It was necessary to reprotect the free hydroxyl group prior to reduction of the

hindered nitrile to avoid formation of a hydrolysis-resistant cyclic aminal. Treatment of **73** with TBSOTf in DCM followed by reduction with DIBAL-H in toluene furnished a critical aldehyde intermediate in excellent yield over two steps. Curiously, when the reduction is performed on a single orthoformate diastereomer of **73**, the orthoformate stereogenic center is equilibrated to a 4:1 mixture (unassigned) in this sequence. Cleavage of the orthoformate and silyl ether protecting groups with TMSCl in methanol resulted in concomitant acetalization to deliver (±)-plebedipene B[29] (**3.16**) in quantitative yield.

Scheme 3. 3: Synthesis of (±)-Plebedipene B.

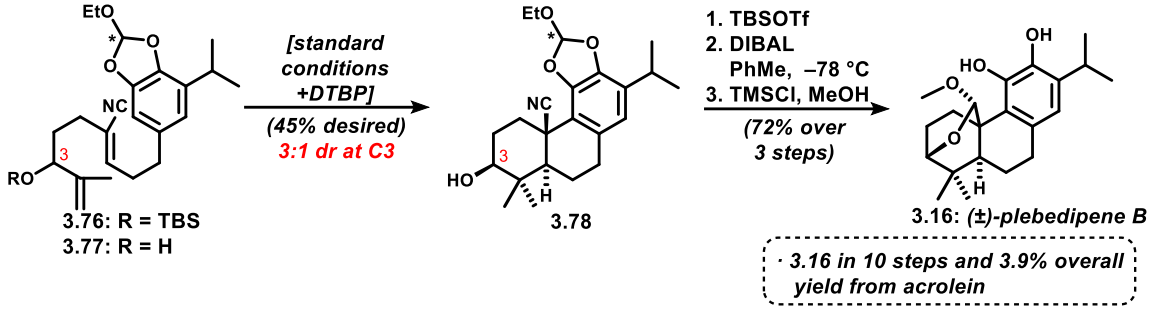

3.6 Outlook

As demonstrated in this work, MHAT-initiated bicyclizations of substrates bearing complex oxygenation patterns can be utilized in the synthesis of highly oxidized terpenoids. Currently, we are pursuing syntheses of **3.19** and **3.21**, using analogous approaches to those utilized en route to the plebedipenes. However, to ensure a long-term future for this project, target-oriented synthesis alone will most likely not be sufficient. Instead, it would be prudent to broaden the scope of terminating groups that can be engaged in these radical cascades. To date, only arenes have been utilized successfully in this context. It is conceivable that other π-systems such as electron rich alkenes or dienes might be suitable (**Scheme 3.4a**). Of course, this would likely necessitate chemoselective HAT to the more accessible 1,1-disubstituted alkene in the cyclization

precursors. Furthermore, nucleophilic trapping of the putative cationic species **3.81** could introduce useful functionalities for late-stage manipulations. The success of such exploratory endeavors would likely aid in development of convergent strategies to access more complex terpenoid targets, given appropriate acceptors can be incorporated into complex fragments (**Scheme 3.4b**).

Scheme 3. 4: a) Proposed termination using various alkenes and nucleophilic trapping of the intermediate cationic species. **b)** A hypothetical convergent approach to complex terpenoid frameworks.

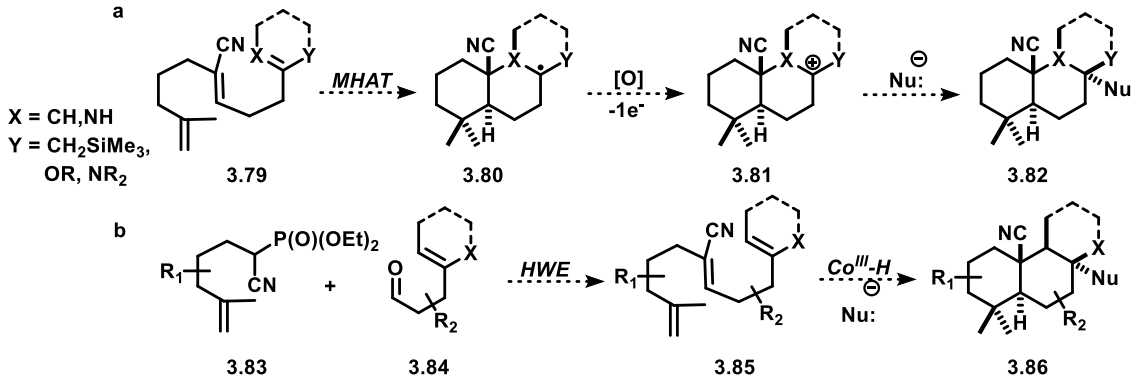

If further studies reveal that only electron rich arenes can terminate the bicyclizations efficiently, development of dearomative cascades could be explored instead. Recently, we showed that submitting substrate **3.87** to the standard bicyclization conditions gave a mixture of three tricyclic products (**Scheme 3.5a**). As in the case of indole substrates (see **Chapter 2**), formation of dearomatized HFIP acetal product **3.90** bolsters our hypothesis that the termination of these bicyclization cascades is oxidative. Although **3.90** wasn't the major isolated product, it is conceivable that dearomatization could become the major pathway under appropriate reaction conditions. Alternatively, oxidative cleavage of electron rich arene bearing products could be considered. Yang and co-workers utilized this strategy to access (–)-antrocin and other terpenoids from naturally abundant abietanes (**scheme 3.5b**).[41]

Scheme 3. 5: a) Dearomative cyclization of a furan bearing substrate. **b)** Oxidative cleavage of carnosic acid in a semisynthetic approach to (–)-antrocin reported by Yang and co-workers.

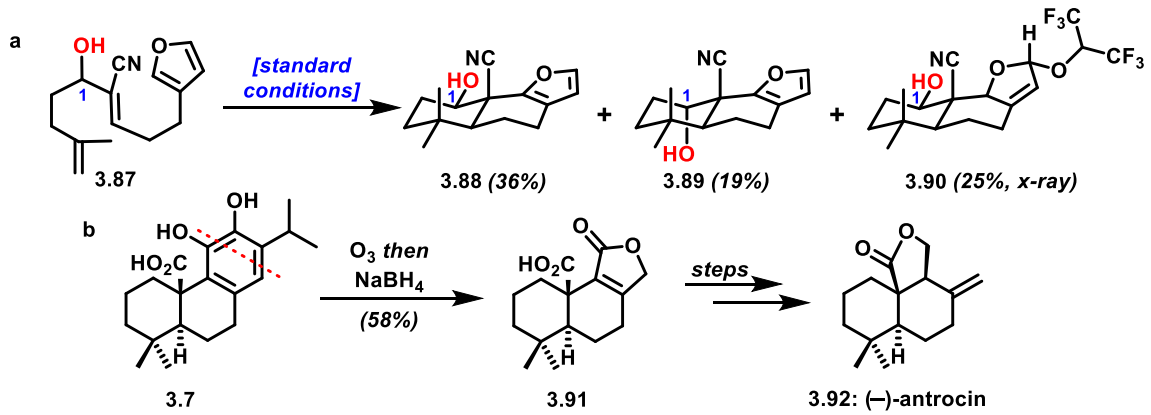

Thus far, our investigations have been limited to construction of the canonical *trans*-decalin systems, which can also be targeted using many other methodologies. Another path to explore in this context could be HAT-initiated (tri)cyclizations to access other polycyclic scaffolds. A systematic investigation of rationally designed dialkenyl arene substrates (**Scheme 3.6**) would dramatically expand the diversity of accessible frameworks. Furthermore, intermolecular variants of this reaction are yet to be investigated. For instance, it should be possible generate radical **3.97** via chemoselective MHAT to the corresponding 1,1-disubstituted alkene which could undergo a Giese addition to **3.99**. The resulting electron deficient radical **3.100** would engage the arene giving the hydroarylated product. Kinetic analysis of such coupling processes might also be possible, providing valuable mechanistic insights into the elementary steps of related MHAT processes.

Scheme 3. 6: Proposed HAT-initiated carbocyclizations of novel dialkenyl arene substrates (**a**) and an intermolecular variant enabling tandem fragment coupling-hydroarylation reactions (**b**).

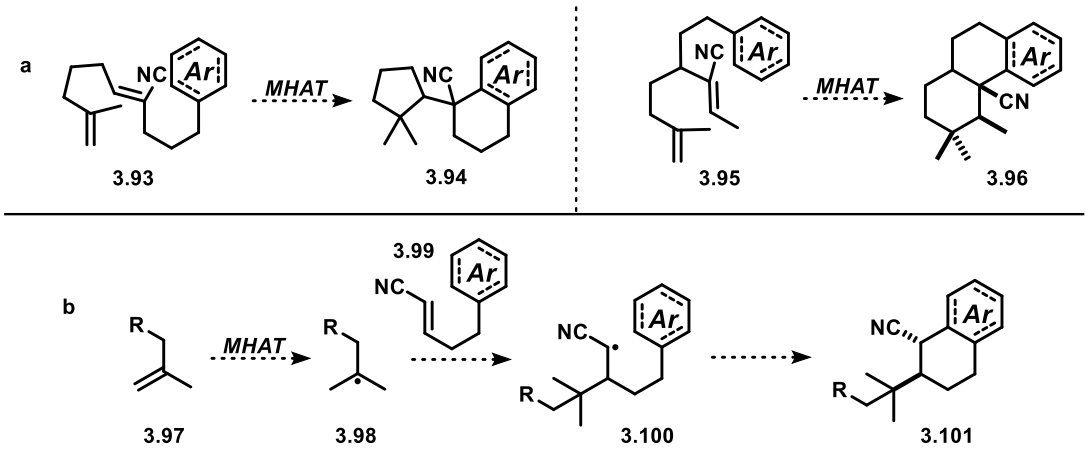

3.7 Conclusions

The ability of pendent oxygen substituents to control the stereochemical outcome of radical bicyclizations was systematically investigated to explore the possibility of using preoxidized polyene precursors to access highly oxidized terpenoids. The degree of stereoselectivity was often high, but varied with oxygenation locus, with free hydroxy groups performing well in most contexts. The stereochemical outcomes of cyclizations of dioxygenated polyenes were dictated by aliphatic chain oxygenation closest to the initiating, 1,1-disubstituted alkene. Simple analyses of nonbonding interactions in the putative cyclization transition states were sufficient to rationalize stereochemical outcomes in most cases. Moreover, in the most complex methodological example, we selectively accessed the functional group arrangement unique to the complex cassane diterpenoid 20-acetoxytaepeenin D. To further validate this proposed approach to bioactive diterpenoid synthesis, we completed the first total syntheses of (+)-2-*O*-deacteyl plebedipene A, (±)-plebedipene B, and (+)-2-*O*-deacetyl plebedipene C.

3.8 Experimental Procedures

General Experimental Information

All reactions were performed in oven-dried (120 °C) or flame-dried glassware under an atmosphere of dry argon unless otherwise noted. Reaction solvents including dichloromethane (CH_2Cl_2, Fisher, HPLC Grade), hexanes (Fisher, HPLC Grade), diethyl ether (Et_2O, Fisher, BHT stabilized, HPLC Grade), benzene (C_6H_6, Fisher, HPLC Grade), tetrahydrofuran (THF, Fisher, HPLC Grade), and toluene ($PhCH_3$, Fisher, HPLC Grade) were dried by percolation through a column packed with neutral alumina and a column packed with Q5 reactant, a supported copper catalyst for scavenging oxygen, under a positive pressure of argon. Solvents for workup and chromatography were: hexanes (Fisher or EMD, ACS Grade), EtOAc (Fisher, ACS Grade), dichloromethane (CH_2Cl_2, Fisher, ACS Grade), and diethyl ether (Fisher, ACS Grade). Column chromatography was performed using EMD Millipore 60 Å (0.040–0.063 mm) mesh silica gel (SiO_2). Analytical and preparatory thin-layer chromatography was performed on Merck silica gel 60 F254 TLC plates. Visualization was accomplished with UV (254 or 210 nm), and *p*-anisaldehyde, vanillin, potassium permanganate, 2,4-dinitrophenylhydrazine, or ceric ammonium molybdate and heat as developing agents. Chloroform-d ($CDCl_3$, D 99.8%, DLM-7) was purchased from Cambridge Isotope Laboratories. K_2CO_3 (anhydrous, 99%, Alfa Aesar), $NaHCO_3$ (ACS grade, Fisher), NaOH (ACS grade, Macron or Fisher), $Na_2S_2O_3$ (ACS grade, Fisher), 1-Fluoro-2,4,6-trimethylpyridinium triflate (95%, EMD or VWR, 95-99%) were purchased and used without further purification. Triethylamine (Et_3N, EMD, CaH_2) and pyridine (Alfa Aesar, CaH_2) were distilled from the indicated drying agents prior to use. Proton and carbon magnetic resonance spectra (^{1}H NMR and ^{13}C NMR) were recorded at 298K on a Bruker CRYO500 (500 MHz, ^{1}H; 125 MHz, ^{13}C) or a Bruker AVANCE600 (600 MHz, ^{1}H; 151 MHz, ^{13}C) spectrometer with solvent

resonance as the internal standard (^{1}H NMR: $CHCl_3$ at 7.26 ppm, ^{13}C NMR: $CDCl_3$ at 77.16 ppm). ^{1}H NMR data are reported as follows: chemical shift, multiplicity (s = singlet, d = doublet, t = triplet, q = quartet, dd = doublet of doublets, ddd = doublet of doublet of doublets, td = triplet of doublets, tdd = triplet of doublet of doublets, qd = quartet of doublets, m = multiplet, br. s. = broad singlet), coupling constants (Hz), and integration. High resolution mass spectra (HRMS) were recorded on a Waters LCT Premier spectrometer using ESI-TOF (electrospray ionization-time of flight) and data are reported in the form of (m/z). Optical rotation was measured on a Jasco P-2000 polarimeter with an optical path of 5 cm at 22-25 °C with the measurement performed in $CHCl_3$. Catalyst **C1**[42] was prepared as described in the literature and was used without further purification.

Substrate Synthesis Overview

Shown below is an overview of synthetic routes for substrates used in the systematic bicyclization study of variously oxygenated substrates. The experimental procedures that follow are sorted in order of oxygenation position, where carbinol derivatizations are also described. Key fragments used in the HWE (Horner–Wadsworth–Emmons) reactions to assemble dioxygenated substrates are in dashed rectangles.

Scheme 3. 7: Synthesis of C1 Oxygenated Substrates**.**

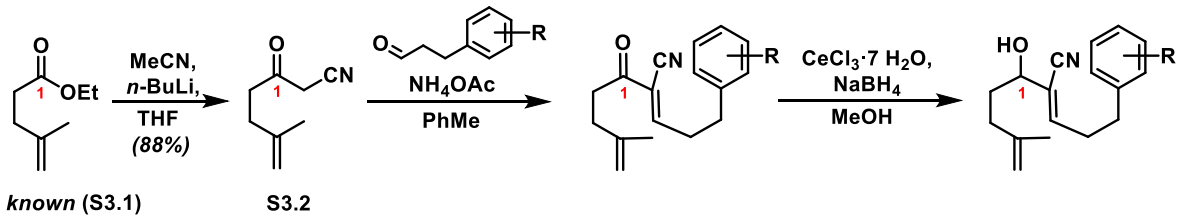

Scheme 3. 8: Synthesis of C2 Oxygenated Substrates.

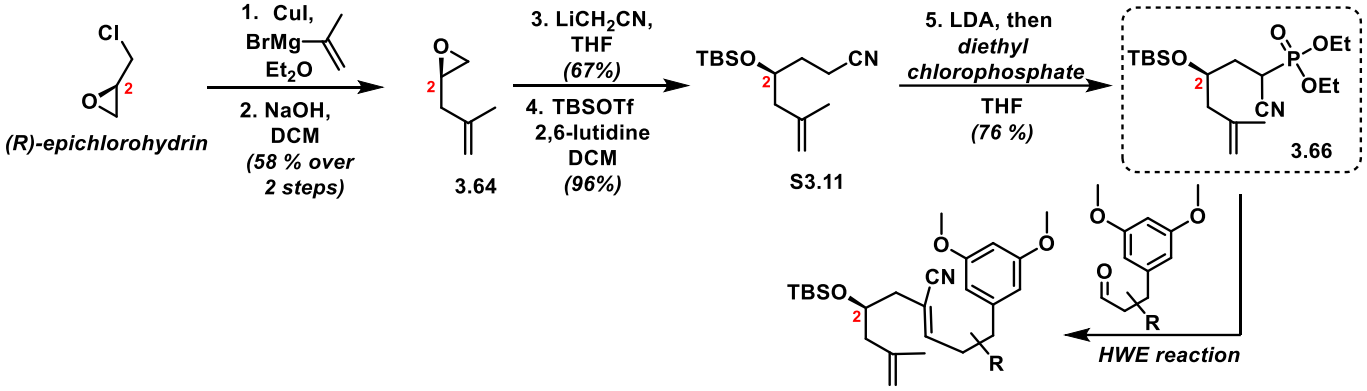

Scheme 3. 9: Synthesis of C3 Oxygenated Substrates.

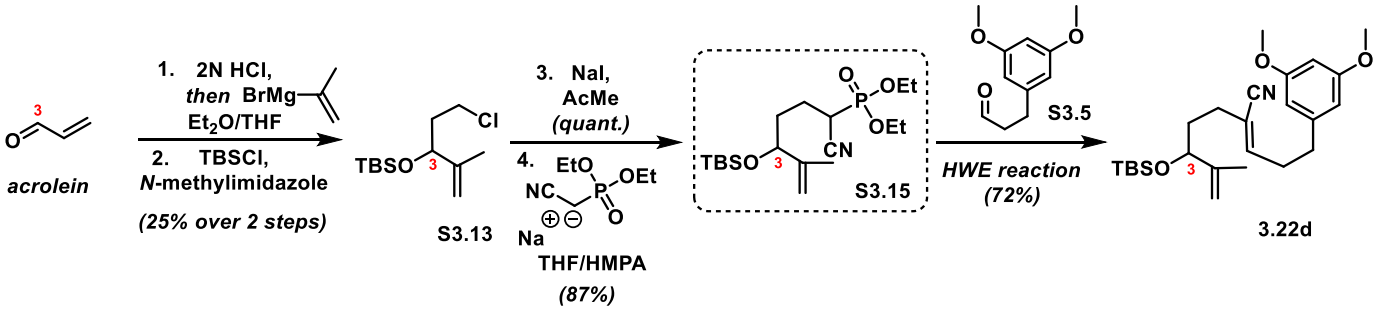

Scheme 3. 10: Synthesis of C18/19 Oxygenated Substrates.

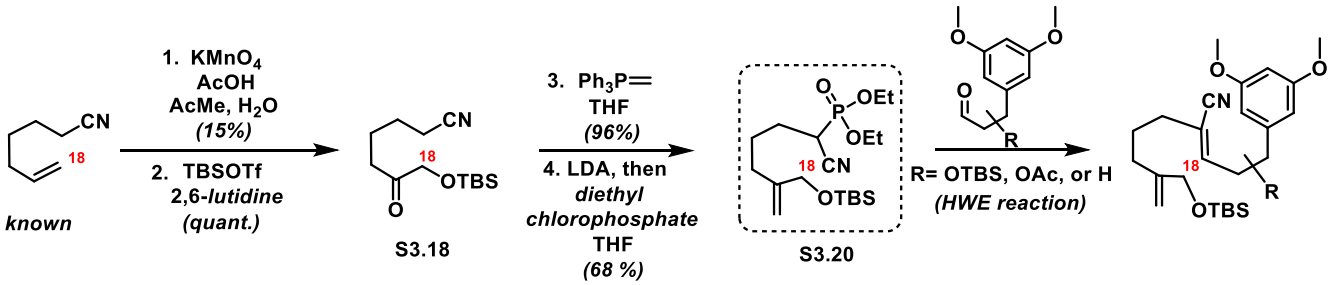

Scheme 3. 11: Synthesis of C6 Oxygenated Substrates.

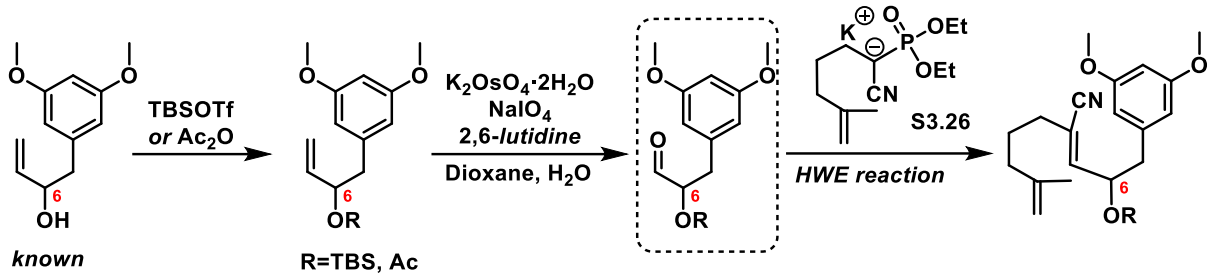

Scheme 3. 12: Synthesis of C7 Oxygenated Substrates.

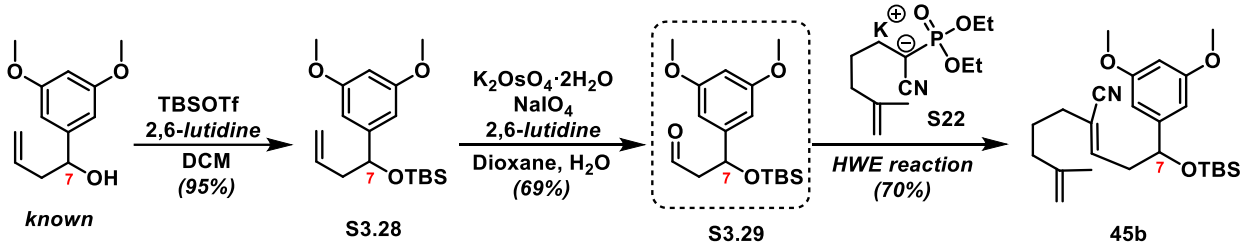

Synthesis and Characterization of C1 Oxygenated Substrates:

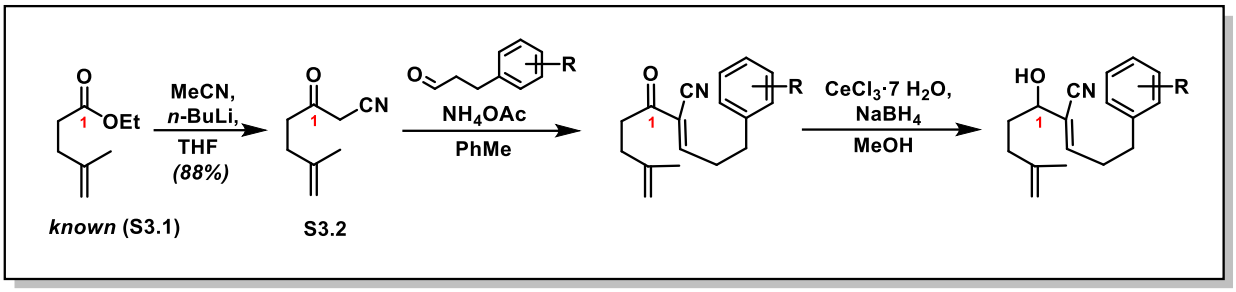

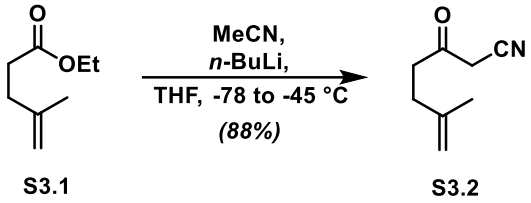

To a cooled (–78 °C) solution of *n*-butyllithium (2.5 M in hexanes, 20.6 mL, 51.5 mmol, 2.0 equiv.) was added THF (200 mL), followed by MeCN (2.7 mL, 51.5 mmol, 2.0 equiv.). The resulting mixture was stirred for 1 hour at –78 °C, then ester **S3.1**[43] (3.3 g, 25.7 mmol, 1.0 equiv.) was added dropwise over a period of 1 minute and the mixture was warmed to –45 °C. After 2 hours, 2 N $HCl_{(aq.)}$ (50 mL) was added and the biphasic mixture was warmed to ambient temperature. The aqueous phase was extracted with Et_2O (3 x 50 mL), the combined organic phases were washed with brine (100 mL), dried over Na_2SO_4, filtered and concentrated *in vacuo.* The resulting crude residue was purified via flash column chromatography, using a mixture of EtOAc/hexanes (1:3, R_f = 0.25) as eluent to give ketonitrile **S3.2** as a colorless oil (3.1 g, 22.6 mmol, 88% yield). **^{1}H NMR** (500 MHz, $CDCl_3$) δ 4.76 (s, 1H), 4.66 (s, 1H), 3.48 (s, 2H), 2.75 (t, *J* = 7.5 Hz, 2H), 2.32 (t, *J* = 7.5 Hz, 2H), 1.73 (s, 3H); **^{13}C NMR** (126 MHz, $CDCl_3$) δ 197.1, 143.4, 113.9, 111.1, 40.4, 32.1, 31.1, 22.6; **HRMS** (ES+) *m/z* calc'd for $C_8H_{11}NONa$ $[M + Na]^+$: 160.0738, found 160.0735.

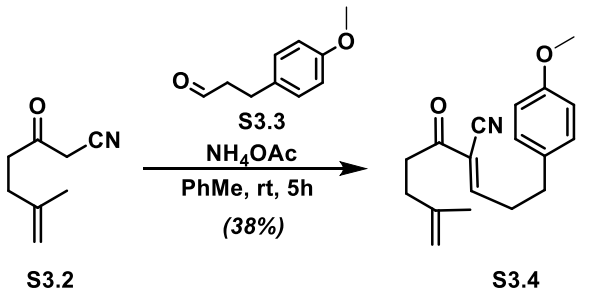

S3.2 S3.4

General procedure A (Ketonitrile Knoevenagel condensation):

To a solution of β-ketonitrile **S3.2** (358 mg, 2.6 mmol, 1.3 equiv.) and aldehyde **S3.3**[44] (330 mg, 2.0 mmol, 1.0 equiv.) in dry toluene (1.5 mL), was added ammonium acetate (31 mg, 0.4 mmol, 0.2 equiv.). The resulting mixture was stirred at ambient temperature for 3 hours (or until complete consumption of aldehyde **S3.3** as indicated by TLC, EtOAc/hexanes 1:9) then concentrated under reduced pressure. The resulting crude residue was directly purified via flash column chromatography on SiO_2, using a mixture of EtOAc/hexanes (8:92, R_f = 0.18) as eluent to give **S3.4** as a colorless oil (215 mg, 0.76 mmol, 38% yield). **^{1}H NMR** (500 MHz, CDCl3) δ 7.54 (t, *J* = 7.3 Hz, 1H), 7.10 (d, *J* = 8.5 Hz, 2H), 6.85 (d, *J* = 8.5 Hz, 2H), 4.76 (s, 1H), 4.67 (s, 1H), 3.79 (s, 3H), 2.91 – 2.80 (m, 6H), 2.34 (t, *J* = 7.5 Hz, 2H), 1.74 (s, 3H); **^{13}C NMR** (151 MHz, $CDCl_3$) δ 192.2, 160.5, 158.5, 143.7, 131.3, 129.4, 117.3, 115.0, 114.3, 110.9, 55.4, 38.7, 33.9, 33.2, 31.3, 22.7; **HRMS** (ES+) *m/z* calc'd for $C_{18}H_{21}NO_2Na$ $[M + Na]^+$: 306.1470, found 306.1460.

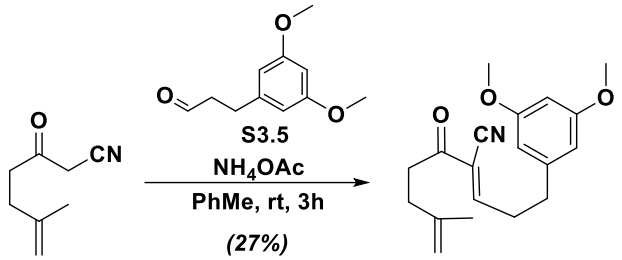

Prepared according to general procedure A, using ketonitrile **S3.2** *(360 mg, 2.62 mmol, 1.3 equiv.), aldehyde* **S3.5**[45] *(392 mg, 2.02 mmol, 1.0 equiv.), and ammonium acetate (31 mg, 0.40 mmol, 0.2 equiv.), in toluene (1.5 mL).* Yield of **S3.6**: 27% (171 mg, 0.54 mmol, colorless oil); R_f= 0.30 (15:85 EtOAc/hexanes); **^{1}H NMR** (500 MHz, $CDCl_3$) δ 7.53 (t, *J* = 7.6 Hz, 1H), 6.33 (s, 3H), 4.75 (s, 1H), 4.66 (s, 1H), 3.78 (s, 6H), 2.89 – 2.85 (m, 4H), 2.82 (t, *J* = 6.8 Hz, 2H), 2.33 (t, *J* = 7.5 Hz, 2H), 1.74 (s, 3H); **^{13}C NMR** (126 MHz, $CDCl_3$) δ 192.2, 161.2, 160.2, 143.7, 141.6, 117.3, 115.0, 110.9, 106.5, 98.8, 55.5, 38.7, 34.2, 33.3, 31.3, 22.7; **HRMS** (ES+) *m/z* calc'd for $C_{19}H_{23}NO_3Na$ $[M + Na]^+$: 336.1576, found 336.1575.

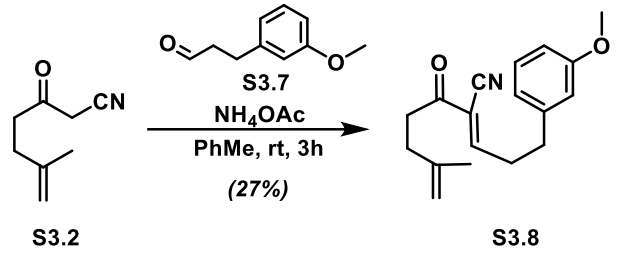

Prepared according to general procedure A, using ketonitrile **S3.2** *(326 mg, 2.38 mmol, 1.3 equiv.), aldehyde* **S3.7**[46] *(300 mg, 1.83 mmol, 1.0 equiv.), and ammonium acetate (28 mg, 0.37 mmol, 0.2 equiv.), in toluene (2.0 mL).* Yield of **S3.8**: 35% (238 mg, 0.84 mmol, colorless oil); R_f= 0.25 (15:85 EtOAc/hexanes); **^{1}H NMR** (600 MHz, $CDCl_3$) δ 7.54 (t, *J* = 7.3 Hz, 1H), 7.23 (t, *J* = 7.9 Hz, 1H), 6.78 (dd, *J* = 5.0, 3.0 Hz, 1H), 6.77 (s, 1H), 6.73 (s, 1H), 4.75 (s, 1H), 4.66 (s, 1H), 3.80 (s, 3H), 2.91 – 2.82 (m, 6H), 2.33 (t, *J* = 7.5 Hz, 2H), 1.74 (s, 3H); **^{13}C NMR** (151 MHz,

$CDCl_3$) δ 192.2, 160.2, 160.0, 143.7, 140.9, 129.9, 120.7, 117.3, 115.0, 114.2, 112.2, 110.9, 55.3, 38.6, 34.0, 33.5, 31.3, 22.7; **HRMS** (ES+) *m/z* calc'd for $C_{18}H_{21}NO_2Na$ [M + Na]$^+$: 306.1470, found 306.1481.

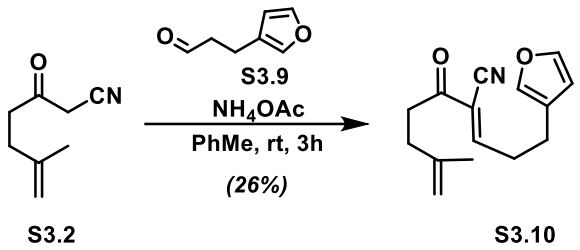

S3.2 **S3.10**

Prepared according to general procedure A, using ketonitrile **S3.2** *(430 mg, 2.62 mmol, 1.3 equiv.), aldehyde* **S3.9**[47] *(250 mg, 2.01 mmol, 1.0 equiv.), and ammonium acetate (31 mg, 0.40 mmol, 0.2 equiv.), in toluene (2.0 mL).* Yield of **S3.10**: 26% (130 mg, 0.53 mmol, colorless oil); R_f= 0.45 (15:85 EtOAc/hexanes); **^{1}H NMR** (500 MHz, $CDCl_3$) δ 7.53 (t, *J* = 7.6 Hz, 1H), 7.38 (s, 1H), 6.29 (s, 1H), 4.76 (s, 1H), 4.67 (s, 1H), 2.92 – 2.87 (m, 2H), 2.82 (q, *J* = 7.3 Hz, 2H), 2.72 (t, *J* = 7.2 Hz, 2H), 2.35 (t, *J* = 7.5 Hz, 2H), 1.75 (s, 3H); **^{13}C NMR** (151 MHz, $CDCl_3$) δ 192.1, 160.2, 143.7, 143.6, 139.4, 122.6, 117.4, 115.1, 110.9, 110.6, 38.7, 32.4, 31.3, 23.3, 22.7; **HRMS** (ES+) *m/z* calc'd for $C_{15}H_{17}NO_2Na$ [M + Na]$^+$: 266.1157, found 266.1152.

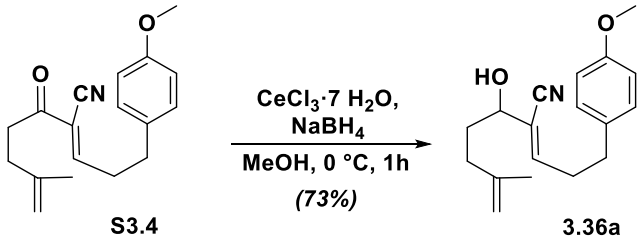

S3.4 **3.36a**

General procedure B (Luche reduction of α,β-unsaturated ketonitriles):

To an ice-cold solution of **S3.4** (350 mg, 1.24 mmol, 1.0 equiv.) in methanol (10 mL), was added $CeCl_3$ •$7H_2O$ (689 mg, 1.9 mmol, 1.5 equiv.) and the resulting solution was stirred for 15 minutes.

Next, sodium borohydride (61 mg, 1.6 mmol, 1.3 equiv.) was added portion-wise. After stirring the mixture for 1 hour at 4 °C, methanol was removed under reduced pressure. The resulting concentrate was taken up in EtOAc (30 mL), diluted with $NH_4Cl_{(aq)}$ (20 mL), and the phases were separated. The aqueous phase was extracted with EtOAc (3 x 20 mL), the combined organic extracts were washed with brine (30 mL), dried over Na_2SO_4, filtered and concentrated *in vacuo*. The resulting crude residue was purified via flash column chromatography, using a mixture of EtOAc/hexanes (1:2, R_f = 0.25) as eluent to give **3.36a** as a colorless oil (260 mg, 0.91 mmol, 73% yield); **^{1}H NMR** (600 MHz, $CDCl_3$) δ 7.10 (d, *J* = 8.2 Hz, 2H), 6.84 (d, *J* = 8.2 Hz, 2H), 6.39 (t, *J* = 7.2 Hz, 1H), 4.75 (s, 1H), 4.69 (s, 1H), 4.16 (dd, *J* = 12.0, 5.9 Hz, 1H), 3.79 (s, 3H), 2.77 – 2.72 (m, 2H), 2.71 – 2.67 (m, 2H), 2.03 (dd, *J* = 16.0, 7.9 Hz, 2H), 1.83 (broad s, 1H), 1.82 – 1.76 (m, 2H), 1.72 (s, 3H); **^{13}C DEPTQ** (151 MHz, $CDCl_3$) δ 158.3, 147.2, 144.7, 132.1, 129.5, 119.5, 115.9, 114.1, 111.1, 72.5, 55.4, 33.8, 33.7, 33.5, 33.1, 22.4; **HRMS** (ES+) *m/z* calc'd for $C_{18}H_{23}NO_2Na$ $[M + Na]^+$: 308.1627, found 308.1626.

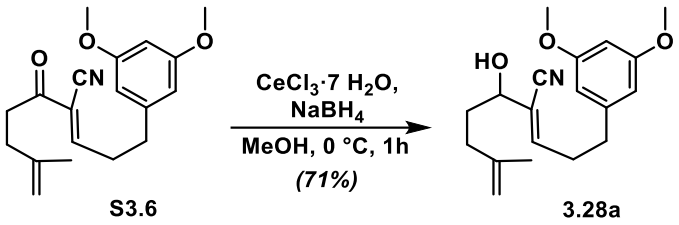

Prepared according to general procedure B, using α,β-unsaturated ketonitrile **S3.6** *(84 mg, 0.27 mmol, 1.0 equiv.),* $CeCl_3 \cdot 7H_2O$ *(150 mg, 0.40 mmol, 1.5 equiv.), sodium borohydride (12 mg, 0.322 mmol, 1.2 equiv.), and methanol (4.0 mL).* Yield of **3.28a**: 71% (60 mg, 0.19 mmol, colorless oil); R_f = 0.28 (3:7 EtOAc/hexanes). **^{1}H NMR** (500 MHz, $CDCl_3$) δ 6.38 (t, *J* = 7.2 Hz, 1H), 6.34 (d, *J* = 2.0 Hz, 2H), 6.32 (d, *J* = 1.9 Hz, 1H), 4.74 (s, 1H), 4.68 (s, 1H), 4.17 – 4.13 (m, 1H), 3.78 (s, 6H), 2.77 – 2.68 (m, 4H), 2.01 (dd, *J* = 16.0, 8.0 Hz, 2H), 1.81 – 1.75 (m, 2H), 1.72 (s, 3H);

^{13}C NMR (126 MHz, $CDCl_3$) δ 161.0, 147.0, 144.7, 142.4, 119.6, 115.9, 111.0, 106.6, 98.5, 72.4, 55.4, 34.8, 33.7, 33.4, 32.4, 22.4; **HRMS** (ES+) *m/z* calc'd for $C_{19}H_{25}NO_3Na$ $[M + Na]^+$: 338.1732, found 338.1735.

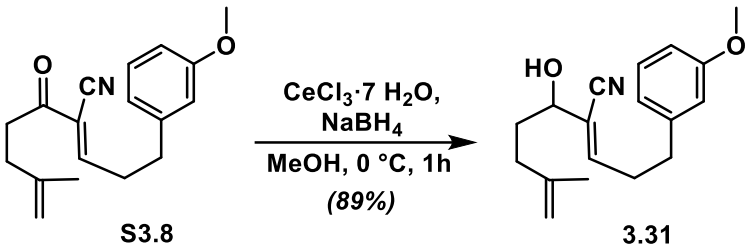

S3.8 3.31

Prepared according to general procedure B, using α,β-unsaturated ketonitrile **S3.8** *(235 mg, 0.83 mmol, 1.0 equiv.),* $CeCl_3 \cdot 7H_2O$ *(466 mg, 1.25 mmol, 1.5 equiv.), sodium borohydride (38 mg, 1.00 mmol, 1.2 equiv.), and methanol (15.0 mL).* Yield of **3.31**: 89% (210 mg, 0.19 mmol, colorless oil); R_f = 0.35 (3:7 EtOAc/hexanes); **^{1}H NMR** (600 MHz, $CDCl_3$) δ 7.21 (t, *J* = 7.8 Hz, 1H), 6.79 – 6.74 (m, 2H), 6.73 (s, 1H), 6.39 (t, *J* = 7.3 Hz, 1H), 4.75 (s, 1H), 4.68 (s, 1H), 4.15 (dd, *J* = 11.9, 5.8 Hz, 1H), 3.80 (s, 3H), 2.80 – 2.70 (m, 4H), 2.02 (tq, *J* = 14.6, 7.4 Hz, 2H), 1.93 (d, *J* = 4.9 Hz, 1H), 1.83 – 1.75 (m, 2H), 1.72 (s, 3H); **^{13}C NMR** (151 MHz, $CDCl_3$) δ 159.9, 147.00, 144.7, 141.6, 129.7, 120.9, 119.6, 115.9, 114.3, 111.9, 111.0, 72.4, 55.3, 34.7, 33.7, 33.5, 32.6, 22.4; **HRMS** (ES+) *m/z* calc'd for $C_{18}H_{23}NO_2Na$ $[M + Na]^+$: 308.1627, found 308.1620.

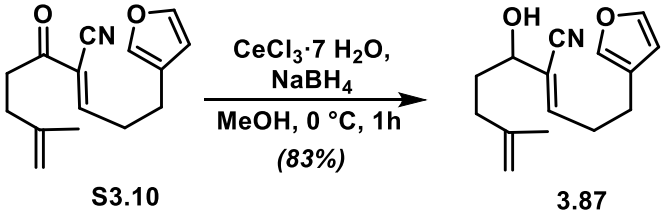

S3.10 3.87

Prepared according to general procedure B, using α,β-unsaturated ketonitrile **S3.10** *(130 mg, 0.53 mmol, 1.0 equiv.),* $CeCl_3 \cdot 7H_2O$ *(298 mg, 0.80 mmol, 1.5 equiv.), sodium borohydride (24 mg, 0.64 mmol, 1.2 equiv.), and methanol (10.0 mL).* Yield of **3.87**: 83% (108 mg, 0.44 mmol, colorless

oil); R_f = 0.38 (3:7 EtOAc/hexanes); **^{1}H NMR** (500 MHz, $CDCl_3$) δ 7.36 (s, 1H), 7.23 (s, 1H), 6.39 (t, *J* = 7.2 Hz, 1H), 6.29 (s, 1H), 4.75 (s, 1H), 4.69 (s, 1H), 4.16 (dd, *J* = 10.6, 5.8 Hz, 1H), 2.70 – 2.64 (m, 2H), 2.63 – 2.59 (m, 2H), 2.13 (d, *J* = 3.8 Hz, 1H), 2.04 (dd, *J* = 13.4, 7.0 Hz, 2H), 1.85 – 1.76 (m, 2H), 1.73 (s, 3H); **^{13}C NMR** (126 MHz, $CDCl_3$) δ 147.0, 144.7, 143.3, 139.2, 123.2, 119.7, 115.9, 111.0, 110.8, 72.3, 33.7, 33.4, 31.5, 23.8, 22.4; **HRMS** (ES+) *m/z* calc'd for $C_{15}H_{19}NO_2$ $[M]^+$: 245.1416, found 245.1422.

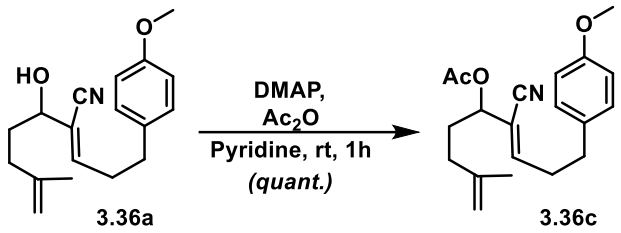

General Procedure C (acetylation of secondary and primary alcohols):

To a solution of alcohol **3.36a** (50 mg, 0.18 mmol, 1.0 equiv.) in pyridine (0.2 mL, solvent), was added acetic anhydride (0.1 mL, co-solvent) in one portion. Then, DMAP (2 mg, 0.016 mmol, 0.09 equiv.) was added and the resulting mixture was stirred at room temperature for one hour. A saturated aqueous solution of $NaHCO_3$ was added carefully in small portions until effervescence stopped (0.5 mL). The resulting mixture was diluted with H_2O (5 mL), and the aqueous phase was extracted with EtOAc (3 x 5 mL). The combined organic extracts were washed with 1N HCl (1 x 10 mL), brine (10 mL), dried over Na_2SO_4, filtered over a plug of cotton, and concentrated *in vacuo.* The resulting crude residue containing **3.36c** was sufficiently pure to carry on to the next synthetic step (EtOAc/hexanes 3:17, R_f = 0.20, colorless oil, 59 mg, 0.18 mmol, quantitative yield). **^{1}H NMR** (600 MHz, $CDCl_3$) δ 7.08 (d, *J* = 8.5 Hz, 2H), 6.83 (d, *J* = 8.6 Hz, 2H), 6.45 (t, *J* = 7.3 Hz, 1H), 5.17 (t, *J* = 6.5 Hz, 1H), 4.74 (s, 1H), 4.63 (s, 1H), 3.78 (s, 3H), 2.76 – 2.71 (m, 2H), 2.71 – 2.66 (m, 2H), 2.06 (s, 3H), 1.96 – 1.89 (m, 3H), 1.84 – 1.77 (m, 1H), 1.70 (s, 3H); **^{13}C NMR**

(151 MHz, $CDCl_3$) δ 170.1, 158.3, 151.0, 143.8, 131.8, 129.5, 115.4, 115.2, 114.1, 111.2, 73.4, 55.3, 33.6, 33.2, 33.1, 30.8, 22.3, 21.1; **HRMS** (ES+) *m/z* calc'd for $C_{20}H_{25}NO_3Na$ $[M + Na]^+$: 350.1732, found 350.1728.

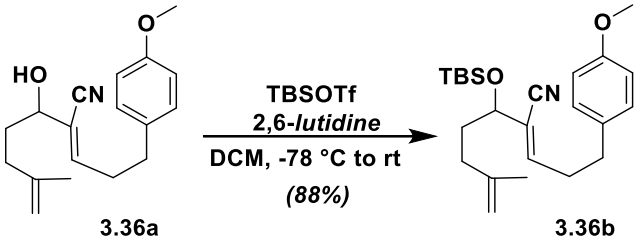

3.36a 3.36b

General Procedure D (silylation of primary and secondary alcohols using TBSOTf):

To a cooled (–78 °C) solution of alcohol **3.36a** (70 mg, 0.25 mmol, 1.0 equiv.) and 2,6-lutidine (0.11 mL, 0.98 mmol, 4.0 equiv.) in DCM (1 mL) was added TBSOTf (86 µL, 0.49 mmol, 2.0 equiv.). The mixture was stirred for one hour at ambient temperature, then methanol (0.1 mL) was added. The volatiles were removed *in vacuo*, and the resulting crude residue was directly purified via flash chromatography using a mixture of EtOAc/hexanes (3:97, R_f = 0.35) as eluent to give silyl ether **3.36b** as a colorless oil (86 mg, 0.22 mmol, 88% yield). **^{1}H NMR** (600 MHz, $CDCl_3$) δ 7.10 (d, *J* = 8.6 Hz, 2H), 6.83 (dd, *J* = 9.1, 2.4 Hz, 2H), 6.30 (t, *J* = 7.2 Hz, 1H), 4.71 (s, 1H), 4.64 (s, 1H), 4.13 (t, *J* = 5.9 Hz, 1H), 3.78 (s, 3H), 2.76 – 2.71 (m, 2H), 2.71 – 2.66 (m, 2H), 1.97 – 1.90 (m, 2H), 1.79 – 1.71 (m, 2H), 1.70 (s, 3H), 0.88 (s, 9H), 0.03 (s, 3H), -0.02 (s, 3H); **^{13}C NMR** (151 MHz, $CDCl_3$) δ 158.3, 146.0, 145.1, 132.2, 129.5, 129.4, 120.1, 116.3, 114.1, 114.0, 110.4, 72.8, 55.4, 35.2, 33.8, 32.9, 32.8, 25.9, 22.6, 18.2, –4.5, –4.8; **HRMS** (ES+) *m/z* calc'd for $C_{24}H_{37}NO_2SiNa$ $[M + Na]^+$: 422.2491, found 422.2479.

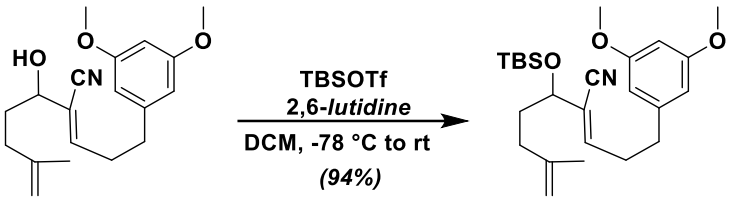

3.28a 3.28b

Prepared according to general procedure D, using alcohol **3.28a** *(50 mg, 0.159 mmol, 1.0 equiv.), TBSOTf (56 µL, 0.32 mmol, 2.0 equiv.) and 2,6-lutidine (73 µL, 0.63 mmol, 4.0 equiv.).* Yield of **3.28b**: 94% (64 mg, 0.15 mmol, colorless oil); R_f = 0.35 (7:93 EtOAc/hexanes). **^{1}H NMR** (500 MHz, $CDCl_3$) δ 6.34 (d, *J* = 2.2 Hz, 2H), 6.32 – 6.27 (m (overlapping), 5H), 4.71 (s, 1H), 4.64 (s, 1H), 4.13 (t, *J* = 5.9 Hz, 1H), 3.78 (s, 6H), 2.73 –2.74 (m, 4H), 1.94 (dd, *J* = 15.8, 6.3 Hz, 2H), 1.79 – 1.70 (m, 2H), 0.88 (s, 9H), 0.03 (s, 3H), -0.03 (s, 3H); **^{13}C NMR** (126 MHz, $CDCl_3$) δ 161.1, 145.7, 145.0, 142.4, 120.3, 116.3, 110.4, 106.5, 98.5, 72.8, 55.4, 35.2, 34.9, 32.9, 32.2, 25.8, 22.6, 18.2, –4.5, –4.9; **HRMS** (ES+) *m/z* calc'd for $C_{25}H_{39}NO_3SiNa$ $[M + Na]^+$: 452.2597, found 452.2592.

Synthesis and Characterization of C2 Oxygenated Substrates:

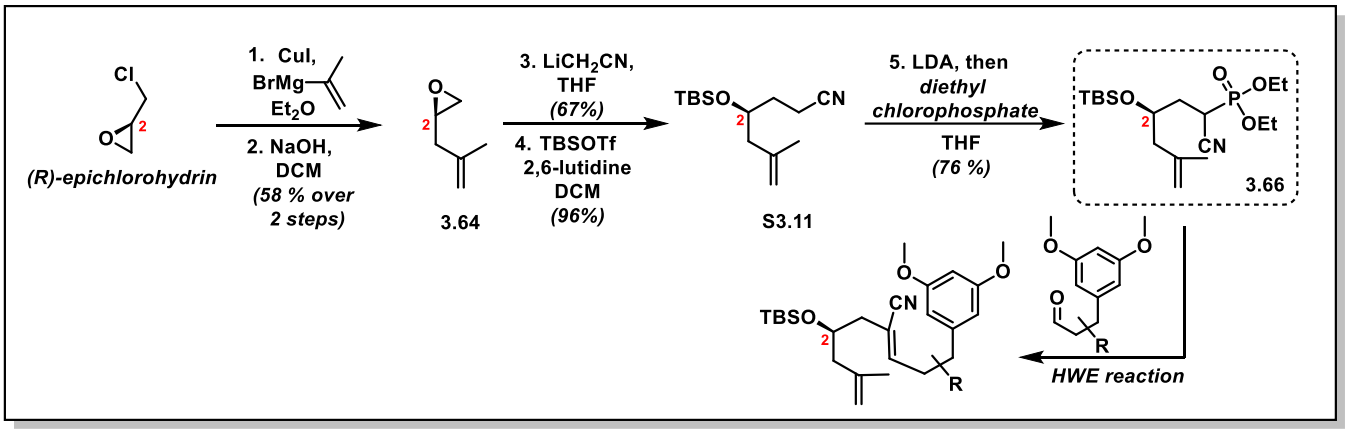

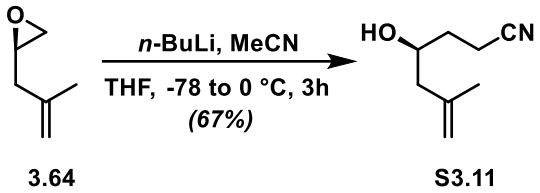

To a solution of acetonitrile (2.24 mL, 41.1 mmol, 2.0 equiv.) in THF (70 mL) was added *n*-butyllithium (1.6 M in hexanes, 18.7 mL, 30.0 mmol, 1.4 equiv.) at –78 °C. The resulting solution was stirred for 1 h, then a solution of epoxide **3.64**[38] (2.1 g, 21.4 mmol, 1.0 equiv.) in THF (10 mL) was added over a period of 3 min. The mixture was warmed to 0 °C, stirred for 3 h and then quenched with satd. $NH_4Cl_{(aq)}$ (30 mL). The aqueous phase was extracted with EtOAc (3 x 20 mL), the combined organic extracts were washed with brine, dried over Na_2SO_4, filtered and concentrated *in vacuo.* The resulting crude residue was purified via flash column chromatography using a mixture of EtOAc/ hexanes (30:70) as eluent to give **S3.11** as a colorless oil (2.00 g, 14.3 mmol, 67% yield). **^{1}H NMR** (600 MHz, $CDCl_3$) δ 4.93 (s, 1H), 4.82 (s, 1H), 3.84 (tt, *J* = 9.2, 3.4 Hz, 1H), 2.54 (td, *J* = 7.1, 3.9 Hz, 2H), 2.21 (dd, *J* = 13.6, 3.6 Hz, 1H), 2.14 (dd, *J* = 13.6, 9.3 Hz, 1H), 1.89 – 1.82 (m, 2H), 1.77 (s, 3H), 1.75 – 1.68 (m, 1H); **^{13}C NMR** (151 MHz, $CDCl_3$) δ 141.8,

120.0, 114.5, 66.6, 46.2, 32.5, 22.5, 13.9; **HRMS** (ES+) *m/z* calc'd for $C_{16}H_{26}N_2O_2Na$ [2M +Na]$^+$: 301.1892, found 301.1892; $[\alpha]_D^{22} = -49.0$ $(c = 1.0, CHCl_3)$.

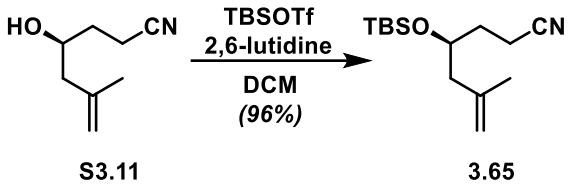

Prepared according to <u>general procedure D</u>, using alcohol **S3.11** *(2.0 g, 14.3 mmol, 1.0 equiv.), TBSOTf (4.96 mL, 21.6 mmol, 1.5 equiv.) and 2,6-lutidine (5.0 mL, 43.2 mmol, 3.0 equiv.).* Yield of **3.65**: 96% (3.5 g, 13.7 mmol, colorless oil); R_f = 0.25 (1:9 EtOAc/hexanes). **^{1}H NMR** (500 MHz, $CDCl_3$) δ 4.80 (s, 1H), 4.72 (s, 1H), 4.01 – 3.82 (m, 1H), 2.46 – 2.34 (m, 2H), 2.28 (dd, *J* = 13.6, 4.9 Hz, 1H), 2.12 (dd, *J* = 13.6, 8.3 Hz, 1H), 1.91 – 1.82 (m, 1H), 1.73 (s, 3H), 1.66 (td, *J* = 14.1, 6.9 Hz, 1H), 0.89 (s, 9H), 0.09 (s, 3H), 0.09 (s, 3H); **^{13}C NMR** (126 MHz, $CDCl_3$) δ 141.8, 120.1, 113.9, 68.8, 46.0, 32.0, 25.9, 23.0, 18.1, 13.2, –4.2, –4.7; **HRMS** (ES+) *m/z* calc'd for $C_{14}H_{27}NOSiNa$ [M +Na]$^+$: 276.1760, found 276.1764; $[\alpha]_D^{22} = -22.7$ $(c = 0.8, CHCl_3)$.

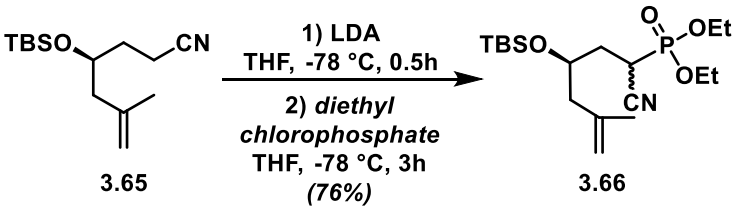

To a solution of diisopropylamine (2.08 mL, 14.7 mmol, 2.2 equiv.) in THF (25 mL) was added *n*-butyllithium (1.6 M in hexanes, 8.79 mL, 14.1 mmol, 2.1 equiv.) at –78 °C. The mixture was allowed to warm to 0 °C, stirred for 30 minutes and cooled back down to –78 °C. A solution of nitrile **3.65** (1.7 g, 6.7 mmol, 1.0 equiv.) in THF (5 mL) was added dropwise and the mixture was stirred for 30 minutes at –78 °C. Diethyl chlorophosphate (1.07 mL, 7.37 mmol, 1.1 equiv.) was added dropwise (neat). After stirring for 3 hours at –78 °C, satd. $NH_4Cl_{(aq)}$ (30 mL) was added to

the reaction mixture. The aqueous phase was extracted with EtOAc (3 x 20 mL), the combined organic extracts were washed with brine, dried over Na_2SO_4, filtered and concentrated *in vacuo.* The resulting crude residue was purified via flash column chromatography, using a mixture of EtOAc/hexanes (30:70) as eluent to give an inconsequential mixture (2:1) of cyanophosphonate **3.66** diastereomers as a colorless oil (1.98 g, 5.1 mmol, 76% yield). *Note: signals are reported for the major diastereomer only*. **^{1}H NMR** (500 MHz, $CDCl_3$) δ4.81 (*major*-s, 1H), 4.74 (*major*-s, 1H), 4.29 – 4.18 (*overlapping* m, 4H), 4.05 – 3.99 (*major*-m, 1H), 3.17 (*overlapping* -ddd, *J* = 23.2, 12.4, 3.3 Hz, 1H), 2.38 (*major*-dd, *J* = 13.6, 4.0 Hz, 1H), 2.27 (*major*-qd, *J* = 13.7, 6.5 Hz, 1H), 2.15 (*overlapping*- dd, *J* = 13.6, 9.0 Hz, 1H), 2.03 – 1.92 (*overlapping* m, 1H), 1.83 – 1.76 (*major*-m, 1H), 1.74 (*major*- s, 3H), 1.37 (*overlapping*- t, *J* = 7.1 Hz, 6H), 0.89 (*overlapping*- s, 9H), 0.14 (*major*-s, 3H), 0.12 (*major*-s, 3H); **^{13}C NMR** (126 MHz, $CDCl_3$) δ141.19 (*major*), 116.24 (*major*-d, *J* = 9.3 Hz), 114.07 (*major*), 67.93 (d, *J* = 13.8 Hz), 64.04 (*major*-d, *J* = 6.9 Hz), 63.72 (*major*-d, *J* = 6.8 Hz), 46.48 (*major*), 33.78 (*major*-d, *J* = 4.0 Hz), 26.96 (*major*-d, *J* = 145.5 Hz), 25.85 (*overlapping*), 22.85 (*major*), 18.01 (*major*), 16.41 (*overlapping*-d, *J* = 3.2 Hz), 16.37 (*overlapping*-d, *J* = 3.2 Hz), –4.05 (*major*), –4.77 (*major*); **HRMS** (ES+) *m/z* calc'd for $C_{18}H_{36}NO_4PSiNa$ $[M+Na]^+$: 412.2044, found 412.2036; $[\alpha]_D^{22} = -18.0\ (c = 0.9, CHCl_3)$.

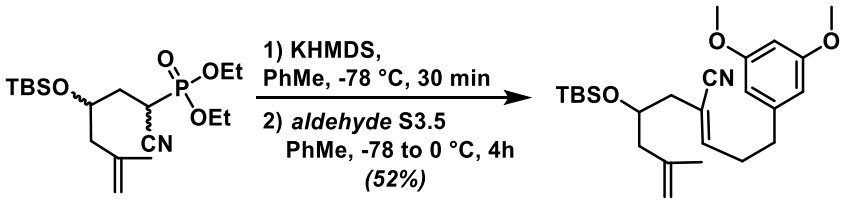

3.66 (*racemic*) **3.25b**

General Procedure E (HWE reaction for the synthesis of α,β-unsaturated nitrile substrates):

To a cooled (−78 °C) solution of racemic cyanoalkylphosphonate **3.66**[27] (1.02 g, 2.62 mmol, 1.0 equiv.) in dry toluene (30 mL) was added dropwise a solution of KHMDS (0.5 M in toluene, 5.2

mL, 2.62 mmol, 1.0 equiv.). After stirring for 30 min at −78 °C, a solution of aldehyde **S5**[45] (509 mg, 2.62 mmol, 1.0 equiv.) in dry toluene (5 mL) was added dropwise. The resulting solution was stirred at −78 °C for 1 h then warmed to 4 °C. After stirring for 3 hours, $NH_4Cl_{(aq)}$ (20 mL) was added and the aqueous layer was extracted with Et_2O (3 x 20 mL). The combined organic extracts were washed with brine (20 mL), dried over Na_2SO_4, filtered and concentrated *in vacuo*. The resulting crude residue was purified via flash column chromatography (EtOAc/hexanes 3:97, R_f= 0.15) to give **3.25b** as a colorless oil (586 mg, 1.36 mmol, 52% yield, 1:4 *E*:*Z*, separable). *Note:* This reaction is selective for *Z-α,β-unsaturated nitrile* products (*E:Z* ranged from 1:4 to 1:20). **^{1}H NMR** (500 MHz, $CDCl_3$) δ 6.34 (d, *J* = 2.1 Hz, 2H), 6.32 (t, *J* = 2.2 Hz, 1H), 6.16 (t, *J* = 6.0 Hz, 1H), 4.79 (s, 1H), 4.69 (s, 1H), 3.98 (tt, *J* = 7.4, 5.3 Hz, 1H), 3.78 (s, 6H), 2.75 – 2.62 (m, 4H), 2.37 (dd, *J* = 14.0, 4.0 Hz, 1H), 2.20 (dd, *J* = 13.9, 5.0 Hz, 1H), 2.17 (dd, *J* = 14.1, 7.6 Hz, 1H), 2.10 (dd, *J* = 13.6, 7.4 Hz, 1H), 1.73 (s, 3H), 0.87 (s, 9H), 0.06 (s, 3H), 0.05 (s, 3H); **^{13}C NMR** (126 MHz, $CDCl_3$) δ 161.1, 149.1, 142.7, 142.1, 117.8, 113.9, 112.8, 106.6, 98.4, 69.0, 55.4, 46.0, 41.7, 35.0, 33.0, 26.0, 23.1, 18.2, –4.4, –4.5; **HRMS** (ES+) *m/z* calc'd for $C_{25}H_{39}NO_3SiNa$ [M + Na]$^+$: 452.2597, found 452.2599.

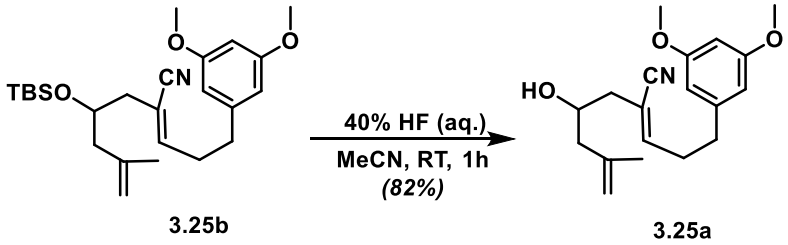

3.25b **3.25a**

General Procedure F (deprotection of silyl-protected secondary and primary alcohols):

To a solution of silyl ether **3.25b** (50 mg, 0.116 mmol, 1.0 equiv.) in acetonitrile (0.25 mL), was added an aqueous solution of hydrofluoric acid (0.2 mL, 40% w/w). The resulting mixture was stirred for 2 hours, then ether (5 mL) and water (5 mL) were added and the phases were separated.

The aqueous phase was extracted with diethyl ether (3 x 5 mL), the combined organic phases were washed with brine, dried over Na_2SO_4 and concentrated *in vacuo*. The resulting crude residue was purified via flash column chromatography (EtOAc/hexanes 7:15, R_f = 0.25) to give **3.25a** as a colorless oil (30 mg, 0.095 mmol, 82%). **^{1}H NMR** (600 MHz, $CDCl_3$) δ 6.34 (s, 2H), 6.31 (s, 1H), 6.22 (t, *J* = 7.2 Hz, 1H), 4.89 (s, 1H), 4.78 (s, 1H), 3.92 – 3.87 (m, 1H), 3.77 (s, 6H), 2.75 – 2.72 (m, 4H), 2.34 (dd, *J* = 14.1, 3.8 Hz, 1H), 2.28 (dd, *J* = 14.1, 8.0 Hz, 1H), 2.13 (dd, *J* = 13.6, 3.5 Hz, 1H), 2.07 (dd, *J* = 13.5, 9.1 Hz, 1H), 1.83 (broad s, 1H), 1.74 (s, 3H); **^{13}C NMR** (151 MHz, $CDCl_3$) δ 161.0, 149.4, 142.5, 142.0, 117.7, 114.2, 112.2, 106.6, 98.4, 66.9, 55.4, 45.4, 41.6, 34.9, 32.9, 22.4; **HRMS** (ES+) *m/z* calc'd for $C_{19}H_{25}NO_3Na$ $[M + Na]^+$: 338.1732, found 338.1730.

E. Synthesis and Characterization of C3 Oxygenated Substrates:

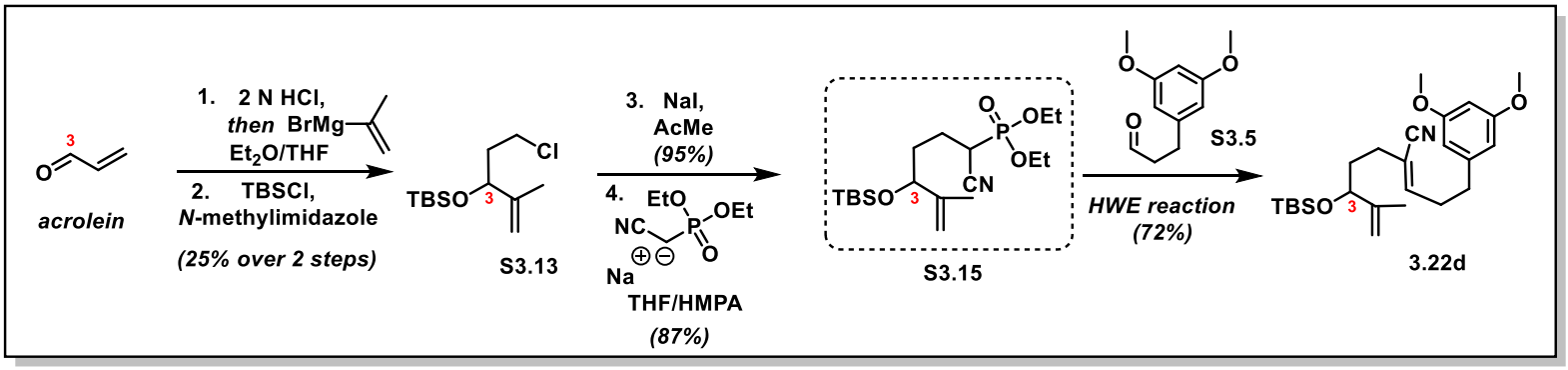

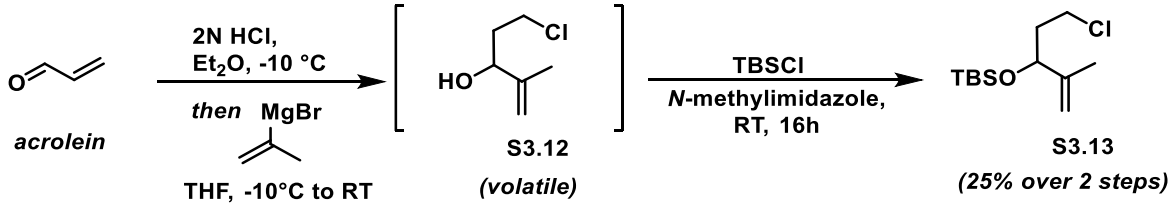

To a solution of acrolein (1.3 mL, 20 mmol, 1.0 equiv) in dry Et_2O (60 mL), 2 N HCl in Et_2O (10 mL, 20 mmol, 1.0 equiv.) was added dropwise while maintaining the ice bath temperature below –10 °C. The mixture was stirred at this temperature for 3 hours, then a solution of isopropenylmagnesium bromide (0.5 M in THF, 21 mmol, 42 mL, 1.05 equiv.) was added

dropwise (keeping ice bath below –10 °C) and the resulting solution was stirred at ambient temperature. After 16 hours, satd. $NH_4Cl_{(aq)}$ (30 mL) was added to the reaction mixture. The aqueous layer was extracted with Et_2O (2 x 20 mL) and the combined organic extracts were concentrated via distillation under atmospheric pressure using a Vigreux condenser (*note: the product is volatile*). The resulting crude residue containing **S3.12** (5-chloro-2-methylpent-1-en-3-ol) was dissolved in *N*-methylimidazole (1.5 mL), then TBSCl (1.2 g, 7.96 mmol) was added and the reaction mixture was stirred vigorously at room temperature. After 12 hours, stirring was stopped and the biphasic mixture was allowed to settle. The top phase was removed using a Pasteur pipette, and the lower phase was extracted twice with hexanes (5 mL). Combined organic extracts were washed with brine, dried over Na_2SO_4, and concentrated in vacuo. The resulting crude residue was purified via flash column chromatography, using Et_2O/hexanes (1:99) as eluent to give silyl ether **S3.13** as a clear colorless oil (1.24 g, 5.0 mmol, 25% yield over 2 steps). **^{1}H NMR** (600 MHz, $CDCl_3$) δ 4.93 (s, 1H), 4.81 (s, 1H), 4.25 (dd, *J* = 8.1, 4.3 Hz, 1H), 3.60 (ddd, *J* = 10.6, 8.2, 6.2 Hz, 1H), 3.56 – 3.51 (m, 1H), 1.98 (ddt, *J* = 14.0, 8.0, 5.8 Hz, 1H), 1.89 – 1.82 (m, 1H), 1.69 (s, 3H), 0.89 (s, 9H), 0.07 (s, 3H), 0.02 (s, 3H); ^{13}C NMR (151 MHz, $CDCl_3$) δ 147.0, 111.6, 73.6, 41.9, 39.3, 26.0, 18.3, 17.3, –4.6, –5.1; **HRMS** (GC-CI) *m/z* calc'd for $C_{12}H_{25}ClOSiH$ $[M + H]^+$: 249.1441, found 249.1444.

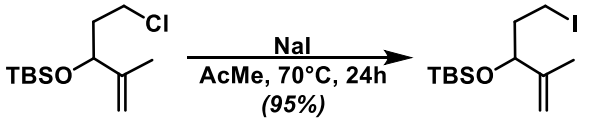

S3.13 **S3.14**

To a solution of chloride **S3.13** (2.6 g, 10.5 mmol, 1.0 equiv.) in dry acetone (20 mL) was added sodium iodide (4.7 g, 31.6 mmol, 3.0 equiv.) and the resulting suspension was heated to reflux under argon for 24 hours. After cooling to ambient temperature, the suspension was carefully

concentrated under reduced pressure, dissolved in H_2O/hexanes (20 mL: 30 mL), separated, and the aqueous phase was extracted with hexanes (2 x 20 mL). The combined organic extracts were washed with brine (10 mL), dried over Na_2SO_4, and concentrated in vacuo to give iodide **S3.14** as a clear colorless oil (3.4 g, 10.0 mmol, 95% yield) which was used in the next step without further purification. **^{1}H NMR** (499 MHz, $CDCl_3$) δ 4.94 (s, 1H), 4.82 (s, 1H), 4.12 (dd, *J* = 7.3, 4.8 Hz, 1H), 3.22 – 3.10 (m, 2H), 2.08 – 2.00 (m, 1H), 1.98 – 1.91 (m, 1H), 1.68 (s, 3H), 0.89 (s, 9H), 0.09 (s, 3H), 0.03 (s, 3H); **^{13}C NMR** (151 MHz, $CDCl_3$) δ 146.6, 111.8, 76.5, 40.3, 26.0, 17.3, 3.2, –4.6, –4.8; **HRMS** (ES+) *m/z* calc'd for $C_{12}H_{25}IOSiH$ $[M + H]^+$: 341.0797, found 341.0799.

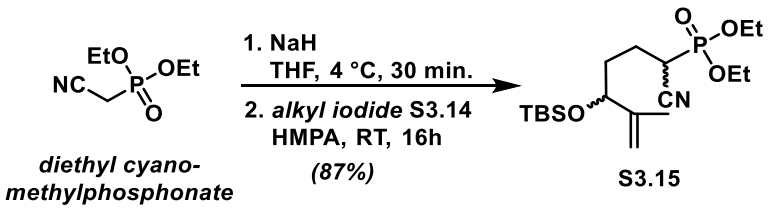

To a cooled (4 °C) suspension of sodium hydride (60% in mineral oil, 680 mg, 17 mmol, 1.7 equiv.) in THF (30 mL), diethyl cyanomethylphosphonate (2.75 mL, 17 mmol, 1.7 equiv.) was added dropwise. After stirring for 1 hour, HMPA (4 mL) and solution of alkyl iodide **S3.14** (3.4 g, 10 mmol, 1.0 equiv.) in THF (5.0 mL) were added. After stirring for 16 hours, H_2O (20 mL) was added and the aqueous phase was extracted with EtOAc (3 x 30 mL). The combined organic extracts were washed with H_2O (3 x 20 mL) and brine (20 mL), dried over Na_2SO_4, filtered and concentrated *in vacuo.* The resulting crude residue was purified via flash column chromatography (EtOAc/hexanes 2:3) to give **S3.15** as a colorless oil (3.38 g, 8.7 mmol, 87% yield). *Note: 1:1 diastereomeric mixture, signals listed for both:* **^{1}H NMR** (500 MHz, $CDCl_3$) δ 4.93 (s, 1H), 4.91 (s, 1H), 4.83 (s, 1H), 4.81 (s, 1H), 4.29 – 4.17 (m, 8H), 4.13 – 4.05 (m, 2H), 3.06 – 2.88 (m, 2H), 2.02 – 1.74 (m, 6H), 1.71 – 1.63 (m, 2H), 1.68 (s, 3H), 1.67 (s, 3H), 1.37 (t, *J* = 7.1 Hz, 12H), 0.90 (s, 9H), 0.89 (s, 9H), 0.05 (s, 6H), 0.01 (s, 3H), 0.01 (s, 3H); **^{13}C NMR** (151 MHz, $CDCl_3$) δ 146.7,

146.2, 116.5 (d, *J* = 3.7 Hz), 116.4 (d, *J* = 3.7 Hz), 111.6, 111.58, 75.7, 75.2, 64.1 – 64.0 (*overlapping* m, 2C), 63.7 (d, *J* = 6.8 Hz), 34.0 (d, *J* = 11.7 Hz), 33.3 (d, *J* = 11.7 Hz), 30.5 (d, *J* = 15.0 Hz), 29.6 (d, *J* = 15.0 Hz), 25.9, 25.8, 23.3 (d, *J* = 4.1 Hz), 22.7 (d, *J* = 4.1 Hz), 17.9, 17.4, 16.50, 16.46, –4.7, –4.8, –5.09, –5.13; **HRMS** (ES+) *m/z* calc'd for $C_{18}H_{36}NO_4PSiNa$ $[M + Na]^+$: 412.2049, found 412.2051.

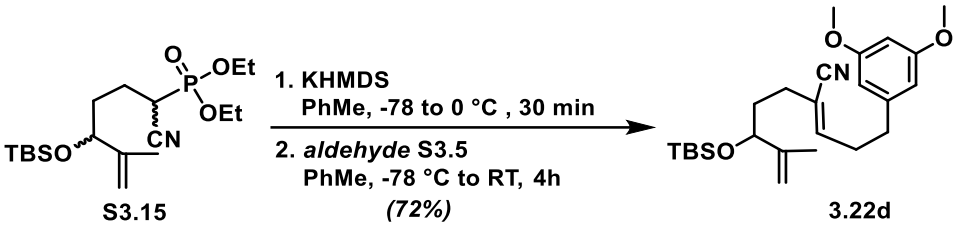

Prepared according to general procedure E, using cyanoalkylphosphonate **S3.15** *(1.03 mmol) and aldehyde* **S3.5**[45] *(1.03 mmol) to give a 1:5 (E:Z) mixture of α,β-unsaturated nitriles*. Yield of **3.22d**: 72% (320 mg, 0.74 mmol, colorless oil); R_f= 0.20 (4:96 EtOAc/hexanes); **^{1}H NMR** (600 MHz, $CDCl_3$) δ 6.34 (d, *J* = 2.2 Hz, 2H), 6.32 (t, *J* = 2.2 Hz, 1H), 6.12 (t, *J* = 7.2 Hz, 1H), 4.86 (s, 1H), 4.79 (s, 1H), 4.03 – 3.99 (m, 1H), 3.78 (s, 6H), 2.73 – 2.63 (m, 4H), 2.23 – 2.10 (m, 2H), 1.74 – 1.67 (m, 1H), 1.66 (s, 3H), 1.65 – 1.61 (m, 1H), 0.88 (s, 9H), 0.03 (s, 3), 0.00 (s, 3H); **^{13}C NMR** (151 MHz, $CDCl_3$) δ 161.0, 146.9, 146.3, 142.7, 117.7, 115.5, 111.5, 106.6, 98.4, 75.5, 55.4, 35.1, 34.6, 32.8, 30.3, 25.9, 18.3, 17.4, –4.6, –5.0; **HRMS** (ES+) *m/z* calc'd for $C_{25}H_{39}NO_3SiNa$ $[M + Na]^+$: 452.2597, found 452.2593.

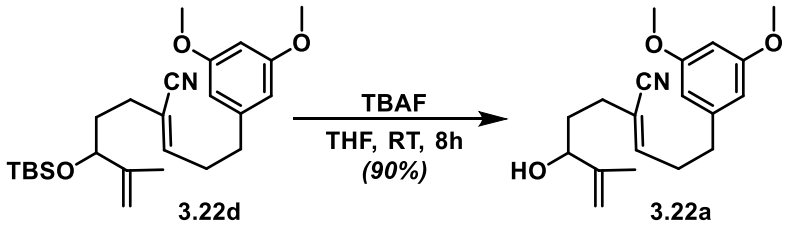

To a cooled (4 °C) solution of silyl ether **3.22d** (150 mg, 0.35 mmol, 1.0 equiv.) in dry THF (1.0 mL) was added TBAF (1 M in THF, 0.47 mL, 0.47 mmol, 1.3 equiv.) and the mixture was stirred while warming to ambient temperature. When the reaction was complete (as indicated by TLC), the volatiles were removed under reduced pressure. The resulting crude residue was directly purified via flash column chromatography on SiO_2, using a mixture of EtOAc/hexanes (4:6, R_f = 0.30) as eluent to give **3.22a** as a colorless oil (99 mg, 0.32 mmol, 90% yield); **^{1}H NMR** (600 MHz, $CDCl_3$) δ 6.33 (d, *J* = 2.0 Hz, 2H), 6.31 (d, *J* = 2.1 Hz, 1H), 6.16 (t, *J* = 6.6 Hz, 1H), 4.92 (s, 1H), 4.84 (s, 1H), 3.87 – 3.84 (m, 1H), 3.78 (s, 6H), 2.77 – 2.65 (m, 4H), 2.30 – 2.24 (m, 2H), 1.77 – 1.71 (m, 1H), 1.70 (s, 3H), 1.68 – 1.62 (m, 1H); **^{13}C NMR** (151 MHz, $CDCl_3$) δ 161.0, 147.4, 147.1, 142.7, 117.6, 115.0, 111.1, 106.7, 98.3, 74.0, 55.4, 35.0, 33.0, 32.8, 30.5, 17.9; **HRMS** (ES+) *m/z* calc'd for $C_{19}H_{25}NO_3Na$ $[M + Na]^+$: 338.1732, found 338.1718.

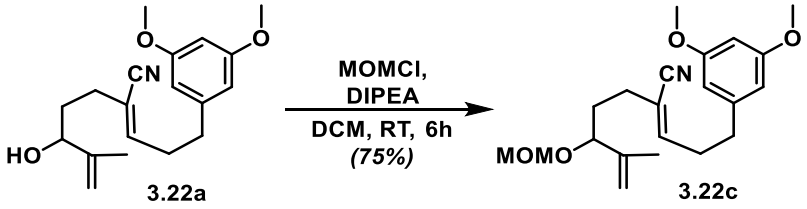

To a solution of secondary alcohol **3.22a** (15 mg, 0.048 mmol, 1 equiv.) in DCM (1.0 mL), was added *N*,*N*-diisopropylethylamine (33 µL, 0.190 mmol, 4 equiv.), followed by chloromethyl methyl ether (technical grade, 7.0 µL, 0.095 mmol, 2.0 equiv.). The reaction mixture was stirred at room temperature for 6 hours until completion (as indicated by TLC), then volatiles were removed under reduced pressure. The resulting crude residue was directly purified via flash column chromatography on SiO_2, using a mixture of EtOAc/hexanes (1:4, R_f = 0.20) as eluent to give methoxymethyl-ether **3.22c** as a colorless oil (13 mg, 0.036 mmol, 75% yield). **^{1}H NMR** (600 MHz, $CDCl_3$) δ 6.34 (d, *J* = 2.1 Hz, 2H), 6.32 (t, *J* = 2.1 Hz, 1H), 6.16 (t, *J* = 6.2 Hz, 1H), 4.94 (s, 1H), 4.91 (s, 1H), 4.59 (d, *J* = 6.7 Hz, 1H), 4.48 (d, *J* = 6.7 Hz, 1H), 3.93 (dd, *J* = 7.6, 5.7 Hz, 1H),

3.78 (s, 6H), 3.36 (s, 3H), 2.72 – 2.66 (m, 4H), 2.32 – 2.26 (m, 1H), 2.23 – 2.15 (m, 1H), 1.84 – 1.76 (m, 1H), 1.73 – 1.67 (m, 1H), 1.65 (s, 3H); **^{13}C NMR** (151 MHz, $CDCl_3$) δ 161.0, 146.8, 143.4, 142.6, 117.6, 115.1, 114.5, 106.6, 98.4, 93.9, 78.8, 55.8, 55.4, 35.1, 32.8, 32.1, 30.7, 17.0; **HRMS** (ES+) *m/z* calc'd for $C_{21}H_{29}NO_4Na$ $[M + Na]^+$: 383.2028, found 383.2019.

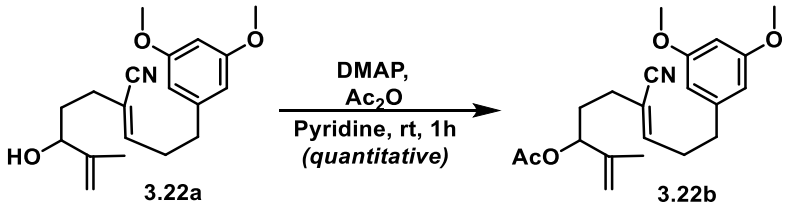

Prepared according to general procedure C, using secondary alcohol **3.22a** *(15 mg, 0.048 mmol, 1.0 equiv.), pyridine (0.15 mL, solvent), acetic anhydride (0.15 mL, co-solvent) and DMAP (1 mg).* Yield of acetate **3.22b**: quantitative (16 mg, 0.048 mmol, colorless oil); R_f= 0.20 (1:9 EtOAc/hexanes). **^{1}H NMR** (600 MHz, $CDCl_3$) δ 6.34 (d, *J* = 1.7 Hz, 1H), 6.32 (t, *J* = 1.9 Hz, 1H), 6.15 (t, *J* = 7.2 Hz, 1H), 5.13 (t, *J* = 6.2 Hz, 1H), 4.93 (s, 1H), 4.91 (s, 1H), 3.78 (s, 6H), 2.72 – 2.65 (m, 4H), 2.24 – 2.12 (m, 2H), 2.07 (s, 3H), 1.89 – 1.77 (m, 2H), 1.72 (s, 3H); **^{13}C NMR** (151 MHz, $CDCl_3$) δ 170.3, 161.0, 147.1, 142.6, 142.5, 117.4, 114.5, 113.3, 106.6, 98.4, 76.0, 55.4, 35.0, 32.8, 31.2, 30.4, 21.3, 18.3; **HRMS** (ES+) *m/z* calc'd for $C_{21}H_{27}NO_4Na$ $[M + Na]^+$: 381.1871, found 381.1857.

Synthesis and Characterization of C18/19 Oxygenated Substrates

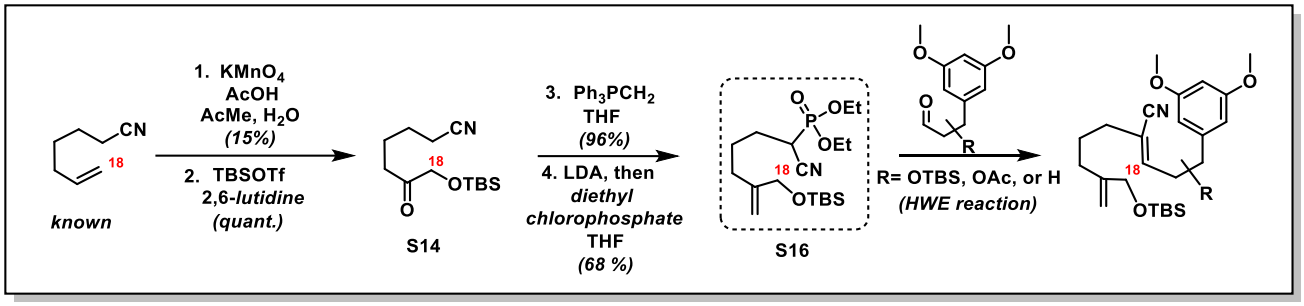

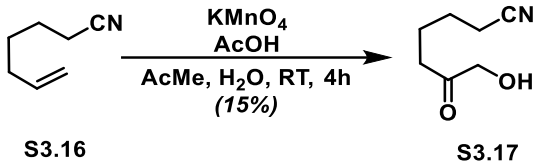

Procedure for the preparation of **S3.17** *was adapted from a report by Bonini et al.*[48]: To a solution of olefin **S3.16**[49] (1.60 g, 14.7 mmol, 1.0 equiv.) in acetone/water/acetic acid (200:50:15 mL) was added $KMnO_4$ (8.53 g, 54.0 mmol, 1.8 equiv.) as a solution in acetone/water (90:30 mL). The resulting mixture was stirred at room temperature for 4 hours, then solid $NaHCO_3$ was added carefully in small portions until effervescence stopped. The mixture was filtered over a pad of Celite, and the acetone was removed under reduced pressure. The resulting aqueous phase was extracted with EtOAc (3 x 100 mL), the combined organic phases were dried over Na_2SO_4, filtered and concentrated *in vacuo.* The resulting crude residue was purified via flash column chromatography, using a mixture of EtOAc/hexanes (4:1, R_f= 0.25) as eluent to give **S3.17** as a colorless oil (650 mg, 4.6 mmol, 15% yield). **^{1}H NMR** (500 MHz, $CDCl_3$) δ 4.24 (d, *J* = 4.3 Hz, 2H), 3.06 (t, *J* = 4.5 Hz, 1H), 2.48 (t, *J* = 7.1 Hz, 2H), 2.37 (t, *J* = 7.0 Hz, 2H), 1.85 – 1.75 (m, 2H), 1.73 – 1.62 (m, 2H); **^{13}C DEPTQ** (126 MHz, $CDCl_3$) δ 208.8, 119.3, 68.3, 37.3, 24.9, 22.5, 17.2; **HRMS** (ES+) *m/z* calc'd for $C_7H_{11}NO_2Na$ $[M + H]^+$: 164.0687, found 164.0690.

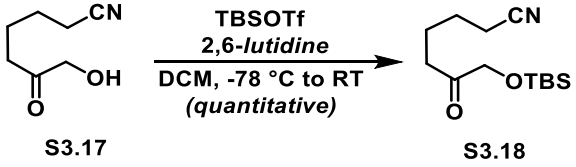

Prepared according to general procedure B, using allylic alcohol **S3.17** *(180 mg, 1.28 mmol, 1.0 equiv.), TBSOTf (446 µL, 2.55 mmol, 2.0 equiv.) and 2,6-lutidine (591 µL, 5.10 mmol).* Yield of **S3.18**: quantitative (327 mg, 1.28 mmol, colorless oil); R_f= 0.30 (1:3 EtOAc/hexanes). **^{1}H NMR** (500 MHz, $CDCl_3$) δ 4.14 (s, 2H), 2.57 (t, *J* = 6.8 Hz, 2H), 2.35 (t, *J* = 6.9 Hz, 2H), 1.78 – 1.64 (m, 4H), 0.92 (s, 9H), 0.08 (s, 6H); **^{13}C DEPTQ** (126 MHz, $CDCl_3$) δ 210.4, 119.5, 69.4, 37.3, 25.9, 25.1, 22.3, 18.4, 17.3, –5.4; **HRMS** (ES+) *m/z* calc'd for $C_{13}H_{25}NO_2SiNa$ $[M + Na]^+$: 278.1552, found 278.1550.

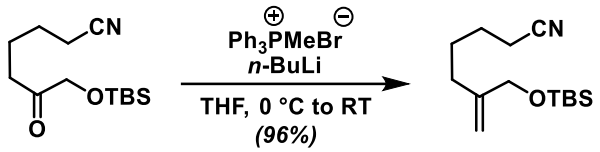

S3.18 **S3.19**

To a cooled (–78 °C) suspension of methyltriphenylphosphonium bromide (1.73 g, 4.84 mmol, 1.3 equiv.) in THF (30 mL) was added *n*-butyllithium (2.5M in hexanes, 1.79 mL, 4.46 mmol, 1.2 equiv.). The dry ice bath was removed and the mixture was stirred for 30 minutes. Then, a solution of **S3.18** (950 mg, 3.72 mmol, 1.0 equiv.) in THF (10 mL) was added and the mixture was warmed to ambient temperature. After 2 hours of stirring, satd. $NH_4Cl_{(aq)}$ (20 mL) was added and the phases were separated. The aqueous phase was extracted with Et_2O (3 x 20 mL), the combined organic extracts were washed with brine (30 mL), dried over Na_2SO_4, filtered and concentrated *in vacuo*. The resulting crude residue was purified via flash column chromatography, using a mixture of EtOAc/hexanes (1:9, R_f= 0.44) as eluent to give **S3.19** as a colorless oil (905 mg, 3.57 mmol, 96% yield); **^{1}H NMR** (600 MHz, $CDCl_3$) δ 5.05 (d, *J* = 1.6 Hz, 1H), 4.82 (dd, *J* = 2.7, 1.3 Hz, 1H), 4.06 (s, 2H), 2.35 (t, *J* = 7.0 Hz, 2H), 2.06 (t, *J* = 7.4 Hz, 2H), 1.71 – 1.65 (m, 2H), 1.64 – 1.60 (m, 2H), 0.91 (s, 9H), 0.07 (s, 6H); **^{13}C DEPTQ** (151 MHz, $CDCl_3$) δ 147.6, 119.8, 109.5, 65.9, 31.9, 26.8,

26.0, 25.2, 18.5, 17.2, –5.3; **HRMS** (ES+) *m/z* calc'd for $C_{14}H_{27}NOSiNa$ [M + Na]$^+$: 276.1760, found 276.1749.

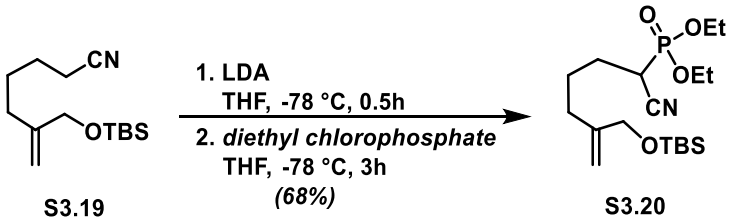

S3.19 S3.20

To a solution of diisopropylamine (337 µL, 2.39 mmol, 2.2 equiv.) in THF (5 mL) was added *n*-butyllithium (2.5M in hexanes, 0.91 mL, 2.27 mmol, 2.1 equiv.) at –78 °C. The mixture was allowed to warm to 0 °C, stirred for 30 minutes and cooled back down to –78 °C. A solution of nitrile **S3.19** (275 mg, 1.08 mmol, 1.0 equiv.) in THF (5 mL) was added dropwise and the mixture was stirred for 30 minutes at –78 °C. Diethyl chlorophosphate (172 µL, 1.19 mmol, 1.1 equiv.) was added dropwise (neat). After stirring for 3 hours at –78 °C, satd. $NH_4Cl_{(aq)}$ (10 mL) was added to the reaction mixture. The aqueous phase was extracted with EtOAc (3 x 10 mL), the combined organic extracts were washed with brine (20 mL), dried over Na_2SO_4, filtered and concentrated *in vacuo.* The resulting crude residue was purified via flash column chromatography, using a mixture of EtOAc/hexanes (30:70) as eluent to give **S3.20** as a colorless oil (287 mg, 0.73 mmol, 68% yield). **^{1}H NMR** (600 MHz, $CDCl_3$) δ 5.06 (s, 1H), 4.83 (s, 1H), 4.30 – 4.17 (m, 4H), 4.06 (s, 2H), 2.90 (ddd, *J* = 23.7, 10.0, 4.7 Hz, 1H), 2.13 – 2.03 (m, 2H), 1.96 – 1.80 (m, 3H), 1.68 – 1.56 (m, 1H), 1.38 (t, *J* = 7.1 Hz, 6H), 0.90 (s, 9H), 0.06 (s, 6H); **^{13}C DEPTQ NMR** (151 MHz, $CDCl_3$) δ 147.2, 116.3 (d, *J* = 9.3 Hz), 109.7, 65.9, 64.2 (d, *J* = 7.0 Hz), 63.8 (d, *J* = 6.8 Hz), 31.8, 30.1 (d, *J* = 143.7 Hz), 26.8 (d, *J* = 4.3 Hz), 26.03, 25.97, 16.54 (d, *J* = 3.1 Hz), 16.50 (d, *J* = 3.1 Hz), –5.2; **HRMS** (ES+) *m/z* calc'd for $C_{18}H_{36}NO_4PSiNa$ [M + Na]$^+$: 412.2049, found 412.2032.

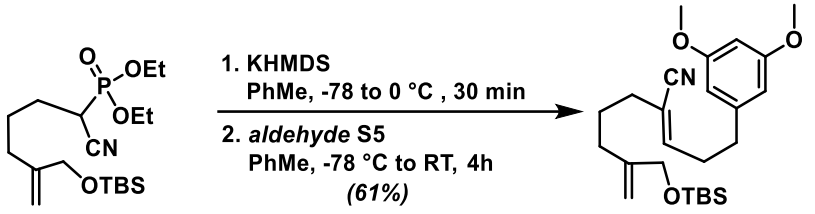

S3.20 3.40

Prepared according to general procedure E, using cyanoalkylphosphonate **S3.20** *(390 mg, 1.0 mmol, 1.0 equiv.) and aldehyde* **S3.5**[45] *(194 mg, 1.0 mmol, 1.0 equiv.) to give a 1:12 (E:Z) mixture of α,β-unsaturated nitriles*. Yield of **3.40**: 61% (262 mg, 0.61 mmol, colorless oil); R_f= 0.20 (1:19 EtOAc/hexanes); **^{1}H NMR** (600 MHz, $CDCl_3$) δ 6.34 (d, *J* = 2.2 Hz, 2H), 6.32 (t, *J* = 2.2 Hz, 1H), 6.12 (t, *J* = 7.3 Hz, 1H), 5.05 (d, *J* = 1.6 Hz, 1H), 4.79 (d, *J* = 1.4 Hz, 1H), 4.04 (s, 2H), 3.78 (s, 6H), 2.72 – 2.65 (m, 4H), 2.18 (t, *J* = 7.5 Hz, 2H), 1.98 (t, *J* = 7.6 Hz, 2H), 1.70 – 1.61 (m, 2H), 0.91 (s, 9H), 0.07 (s, 6H); **^{13}C DEPTQ** (151 MHz, $CDCl_3$) δ 161.0, 147.6, 146.7, 142.7, 117.6, 115.3, 109.4, 106.6, 98.4, 65.9, 55.4, 35.1, 33.9, 32.8, 31.6, 26.2, 26.0, 18.5, –5.2; **HRMS** (ES+) *m/z* calc'd for $C_{25}H_{39}NO_3SiNa$ $[M + Na]^+$: 452.2597, found 452.2595.

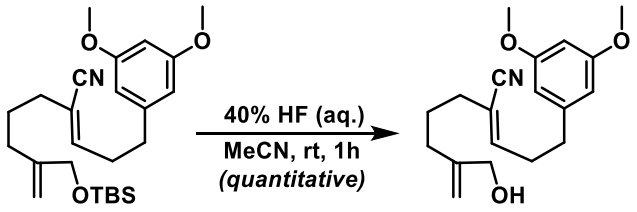

S3.40 S3.45

Prepared according to general procedure F, using secondary alcohol **3.40** *(25 mg, 0.058 mmol, 1.0 equiv.), acetonitrile (0.2 mL), and 40% w/w aq. hydrofluoric acid (0.2 mL, excess).* Yield of alcohol **3.45**: quantitative (18 mg, 0.058 mmol, colorless oil); R_f= 0.24 (3:7 EtOAc/hexanes). **^{1}H NMR** (500 MHz, $CDCl_3$) δ 6.34 (d, *J* = 2.2 Hz, 2H), 6.32 (t, *J* = 2.2 Hz, 1H), 6.12 (t, *J* = 6.4 Hz, 1H), 5.04 (s, 1H), 4.85 (s, 1H), 4.05 (s, 2H), 3.78 (s, 6H), 2.74 – 2.65 (m, 4H), 2.19 (t, *J* = 7.4 Hz, 2H), 2.01 (t, *J* = 7.6 Hz, 2H), 1.70 – 1.62 (m, 2H), 1.59 (*br* s, 1H); **^{13}C DEPTQ** (126 MHz, $CDCl_3$)

δ 161.0, 148.0, 146.9, 142.6, 117.6, 115.2, 110.2, 106.6, 98.4, 65.9, 55.4, 35.1, 33.8, 32.7, 31.7, 26.1; **HRMS** (ES+) *m/z* calc'd for $C_{25}H_{39}NO_3SiNa$ $[M + Na]^+$: 338.1732, found 338.1725.

Synthesis and Characterization of C6 Oxygenated Substrates

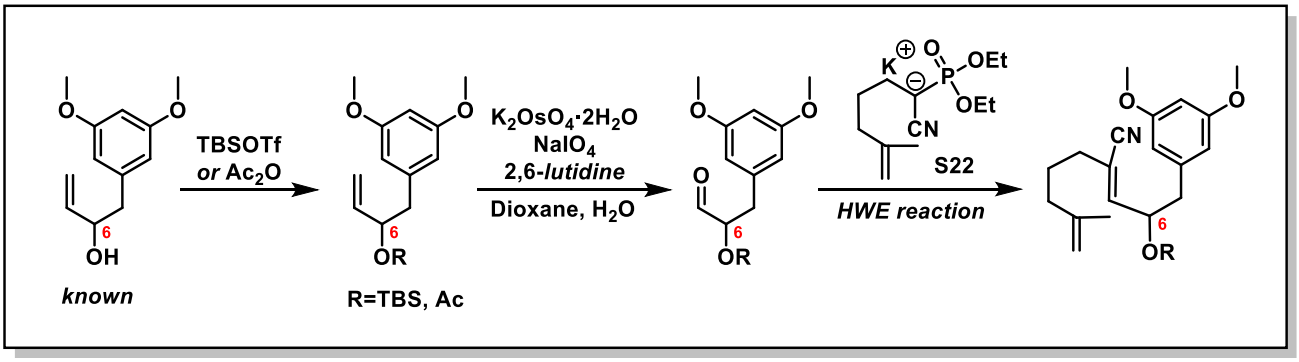

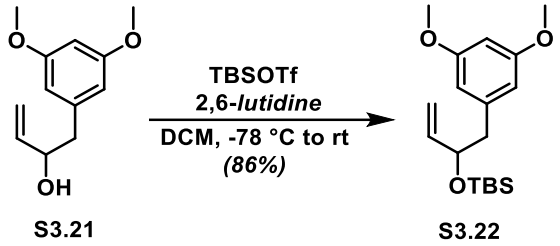

Prepared according to general procedure D, using allylic alcohol **S3.21**[50] *(190 mg, 0.91 mmol, 1.0 equiv.), TBSOTf (320 µL, 1.82 mmol) and 2,6-lutidine (423 µL, 3.65 mmol).* Yield of **S3.22**: 86% (250 mg, 0.78 mmol, colorless oil); R_f= 0.35 (5:95 EtOAc/hexanes). **^{1}H NMR** (500 MHz, $CDCl_3$) δ 6.36 (d, *J* = 2.0 Hz, 2H), 6.32 (t, *J* = 2.2 Hz, 1H), 5.87 (ddd, *J* = 17.1, 10.6, 5.9 Hz, 1H), 5.17 (d, *J* = 17.1 Hz, 1H), 5.03 (d, *J* = 10.4 Hz, 1H), 4.28 (q, *J* = 6.2 Hz, 1H), 3.78 (s, 6H), 2.70 (d, *J* = 6.1 Hz, 2H), 0.85 (s, 9H), -0.07 (s, 3H), -0.16 (s, 3H); **^{13}C NMR** (126 MHz, $CDCl_3$) δ 160.7, 141.3, 141.2, 114.0, 108.1, 98.5, 75.1, 55.4, 45.6, 26.0, 18.4, –4.6, –5.0; **HRMS** (ES+) *m/z* calc'd for $C_{18}H_{30}O_3SiNa$ $[M + Na]^+$: 345.1862, found 345.1873.

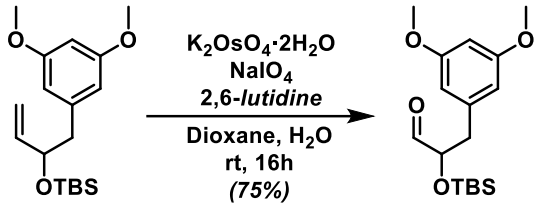

S3.22 **S3.23**

General Procedure G (one-pot oxidative cleavage of olefins)[51]:

To a solution of **S3.22** (250 mg, 0.78 mmol, 1.0 equiv.) in dioxane and water (3:1, 4 mL) was added 2,6-lutidine (180 µL, 1.55 mmol, 2.0 equiv.), K_2OsO_4 dihydrate (9 mg, 0.024 mmol, 0.03 equiv.) and $NaIO_4$ (663 mg, 3.10 mmol, 4.0 equiv.). After 16 hours of vigorous stirring, H_2O (10 mL) and CH_2Cl_2 (20 mL) were added, and the phases were separated. The aqueous phase was extracted with CH_2Cl_2 (3 x 10 mL), combined organic phases were washed with brine, dried over Na_2SO_4, and concentrated *in vacuo*. The resulting crude residue was purified via flash column chromatography on SiO_2, using a mixture of EtOAc/hexanes (1:9) as eluent to give aldehyde **S3.23** as a colorless oil (190 mg, 0.59 mmol, 75% yield). **^{1}H NMR** (500 MHz, $CDCl_3$) δ 9.64 (d, *J* = 1.2 Hz, 1H), 6.37 (d, *J* = 1.9 Hz, 2H), 6.34 (t, *J* = 2.0 Hz, 1H), 4.14 (dd, *J* = 8.8, 2.6 Hz, 1H), 3.77 (s, 6H), 2.94 (dd, *J* = 13.6, 3.9 Hz, 1H), 2.72 (dd, *J* = 13.6, 8.8 Hz, 1H), 0.85 (s, 9H), –0.07 (s, 3H), –0.17 (s, 3H); **^{13}C NMR** (126 MHz, $CDCl_3$) δ 203.7, 160.9, 139.2, 108.0, 99.1, 79.1, 55.5, 39.7, 25.8, 18.3, –4.9; **HRMS** (ES+) *m/z* calc'd for $C_{17}H_{28}O_4SiNa$ $[M + Na]^+$: 347.1655, found 347.1763.

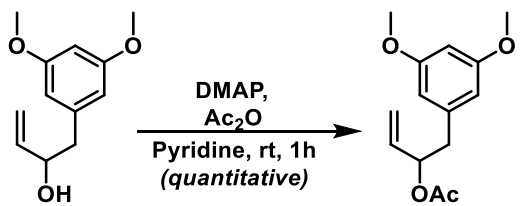

S3.21 **S3.24**

Prepared according to general procedure C, using secondary alcohol **S3.21** *(120 mg, 0.58 mmol, 1.0 equiv.), pyridine (0.2 mL, solvent), acetic anhydride (0.2 mL, co-solvent) and DMAP (7 mg, 0.058, 0.1 equiv.).* Yield of secondary allylic acetate **S3.24**: quantitative (144 mg, 0.58 mmol, colorless oil); R_f= 0.20 (3:17 EtOAc/hexanes). **^{1}H NMR** (600 MHz, $CDCl_3$) δ 6.36 (d, *J* = 1.9 Hz, 2H), 6.33 (d, *J* = 1.8 Hz, 1H), 5.81 (ddd, *J* = 17.0, 10.5, 6.2 Hz, 1H), 5.46 (q, *J* = 6.6 Hz, 1H), 5.22 (d, *J* = 17.2 Hz, 1H), 5.16 (d, *J* = 10.5 Hz, 1H), 3.77 (s, 6H), 2.91 (dd, *J* = 13.7, 7.3 Hz, 1H), 2.81 (dd, *J* = 13.7, 6.3 Hz, 1H), 2.03 (s, 3H); **^{13}C NMR** (151 MHz, $CDCl_3$) δ 170.2, 160.8, 139.3, 135.9, 117.1, 107.7, 98.7, 75.0, 55.4, 41.2, 21.3; **HRMS** (ES+) *m/z* calc'd for $C_{14}H_{18}O_4Na$ $[M + Na]^+$: 273.1103, found 273.1319.

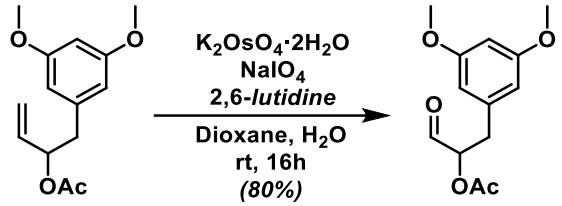

S3.24 **S3.25**

Prepared according to general procedure G, using allylic acetate **S3.24** *(272 mg, 1.09 mmol), K_2OsO_4 dihydrate (12 mg, 0.032 mmol), $NaIO_4$ (930 mg, 4.35 mmol) and 2,6-lutidine (251 µL, 2.17 mmol).* NOTE: this material was unstable to purification on acidic SiO_2. Crude yield of **S3.25**: 80 % (220 mg, 0.872 mmol, dark brown oil). **^{1}H NMR** (500 MHz, $CDCl_3$) δ 9.54 (s, 1H), 6.36 – 6.35 (m (2 overlapping signals), 3H), 5.21 (dd, *J* = 8.5, 4.9 Hz, 1H), 3.78 (s, 6H), 3.10 (dd, *J* = 14.4, 4.9 Hz, 1H), 2.96 (dd, *J* = 14.4, 8.5 Hz, 1H), 2.14 (s, 3H); **^{13}C NMR** (126 MHz, $CDCl_3$) δ 198.0, 170.5, 161.0, 137.7, 107.5, 99.0, 78.6, 55.3, 35.4, 20.6; **HRMS** (ES+) *m/z* calc'd for $C_{13}H_{16}O_5Na$ $[M + Na]^+$: 275.0895, found 275.0902.

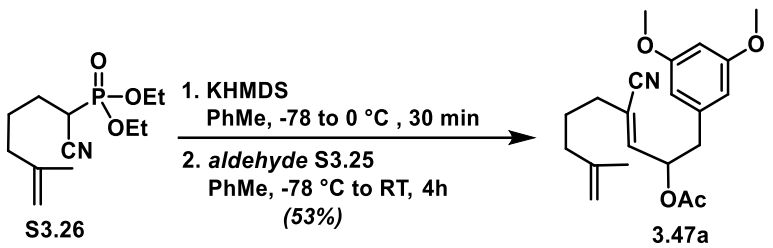

Prepared according to general procedure E, using cyanoalkylphosphonate **S3.26** *(82 mg, 0.32 mmol, 1.0 equiv.) and aldehyde* **S3.25** *(80 mg, 0.32 mmol, 1.0 equiv.) to give a 1:5 (E:Z) mixture of α,β-unsaturated nitriles*. Yield of **3.47a**: 53% (60 mg, 0.17 mmol, colorless oil); R_f= 0.25 (1:9 EtOAc/hexanes); **^{1}H NMR** (600 MHz, $CDCl_3$) δ 6.36 – 6.34 (m, 3H), 5.99 (d, *J* = 8.0 Hz, 1H), 5.75 (q, *J* = 7.2 Hz, 1H), 4.72 (s, 1H), 4.63 (s, 1H), 3.77 (s, 6H), 3.04 (dd, *J* = 13.7, 6.9 Hz, 1H), 2.83 (dd, *J* = 13.7, 6.8 Hz, 1H), 2.21 – 2.11 (m, 2H), 2.06 (s, 3H), 1.97 – 1.89 (m, 2H), 1.68 (s, 3H), 1.65 – 1.57 (m, 2H); **^{13}C NMR** (151 MHz, $CDCl_3$) δ 169.9, 160.9, 144.6, 143.4, 137.8, 117.3, 116.5, 110.9, 107.7, 99.1, 72.9, 55.4, 40.6, 36.5, 34.0, 25.6, 22.2, 21.1; **HRMS** (ES+) *m/z* calc'd for $C_{21}H_{27}NO_4Na$ $[M + Na]^+$: 380.1838, found 380.1837.

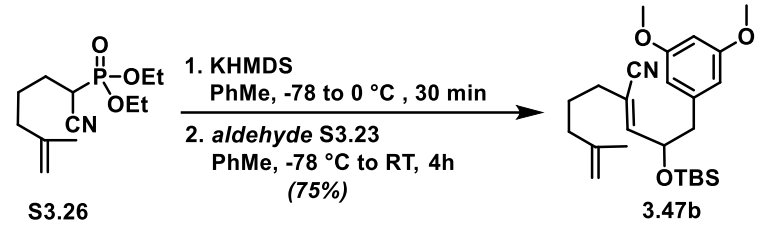

Prepared according to general procedure E, using cyanoalkylphosphonate **S3.26** *(152 mg, 0.59 mmol, 1.0 equiv.) and aldehyde* **S3.23** *(190 mg, 0.59 mmol, 1.0 equiv.) to give a 1:15 (E:Z) mixture of α,β-unsaturated nitriles*. Yield of **3.47b**: 75% (190 mg, 0.44 mmol, colorless oil); R_f= 0.15 (3:97 EtOAc/hexanes); **^{1}H NMR** (600 MHz, $CDCl_3$) δ 6.42 (d, *J* = 2.1 Hz, 2H), 6.39 (t, *J* = 2.0 Hz, 1H), 6.12 (d, *J* = 8.8 Hz, 1H), 4.85 – 4.76 (m, 2H), 4.72 (s, 1H), 3.83 (s, 6H), 2.86 (dd, *J* = 13.3, 7.5 Hz, 1H), 2.79 (dd, *J* = 13.4, 5.3 Hz, 1H), 2.22 (t, *J* = 7.5 Hz, 2H), 2.07 – 1.99 (m, 2H), 1.76 (s, 3H),

1.68 (p, *J* = 7.6 Hz, 2H), 0.89 (s, 9H), 0.01 (s, 3H), -0.02 (s, 3H); **^{13}C NMR** (151 MHz, $CDCl_3$) δ 160.8, 149.6, 144.7, 139.3, 117.0, 114.0, 110.9, 108.0, 99.0, 72.8, 55.4, 44.7, 36.6, 33.6, 25.9, 25.8, 22.3, 18.2, –4.6, –5.0; **HRMS** (ES+) *m/z* calc'd for $C_{25}H_{39}NO_3SiNa$ $[M + Na]^+$: 452.2597, found 452.2592.

Synthesis and Characterization of C7 Oxygenated Substrates

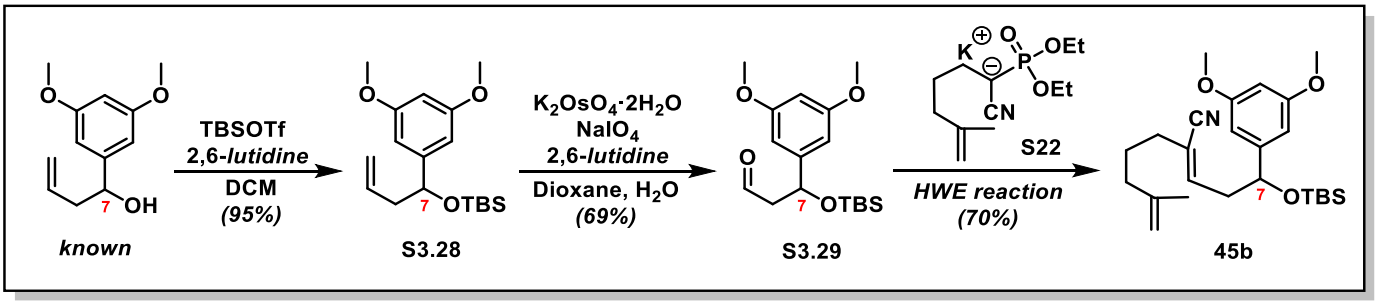

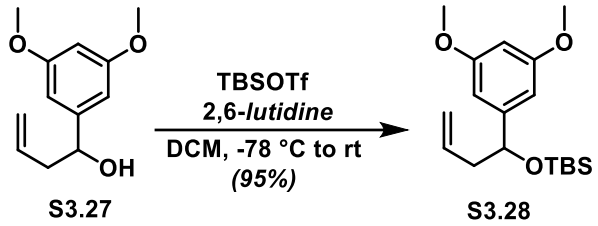

Prepared according to general procedure D, using alcohol **S3.27**[52] *(1.0 g, 4.8 mmol, 1.0 equiv.), TBSOTf (1.0 mL 5.8 mmol, 1.2 equiv.) and 2,6-lutidine (1.1 mL, 9.6 mmol, 2.0 equiv.).* Yield of **S3.28**: 95 % (1.5 g, 4.7 mmol, colorless oil); R_f= 0.45 (1:9 EtOAc/hexanes). **^{1}H NMR** (600 MHz, $CDCl_3$) δ 6.48 (d, *J* = 2.2 Hz, 2H), 6.33 (t, *J* = 2.2 Hz, 1H), 5.79 (ddt, *J* = 17.3, 10.2, 7.1 Hz, 1H), 5.03 (d, *J* = 9.6 Hz, 1H), 5.01 (d, *J* = 1.3 Hz, 1H), 4.61 (dd, *J* = 7.3, 5.0 Hz, 1H), 3.78 (s, 6H), 2.46 – 2.40 (m, 1H), 2.40 – 2.34 (m, 1H), 0.89 (s, 9H), 0.03 (s, 3H), –0.09 (s, 3H); **^{13}C DEPTQ** (151 MHz, $CDCl_3$) δ 160.6, 148.0, 135.4, 117.0, 103.9, 99.0, 75.1, 55.4, 45.6, 26.0, 18.4, –4.5, –4.8; **HRMS** (ES+) *m/z* calc'd for $C_{18}H_{30}O_3SiNa$ $[M + Na]^+$: 345.1862, found 345.1870.

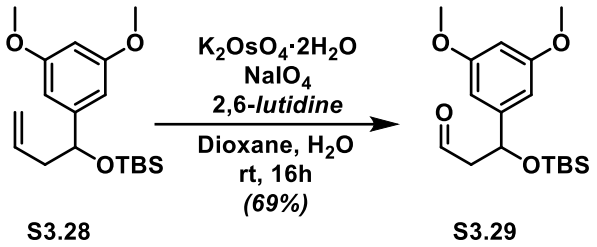

Prepared according to general procedure G, using allylic silyl ether **S3.28** *(750 mg, 2.33 mmol, 1.0 equiv.), K_2OsO_4 dihydrate (26 mg, 0.07 mmol, 0.03 equiv.), $NaIO_4$ (2.0 g, 9.32 mmol, 4.0 equiv.) and 2,6-lutidine (540 µL, 4.66 mmol, 2.0 equiv.).* Yield of **S3.29**: 69% (520 mg, 1.60 mmol, colorless oil); R_f= 0.25 (1:9 EtOAc/hexanes). **^{1}H NMR** (600 MHz, $CDCl_3$) δ 9.78 (s, 1H), 6.50 (d, *J* = 2.1 Hz, 2H), 6.35 (s, 1H), 5.14 (dd, *J* = 8.1, 4.0 Hz, 1H), 3.78 (s, 6H), 2.82 (ddd, *J* = 15.8, 8.1, 2.7 Hz, 1H), 2.61 (ddd, *J* = 15.8, 3.8, 1.9 Hz, 1H), 0.88 (s, 9H), 0.05 (s, 3H), -0.08 (s, 3H); **^{13}C DEPTQ** (151 MHz, $CDCl_3$) δ 201.48, 160.99, 146.53, 103.64, 99.54, 70.77, 55.45, 54.03, 25.85, 18.25, –4.47, –5.03; **HRMS** (ES+) *m/z* calc'd for $C_{17}H_{28}O_4SiNa$ $[M + Na]^+$: 347.1655, found 347.1661.

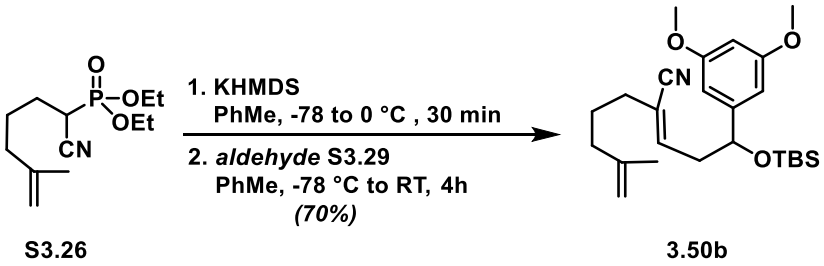

Prepared according to general procedure E, using cyanoalkylphosphonate **S3.26** *(166 mg, 0.64 mmol, 1.0 equiv.) and aldehyde* **S3.29** *(208 mg, 0.64 mmol, 1.0 equiv.) to give a 1:4 (E:Z) mixture of α,β-unsaturated nitriles*. Yield of **3.50b**: 70% (193 mg, 0.45 mmol, colorless oil); R_f= 0.20 (3:97 EtOAc/hexanes); **^{1}H NMR** (600 MHz, $CDCl_3$) δ 6.47 (d, *J* = 2.2 Hz, 2H), 6.34 (t, *J* = 2.2 Hz, 1H),

6.13 (t, *J* = 7.5 Hz, 1H), 4.75 (t, *J* = 5.7 Hz, 1H), 4.72 (s, 1H), 4.65 (s, 1H), 3.78 (s, 6H), 2.72 (t, *J* = 6.6 Hz, 2H), 2.16 (t, *J* = 7.6 Hz, 2H), 1.97 (t, *J* = 7.6 Hz, 2H), 1.70 (s, 3H), 1.66 – 1.59 (m, 2H), 0.90 (s, 9H), 0.05 (s, 3H), –0.07 (s, 3H); **^{13}C NMR** (151 MHz, $CDCl_3$) δ 160.8, 146.6, 144.8, 143.9, 117.8, 116.5, 110.8, 103.7, 99.4, 73.7, 55.4, 42.4, 36.7, 33.9, 26.0, 25.9, 22.3, 18.3, –4.6, –4.9; **HRMS** (ES+) *m/z* calc'd for $C_{25}H_{39}NO_3SiNa$ $[M + Na]^+$: 452.2597, found 452.2591.

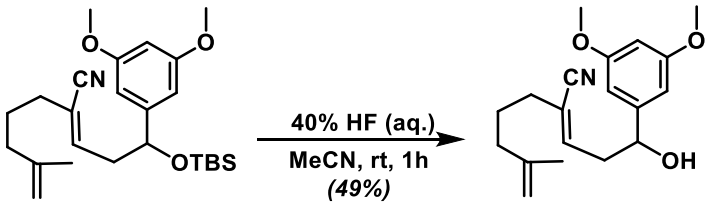

3.50b **3.50a**

Prepared according to general procedure F, using silyl ether **3.50b** *(50 mg, 0.12 mmol), acetonitrile (0.3 mL), and 40% w/w aq. hydrofluoric acid (0.2 mL, excess).* Yield of **3.50a**: 49% (18 mg, 0.057 mmol, colorless oil); R_f= 0.22 (3:7 EtOAc/hexanes); **^{1}H NMR** (500 MHz, $CDCl_3$) δ 6.50 (d, *J* = 2.2 Hz, 2H), 6.38 (t, *J* = 2.2 Hz, 1H), 6.19 (t, *J* = 7.5 Hz, 1H), 4.75 (t, *J* = 6.3 Hz, 1H), 4.72 (s, 1H), 4.65 (s, 1H), 3.79 (s, 6H), 2.80 (t, *J* = 7.0 Hz, 2H), 2.19 (t, *J* = 7.6 Hz, 2H), 2.04 (broad s, 1H), 1.97 (t, *J* = 7.5 Hz, 2H), 1.70 (s, 3H), 1.68 – 1.60 (m, 2H); **^{13}C NMR** (151 MHz, $CDCl_3$) δ 161.2, 145.7, 144.8, 143.4, 117.7, 116.9, 110.8, 103.7, 100.0, 73.4, 55.5, 40.7, 36.6, 33.8, 25.9, 22.3; **HRMS** (ES+) *m/z* calc'd for $C_{25}H_{39}NO_3SiNa$ $[M + Na]^+$: 338.1732, found 338.1739.

Synthesis and Characterization of Di-Oxygenated Substrates

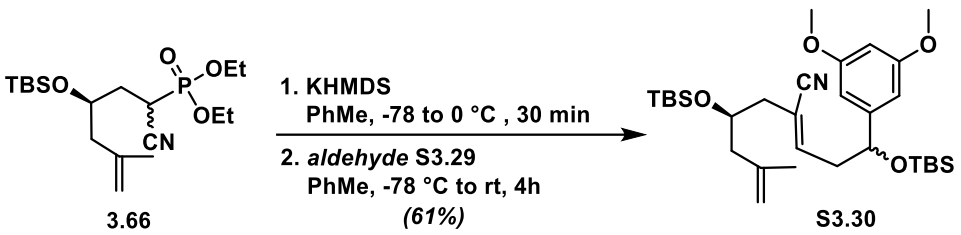

3.66 S3.30

Prepared according to general procedure E, using cyanoalkylphosphonate **3.66** *(400 mg, 1.03 mmol, 1.0 equiv.) and aldehyde* **S3.29** *(333 mg, 1.03 mmol, 1.0 equiv.) to give a 1:7 (E:Z) mixture of α,β-unsaturated nitriles as a 1:1 mixture of diastereomers at C7*. Yield of pure *Z*-**S3.30** diastereomers: 61% (350 mg, 0.63 mmol, colorless oil); R_f= 0.20 (2:98 EtOAc/hexanes); **^{1}H NMR** (500 MHz, $CDCl_3$) (*NOTE: integration values are for the mixture diastereomers*) δ 6.47 (d, *J* = 2.2 Hz, 2H), 6.46 (d, *J* = 2.2 Hz, 2H), 6.36 – 6.32 (m, 2H), 6.17 (t, *J* = 7.2 Hz, 2H), 4.79 (s, 2H), 4.77 – 4.71 (m, 2H), 4.70 (s, 2H), 3.96 (dd, *J* = 11.4, 6.0 Hz, 2H), 3.78 (s, 6H), 3.78 (s, 6H), 2.81 – 2.78 (m, 1H), 2.70 – 2.66 (m, 1H), 2.39 – 2.32 (m, 1H), 2.18 (dd, *J* = 13.6, 6.0 Hz, 2H), 2.13 – 2.06(m, 1H), 1.73 (s, 3H), 1.72 (s, 3H), 0.90 (s, 18H), 0.86 (s, 9H), 0.85 (s, 9H), 0.05 (s, 12H), 0.03 (s, 3H), 0.03 (s, 3H), –0.07 (s, 3H); **^{13}C NMR** (126 MHz, $CDCl_3$) (*NOTE: all observed signals for a 1:1 mixture of diastereomers are reported*) δ 160.88, 160.87, 146.6, 146.5, 146.48, 146.4, 142.1, 117.9, 113.9, 113.7, 103.8, 103.7, 99.49, 99.45, 73.8, 73.5, 69.1, 55.4, 45.9, 45.8, 42.5, 41.9, 27.0, 25.95, 25.9, 23.1, 23.0, 18.3, 18.2, –4.4, –4.5, –4.6, –4.88, –4.91; **HRMS** (ES+) *m/z* calc'd for $C_{31}H_{53}NO_4Si_2Na$ $[M + Na]^+$: 582.3411, found 582.3391; $[\alpha]_D^{22} = -8.6$ $(c = 0.1, CHCl_3)$.

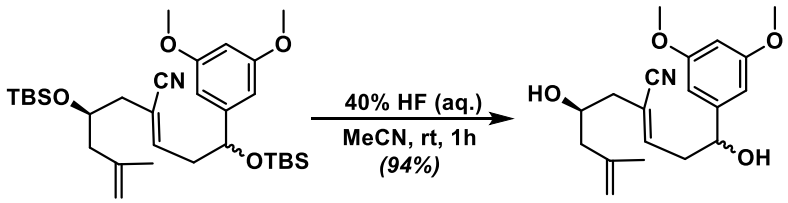

S3.30 3.59

Prepared according to general procedure F, using silyl ether **S3.30** *(74 mg, 0.132 mmol, 1.0 equiv.), acetonitrile (3.0 mL), and 40% w/w aq. hydrofluoric acid (0.20 mL, excess).* Yield of **3.59**: 94% (41 mg, 0.124 mmol, colorless oil); R_f= 0.30 (9:11 EtOAc/hexanes); **^{1}H NMR** (500 MHz, $CDCl_3$) (*NOTE: all signals for a 1:1 mixture of diastereomers are reported as observed*) δ 6.50 (apparent t, *J* = 2.0 Hz, 2H), 6.36 (apparent t, *J* = 1.9 Hz, 1H), 6.31 – 6.27 (m, 1H), 4.88 (s, 1H), 4.81 – 4.73 (m, 2H), 3.95 – 3.87 (m, 1H), 3.78 (s, 6H), 2.87 – 2.75 (m, 2H), 2.37 (dt, *J* = 13.3, 4.4 Hz, 1H), 2.26 (dd, *J* = 14.2, 8.6 Hz, 1H), 2.17 – 2.08 (m, 2H), 1.74 (s, 3H); **^{13}C NMR** (125 MHz, $CDCl_3$) (*NOTE: all observed signals for a 1:1 mixture of diastereomers are reported*) δ 161.13, 161.12, 146.34, 146.26, 145.7, 141.99, 141.98, 117.7, 114.2, 114.1, 113.9, 113.7, 103.75, 103.71, 99.94, 99.87, 73.04, 73.02, 67.0, 66.9, 55.49, 45.47, 45.4, 41.8, 41.7, 41.1, 40.9, 22.5; **HRMS** (ES+) *m/z* calc'd for $C_{19}H_{25}NO_4Na$ $[M + Na]^+$: 354.1681, found 354.1677; $[\alpha]_D^{22} = -50.1$ $(c = 0.1, CHCl_3)$.

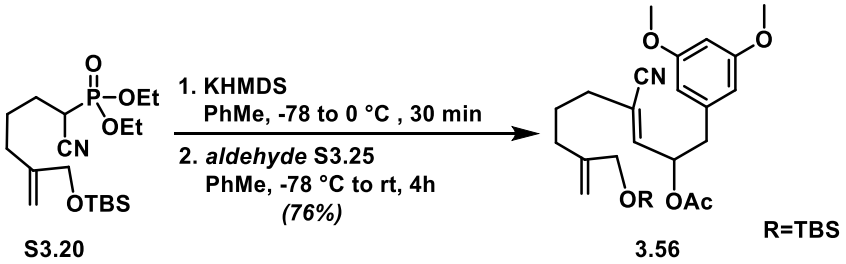

Prepared according to general procedure E, using cyanoalkylphosphonate **S3.20** *(287 mg, 0.74 mmol, 1.0 equiv.) and aldehyde* **S3.25** *(186 mg, 0.74 mmol, 1.0 equiv.) to give a 1:10 (E:Z) mixture of α,β-unsaturated nitriles*. Yield of **3.56**: 76% (273 mg, 0.56 mmol, colorless oil); R_f= 0.20 (1:9 EtOAc/hexanes); **^{1}H NMR** (600 MHz, $CDCl_3$) δ 6.36 – 6.33 (m (2 signals overlapping) 3H), 5.99 (d, *J* = 8.0 Hz, 1H), 5.75 (q, *J* = 7.1 Hz, 1H), 5.05 (s, 1H), 4.78 (s, 1H), 4.03 (s, 2H), 3.77 (s, 6H), 3.03 (dd, *J* = 13.7, 7.0 Hz, 1H), 2.83 (dd, *J* = 13.7, 6.7 Hz, 1H), 2.23 – 2.14 (m, 1H), 2.06 (s, 2H), 1.95 (t, *J* = 7.6 Hz, 2H), 1.67 – 1.60 (m, 2H), 0.91 (s, 9H), 0.07 (s, 6H); **^{13}C DEPT NMR** (151

MHz, $CDCl_3$) δ 169.9, 161.0, 147.4, 143.5, 137.8, 117.2, 116.5, 109.5, 107.7, 99.2, 72.9, 65.8, 55.5, 40.7, 34.2, 31.5, 26.1, 25.9, 21.1, 18.5, –5.2; **HRMS** (ES+) *m/z* calc'd for $C_{27}H_{41}NO_5SiNa$ $[M + Na]^+$: 510.2652, found 510.2640.

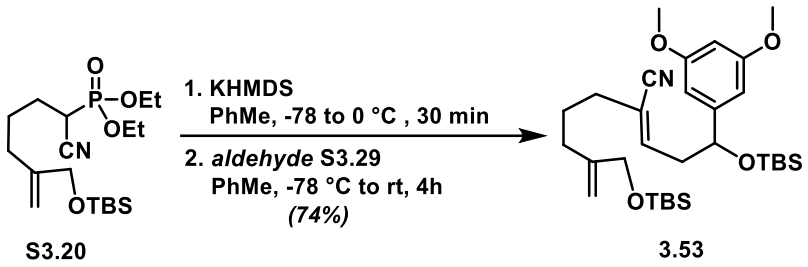

Prepared according to general procedure E, using cyanoalkylphosphonate **S3.20** *(300 mg, 0.77 mmol, 1.0 equiv.) and aldehyde* **S3.29** *(208 mg, 0.77 mmol, 1.0 equiv.) to give a 1:10 (E:Z) mixture of α,β-unsaturated nitriles*. Yield of **3.53**: 74% (320 mg, 0.57 mmol, colorless oil); R_f= 0.25 (3:98 EtOAc/hexanes); **^{1}H NMR** (500 MHz, $CDCl_3$) δ 6.47 (d, *J* = 1.7 Hz, 2H), 6.34 (s, 1H), 6.14 (t, *J* = 7.5 Hz, 1H), 5.05 (s, 1H), 4.80 (s, 1H), 4.74 (t, *J* = 5.7 Hz, 1H), 4.05 (s, 2H), 3.78 (s, 6H), 2.72 (t, *J* = 6.6 Hz, 2H), 2.18 (t, *J* = 7.6 Hz, 2H), 1.98 (t, *J* = 7.6 Hz, 2H), 1.69 – 1.61 (m, 2H), 0.915 (s, 9H), 0.913 (s, 9H), 0.07 (s, 6H), 0.05 (s, 3H), –0.07 (s, 3H); **^{13}C NMR** (126 MHz, $CDCl_3$) δ 160.8, 147.5, 146.5, 143.8, 117.6, 116.3, 109.2, 103.6, 99.4, 73.6, 65.8, 55.3, 42.3, 34.0, 31.6, 26.1, 26.0, 25.8, 18.4, 18.2, –4.7, –5.0, –5.3; **HRMS** (ES+) *m/z* calc'd for $C_{31}H_{53}NO_4Si_2Na$ $[M + Na]^+$: 582.3411, found 582.3399.

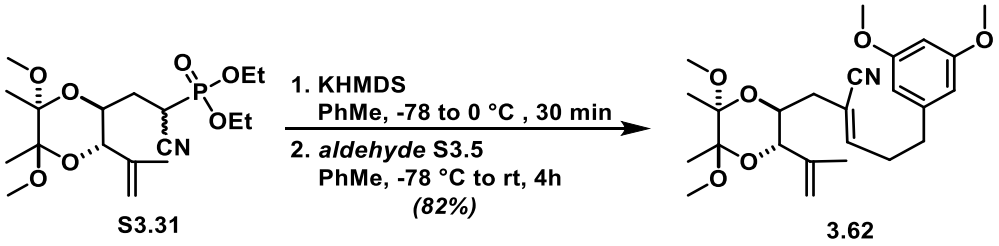

Prepared according to general procedure E, using cyanoalkylphosphonate **S3.31** *(18 mg, 0.044 mmol, 1.0 equiv.) and aldehyde* **S3.5** *(9 mg, 0.044 mmol, 1.0 equiv.) to give a 1:20 (E:Z) mixture*

of α,β-unsaturated nitriles. Yield of **3.62**: 82% (16 mg, 0.61 mmol, colorless oil); R_f= 0.21 (3:17 EtOAc/hexanes); **^{1}H NMR** (600 MHz, $CDCl_3$) δ 6.34 (d, *J* = 2.2 Hz, 2H), 6.31 – 6.30 (m, 1H), 6.25 (t, *J* = 6.2 Hz, 1H), 5.00 – 4.98 (m, 2H), 3.94 – 3.89 (m, 2H), 3.77 (s, 6H), 3.25 (s, 3H), 3.20 (s, 3H), 2.73 – 2.66 (m, 4H), 2.24 (d, *J* = 14.4 Hz, 1H), 2.17 (dd, *J* = 14.4, 8.9 Hz, 1H), 1.79 (s, 3H), 1.27 (s, 4H), 1.24 (s, 3H); **^{13}C NMR** (151 MHz, $CDCl_3$) δ 161.0, 149.4, 142.6, 141.8, 117.5, 116.8, 111.6, 106.5, 98.4, 77.4, 77.2, 77.0, 76.5, 67.2, 55.4, 48.2, 48.1, 35.9, 35.1, 32.8, 18.1, 17.8, 17.7; **HRMS** (ES+) *m/z* calc'd for $C_{25}H_{35}NO_6Na$ $[M + Na]^+$: 468.2362, found 468.2371.

Bicyclization Experiments and Product Characterization

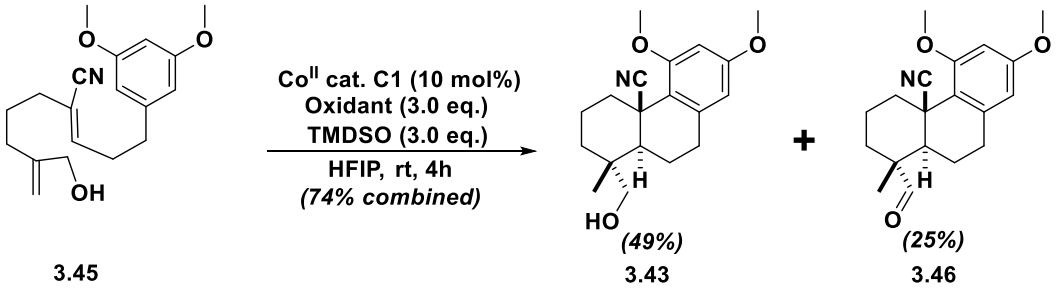

<u>*General procedure I (Cobalt catalyzed bicyclization of oxygenated polyenes):*</u>

A dry round-bottom flask was charged with a magnetic stirring bar, allylic alcohol **3.45** (18 mg, 0.057 mmol, 1.0 equiv.), cobalt catalyst **C1** (3 mg, 0.006 mmol, 0.1 equiv.), and 1-fluoro-2,4,6-trimethylpyridinium triflate (49 mg, 0.17 mmol, 3.0 equiv.). The reagents were dissolved in HFIP (0.5 mL), and the flask was capped with a rubber septum. A balloon equipped with a syringe needle was used to bubble argon through the solution for 10 minutes (a syringe needle was used as an outlet). The flask was sealed from the atmosphere and 1,1,3,3-tetramethyldisiloxane (30 µL, 0.17 mmol, 3.0 equiv.) was added dropwise at a rate of 1 drop per 3 seconds. The resulting solution gradually turned dark red from its initial, dark green color. After 4 hours, the volatiles were removed *in vacuo* and the resulting residue was directly purified via flash via flash column

chromatography on SiO_2, using a mixture of EtOAc/hexanes (1:1) as eluent to give carbinol **3.43** (9 mg, 0.016 mmol, R_f =0.32, 49%) and aldehyde **3.46** (5 mg, 0.016 mmol, R_f =0.61, 25% yield). *Data for carbinol* **3.43**: **^{1}H NMR** (500 MHz, $CDCl_3$) δ 6.32 (d, *J* = 2.3 Hz, 1H), 6.22 (d, *J* = 2.1 Hz, 1H), 3.85 (s, 3H), 3.77 (s, 3H), 3.59 (d, *J* = 10.9 Hz, 1H), 3.47 (d, *J* = 13.3 Hz, 1H), 3.23 (d, *J* = 10.9 Hz, 1H), 2.90 (ddd, *J* = 17.7, 12.6, 5.5 Hz, 1H), 2.81 (dd, *J* = 16.9, 3.4 Hz, 1H), 2.04 (dtd, *J* = 13.7, 10.4, 3.5 Hz, 1H), 1.95 (dd, *J* = 13.1, 5.1 Hz, 1H), 1.80 (d, *J* = 11.9 Hz, 1H), 1.77 – 1.71 (m, 1H), 1.70 – 1.62 (m, 1H), 1.62 – 1.56 (m, 1H), 1.55 (s, 1H), 1.41 (d, *J* = 13.2 Hz, 1H), 1.17 (td, *J* = 13.4, 3.2 Hz, 1H), 1.11 (s, 3H); **^{13}C NMR** (151 MHz, $CDCl_3$) δ 160.1, 159.9, 140.0, 123.7, 119.3, 105.3, 97.8, 71.2, 55.7, 55.4, 46.5, 39.6, 38.5, 34.9, 34.6, 32.5, 20.9, 20.0, 16.7; **HRMS** (ES+) *m/z* calc'd for $C_{19}H_{25}NO_3Na$ $[M + Na]^+$: 338.1732, found 338.1736.

Data for aldehyde **3.46**: **^{1}H NMR** (600 MHz, $CDCl_3$) δ 9.33 (s, 1H), 6.33 (d, *J* = 2.3 Hz, 1H), 6.23 (d, *J* = 2.0 Hz, 1H), 3.85 (s, 3H), 3.78 (s, 3H), 3.53 (d, *J* = 13.6 Hz, 1H), 3.00 – 2.90 (m, 1H), 2.80 (dd, *J* = 16.9, 4.1 Hz, 1H), 2.06 (qt, *J* = 13.6, 3.5 Hz, 1H), 1.98 (d, *J* = 11.9 Hz, 1H), 1.86 – 1.81 (m, 1H), 1.77 (ddd, *J* = 25.3, 12.8, 4.9 Hz, 1H), 1.51 – 1.53 (m, 2H), 1.47 (td, *J* = 13.4, 3.4 Hz, 1H), 1.44 (s, 3H), 1.24 (td, *J* = 13.4, 3.4 Hz, 1H); **^{13}C NMR** (151 MHz, $CDCl_3$) δ 205.0, 160.1, 139.6, 122.9, 118.2, 105.5, 97.9, 55.7, 55.4, 50.2, 45.4, 38.7, 34.5, 32.0, 32.0, 23.6, 19.2, 13.8; **HRMS** (ES+) *m/z* calc'd for $C_{19}H_{23}NO_3Na$ $[M + Na]^+$: 336.1576, found 336.1585. *Note: Our stereochemical assignment is based on the observation that subjecting aldehyde **3.46** to reduction with sodium borohydride in methanol, resulted in clean formation of carbinol **3.43** described above.*

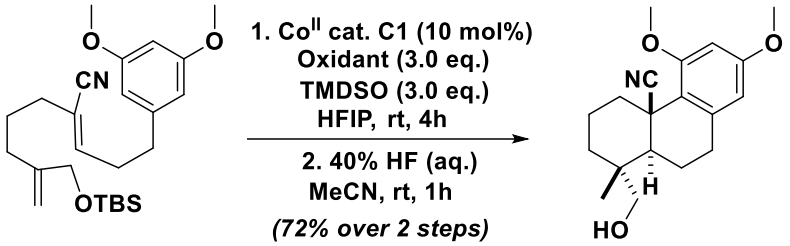

Prepared according to general procedure I, using α,β-unsaturated nitrile **3.40** *(36 mg, 0.084 mmol, 1.0 equiv.), cobalt catalyst* **C1** *(5 mg, 0.008 mmol, 0.1 equiv.), 1-fluoro-2,4,6-trimethylpyridinium triflate (73 mg, 0.252 mmol, 3.0 equiv.), TMDSO (44 µL, 0.252 mmol, 3.0 equiv.), and HFIP (1.0 mL). The crude residue was subjected to general procedure E for desilylation, using 40% w/w aq. hydrofluoric acid (0.2 mL, excess) and acetonitrile (1 mL).* Yield of **3.43**: 72% over two steps (19 mg, 0.060 mmol, white solid) – *please see the above experiment for characterization data*.

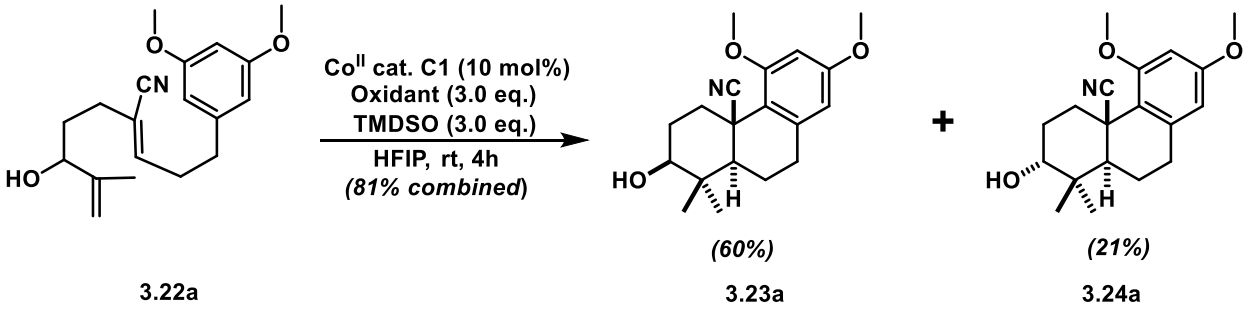

Prepared according to general procedure I, using α,β-unsaturated nitrile **3.22a** *(25 mg, 0.079 mmol, 1.0 equiv.), cobalt catalyst* **C1** *(5 mg, 0.008 mmol, 0.1 equiv.), 1-fluoro-2,4,6-trimethylpyridinium triflate (69 mg, 0.238 mmol, 3.0 equiv.), TMDSO (42 µL, 0.238 mmol, 3.0 equiv.), and HFIP (1.0 mL). NOTE: for experiments with TBS, MOM, and Ac protected substrates, the diastereomeric ratio and yields were estimated via ^1H NMR spectroscopy using dibromomethane as an internal standard.* Yield of isomer with equatorial hydroxyl group **3.23a:**

60% (15 mg, 0.048 mmol, white solid); R_f=0.14 (20:80 EtOAc/hexanes); **^{1}H NMR** (500 MHz, $CDCl_3$) δ 6.32 (d, *J* = 2.0 Hz, 1H), 6.23 (d, *J* = 1.1 Hz, 1H), 3.85 (s, 3H), 3.77 (s, 3H), 3.52 (d, *J* = 13.7 Hz, 1H), 3.32 (dd, *J* = 11.8, 4.1 Hz, 1H), 2.93 – 2.79 (m, 2H), 2.06 – 1.94 (m, 1H), 1.92 – 1.86 (m, 2H), 1.72 (ddd, *J* = 25.1, 11.7, 5.9 Hz, 1H), 1.35 – 1.25 (m, 3H), 1.14 (s, 3H), 1.13 (s, 3H); **^{13}C DEPTQ** (151 MHz, $CDCl_3$) δ 160.1, 160.0, 139.8, 122.8, 118.7, 105.3, 97.9, 77.8, 55.7, 55.4, 52.4, 39.8, 39.2, 33.1, 32.9, 29.1, 27.8, 21.1, 14.3; **HRMS** (ES+) *m/z* calc'd for $C_{19}H_{25}NO_3Na$ $[M + Na]^+$: 338.1732, found 338.1739. Yield of isomer with axial hydroxyl group **3.24a:** 21% (5.3 mg, 0.016 mmol, white solid); R_f=0.15 (1:4 EtOAc/hexanes); **^{1}H NMR** (600 MHz, $CDCl_3$) δ 6.31 (d, *J* = 2.4 Hz, 1H), 6.22 (d, *J* = 2.2 Hz, 1H), 3.84 (s, 3H), 3.77 (s, 3H), 3.58 (s, 1H), 3.28 (dt, *J* = 13.6, 3.5 Hz, 1H), 2.93 – 2.82 (m, 2H), 1.94 – 1.88 (m, 1H), 1.86 (d, *J* = 12.1 Hz, 1H), 1.77 (ddd, *J* = 14.7, 6.6, 3.3 Hz, 1H), 1.75 – 1.65 (m, 2H), 1.55 (s, 1H), 1.43 (broad s, 1H), 1.20 (s, 3H), 1.08 (s, 3H); **^{13}C DEPTQ** (151 MHz, $CDCl_3$) δ 160.1, 159.9, 139.9, 123.4, 119.1, 105.3, 97.8, 74.8, 55.7, 55.4, 46.0, 39.5, 38.3, 32.7, 28.1, 27.8, 27.5, 21.1, 20.9; **HRMS** (ES+) *m/z* calc'd for $C_{19}H_{25}NO_3Na$ $[M + Na]^+$: 338.1732, found 338.1728.

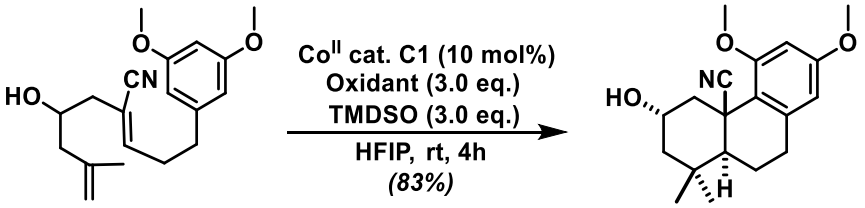

3.25a **3.26a**

Prepared according to general procedure I, using α,β-unsaturated nitrile **3.25a** *(30 mg, 0.095 mmol, 1.0 equiv.), cobalt catalyst* **C1** *(6 mg, 0.010 mmol, 0.1 equiv.), 1-fluoro-2,4,6-trimethylpyridinium triflate (83 mg, 0.285 mmol, 3.0 equiv.), TMDSO (50 µL, 0.285 mmol, 3.0 equiv.), and HFIP (1.0 mL).* Yield of **3.26a**: 83% (25 mg, 0.079 mmol, white solid); R_f=0.25 (5:6:9 EtOAc/benzene/hexanes – purified via PTLC); **^{1}H NMR** (500 MHz, $CDCl_3$) δ 6.32 (d, *J* = 2.5 Hz,

1H), 6.23 (d, *J* = 2.4 Hz, 1H), 4.26 (tt, *J* = 11.5, 4.0 Hz, 1H), 3.86 (s, 3H), 3.80 – 3.76 (m, 1H), 3.77 (s, 3H), 2.88 – 2.86 (m, 2H), 1.99 (dd, *J* = 10.0, 6.6 Hz, 1H), 1.92 (ddd, *J* = 12.5, 4.1, 2.2 Hz, 1H), 1.72 – 1.62 (m, 1H), 1.61 (broad s, 1H), 1.34 (d, *J* = 11.0 Hz, 1H), 1.26 (t, *J* = 12.1 Hz, 1H), 1.20 (s, 3H), 1.16 (t, *J* = 11.0 Hz, 1H), 1.07 (s, 3H); **^{13}C NMR** (151 MHz, $CDCl_3$) δ 160.04, 159.98, 139.8, 122.7, 118.4, 105.4, 97.8, 65.5, 55.7, 55.4, 52.5, 49.9, 43.0, 39.3, 35.0, 32.9, 32.8, 21.5, 20.9; **HRMS** (ES+) *m/z* calc'd for $C_{19}H_{25}NO_3Na$ $[M + Na]^+$: 338.1732, found 338.1732.

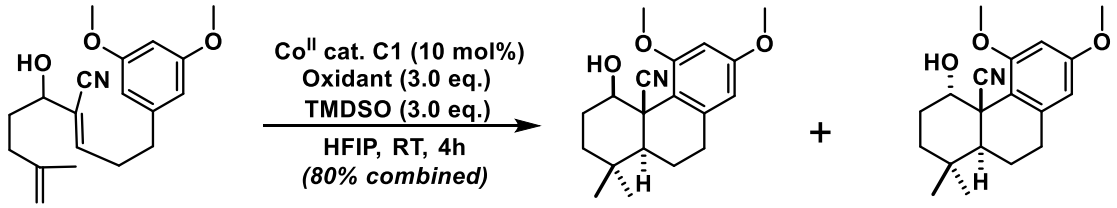

3.28a **3.29a** **3.30a**

Prepared according to general procedure I, using α,β-unsaturated nitrile **3.28a** *(10 mg, 0.032 mmol, 1.0 equiv.), cobalt catalyst* **C1** *(2 mg, 0.003 mmol, 0.1 equiv.), 1-fluoro-2,4,6-trimethylpyridinium triflate (28 mg, 0.095 mmol, 3.0 equiv.), TMDSO (17 µL, 0.095 mmol, 3.0 equiv.), and HFIP (0.5 mL).* Yield of isomer with equatorial hydroxyl group **3.29a:** 60% (6 mg, 0.019 mmol, white solid); R_f=0.15 (18:32:50 EtOAc/benzene/hexanes – purified via PTLC); **^{1}H NMR** (500 MHz, C_6D_6) δ 6.15 – 6.14 (m- overlapping arene doublets, 2H), 4.99 (s -OH, 1H), 3.85 (s-broad, 1H), 3.32 (s, 3H), 3.04 (s, 3H), 2.63 (ddd, *J* = 16.6, 4.8, 3.7 Hz, 1H), 2.42 (ddd, *J* = 16.9, 11.3, 5.9 Hz, 1H), 2.16 (ddd, *J* =13.9, 11.7, 2.2 Hz, 1H), 1.99 – 1.93 (m, 1H), 1.70 (ddd, *J* = 24.7, 11.5, 5.3 Hz, 1H), 1.65 – 1.57 (m, 1H), 1.54 (dtd, *J* = 9.0, 6.0, 3.1 Hz, 1H), 1.30 (s, 3H), 1.19 (ddd, *J* = 13.7, 6.8, 2.3 Hz, 1H), 1.10 (dd, *J* = 11.6, 2.8 Hz, 1H), 0.73 (s, 3H); **^{13}C NMR** (126 MHz, $CDCl_3$) δ 160.0, 158.8, 140.9, 120.6, 120.6, 107.0, 98.8, 74.7, 55.9, 54.9, 47.6, 46.8, 33.8, 33.0, 32.3, 30.3, 28.2, 23.1, 21.9; *See spectra for 2D NMR experiments*; **HRMS** (ES+) *m/z* calc'd for $C_{19}H_{25}NO_3Na$ $[M + Na]^+$: 338.1732, found 338.1737. Yield of isomer with axial hydroxyl group

3.30a: 20% (2 mg, 0.006 mmol, white solid); R_f=0.14 (18:32:50 EtOAc/benzene/hexanes – purified via PTLC); **^{1}H NMR** (500 MHz, $CDCl_3$) δ 6.33 (d, *J* = 2.4 Hz, 1H), 6.26 (d, *J* = 2.3 Hz, 1H), 5.38 (s-broad, 1H), 3.86 (s, 3H), 3.78 (s, 3H), 2.87 – 2.83 (m-overlapping benzylic C-H signals, 2H), 2.25 – 2.17 (m, 1H), 2.00 (d-broad, *J* = 13.4 Hz, 1H), 1.88 (d, *J* = 12.1 Hz, 1H), 1.82 (ddd, *J* = 14.4, 7.3, 3.5 Hz, 1H), 1.74 – 1.67 (m, 2H), 1.45 (s-broad, 1H), 1.32 (dt, *J* = 13.6, 3.6 Hz, 1H), 1.18 (s, 3H), 1.03 (s, 3H); **^{13}C NMR** (126 MHz, $CDCl_3$) δ 160.3, 159.5, 142.4, 122.4, 115.6, 106.3, 97.8, 68.0, 55.9, 55.4, 45.0, 44.7, 33.7, 33.6, 32.7, 32.3, 26.1, 21.0, 20.1; *See spectra for 2D NMR experiments*; **HRMS** (ES+) *m/z* calc'd for $C_{19}H_{25}NO_3Na$ $[M + Na]^+$: 338.1732, found 338.1720.

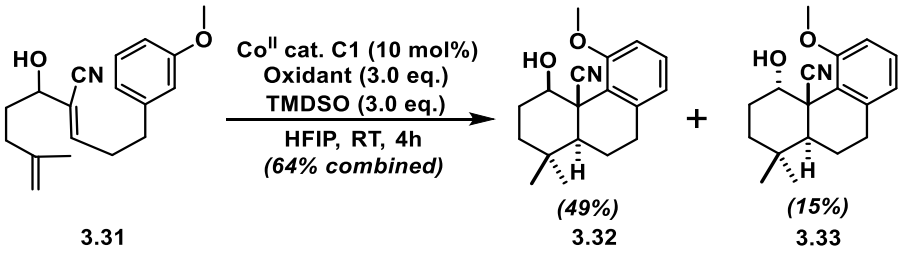

Prepared according to general procedure I, using α,β-unsaturated nitrile **3.31** *(20 mg, 0.070 mmol, 1.0 equiv.), cobalt catalyst* **C1** *(4.2 mg, 0.007 mmol, 0.1 equiv.), 1-fluoro-2,4,6-trimethylpyridinium tetrafluoroborate (48 mg, 0.210 mmol, 3.0 equiv.), TMDSO (37 µL, 0.210 mmol, 3.0 equiv.), and HFIP (1.6 mL).* Yield of isomer with equatorial hydroxyl group **3.32:** 49% (9.8 mg, 0.034 mmol, white solid); R_f=0.20 (15:25:60 EtOAc/benzene/cyclohexane – purified via PTLC); **^{1}H NMR** (600 MHz, $CDCl_3$) δ 7.21 (t, *J* = 7.9 Hz, 1H), 6.85 (d, *J* = 8.1 Hz, 1H), 6.82 (d, *J* = 7.6 Hz, 1H), 5.02 (s, 1H), 3.99 – 3.98 (m, 1H), 3.97 (s, 3H), 3.03 – 2.97 (m, 1H), 2.83 (ddd, *J* = 16.6, 10.6, 6.1 Hz, 1H), 1.96 – 1.90 (m, 2H), 1.83 – 1.76 (m, 3H), 1.42 (dd, *J* = 11.4, 3.4 Hz, 1H), 1.39 – 1.35 (m, 1H), 1.23 (s, 3H), 0.99 (s, 3H); **^{13}C NMR** (151 MHz, $CDCl_3$) δ 157.2, 140.3, 128.9, 127.0, 123.7, 120.4, 110.5, 74.0, 56.8, 47.7, 46.9, 34.0, 33.1, 31.5, 30.5, 27.8, 22.8, 21.6;

HRMS (ES+) *m/z* calc'd for $C_{18}H_{23}NO_2Na$ $[M+Na]^+$: 308.1627, found 308.1622; Yield of isomer with equatorial hydroxyl group **3.33:** 15% (3.0 mg, 0.011 mmol, white solid); R_f=0.19 (15:25:60 EtOAc/benzene/cyclohexane – purified via PTLC); **^{1}H NMR** (600 MHz, $CDCl_3$) δ 7.20 (t, *J* = 7.9 Hz, 1H), 6.76 (overlapping d, *J* = 7.9 Hz, 2H), 5.47 (s, 1H), 3.90 (s, 3H), 2.91 – 2.86 (m, 2H), 2.23 (tt, *J* = 14.6, 3.5 Hz, 1H), 2.05 – 1.99 (m, 2H), 1.92 (d, *J* = 12.2 Hz, 1H), 1.83 (dq, *J* = 15.0, 3.9 Hz, 1H), 1.74 – 1.67 (m, 3H), 1.44 (br s, 1H), 1.33 (dt, *J* = 13.6, 3.7 Hz, 1H), 1.19 (s, 3H), 1.04 (s, 3H); **^{13}C NMR** (151 MHz, $CDCl_3$) δ 158.5, 141.4, 129.3, 123.2, 123.1, 122.2, 109.6, 68.0, 55.9, 45.0, 44.9, 33.8, 33.6, 32.3, 32.2, 26.2, 20.9, 20.2; **HRMS** (ES+) *m/z* calc'd for $C_{18}H_{23}NO_2Na$ $[M+Na]^+$: 308.1627, found 308.1624.

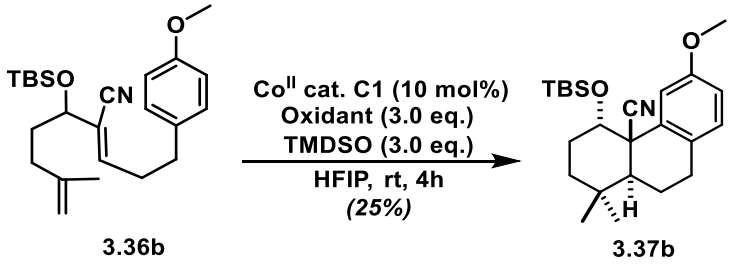

3.36b 3.37b

Prepared according to general procedure I, using α,β-unsaturated nitrile **3.36b** *(50 mg, 0.125 mmol, 1.0 equiv.), cobalt catalyst* **C1** *(8 mg, 0.013 mmol, 0.1 equiv.), 1-fluoro-2,4,6-trimethylpyridinium triflate (109 mg, 0.375 mmol, 3.0 equiv.), TMDSO (66 µL, 0.375 mmol, 3.0 equiv.), and HFIP (1.0 mL).* Yield of **3.37b**: 25% (12.5 mg, 0.031 mmol, white foam); R_f=0.15 (1:25:74 EtOAc/benzene/cyclohexane – purified via PTLC); **^{1}H NMR** (600 MHz, $CDCl_3$) δ 6.99 (d, *J* = 8.5 Hz, 1H), 6.88 (d, *J* = 2.5 Hz, 1H), 6.74 (dd, *J* = 8.4, 2.5 Hz, 1H), 4.71 (s, 1H), 3.79 (s, 3H), 2.83 (dd, *J* = 16.4, 3.7 Hz, 1H), 2.79 – 2.71 (m, 1H), 2.33 – 2.27 (m, 1H), 2.00 (dd, *J* = 13.2, 5.5 Hz, 1H), 1.96 (d, *J* = 12.5 Hz, 1H), 1.80 – 1.75 (m, 2H), 1.74 – 1.69 (m, 1H), 1.30 (dt, *J* = 6.3, 3.6 Hz, 1H), 1.17 (s, 3H), 1.02 (s, 3H), 0.59 (s, 9H), 0.06 (s, 3H), –0.18 (s, 3H); **^{13}C NMR** (151 MHz, $CDCl_3$) δ 158.2, 136.6, 130.8, 129.8, 123.4, 113.8, 112.0, 70.9, 55.5, 43.9, 33.9, 33.4, 32.3,

30.2, 27.6, 25.4, 21.4, 20.1, 17.9, –3.9, –5.4; **HRMS** (ES+) *m/z* calc'd for $C_{24}H_{37}NO_2SiNa$ [M + Na]$^+$: 422.2491, found 422.2486.

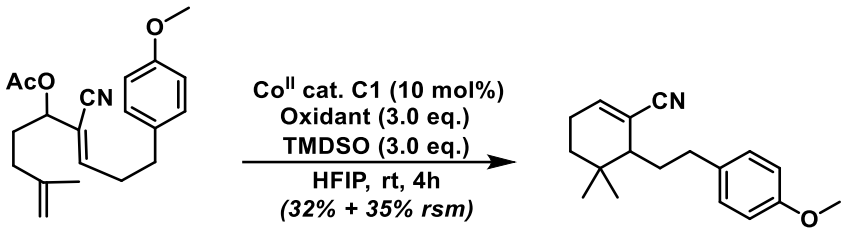

3.36c **3.39**

Prepared according to general procedure I, using α,β-unsaturated nitrile **3.36c** *(20 mg, 0.061 mmol, 1.0 equiv.), cobalt catalyst* **C1** *(3.7 mg, 0.006 mmol, 0.1 equiv.), 1-fluoro-2,4,6-trimethylpyridinium triflate (53 mg, 0.183 mmol, 3.0 equiv.), TMDSO (32 µL, 0.183 mmol, 3.0 equiv.), and HFIP (1.0 mL).* Yield of **3.39**: 32% (6.4 mg, 0.020 mmol, colorless oil); R_f=0.20 (3:22 EtOAc/hexanes – purified via PTLC); **^{1}H NMR** (500 MHz, $CDCl_3$) δ 7.15 (d, *J* = 8.5 Hz, 2H), 6.84 (d, *J* = 8.6 Hz, 2H), 6.64 (td, *J* = 3.7, 1.1 Hz, 1H), 3.79 (s, 3H), 2.91 (ddd, *J* = 13.4, 11.2, 5.1 Hz, 1H), 2.66 (ddd, *J* = 13.8, 11.2, 6.1 Hz, 1H), 2.23 – 2.17 (m, 2H), 1.95 – 1.87 (m, 2H), 1.67 – 1.58 (m, 1H), 1.49 (dt, *J* = 13.6, 6.8 Hz, 1H), 1.34 – 1.28 (m, 1H), 0.91 (s, 3H), 0.89 (s, 3H); **^{13}C NMR** (150 MHz, $CDCl_3$) δ 158.0, 145.2, 134.3, 129.6, 120.6, 116.6, 114.0, 55.4, 45.4, 34.5, 33.7, 32.2, 27.8, 24.6, 24.1; **HRMS** (ES+) *m/z* calc'd for $C_{18}H_{23}NONa$ [M + Na]$^+$: 292.1677, found 292.1678.

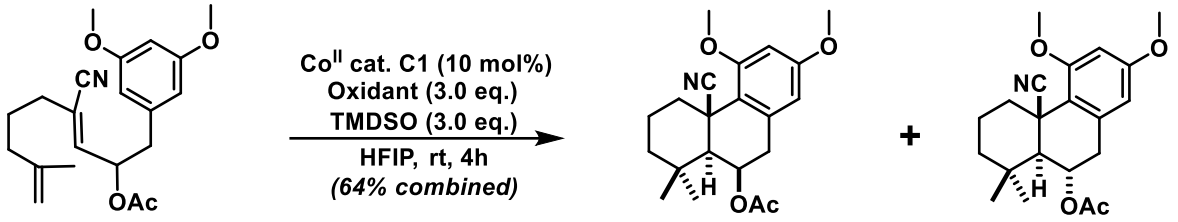

3.47a **3.48a** **3.49a**

Prepared according to general procedure I, using α,β-unsaturated nitrile **3.47a** *(30 mg, 0.084 mmol, 1.0 equiv.), cobalt catalyst* **C1** *(5 mg, 0.008 mmol, 0.1 equiv.), 1-fluoro-2,4,6-trimethylpyridinium triflate (73 mg, 0.252 mmol, 3.0 equiv.), TMDSO (44 µL, 0.252 mmol, 3.0 equiv.), and HFIP (1.0 mL).* Yield of isomer with axial OAc group **3.48a**: 34% (10 mg, 0.028 mmol, white solid); R_f=0.15 (3:22 EtOAc/hexanes); **^{1}H NMR** (600 MHz, $CDCl_3$) δ 6.38 (d, *J* = 1.8 Hz, 1H), 6.19(d, *J* = 1.8 Hz, 1H), 5.62 (s, 1H), 3.89 (s, 3H), 3.78 (s, 3H), 3.52 (d, *J* = 13.3 Hz, 1H), 3.02 (dd, *J* = 17.7, 3.4 Hz, 1H), 2.96 (d, *J* = 17.5 Hz, 1H), 2.12 – 2.08 (qt, *J* = 13.6, 3.5 Hz, 1H), 2.04 (s, 3H), 1.73 – 1.65 (m, 1H), 1.62 – 1.52 (m, 2H), 1.30 (*J* = 13.6, 3.6 Hz, 1H), 1.25 (s, 3H), 1.21 *J* = 13.6, 3.6 Hz, 1H), 1.08 (s, 3H); **^{13}C NMR** (151 MHz, $CDCl_3$) δ 171.2, 160.2, 159.9, 135.3, 123.4, 117.9, 105.7, 98.4, 65.0, 55.7, 55.4, 53.8, 42.2, 38.1, 37.2, 35.8, 34.4, 33.0, 21.4, 21.3, 20.4; **HRMS** (ES+) *m/z* calc'd for $C_{21}H_{27}NO_4Na$ $[M + Na]^+$: 380.1838, found 380.1830. Yield of isomer with equatorial OAc group **3.49a**: 30% (9 mg, 0.025 mmol, white solid); R_f=0.20 (5:55:40 EtOAc/benzene/hexanes – purified via PTLC); **^{1}H NMR** (500 MHz, $CDCl_3$) δ 6.36 (d, *J* = 2.5 Hz, 1H), 6.24 (d, *J* = 2.5 Hz, 1H), 5.39 (dt, *J* = 7.9, 5.5 Hz, 1H), 3.80 (s, 3H), 3.78 (s, 3H), 3.39 (d, *J* = 10.3, 1H), 3.31 (dd, *J* = 16.1, 5.0 Hz, 1H), 2.87 (dd, *J* = 16.2, 5.8 Hz, 1H), 2.03 (s, 3H), 2.00 – 1.89 (m, 1H), 1.74 – 1.64 (m, 3H), 1.60 (dt, *J* = 7.7, 3.1 Hz, 1H), 1.31 (td, *J* = 13.3, 3.7 Hz, 1H), 1.26 (s, 3H), 1.04 (s, 3H); **^{13}C NMR** (151 MHz, $CDCl_3$) δ 170.3, 160.3, 159.1, 137.8, 123.0, 117.6, 105.8, 98.7, 70.5, 55.9, 55.7, 55.5, 41.4, 39.7, 37.4, 36.3, 34.6, 33.2, 21.7, 21.3, 20.0; **HRMS** (ES+) *m/z* calc'd for $C_{21}H_{27}NO_4Na$ $[M + Na]^+$: 380.1838, found 380.1844.

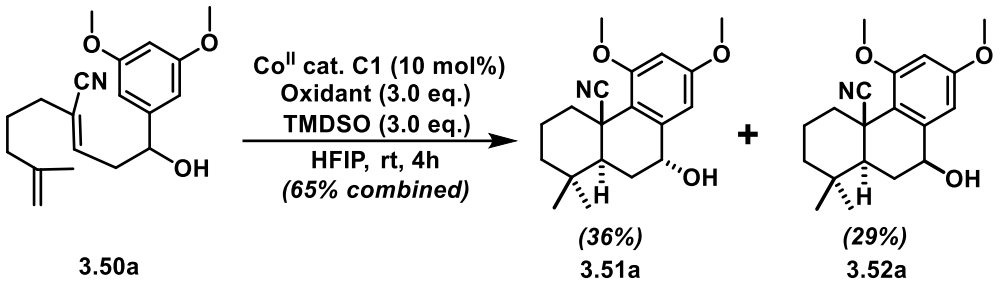

3.50a 3.51a 3.52a

Prepared according to general procedure I, using α,β-unsaturated nitrile **3.50a** *(18 mg, 0.057 mmol, 1.0 equiv.), cobalt catalyst* **C1** *(3.5 mg, 0.006 mmol, 0.1 equiv.), 1-fluoro-2,4,6-trimethylpyridinium triflate (50 mg, 0.171 mmol, 3.0 equiv.), TMDSO (30 µL, 0.171 mmol, 3.0 equiv.), and HFIP (1.0 mL).* Yield of isomer with axial hydroxyl group **3.51a**: 36% (6.5 mg, 0.021 mmol, white solid); R_f = 0.21 (3:7 EtOAc/hexanes); **^{1}H NMR** (600 MHz, $CDCl_3$) δ 6.50 (d, *J* = 2.4 Hz, 1H), 6.43 (d, *J* = 2.4 Hz, 1H), 4.79 (s, 1H), 3.85 (s, 3H), 3.81 (s, 3H), 3.50 (d, *J* = 13.4 Hz, 1H), 2.09 (d, *J* = 13.1 Hz, 1H), 1.98 (qt, *J* = 13.9, 3.3 Hz, 1H), 1.92 – 1.87 (m, 3H), 1.72 – 1.66 (m, 1H), 1.60 (d, *J* = 13.3 Hz, 1H), 1.32 (td, *J* = 13.5, 3.9 Hz, 1H), 1.20 (td, *J* = 13.5, 3.9 Hz, 1H), 1.17 (s, 3H), 1.02 (s, 3H); **^{13}C NMR** (151 MHz, $CDCl_3$) δ 160.5, 160.0, 140.1, 122.8, 119.3, 106.2, 100.1, 68.6, 55.8, 55.6, 45.3, 41.0, 39.7, 34.9, 33.6, 32.5, 29.6, 20.6, 20.5; **HRMS** (ES+) *m/z* calc'd for $C_{19}H_{25}NO_3Na$ $[M + Na]^+$: 338.1732, found 338.1737. Yield of isomer with equatorial hydroxyl group **3.52a**: 29% (5.2 mg, 0.017 mmol, white solid); R_f=0.19 (3:7 EtOAc/ hexanes); **^{1}H NMR** (600 MHz, $CDCl_3$) δ 6.79 (d, *J* = 2.3 Hz, 1H), 6.40 (d, *J* = 2.3 Hz, 1H), 4.70 – 4.68 (m, 1H), 3.85 (s, 3H), 3.81 (s, 3H), 3.44 (d, *J* = 13.4 Hz, 1H), 2.36 (dd, *J* = 12.5, 5.9 Hz, 1H), 1.97 (qt, *J* = 13.7, 3.1 Hz, 1H), 1.69 – 1.63 (m, 3H), 1.59 (d, *J* = 13.9 Hz, 1H), 1.36 (d, *J* = 12.1 Hz, 1H), 1.26 (td, *J* = 13.4, 3.1 Hz, 1H), 1.18 (s, 3H), 1.14 (td, *J* = 13.4, 3.1 Hz, 1H), 1.01 (s, 3H); **^{13}C NMR** (151 MHz, $CDCl_3$) δ 160.6, 159.5, 143.3, 123.0, 119.0, 102.9, 99.5, 71.4, 55.8, 55.6, 49.9, 40.8, 40.4, 35.2, 33.8, 32.7, 32.2, 20.6, 20.4; **HRMS** (ES+) *m/z* calc'd for $C_{19}H_{25}NO_3Na$ $[M + Na]^+$: 338.1732, found 338.1730.

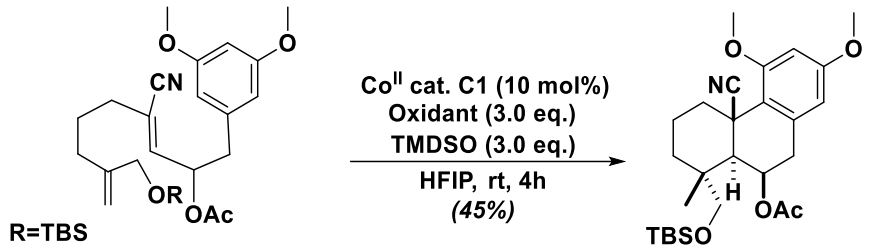

3.56 3.57

Prepared according to general procedure D, using α,β-unsaturated nitrile **3.56** *(20 mg, 0.041 mmol, 1.0 equiv.), cobalt catalyst* **C1** *(2.5 mg, 0.004 mmol, 0.1 equiv.), 1-fluoro-2,4,6-trimethylpyridinium triflate (36 mg, 0.123 mmol, 3.0 equiv.), TMDSO (30 µL, 0.123 mmol, 3.0 equiv.), and HFIP (1.0 mL).* Yield of **3.57**: 45% (9 mg, 0.018 mmol, white solid); R_f=0.15 (8:92 EtOAc/hexanes); *Note: Contains approximately 7% of a minor diastereomer*; **^{1}H NMR** (500 MHz, $CDCl_3$) δ 6.39 (d, *J* = 2.1 Hz, 1H), 6.20 (d, *J* = 1.9 Hz, 1H), 5.50 (broad s, 1H), 3.89 (s, 3H), 3.78 (s, 3H), 3.69 (d, *J* = 10.2 Hz, 1H), 3.46 (d, *J* = 13.1 Hz, 1H), 3.08 (d, *J* = 10.3 Hz, 1H), 2.99 (dd, *J* = 17.7, 3.2 Hz, 1H), 2.92 (d, *J* = 17.3 Hz, 1H), 2.18 – 2.07 (m, 2H), 2.04 (s, 3H), 1.79 – 1.69 (m, 2H), 1.27 – 1.16 (m, 3H), 1.12 (s, 3H), 0.87 (s, 9H), 0.07 (s, 3H), 0.05 (s, 3H); **^{13}C NMR** (151 MHz, $CDCl_3$) δ 171.2, 160.2, 159.8, 135.6, 123.8, 118.0, 105.8, 98.3, 70.6, 64.9, 55.8, 55.4, 46.8, 38.9, 37.7, 36.8, 35.9, 35.8, 26.0, 21.3, 20.1, 17.6, –5.3, –5.6; NOTE: *see spectra for 2D NMR experiments*. **HRMS** (ES+) *m/z* calc'd for $C_{27}H_{41}NO_5SiNa$ $[M + Na]^+$: 510.2652, found 510.2543.

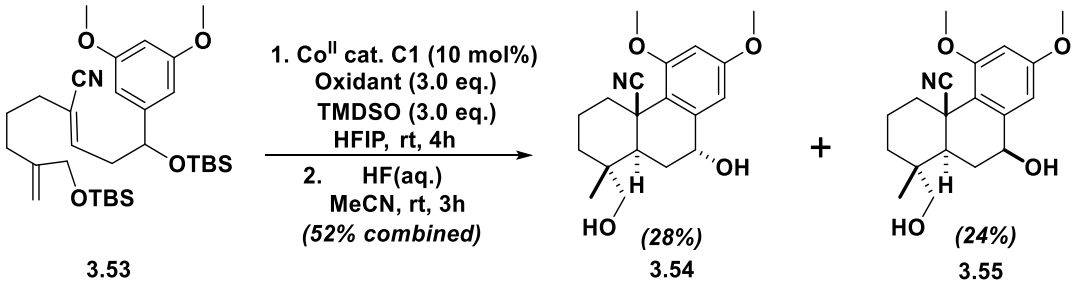

3.53 3.54 3.55

Prepared according to general procedure D, using α,β-unsaturated nitrile **3.53** *(20 mg, 0.036 mmol, 1.0 equiv.), cobalt catalyst* **C1** *(2.2 mg, 0.004 mmol, 0.1 equiv.), 1-fluoro-2,4,6-*

trimethylpyridinium triflate (31 mg, 0.107 mmol, 3.0 equiv.), TMDSO (19 µL, 0.107 mmol, 3.0 equiv.) and HFIP (1.0 mL). The crude residue was subjected to general procedure E for desilylation, using 40% w/w aq. hydrofluoric acid (0.2 mL, excess) and acetonitrile (1.0 mL). Yield of isomer with axial C7 hydroxyl group **3.54**: 28% (5.6 mg, 0.012 mmol, white solid); R_f=0.35 (4:1 EtOAc/hexanes); **^{1}H NMR** (600 MHz, $CDCl_3$) δ 6.48 (d, *J* = 2.4 Hz, 1H), 6.44 (d, *J* = 2.4 Hz, 1H), 4.77 (s, 1H), 3.86 (s, 3H), 3.81 (s, 3H), 3.66 (d, *J* = 11.5 Hz, 1H), 3.45 (d, *J* = 13.5 Hz, 1H), 3.13 (d, *J* = 11.5 Hz, 1H), 2.38 (broad s, 1H), 2.29 (d, *J* = 12.4 Hz, 1H), 2.08 – 1.98 (m, 2H), 1.92 – 1.85 (m, 1H), 1.79 – 1.72 (m, 2H), 1.60 (broad s, 1H), 1.36 (d, *J* = 13.5 Hz, 1H), 1.20 (td, *J* = 13.6, 3.0 Hz, 1H), 1.06 (s, 3H); **^{13}C NMR** (151 MHz, $CDCl_3$) δ 160.6, 159.9, 140.1, 122.8, 119.2, 106.3., 100.0, 70.5, 68.9, 55.8, 55.6, 39.6, 38.9, 37.9, 34.5, 34.2, 28.9, 20.0, 16.6; **HRMS** (ES+) *m/z* calc'd for $C_{19}H_{25}NO_4Na$ $[M + Na]^+$: 354.1681, found 354.1685. Yield of isomer with equatorial C7 hydroxyl group **3.55**: 24% (4.8 mg, 0.009 mmol, white solid); R_f=0.40 (4:1 EtOAc/ hexanes); **^{1}H NMR** (600 MHz, $CDCl_3$) δ 6.80 (d, *J* = 2.4 Hz, 1H), 6.41 (d, *J* = 2.4 Hz, 1H), 4.77 – 4.71 (m, 1H), 3.86 (s, 3H), 3.81 (s, 3H), 3.60 (d, *J* = 10.8 Hz, 1H), 3.43 (d, *J* = 13.3 Hz, 1H), 3.22 (d, *J* = 10.8 Hz, 1H), 2.32 (dd, *J* = 12.3, 5.9 Hz, 1H), 1.87 (d, *J* = 12.1 Hz, 1H), 1.68 – 1.60 (m, 2H), 1.40 (d, *J* = 12.9 Hz, 1H), 1.15 (td, *J* = 13.5, 3.2 Hz, 1H), 1.11 (s, 3H); **^{13}C NMR** (151 MHz, $CDCl_3$) δ 160.6, 159.4, 143.4, 123.3, 118.9, 102.8, 99.5, 71.0, 70.7, 55.8, 55.6, 43.2, 40.3, 38.1, 34.7, 34.3, 31.7, 29.9, 19.8, 16.7; **HRMS** (ES+) *m/z* calc'd for $C_{19}H_{25}NO_4Na$ $[M + Na]^+$: 354.1681, found 354.1685.

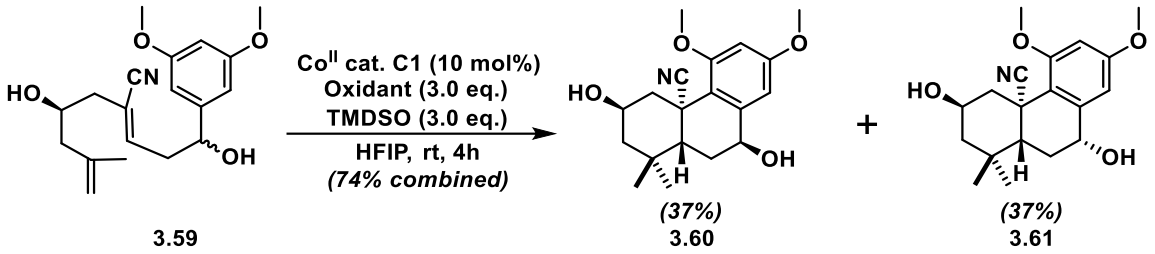

3.59 3.60 3.61

Prepared according to general procedure D, using α,β-unsaturated nitrile **3.59** *(38 mg, 0.124 mmol, 1.0 equiv.), cobalt catalyst* **C1** *(7.5 mg, 0.012 mmol, 0.1 equiv.), 1-fluoro-2,4,6-trimethylpyridinium triflate (107 mg, 0.371 mmol, 3.0 equiv.), TMDSO (65 µL, 0.371 mmol, 3.0 equiv.), and HFIP (4.0 mL)*. Yield of isomer with axial C7 hydroxyl group **3.60**: 37% (14 mg, 0.046 mmol, white solid); R_f=0.32 (3:2 EtOAc/hexanes); **^{1}H NMR** (500 MHz, $CDCl_3$) δ 6.50 (d, *J* = 2.1 Hz, 1H), 6.43 (d, *J* = 2.1 Hz, 1H), 4.80 (s-broad, 1H), 4.24 (tt, *J* = 11.4, 3.9 Hz, 1H), 3.86 (s, 3H), 3.80 (s, 3H), 3.76 (d, *J* = 12.8 Hz, 1H), 2.11 (s, 1H), 2.08 (d, *J* = 12.8 Hz, 1H), 1.93 (d, *J* = 12.5 Hz, 1H), 1.89 – 1.82 (m, 2H), 1.29 (d, *J* = 12.1 Hz, 2H), 1.19 (s, 3H), 1.15 (d, *J* = 12.1 Hz, 1H), 1.06 (s, 3H); **^{13}C NMR** (126 MHz, C_6D_6) δ 160.7, 159.7, 140.1, 122.1, 118.3, 106.3, 100.0, 68.5, 65.4, 55.8, 55.6, 49.89, 44.85, 42.5, 39.3, 34.4, 32.6, 29.3, 21.5; **HRMS** (ES+) *m/z* calc'd for $C_{19}H_{25}NO_4Na$ $[M + Na]^+$: 354.1681, found 354.1682; $[\alpha]_D^{22} = -59.8$ $(c = 0.1, CHCl_3)$. Yield of isomer with equatorial C7 hydroxyl group **3.61**: 37% (14 mg, 0.046 mmol, white solid); R_f=0.35 (3:2 EtOAc/hexanes); **^{1}H NMR** (500 MHz, $CDCl_3$) δ 6.80 (d, *J* = 2.0 Hz, 1H), 6.40 (d, *J* = 2.5 Hz, 1H), 4.71 – 4.66 (m, 1H), 4.22 (tt, *J* = 11.4, 3.9 Hz, 1H), 3.86 (s, 3H), 3.81 (s, 3H), 3.73 (ddd, *J* = 12.6, 3.4, 2.2 Hz, 1H), 2.36 (dd, *J* = 12.5, 6.0 Hz, 1H), 1.95 – 1.90 (m, 1H), 1.65 (dd, *J* = 23.6, 12.3 Hz, 1H), 1.33 (d, *J* = 12.0 Hz, 1H), 1.28 – 1.23 (m, 1H), 1.20 (s, 3H), 1.12 (t, *J* = 12.1 Hz, 1H), 1.07 (s, 3H); **^{13}C NMR** (126 MHz, $CDCl_3$) δ 160.8, 159.2, 143.3, 122.3, 117.9, 103.1, 99.4, 71.2, 65.2, 55.9, 55.6, 49.7, 49.4, 42.9, 39.9, 34.8, 32.8, 31.7, 21.4; **HRMS** (ES+) *m/z* calc'd for $C_{19}H_{25}NO_4Na$ $[M + Na]^+$: 354.1681, found 354.1690; $[\alpha]_D^{22} = -54.9$ $(c = 0.1, CHCl_3)$.

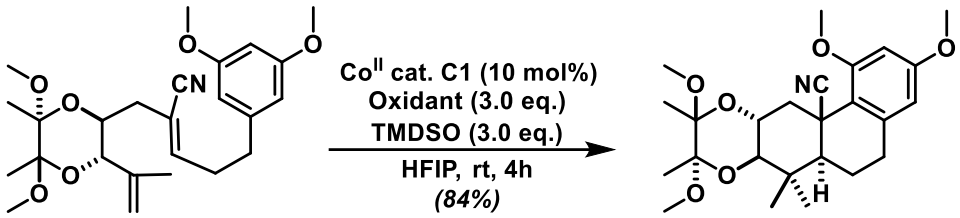

3.62 **3.63**

Prepared according to general procedure D, using α,β-unsaturated nitrile **3.62** *(15 mg, 0.034 mmol, 1.0 equiv.), cobalt catalyst* **C1** *(2.0 mg, 0.003 mmol, 0.1 equiv.), 1-fluoro-2,4,6-trimethylpyridinium triflate (29 mg, 0.101 mmol, 3.0 equiv.), TMDSO (18 µL, 0.101 mmol, 3.0 equiv.), and HFIP (0.7 mL).* Yield of **3.63**: 84% (12.6 mg, 0.028 mmol, white solid); R_f=0.15 (1:9 EtOAc/hexanes); **^{1}H NMR** (600 MHz, $CDCl_3$) δ 6.31 (d, *J* = 2.3 Hz, 1H), 6.23 (d, *J* = 2.2 Hz, 1H), 4.14 (ddd, *J* = 12.3, 10.3, 4.1 Hz, 1H), 3.85 (s, 3H), 3.78 (s, 3H), 3.60 (dd, *J* = 12.9, 4.0 Hz, 1H), 3.34 (s, 3H), 3.23 (s, 3H), 3.22 (m, 1H), 2.91 – 2.81 (m, 2H), 2.02 – 1.97 (m, 1H), 1.74 (qd, *J* = 12.0, 6.0 Hz, 1H), 1.39 (t, *J* = 11.7 Hz, 2H), 1.31 (s, 3H), 1.30 (s, 2H), 1.20 (s, 3H), 1.12 (s, 3H); **^{13}C NMR** (151 MHz, $CDCl_3$) δ 160.1, 160.0, 139.6, 122.4, 118.1, 105.3, 99.8, 99.4, 97.7, 77.6, 65.1, 55.8, 55.4, 52.6, 48.2, 47.8, 38.9, 38.3, 37.7, 32.8, 29.9, 27.5, 20.7, 17.97, 17.96, 15.7; **HRMS** (ES+) *m/z* calc'd for $C_{25}H_{35}NO_6Na$ $[M + Na]^+$: 468.2362, found 468.2366.

Total Syntheses of 2-O-Deacetyl Plebedipenes A and C

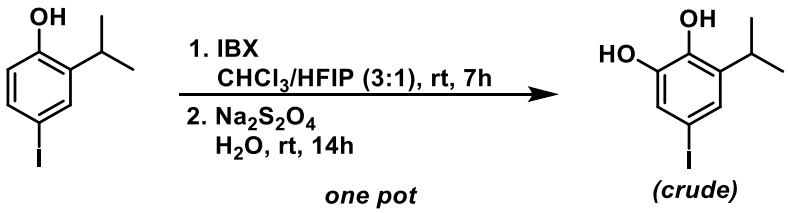

3.67 **S3.32**

Experimental procedure adapted from a report by Pettus et al.[53]: To a solution of 4-iodo-2-isopropylphenol **3.67**[54] (5.39 g, 20.6 mmol, 1 equiv.) in a mixture of $CHCl_3$/HFIP (3:1, 96 mL)

was added 2-iodoxybenzoic acid (8.65 g, 30.9 mmol, 1.5 equiv.). The reaction mixture was stirred for 7 h at room temperature or until complete consumption of starting material (as indicated by TLC). Water (90 mL) and solid $Na_2S_2O_4$ (15 equiv.) were subsequently added and the biphasic mixture was stirred vigorously for 16 h. The reaction mixture was diluted with EtOAc (100 mL) and water (70 mL) and the phases were separated. The organic phase was washed with a mixture of sat. $NaHCO_3$, brine and water (1:5:2, 4 x 60 mL) and the combined aqueous phases were back-extracted with EtOAc (2 x 50 mL). The combined organic phases were dried over $MgSO_4$, filtered and concentrated in vacuo. The crude product was used without further purification for the next reaction (**S3.32**, R_f= 0.20 in 1:4 EtOAc/hexanes). *Note: This compound is sensitive and should be stored under inert gas. Purification via flash column chromatography on SiO_2 leads to partial decomposition.* **^{1}H NMR** (500 MHz, $CDCl_3$) δ 7.08 (d, *J* = 1.9 Hz, 1H), 7.02 (d, *J* = 1.9 Hz, 1H), 5.30, (s, 1H), 5.26 (s, 1H), 3.15 (sept, *J* = 6.9 Hz, 1H), 1.23 (s, 3H), 1.22 (s, 3H); **^{13}C NMR** (151 MHz, $CDCl_3$): δ 143.8, 141.6, 137.6, 127.9, 121.7, 81.8, 27.2, 22.5; **HRMS** (ESI): *m/z* calcd for $C_9H_{11}IO_2^+$: 277.9804 $[M]^+$; found: 277.9804.

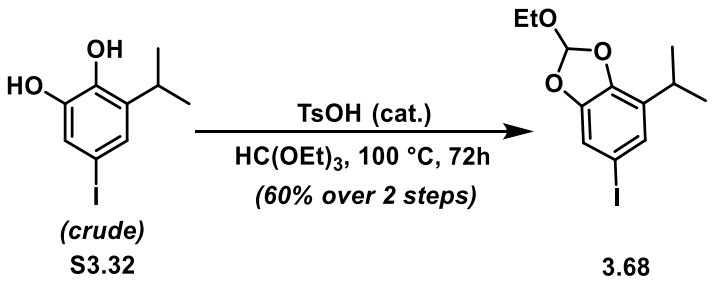

To a solution of crude 4-iodo-2-isopropylcatechol **S3.32** in triethyl orthoformate (50 mL, solvent) was added a catalytic amount of *p*-toluenesulfonic acid (458 mg, 2.66 mmol, 0.1 equiv.). The reaction mixture was heated to 100°C for 72 h or until complete consumption of starting material (monitored by TLC). The resulting solution was cooled to room temperature, concentrated under

reduced pressure, and directly purified via flash column chromatography (EtOAc:hexanes = 1:50) to give **3.68** as an orange oil (4.14 g, 12.38 mmol, 60% yield over two steps). **^{1}H NMR** (500 MHz, $CDCl_3$) δ 7.07 (d, *J* = 1.4 Hz, 1H), 7.03 (d, *J* = 1.4 Hz, 1H), 6.85 (s, 1H), 3.69 (q, *J* = 7.4 Hz, 2H), 2.99 (sept, *J* = 7.1 Hz, 1H), 1.27 (t, *J* = 7.1 Hz, 3H), 1.25 (s, 3H), 1.24 (s, 3H); **^{13}C NMR** (151 MHz, $CDCl_3$) δ 146.8, 143.8, 132.1, 128.9, 119.1, 115.1, 82.8, 59.4, 29.0, 22.2, 22.1, 15.0; HRMS (ESI): *m/z* calcd for $C_{12}H_{15}IO_3^+$: 334.0066 $[M]^+$; found: 334.0066.

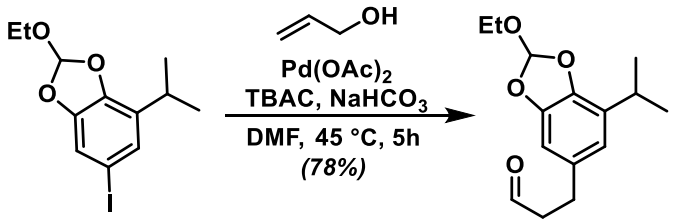

3.68 **3.69**

To a solution of **3.68** (2.4 g, 7.2 mmol, 1.0 equiv.) in degassed DMF (20 mL) was added tetrabutylammonium chloride (2.01 g, 7.2 mmol, 1.0 equiv.), allyl alcohol (0.98 mL, 14.4 mmol, 2.0 equiv.), sodium bicarbonate (1.81 g, 21.6 mmol, 3.0 equiv.), and finally $Pd(OAc)_2$ (80 mg, 0.36 mmol, 0.05 equiv.). The resulting mixture was stirred at 45 °C for 6 hours. After cooling to room temperature, Et_2O (80 mL) was added and the organic phase was washed with H_2O (3x 30 mL). The combined organic extracts were washed with brine (30 mL), dried over Na_2SO_4, filtered and concentrated *in vacuo.* The crude residue was purified via flash column chromatography (EtOAc/hexanes 7:93) to give aldehyde **3.69** as a clear yellow oil (1.49 g, 5.63 mmol, 78% yield); **^{1}H NMR** (600 MHz, $CDCl_3$) δ 9.81 (t, *J* = 1.3 Hz, 1H), 6.84 (s, 1H), 6.57 (d, *J* = 1.7 Hz, 1H), 6.55 (d, *J* = 1.1 Hz, 1H), 3.70 (q, *J* = 7.1 Hz, 2H), 3.01 (sept, *J* = 6.9 Hz, 1H), 2.87 (t, *J* = 7.5 Hz, 2H), 2.73 (td, *J* = 7.4, 1.0 Hz, 2H), 1.26 (t, *J* = 7.1 Hz, 3H), 1.26 (d, *J* = 6.9 Hz, 6H); **^{13}C NMR** (151

MHz, $CDCl_3$) δ 201.7, 145.9, 141.8, 134.0, 129.6, 119.3, 118.8, 105.9, 59.1, 45.7, 29.2, 28.2, 22.3, 22.2, 15.0; **HRMS** (ESI): *m/z* calcd for $C_{15}H_{20}O_4$+Na^+: 287.1259 $[M+Na]^+$; found: 287.1259.

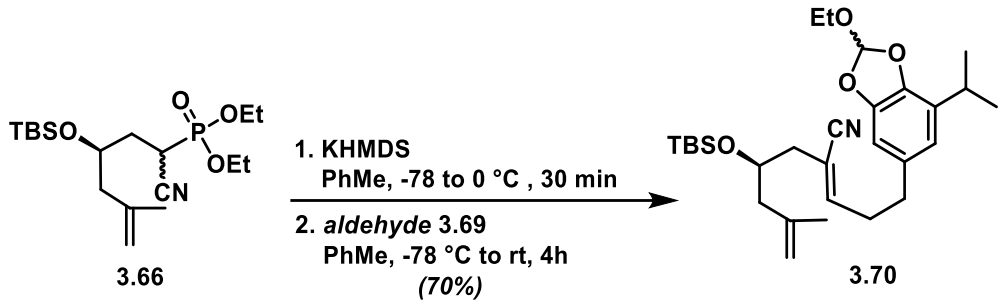

Prepared according to general procedure E, using cyanoalkylphosphonate **3.66** *(736 mg, 1.89 mmol, 1.0 equiv.) and aldehyde* **3.69** *(500mg, 1.89 mmol, 1.0 equiv.) to give a (1:6 E:Z, separable) mixture of α,β-unsaturated nitriles*. Yield of **3.70**: 70% (665 mg, 1.33 mmol, colorless oil); R_f = 0.15 (1:99 EtOAc/hexanes). *Note: 1:1 mixture of diastereomers – most signals overlap;* **^{1}HNMR** (500 MHz, $CDCl_3$): δ 6.84 (s, 1H), 6.56 (s, 1H), 6.54 (s, 1H) 6.15 (t, *J* = 6.4 Hz, 1H), 4.79 (s, 1H), 4.69 (s, 1H), 4.02 (m, 1H), 3.70 (q, *J* = 7.2 Hz, 2H), 3.02 (sept, *J* = 7.0 Hz, 1H), 2.60 – 2.69 (m, 4H), 2.37 (dd, *J* = 14.1, 3.7 Hz, 1H), 2.22 (dd, *J* = 13.5, 5.2 Hz, 1H) 2.21 – 2.10 (m, 2H), 1.73 (s, 3H), 1.26 (*overlapping* t, *J* = 7.1 Hz, 3H) 1.26 (d, *J* = 6.9 Hz, 6H), 0.86 (s, 9H), 0.06 (s, 3H), 0.05 (s, 3H); **^{13}C NMR** (151 MHz, $CDCl_3$) δ 149.1, 145.9, 141.9, 141.9, 141.9, 133.9, 129.5, 119.4, 118.7, 117.7, 113.9, 112.6, 105.97, 105.95, 68.9, 59.0, 45.9, 45.9, 41.7, 34.7, 33.6, 29.2, 25.9, 25.9, 23.0, 22.3, 22.2, 18.1, 15.0, –4.4, –4.6; **HRMS** (ESI): *m/z* calcd for $C_{29}H_{45}NO_4Si$+Na^+: 522.3016 $[M+Na]^+$; found: 522.3016; $[\alpha]_D^{22} = -23.7$ $(c = 1.2, CHCl_3)$.

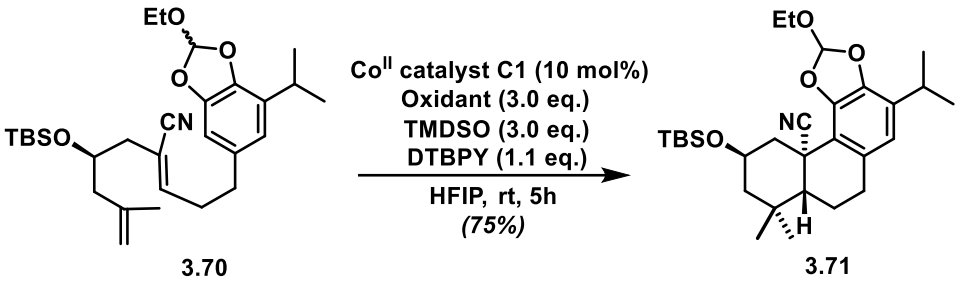

3.70 3.71

A dry round-bottom flask was charged with a magnetic stirring bar, **3.70** (1.0 g, 2.0 mmol, 1.0 equiv.) catalyst **C1** (113 mg, 0.2 mmol, 0.1 equiv.), 2,6-di-*tert*-butylpyridine (421 mg, 2.2 mmol, 1.1 equiv.) and 1-fluoro-2,4,6-trimethylpyridinium triflate (1.73 g, 6.0 mmol, 3.0 equiv.). The reagents were dissolved in HFIP (50 mL), and the flask was capped with a rubber septum. A balloon equipped with a syringe needle was used to bubble Ar through the solution for 10 minutes (a syringe needle was used as an outlet). The flask was sealed from the atmosphere and TMDSO (1.1 mL, 6.0 mmol, 3.0 equiv.) was added dropwise at a rate of 1 drop per 3 seconds. The resulting solution gradually turned dark red from its initial, dark green color. After 4 hours, the volatiles were removed *in vacuo* and the resulting residue was directly purified via flash via flash column chromatography on SiO_2, using a mixture of EtOAc/hexanes (2:98) as eluent to give **3.71** as an amorphous white foam (single, unassigned diastereomer with respect to orthoformate stereogenic center, 750 mg, 0.15 mmol, 75% yield); **^{1}HNMR** (500 MHz, CDCl3) δ 6.94 (s, 1H), 6.51 (s, 1H), 4.22 (tt, *J* = 11.3, 3.8 Hz, 1H), 3.73 – 3.67 (m, 1H), 3.64 – 3.58 (m, 1H), 3.48 (d, *J* = 12.7 Hz, 1H), 3.00 (sept, *J* = 7.1 Hz, 1H), 2.91 (dd, *J* = 4.4 Hz, 16.6 Hz, 1H), 2.75 – 2.84 (m, 1H), 1.99 – 2.05 (m, 1H), 1.81 (d, *J* = 12.1 Hz, 1H), 1.73 (dd, *J* = 12.7, 5.1 Hz, 1H)., 1.43 – 1.32 (m, 2H), 1.23–1.27 (*overlapping* m, 9H), 1.18 (s, 3H), 1.03 (s, 3H), 0.93 (s, 9 H), 0.15 (s, 6H); **^{13}C NMR** (126 MHz, CDCl3) δ 143.4, 142.2, 129.83, 129.77, 122.2, 120.3, 118.5, 117.0, 65.9, 58.4, 50.9, 50.5, 43.3, 39.3, 34.9, 32.5, 31.0, 29.0, 26.1, 22.2, 22.1, 21.6, 21.3, 18.4, 15.1, –4.4, –4.5; **HRMS** (ESI):

m/z calcd for $C_{29}H_{45}NO_4Si+Na^+$: 522.3016 $[M+Na]^+$; found: 522.3016; $[\alpha]_D^{22} = -14.5$ ($c = 0.9, CHCl_3$).

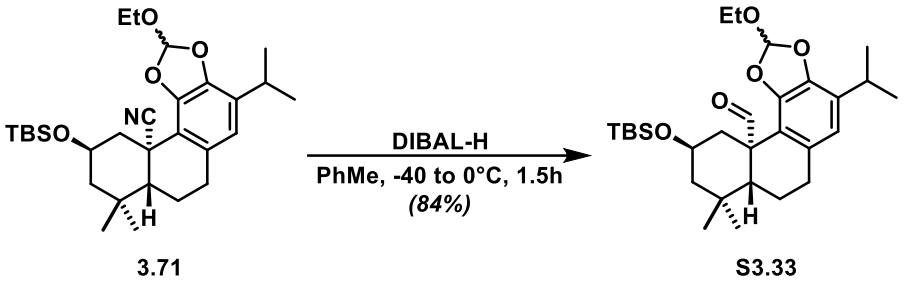

3.71 S3.33

To a cooled (–40 °C) solution of nitrile **3.71** (0.50 g, 1.1 mmol, 1.0 equiv.) in toluene (40 mL), a solution of diisobutylaluminum hydride (1.0M in toluene, 6.6 mmol, 6.0 equiv.) was added dropwise. The resulting mixture was stirred at –40 °C for 1.5 h, warmed to (4 °C) and diluted with ether (20 mL). Then 0.26 mL of water, 0.26 mL 15% KOH, followed by another 0.66 mL of water were added sequentially with care (slowly, dropwise). The resulting suspension was stirred vigorously for 30 min, then anhydrous magnesium sulfate (0.5 g) was added and the suspension was stirred for another 1 h at ambient temperature. The insoluble salts were removed via filtration over cotton and washed with diethyl ether (3 x 10 mL). The filtrate was concentrated *in vacuo* and the crude residue was purified via flash column chromatography on SiO_2, using a mixture of EtOAc/ hexanes (2:98) as eluent to give **S3.33** as an amorphous white foam (0.47 g, 0.92 mmol, 84 % yield). *Note: The orthoformate stereogenic was partially epimerized. Spectral data reported for the major isolated stereoisomer*: **^{1}H NMR** (500 MHz, $CDCl_3$) δ 9.82 (s, 1H), 6.80 (s, 1H), 6.56 (s, 1H), 4.09 – 4.01 (m, 1H), 3.65 (dd, *J* = 7.2 Hz, 2H), 3.62 – 3.58 (m, 1H), 3.03 – 2.95 (m, 2H), 2.95 – 2.86 (m, 1H), 2.07 – 1.95 (m, 2H), 1.71 (d, *J* = 12.5 Hz, 2H), 1.63 (d, *J* = 12.6 Hz, 2H), 1.32 – 1.28 (m, 1H), 1.23 (m, 9H), 1.14 (t, *J* = 11.9 Hz, 1H), 1.02 (s, 3H), 0.93 (s, 9H), 0.84 (s, 3H), 0.16 (s, 6H); **^{13}C NMR** (151 MHz, $CDCl_3$) δ 197.8, 144.5, 142.1, 131.4, 129.3, 120.2, 118.3,

114.5, 64.9, 58.8, 53.1, 52.1, 50.8, 39.2, 34.7, 32.0, 31.1, 28.7, 26.0, 22.1, 22.0, 21.7, 18.4, 18.3, 14.9, –4.5, –4.6; **HRMS** (ESI): *m/z* calcd for $C_{29}H_{46}O_5Si+Na^+$: 525.3012 $[M+Na]^+$; found: 525.3012; $[\alpha]_D^{22} = -56.6\ (c = 1.5, CHCl_3)$.

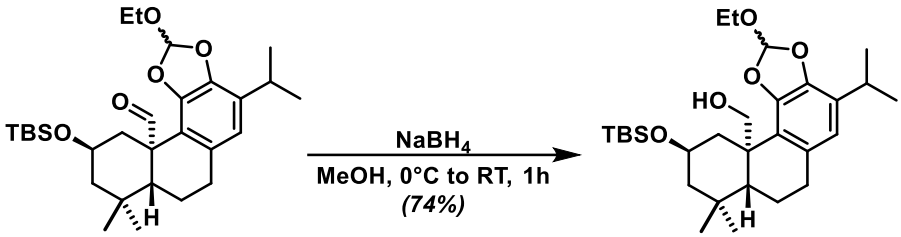

S3.33 **3.72**

To a cooled (0 °C) solution of **S3.33** (128 mg, 0.25 mmol, 1.0 equiv.) in MeOH (3 mL) was added $NaBH_4$ (47.3 mg, 1.25 mmol, 5 equiv.). The reaction mixture was stirred for 1 h while warming to ambient temperature then EtOAc (6 mL), and satd. aqueous NH_4Cl solution (6 mL) were added. After stirring the biphasic mixture for 14 hours, water (5 mL) was added and the aqueous phase was extracted with EtOAc (3 x 20 mL). The combined organic phases were dried over Na_2SO_4, filtered and concentrated in vacuo. The resulting crude residue was purified via flash column chromatography (EtOAc/hexanes = 2:98, R_f=0.15) to afford carbinol **3.72** as a colorless foam (93 mg, 0.19 mmol, 74% yield); **^{1}H NMR** (600 MHz, $CDCl_3$) δ 6.83 (s, 1H), 6.53 (s, 1H), 4.02 – 3.95 (m, 2H), 3.92 (d, *J* = 11.1 Hz, 1H), 3.65 (q, *J* = 7.0 Hz, 2H), 3.24 (d, *J* = 12.3 Hz, 1H), 3.00 (sept, *J* = 7.1 Hz, 1H), 2.93 (dd, *J* = 16.7, 6.1 Hz, 1H), 2.87 – 2.79 (m, 1H), 1.91 – 1.80 (m, 2H), 1.77 (d, *J* = 13.2 Hz, 1H), 1.47 – 1.40 (m, 2H), 1.30 (t, *J* = 12.1 Hz, 1H), 1.26 – 1.22 (m, 9H), 1.00 (s, 6H), 0.92 (s, 9H), 0.13 (s, 6H); **^{13}C NMR** (151 MHz, $CDCl_3$) δ 143.0, 141.4, 130.8, 128.1, 123.4, 120.3, 117.7, 66.8, 65.4, 58.6, 51.0, 50.9, 44.9, 42.5, 34.6, 34.0, 30.6, 28.8, 26.0, 23.2, 22.3, 22.2, 18.7, 18.4, 15.0, –4.38, –4.41; **HRMS** (ESI): *m/z* calcd for $C_{29}H_{48}O_5Si+Na^+$: 527.3169 $[M+Na]^+$; found: 527.3169; $[\alpha]_D^{22} = -1.3\ (c = 1.1, CHCl_3)$.

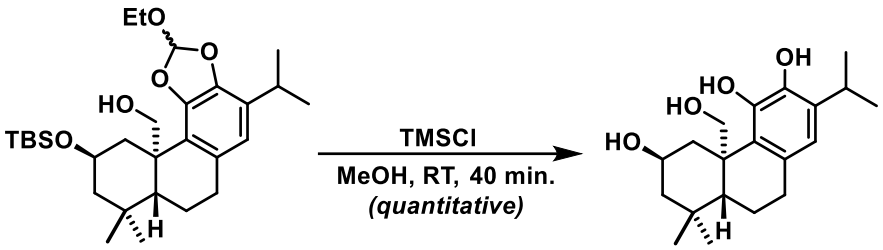

3.72 **3.73**

To a solution of **3.72** (15.0 mg, 0.035 mmol, 1 equiv.) in MeOH (3 mL) was added chlorotrimethylsilane (50 µL, 0.39 mmol, ~10 equiv.). After stirring for 1 hour at room temperature the reaction mixture was concentrated under pressure to afford **3.73** (10 mg, 0.035 mmol, quantitative). *Note:* **3.73** *was submitted to oxidative cyclization conditions without further purification;* **^{1}H NMR** (500 MHz, $CDCl_3$) δ 6.52 (s, 1H), 4.31 (d, *J* = 9.9 Hz, 1H), 4.23 – 4.13 (m, 1H), 3.91 (d, *J* = 9.9 Hz, 1H), 3.61 (d, *J* = 11.9 Hz, 1H), 3.20 (sept, *J* = 6.8 Hz, 1H), 2.88 – 2.81 (m, 2H) 1.90 (d, *J* = 11.4 Hz, 1H), 1.79 – 1.74 (m, 1H), 1.43 – 1.37 (m, 2H), 1.31 – 1.23 (m, 2H), 1.21 (d, *J* = 7.4 Hz, 3H), 1.20 (d, *J* = 7.4 Hz, 3H), 1.02 (s, 3H), 0.91 (s, 3H). *Note: exchangeable proton signals were not observed clearly, owing to the presence of water;* **^{13}C NMR** (151 MHz, $CDCl_3$) δ 142.3, 142.0, 132.9, 129.7, 127.3, 119.14, 67.7, 65.2, 52.5, 50.2, 45.5, 40.5, 34.7, 34.3, 32.0, 27.3, 23.7, 22.7, 22.4, 18.7; **HRMS** (ESI): *m/z* calcd for $C_{20}H_{30}O_4$+Na^+: 357.2042 $[M+Na]^+$; found: 357.2042; $[\alpha]_D^{22} = -20.9$ $(c = 0.6, CHCl_3)$.

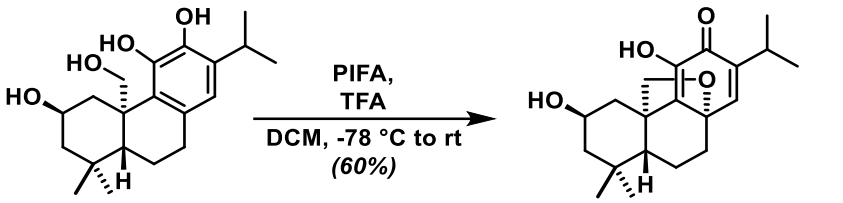

3.73 **3.14**

(+)-2-O-deacetyl plebedipene A

To a solution of **3.73** (7.0 mg, 0.021 mmol, 1.0 equiv.) in DCM (2 mL) was added trifluoroacetic acid (0.010 mL, 0.11 mmol, 5.0 equiv.). The reaction mixture was cooled to –78 °C and a solution of PIFA (12 mg, 0.027 mmol, 1.3 equiv.) in DCM (1 mL) was added dropwise. After stirring for 1 h while warming to ambient temperature, the volatiles were removed under reduced pressure. The resulting crude residue was purified via flash column chromatography (R_f= 0.22 in 4:1 EtOAc/hexanes) to afford **3.14** (2–*O*-deacetyl plebedipene A) as a yellow oil (4.0 mg, 0.012 mmol, 60%); **^{1}H NMR** (500 MHz, $CDCl_3$) δ 6.78 (s, 1H), 6.38 (s, 1H), 4.46 (d, *J* = 7.9 Hz, 1H), 3.74 (d, *J* = 7.9 Hz, 1H), 3.61 (tt, *J* = 11.8, 3.7 Hz, 1H), 2.95 (sept, *J* = 6.9 Hz, 1H), 2.58 (t, *J* = 12.4 Hz, 1H), 2.20 (dt, *J* = 12.4, 3.9 Hz, 1H), 2.14 (dt, *J* =12.4, 2.8 Hz, 1H), 1.85 – 1.77 (m, 3H), 1.62 (t, *J* = 8.6 Hz, 1H), 1.35 – 1.28 (m, 2H) 1.09 (d, *J* = 6.9 Hz, 6H), 1.05 (s, 3H), 1.01 (s, 2H); **^{13}C NMR** (151 MHz, $CDCl_3$) δ 182.7, 142.6 (2C), 137.0, 135.3, 78.8, 78.1, 65.6, 50.8, 49.69, 49.66, 41.9, 40.4, 35.7, 33.0, 27.0, 23.1, 21.9, 21.4, 20.1; **HRMS (ESI)**: *m/z* calcd for $C_{20}H_{28}O_4$+Na^+: 355.1885 $[M+Na]^+$; found: 355.1885; $[\alpha]_D^{22} = 205.5$ $(c = 0.8, CHCl_3)$.

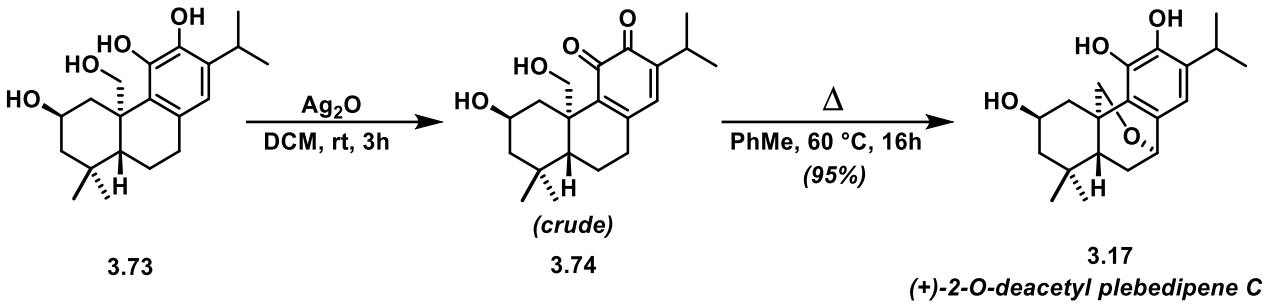

3.73 (crude) 3.74 3.17 (+)-2-O-deacetyl plebedipene C

Experimental procedure adapted from a report by Majetich and Zou[40]: To a solution of tetraol **3.73** (19 mg, 0.055 mmol, 1.0 equiv.) in DCM (1.0 mL) was added silver(I) oxide (26 mg, 0.11 mmol, 2.0 equiv.) and the resulting suspension was stirred at room temperature in the dark. After 3 hours, the solution turned dark red, indicating formation of the *ortho*-quinone moiety (R_f= 0.20 in 7:3 EtOAc/hexanes. *NOTE: This material decomposes on SiO_2*). Upon complete consumption of starting material (determined by TLC analysis), the contents of the reaction vessel were filtered over a short plug of celite and washed with DCM (10 mL). The filtrate was concentrated under reduced pressure, and the crude residue (23 mg, partially characterized via ^{13}C NMR and HRMS, see below) was re-dissolved in toluene (2 mL). The resulting dark red solution was stirred and heated at 60 °C for 16 hours, the volatiles were removed under reduced pressure and the crude residue was purified via flash column chromatography (R_f= 0.20 in 4:1 EtOAc/hexanes) to afford **3.17** ((+)-2-*O*-deacetyl plebedipene C) as a white solid (18 mg, 0.055 mmol, 95%); *Partial characterization of orthoquinone intermediate* **3.74**: **^{13}C NMR** (126 MHz, $CDCl_3$) δ 182.6, 181.4, 151.5, 147.4, 141.3, 137.5, 66.1, 64.5, 50.8, 49.9, 44.8, 42.0, 34.4, 34.0, 33.9, 29.8, 27.1, 22.9, 21.5, 17.8; **HRMS** (ES+) *m/z* calc'd for $C_{20}H_{28}O_4Na$ $[M + Na]^+$: 355.1885, found 355.1898; *2-O-deacetyl plebedipene C* (**17**): **^{1}H NMR** (600 MHz, DMSO-d_6) δ 8.06 (s, 1H), 7.73 (s, 1H), 4.61 (d, *J* = 1.7 Hz, 1H), 4.48 (d, *J* = 4.2 Hz, 1H), 4.07 (d, *J* = 8.6 Hz, 1H), 3.72 (ddd, *J* = 12.4, 11.9, 3.6 Hz, 1H), 3.23 (d, *J* = 6.9 Hz, 1H), 2.53 (dd, *J* = 13.0, 12.6 Hz, 1H) 2.90 (sept, *J* = 7.6 Hz, 1H),

2.16 (d, *J* = 13.0 Hz, 1H), 1.85 (ddd, *J* = 12.9, 5.5, 3.7 Hz, 1H), 1.70 (d, *J* = 11.7 Hz, 1H), 1.40 (t, *J* = 11.8 Hz, 1H), 1.25 (dd, *J* = 11.7, 4.8 Hz, 1H), 1.13 (d, *J* = 6.9 Hz, 3H), 1.11 (d, *J* = 6.9 Hz, 3H), 1.10 (m, 1H), 1.07 (s, 3H), 0.82 (s, 3H); **^{13}C NMR** (151 MHz, DMSO-d_6) δ 142.1, 140.8, 133.1, 132.3, 128.2, 111.2, 69.8, 68.6, 63.0, 50.4, 42.7, 40.7, 40.1, 34.5, 32.9, 29.5, 26.1, 22.89, 22.88, 22.0; **HRMS** (ES+) *m/z* calc'd for $C_{20}H_{28}O_4Na$ $[M + Na]^+$: 355.1885, found 355.1898; $[\alpha]_D^{22} = 78.6\ (c = 0.1, \mathrm{MeOH})$.

Table 3. 1: Reaction conditions screened for the dearomative oxidative cyclization of **3.73**. The presence of acid was critical (DDQ likely contained trace amounts of HCN), whereas inclusion of bases led to decomposition. [a]Under these conditions, 2-*O*-deacetyl plebedipene C (**3.17**) was also observed (~20%).

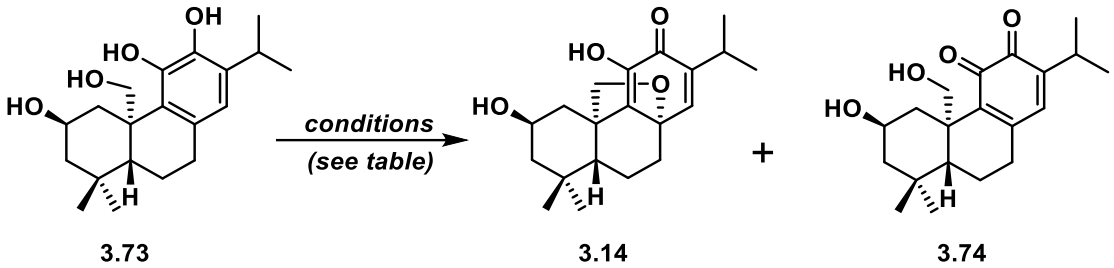

3.73 **3.14** **3.74**

entry	*conditions*	*yield of 3.14 (%)*	*3.74 (%)*
1[a]	DDQ (2.5 equiv.), THF, rt, 30 min.	43	<5
2	PbO_2, AcMe/Et_2O, rt, 2h	<5	0
3	$PhI(OAc)_2$, $CDCl_3$, rt, 1h	0	99
4	$PhI(OAc)_2$, $CDCl_3$, rt, 1.5h, then PhMe, DBU, 110°C, 16h	0	0
5	$PhI(OCOCF_3)_2$, DCM,– 25°C to rt, 1h	21	0
6	$PhI(OCOCF_3)_2$, TFA (5.0 equiv.), DCM,– 78°C to rt, 1h	60	0
7	$PhI(OCOCF_3)_2$, $NaHCO_3$ (3.0 equiv.), DCM,– 25°C to rt, 1h	<5	<5
8	$PhI(OCOCF_3)_2$, HFIP, rt, 1h	<5	0

Chemical Shift Comparison Tables for 2-O-Deacetyl Plebedipene A and C

Table 3. 2: Comparison of ^{1}H NMR chemical shifts

of natural and synthetic **(+)-*2-O-deacetylplebedipene A*** in $CDCl_3$.

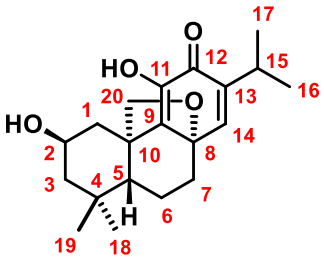

position	***natural*** δ ^{1}H (ppm), multiplicity, *J* (Hz) 400 MHz	***our synthetic*** δ ^{1}H (ppm), multiplicity, *J* (Hz) 600 MHz
1	2.59, t (12.8); 2.14, dt (12.8, 3.2)	2.58, t (12.4); 2.14, dt (12.4, 2.8)
2	3.61, tt (12.8, 3.2)	3.61, tt (11.8, 3.7)
3	1.81, m; 1.32, m	1.81, m; 1.32, m
5	1.62, t (8.6)	1.62, t (8.6)
6	1.61, m; 1.81, m	1.61, m; 1.81, m
7	2.21, dt (12.5, 3.4); 1.31, m	2.20, dt (12.4, 3.9); 1.31 m
14	6.78, s	6.78, s
15	2.95, sept (6.9)	2.95, sept (6.9)
16	1.09, d (6.9)	1.09, d (6.9)
17	1.09, d (6.9)	1.09, d (6.9)
18	1.01, s	1.01, s
19	1.05, s	1.05, s
20	4.46, d (7.8), 3.74, d (7.8)	4.46, d (7.9), 3.74, d (7.9)

Table 3. 3: Comparison of ^{13}C NMR chemical shifts

of natural and synthetic **(+)-*2-O-deacetylplebedipene A*** in $CDCl_3$.

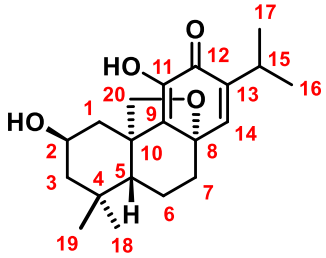

position	***natural*** δ ^{13}C (ppm) 100 MHz	***our synthetic*** δ ^{13}C (ppm) 150 MHz
1	40.2	40.4
2	65.4	65.6
3	50.6	50.8
4	35.6	35.7
5	49.5	49.69
6	19.9	20.1
7	41.7	41.9
8	78.6	78.8
9	135.2	135.3
10	49.5	49.66
11	142.4	142.6
12	182.6	182.7
13	136.8	137.0
14	142.4	142.6
15	26.9	27.0
16	21.8	21.9
17	21.2	21.4
18	32.9	33.0
19	23.0	23.1
20	78.0	78.1

Table 3. 4: Comparison of ^{1}H NMR chemical shifts

of natural and synthetic **(+)-*2-O-deacetylplebedipene C*** in DMSO-d_6.

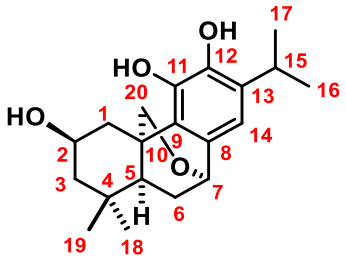

position	***natural*** δ ^{1}H (ppm), multiplicity, *J* (Hz) 400 MHz	***our synthetic*** δ ^{1}H (ppm), multiplicity, *J* (Hz) 600 MHz
1	2.54, dd (12.8, 12.2); 2.15, br d	2.53, dd (13.0, 12.6); 2.15, br d (13.0)
2	3.71, ddd (12.2, 11.8, 3.4)	3.72, ddd (12.4, 11.9, 3.6)
3	1.10, m; 1.70, dt (11.8, 2.8)	1.10, m; 1.70, dt (11.7, 2.9)
5	1.24, dd (11.5, 5.3)	1.25, dd (11.7, 4.8)
6	1.84, ddd (13.2, 5.3, 3.9); 1.39, dd (13.2, 11.5)	1.85, ddd (12.9, 5.5, 3.7); 1.40, t (11.8)
7	4.60, dd (3.9, 1.5)	4.61, d (1.7)
14	6.52, s	6.53, s
15	3.22, sept (6.8)	3.23, sept (6.9)
16	1.10, d (6.8)	1.11, d (6.9)
17	1.12, d (6.8)	1.13, d (6.9)
18	0.81, s	0.82, s
19	1.06, s	1.07, s
20	4.06, d (8.5); 2.89 d (8.5)	4.07, d (8.6); 2.90 d (8.6)
-OH (2)	4.48, d (3.4)	4.48, d (4.2)
-OH	7.72, s	7.73, s
-OH	8.04, s	8.06, s

Table 3. 5: Comparison of ^{13}C NMR chemical shifts

of natural and synthetic **(+)-*2-O-deacetylplebedipene C*** in DMSO-d_6.

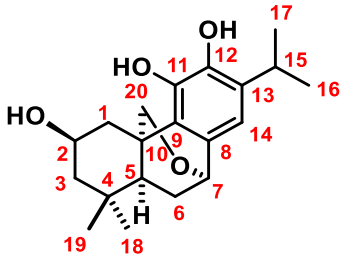

position	***natural*** δ ^{13}C (ppm) 100 MHz	***our synthetic*** δ ^{13}C (ppm)
1	40.0	40.1
2	63.1	63.0
3	50.4	50.4
4	34.5	34.5
5	42.7	42.7
6	29.5	29.5
7	69.8	69.8
8	132.3	132.3
9	128.2	128.2
10	40.7	40.7
11	140.7	140.8
12	142.0	142.1
13	133.1	133.1
14	111.2	111.2
15	26.1	26.1
16	22.9	22.9
17	22.9	22.9
18	32.9	32.9
19	22.0	22.0
20	68.6	68.6

Total Synthesis of Plebedipene B

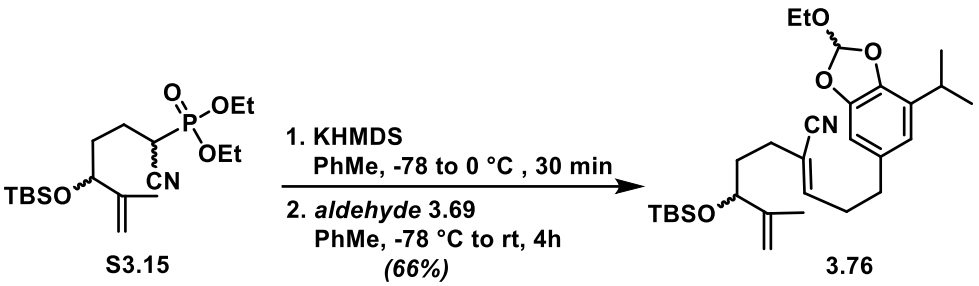

Prepared according to general procedure E, using cyanoalkylphosphonate **S3.15** *(736 mg, 1.89 mmol, 1.0 equiv.) and aldehyde* **S3.69** *(500 mg, 1.89 mmol, 1.0 equiv.) to give a (1:6 E:Z, separable) mixture of α,β-unsaturated nitriles*. Yield of **3.76**: 66% (624 mg, 1.25 mmol, colorless oil); R_f= 0.15 (1.5:98.5 EtOAc/hexanes); *NOTE: 1:1 mixture of diastereomers:* **^{1}H NMR** (600 MHz, $CDCl_3$) δ 6.85 (s, 1H), 6.56 (d, *J* = 1.6 Hz, 1H), 6.53 (s, 1H), 6.12 (t, *J* = 7.2 Hz, 1H), 4.87 (s, 1H), 4.79 (s, 1H), 4.02 (t, *J* = 6.0 Hz, 1H), 3.70 (q, *J* = 7.1 Hz, 1H), 3.02 (sept, *J* = 7.0 Hz, 1H), 2.68 – 2.64 (m, 1H), 2.64 – 2.60 (m, 1H), 2.24 – 2.17 (m, 1H), 2.16 – 2.10 (m, 1H), 1.74 – 1.68 (m, 1H), 1.66 (s, 1H), 1.66 – 1.61 (m, 1H), 1.26 (d, *J* = 7.0 Hz, 6H), 1.26 (t, *J* = 7.1 Hz, 3H), 0.89 (s, 9H), 0.03 (s, 3H), 0.00 (s, 3H); **^{13}C NMR** (151 MHz, $CDCl_3$) δ 146.9, 146.4, 146.0, 141.9, 134.0, 129.6, 119.4, 118.8, 117.7, 115.4, 111.5, 106.1, 75.6, 59.1, 34.9, 34.6, 33.5, 30.3, 29.2, 26.0, 22.4, 22.3, 18.3, 17.4, 15.1, –4.6, –5.0; **HRMS** (ES+) *m/z* calc'd for $C_{29}H_{45}NO_4SiNa$ $[M + Na]^+$: 522.3016, found 522.3007.

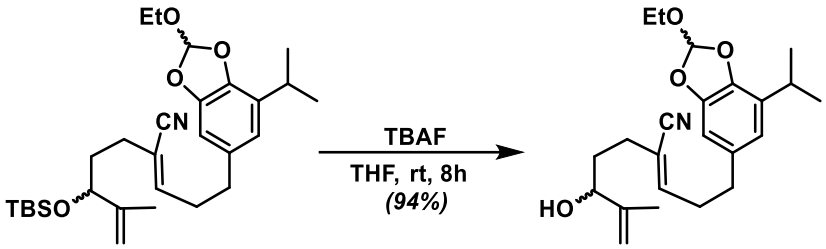

3.76 **3.77**

To a cooled (4 °C) solution of silyl ether **3.76** (560 mg, 1.12 mmol, 1.0 equiv.) in dry THF (3.0 mL) was added TBAF (1.0 M solution THF, 1.50 mL, 1.50 mmol, 1.34 equiv.) and the mixture was stirred while warming to ambient temperature. When the reaction was complete (as indicated by TLC), the volatiles were removed under reduced pressure. The resulting crude residue was directly purified via flash column chromatography on SiO_2, using a mixture of EtOAc/hexanes (3:7, R_f = 0.25) as eluent to give **3.77** as a colorless oil (406 mg, 1.05 mmol, 94% yield); *NOTE: 1:1 mixture of diastereomers:* **^{1}H NMR** (500 MHz, $CDCl_3$) δ 6.83 (apparent d, *J* = 3.1 Hz, 1H), 6.55 (s, 2H), 6.16 (t, *J* = 6.9 Hz, 1H), 4.92 (s, 1H), 4.85 (s, 1H), 4.04 – 3.89 (m, 1H), 3.70 (q, *J* = 7.1 Hz, 2H), 3.02 (sept, *J* = 6.9 Hz, 1H), 2.72 – 2.60 (m, 4H), 2.33 – 2.18 (m, 2H), 1.80 – 1.73 (m, 1H), 1.72 (s, 3H), 1.69 – 1.64 (m, 1H), 1.29 – 1.22 (m, 9H); **^{13}C NMR** (151 MHz, $CDCl_3$) δ 147.1, 147.0, 146.97, 146.95, 145.8, 145.7, 141.8, 133.8, 129.6, 129.5, 119.39, 119.36, 118.7, 117.50, 117.47, 114.9, 114.8, 111.4, 111.3, 106.1, 106.0, 74.4, 74.2, 59.14, 59.13, 34.7, 33.4, 33.3, 33.1, 33.0, 30.4, 29.14, 29.12, 22.3, 22.23, 22.18, 22.15, 17.7, 15.0; **HRMS** (ES+) *m/z* calc'd for $C_{23}H_{31}NO_4Na$ $[M + Na]^+$: 408.2151, found 408.2159.

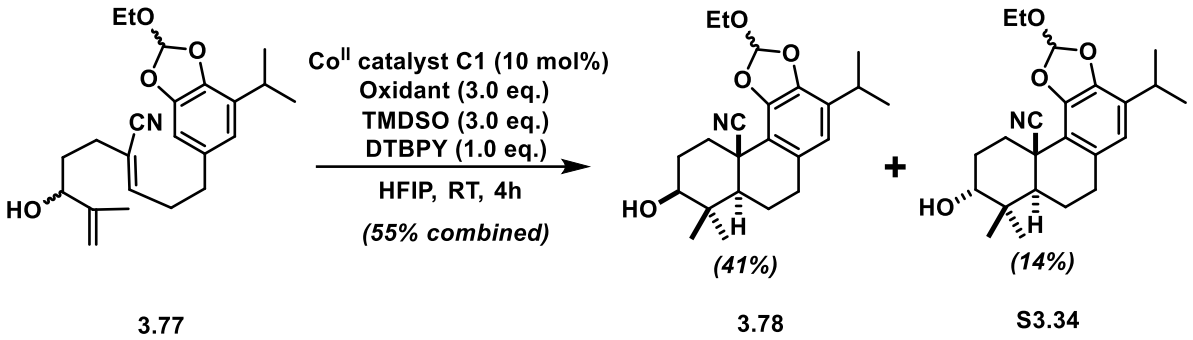

3.77 **3.78** **S3.34**

A dry round-bottom flask was charged with a magnetic stirring bar, allylic alcohol **72** (360 mg, 0.934 mmol, 1.0 equiv.) catalyst **C1** (56 mg, 0.093 mmol, 0.1 equiv.), 2,6-di-*tert*-butylpyridine (179 mg, 0.934 mmol, 1.0 equiv.) and 1-fluoro-2,4,6-trimethylpyridinium triflate (810 mg, 2.80 mmol, 3.0 equiv.). The reagents were dissolved in HFIP (15 mL), and the flask was capped with a rubber septum. A balloon equipped with a syringe needle was used to bubble argon through the solution for 10 minutes (a syringe needle was used as an outlet). The flask was sealed from the atmosphere and TMDSO (0.5 mL, 2.8 mmol, 3.0 equiv.) was added dropwise at a rate of 1 drop per 3 seconds. The resulting solution gradually turned dark red from its initial, dark green color. After 4 hours, the volatiles were removed *in vacuo* and the resulting residue was directly purified via flash via flash column chromatography on SiO_2, using a mixture of EtOAc/hexanes (15:85) as eluent to give **73** as an amorphous white foam (2:1 mixture of orthoformate diastereomers, 162 mg, 0.420 mmol, 45% yield); *NOTE: Only the isolated major diastereomer is reported for clarity:* **^{1}H NMR** (500 MHz, CDCl3) δ 6.93 (s, 1H), 6.52 (s, 1H), 3.71 – 3.65 (m, 1H), 3.61 – 3.55 (m, 1H), 3.37 – 3.30 (m, 2H), 3.00 (sept, *J* = 6.9 Hz, 1H), 2.93 (dd, *J* = 16.7, 3.7 Hz, 1H), 2.83 – 2.75 (m, 1H), 2.06 (dd, *J* = 13.4, 5.4 Hz, 1H), 2.02 – 1.97 (m, 1H), 1.97 – 1.91 (m, 1H), 1.80 (qd, *J* = 12.8, 5.1 Hz, 1H), 1.54 (td, *J* = 13.6, 3.8 Hz, 1H), 1.36 (d, *J* = 11.7 Hz, 1H), 1.25 (d, *J* = 3.8 Hz, 3H), 1.24 (d, *J* = 4.0 Hz, 3H), 1.24 (t, *J* = 7.3 Hz, 3H), 1.12 (s, 6H). **^{13}C NMR** (126 MHz, $CDCl_3$) δ 143.5, 142.2, 129.8, 122.1, 120.3, 118.4, 117.0, 77.5, 58.0, 50.9, 39.6, 39.0, 33.0, 31.1,

29.0, 28.7, 27.3, 22.14, 22.12, 21.7, 15.0, 13.9; **HRMS** (ES+) *m/z* calc'd for $C_{23}H_{31}NO_4Na$ [M + Na]$^+$: 408.2151, found 408.2151.

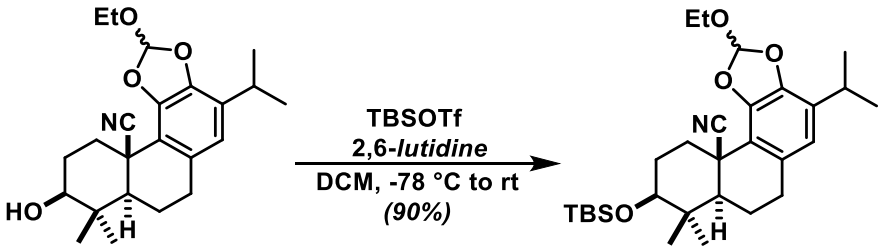

3.78 S3.35

To a solution of alcohol **3.78** (60 mg, 0.156 mmol, 1.0 equiv.) and 2,6-lutidine (54 µL, 0.468 mmol, 3.0 equiv.) in DCM (3 mL) was added TBSOTf (30 µL, 0.171 mmol, 1.5 equiv.). The mixture stirred for 1 hour at ambient temperature, then methanol (0. 5 mL) was added. The volatiles were removed *in vacuo,* and the resulting crude residue was directly purified via flash chromatography using a mixture of EtOAc/hexanes (2:98, R_f = 0.20) as eluent to give silyl ether **S3.35** as amorphous white foam (70 mg, 0.140 mmol, 90% yield); **^{1}H NMR** (500 MHz, $CDCl_3$) δ 6.92 (s, 1H), 6.51 (s, 1H), 3.68 (dq, *J* = 14.2, 7.1 Hz, 1H), 3.57 (dq, *J* = 14.2, 7.1 Hz, 1H), 3.33 – 3.26 (m, 2H), 3.00 (sept, *J* = 6.9 Hz, 1H), 2.92 (dd, *J* = 16.6, 4.0 Hz, 1H), 2.78 (ddd, *J* = 17.9, 12.6, 5.8 Hz, 1H), 2.08 – 1.96 (m, 2H), 1.84 – 1.74 (m, 2H), 1.50 (td, *J* = 13.9, 3.2 Hz, 1H), 1.33 (d, *J* = 11.7 Hz, 1H), 1.28 – 1.21 (m, 9H), 1.09 (s, 3H), 1.03 (s, 3H), 0.91 (s, 9H), 0.07 (s, 3H), 0.05 (s, 3H); **^{13}C NMR** (126 MHz, $CDCl_3$) δ 143.5, 142.1, 129.9, 129.7, 122.2, 120.3, 118.4, 117.3, 78.1, 58.0, 50.9, 40.2, 38.9, 32.9, 31.1, 29.9, 29.0, 27.7, 26.0, 22.2, 22.1, 21.9, 18.2, 15.0, 14.4, -3.7, -4.8; **HRMS** (ES+) *m/z* calc'd for $C_{29}H_{45}NO_4SiNa$ [M + Na]$^+$: 522.3016, found 522.3029.

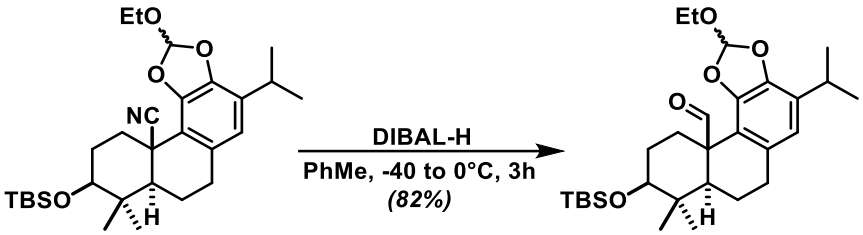

S3.35 S3.36(a,b)

To a cooled (–78 °C) solution of nitrile **S3.35** (10 mg, 0.02 mmol, 1 equiv.) in toluene (0.5 mL), a solution of DIBAL-H (1.0 M in toluene, 0.16 mL, 0.16 mmol, 8.0 equiv.) was added dropwise. The resulting mixture was stirred at –78 °C for 10 minutes then warmed to – 40 °C, stirred for another 3h and diluted with ether (3 mL). Then 10 µL water, 10 µL of 15% w/v $NaOH_{(aq.)}$, followed by another 40 µL of water were added. The resulting suspension was stirred vigorously for 30 minutes, then anhydrous magnesium sulfate (0.25 g) was added and the suspension was stirred for another 1 h at ambient temperature. The insoluble salts were removed via filtration over cotton and washed with ether (3 x 3 mL). The filtrate was concentrated *in vacuo* and the crude residue was purified via flash column chromatography on SiO_2, using a mixture of EtOAc/hexanes (6:94, R_f = 0.20) as eluent to give **S3.36a** and **S3.36b** (4:1 mixture of unassigned diastereomers) as an amorphous white foam (8.2 mg, 82% yield); *Major diastereomer* **S3.36a** *(relative configuration unassigned)*: **^{1}H NMR** (500 MHz, $CDCl_3$) δ 9.85 (s, 1H), 6.78 (s, 1H), 6.56 (s, 1H), 3.66 (q, *J* = 7.1 Hz, 2H), 3.39 (dt, *J* = 13.4, 3.3 Hz, 1H), 3.29 (dd, *J* = 11.0, 5.2 Hz, 1H), 3.02 – 2.95 (m, 2H), 2.86 (ddd, *J* = 17.9, 12.6, 6.0 Hz, 1H), 2.10 (ddd, *J* = 25.8, 12.8, 5.6 Hz, 1H), 1.98 (dd, *J* = 13.6, 6.0 Hz, 1H), 1.79 – 1.68 (m, 2H), 1.59 (d, *J* = 11.5 Hz, 1H), 1.29–1.23 (m, overlapping, 10H), 1.01 (s, 3H), 0.89 (s, 9H), 0.76 (s, 3H), 0.05 (s, 3H), 0.04 (s, 3H); **^{13}C NMR** (126 MHz, $CDCl_3$) δ 197.9, 144.7, 142.1, 131.7, 129.3, 120.2, 118.4, 114.9, 78.5, 59.1, 52.0, 51.7, 40.2, 31.3, 28.8, 28.7, 28.4, 27.1, 26.0 (3C), 22.2, 22.1, 18.5, 18.3, 15.5, 15.1, –3.6, –4.8; **HRMS** (ES+) *m/z* calc'd for $C_{29}H_{46}O_5SiNa$ $[M + Na]^+$: 525.3012, found 525.3029.

Data for the minor orthoformate diastereomer **S3.36b** *(relative configuration unassigned)*: **^{1}H NMR** (500 MHz, $CDCl_3$) δ 9.85 (s, 1H), 6.82 (s, 1H), 6.56 (s, 1H), 3.52 – 3.43 (m, 2H), 3.36 (dt, *J* = 13.4, 3.3 Hz, 1H), 3.30 (dd, *J* = 11.1, 5.2 Hz, 1H), 3.03 – 2.94 (m, 2H), 2.87 (ddd, *J* = 17.9, 12.6, 6.0 Hz, 1H), 2.09 (ddd, *J* = 25.8, 12.8, 5.2 Hz, 1H), 1.98 (dd, *J* = 13.5, 5.8 Hz, 1H), 1.78 – 1.67 (m, 2H), 1.59 (d, *J* = 12.5 Hz, 1H), 1.25 – 1.24 (m, 1H) 1.24 (d, *J* = 6.9 Hz, 6H), 1.19 (t, *J* = 7.1 Hz, 3H), 1.02 (s, 3H), 0.89 (s, 9H), 0.76 (s, 3H), 0.04 (s, 3H), 0.04 (s, 3H); **^{13}C NMR** (150 MHz, $CDCl_3$) δ 197.7, 144.7, 142.0, 131.7, 129.3, 120.2, 118.1, 114.9, 78.5, 58.2, 52.0, 51.7, 40.2, 31.6, 29.9, 28.9, 28.8, 28.7, 27.0, 26.0, 22.2, 22.1, 18.5, 18.3, 15.5, 14.9, –3.6, –4.8; **HRMS** (ES+) *m/z* calc'd for $C_{29}H_{46}O_5SiNa$ $[M + Na]^+$: 525.3012, found 525.3009.

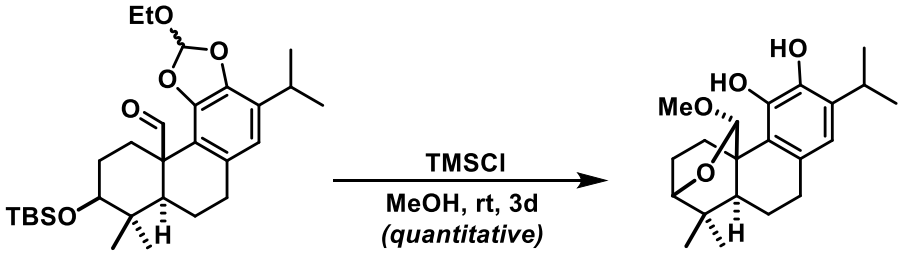

S3.36(a,b) **3.16**

(±)-plebedipene B

To a solution of aldehydes **S3.36(a,b)** (3 mg, 0.006 mmol, 1.0 equiv.) in MeOH, chlorotrimethylsilane (50 µL, 0.394 mmol, ~70 equiv.) was added and the resulting mixture was stirred for 3 days at ambient temperature. The volatiles were removed in vacuo, and the resulting residue was concentrated from $CDCl_3$ (1 mL) to give (**±**)***plebedipene B*** **(3.16)** as a white solid (2.1 mg, 0.006 mmol, quantitative yield, R_f = 0.18 [6:94 EtOAc/hexanes]); **^{1}H NMR** (600 MHz, $CDCl_3$) δ 9.41 (s, 1H), 6.52 (s, 1H), 5.97 (s, 1H), 4.93 (s, 1H), 3.51 (s, 3H), 3.46 (t, *J* = 2.6 Hz, 1H), 3.23 (sept, *J* = 7.1 Hz, 1H), 3.06 (dd, *J* = 11.6, 1.6 Hz, 1H), 2.84 – 2.76 (m, 2H), 2.13 (dddd, *J* = 14.1, 11.1, 8.0, 3.1 Hz, 1H *axial*), 1.96 (ddt, *J* = 13.8, 11.5, 2.0 Hz, 1H), 1.83 – 1.80 (m, 1H),

1.61– 1.52 (m, 1H), 1.55 – 1.52 (m, 1H), 1.25 – 1.22 (overlapping m, 1H), 1.24 (d, *J* = 7.1 Hz, 3H), 1.22 (d, *J* = 7.1 Hz, 3H), 1.10 (s, 3H), 1.06 (s, 3H); **^{13}C NMR** (151 MHz, $CDCl_3$) δ 142.8, 142.4, 133.1, 128.6, 122.3, 118.4, 103.6, 76.9, 55.2, 51.4, 40.3, 36.8, 31.8, 29.6, 27.3, 24.4, 23.4, 22.9, 22.6, 22.3, 21.1; **HRMS** (ES+) *m/z* calc'd for $C_{21}H_{30}O_4Na$ $[M + Na]^+$: 369.2042, found 369.2027.

Chemical Shift Comparison Tables for Plebedipene B

Table 3. 6: Comparison of ^{1}H NMR chemical shifts of natural and synthetic **(±)-*plebedipene B*** in $CDCl_3$.

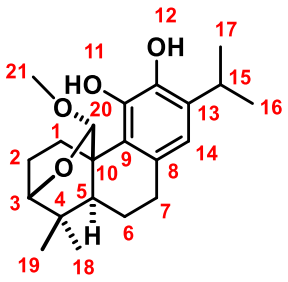

position	***natural*** δ ^{1}H (ppm), multiplicity, *J* (Hz) 400 MHz	***our synthetic*** δ ^{1}H (ppm), multiplicity, *J* (Hz) 600 MHz
1	3.07, dd (11.5, 1.7); 3.04, dd (11.5,	3.06, dd (11.6, 1.6); 1.23, m*
2	2.13, m; 1.96, m	2.13, dddd (14.1, 11.1, 8.0, 3.1); 1.96, ddt (13.8, 11.5,
3	3.46, t (2.6)	3.46, t (2.6)
5	1.58, m	1.58, m
6	1.55, m; 1.81, m	1.55, m; 1.81, m
7	2.80, m (2H)	2.80, m (2H)
14	6.52, s	6.52, s
15	3.22, sept (6.9)	3.23, sept (7.1)
16	1.22, d (6.9)	1.22, d (7.1)
17	1.24, d (6.9)	1.24, d (7.1)
18	1.05, s	1.06, s
19	1.10, s	1.10, s
20	4.93, s	4.93, s
21	3.51, s	3.51, s
-OH	*not reported*	9.41, s
-OH	*not reported*	5.97, s

*We believe that the authors of the paper describing the isolation and characterization of plebedipene B made an error in the assignments of resonances attributed to the protons on C1. Our spectra are excellent matches for theirs, and the resonance at around 3.05 ppm integrates for only one proton. We know from our work in this area that the diastereotopic protons attached to C1 have dramatically different resonances owing to the proximity of the phenol to α-proton, which typically appears around 3 ppm; the β-proton, however, is found in a more typical "alkane" range, near 1.2 ppm. For plebedipene B, this resonance is essentially coincident with the isopropyl methyl groups, and cannot be resolved.

Table 3. 7: Comparison of ^{13}C NMR chemical shifts of natural and synthetic **(±)-*plebedipene B*** in $CDCl_3$.

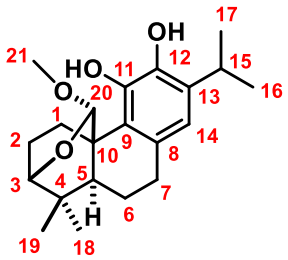

position	***natural*** δ ^{13}C (ppm) 100 MHz	***our synthetic*** δ ^{13}C (ppm)
1	23.3	23.4
2	22.8	22.9
3	76.8	76.9
4	36.7	36.8
5	51.3	51.4
6	21.0	21.1
7	31.7	31.8
8	128.5	128.6
9	122.2	122.3
10	40.2	40.3
11	142.2	142.4
12	142.7	142.8
13	132.9	133.1
14	118.3	118.4
15	27.2	27.3
16	22.5	22.6
17	22.2	22.3
18	29.5	29.6
19	24.3	24.4
20	103.5	103.6
21	55.1	55.2

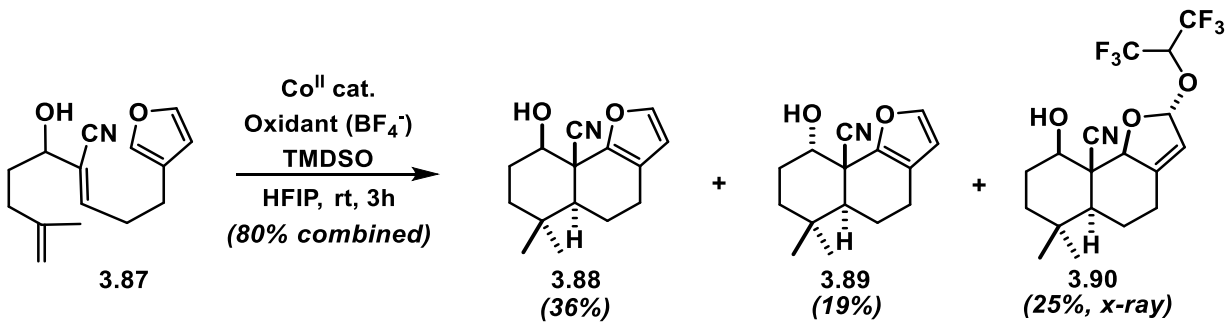

Prepared according to general procedure I, using α,β-unsaturated nitrile **3.87** *(55 mg, 0.22 mmol, 1.0 equiv.), cobalt catalyst* **C1** *(14 mg, 0.022 mmol, 0.1 equiv.), 1-fluoro-2,4,6-trimethylpyridinium tetrafluoroborate (150 mg, 0.66 mmol, 3.0 equiv.), TMDSO (120 µL, 0.66 mmol, 3.0 equiv.), and HFIP (7 mL).* Yield of isomer with equatorial hydroxyl group **3.88:** 36% (19.8 mg, 0.081 mmol, white solid); R_f=0.25 (3:7 EtOAc/hexanes); **^{1}H NMR** (600 MHz, $CDCl_3$) δ 7.33 (d, *J* = 1.9 Hz, 1H), 6.25 (d, *J* = 1.9 Hz, 1H), 3.75 (ddd, *J* = 11.2, 4.2, 2.0 Hz, 1H), 3.33 (d, *J* = 2.2 Hz, 1H), 2.63 (ddd, *J* = 16.4, 5.7, 1.2 Hz, 1H), 2.47 – 2.40 (m, 1H), 2.06 – 1.98 (m, 2H), 1.97 – 1.92 (m, 1H), 1.91 – 1.83 (m, 1H), 1.64 (dt, *J* = 14.0, 3.5 Hz, 1H), 1.48 (dd, *J* = 12.1, 1.5 Hz, 1H), 1.38 (td, *J* = 13.9, 4.1 Hz, 1H), 1.17 (s, 3H), 0.99 (s, 3H); **^{13}C NMR** (151 MHz, $CDCl_3$) δ 148.2, 142.8, 119.8, 119.1, 110.9, 74.8, 50.6, 46.2, 39.4, 32.9, 31.8, 27.5, 22.2, 21.7, 20.0; **HRMS** (ES+) *m/z* calc'd for $C_{15}H_{19}NO_2Na$ $[M+Na]^+$: 268.1313, found 268.1307. Yield of isomer with axial hydroxyl group **3.89:** 19% (10.5 mg, 0.042 mmol, white solid); R_f=0.27 (3:7 EtOAc/hexanes); **^{1}H NMR** (600 MHz, $CDCl_3$) δ 7.34 (d, *J* = 1.9 Hz, 1H), 6.25 (d, *J* = 1.8 Hz, 1H), 4.70 (s, 1H), 2.60 (ddd, *J* = 16.3, 5.6, 1.2 Hz, 1H), 2.49 – 2.41 (m, 1H), 2.23 – 2.15 (m, 1H), 2.06 (dd, *J* = 13.5, 5.9 Hz, 1H), 1.97 (dd, *J* = 12.4, 1.3 Hz, 1H), 1.91 – 1.86 (m, 1H), 1.85 – 1.79 (m, 1H), 1.78 – 1.72 (m, 3H), 1.36 – 1.31 (m, 1H), 1.17 (s, 3H), 1.02 (s, 3H); **^{13}C NMR** (151 MHz, $CDCl_3$) δ 145.9, 143.1, 121.7, 120.6, 111.3, 67.5, 44.6, 43.7, 34.0, 33.0, 32.0, 25.5, 22.1, 21.5, 19.6; **HRMS** (ES+) *m/z* calc'd for $C_{15}H_{19}NO_2Na$ $[M+Na]^+$: 268.1313, found 268.1309.; Yield of dearomatized HFIP acetal **3.90:**

26% (24 mg, 0.057 mmol, colorless needles); R_f=0.45 (3:7 EtOAc/hexanes, recrystallized using the vapor diffusion method from DCM and hexanes); **^{1}H NMR** (600 MHz, $CDCl_3$) δ 6.15 (d, *J* = 3.5 Hz, 1H), 5.72 (d, *J* = 1.1 Hz, 1H), 4.69 (s, 1H), 4.43 (d, *J* = 6.0 Hz, 1H), 3.74 (dd, *J* = 11.4, 4.4 Hz, 1H), 3.36 (s, 1H), 2.78 (ddd, *J* = 14.5, 4.5, 1.7 Hz, 1H), 2.17 (td, *J* = 14.2, 5.9 Hz, 1H), 1.99 – 1.93 (m, 1H), 1.89 (dq, *J* = 13.7, 3.8 Hz, 1H), 1.85 – 1.77 (m, 1H), 1.65 – 1.58 (m, 1H), 1.59 – 1.54 (m, 1H), 1.34 (td, *J* = 13.9, 3.7 Hz, 1H), 1.21 (dd, *J* = 12.4, 2.6 Hz, 1H), 1.07 (s, 2H), 0.98 (s, 2H); **^{13}C NMR** (151 MHz, $CDCl_3$) δ 145.0, 118.7, 117.4, 110.5, 91.8, 76.7, 72.5 (sept, *J* = 33 Hz), 72.1, 53.6, 47.6, 39.0, 33.1, 31.8, 27.4, 25.7, 24.0, 20.6; **HRMS** (ES+) *m/z* calc'd for $C_{18}H_{21}F_6NO_3Na$ $[M+Na]^+$: 436.1323, found 436.1336.

3.9 Notes and References

(1) Yoder, R. A.; Johnston, J. N. *Chem. Rev.* **2005**, *105*, 4730–4756.

(2) a) Ignea, C.; Athanasakoglou, A.; Ioannou, E.; Georgantea, P.; Trikka, F. A.; Loupassaki, S.; Roussis, V.; Makris, A. M.; Kampranis, S. C. *Proc. Natl. Ac. Sci.* **2016**, *113*, 3681–3686; b) Scheler, U.; Brandt, W.; Porzel, A.; Rothe, K.; Manzano, D.; Božić, D.; Papaefthimiou, D.; Balcke, G. U.; Henning, A.; Lohse, S.; Marillonnet, S.; Kanellis, A. K.; Ferrer, A.; Tissier, A. *Nat. Commun.* **2016**, *7*, 12942.

(3) For recent relevant reviews, see: a) Bathe, U.; Tissier, A. *Phytochemistry* **2019**, *161*, 149–162; b) Banerjee, A.; Hamberger, B. *Phytochemistry Reviews* **2018**, *17*, 81–111.

(4) González, M. A. *Nat. Prod. Rep.* **2015**, *32*, 684–704.

(5) For some key examples, see: a) Chen, K.; Baran, P. S. *Nature* **2009**, *459*, 824–828; b) Jørgensen, L.; McKerrall, S. J.; Kuttruff, C. A.; Ungeheuer, F.; Felding, J.; Baran, P. S. *Science* **2013**, *341*, 878–882; c) Kanda, Y.; Nakamura, H.; Umemiya, S.; Puthukanoori, R. K.; Murthy Appala, V. R.; Gaddamanugu, G. K.; Paraselli, B. R.; Baran, P. S. *J. Am. Chem. Soc.* **2020**, *142*, 10526–10533; d) Kanda, Y.; Ishihara, Y.; Wilde, N. C.; Baran, P. S. *J. Org. Chem.* **2020**, *85*, 10293–10320.

(6) For excellent achievements in semisynthesis featuring multiple late-stage oxidations, see: a) Hung, K.; Condakes, M. L.; Novaes, L. F. T.; Harwood, S. J.; Morikawa, T.; Yang, Z.; Maimone, T. J. *J. Am. Chem. Soc.* **2019**, *141*, 3083–3099; b) Zhang, X.; King-Smith, E.; Dong, L.-B.; Yang, L.-C.; Rudolf, J. D.; Shen, B.; Renata, H. *Science* **2020**, *369*, 799.

(7) For selected recent reviews of late-stage oxidations, see: a) White, M. C.; Zhao, J. *J. Am. Chem. Soc.* **2018**, *140*, 13988–14009; b) Li, J.; Amatuni, A.; Renata, H. *Curr. Opin. Chem. Biol.* **2020**, *55*, 111–118.

(8) For a recent review that includes some examples of functionalized substrates engaged in polyene cyclizations, see: Barrett, A. G. M.; Ma, T.-K.; Mies, T. *Synthesis* **2019**, *51*, 67–82.

(9) It is unfortunately not yet possible to make a data-based comparison of cyclization-then-oxidation versus oxidation-then-cyclization approaches. There are few instances of bioinspired polyene cyclizations with high levels of oxygenation in the substrate, and a relatively small number of syntheses that involve an early-stage polycyclization and multiple late-stage oxidations, and none of them overlap with respect to targets. For an example where a highly-oxidized substrate is engaged in a radical polyene cyclization, see: Yamaoka, M.; Nakazaki, A.; Kobayashi, S. *Tetrahedron Lett.* **2009**, *50*, 6764–6768.

(10) It is likely that some transition-metal-catalyzed approaches might also function well in highly functionalized situations. Carreira's Ir-catalyzed enantioselective polycyclizations of allylic alcohols is a likely candidate for application in complex settings, because of the tolerance of the catalyst system for numerous functional groups: Schafroth, M. A.; Sarlah, D.; Krautwald, S.; Carreira, E. M. *J. Am. Chem. Soc.* **2012**, *134*, 20276–20278.

(11) Breslow, R.; Olin, S. S.; Groves, J. T. *Tetrahedron Lett.* **1968**, *9*, 1837–1840.

(12) For a review, see: Justicia, J.; Álvarez de Cienfuegos, L.; Campaña, A. G.; Miguel, D.; Jakoby, V.; Gansäuer, A.; Cuerva, J. M. *Chem. Soc. Rev.* **2011**, *40*, 3525–3537.

(13) a) Boger, D. L.; Mathvink, R. J. *J. Am. Chem. Soc.* **1990**, *112*, 4003–4008; b) Chen, L.; Gill, G. B.; Pattenden, G. *Tetrahedron Lett.* **1994**, *35*, 2593–2596; c) Pattenden, G.; Roberts, L.; J. Blake, A. *J. Chem. Soc., Perkin Trans. 1* **1998**, 863–868.

(14) For select relevant examples, see: a) Snider, B. B.; Mohan, R.; Kates, S. A. *J. Org. Chem.* **1985**, *50*, 3659–3661; b) Kates, S. A.; Dombroski, M. A.; Snider, B. B. *J. Org. Chem.*

1990, *55*, 2427–2436; c) Zoretic, P. A.; Weng, X.; Caspar, M. L.; Davis, D. G. *Tetrahedron Lett.* **1991**, *32*, 4819–4822; d) Zoretic, P. A.; Wang, M.; Zhang, Y.; Shen, Z.; Ribeiro, A. A. *J. Org. Chem.* **1996**, *61*, 1806–1813.

(15) a) Heinemann, C.; Xing, X.; Warzecha, K. D.; Ritterskamp, P.; Görner, H.; Demuth, M. *Pure Appl. Chem.* **1998**, *70*, 2167–2176; b) Heinemann, C.; Demuth, M. *J. Am. Chem. Soc.* **1999**, *121*, 4894–4895.

(16) RajanBabu, T. V.; Nugent, W. A. *J. Am. Chem. Soc.* **1994**, *116*, 986–997.

(17) a) Gansäuer, A.; Bluhm, H.; Pierobon, M. *J. Am. Chem. Soc.* **1998**, *120*, 12849–12859; b) Barrero, A. F.; Cuerva, J. M.; Herrador, M. M.; Valdivia, M. V. *J. Org. Chem.* **2001**, *66*, 4074–4078; c) Justicia, J.; Rosales, A.; Buñuel, E.; Oller-López, J. L.; Valdivia, M.; Haïdour, A.; Oltra, J. E.; Barrero, A. F.; Cárdenas, D. J.; Cuerva, J. M. *Chem. Eur. J.* **2004**, *10*, 1778–1788.

(18) Rendler, S.; MacMillan, D. W. C. *J. Am. Chem. Soc.* **2010**, *132*, 5027–5029.

(19) a) Crossley, S. W. M.; Obradors, C.; Martinez, R. M.; Shenvi, R. A. *Chem. Rev.* **2016**, *116*, 8912–9000; b) Shevick, S. L.; Wilson, C. V.; Kotesova, S.; Kim, D.; Holland, P. L.; Shenvi, R. A. *Chem. Sci.* **2020**, *11*, 12401–12422.

(20) a) Deng, H.; Cao, W.; Liu, R.; Zhang, Y.; Liu, B. *Angew. Chem. Int. Ed.* **2017**, *56*, 5849–5852; b) Cao, W.; Deng, H.; Sun, Y.; Liu, B.; Qin, S. *Chem. Eur. J.* **2018**, *24*, 9120–9129.

(21) a) Lo, J. C.; Yabe, Y.; Baran, P. S. *J. Am. Chem. Soc.* **2014**, *136*, 1304–1307; b) Lo, J. C.; Gui, J.; Yabe, Y.; Pan, C.-M.; Baran, P. S. *Nature* **2014**, *516*, 343–348; c) Lo, J. C.; Kim, D.; Pan, C.-M.; Edwards, J. T.; Yabe, Y.; Gui, J.; Qin, T.; Gutiérrez, S.; Giacoboni, J.; Smith, M. W.; Holland, P. L.; Baran, P. S. *J. Am. Chem. Soc.* **2017**, *139*, 2484–2503.

(22) a) Ishikawa, H.; Colby, D. A.; Boger, D. L. *J. Am. Chem. Soc.* **2008**, *130*, 420–421; b) Barker, T. J.; Boger, D. L. *J. Am. Chem. Soc.* **2012**, *134*, 13588–13591.

(23) MHAT-initiated cyclizations have played key roles in the synthesis of a growing number of natural products: a) George, D. T.; Kuenstner, E. J.; Pronin, S. V. *J. Am. Chem. Soc.* **2015**, *137*, 15410–15413; b) Zhang, B.; Zheng, W.; Wang, X.; Sun, D.; Li, C. *Angew. Chem. Int. Ed.* **2016**, *55*, 10435–10438; c) Xu, G.; Elkin, M.; Tantillo, D. J.; Newhouse, T. R.; Maimone, T. J. *Angew. Chem. Int. Ed.* **2017**, *56*, 12498–12502; d) Lu, Z.; Zhang, X.; Guo, Z.; Chen, Y.; Mu, T.; Li, A. *J. Am. Chem. Soc.* **2018**, *140*, 9211–9218; e) Godfrey, N. A.; Schatz, D. J.; Pronin, S. V. *J. Am. Chem. Soc.* **2018**, *140*, 12770–12774; f) Liu, J.; Ma, D. *Angew. Chem. Int. Ed.* **2018**, *57*, 6676–6680; g) Thomas, W. P.; Schatz, D. J.; George, D. T.; Pronin, S. V. *J. Am. Chem. Soc.* **2019**, *141*, 12246–12250; h) Xu, G.; Wu, J.; Li, L.; Lu, Y.; Li, C. *J. Am. Chem. Soc.* **2020**, *142*, 15240–15245; i) Li, J.; Li, F.; King-Smith, E.; Renata, H. *Nat. Chem.* **2020**, *12*, 173–179; j) Bartels, F.; Weber, M.; Christmann, M. *Org. Lett.* **2020**, *22*, 552–555; k) Zeng, X.; Shukla, V.; Boger, D. L. *J. Org. Chem.* **2020**, *85*, 14817–14826; l) Chen, P.; Wang, C.; Yang, R.; Xu, H.; Wu, J.; Jiang, H.; Chen, K.; Ma, Z. *Angew. Chem. Int. Ed.* **2021**, *60*, 5512–5518.

(24) Shigeru, I.; Teruaki, M. *Chem. Lett.* **1989**, *18*, 1071–1074.

(25) a) Waser, J.; Carreira, E. M. *J. Am. Chem. Soc.* **2004**, *126*, 5676–5677; b) Waser, J.; Nambu, H.; Carreira, E. M. *J. Am. Chem. Soc.* **2005**, *127*, 8294–8295; c) Gaspar, B.; Carreira, E. M. *Angew. Chem. Int. Ed.* **2007**, *46*, 4519–4522; d) Gaspar, B.; Carreira, E. M. *Angew. Chem. Int. Ed.* **2008**, *47*, 5758–5760.

(26) Norton and co-workers have reported a single example of a decalin-forming radical bicyclization initiated by $CpCr(CO)_3H$-catalyzed HAT to an electron deficient alkene; the

yield was low and there was no discussion of stereochemical control by the resident stereogenic center: Hartung, J.; Pulling, M. E.; Smith, D. M.; Yang, D. X.; Norton, J. R. *Tetrahedron* **2008**, *64*, 11822–11830.

(27) Vrubliauskas, D.; Vanderwal, C. D. *Angew. Chem. Int. Ed.* **2020**, *59*, 6115–6121.

(28) Michalak, S. E.; Nam, S.; Kwon, D. M.; Horne, D. A.; Vanderwal, C. D. *J. Am. Chem. Soc.* **2019**, *141*, 9202–9206.

(29) Xu, J.; Wang, M.; Sun, X.; Ren, Q.; Cao, X.; Li, S.; Su, G.; Tuerhong, M.; Lee, D.; Ohizumi, Y.; Bartlam, M.; Guo, Y. *J. Nat. Prod.* **2016**, *79*, 2924–2932.

(30) a) Xiong, Y.; Qu, W.; Sun, J.-b.; Wang, M.-h.; Liang, J.-y. *Phytochem. Lett.* **2013**, *6*, 457–460; b) Radulović, N.; Denić, M.; Stojanović-Radić, Z. *Bioorg. Med. Chem. Lett.* **2010**, *20*, 4988–4991; c) Qiao, Y.; Xu, Q.; Hu, Z.; Li, X.-N.; Xiang, M.; Liu, J.; Huang, J.; Zhu, H.; Wang, J.; Luo, Z.; Xue, Y.; Zhang, Y. *J. Nat. Prod.* **2016**, *79*, 3134–3142.

(31) Morcillo, S. P.; Miguel, D.; Resa, S.; Martín-Lasanta, A.; Millán, A.; Choquesillo-Lazarte, D.; García-Ruiz, J. M.; Mota, A. J.; Justicia, J.; Cuerva, J. M. *J. Am. Chem. Soc.* **2014**, *136*, 6943–6951.

(32) Surendra, K.; Qiu, W.; Corey, E. J. *J. Am. Chem. Soc.* **2011**, *133*, 9724–9726.

(33) Tada, M.; Nishiiri, S.; Zhixiang, Y.; Imai, Y.; Tajima, S.; Okazaki, N.; Kitano, Y.; Chiba, K. *J. Chem. Soc., Perkin Trans. 1* **2000**, 2657–2664.

(34) Matsushita, Y.-i.; Sugamoto, K.; Iwakiri, Y.; Yoshida, S.; Chaen, T.; Matsui, T. *Tetrahedron Lett.* **2010**, *51*, 3931–3934.

(35) Montchamp, J.-L.; Tian, F.; Hart, M. E.; Frost, J. W. *J. Org. Chem.* **1996**, *61*, 3897–3899.

(36) a) Shigemori, H.; Komaki, H.; Yazawa, K.; Mikami, Y.; Nemoto, A.; Tanaka, Y.; Sasaki, T.; In, Y.; Ishida, T.; Kobayashi, J. *J. Org. Chem.* **1998**, *63*, 6900–6904; b) Lin, S.; Zhang,

X.; Shen, L.; Mo, S.; Liu, J.; Wang, J.; Hu, Z.; Zhang, Y. *Nat. Prod. Res.* **2020**, 1–8; c) Zeng, N.; Shen, Y.; Li, L.-Z.; Jiao, W.-H.; Gao, P.-Y.; Song, S.-J.; Chen, W.-S.; Lin, H.-W. *J. Nat. Prod.* **2011**, *74*, 732–738.

(37) Gao, C.; Han, L.; Zheng, D.; Jin, H.; Gai, C.; Wang, J.; Zhang, H.; Zhang, L.; Fu, H. *J. Nat. Prod.* **2015**, *78*, 630–638.

(38) Dai, M.; Krauss, I. J.; Danishefsky, S. J. *J. Org. Chem.* **2008**, *73*, 9576–9583.

(39) Peters, M.; Trobe, M.; Tan, H.; Kleineweischede, R.; Breinbauer, R. *Chem. Eur. J.* **2013**, *19*, 2442–2449.

(40) Majetich, G.; Zou, G. *Org. Lett.* **2008**, *10*, 81–83.

(41) We have made the unnatural enantiomers of these natural products. This was only because we had large quantities of the corresponding enantiomer of epichclorohydrin in our labarotories. Both enantiomers of epichlorohydrin are commercially available. Li, F.-Z.; Li, S.; Zhang, P.-P.; Huang, Z.-H.; Zhang, W.-B.; Gong, J.; Yang, Z. *Chem. Commun.* **2016**, *52*, 12426–12429.

(42) Girijavallabhan, V.; Arasappan, A.; Bennett, F.; Chen, K.; Dang, Q.; Huang, Y.; Kerekes, A.; Nair, L.; Pissarnitski, D.; Verma, V.; Alvarez, C.; Chen, P.; Cole, D.; Esposite, S.; Huang, Y.; Hong, Q.; Liu, Z.; Pan, W.; Pu, H.; Rossman, R.; Truong, Q.; Vibulbhan, B.; Wang, J.; Zhao, Z.; Olsen, D.; Stamford, A.; Bogen, S.; Njoroge, F. G. *Nucleosides, Nucleotides and Nucleic Acids* **2016**, *35*, 277–294.

(43) Green, J. C.; Brown, E. R.; Pettus, T. R. R. *Org. Lett.* **2012**, *14*, 2929–2931.

(44) Satyanarayana, G.; Maier, M. E. *Tetrahedron* **2012**, *68*, 1745–1749.

(45) Nikas, S. P.; Thakur, G. A.; Makriyannis, A. *Synth. Commun.* **2002**, *32*, 1751–1756.

(46) Lee, J.-H.; Shin, S. C.; Seo, S. H.; Seo, Y. H.; Jeong, N.; Kim, C.-W.; Kim, E. E.; Keum, G. *Bioorg. Med. Chem. Lett.* **2017**, *27*, 237–241.

(47) Mihelcic, J.; Moeller, K. D. *J. Am. Chem. Soc.* **2004**, *126*, 9106–9111.

(48) Bonini, C.; Chiummiento, L.; Funicello, M.; Lupattelli, P.; Pullez, M. *Eur. J. Org. Chem.* **2006**, *2006*, 80–83.

(49) Pearson, W. H.; Walters, M. A.; Oswell, K. D. *J. Am. Chem. Soc.* **1986**, *108*, 2769–2771.

(50) Namba, K.; Yamamoto, H.; Sasaki, I.; Mori, K.; Imagawa, H.; Nishizawa, M. *Org. Lett.* **2008**, *10*, 1767–1770.

(51) Yu, W.; Mei, Y.; Kang, Y.; Hua, Z.; Jin, Z. *Org. Lett.* **2004**, *6*, 3217–3219.

(52) Kong, W.; Guo, Q.; Xu, Z.; Wang, G.; Jiang, X.; Wang, R. *Org. Lett.* **2015**, *17*, 3686–3689.

(53) Magdziak, D.; Rodriguez, A. A.; Van De Water, R. W.; Pettus, T. R. R. *Org. Lett.* **2002**, *4*, 285–288.

(54) Devereaux, J.; Ferrara, S. J.; Banerji, T.; Placzek, A. T.; Scanlan, T. S. *ChemMedChem* **2016**, *11*, 2459–2465.

APPENDIX A: ^{1}H, ^{13}C, 2D NMR & ISOTOPE MASS RATIO SPECTRA

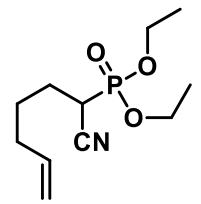

S2.1

^{1}H NMR

500 MHz, $CDCl_3$

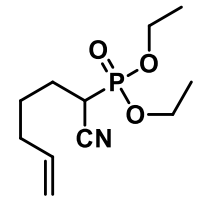

S2.1

^{13}C NMR

126 MHz, $CDCl_3$

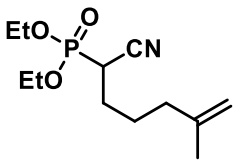

S2.2

^{1}H NMR

600 MHz, $CDCl_3$

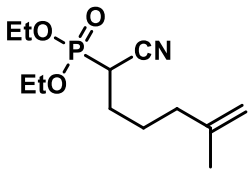

S2.2

^{13}C NMR

151 MHz, $CDCl_3$

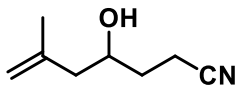

S2.4
^{13}C NMR
151 MHz, $CDCl_3$

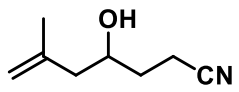

S2.4

^{13}C NMR

151 MHz, $CDCl_3$

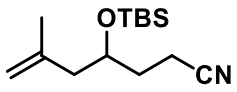

S2.5
^{1}H NMR
600 MHz, $CDCl_3$

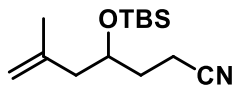

S2.5
^{13}C NMR
151 MHz, $CDCl_3$

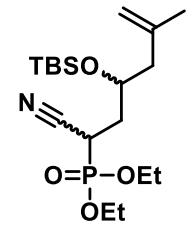

S2.6 (mixture of diastereomers)

^{1}H NMR

600 MHz, $CDCl_3$

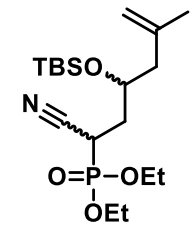

S2.6 (mixture of diastereomers)

^{13}C NMR

126 MHz, $CDCl_3$

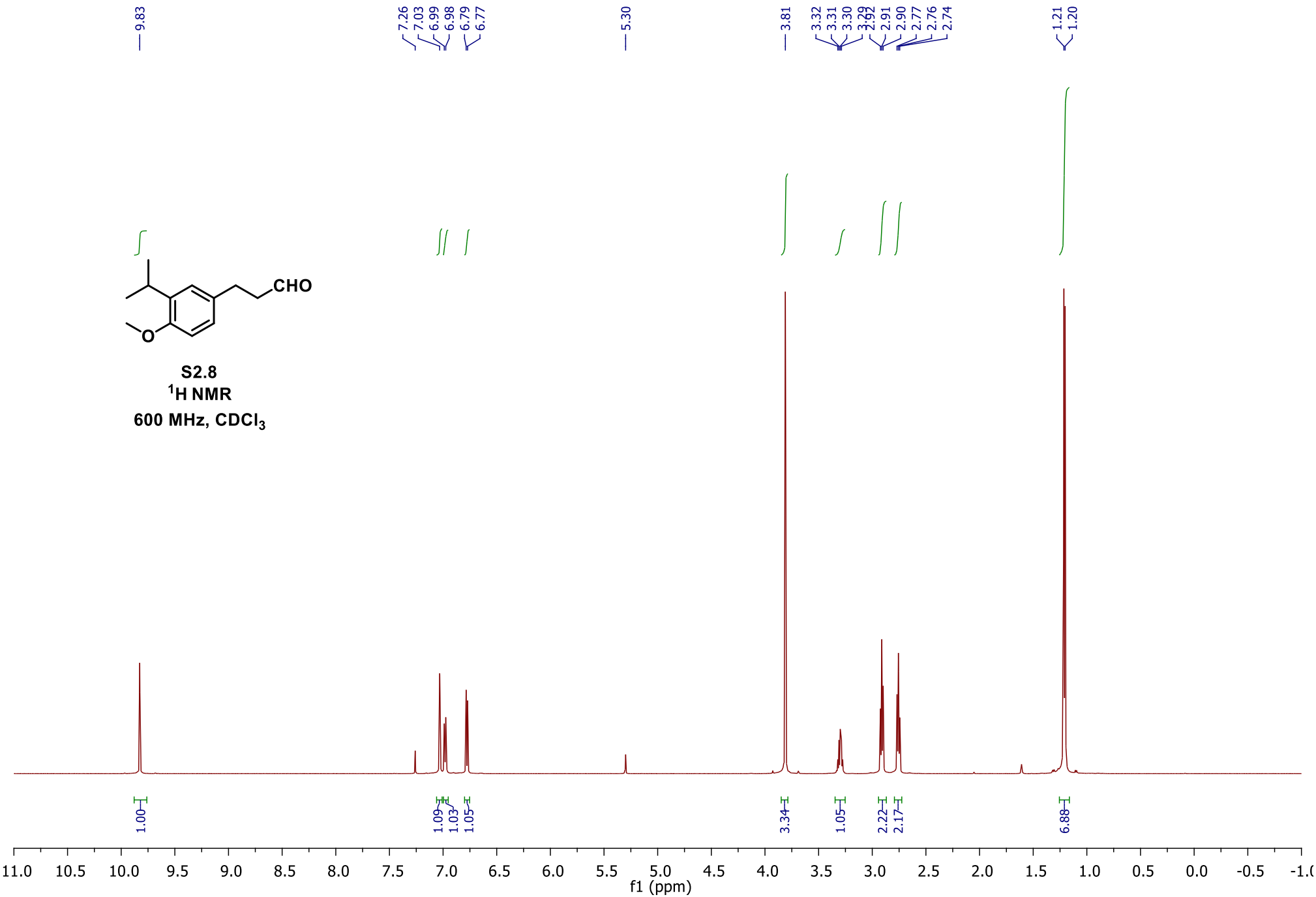
9.83
7.26
7.03
6.99
6.98
6.79
6.77
5.30
3.81
3.32
3.31
3.30
2.91
2.90
2.77
2.76
2.74
1.21
1.20
CHO
O
S2.8
1H NMR
600 MHz, CDCl3
1.00
1.09
1.03
1.05
3.34
1.05
2.22
2.17
6.88
f1 (ppm)

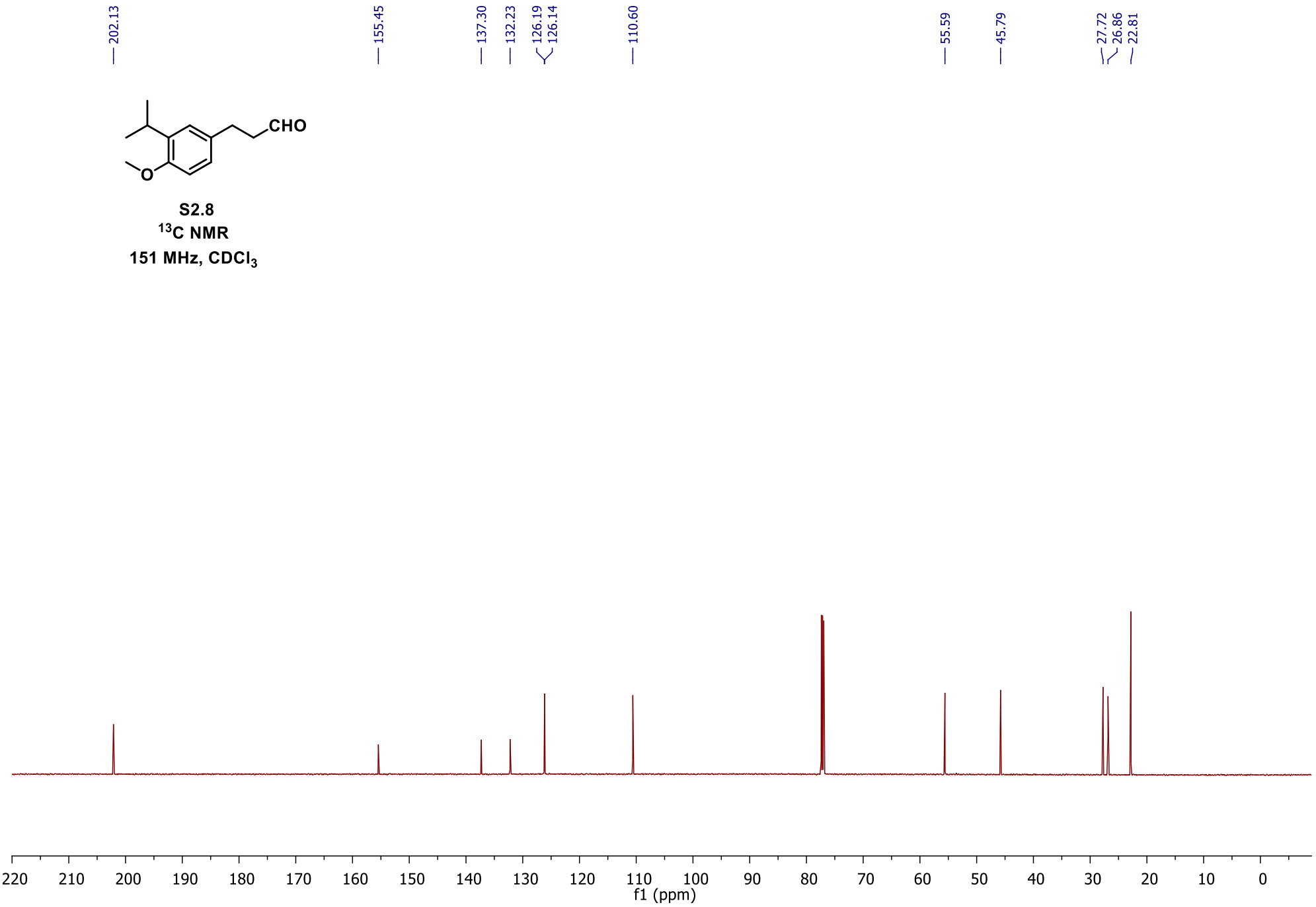

S2.8
^{13}C NMR
151 MHz, $CDCl_3$

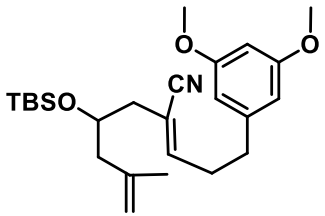

2.5a
^{1}H NMR
500 MHz, $CDCl_3$

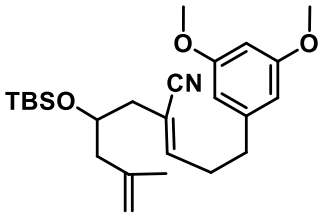

2.5a
^{13}C NMR
126 MHz, $CDCl_3$

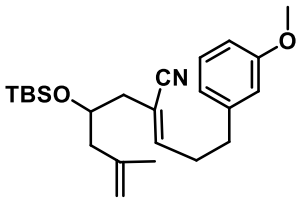

S2.11
^{1}H NMR
500 MHz, $CDCl_3$

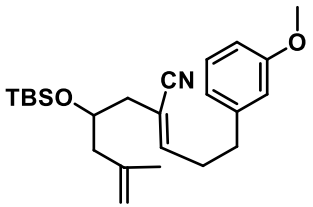

S2.11

^{13}C NMR

126 MHz, $CDCl_3$

159.93
149.13
142.05
142.00
129.69
120.88
117.81
114.25
113.88
112.78
111.81
77.41
77.16
76.91
69.00
55.32
46.00
41.73
34.79
33.13
25.97
23.07
18.17
-4.35
-4.51

230 220 210 200 190 180 170 160 150 140 130 120 110 100 90 80 70 60 50 40 30 20 10 0 -10

f1 (ppm)

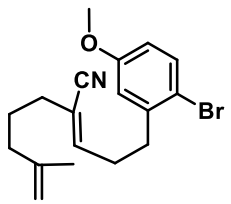

S2.13
^{1}H NMR
500 MHz, $CDCl_3$

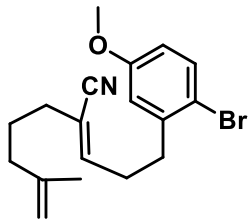

S2.13
^{13}C NMR
126 MHz, $CDCl_3$

159.17
146.05
144.79
140.59
133.55
117.54
116.16
115.67
114.93
113.89
110.80
77.41
77.16
76.91
55.58
36.69
35.18
33.78
31.69
25.91
22.33

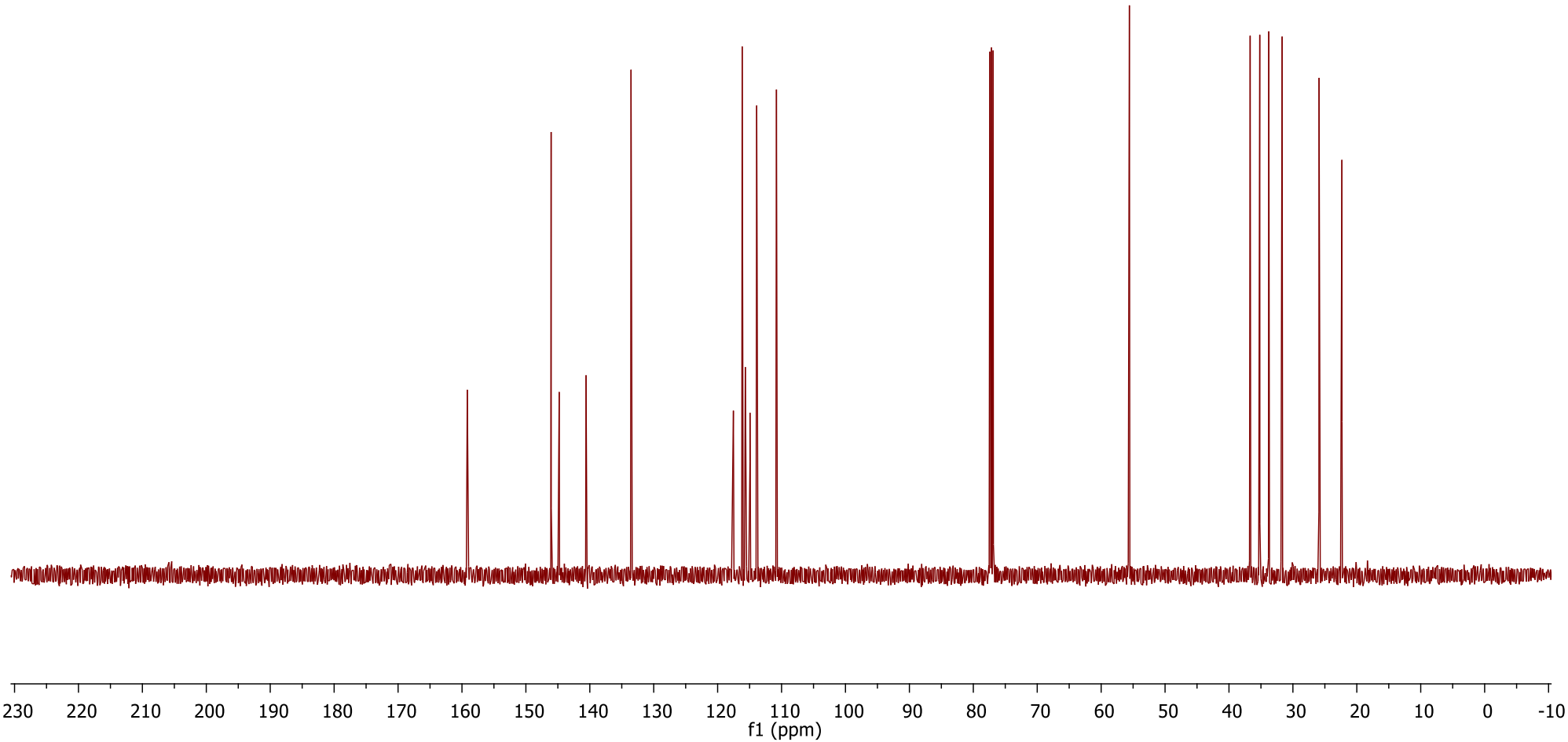

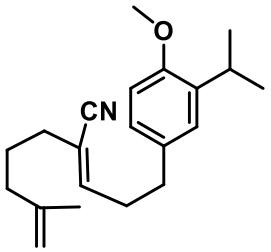

S2.14
^{1}H NMR
600 MHz, $CDCl_3$

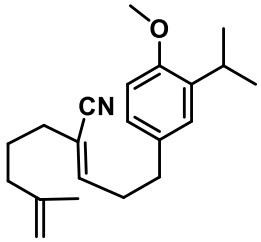

S2.14
^{13}C NMR
151 MHz, $CDCl_3$

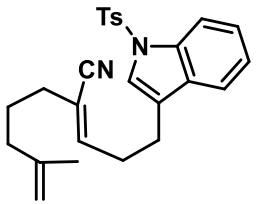

S2.16
^{1}H NMR
600 MHz, $CDCl_3$

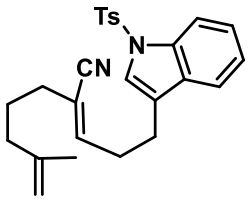

S2.16
^{13}C NMR
151 MHz, $CDCl_3$

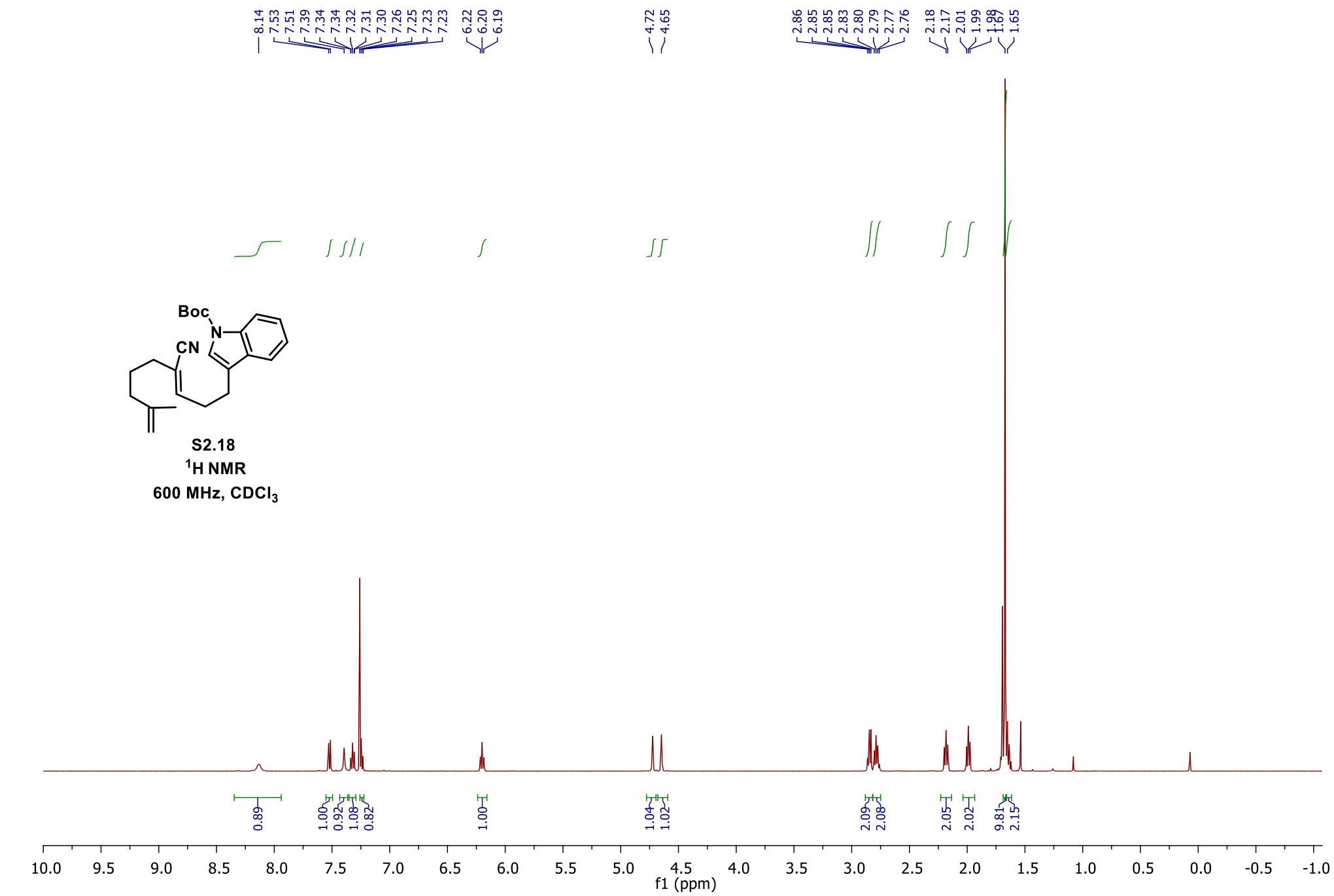
8.14
7.53
7.51
7.39
7.34
7.34
7.32
7.31
7.30
7.26
7.25
7.23
7.23
6.22
6.20
6.19
4.72
4.65
2.86
2.85
2.85
2.83
2.80
2.79
2.77
2.76
2.18
2.17
2.01
1.99
1.98
1.67
1.65
Boc
N
CN
S2.18
1H NMR
600 MHz, CDCl3
0.89
1.00
0.92
1.08
0.82
1.00
1.04
1.02
2.09
2.08
2.05
2.02
9.81
2.15
10.0
9.5
9.0
8.5
8.0
7.5
7.0
6.5
6.0
5.5
5.0
4.5
4.0
3.5
3.0
2.5
2.0
1.5
1.0
0.5
0.0
-0.5
-1.0
f1 (ppm)

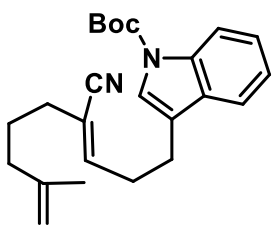

S2.18
^{13}C NMR
126 MHz, $CDCl_3$

149.83
146.75
144.72
135.69
130.43
124.60
122.81
122.60
119.29
118.94
117.62
115.53
115.45
110.85
83.65
77.41
77.16
76.91
36.65
33.74
31.14
28.35
25.89
24.21
22.31

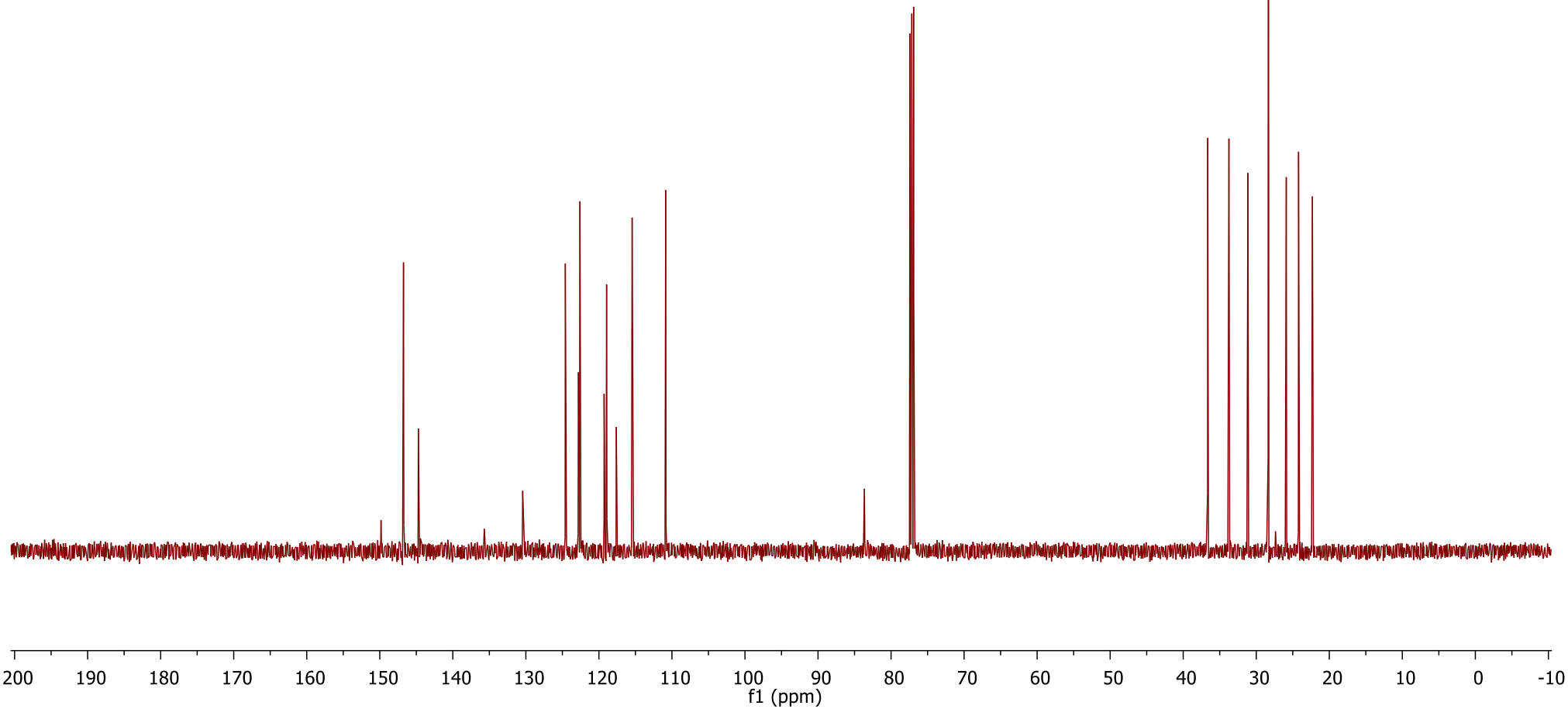

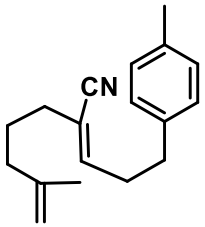

S2.20
^{1}H NMR
500 MHz, $CDCl_3$

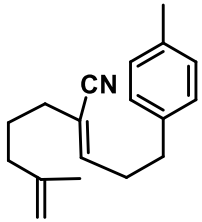

S2.20
^{13}C NMR
126 MHz, $CDCl_3$

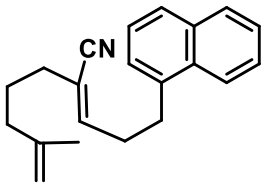

S2.22
^{1}H NMR
600 MHz, $CDCl_3$

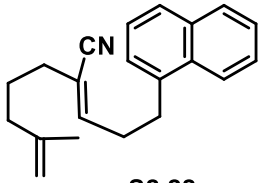

S2.22
^{13}C NMR
151 MHz, $CDCl_3$

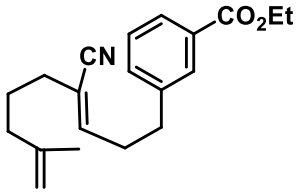

S2.24
^{1}H NMR
500 MHz, $CDCl_3$

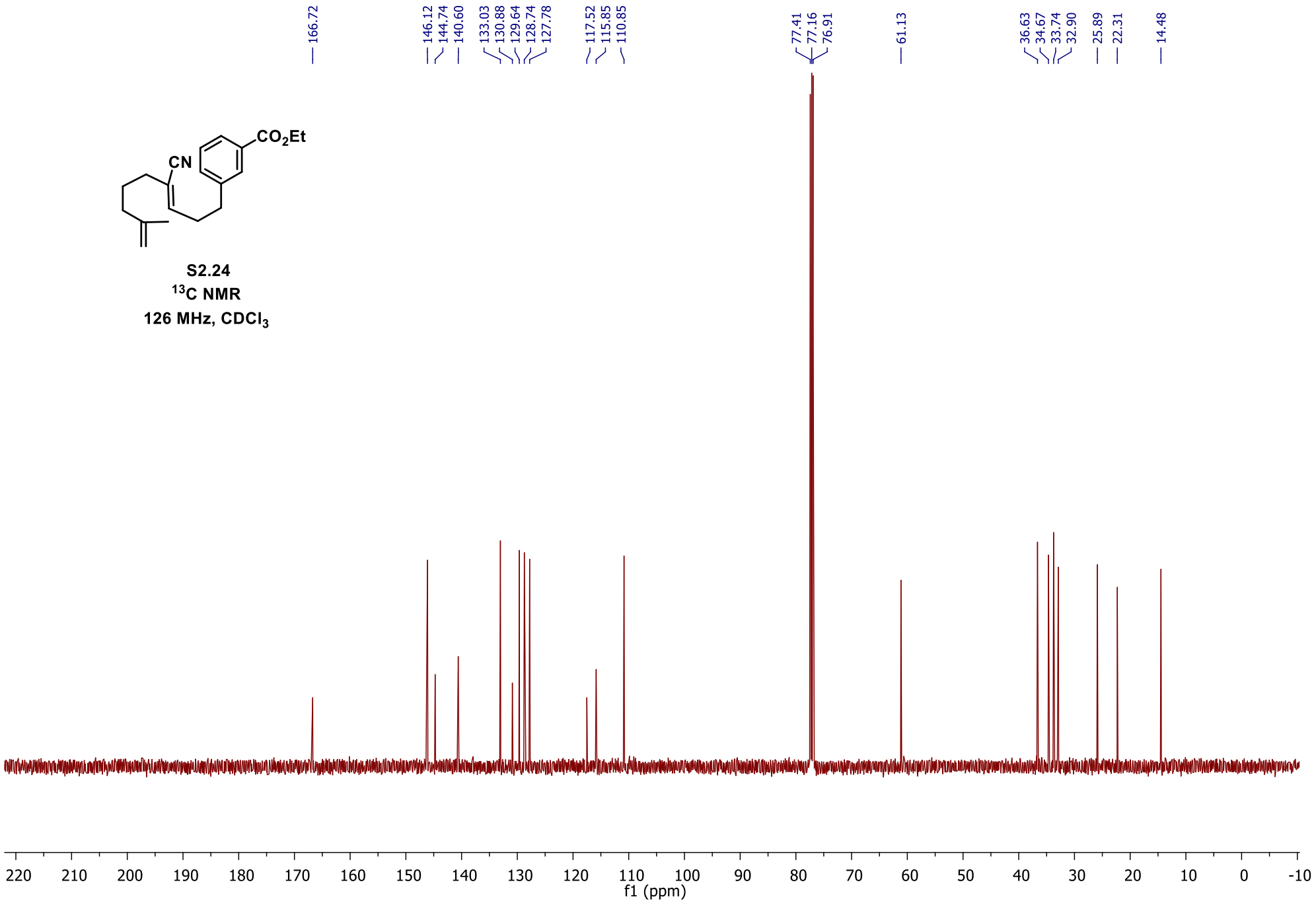
166.72
146.12
144.74
140.60
133.03
130.88
129.64
128.74
127.78
117.52
115.85
110.85
77.41
77.16
76.91
61.13
36.63
34.67
33.74
32.90
25.89
22.31
14.48
CO2Et
CN
S2.24
13C NMR
126 MHz, CDCl3
220 210 200 190 180 170 160 150 140 130 120 110 100 90 80 70 60 50 40 30 20 10 0 -10
f1 (ppm)

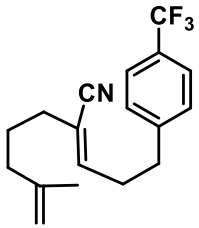

S2.26
^{1}H NMR
600 MHz, $CDCl_3$

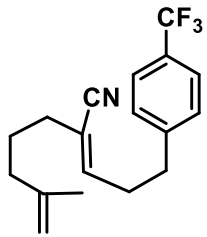

S2.26

^{13}C NMR

151 MHz, $CDCl_3$

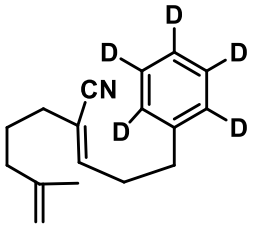

2.28
^{1}H NMR
600 MHz, $CDCl_3$

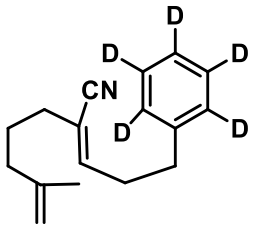

2.28
^{13}C DEPTQ
151 MHz, $CDCl_3$

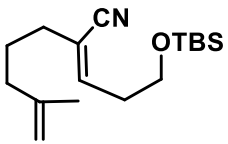

S2.53
^{1}H NMR
600 MHz, $CDCl_3$

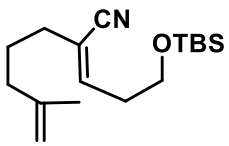

S2.53
^{13}C DEPTQ
151 MHz, $CDCl_3$

144.97
144.75
117.73
116.04
110.81
77.37
77.16
76.95
61.64
36.67
35.10
33.83
26.06
25.96
25.87
22.32
-5.27

230 220 210 200 190 180 170 160 150 140 130 120 110 100 90 80 70 60 50 40 30 20 10 0
f1 (ppm)

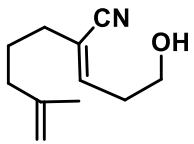

2.26
^{1}H NMR
600 MHz, $CDCl_3$

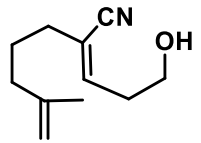

2.26
^{13}C DEPTQ
151 MHz, $CDCl_3$

144.73
144.25
117.68
116.76
110.85
77.37
77.16
76.95
61.29
36.67
34.93
33.80
25.84
22.31

230 220 210 200 190 180 170 160 150 140 130 120 110 100 90 80 70 60 50 40 30 20 10 0
f1 (ppm)

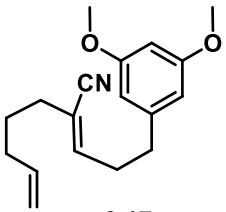

2.17
^{1}H NMR
500 MHz, $CDCl_3$

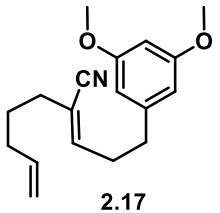

2.17
^{13}C NMR
126 MHz, $CDCl_3$

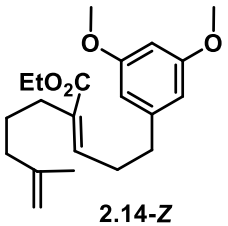

2.14-*Z*

^{1}H NMR

500 MHz, $CDCl_3$

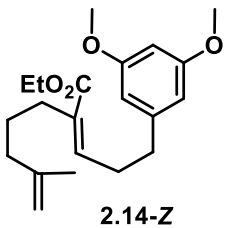

2.14-*Z*

^{13}C NMR

126 MHz, $CDCl_3$

168.22
160.91
145.74
144.09
140.27
132.93
110.15
106.66
98.09
77.41
77.16
76.91
60.24
55.39
37.34
36.00
34.33
30.99
27.14
22.45
14.47

220 210 200 190 180 170 160 150 140 130 120 110 100 90 80 70 60 50 40 30 20 10 0 -10

f1 (ppm)

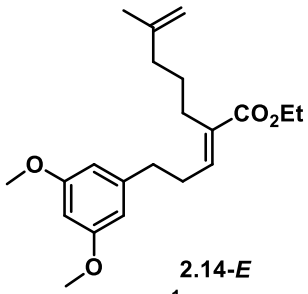

2.14-*E*
^{1}H NMR
500 MHz, $CDCl_3$

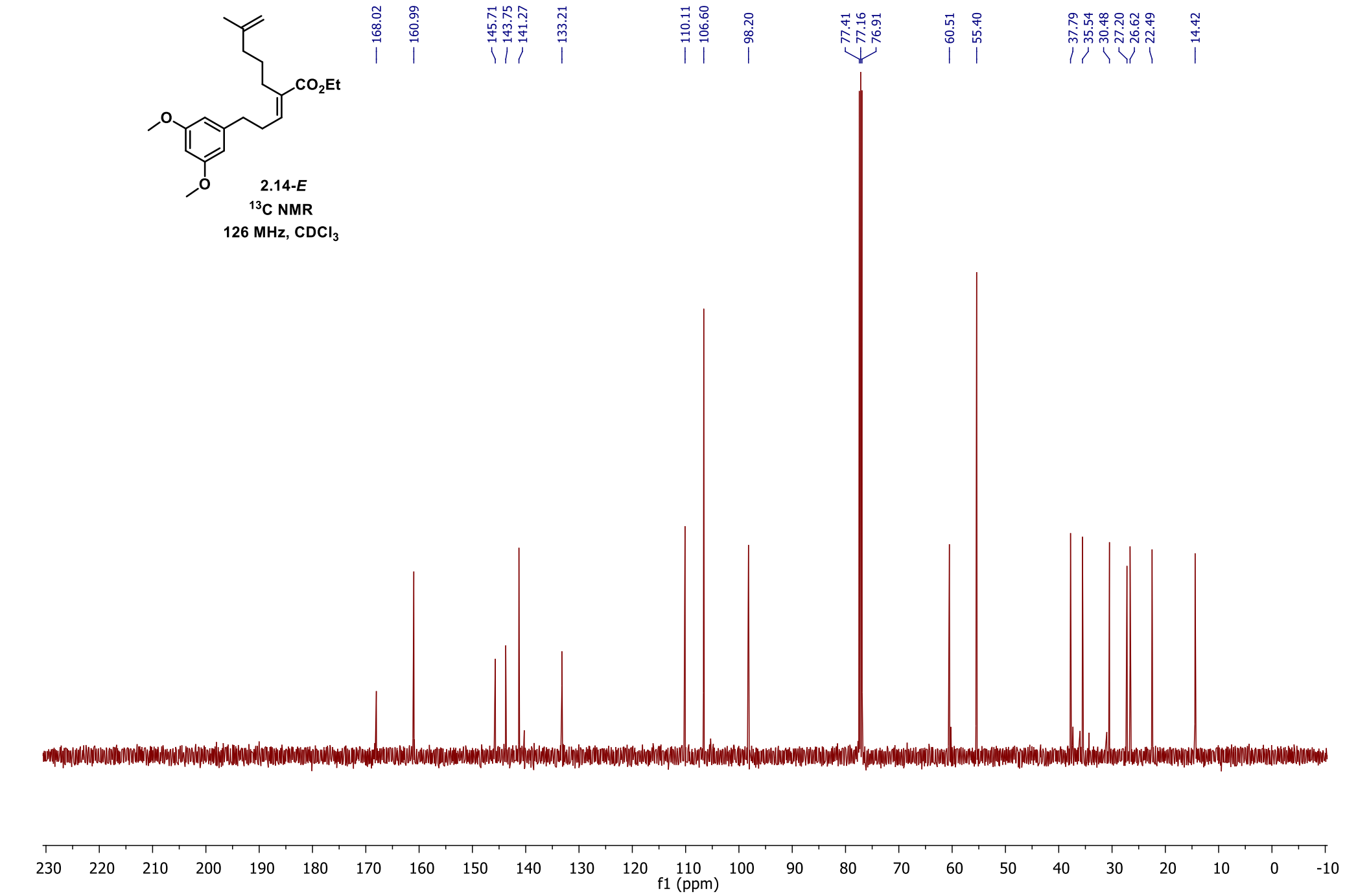
168.02
160.99
145.71
143.75
141.27
133.21
110.11
106.60
98.20
77.41
77.16
76.91
60.51
55.40
37.79
35.54
30.48
27.20
26.62
22.49
14.42
CO2Et
O
O
2.14-E
13C NMR
126 MHz, CDCl3
230 220 210 200 190 180 170 160 150 140 130 120 110 100 90 80 70 60 50 40 30 20 10 0 -10
f1 (ppm)

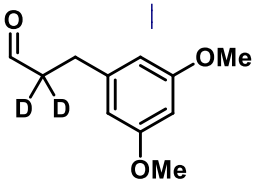

S2.9-d_2

^{1}H NMR

500 MHz, $CDCl_3$

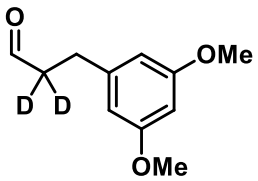

S2.9-d_2
^{13}C NMR
151 MHz, $CDCl_3$

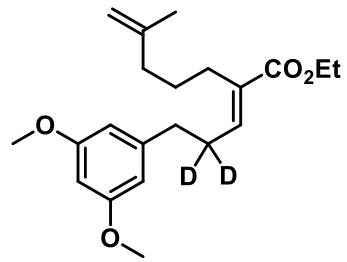

2.14-*E*-d_2 (~90% d_2)
^{1}H NMR
600 MHz, $CDCl_3$

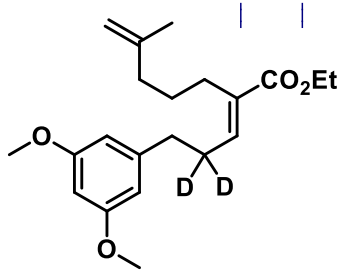

2.14-*E*-d_2 (~90% d_2)

^{13}C NMR

151 MHz, $CDCl_3$

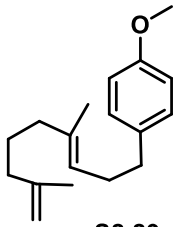

S2.29

^{1}H NMR

500 MHz, $CDCl_3$

(contains ~11% of trisubstituted alkene isomer)

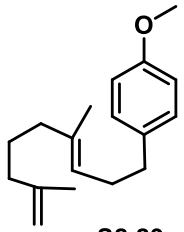

S2.29

^{13}C NMR

126 MHz, $CDCl_3$

(contains ~11% of trisubstituted alkene isomer)

157.83
146.28
135.82
134.67
129.48
123.95
113.78
109.83
77.41
77.16
76.91
55.40
39.42
37.51
35.36
30.31
26.07
22.58
16.01

230 220 210 200 190 180 170 160 150 140 130 120 110 100 90 80 70 60 50 40 30 20 10 0 -10

f1 (ppm)

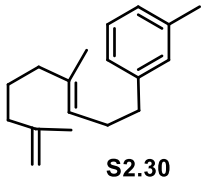

S2.30
^{1}H NMR
600 MHz, $CDCl_3$

(contains ~11% of trisubstituted alkene isomer)

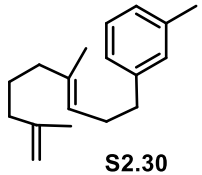

S2.30
^{13}C NMR
151 MHz, $CDCl_3$

(contains ~11% of trisubstituted alkene isomer)

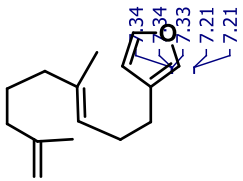

S2.31
^{1}H NMR
500 MHz, $CDCl_3$

(contains ~11% of trisubstituted alkene isomer)

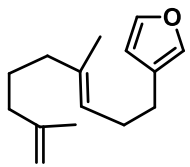

S2.31

^{13}C NMR

126 MHz, $CDCl_3$

(contains ~11% of trisubstituted alkene isomer)

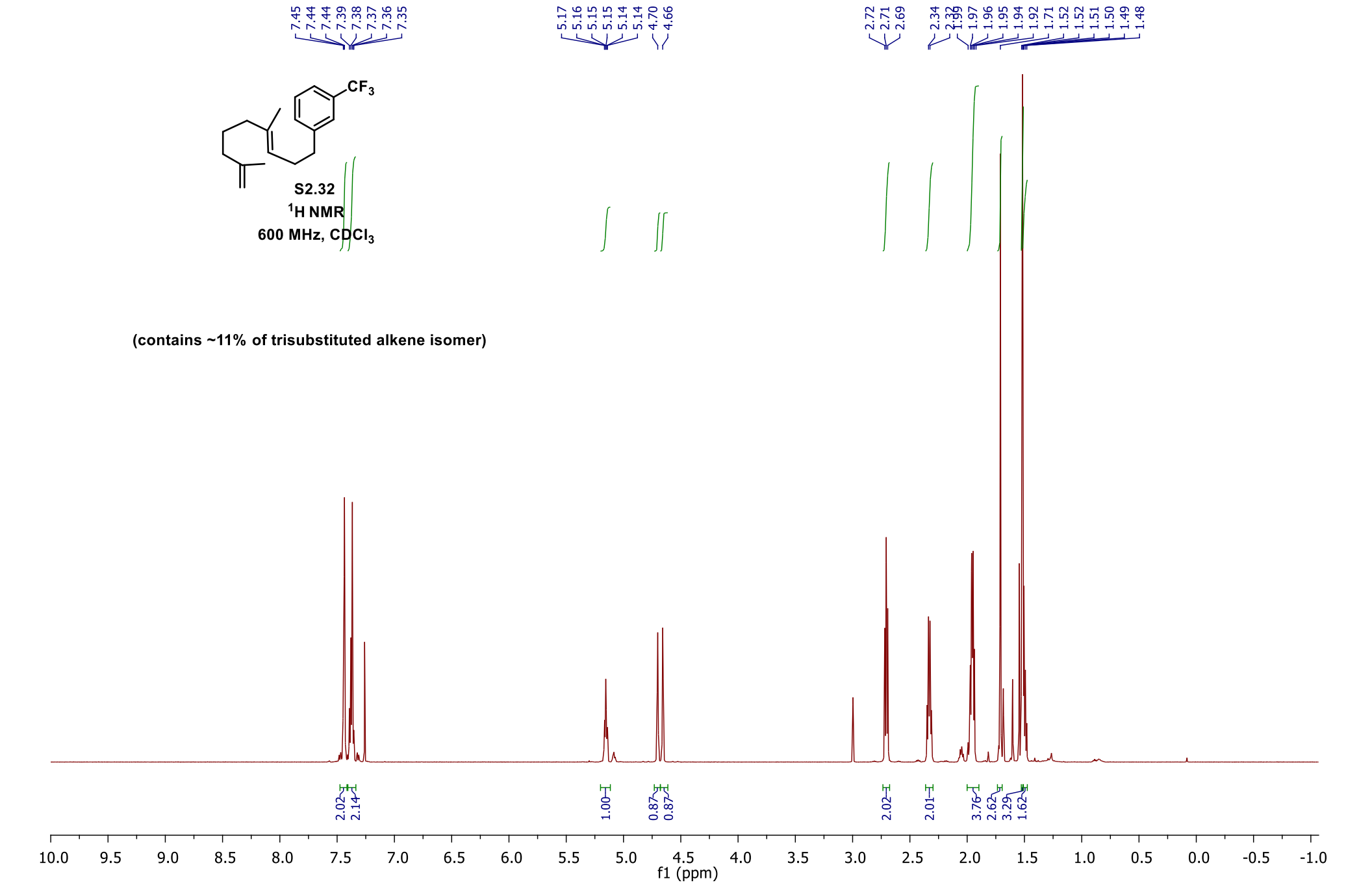
7.45
7.44
7.44
7.39
7.38
7.37
7.36
7.35
5.17
5.16
5.15
5.15
5.14
5.14
4.70
4.66
2.72
2.71
2.69
2.34
1.97
1.96
1.95
1.94
1.92
1.71
1.52
1.52
1.51
1.50
1.49
1.48
CF3
S2.32
1H NMR
600 MHz, CDCl3
(contains ~11% of trisubstituted alkene isomer)
2.02
2.14
1.00
0.87
0.87
2.02
2.01
3.76
2.62
3.29
1.62
10.0
9.5
9.0
8.5
8.0
7.5
7.0
6.5
6.0
5.5
5.0
4.5
4.0
3.5
3.0
2.5
2.0
1.5
1.0
0.5
0.0
-0.5
-1.0
f1 (ppm)

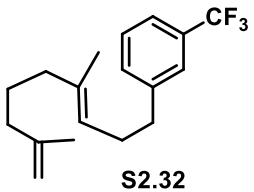

S2.32

^{13}C NMR

151 MHz, $CDCl_3$

(contains ~11% of trisubstituted alkene isomer)

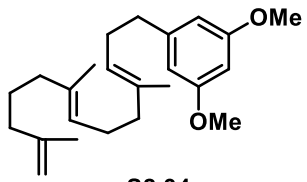

S2.34
^{1}H NMR
500 MHz, $CDCl_3$

(contains ~11% of trisubstituted alkene isomer)

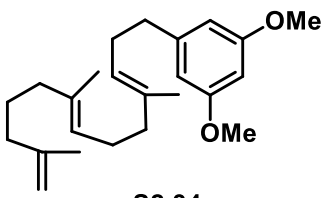

S2.34
^{13}C NMR
126 MHz, $CDCl_3$

(contains ~11% of trisubstituted alkene isomer)

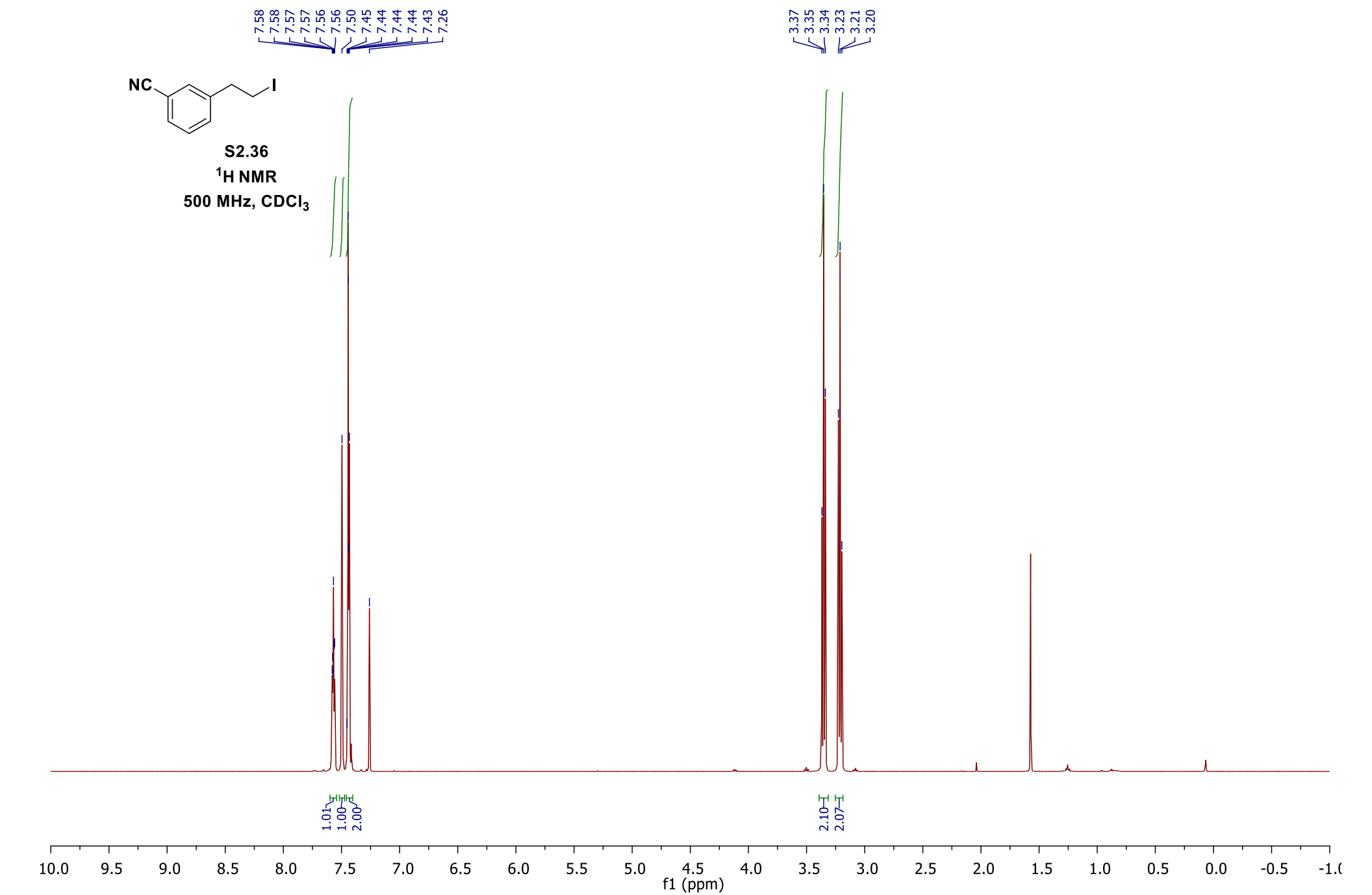
7.58
7.58
7.57
7.57
7.56
7.56
7.50
7.45
7.44
7.44
7.44
7.43
7.26
3.37
3.35
3.34
3.23
3.21
3.20
NC
I
S2.36
1H NMR
500 MHz, CDCl3
1.01
1.00
2.00
2.10
2.07
10.0
9.5
9.0
8.5
8.0
7.5
7.0
6.5
6.0
5.5
5.0
4.5
4.0
3.5
3.0
2.5
2.0
1.5
1.0
0.5
0.0
-0.5
f1 (ppm)

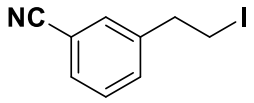

S2.36

^{13}C NMR

126 MHz, $CDCl_3$

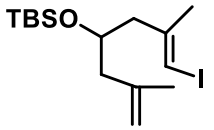

S2.38
^{1}H NMR
500 MHz, $CDCl_3$

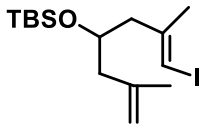

S2.38
^{13}C NMR
126 MHz, $CDCl_3$

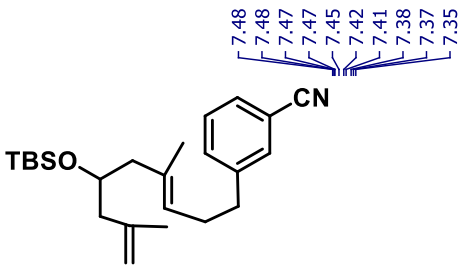

S2.40
^{1}H NMR
600 MHz, $CDCl_3$

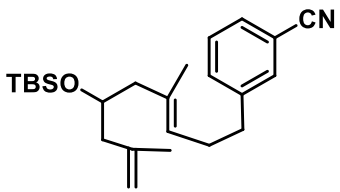

S2.40
^{13}C NMR
151 MHz, $CDCl_3$

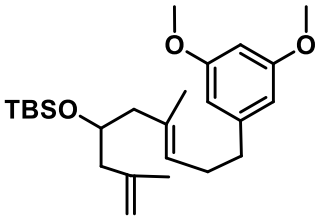

S2.42
^{1}H NMR
500 MHz, $CDCl_3$

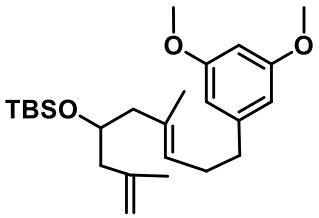

S2.42

^{13}C NMR

151 MHz, $CDCl_3$

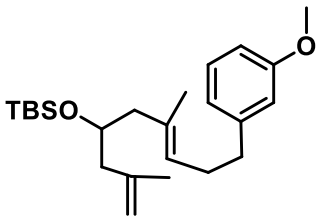

S2.44
^{1}H NMR
600 MHz, $CDCl_3$

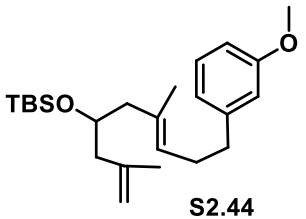

S2.44

^{13}C NMR

151 MHz, $CDCl_3$

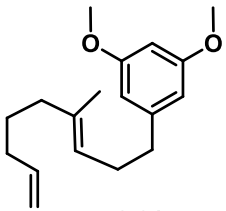

2.21
^{1}H NMR
600 MHz, $CDCl_3$

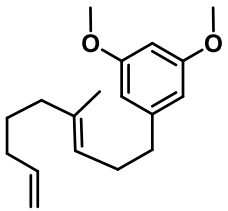

2.21

^{13}C DEPTQ

151 MHz, $CDCl_3$

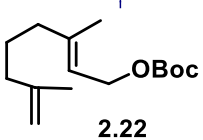

2.22

^{1}H NMR

500 MHz, $CDCl_3$

(contains ~11% of trisubstituted alkene isomer)

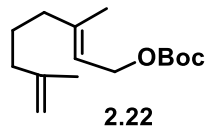

153.79
145.82
142.69
118.33
110.10
81.97
77.41
77.16
76.91
63.88
39.17
37.42
27.95
25.56
22.50
16.54

2.22

^{13}C NMR

126 MHz, $CDCl_3$

(contains ~11% of trisubstituted alkene isomer)

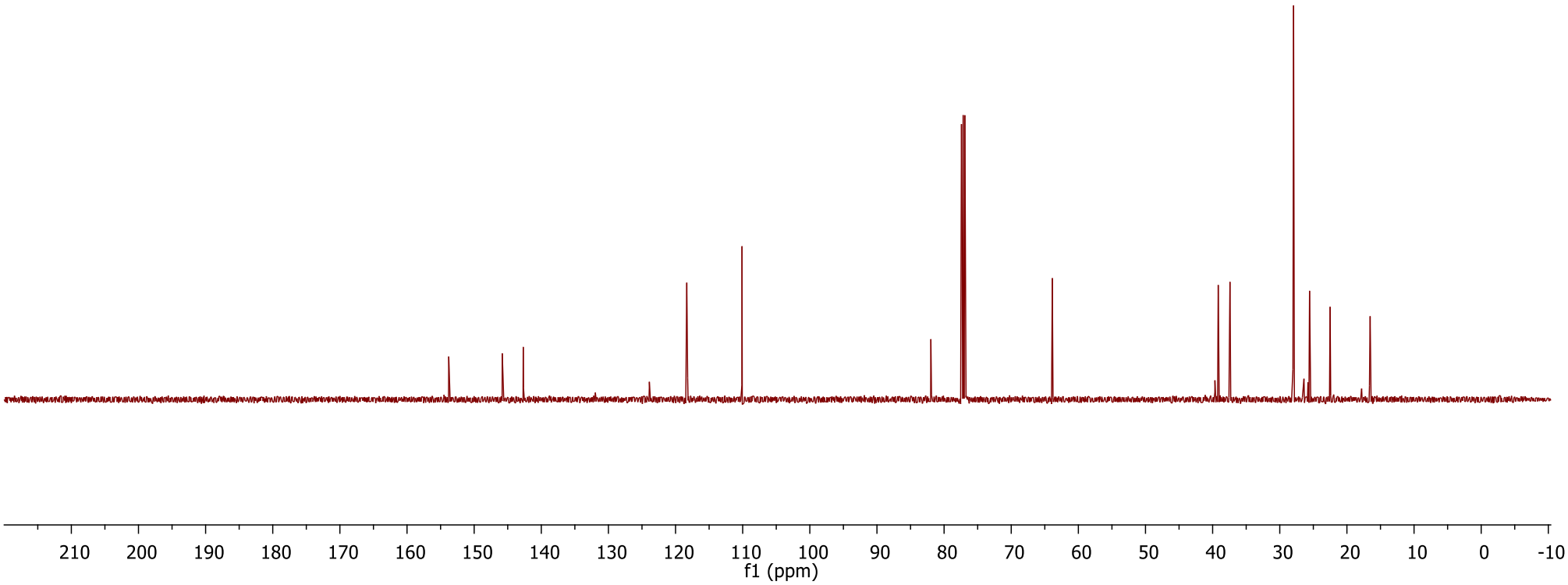

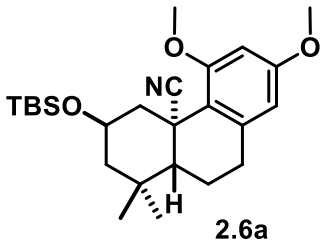

2.6a

^{1}H NMR

500 MHz, $CDCl_3$

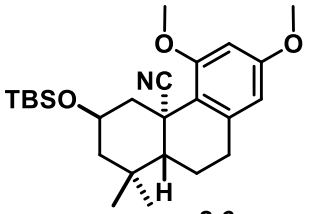

2.6a

^{13}C NMR

151 MHz, $CDCl_3$

159.97
159.90
139.79
122.81
118.55
105.41
97.81
77.37
77.16
76.95
66.22
55.57
55.38
52.50
50.54
43.32
39.36
34.92
32.95
32.80
26.12
21.58
20.95
18.48
-4.49

230 220 210 200 190 180 170 160 150 140 130 120 110 100 90 80 70 60 50 40 30 20 10 0

f1 (ppm)

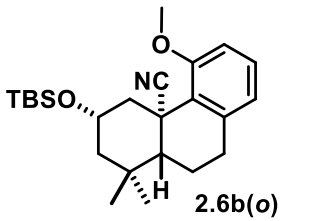

2.6b(*o*)
^{1}H NMR
600 MHz, $CDCl_3$

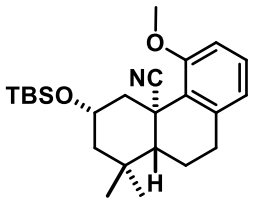

2.6b(*o*)
^{13}C NMR
151 MHz, $CDCl_3$

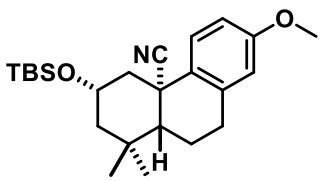

2.6b(*p*)
^{1}H NMR
600 MHz, $CDCl_3$

(contains ~10% of *ortho* regioisomer)

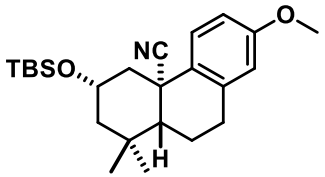

2.6b(*p*)

^{13}C NMR

151 MHz, $CDCl_3$

(contains ~10% of the *ortho* regioisomer)

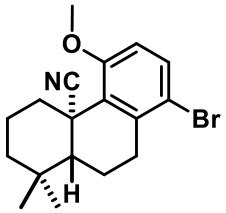

2.6c

^{1}H NMR

600 MHz, $CDCl_3$

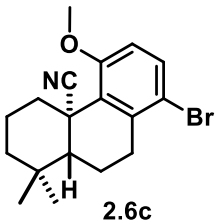

2.6c

^{13}C NMR

151 MHz, $CDCl_3$

158.40
138.28
132.45
129.06
122.59
117.03
111.19
77.37
77.16
76.95
55.89
52.31
40.92
40.23
34.98
34.19
34.15
32.66
21.18
20.58
20.54

230 220 210 200 190 180 170 160 150 140 130 120 110 100 90 80 70 60 50 40 30 20 10 0

f1 (ppm)

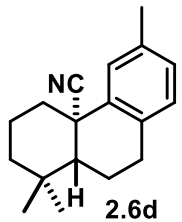

2.6d

^{1}H NMR

600 MHz, $CDCl_3$

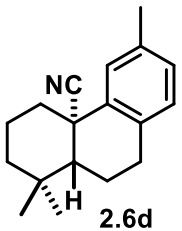

2.6d

^{13}C NMR

151 MHz, $CDCl_3$

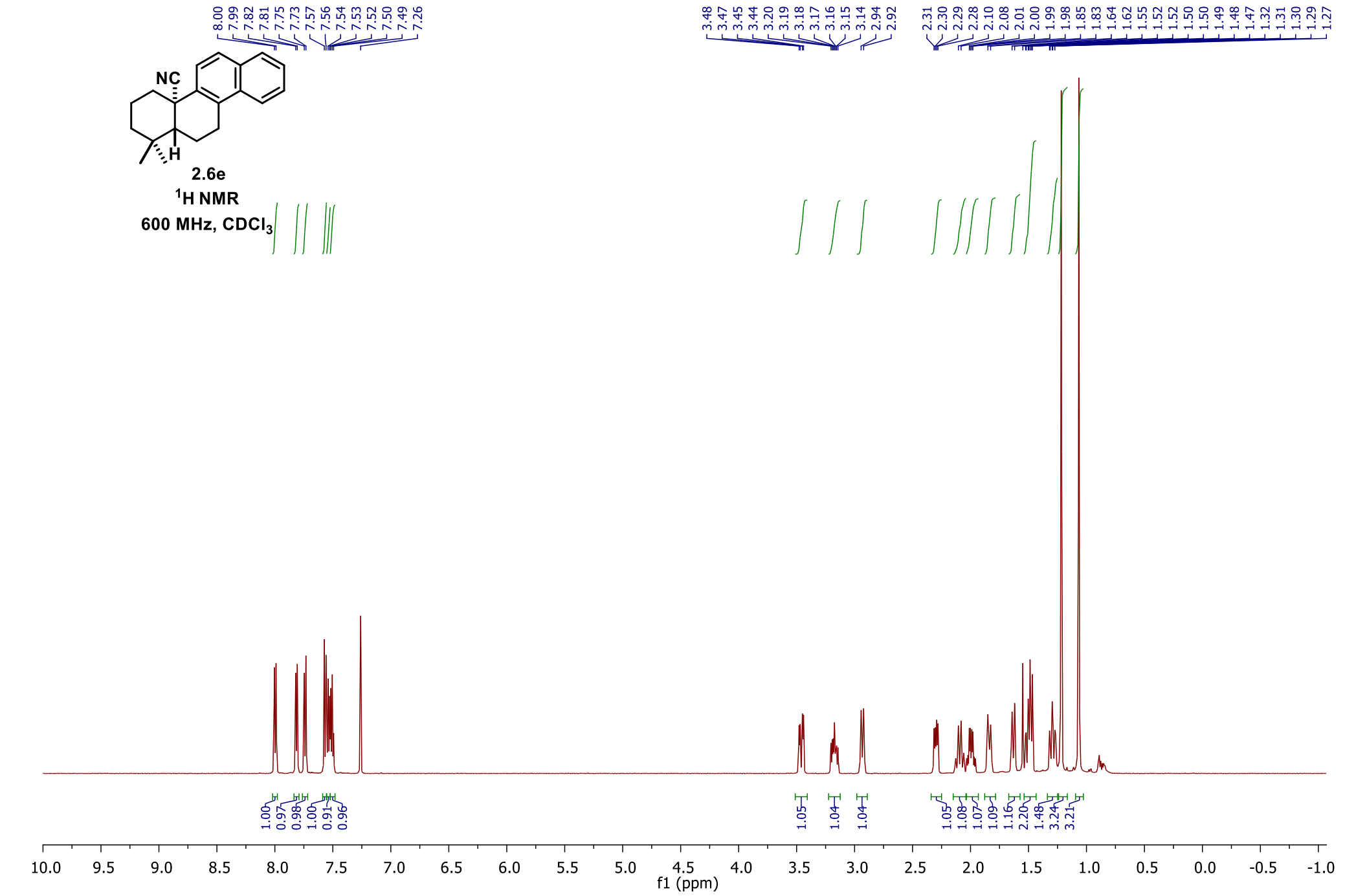
8.00
7.99
7.82
7.81
7.75
7.73
7.57
7.56
7.54
7.53
7.52
7.50
7.49
7.26
3.48
3.47
3.45
3.44
3.20
3.19
3.18
3.17
3.16
3.15
3.14
2.94
2.92
2.31
2.30
2.29
2.28
2.10
2.08
2.01
2.00
1.99
1.98
1.85
1.83
1.64
1.62
1.55
1.52
1.52
1.50
1.50
1.49
1.48
1.47
1.32
1.31
1.30
1.29
1.27
NC
H
2.6e
1H NMR
600 MHz, CDCl3
1.00
0.97
0.98
1.00
0.91
0.96
1.05
1.04
1.04
1.05
1.08
1.07
1.09
1.16
2.20
1.48
3.24
3.21
10.0
9.5
9.0
8.5
8.0
7.5
7.0
6.5
6.0
5.5
5.0
4.5
4.0
3.5
3.0
2.5
2.0
1.5
1.0
0.5
0.0
-0.5
-1.0
f1 (ppm)

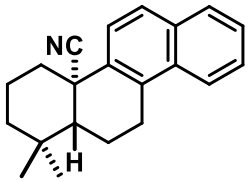

2.6e

^{13}C NMR

151 MHz, $CDCl_3$

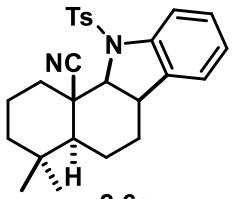

2.6g

^{1}H NMR

600 MHz, $CDCl_3$

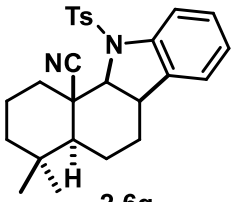

2.6g

^{13}C NMR

151 MHz, $CDCl_3$

144.21
142.88
135.93
135.83
129.76
128.53
127.05
126.28
122.01
121.21
120.26
77.37
77.16
76.95
72.24
49.67
43.07
41.15
39.52
37.14
33.45
32.30
24.37
21.70
20.58
20.11
18.91

220 210 200 190 180 170 160 150 140 130 120 110 100 90 80 70 60 50 40 30 20 10 0

f1 (ppm)

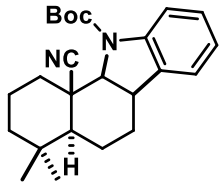

(mixture of rotamers)

2.6f
^{1}H NMR
600 MHz, $CDCl_3$

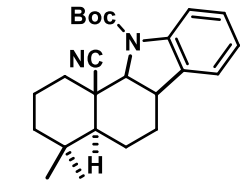

(mixture of rotamers)

2.6f

^{13}C NMR

151 MHz, $CDCl_3$

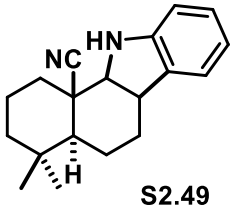

S2.49
^{1}H NMR
600 MHz, $CDCl_3$

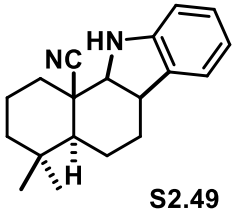

S2.49
^{13}C NMR
151 MHz, $CDCl_3$

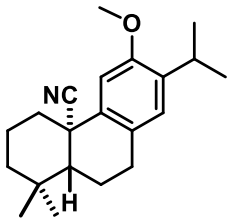

2.6h
^{1}H NMR
600 MHz, $CDCl_3$

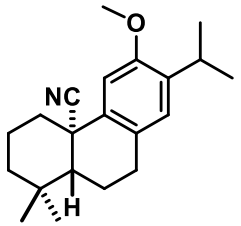

2.6h
^{13}C NMR
151 MHz, $CDCl_3$

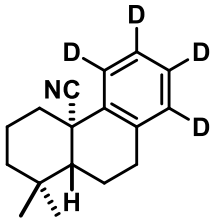

2.29
^{1}H NMR
600 MHz, $CDCl_3$

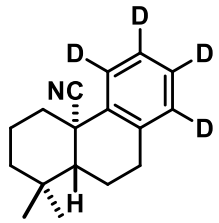

2.29
^{13}C DEPTQ
151 MHz, $CDCl_3$

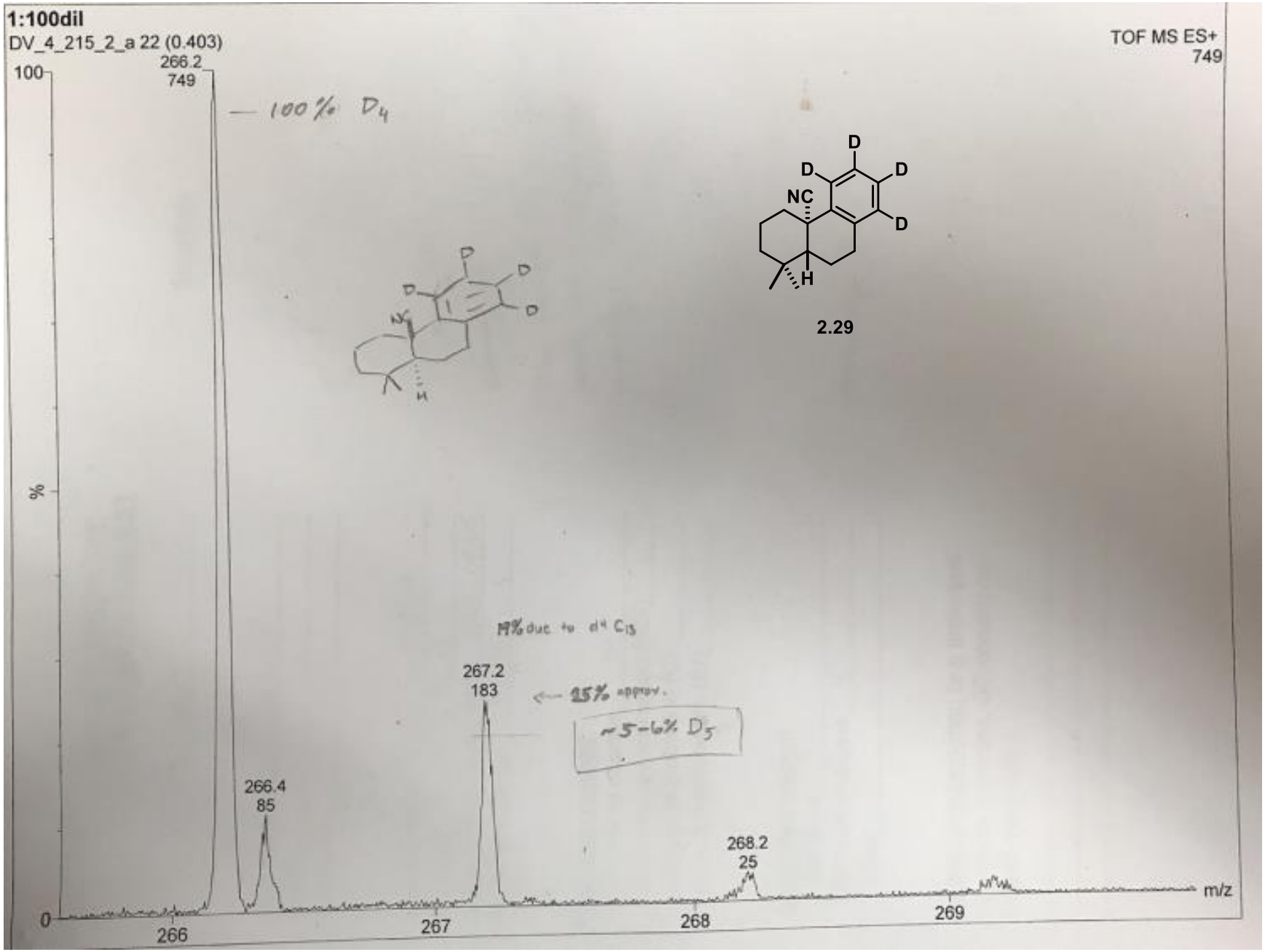
1:100dil
DV_4_215_2_a 22 (0.403)
TOF MS ES+
749
100
%
0
266.2
749
— 100% D4
266.4
85
267.2
183
~5-6% D5
268.2
25
266
267
268
269
m/z
D
D
D
D
NC
H
2.29

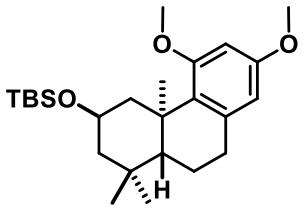

2.8a
^{1}H NMR
600 MHz, $CDCl_3$

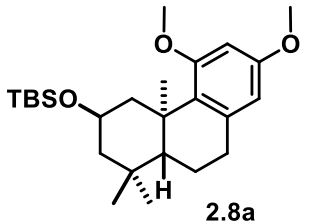

2.8a

^{13}C NMR

151 MHz, $CDCl_3$

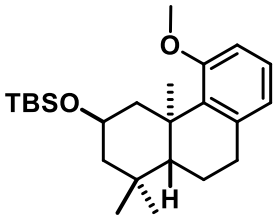

2.8b(*o*)
^{1}H NMR
600 MHz, $CDCl_3$

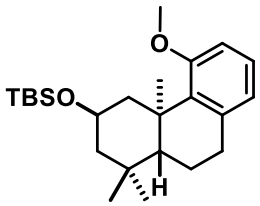

2.8b(*o*)
^{13}C NMR
151 MHz, $CDCl_3$

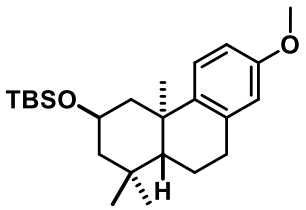

2.8b(*p*)
^{1}H NMR
600 MHz, $CDCl_3$

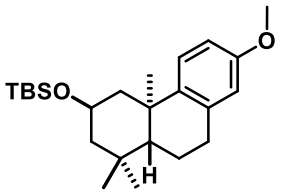

8b(*p*)
^{13}C NMR
151 MHz, $CDCl_3$

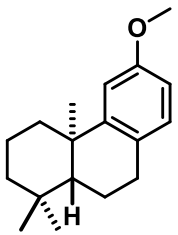

2.8d

^{1}H NMR

600 MHz, $CDCl_3$

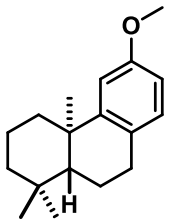

2.8d
^{13}C NMR
151 MHz, $CDCl_3$

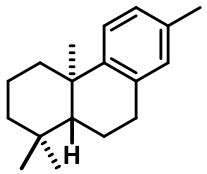

2.8c

^{1}H NMR

500 MHz, $CDCl_3$

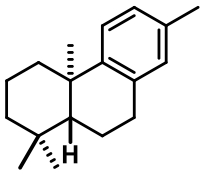

2.8c
^{13}C NMR
151 MHz, $CDCl_3$

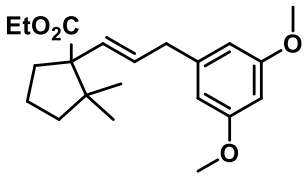

2.16
^{1}H NMR
500 MHz, $CDCl_3$

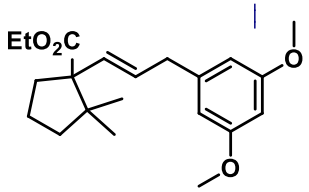

2.16
^{13}C NMR
126 MHz, $CDCl_3$

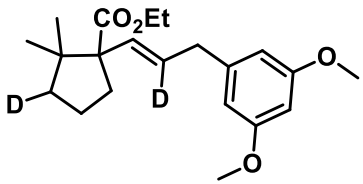

2.16-d_2 (~38% d_2)
^{1}H NMR
600 MHz, $CDCl_3$

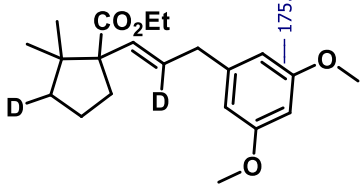

2.16-d_2 (~38% d_2)
^{1}H NMR
151 MHz, $CDCl_3$

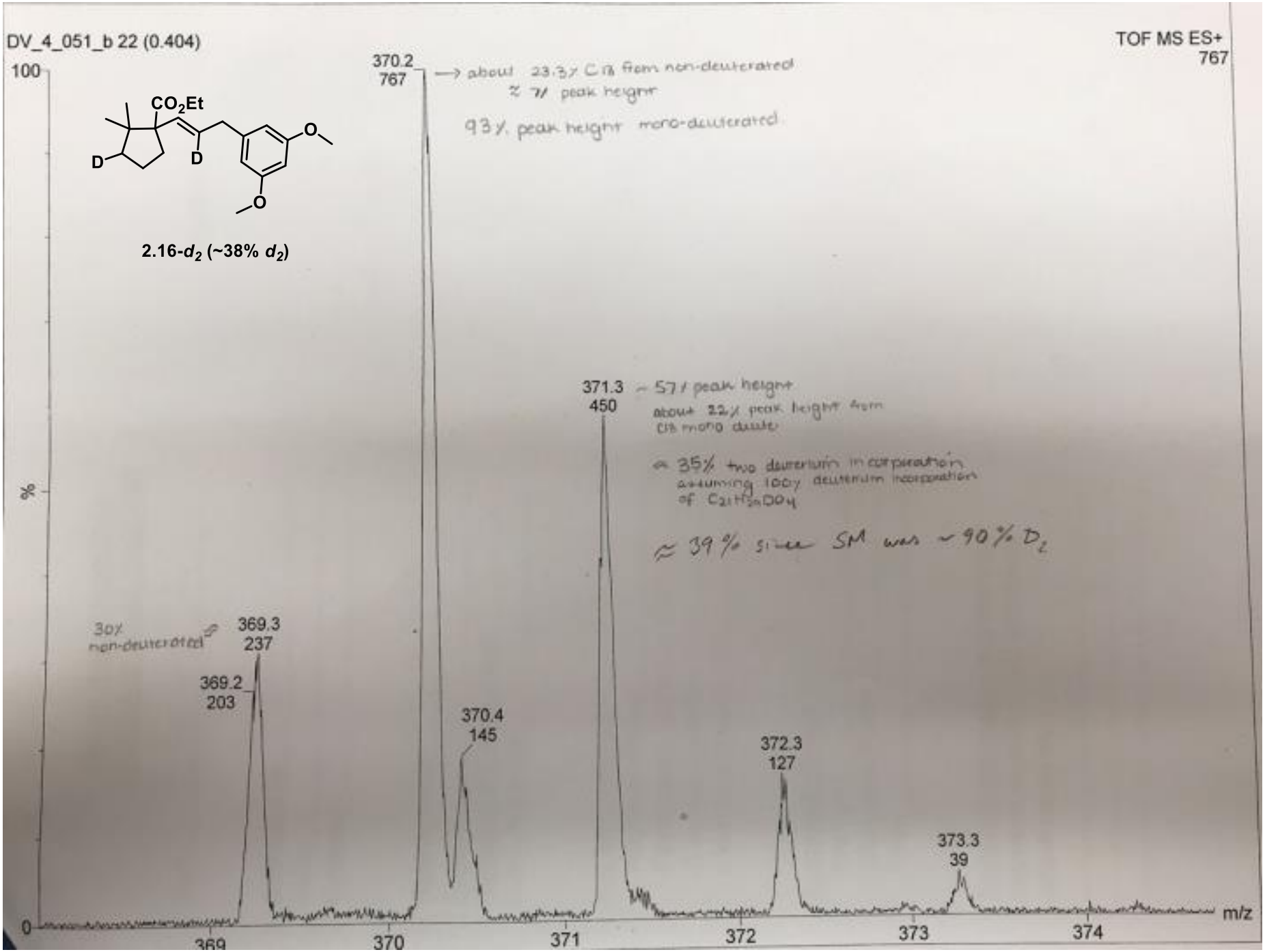
DV_4_051_b 22 (0.404)
TOF MS ES+
767
100
%
0
CO2Et
D
D
O
O
2.16-d2 (~38% d2)
370.2
767
→ about 23.3% C13 from non-deuterated
≈ 7% peak height
93% peak height mono-deuterated
371.3
450
~ 57% peak height
about 22% peak height from C13 mono deute
≈ 35% two deuterium incorporation assuming 100% deuterium incorporation of C21H28D04
≈ 39% since SM was ~90% D2
30% non-deuterated
369.3
237
369.2
203
370.4
145
372.3
127
373.3
39
m/z
369
370
371
372
373
374

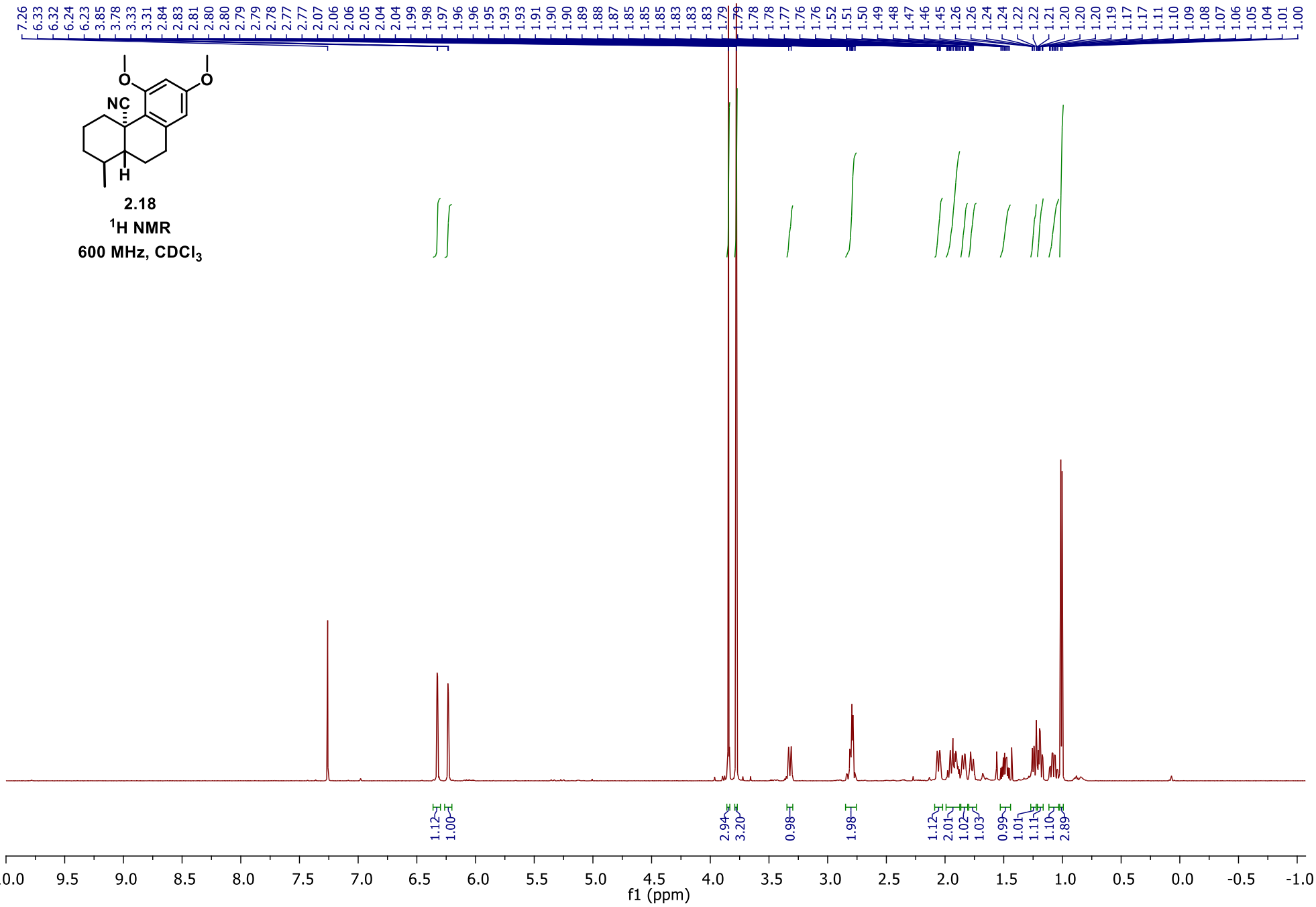
7.26 6.33 6.32 6.24 6.23 3.85 3.78 3.33 3.31 2.84 2.83 2.81 2.80 2.80 2.79 2.79 2.78 2.77 2.77 2.07 2.06 2.06 2.05 2.04 2.04 1.99 1.98 1.97 1.96 1.96 1.95 1.93 1.93 1.91 1.90 1.90 1.89 1.88 1.87 1.85 1.85 1.85 1.83 1.83 1.83 1.79 1.79 1.78 1.78 1.77 1.76 1.76 1.52 1.51 1.50 1.49 1.48 1.47 1.46 1.45 1.26 1.26 1.24 1.24 1.22 1.22 1.21 1.20 1.20 1.20 1.19 1.17 1.17 1.11 1.10 1.09 1.08 1.07 1.06 1.05 1.04 1.01 1.00
O
O
NC
H
2.18
1H NMR
600 MHz, CDCl3
1.12 1.00 2.94 3.20 0.98 1.98 1.12 2.01 1.02 1.03 0.99 1.01 1.11 1.10 2.89
10.0 9.5 9.0 8.5 8.0 7.5 7.0 6.5 6.0 5.5 5.0 4.5 4.0 3.5 3.0 2.5 2.0 1.5 1.0 0.5 0.0 -0.5 -1.0
f1 (ppm)

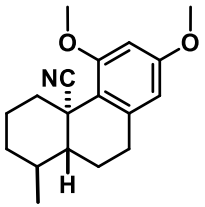

2.18
^{13}C NMR
151 MHz, $CDCl_3$

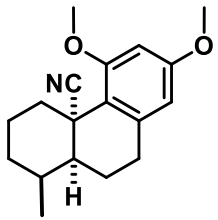

2.19
^{1}H NMR
600 MHz, $CDCl_3$

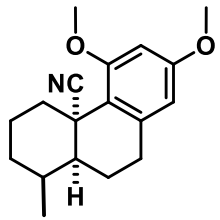

2.19

^{13}C NMR

151 MHz, $CDCl_3$

159.75
158.81
138.36
124.32
118.33
105.30
97.86
77.37
77.16
76.95
55.81
55.40
45.29
40.13
31.88
30.92
30.28
28.50
23.64
19.83
16.91

230 220 210 200 190 180 170 160 150 140 130 120 110 100 90 80 70 60 50 40 30 20 10 0

f1 (ppm)

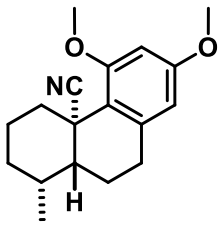

2.20
^{1}H NMR
600 MHz, $CDCl_3$

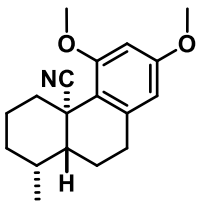

2.20
^{13}C NMR
151 MHz, $CDCl_3$

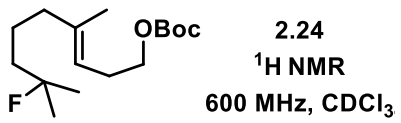

2.24
^{1}H NMR
600 MHz, $CDCl_3$

(contains ~30% of regioisomeric impurities)

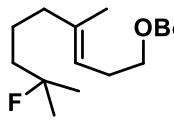

2.24
^{13}C NMR
151 MHz, $CDCl_3$

(contains ~30% of regioisomeric impurities)

153.76
142.35
118.55
96.27
95.18
82.03
63.82
41.05
40.90
39.71
27.94
26.87
26.70
21.93
21.90
16.44

230 220 210 200 190 180 170 160 150 140 130 120 110 100 90 80 70 60 50 40 30 20 10 0
f1 (ppm)

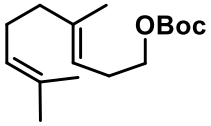

2.25

^{1}H NMR

600 MHz, $CDCl_3$

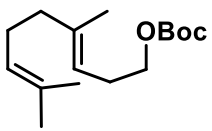

2.25

^{13}C NMR

151 MHz, $CDCl_3$

153.79
142.69
131.98
123.90
118.17
82.00
77.37
77.16
76.95
63.92
39.66
27.95
26.39
25.82
17.82
16.65

230 220 210 200 190 180 170 160 150 140 130 120 110 100 90 80 70 60 50 40 30 20 10 0

f1 (ppm)

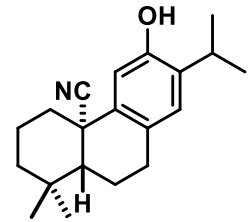

S2.50
^{1}H NMR
600 MHz, $CDCl_3$

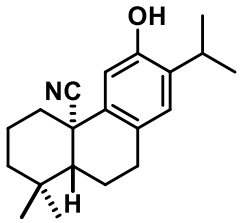

S2.50
^{13}C DEPT
151 MHz, $CDCl_3$

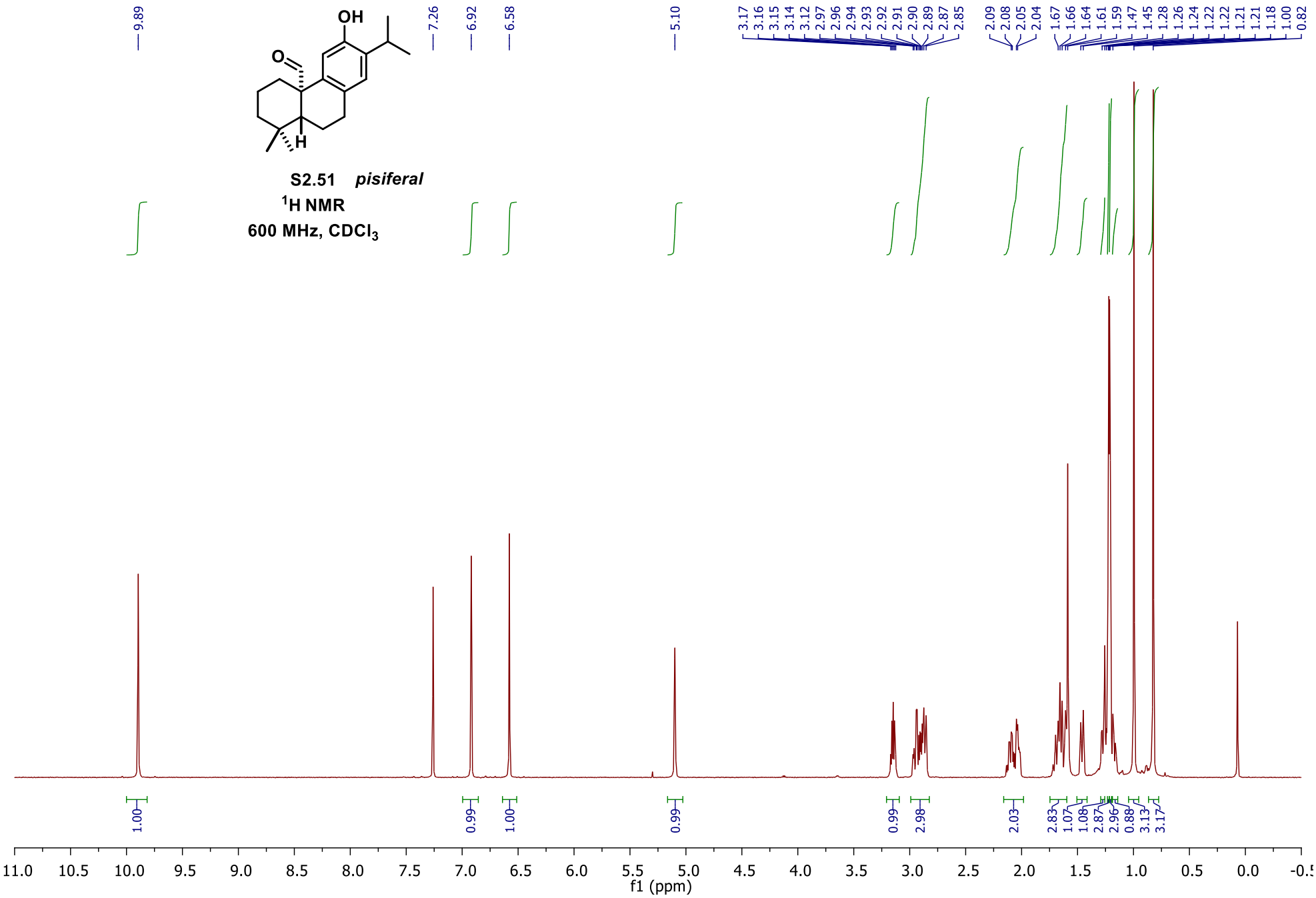
9.89
7.26
6.92
6.58
5.10
3.17
3.16
3.15
3.14
3.12
2.97
2.96
2.94
2.93
2.92
2.91
2.90
2.89
2.87
2.85
2.09
2.08
2.05
2.04
1.67
1.66
1.64
1.61
1.59
1.47
1.45
1.28
1.26
1.24
1.22
1.22
1.21
1.21
1.18
1.00
0.82
OH
O
H
S2.51 pisiferal
1H NMR
600 MHz, CDCl3
1.00
0.99
1.00
0.99
0.99
2.98
2.03
2.83
1.07
1.08
2.87
2.96
0.88
3.13
3.17
11.0
10.5
10.0
9.5
9.0
8.5
8.0
7.5
7.0
6.5
6.0
5.5
5.0
4.5
4.0
3.5
3.0
2.5
2.0
1.5
1.0
0.5
0.0
f1 (ppm)

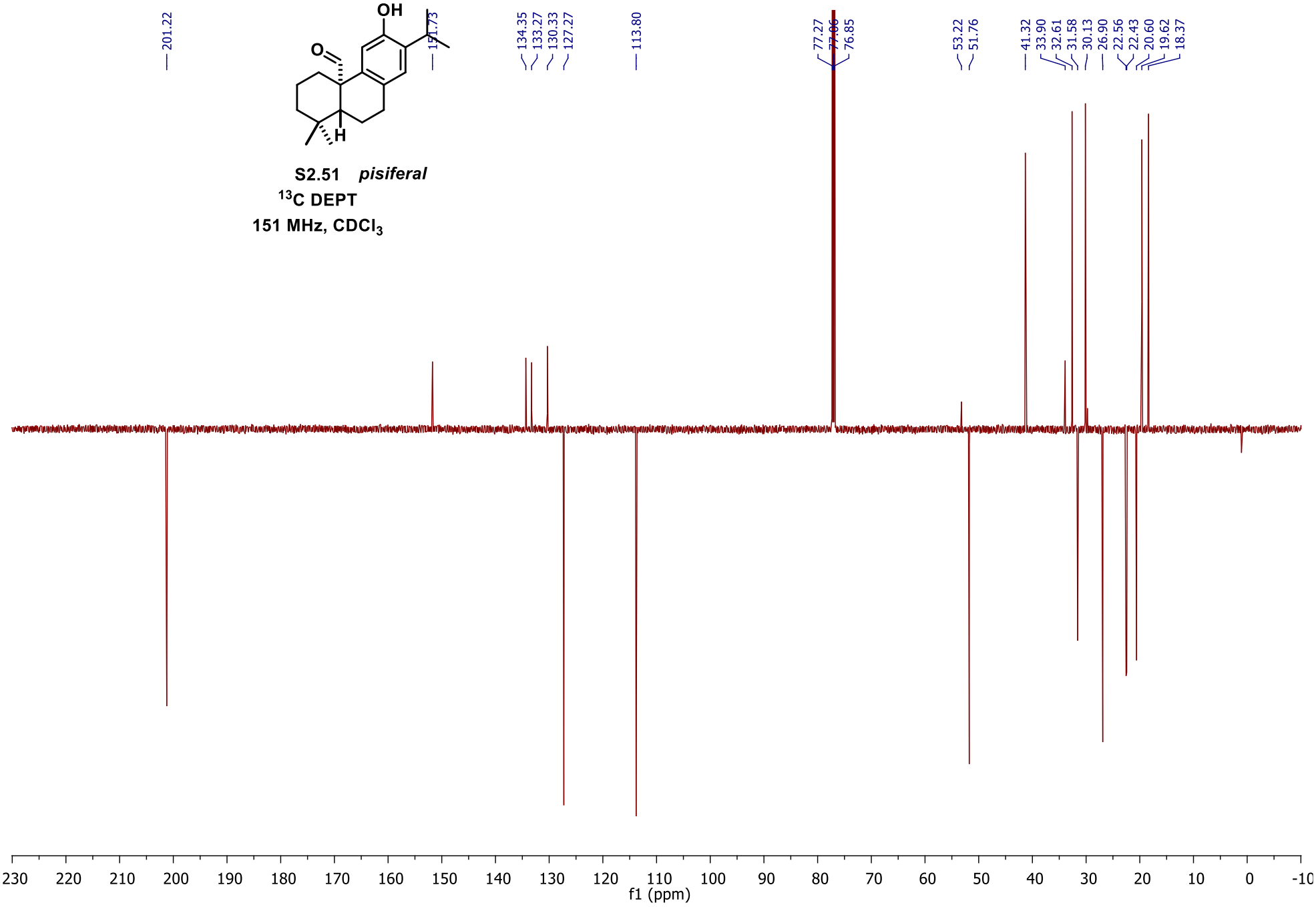
201.22
151.73
134.35
133.27
130.33
127.27
113.80
77.27
77.06
76.85
53.22
51.76
41.32
33.90
32.61
31.58
30.13
26.90
22.56
22.43
20.60
19.62
18.37
OH
O
H
S2.51 pisiferal
13C DEPT
151 MHz, CDCl3
230 220 210 200 190 180 170 160 150 140 130 120 110 100 90 80 70 60 50 40 30 20 10 0 -10
f1 (ppm)

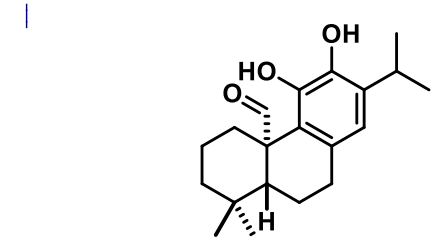

carnosaldehyde

^{1}H NMR

600 MHz, $CDCl_3$

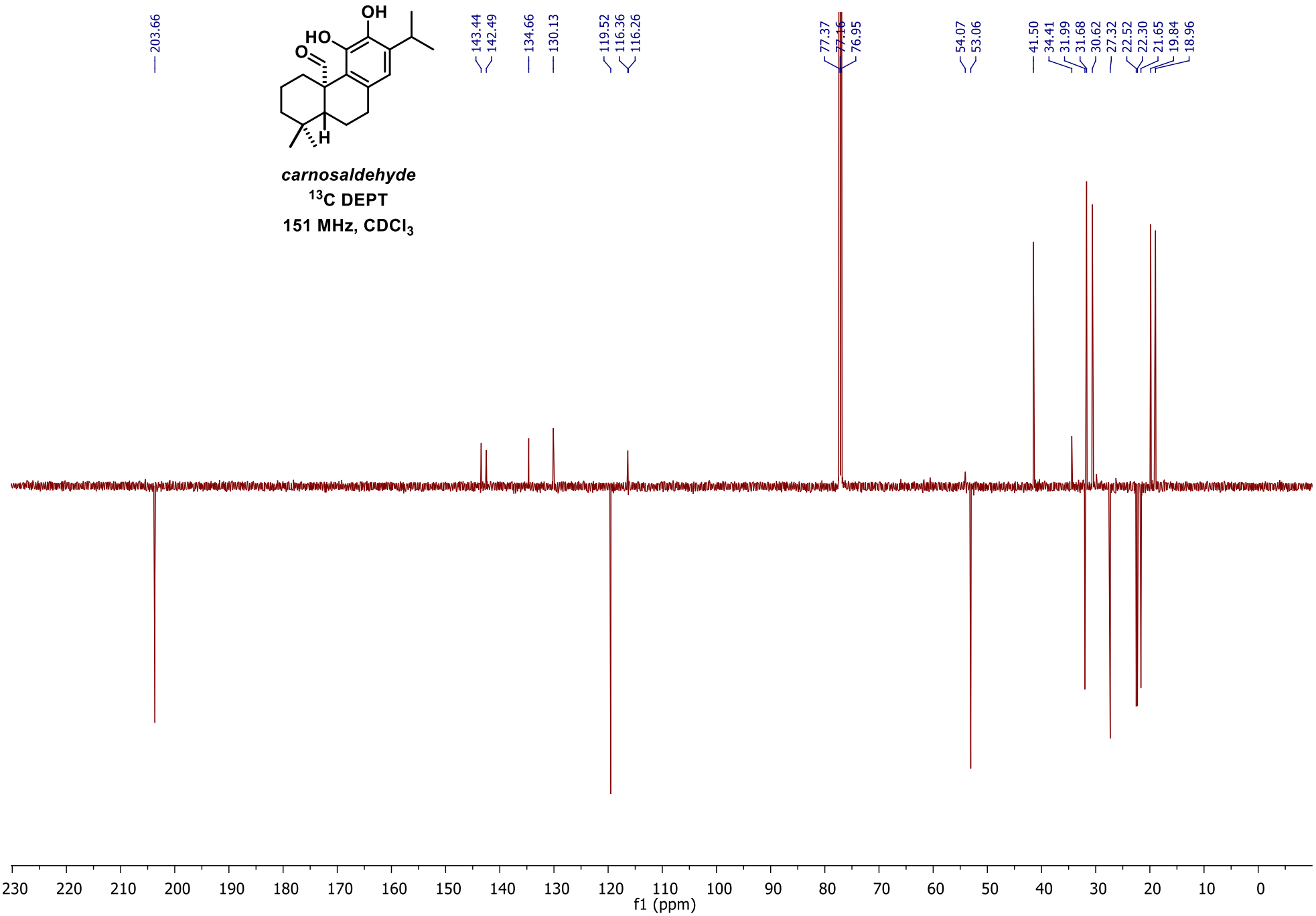
203.66
143.44
142.49
134.66
130.13
119.52
116.36
116.26
77.37
77.16
76.95
54.07
53.06
41.50
34.41
31.99
31.68
30.62
27.32
22.52
22.30
21.65
19.84
18.96
OH
HO
O
H
carnosaldehyde
13C DEPT
151 MHz, CDCl3
230 220 210 200 190 180 170 160 150 140 130 120 110 100 90 80 70 60 50 40 30 20 10 0
f1 (ppm)

^{1}H COSY

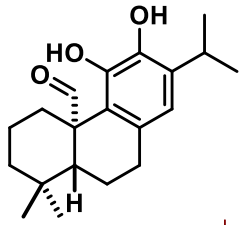

carnosaldehyde

^{1}H COSY

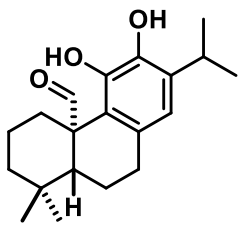

carnosaldehyde

HSQC

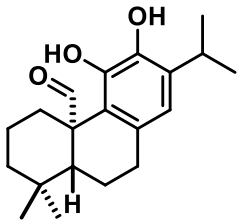

carnosaldehyde

HSQC

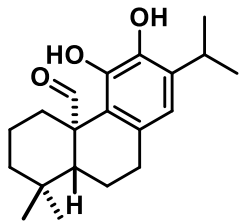

carnosaldehyde

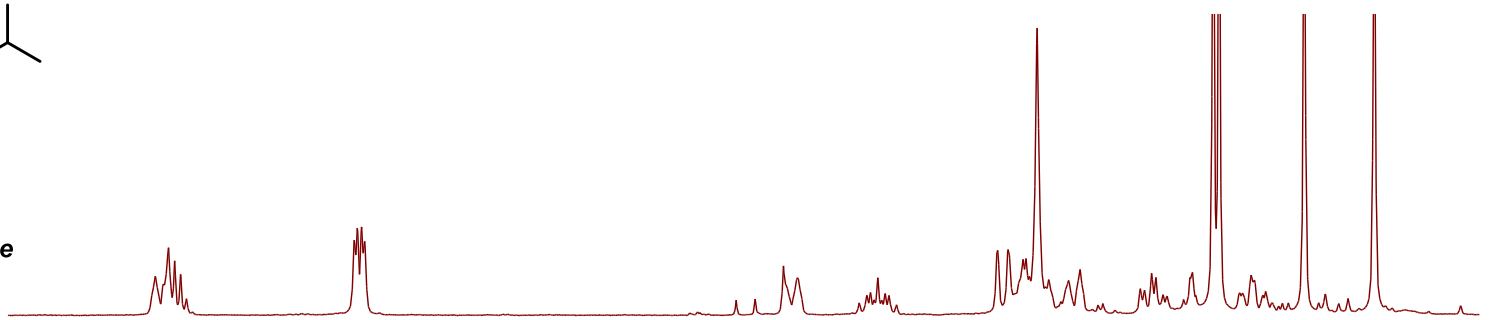

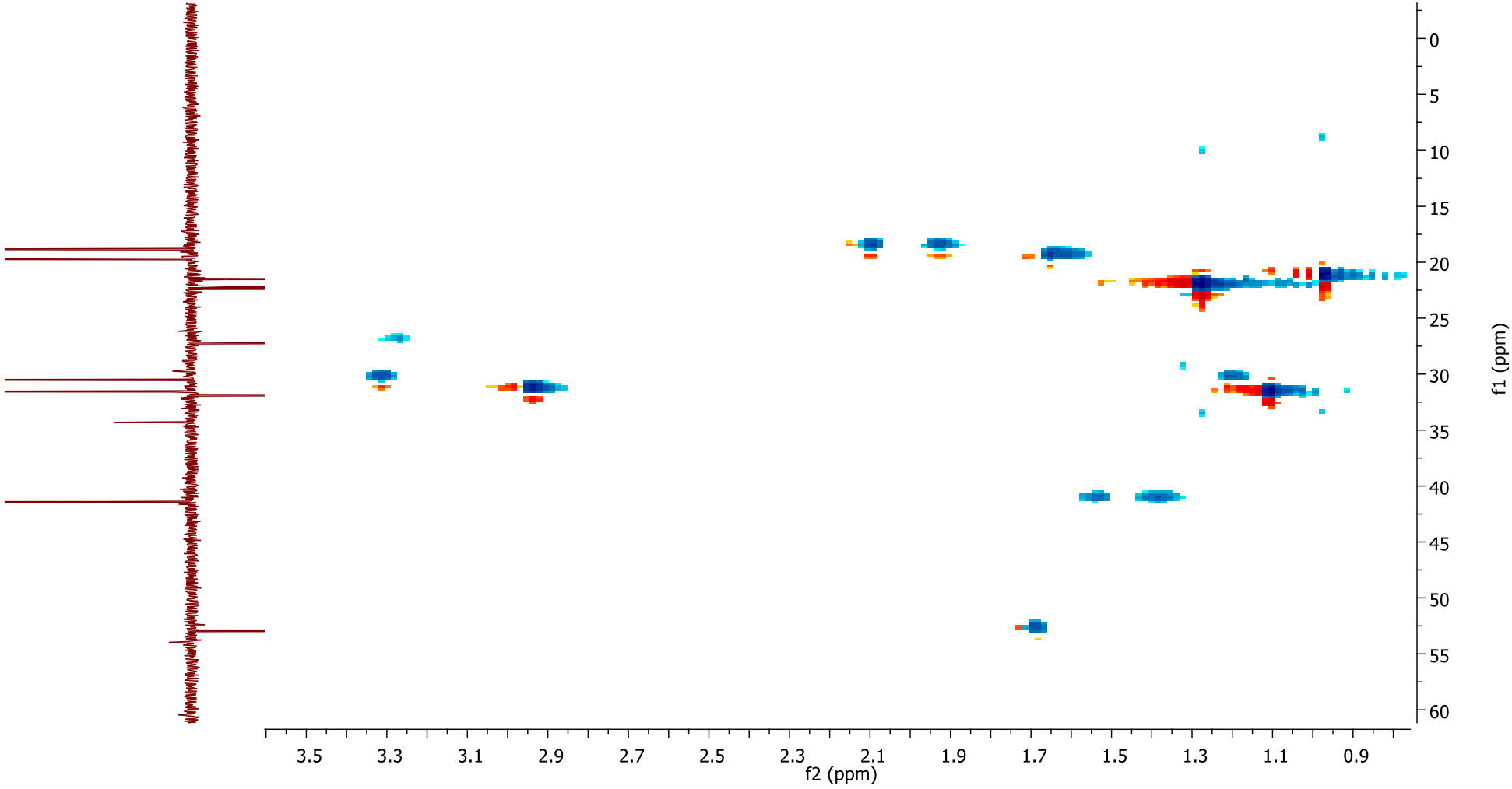

^{1}H NOESY

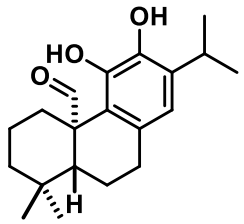

carnosaldehyde

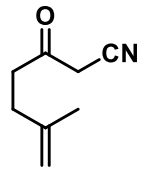

S3.2
^{1}H NMR
500 MHz, $CDCl_3$

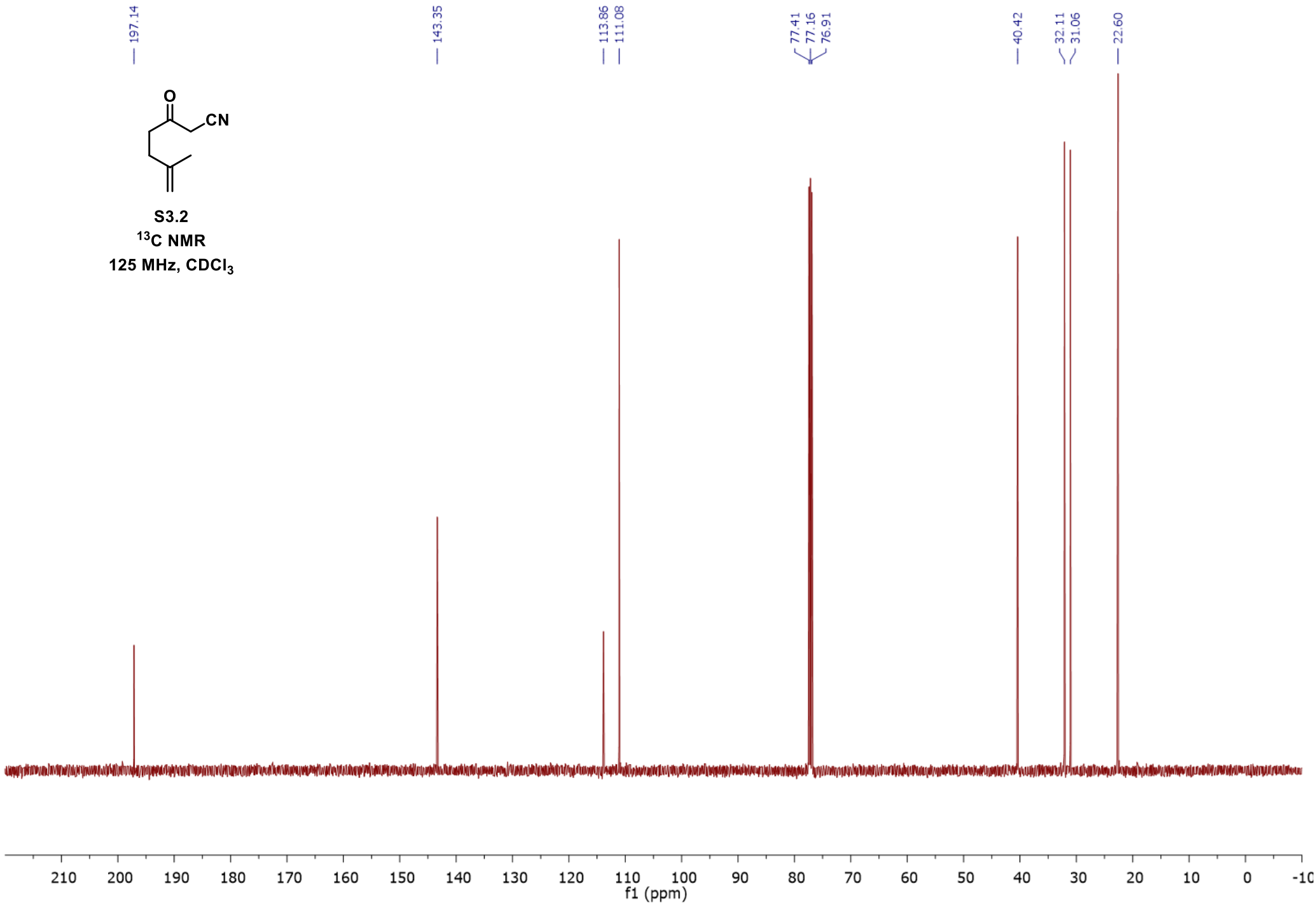
197.14
143.35
113.86
111.08
77.41
77.16
76.91
40.42
32.11
31.06
22.60
O
CN
S3.2
13C NMR
125 MHz, CDCl3
210
200
190
180
170
160
150
140
130
120
110
100
90
80
70
60
50
40
30
20
10
0
-10
f1 (ppm)

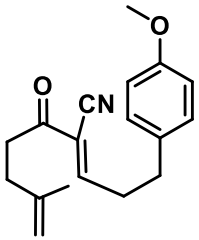

S3.4
^{1}H NMR
500 MHz, $CDCl_3$

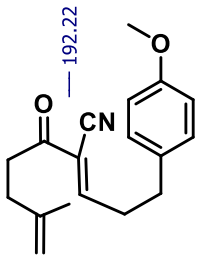

S3.4
^{13}C DEPTQ
150 MHz, $CDCl_3$

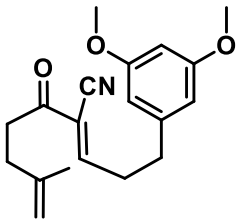

S3.6
^{1}H NMR
500 MHz, $CDCl_3$

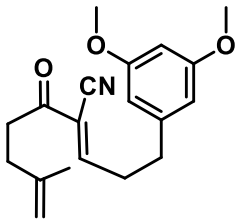

S3.6
^{13}C NMR
125 MHz, $CDCl_3$

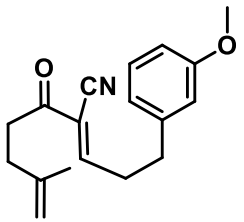

S3.8
^{1}H NMR
600 MHz, $CDCl_3$

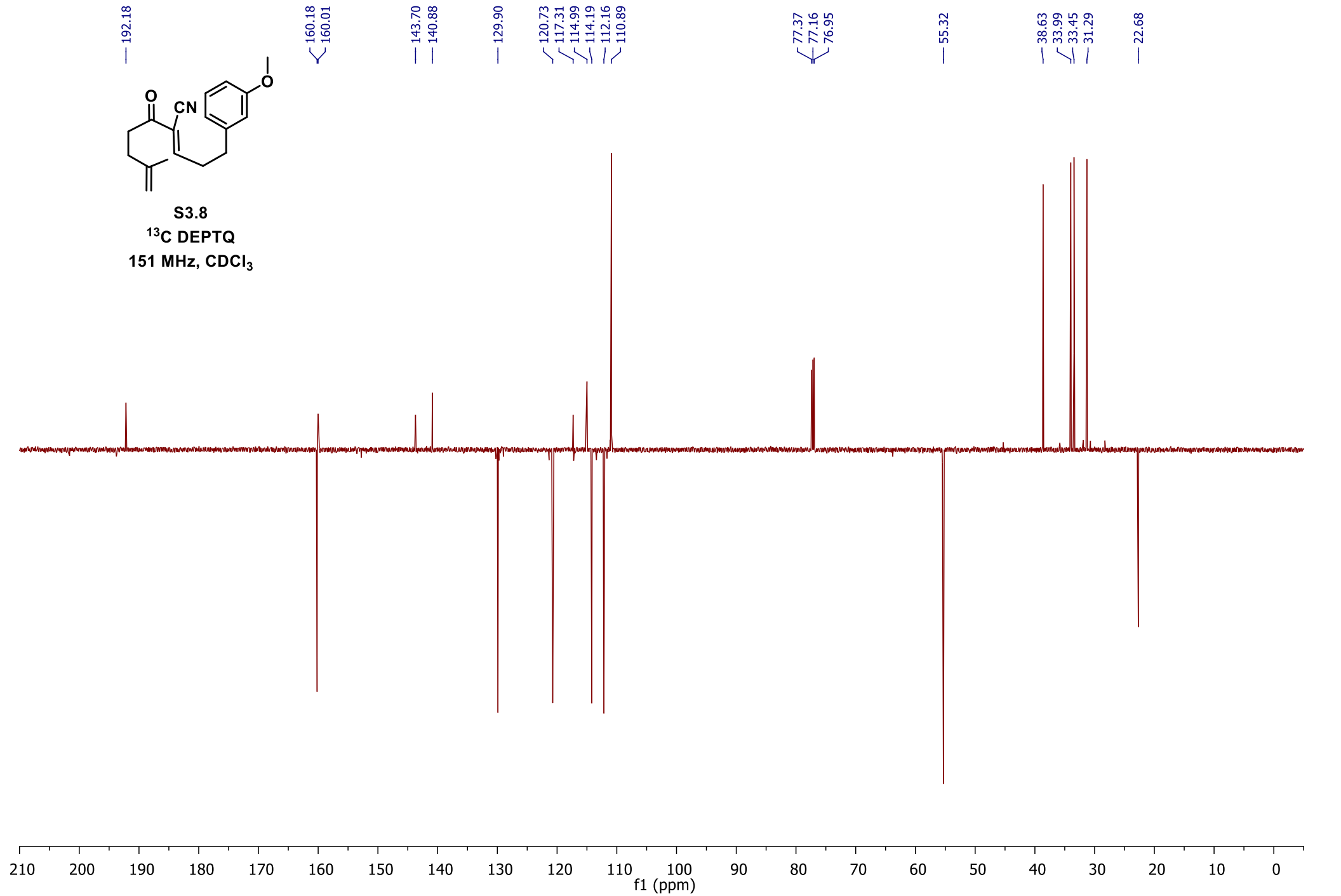
192.18
160.18
160.01
143.70
140.88
129.90
120.73
117.31
114.99
114.19
112.16
110.89
77.37
77.16
76.95
55.32
38.63
33.99
33.45
31.29
22.68
O
CN
O
S3.8
13C DEPTQ
151 MHz, CDCl3
210
200
190
180
170
160
150
140
130
120
110
100
90
80
70
60
50
40
30
20
10
0
f1 (ppm)

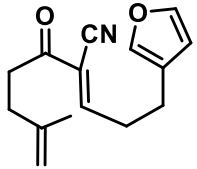

S3.10
^{1}H NMR
600 MHz, $CDCl_3$

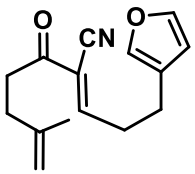

S3.10
^{13}C NMR
151 MHz, $CDCl_3$

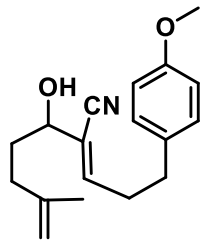

3.36a
^{1}H NMR
600 MHz, $CDCl_3$

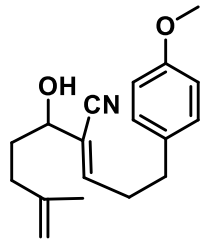

3.36a
^{13}C DEPTQ
150 MHz, $CDCl_3$

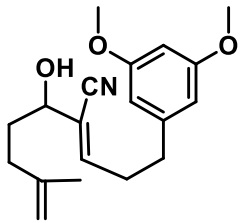

3.28a
^{1}H NMR
500 MHz, $CDCl_3$

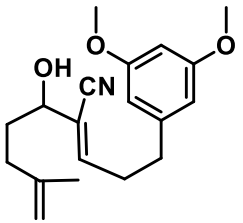

3.28a
^{13}C NMR
125 MHz, $CDCl_3$

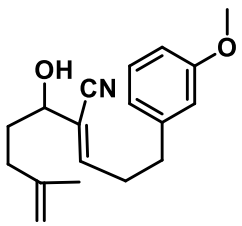

3.31
^{1}H NMR
600 MHz, $CDCl_3$

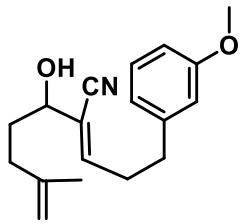

3.31
^{13}C NMR
151 MHz, $CDCl_3$

159.89
146.99
144.71
141.63
129.71
120.90
119.63
115.91
114.30
111.86
111.04
77.37
77.16
76.95
72.43
55.31
34.65
33.72
33.45
32.61
22.42

230 220 210 200 190 180 170 160 150 140 130 120 110 100 90 80 70 60 50 40 30 20 10 0
f1 (ppm)

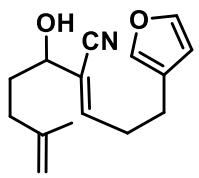

S3.87
^{1}H NMR
500 MHz, $CDCl_3$

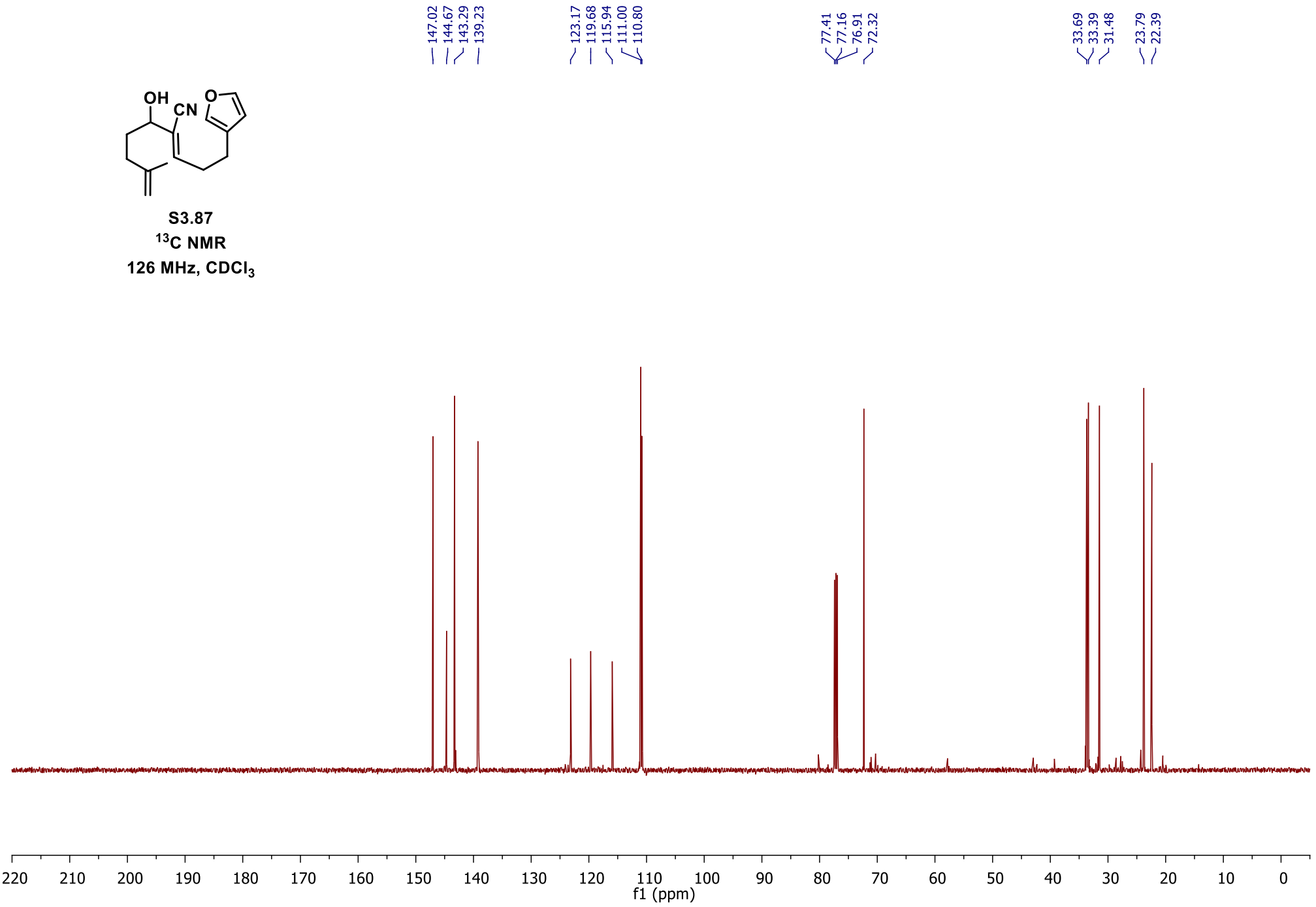

S3.87
^{13}C NMR
126 MHz, $CDCl_3$

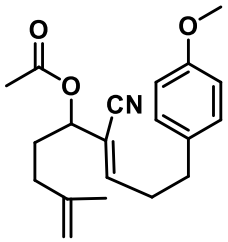

3.36c
^{1}H NMR
600 MHz, $CDCl_3$

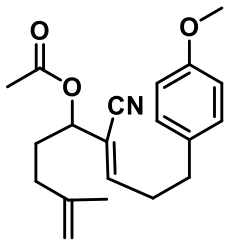

3.36c
^{13}C DEPTQ
150 MHz, $CDCl_3$

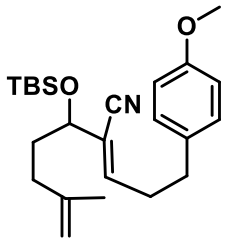

3.36b
^{1}H NMR
600 MHz, $CDCl_3$

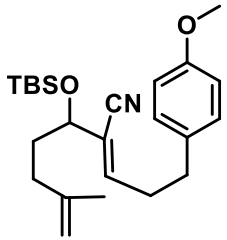

3.36b
^{13}C DEPTQ
150 MHz, $CDCl_3$

158.30
145.96
145.07
132.18
129.46
120.14
116.28
114.12
110.37
77.37
77.16
76.95
72.75
55.40
35.19
33.84
32.92
32.84
25.85
22.64
18.22
-4.49
-4.82

220 210 200 190 180 170 160 150 140 130 120 110 100 90 80 70 60 50 40 30 20 10 0
f1 (ppm)

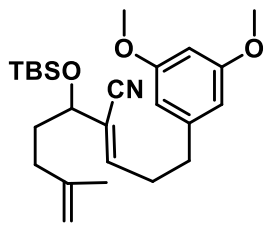

3.28b
^{1}H NMR
500 MHz, $CDCl_3$

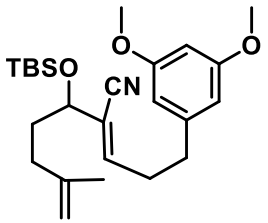

3.28b
^{13}C NMR
125 MHz, $CDCl_3$

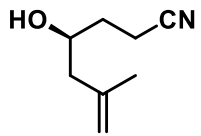

S3.11
^{1}H NMR
600 MHz, $CDCl_3$

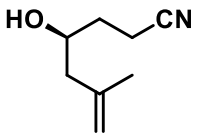

S3.11
^{13}C NMR
150 MHz, $CDCl_3$

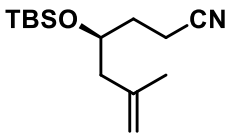

3.65
^{1}H NMR
500 MHz, $CDCl_3$

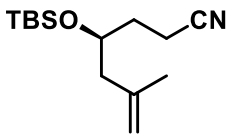

3.65
^{13}C NMR
125 MHz, $CDCl_3$

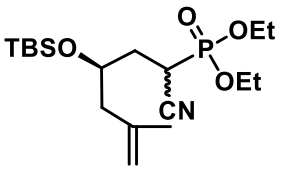

3.66

^{1}H NMR

500 MHz, $CDCl_3$

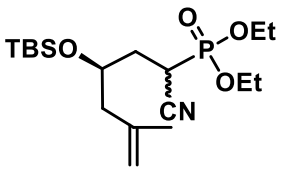

3.66
^{13}C NMR
125 MHz, $CDCl_3$

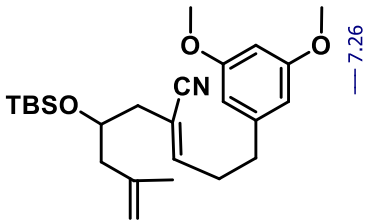

3.25b
^{1}H NMR
500 MHz, $CDCl_3$

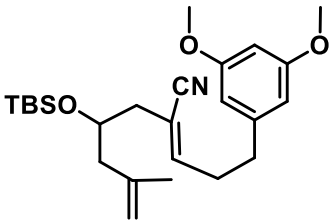

3.25b
^{13}C NMR
125 MHz, $CDCl_3$

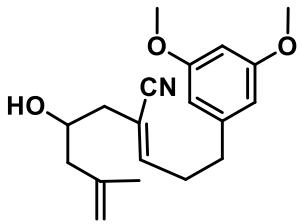

3.25a
^{1}H NMR
600 MHz, $CDCl_3$

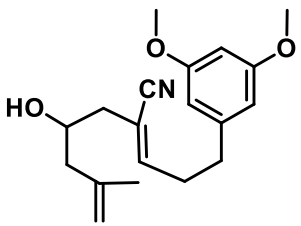

3.25a
^{13}C DEPTQ
150 MHz, $CDCl_3$

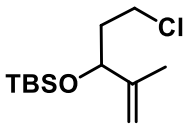

S3.13
^{1}H NMR
600 MHz, $CDCl_3$

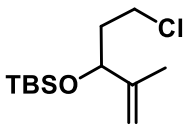

S3.13
^{13}C DEPTQ
150 MHz, $CDCl_3$

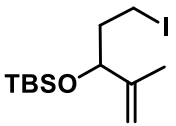

S3.14
^{1}H NMR
500 MHz, $CDCl_3$

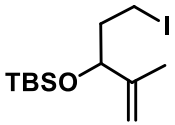

S3.14
^{13}C DEPTQ
150 MHz, $CDCl_3$

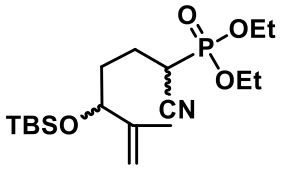

S3.15
^{1}H NMR
500 MHz, $CDCl_3$

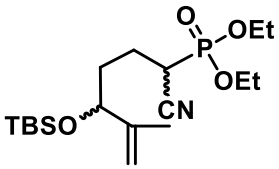

S3.15
^{13}C DEPTQ
150 MHz, $CDCl_3$

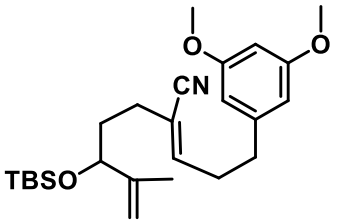

3.22d
^{1}H NMR
600 MHz, $CDCl_3$

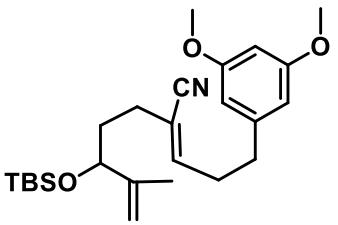

3.22d
^{13}C DEPTQ
150 MHz, $CDCl_3$

161.03
146.92
146.34
142.72
117.68
115.48
111.47
106.55
98.40
77.37
77.16
76.95
75.52
55.42
35.11
34.58
32.78
30.28
25.94
18.32
17.39
-4.63
-4.97

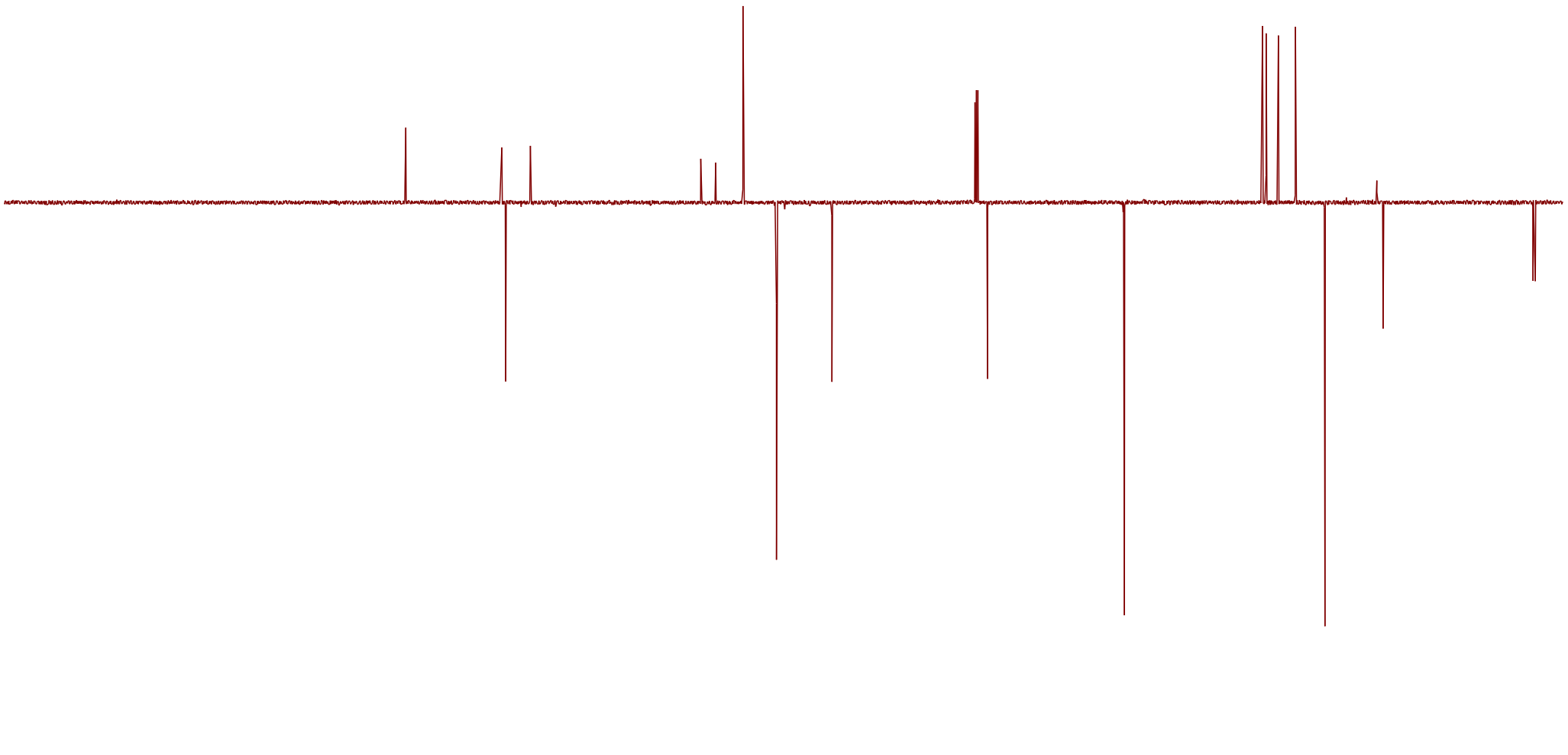

220 210 200 190 180 170 160 150 140 130 120 110 100 90 80 70 60 50 40 30 20 10 0
f1 (ppm)

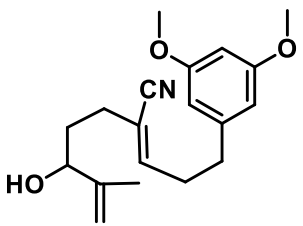

3.22a
^{1}H NMR
600 MHz, $CDCl_3$

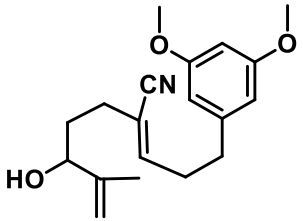

3.22a
^{13}C DEPTQ
150 MHz, $CDCl_3$

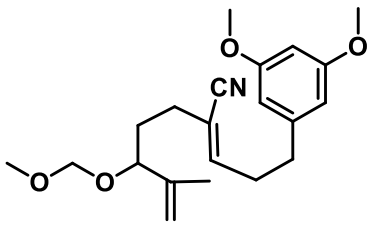

3.22c

^{1}H NMR

600 MHz, $CDCl_3$

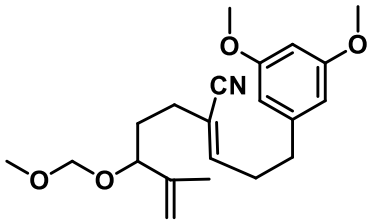

3.22c

^{13}C DEPTQ

150 MHz, $CDCl_3$

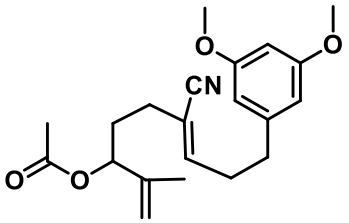

3.22b
^{1}H NMR
600 MHz, $CDCl_3$

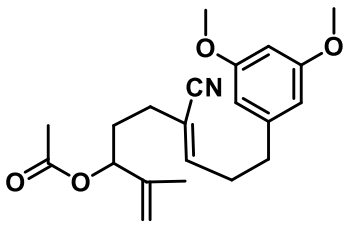

3.22b
^{13}C DEPTQ
150 MHz, $CDCl_3$

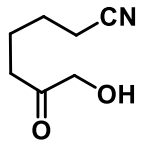

S3.17
^{1}H NMR
500 MHz, $CDCl_3$

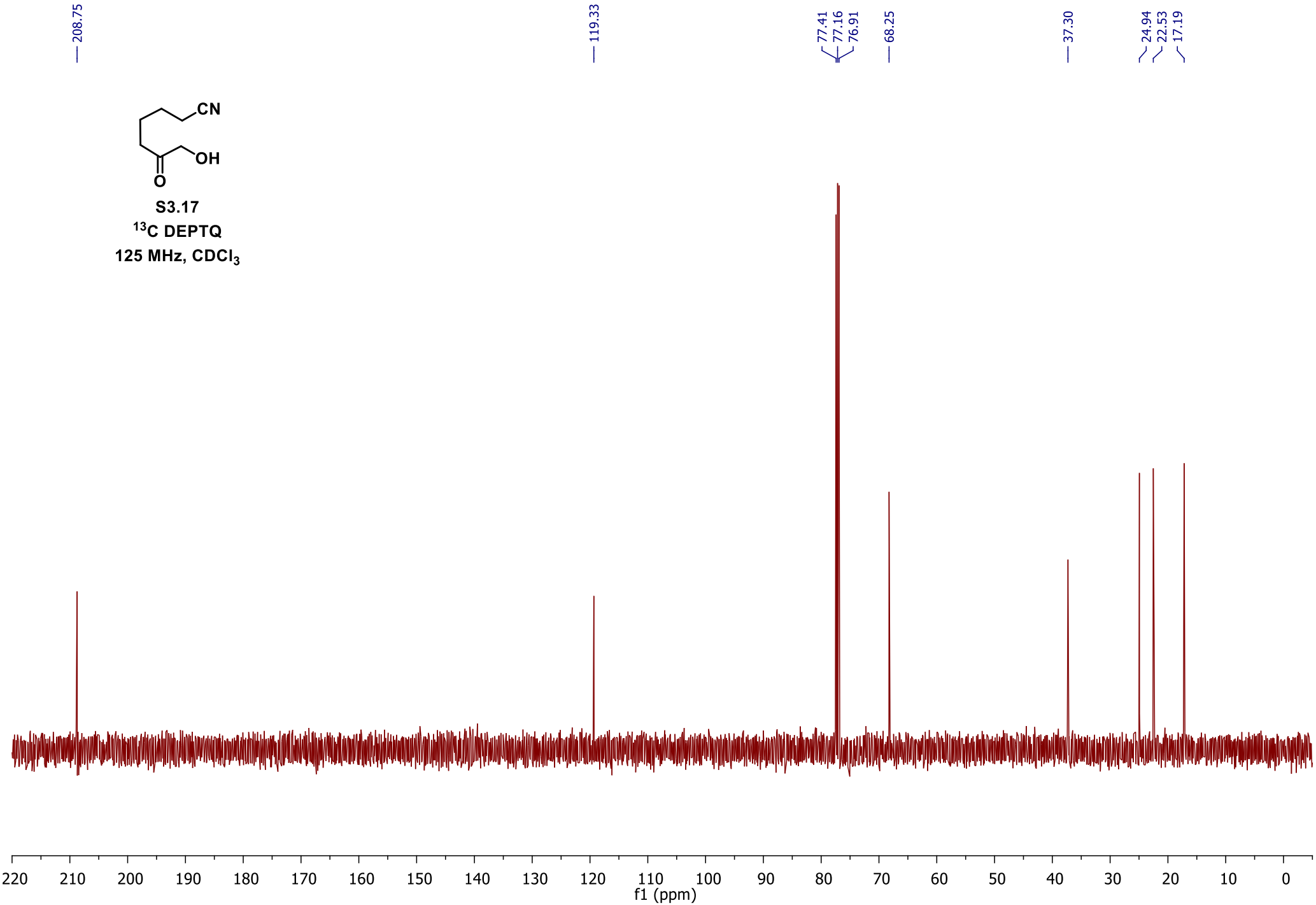
208.75
119.33
77.41
77.16
76.91
68.25
37.30
24.94
22.53
17.19
CN
OH
O
S3.17
13C DEPTQ
125 MHz, CDCl3
220
210
200
190
180
170
160
150
140
130
120
110
100
90
80
70
60
50
40
30
20
10
0
f1 (ppm)

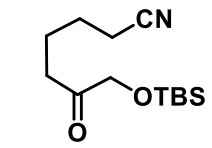

S3.18
^{1}H NMR
500 MHz, $CDCl_3$

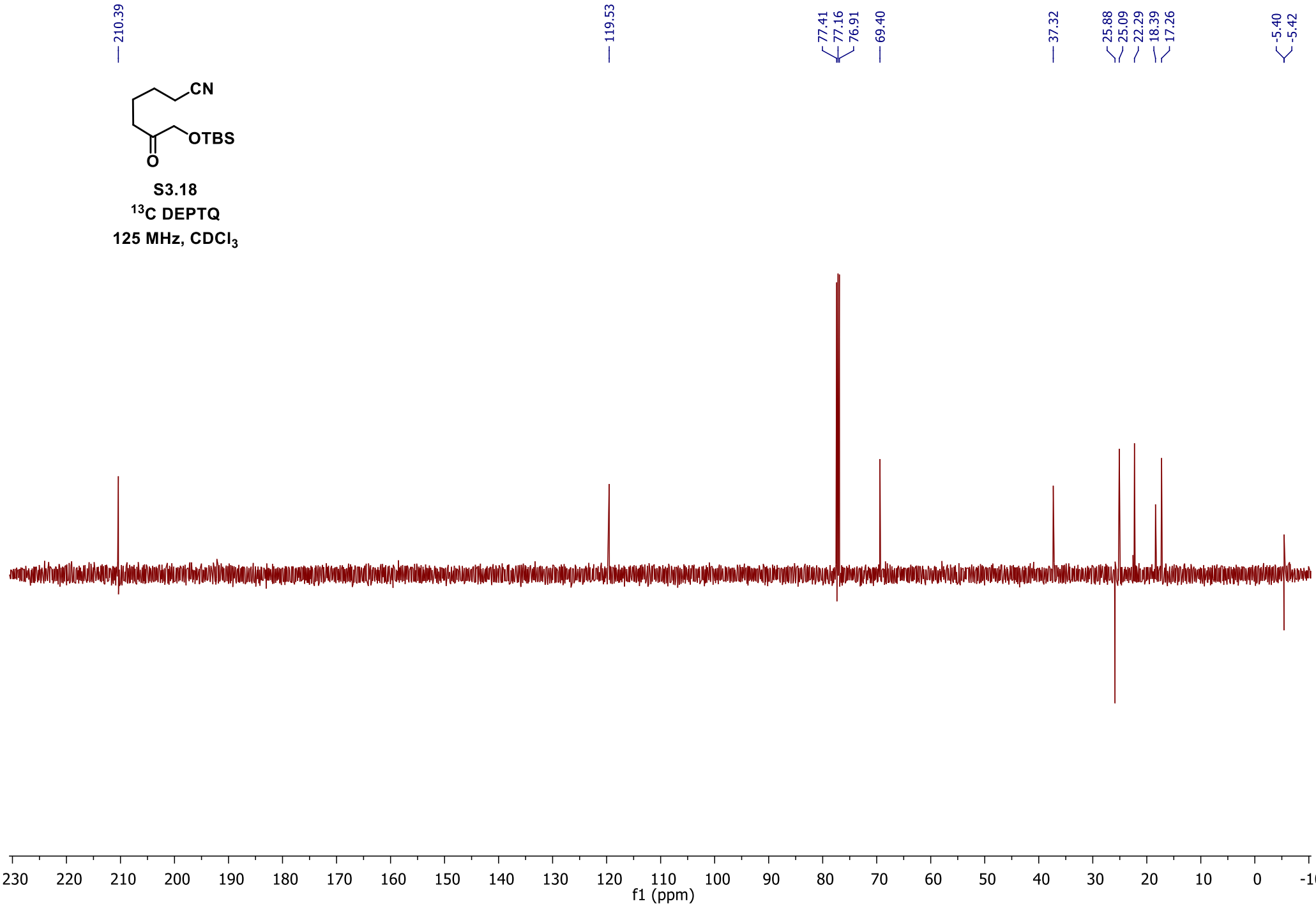
210.39
119.53
77.41
77.16
76.91
69.40
37.32
25.88
25.09
22.29
18.39
17.26
-5.40
-5.42
CN
OTBS
O
S3.18
13C DEPTQ
125 MHz, CDCl3
230 220 210 200 190 180 170 160 150 140 130 120 110 100 90 80 70 60 50 40 30 20 10 0 -10
f1 (ppm)

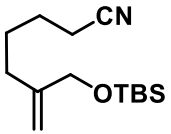

S3.19
^{1}H NMR
600 MHz, $CDCl_3$

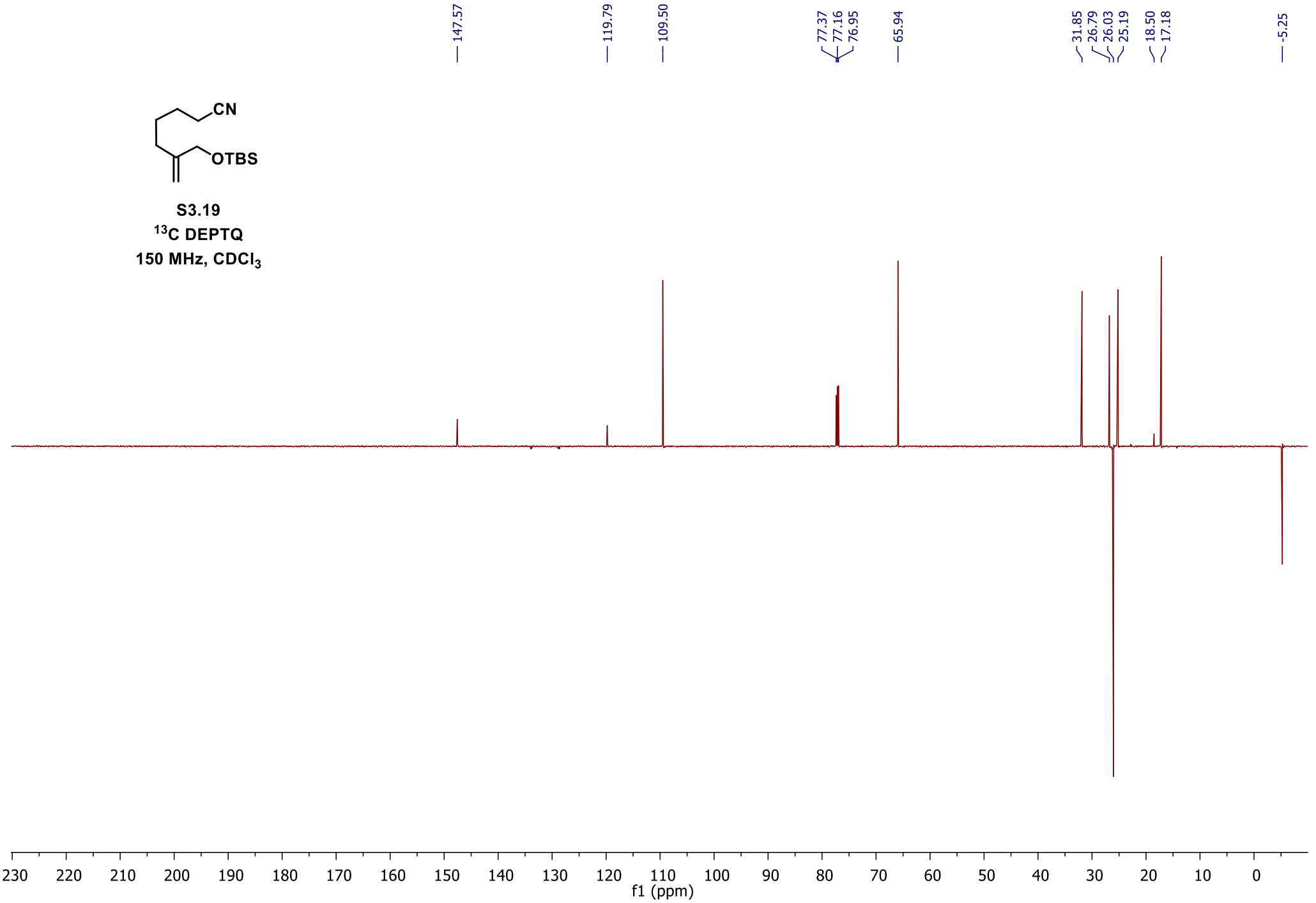
147.57
119.79
109.50
77.37
77.16
76.95
65.94
31.85
26.79
26.03
25.19
18.50
17.18
-5.25
CN
OTBS
S3.19
13C DEPTQ
150 MHz, CDCl3
230 220 210 200 190 180 170 160 150 140 130 120 110 100 90 80 70 60 50 40 30 20 10 0
f1 (ppm)

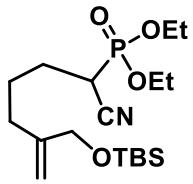

S3.20
^{1}H NMR
600 MHz, $CDCl_3$

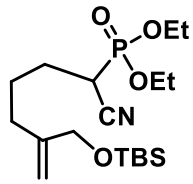

S3.20
^{13}C DEPTQ
150 MHz, $CDCl_3$

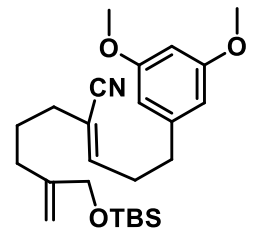

3.40
^{1}H NMR
600 MHz, $CDCl_3$

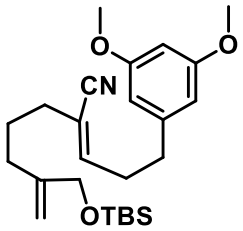

3.40
^{13}C DEPTQ
150 MHz, $CDCl_3$

161.03
147.58
146.68
142.66
117.64
115.32
109.40
106.55
98.39
77.37
77.16
76.95
65.87
55.41
35.11
33.93
32.75
31.62
26.18
26.04
18.51
-5.24

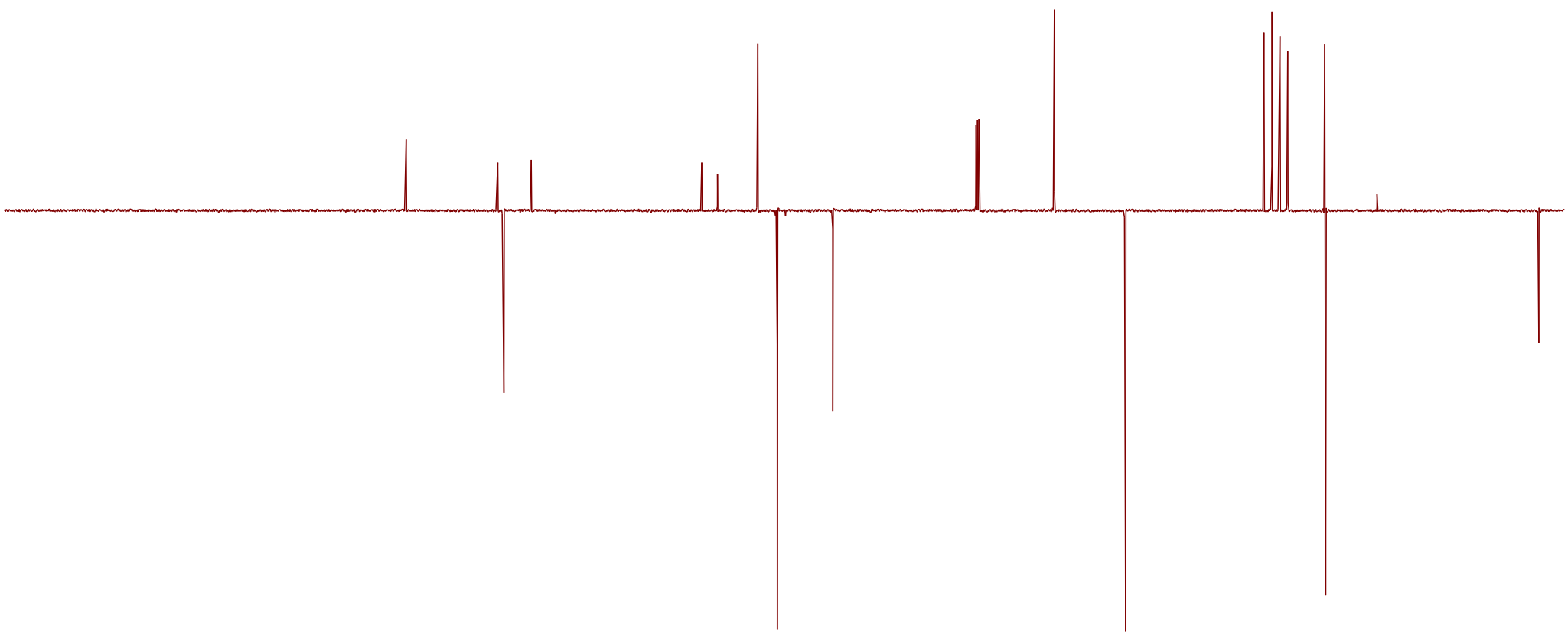

220 210 200 190 180 170 160 150 140 130 120 110 100 90 80 70 60 50 40 30 20 10 0
f1 (ppm)

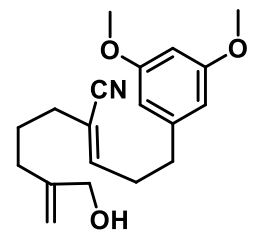

3.45
^{1}H NMR
500 MHz, $CDCl_3$

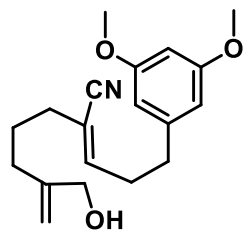

S3.45
^{13}C DEPTQ
125 MHz, $CDCl_3$

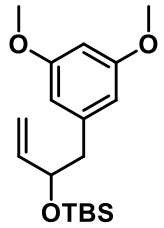

S3.22
^{1}H NMR
500 MHz, $CDCl_3$

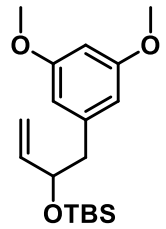

S3.22
^{13}C NMR
125 MHz, $CDCl_3$

160.65
141.25
141.15
113.95
108.13
98.45
77.41
77.16
76.91
55.41
45.59
25.98
18.35
-4.62
-5.04

220 210 200 190 180 170 160 150 140 130 120 110 100 90 80 70 60 50 40 30 20 10 0 -10
f1 (ppm)

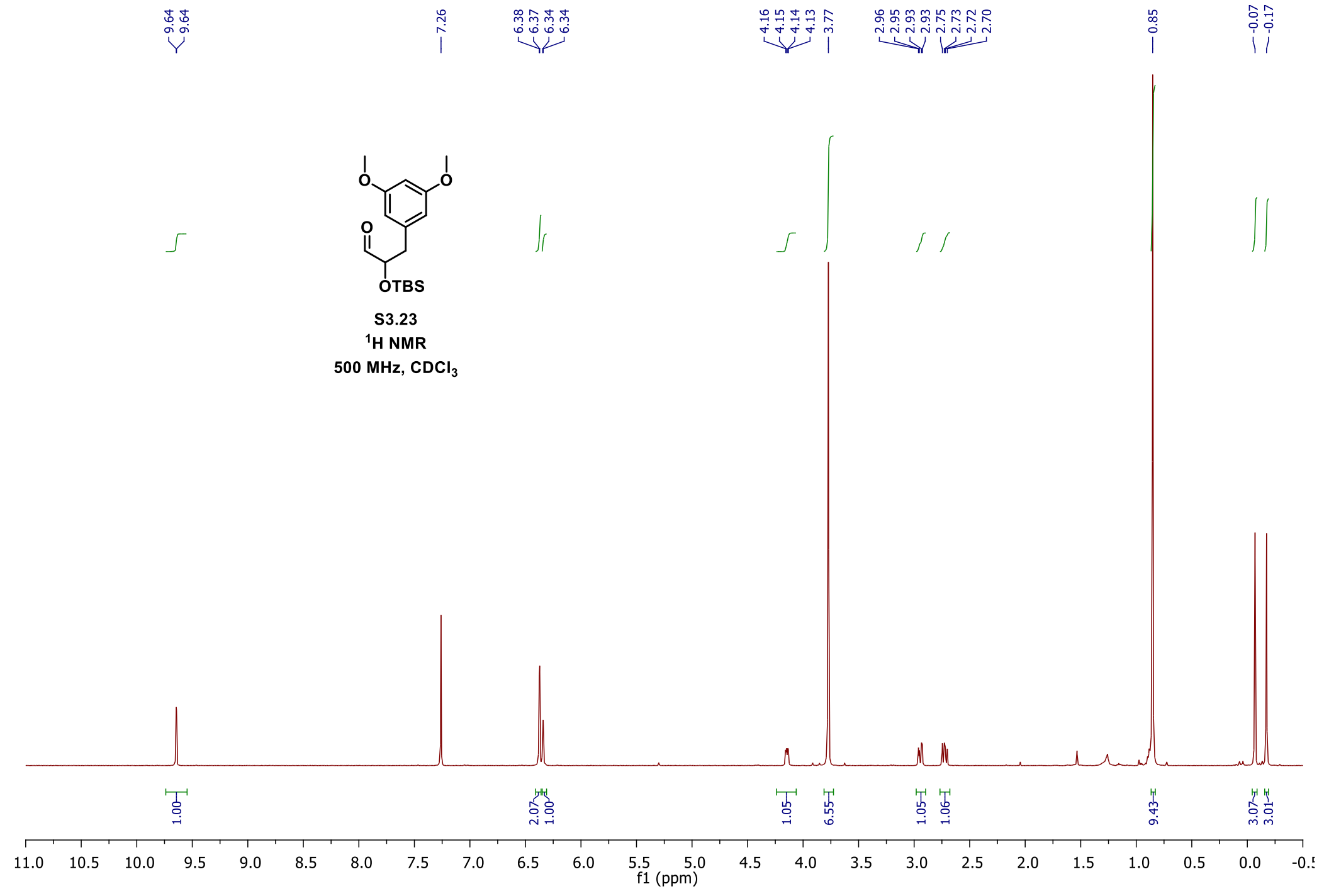
9.64
9.64
7.26
6.38
6.37
6.34
6.34
4.16
4.15
4.14
4.13
3.77
2.96
2.95
2.93
2.93
2.75
2.73
2.72
2.70
0.85
-0.07
-0.17
O
O
O
OTBS
S3.23
1H NMR
500 MHz, CDCl3
1.00
2.07
1.00
1.05
6.55
1.05
1.06
9.43
3.07
3.01
11.0
10.5
10.0
9.5
9.0
8.5
8.0
7.5
7.0
6.5
6.0
5.5
5.0
4.5
4.0
3.5
3.0
2.5
2.0
1.5
1.0
0.5
0.0
f1 (ppm)

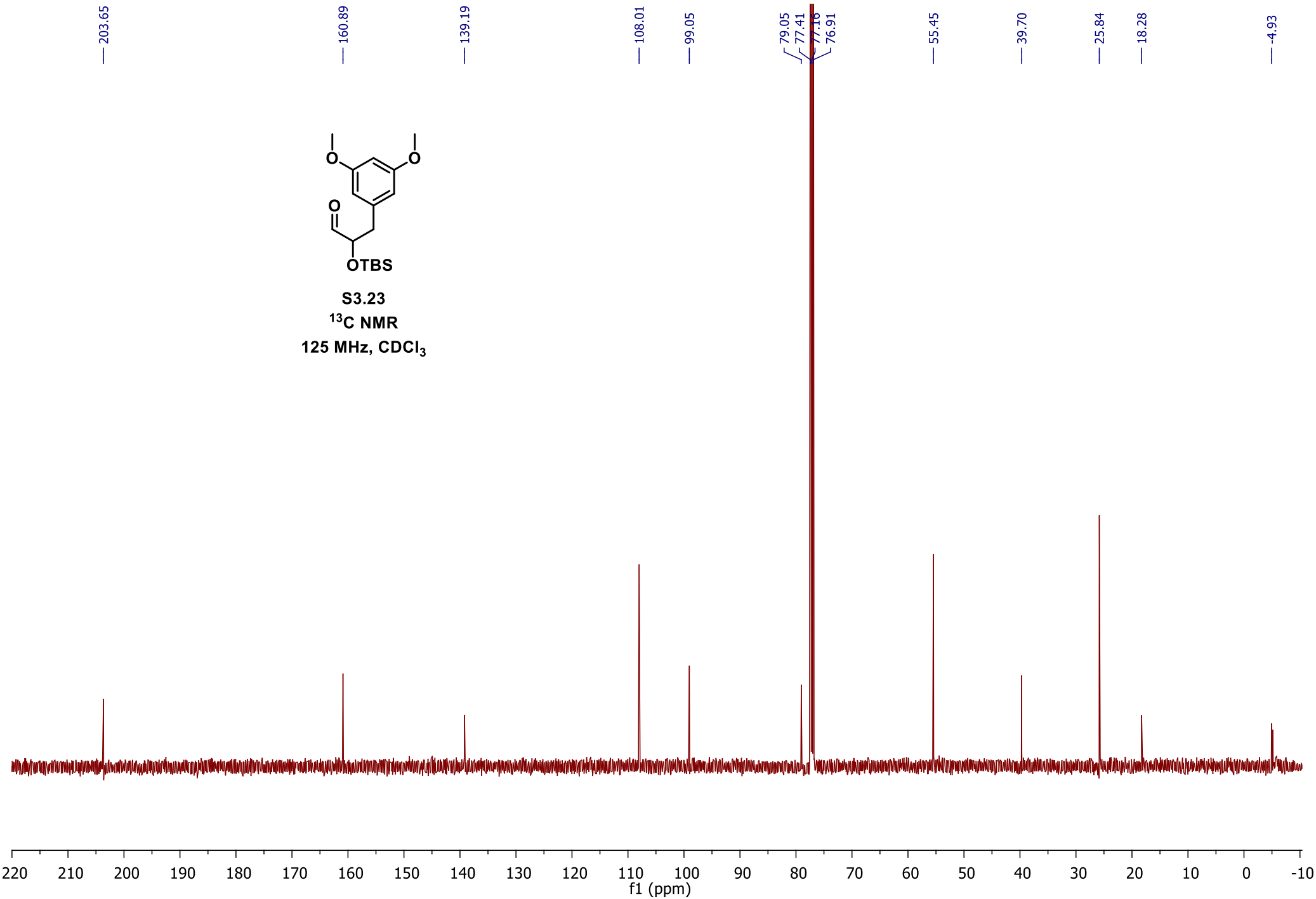
203.65
160.89
139.19
108.01
99.05
79.05
77.41
77.16
76.91
55.45
39.70
25.84
18.28
-4.93
O
O
O
OTBS
S3.23
13C NMR
125 MHz, CDCl3
220
210
200
190
180
170
160
150
140
130
120
110
100
90
80
70
60
50
40
30
20
10
0
-10
f1 (ppm)

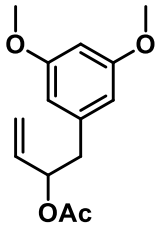

S3.24 (*~80% pure*)
^{1}H NMR
500 MHz, $CDCl_3$

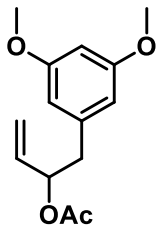

S3.24 (~*80% pure*)
^{13}C DEPTQ
125 MHz, $CDCl_3$

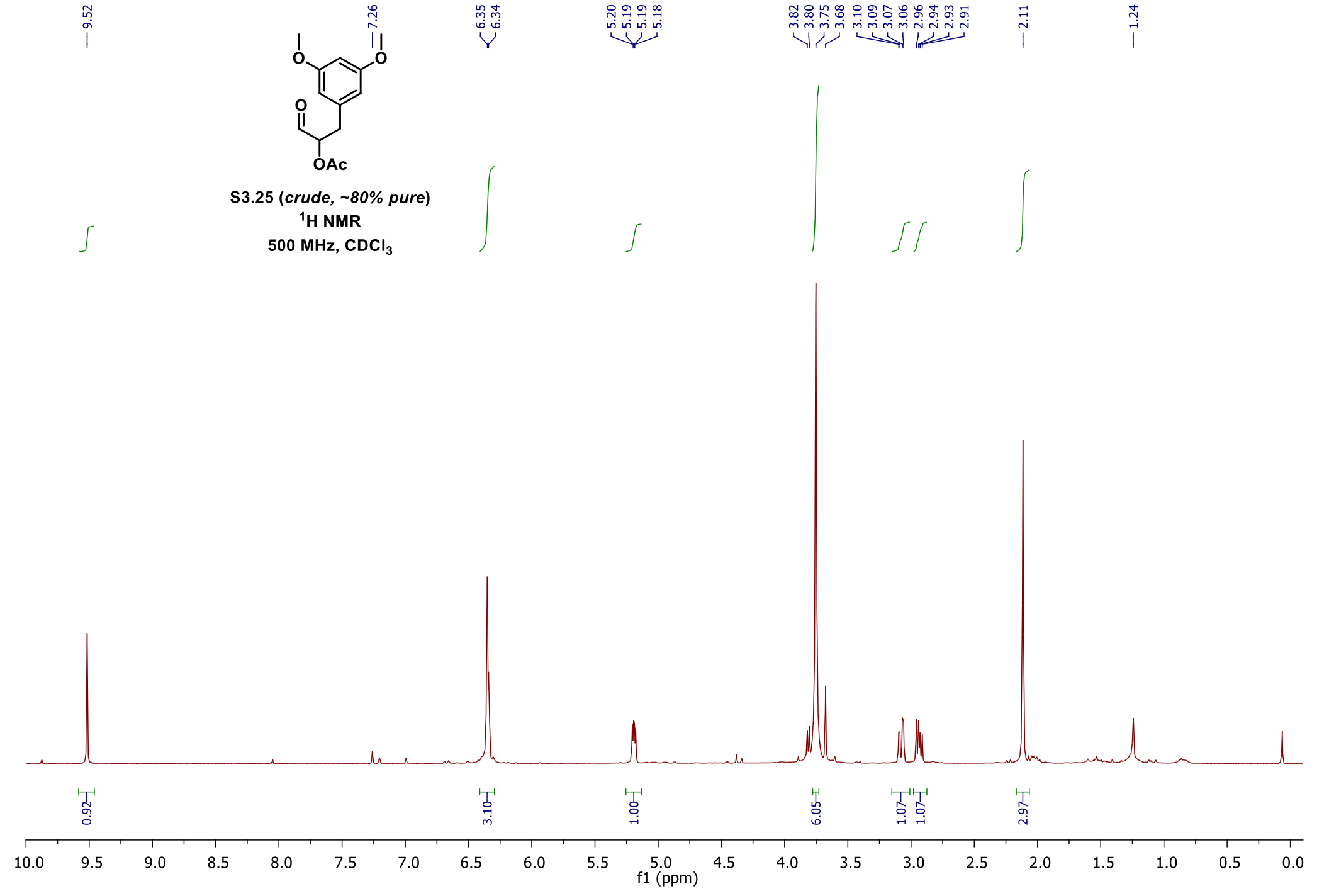
9.52
7.26
6.35
6.34
5.20
5.19
5.19
5.18
3.82
3.80
3.75
3.68
3.10
3.09
3.07
3.06
2.96
2.94
2.93
2.91
2.11
1.24
O
O
O
OAc
S3.25 (crude, ~80% pure)
1H NMR
500 MHz, CDCl3
0.92
3.10
1.00
6.05
1.07
1.07
2.97
10.0
9.5
9.0
8.5
8.0
7.5
7.0
6.5
6.0
5.5
5.0
4.5
4.0
3.5
3.0
2.5
2.0
1.5
1.0
0.5
0.0
f1 (ppm)

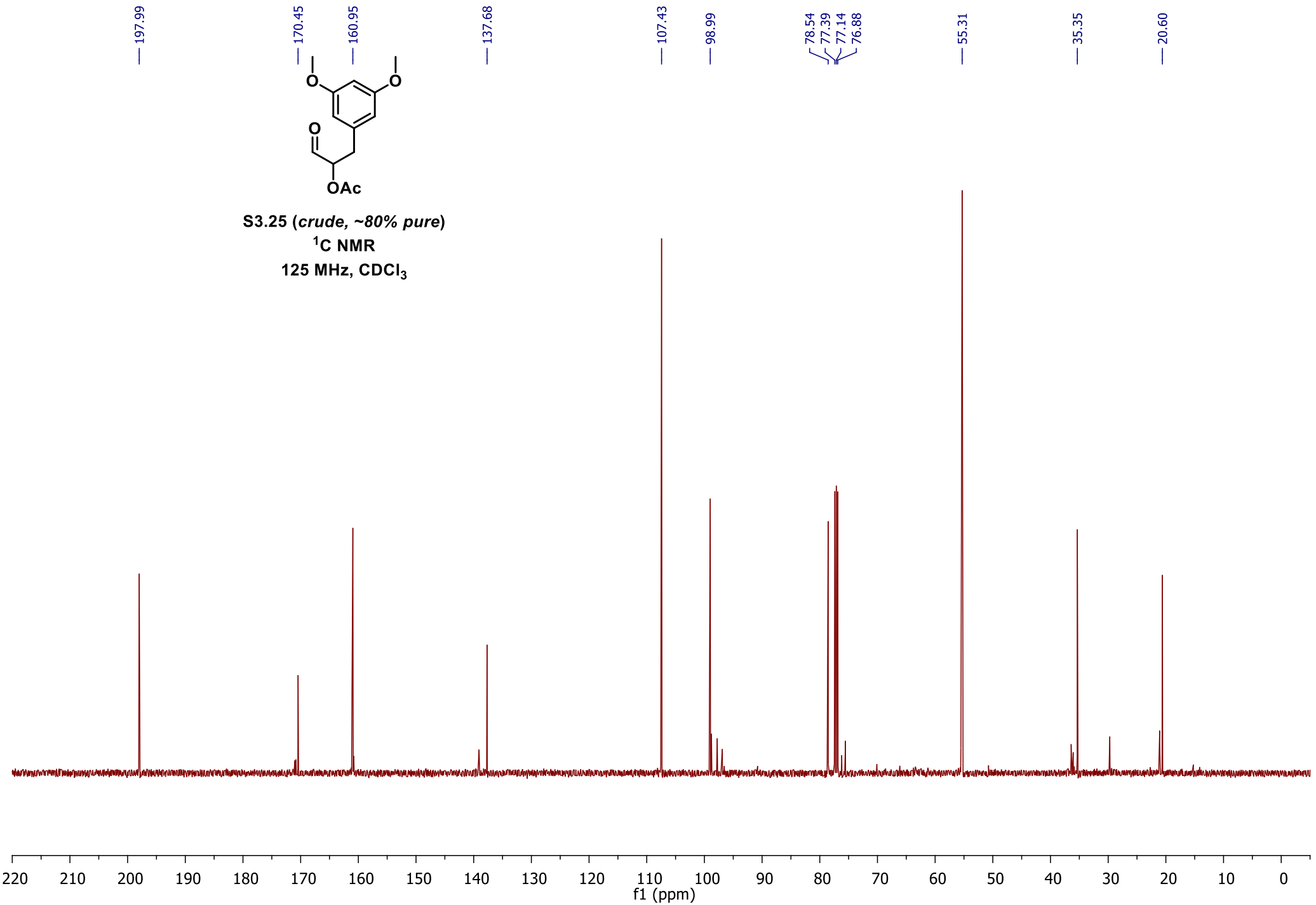
197.99
170.45
160.95
137.68
107.43
98.99
78.54
77.39
77.14
76.88
55.31
35.35
20.60
O
O
O
OAc
S3.25 (crude, ~80% pure)
1C NMR
125 MHz, CDCl3
220
210
200
190
180
170
160
150
140
130
120
110
100
90
80
70
60
50
40
30
20
10
0
f1 (ppm)

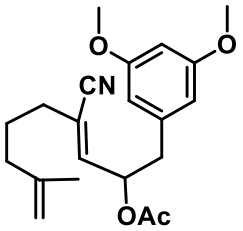

3.47a
^{1}H NMR
600 MHz, $CDCl_3$

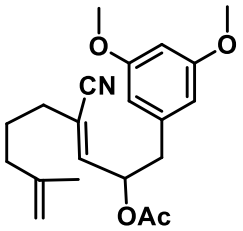

3.47a
^{13}C DEPTQ
150 MHz, $CDCl_3$

169.93
160.94
144.57
143.40
137.77
117.31
116.49
110.94
107.69
99.12
72.88
55.42
40.62
36.47
34.00
25.58
22.22
21.06

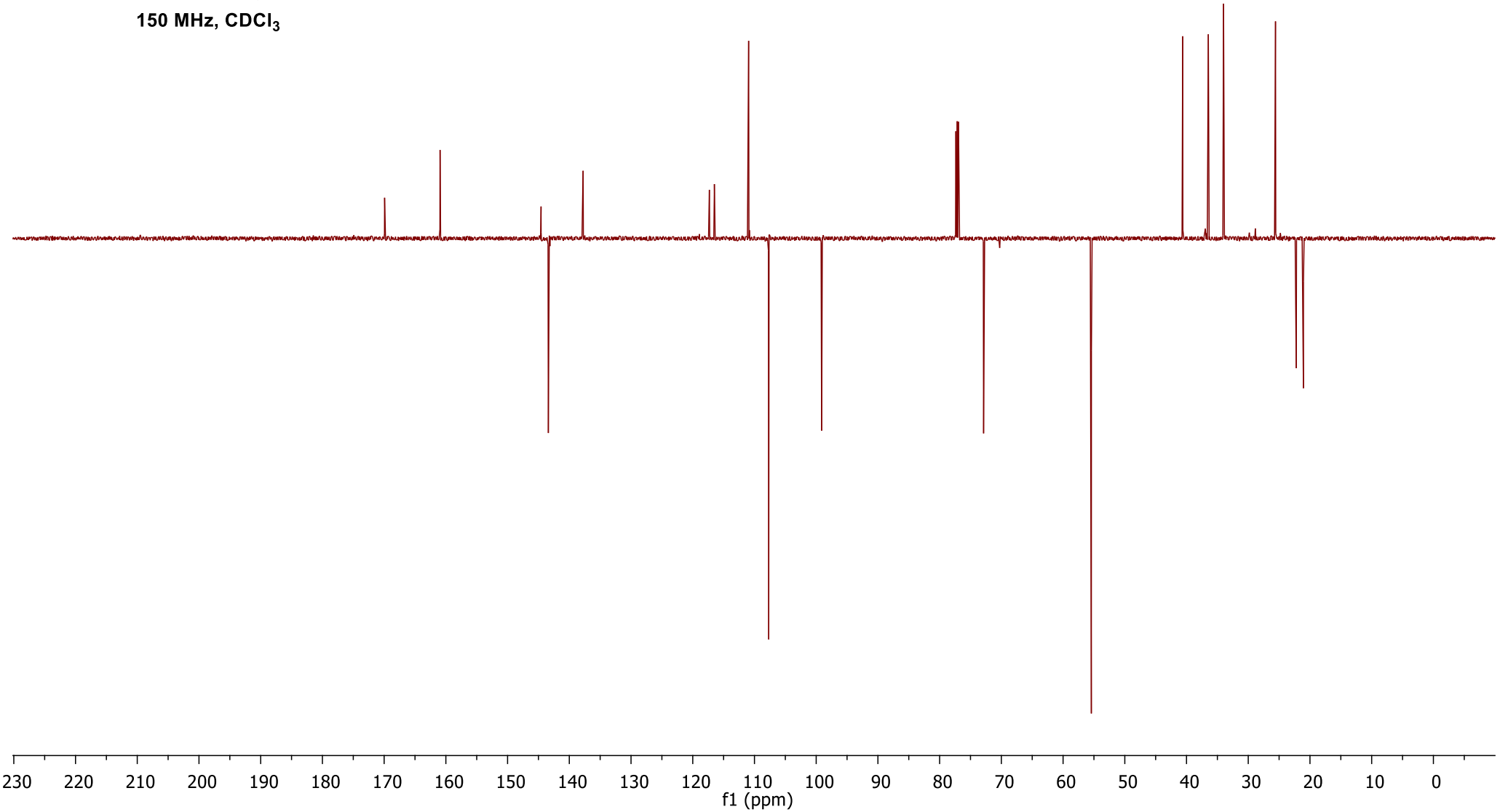

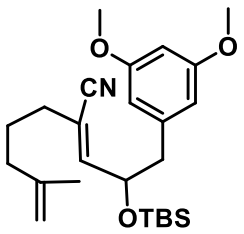

3.47b
^{1}H NMR
600 MHz, $CDCl_3$

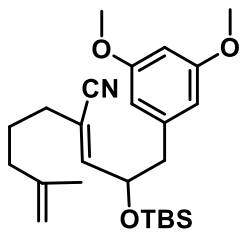

3.47b
^{13}C DEPTQ
150 MHz, $CDCl_3$

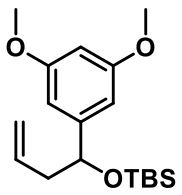

S3.28
^{1}H NMR
600 MHz, $CDCl_3$

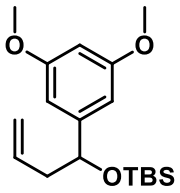

S3.28
^{13}C DEPTQ
150 MHz, $CDCl_3$

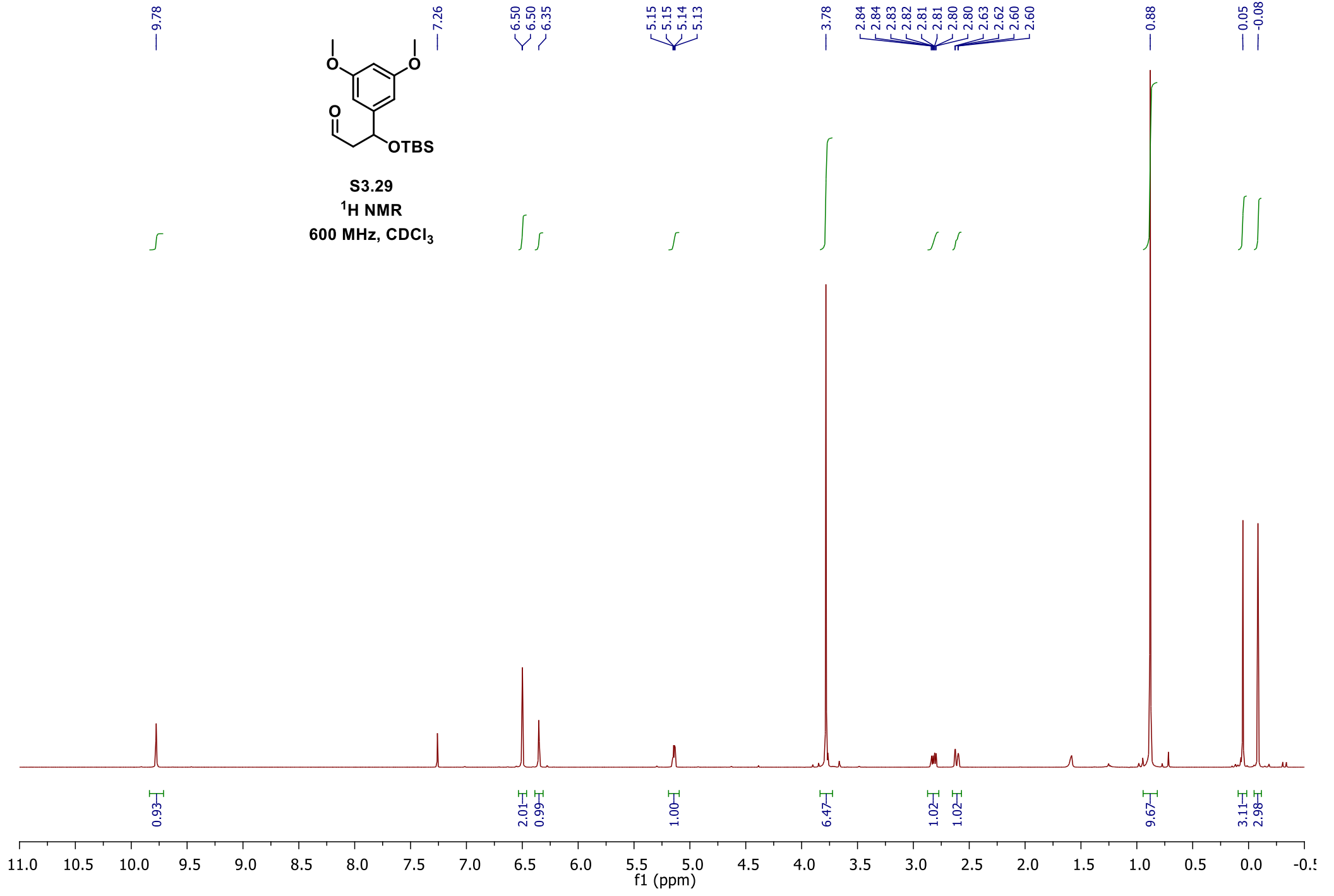
9.78
7.26
6.50
6.50
6.35
5.15
5.15
5.14
5.13
3.78
2.84
2.84
2.83
2.82
2.81
2.81
2.80
2.80
2.63
2.62
2.60
2.60
0.88
0.05
-0.08
O
O
O
OTBS
S3.29
1H NMR
600 MHz, CDCl3
0.93
2.01
0.99
1.00
6.47
1.02
1.02
9.67
3.11
2.98
11.0
10.5
10.0
9.5
9.0
8.5
8.0
7.5
7.0
6.5
6.0
5.5
5.0
4.5
4.0
3.5
3.0
2.5
2.0
1.5
1.0
0.5
0.0
-0.5
f1 (ppm)

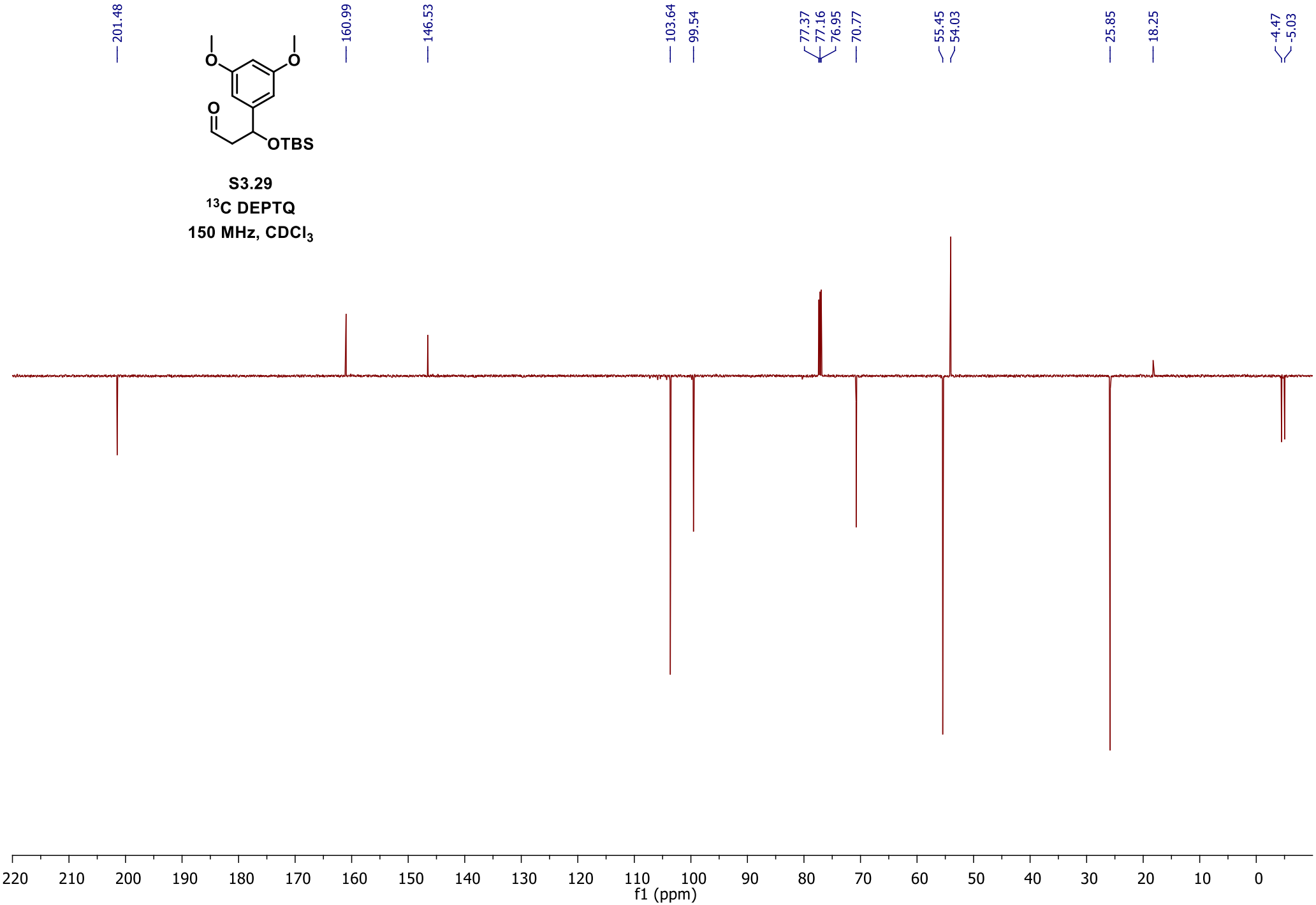
201.48
160.99
146.53
103.64
99.54
77.37
77.16
76.95
70.77
55.45
54.03
25.85
18.25
-4.47
-5.03
O
O
O
OTBS
S3.29
13C DEPTQ
150 MHz, CDCl3
220
210
200
190
180
170
160
150
140
130
120
110
100
90
80
70
60
50
40
30
20
10
0
f1 (ppm)

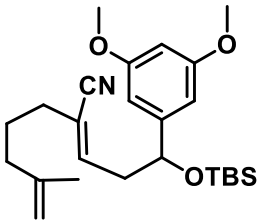

3.50b
^{1}H NMR
600 MHz, $CDCl_3$

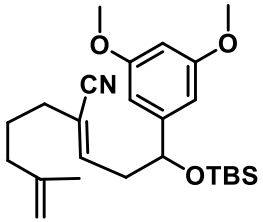

3.50b
^{13}C DEPTQ
150 MHz, $CDCl_3$

160.83
146.59
144.84
143.87
117.79
116.48
110.75
103.72
99.42
77.37
77.16
76.95
73.70
55.44
42.40
36.69
33.92
25.95
25.91
22.34
18.32
-4.59
-4.91

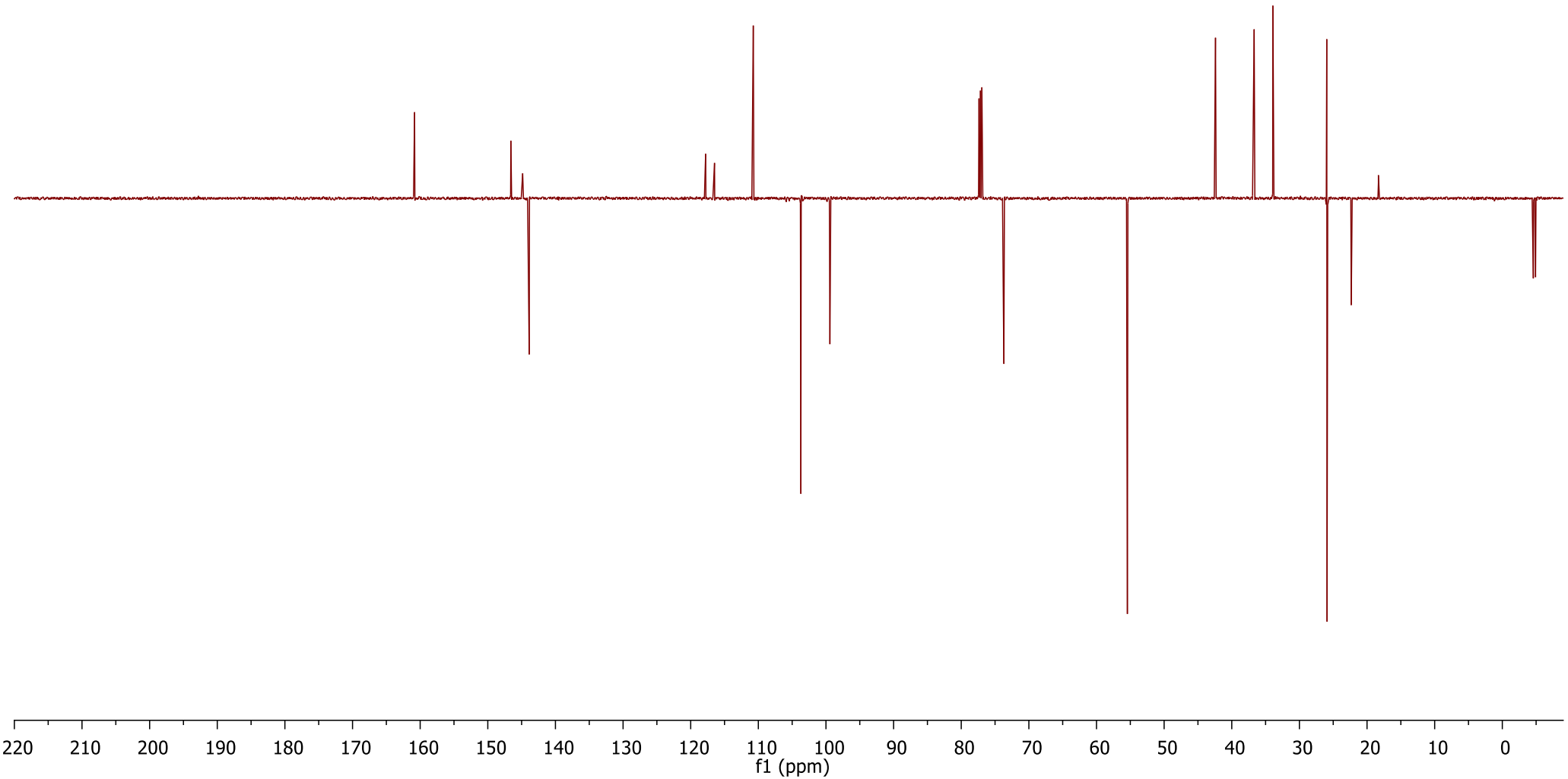

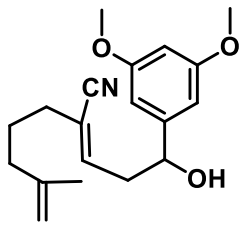

3.50a
^{1}H NMR
500 MHz, $CDCl_3$

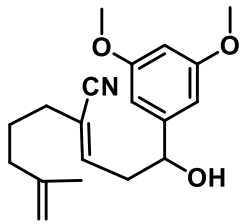

3.50a
^{13}C DEPTQ
150 MHz, $CDCl_3$

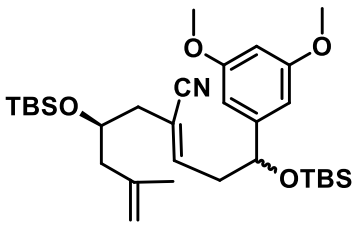

S3.30
^{1}H NMR
500 MHz, $CDCl_3$

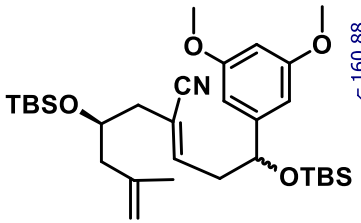

S3.30
^{13}C NMR
125 MHz, $CDCl_3$

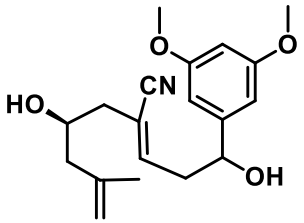

3.59
^{1}H NMR
500 MHz, $CDCl_3$

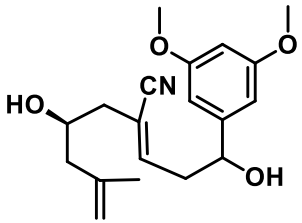

3.59
^{13}C NMR
125 MHz, $CDCl_3$

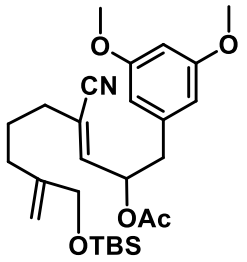

3.56

^{1}H NMR

600 MHz, $CDCl_3$

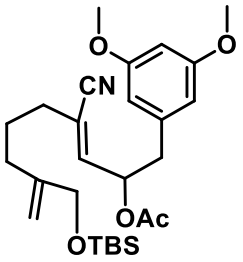

3.56
^{13}C DEPTQ
150 MHz, $CDCl_3$

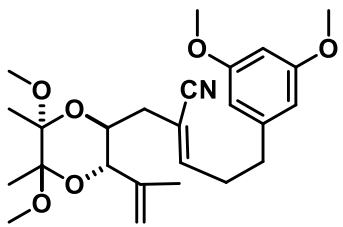

3.62

^{1}H NMR

600 MHz, $CDCl_3$

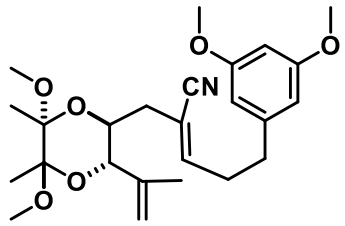

3.62

^{13}C DEPTQ

151 MHz, $CDCl_3$

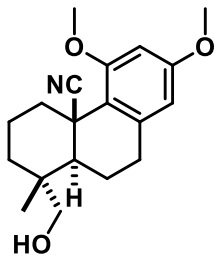

3.43
^{1}H NMR
500 MHz, $CDCl_3$

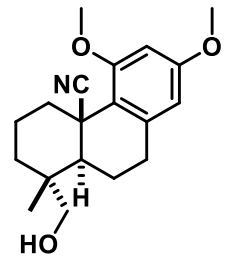

3.43
^{13}C DEPTQ
151 MHz, $CDCl_3$

160.14
159.86
140.00
123.67
119.27
105.32
97.82
77.37
77.16
76.95
71.18
55.65
55.39
46.54
39.56
38.48
34.86
34.55
32.47
20.89
20.01
16.67

220 210 200 190 180 170 160 150 140 130 120 110 100 90 80 70 60 50 40 30 20 10 0
f1 (ppm)

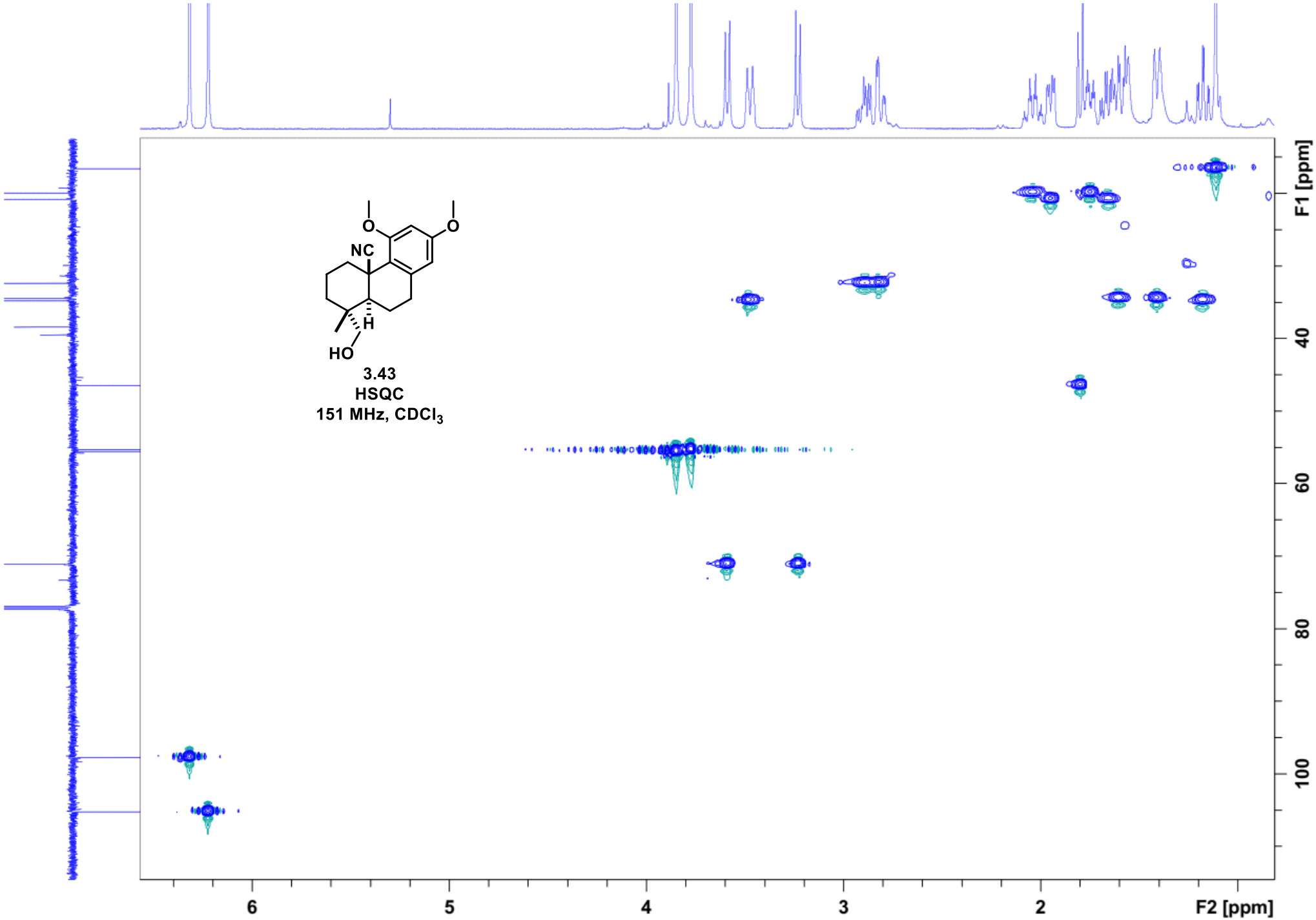
O
O
NC
H
HO
3.43
HSQC
151 MHz, CDCl3
F1 [ppm]
40
60
80
100
6
5
4
3
2
F2 [ppm]

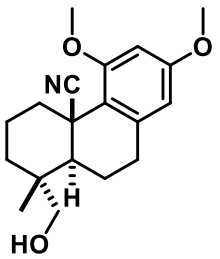

3.43

^{1}H COSY

500 MHz, $CDCl_3$

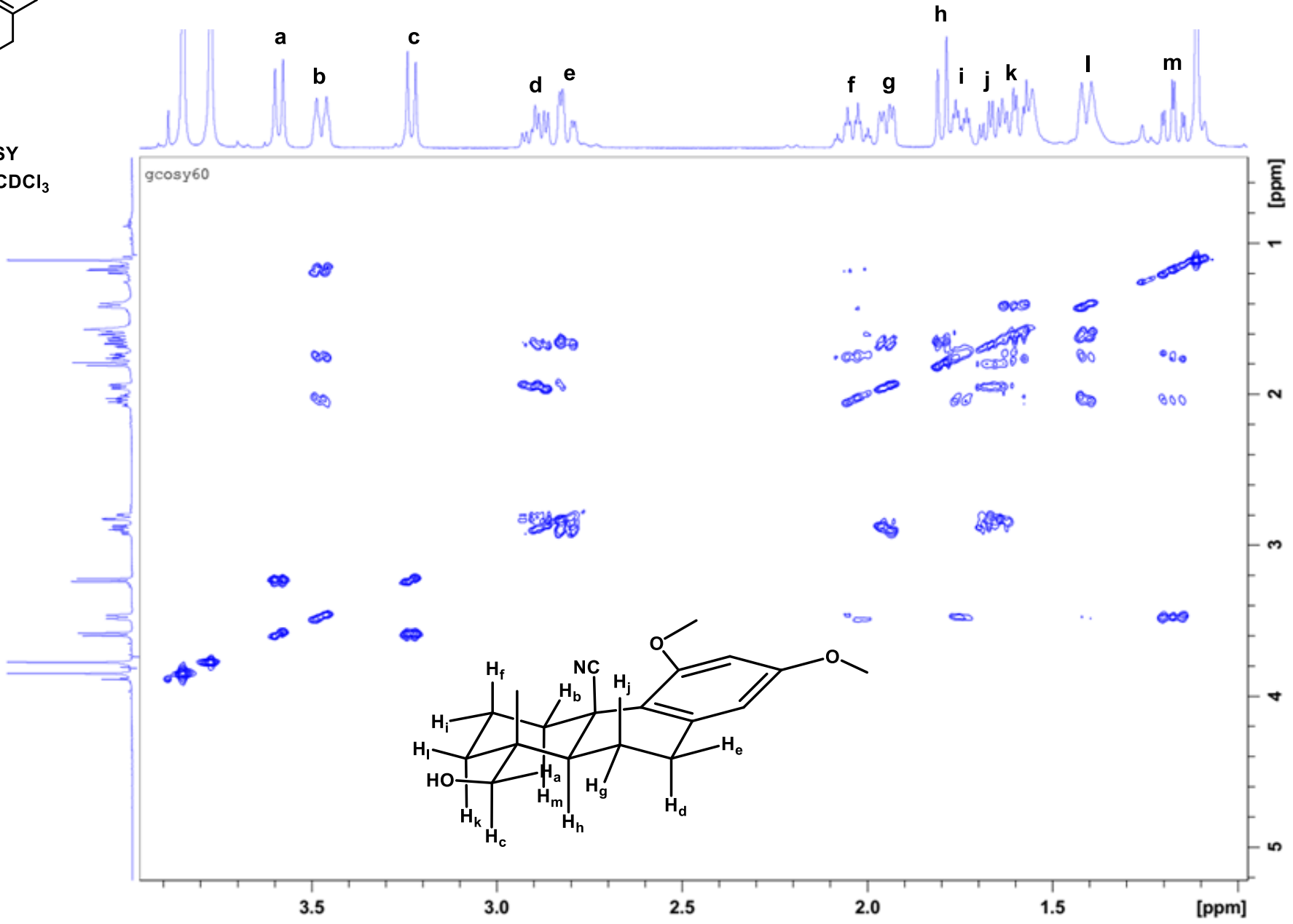

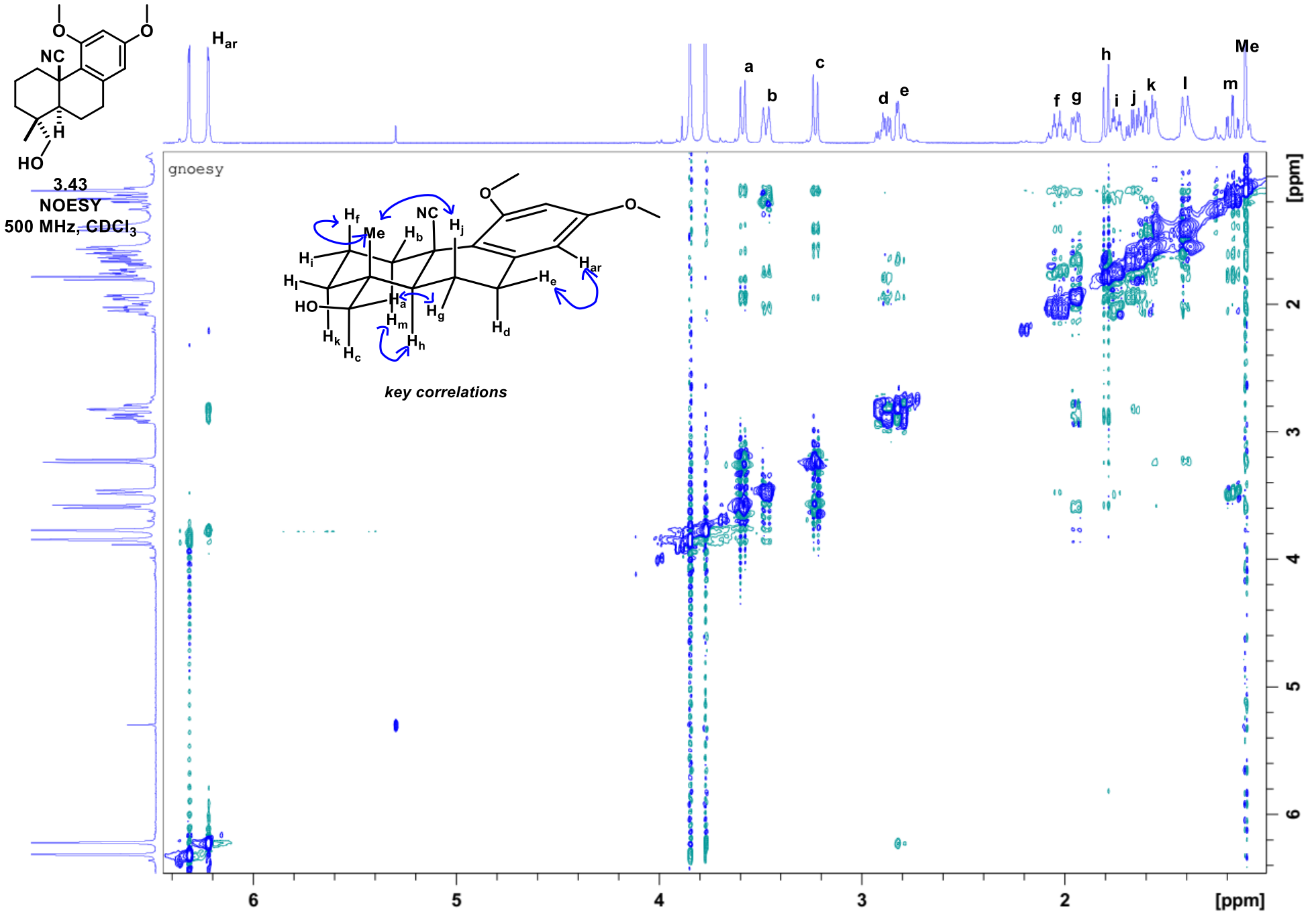
3.43
NOESY
500 MHz, CDCl3
gnoesy
key correlations
[ppm]

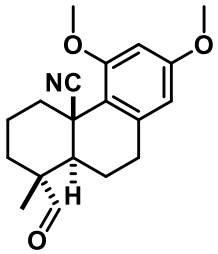

3.46
^{1}H NMR
600 MHz, $CDCl_3$

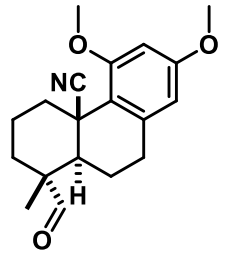

3.46

^{13}C DEPTQ

151 MHz, $CDCl_3$

205.01 160.14 139.61 122.85 118.23 105.45 97.92 77.37 77.16 76.95 55.68 55.43 50.17 45.40 38.73 34.47 32.04 32.02 23.58 19.15 13.76

220 210 200 190 180 170 160 150 140 130 120 110 100 90 80 70 60 50 40 30 20 10 0

f1 (ppm)

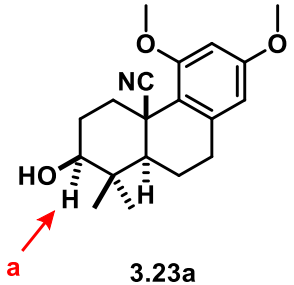

3.23a
^{1}H NMR
500 MHz, $CDCl_3$

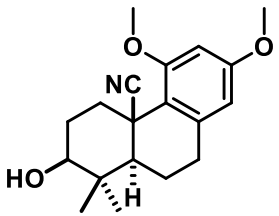

3.23a
^{13}C DEPTQ
151 MHz, $CDCl_3$

160.14
159.99
139.81
122.79
118.74
105.31
97.86
77.79
77.37
77.16
76.95
55.67
55.41
52.39
39.76
39.21
33.09
32.93
29.12
27.76
21.07
14.31

220 210 200 190 180 170 160 150 140 130 120 110 100 90 80 70 60 50 40 30 20 10 0
f1 (ppm)

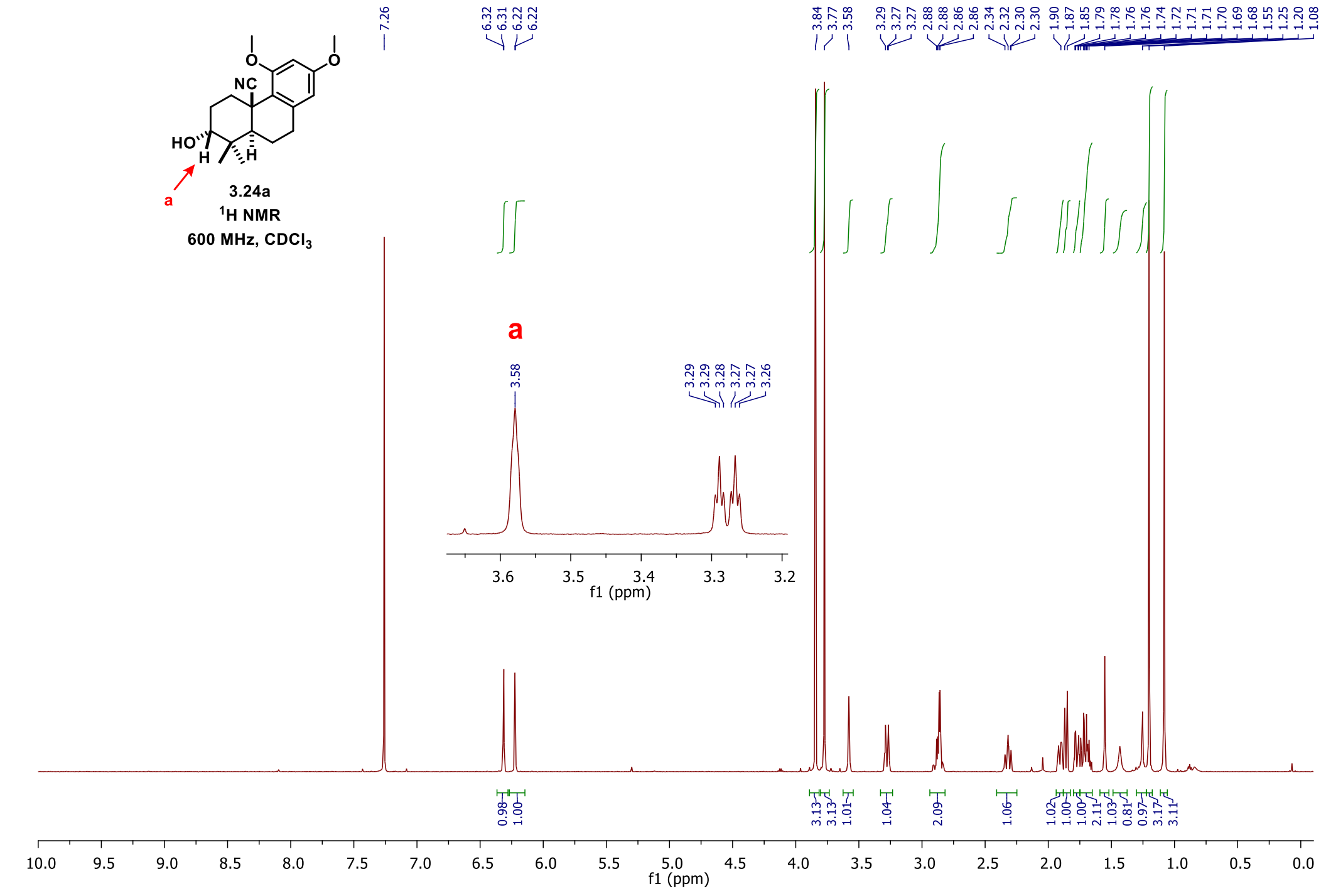
7.26
6.32
6.31
6.22
6.22
3.84
3.77
3.58
3.29
3.27
3.27
2.88
2.88
2.86
2.86
2.34
2.32
2.30
2.30
1.90
1.87
1.85
1.79
1.78
1.76
1.76
1.74
1.72
1.71
1.71
1.70
1.69
1.68
1.55
1.25
1.20
1.08
O
O
NC
HO
H
H
a
3.24a
1H NMR
600 MHz, CDCl3
a
3.58
3.29
3.29
3.28
3.27
3.27
3.26
3.6
3.5
3.4
3.3
3.2
f1 (ppm)
0.98
1.00
3.13
3.13
1.01
1.04
2.09
1.06
1.02
1.00
1.00
2.11
1.03
0.81
0.97
3.17
3.11
10.0
9.5
9.0
8.5
8.0
7.5
7.0
6.5
6.0
5.5
5.0
4.5
4.0
3.5
3.0
2.5
2.0
1.5
1.0
0.5
0.0
f1 (ppm)

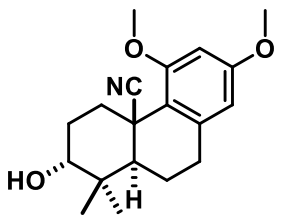

3.24a
^{13}C DEPTQ
151 MHz, $CDCl_3$

160.14
159.89
139.92
123.44
119.11
105.34
97.84
77.37
77.16
76.95
74.75
55.66
55.39
45.99
39.46
38.26
32.74
28.14
27.75
27.47
21.11
20.88

220 210 200 190 180 170 160 150 140 130 120 110 100 90 80 70 60 50 40 30 20 10 0
f1 (ppm)

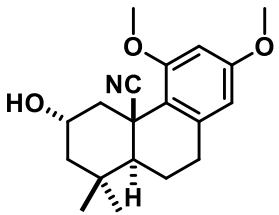

3.26a
^{1}H NMR
500 MHz, $CDCl_3$

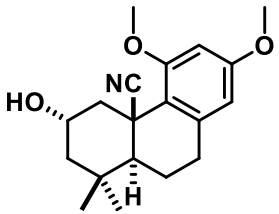

3.26a
^{13}C DEPTQ
151 MHz, $CDCl_3$

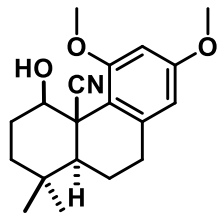

3.29a
^{1}H NMR
500 MHz, C_6D_6

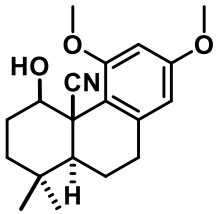

3.29a
^{13}C NMR
126 MHz, C_6D_6

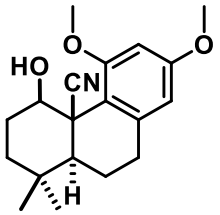

3.29a
HMQC
126 MHz, C_6D_6

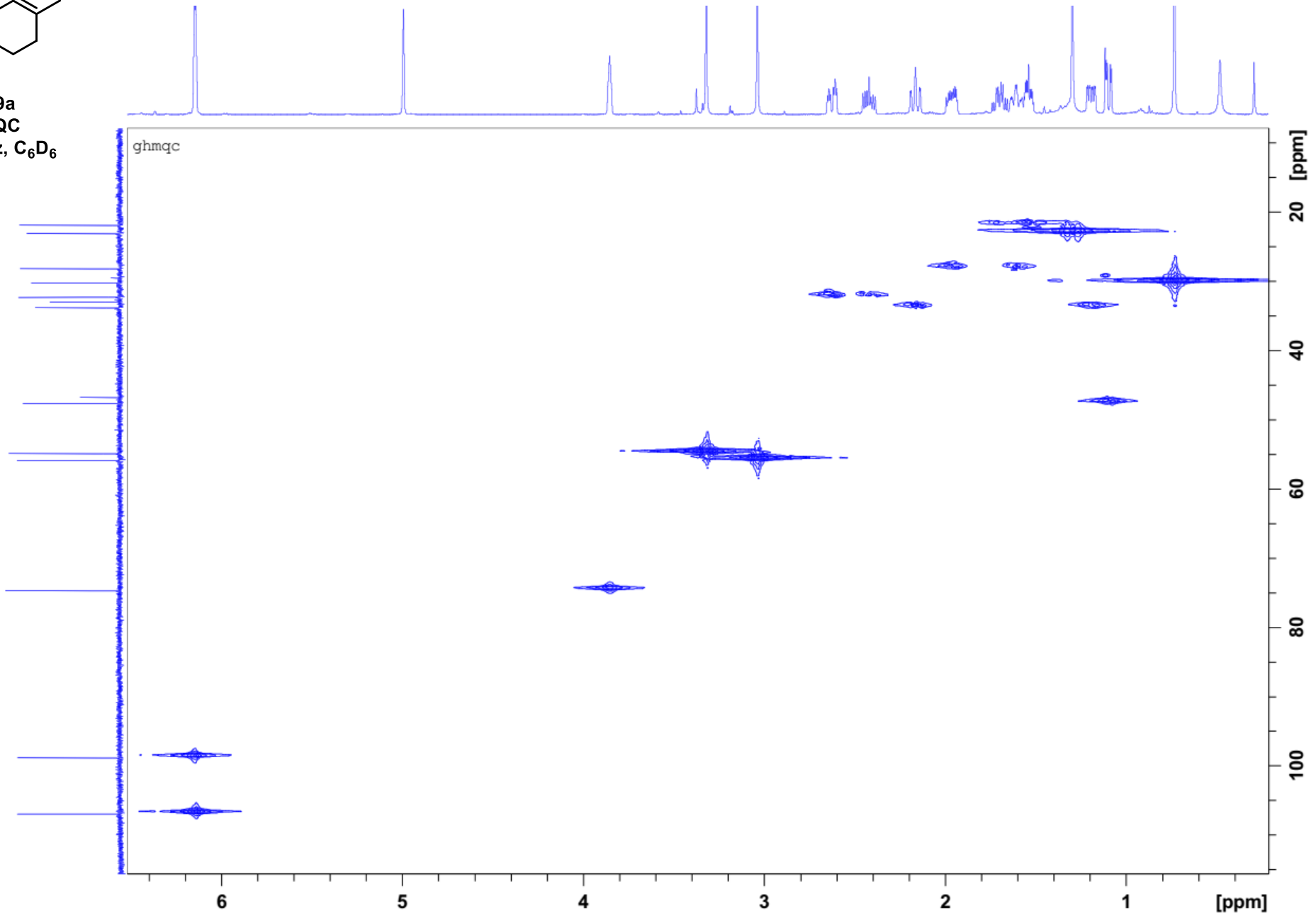

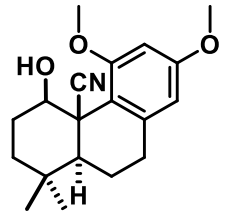

3.29a
^{1}H COSY
500 MHz, C_6D_6

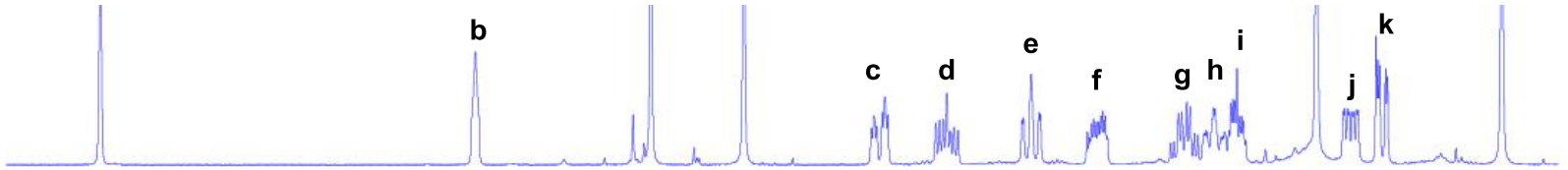

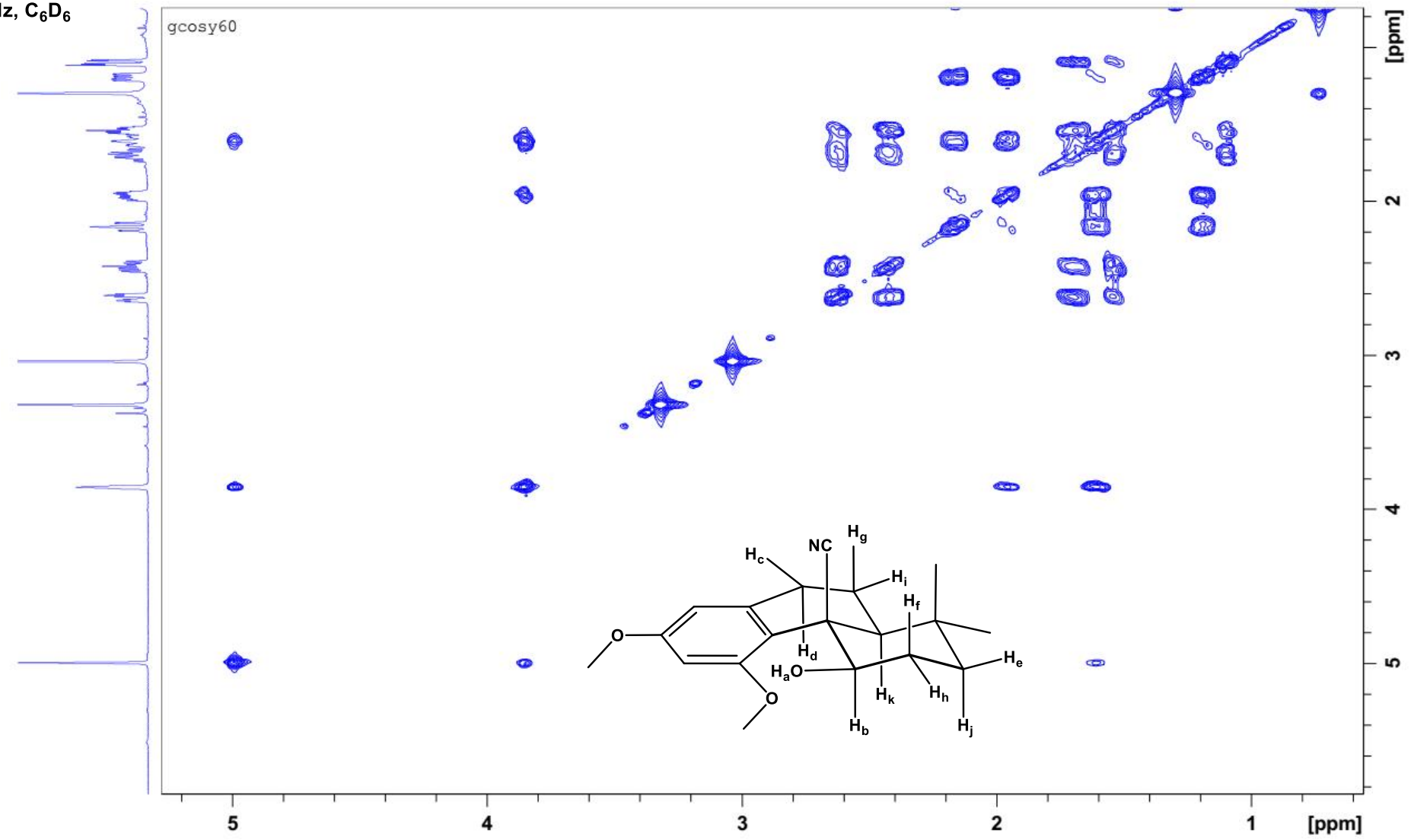

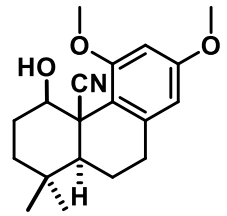

3.29a
NOESY
500 MHz, C_6D_6

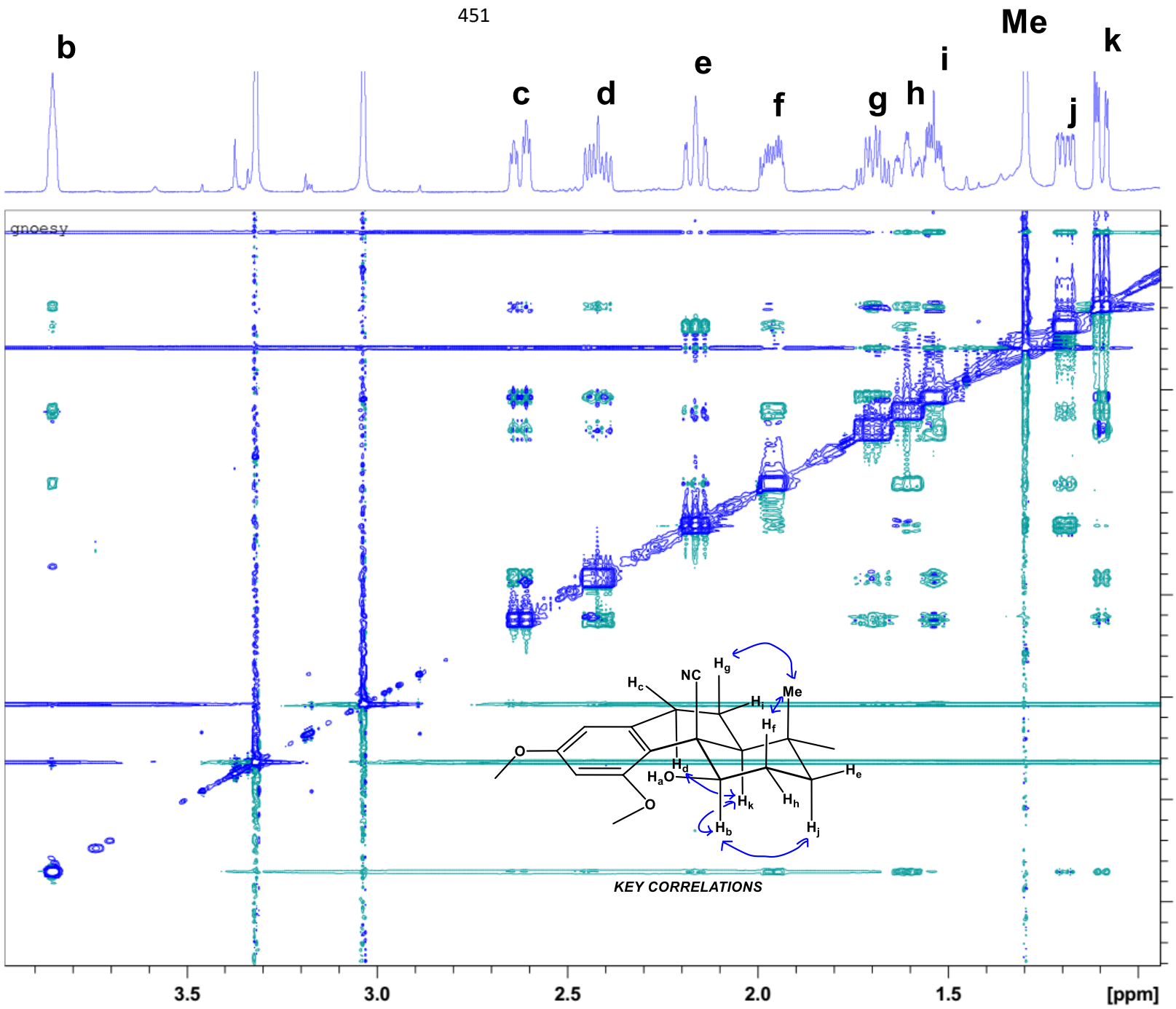

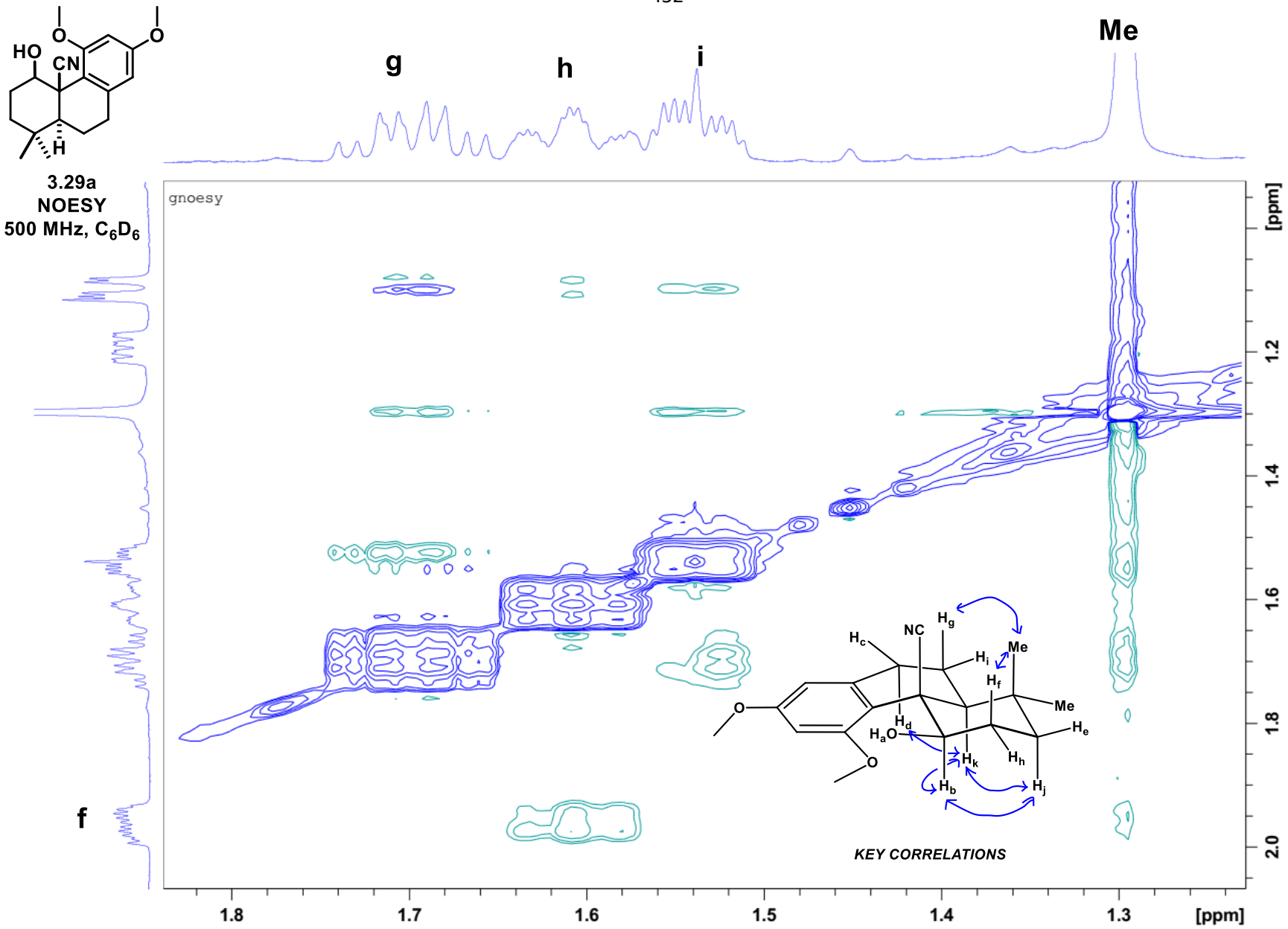
HO
O
O
CN
H
3.29a
NOESY
500 MHz, C6D6
gnoesy
g
h
i
Me
f
[ppm]
1.2
1.4
1.6
1.8
2.0
1.8
1.7
1.6
1.5
1.4
1.3
[ppm]
Hg
NC
Hc
Hi
Me
Hf
Me
Hd
Ha
O
He
Hk
Hh
Hb
Hj
O
KEY CORRELATIONS

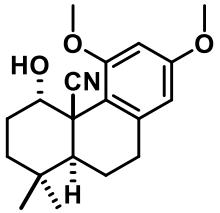

3.30a
^{1}H NMR
500 MHz, $CDCl_3$

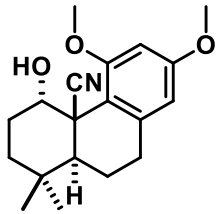

3.30a
^{13}C NMR
126 MHz, $CDCl_3$

160.31
159.52
142.35
122.44
115.58
106.30
97.83
77.41
77.16
76.91
67.96
55.92
55.42
44.97
44.66
33.70
33.61
32.67
32.33
29.86
26.10
20.99
20.13

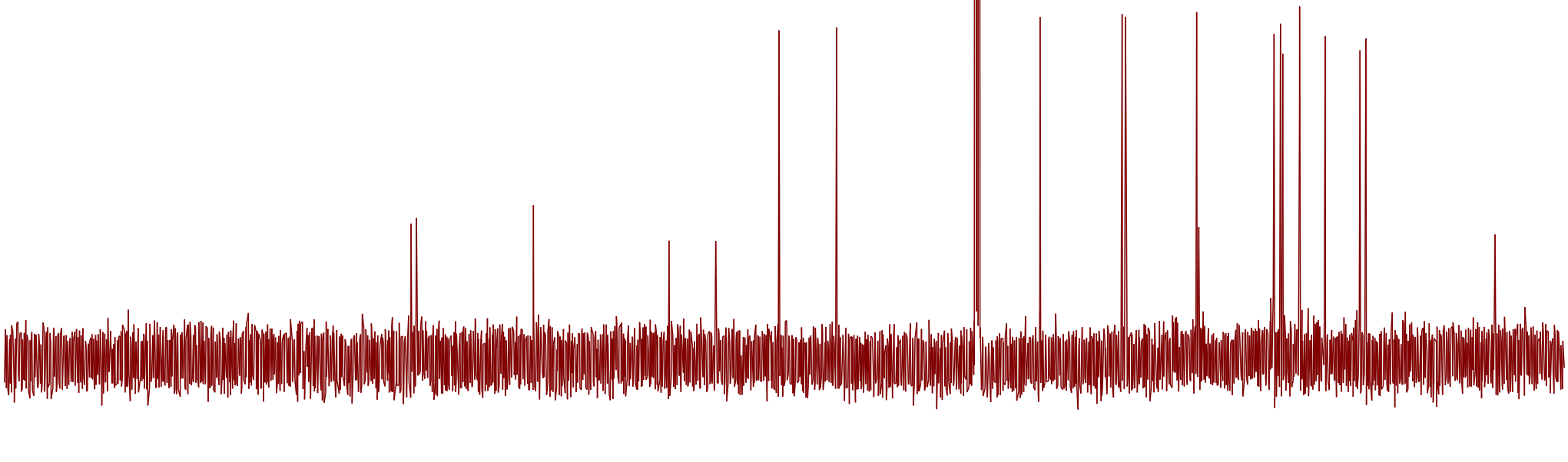

220 210 200 190 180 170 160 150 140 130 120 110 100 90 80 70 60 50 40 30 20 10 0
f1 (ppm)

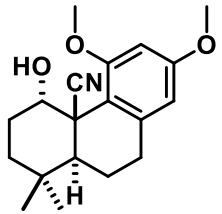

3.30a

^{1}H COSY

500 MHz, $CDCl_3$

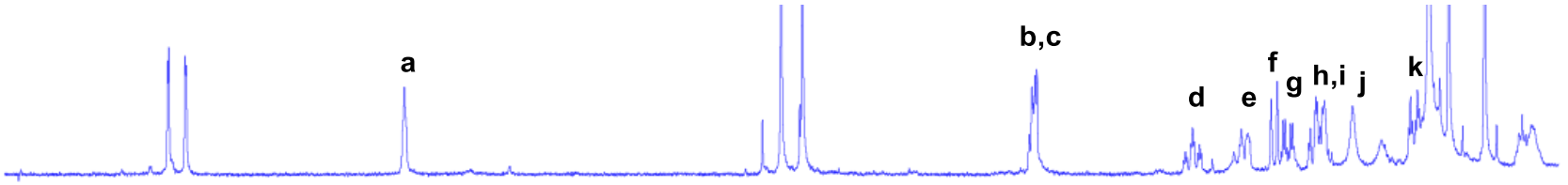

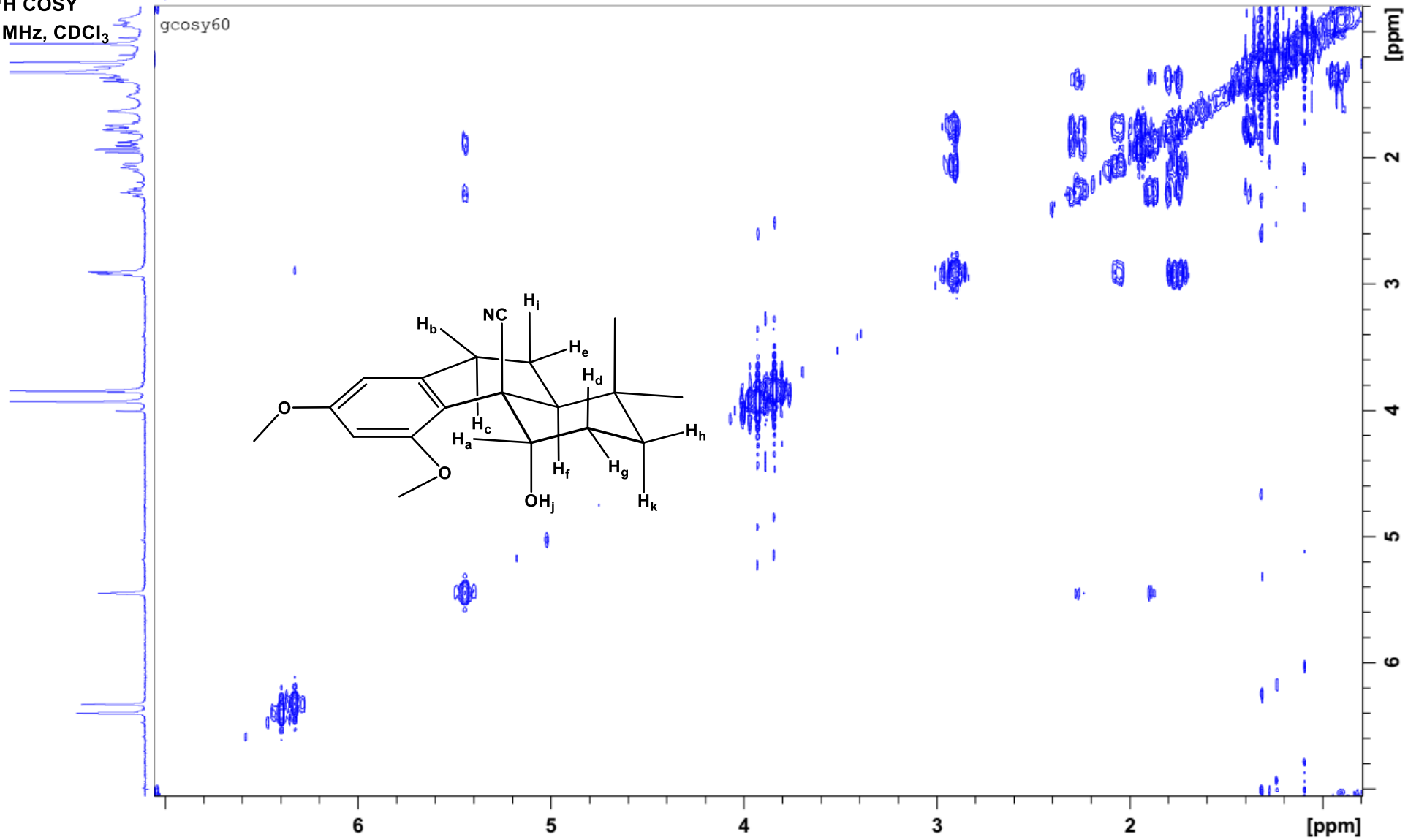

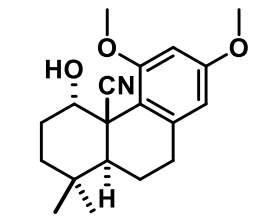

3.30a
NOESY
500 MHz, $CDCl_3$

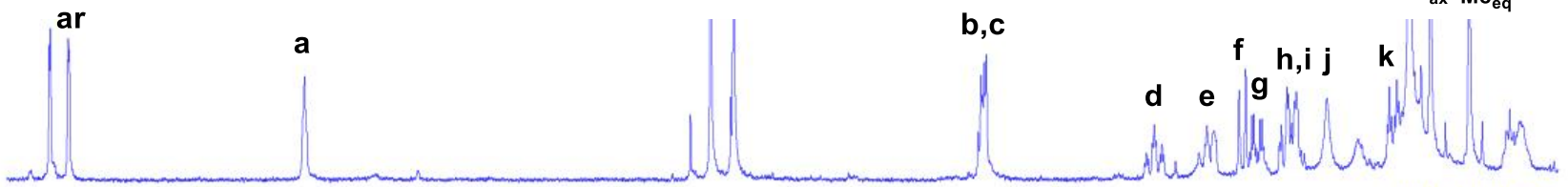

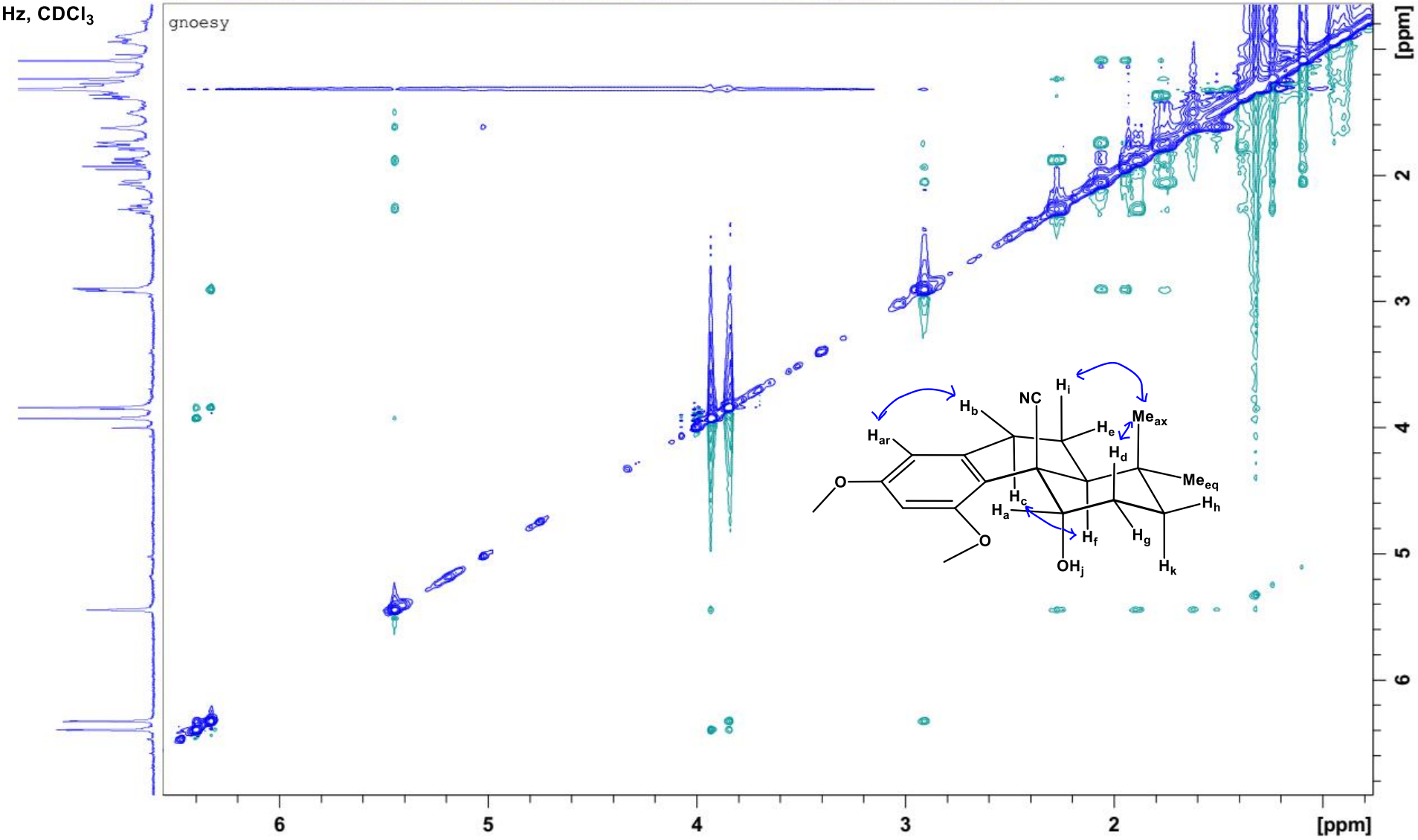

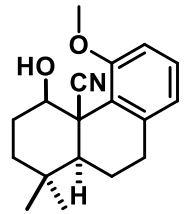

3.32
^{1}H NMR
600 MHz, $CDCl_3$

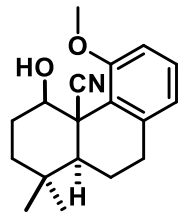

3.32

^{13}C NMR

126 MHz, $CDCl_3$

157.18
140.32
128.86
126.96
123.68
120.38
110.53
77.37
77.16
76.95
74.04
56.84
47.69
46.91
33.95
33.14
31.53
30.50
27.76
22.82
21.58

220 210 200 190 180 170 160 150 140 130 120 110 100 90 80 70 60 50 40 30 20 10 0

f1 (ppm)

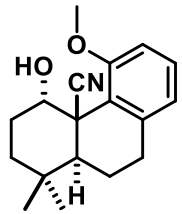

3.33
^{1}H NMR
600 MHz, $CDCl_3$

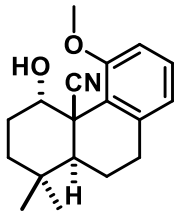

3.33
^{13}C NMR
126 MHz, $CDCl_3$

158.45
141.41
129.25
123.24
123.08
122.22
109.55
77.37
77.16
76.95
68.01
55.94
45.00
44.85
33.75
33.57
32.29
32.17
26.22
20.93
20.15

230 220 210 200 190 180 170 160 150 140 130 120 110 100 90 80 70 60 50 40 30 20 10 0
f1 (ppm)

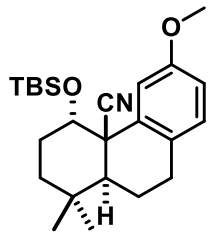

3.37b
^{1}H NMR
600 MHz, $CDCl_3$

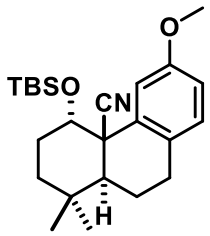

3.37b
^{13}C DEPTQ
151 MHz, $CDCl_3$

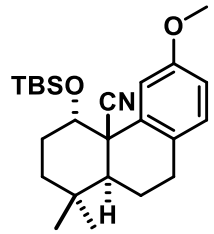

3.37b
HSQC
151 MHz, $CDCl_3$

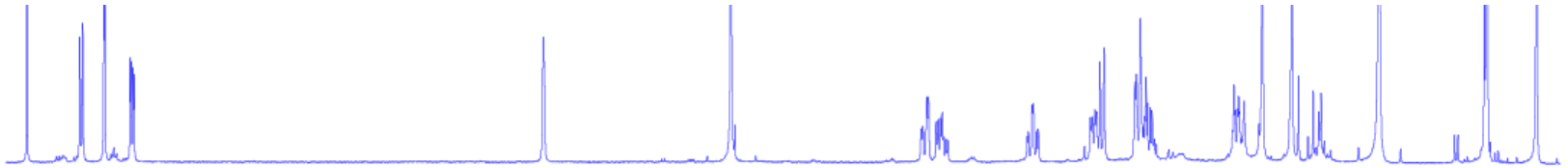

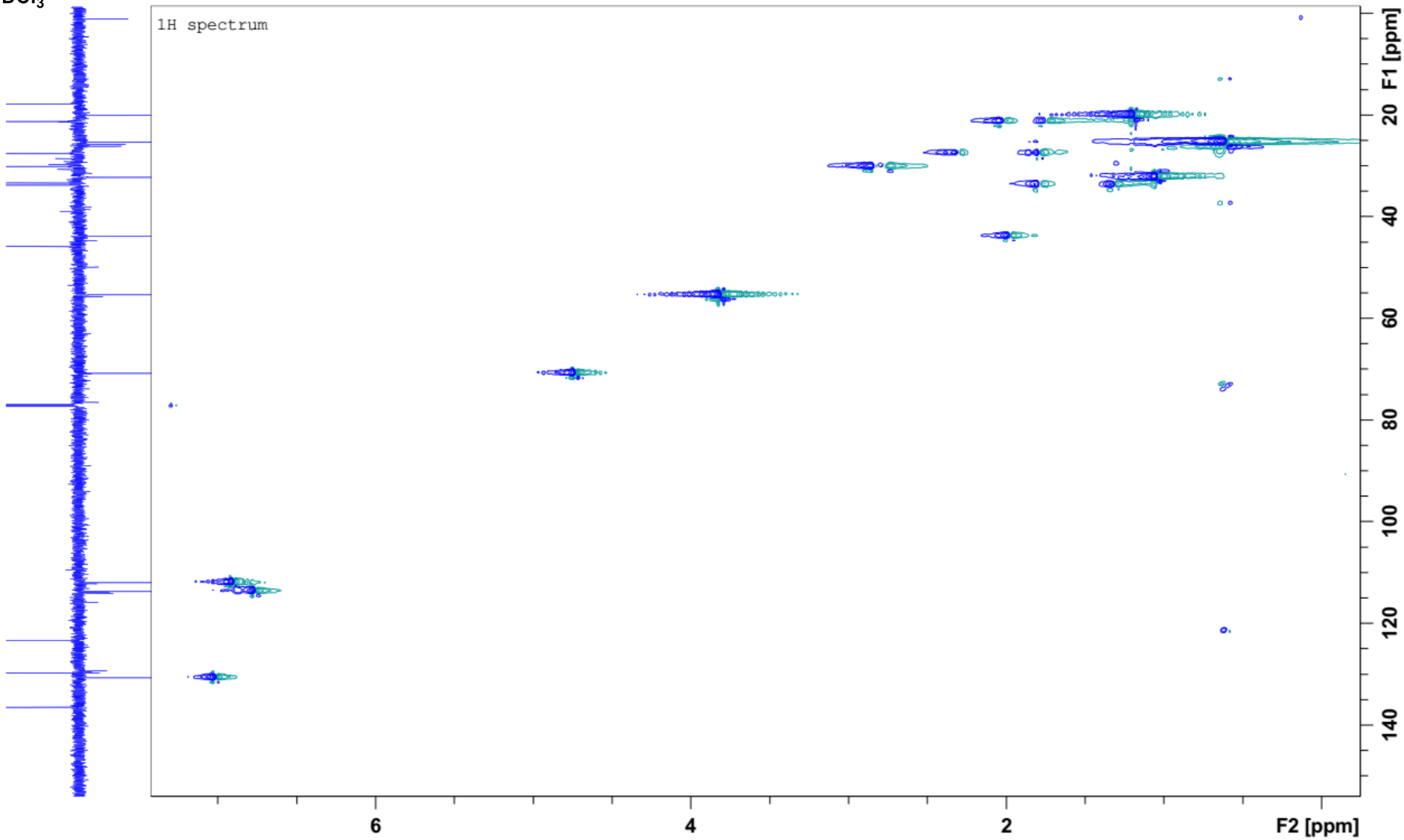

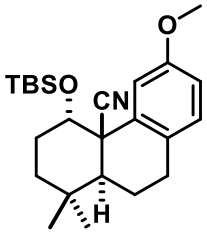

3.37b
^{1}H COSY
600 MHz, $CDCl_3$

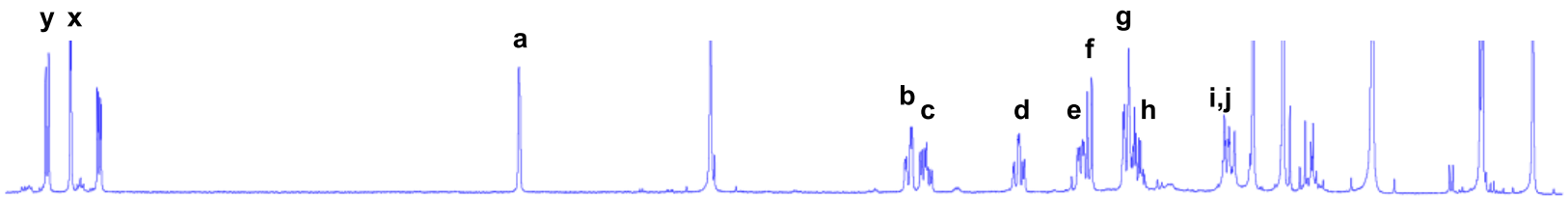

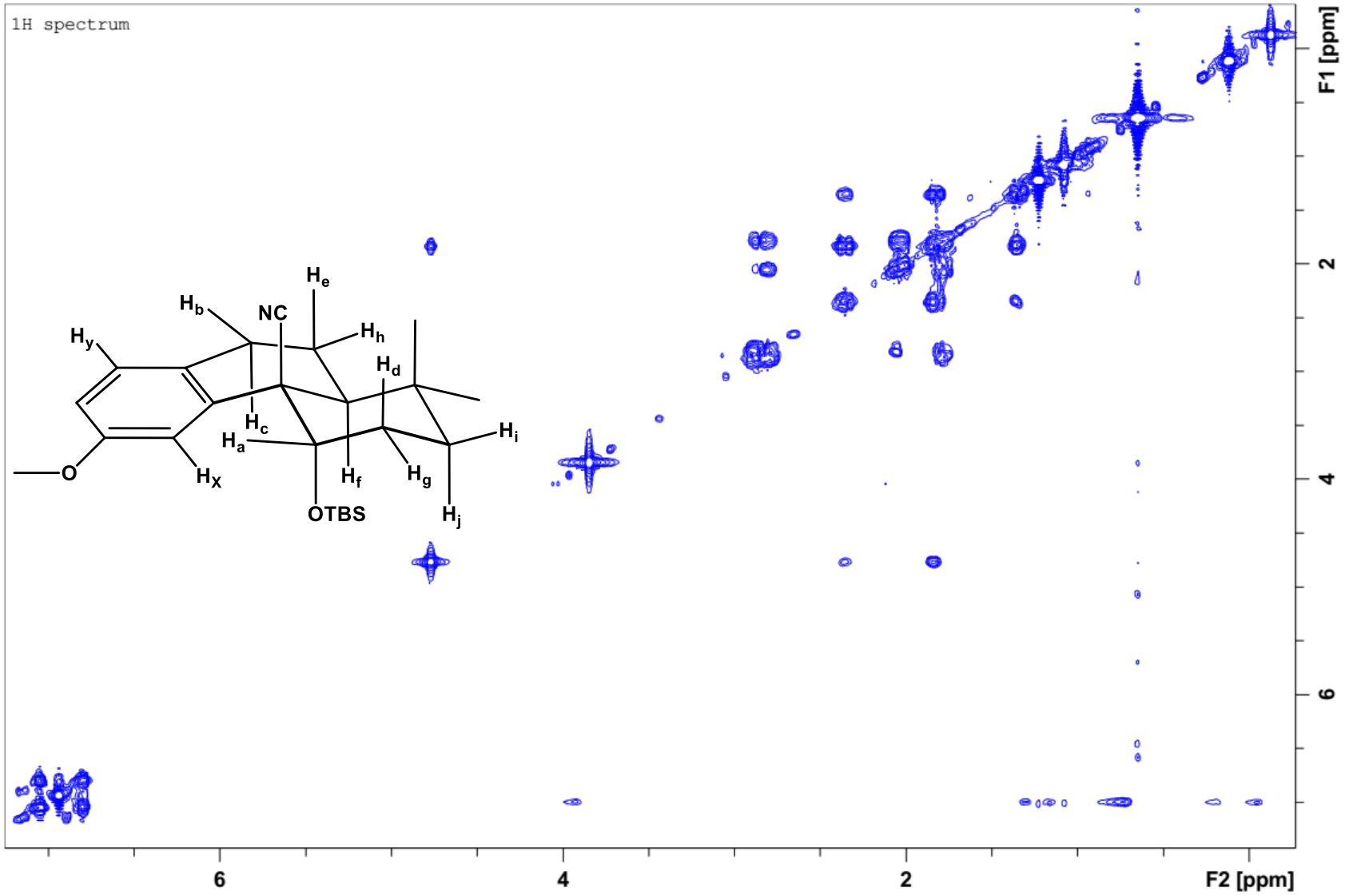

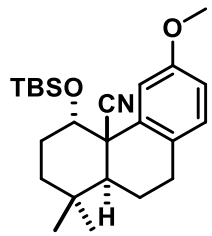

3.37b
NOESY
600 MHz, $CDCl_3$

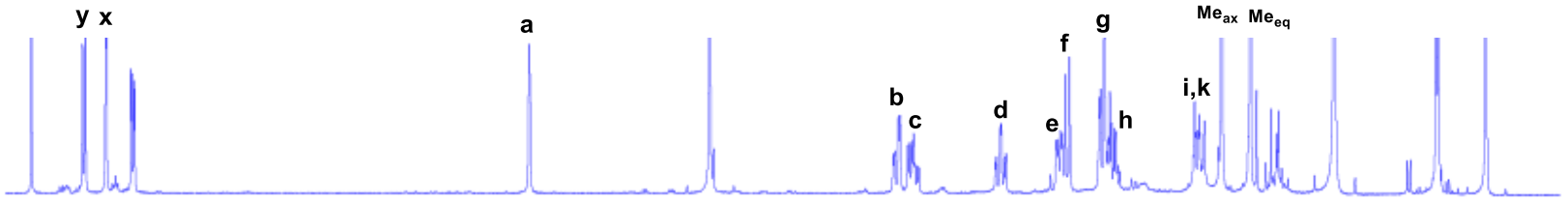

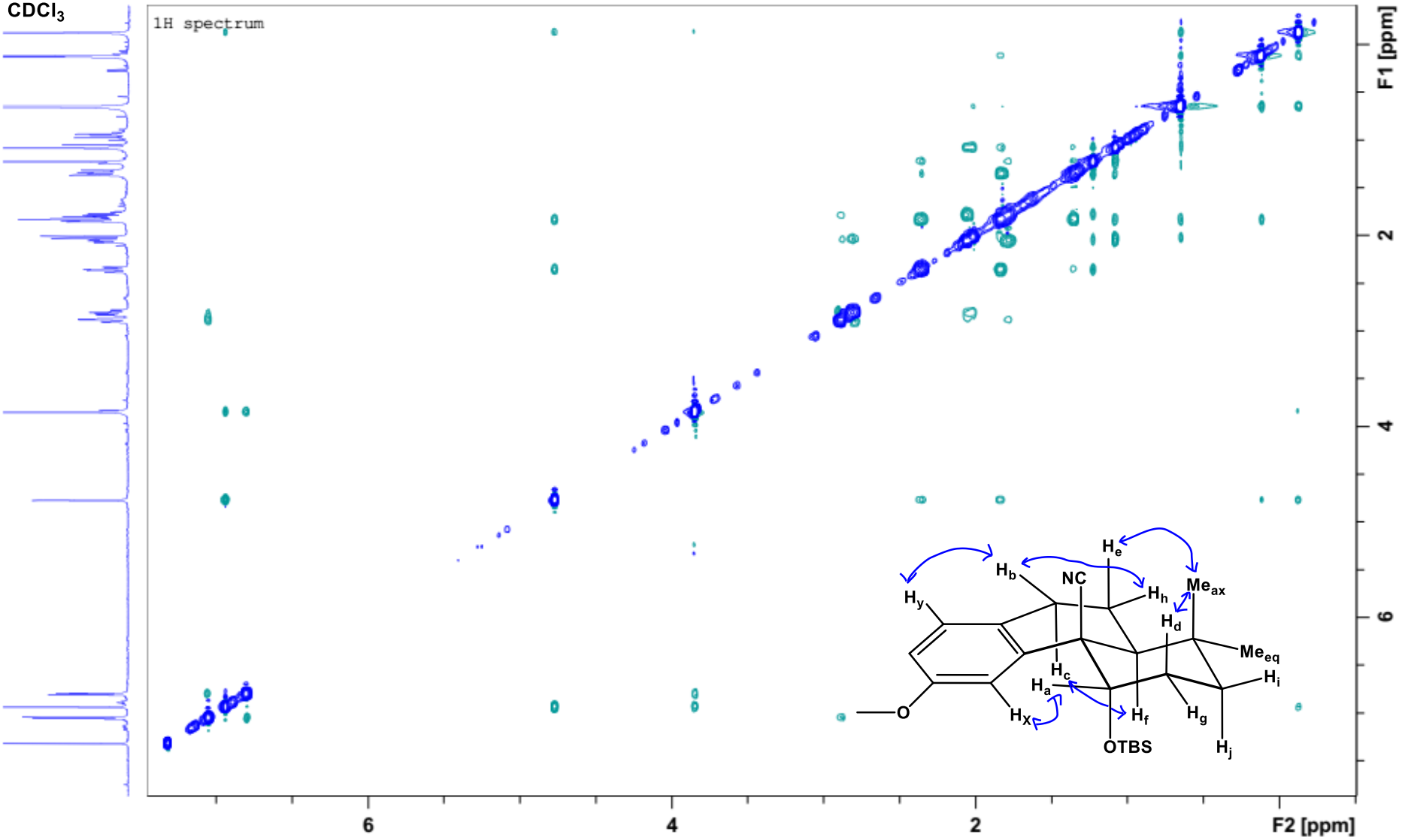

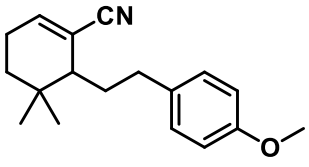

3.39
NOESY
500 MHz, $CDCl_3$

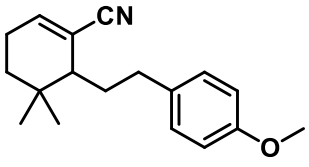

3.39
^{13}C DEPTQ
151 MHz, $CDCl_3$

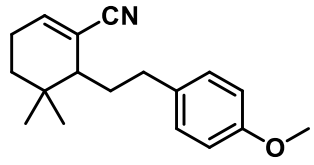

3.39
^{1}H COSY
600 MHz, $CDCl_3$

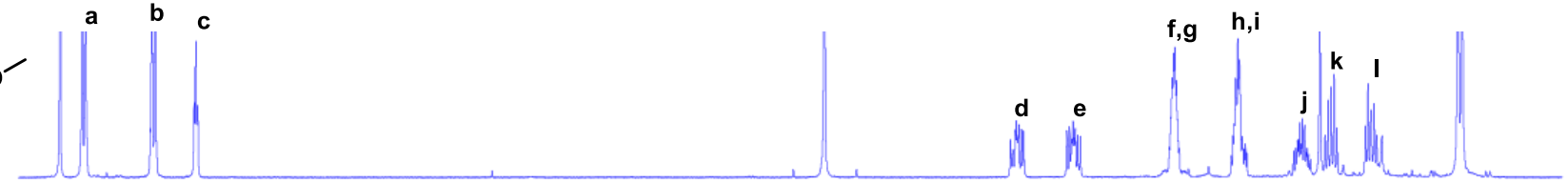

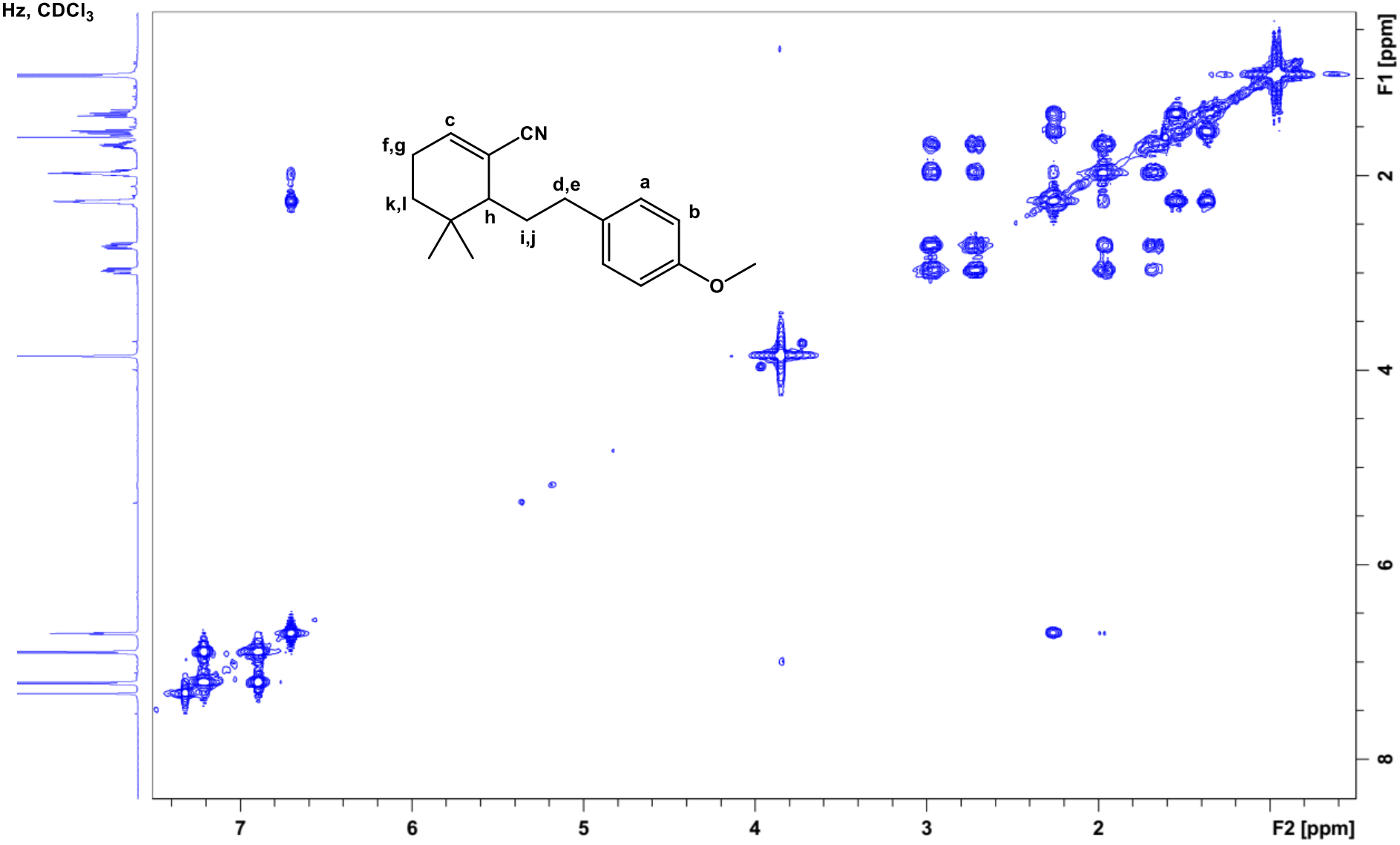

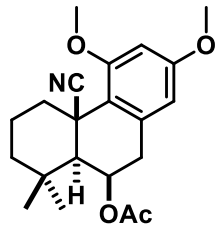

3.48a
^{1}H NMR
600 MHz, $CDCl_3$

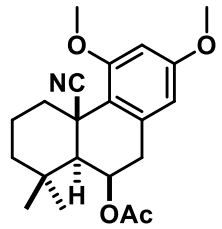

3.48a
^{13}C DEPTQ
151 MHz, $CDCl_3$

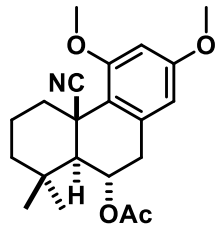

3.49a
^{1}H NMR
500 MHz, $CDCl_3$

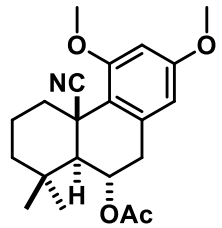

3.49a
^{13}C DEPTQ
151 MHz, $CDCl_3$

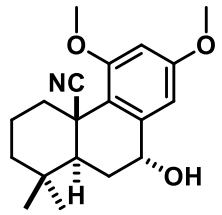

3.51a
^{1}H NMR
600 MHz, $CDCl_3$

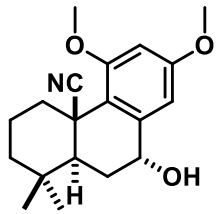

3.51a
^{13}C DEPTQ
151 MHz, $CDCl_3$

160.53
159.95
140.12
122.75
119.32
106.17
100.06
77.37
77.16
76.95
68.59
55.78
55.55
45.28
40.98
39.71
34.85
33.56
32.46
29.63
20.64
20.51

220 210 200 190 180 170 160 150 140 130 120 110 100 90 80 70 60 50 40 30 20 10 0
f1 (ppm)

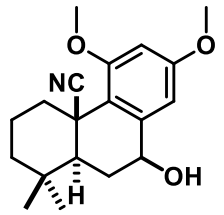

3.52a
^{1}H NMR
600 MHz, $CDCl_3$

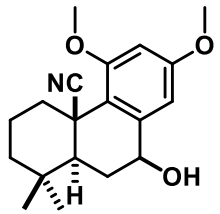

3.52a
^{13}C DEPTQ
151 MHz, $CDCl_3$

160.58
159.45
143.33
122.96
119.03
102.90
99.49
71.36
55.82
55.55
49.90
40.81
40.38
35.15
33.79
32.65
32.17
20.55
20.35

220 210 200 190 180 170 160 150 140 130 120 110 100 90 80 70 60 50 40 30 20 10 0
f1 (ppm)

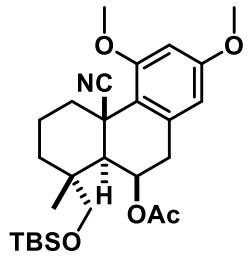

3.57
^{1}H NMR
500 MHz, $CDCl_3$

minor diastereomer

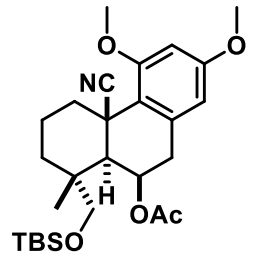

3.57

^{13}C DEPTQ

151 MHz, $CDCl_3$

171.24
160.16
159.84
135.56
123.75
118.01
105.81
98.33
77.37
77.16
76.95
70.62
64.94
55.75
55.40
46.81
38.87
37.73
36.80
35.85
35.75
26.04
21.31
20.07
17.56
-5.31
-5.55

220 210 200 190 180 170 160 150 140 130 120 110 100 90 80 70 60 50 40 30 20 10 0

f1 (ppm)

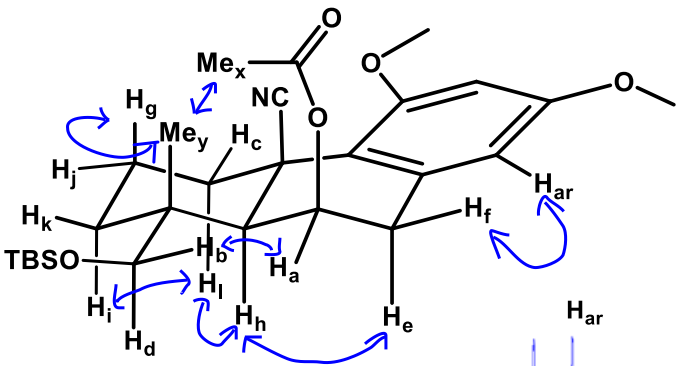

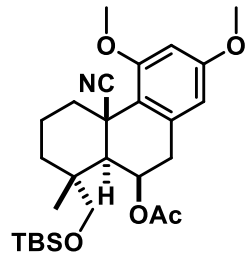

3.57
NOESY
600 MHz, $CDCl_3$

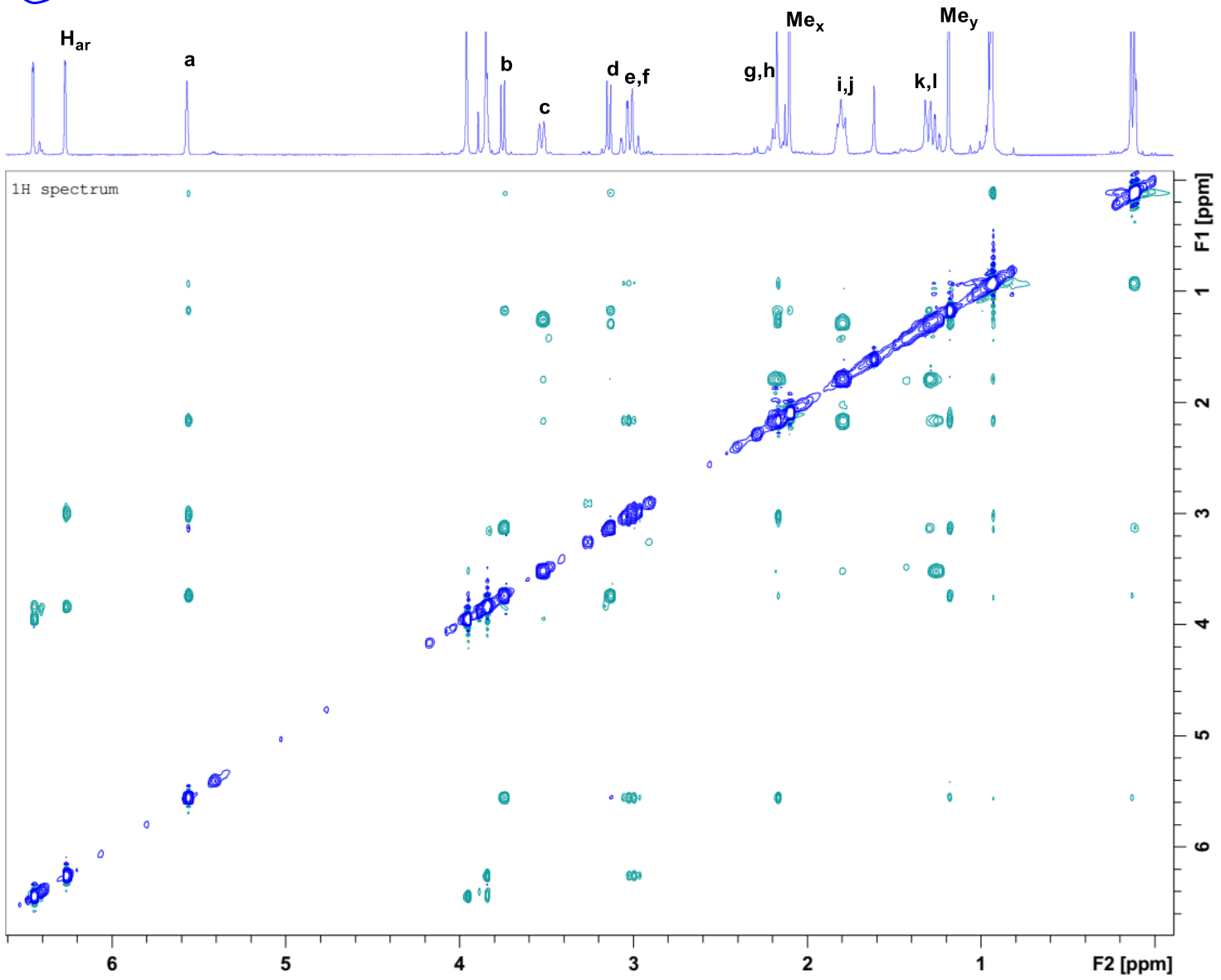

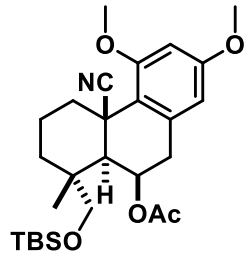

3.57
NOESY
600 MHz, $CDCl_3$

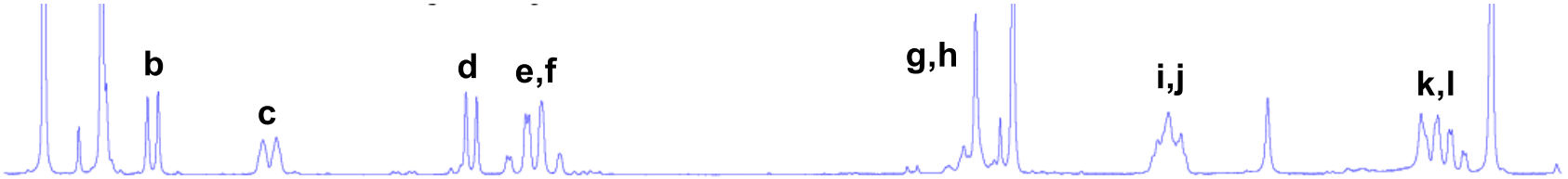

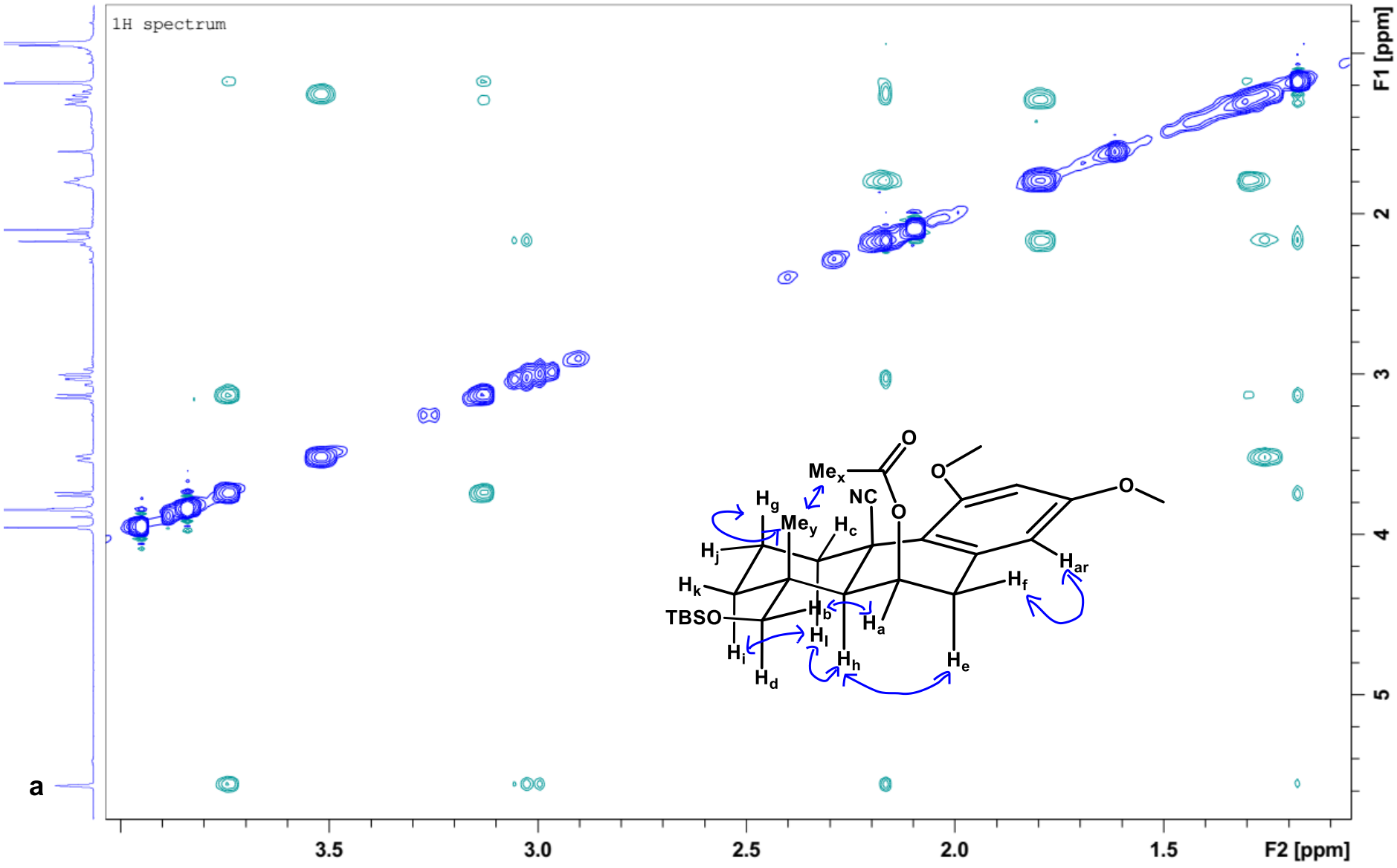

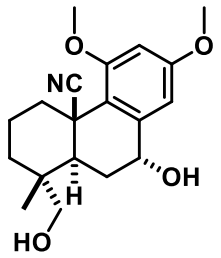

3.54
^{1}H NMR
600 MHz, $CDCl_3$

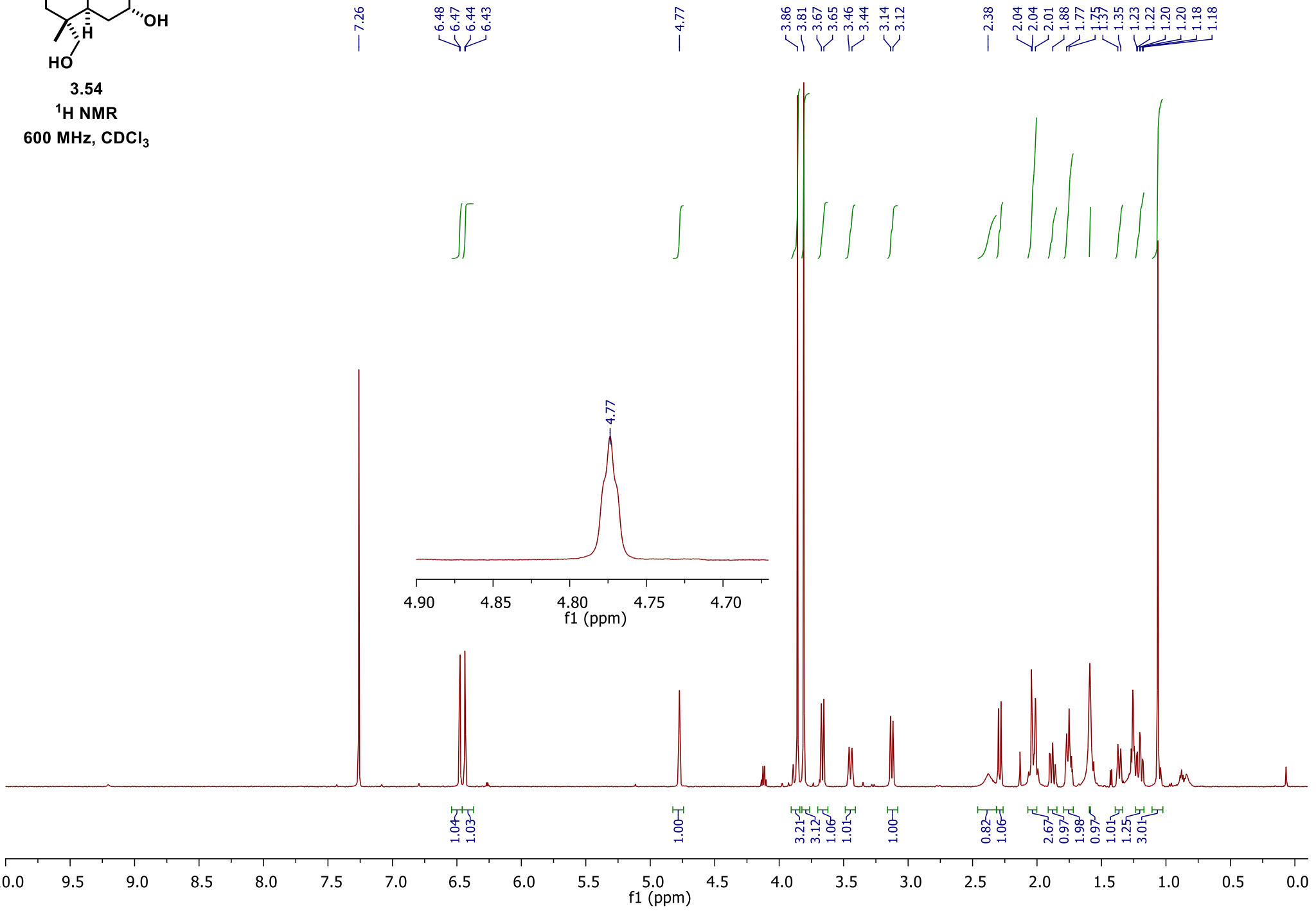

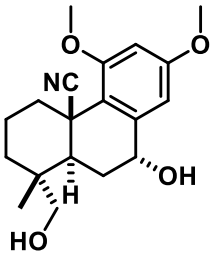

3.54

^{13}C DEPTQ

151 MHz, $CDCl_3$

160.63
159.94
140.14
122.84
119.23
106.29
100.02
77.37
77.16
76.95
70.49
68.88
55.81
55.57
39.61
38.90
37.87
34.52
34.24
28.86
19.95
16.63

220 210 200 190 180 170 160 150 140 130 120 110 100 90 80 70 60 50 40 30 20 10 0

f1 (ppm)

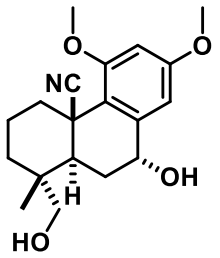

3.54
HSQC
151 MHz, $CDCl_3$

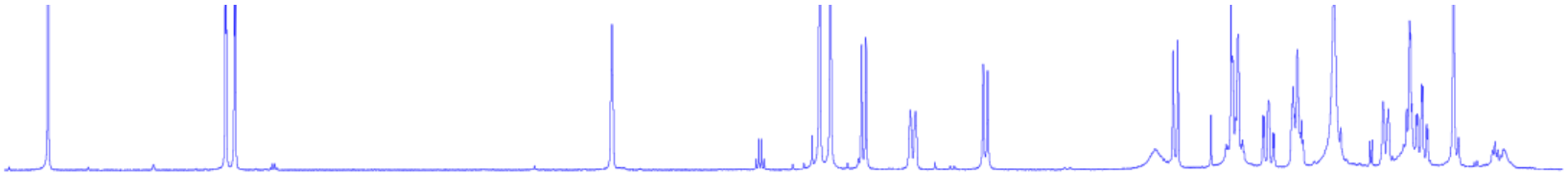

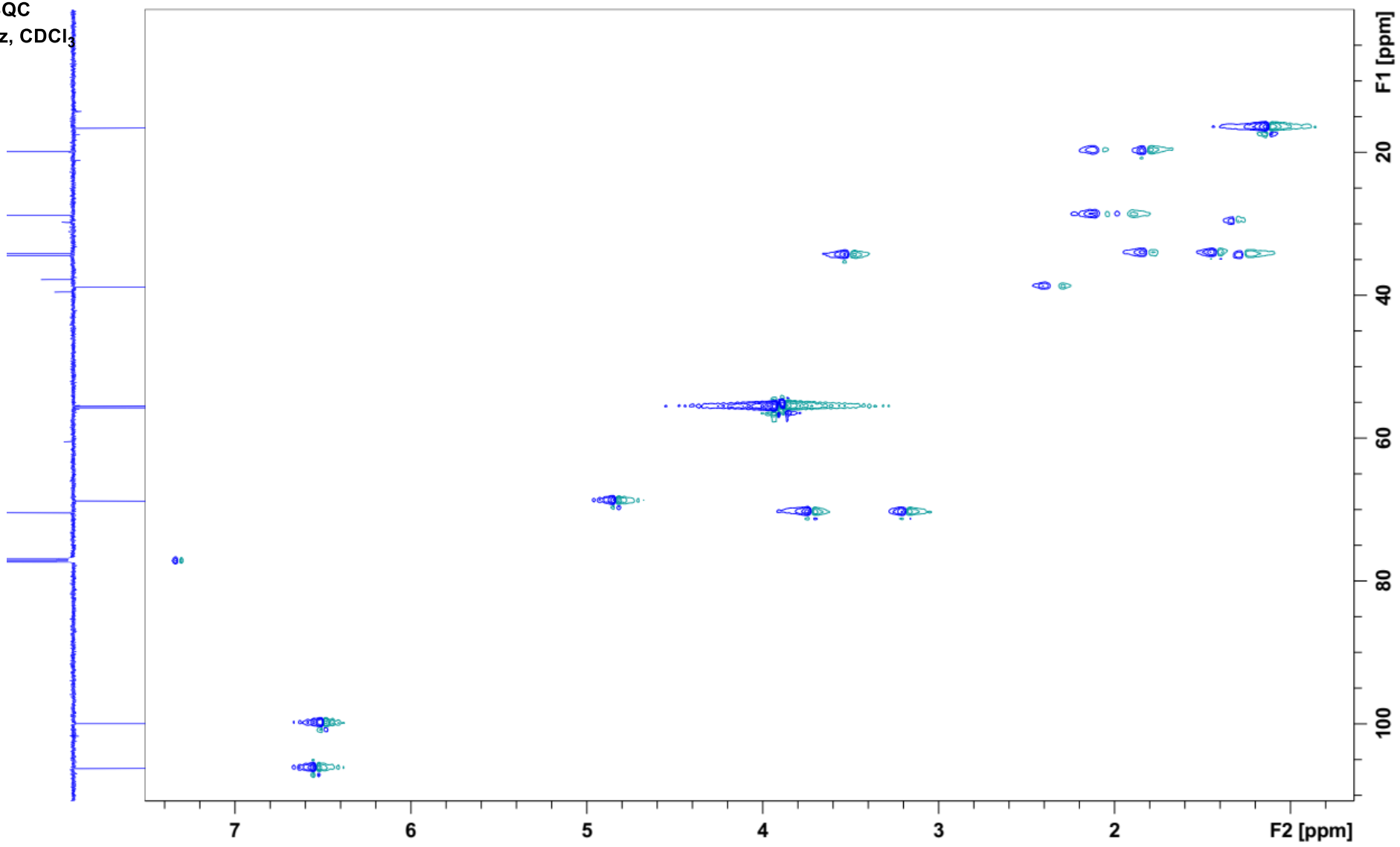

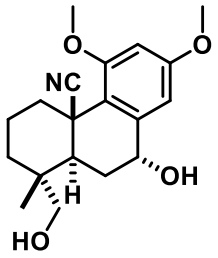

3.54
^{1}H COSY
600 MHz, $CDCl_3$

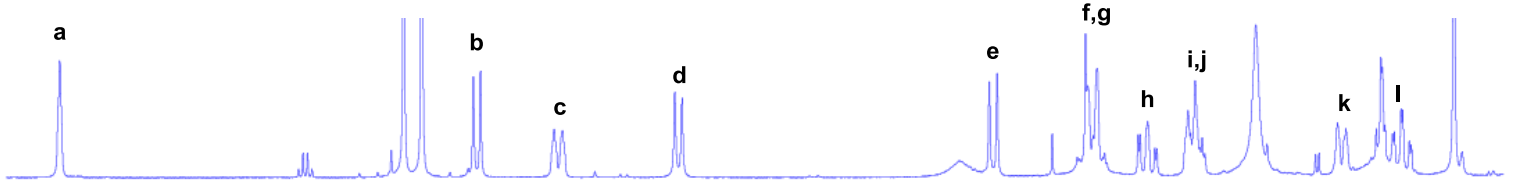

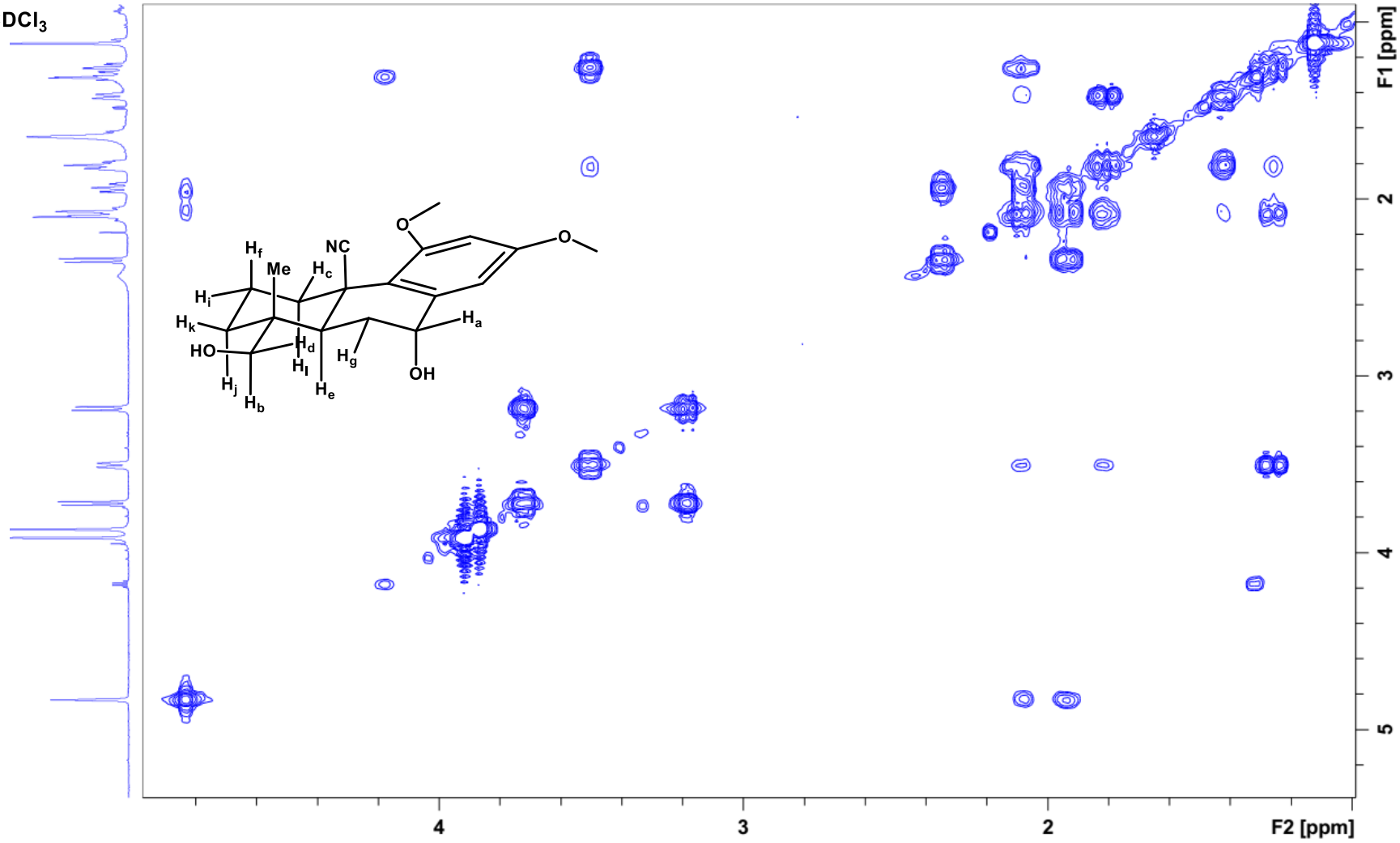

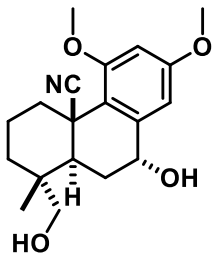

3.54
NOESY
600 MHz, $CDCl_3$

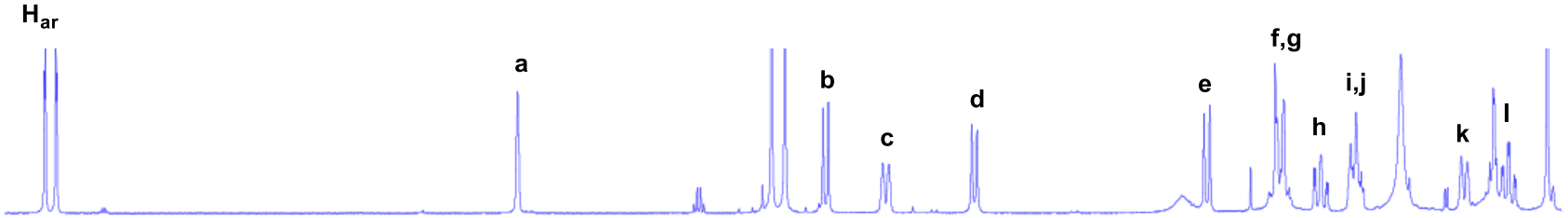

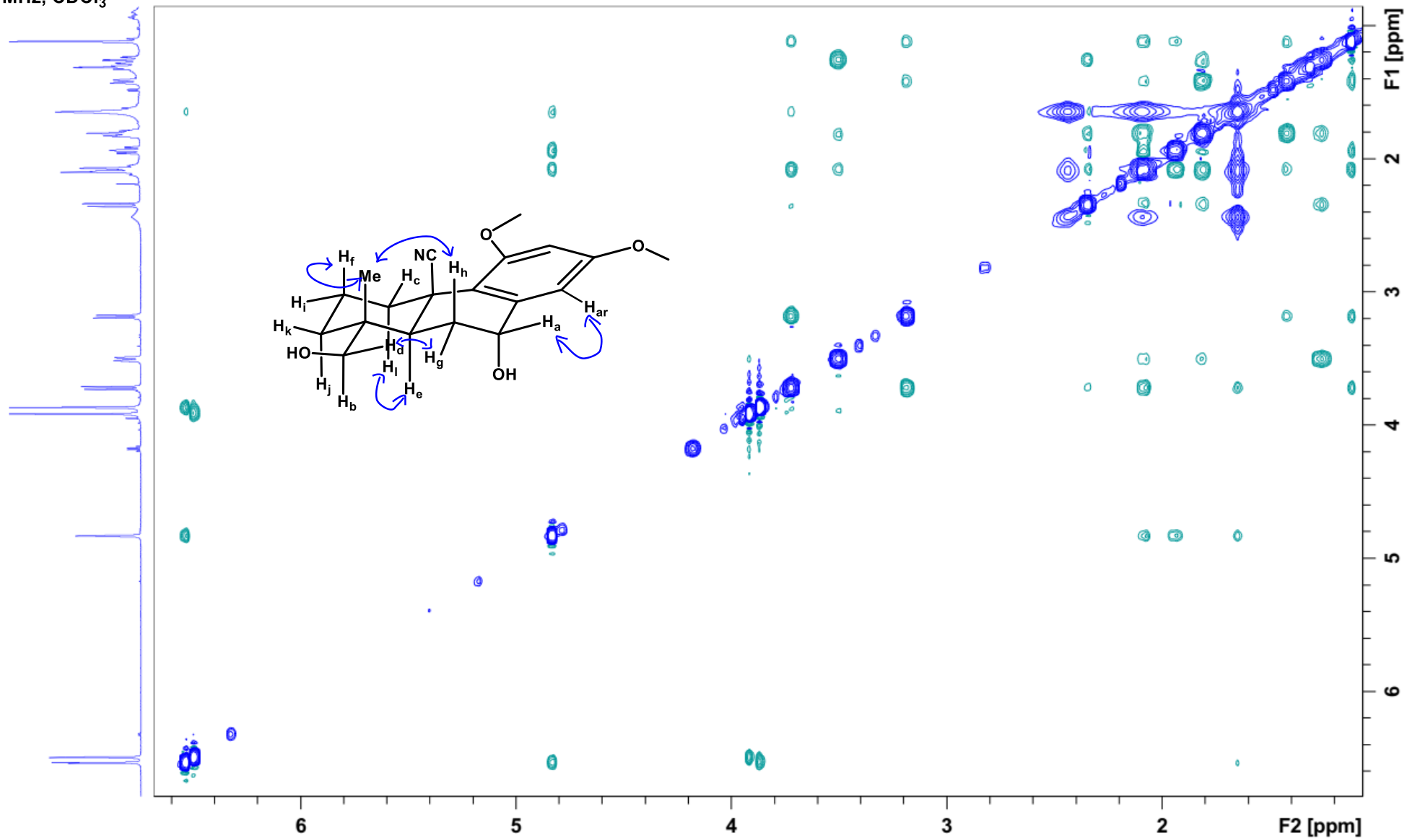

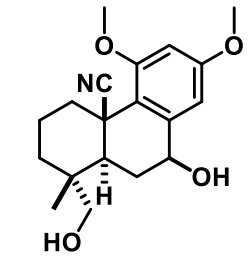

3.55
^{1}H NMR
600 MHz, $CDCl_3$

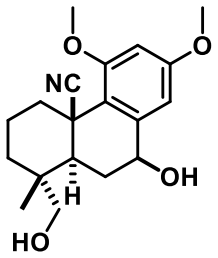

3.55
^{13}C DEPTQ
151 MHz, $CDCl_3$

160.62
159.42
143.38
123.29
118.90
102.83
99.46
77.37
77.16
76.95
70.96
70.73
55.84
55.56
43.15
40.27
38.11
34.72
34.31
31.73
29.85
19.84
16.72

220 210 200 190 180 170 160 150 140 130 120 110 100 90 80 70 60 50 40 30 20 10 0
f1 (ppm)

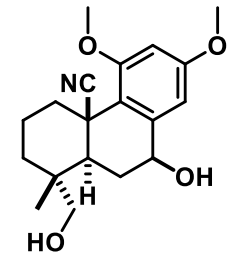

3.55
^{1}H COSY
600 MHz, $CDCl_3$

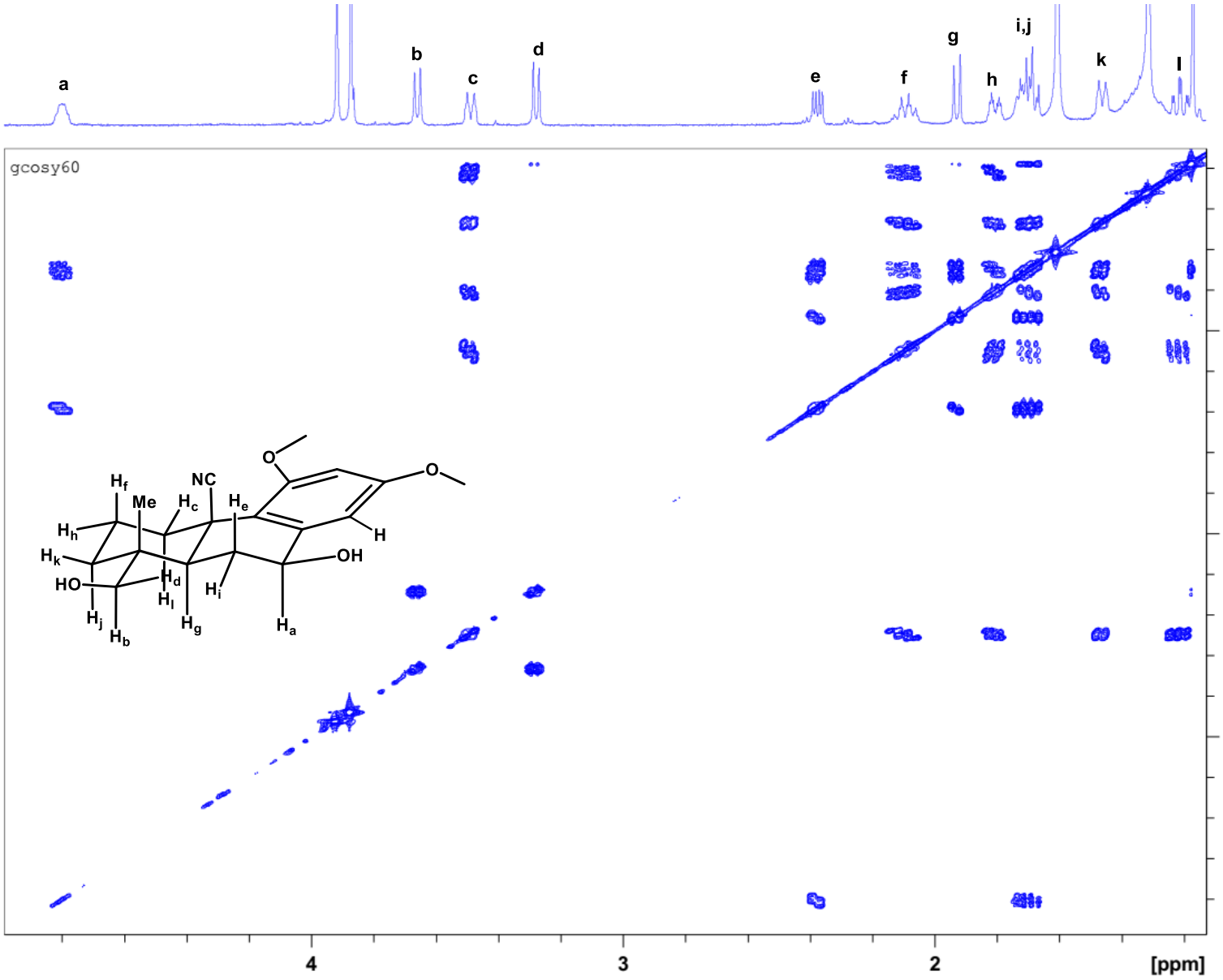

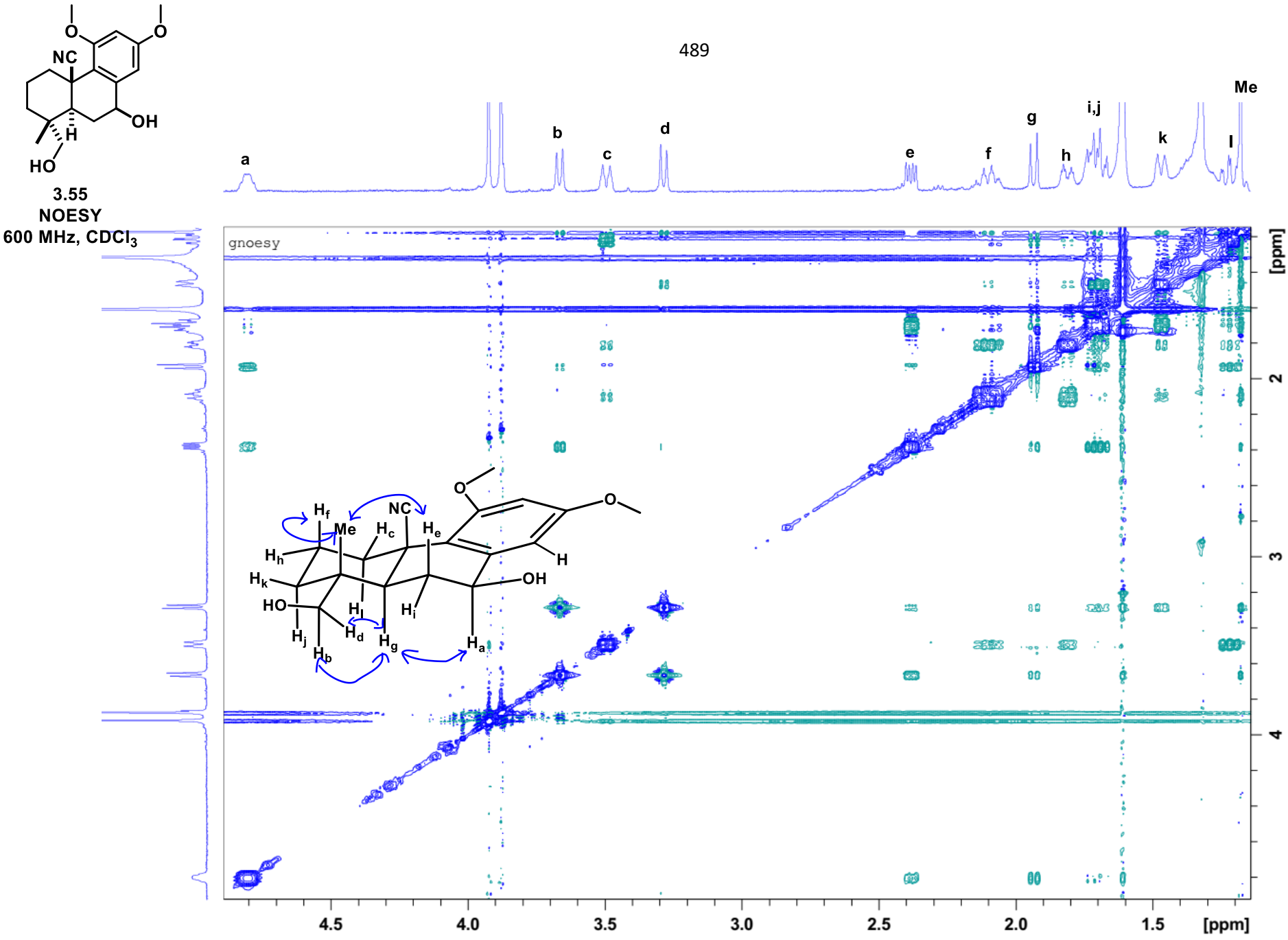
3.55
NOESY
600 MHz, CDCl3
gnoesy
a
b
c
d
e
f
g
h
i,j
k
l
Me
[ppm]
4.5
4.0
3.5
3.0
2.5
2.0
1.5
[ppm]
2
3
4
NC
OH
HO
H
O
Me
Hf
Hc
He
Hh
Hk
Hl
Hi
Hj
Hd
Hg
Hb
Ha

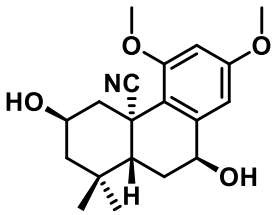

3.60
^{1}H NMR
500 MHz, $CDCl_3$

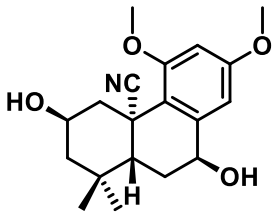

3.60

^{13}C NMR

126 MHz, $CDCl_3$

160.70
159.73
140.08
122.11
118.29
106.34
100.02
77.41
77.16
76.91
68.54
65.44
55.82
55.55
49.89
44.85
42.51
39.33
34.43
32.56
29.31
21.53

210 200 190 180 170 160 150 140 130 120 110 100 90 80 70 60 50 40 30 20 10 0

f1 (ppm)

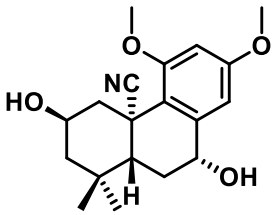

3.61
^{1}H NMR
500 MHz, $CDCl_3$

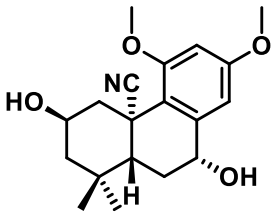

3.61
^{13}C NMR
126 MHz, $CDCl_3$

160.80
159.24
143.25
122.34
117.94
103.14
99.44
77.41
77.16
76.91
71.20
65.15
55.85
55.56
49.67
49.40
42.87
39.91
34.78
32.77
31.72
21.44

220 210 200 190 180 170 160 150 140 130 120 110 100 90 80 70 60 50 40 30 20 10 0
f1 (ppm)

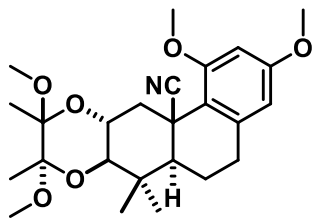

3.63
^{1}H NMR
600 MHz, $CDCl_3$

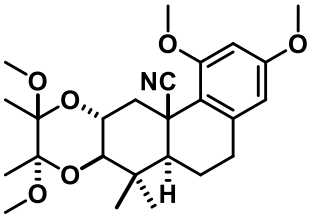

3.63
^{13}C DEPTQ
151 MHz, $CDCl_3$

160.08
160.01
139.64
122.43
118.07
105.33
99.82
99.42
97.72
77.63
77.37
77.16
76.95
65.06
55.75
55.39
52.59
48.23
47.83
38.88
38.30
37.65
32.79
29.85
27.51
20.68
17.97
17.96
15.71

220 210 200 190 180 170 160 150 140 130 120 110 100 90 80 70 60 50 40 30 20 10 0
f1 (ppm)

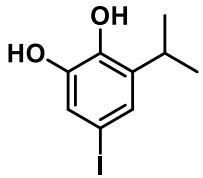

S3.32
^{1}H NMR
500 MHz, $CDCl_3$

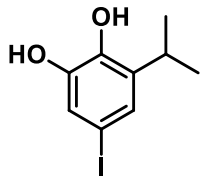

S3.32
^{13}C NMR
151 MHz, $CDCl_3$

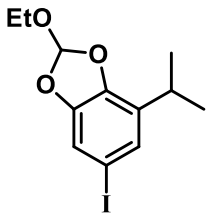

3.68
^{1}H NMR
500 MHz, $CDCl_3$

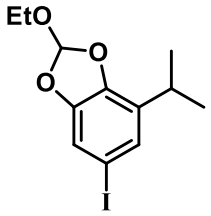

3.68

^{13}C NMR

151 MHz, $CDCl_3$

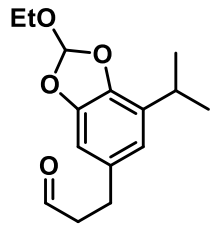

3.69
^{1}H NMR
600 MHz, $CDCl_3$

f1 (ppm)

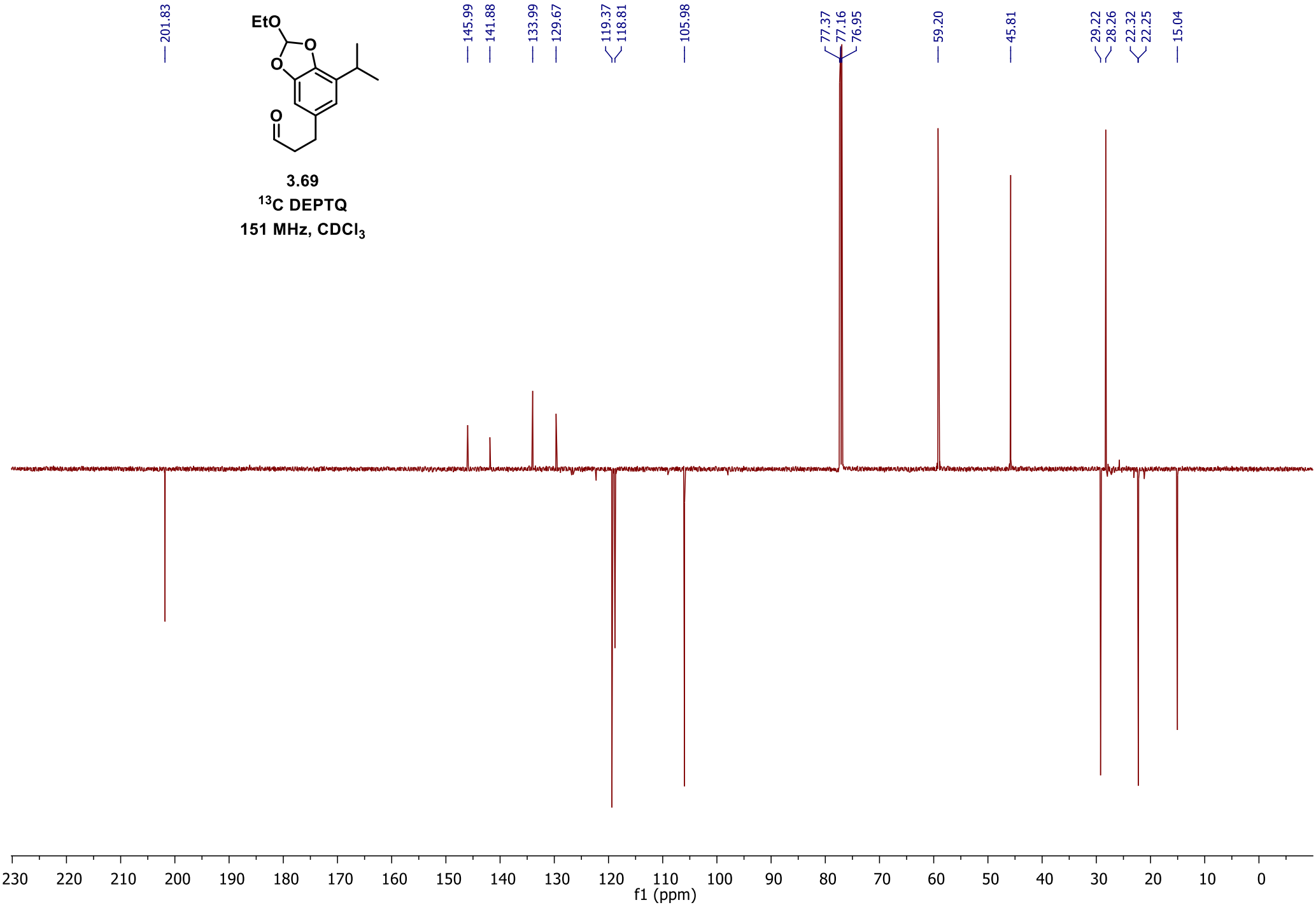
201.83
145.99
141.88
133.99
129.67
119.37
118.81
105.98
77.37
77.16
76.95
59.20
45.81
29.22
28.26
22.32
22.25
15.04
EtO
O
O
O
3.69
13C DEPTQ
151 MHz, CDCl3
230 220 210 200 190 180 170 160 150 140 130 120 110 100 90 80 70 60 50 40 30 20 10 0
f1 (ppm)

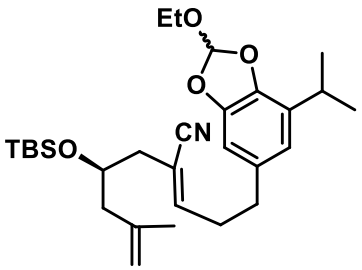

3.70
^{1}H NMR
500 MHz, $CDCl_3$

f1 (ppm)

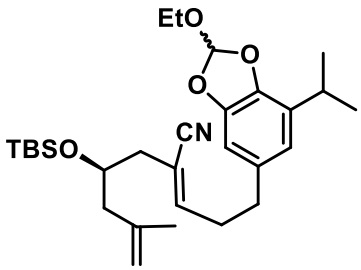

3.70

^{13}C NMR

151 MHz, $CDCl_3$

149.10
145.93
141.93
141.92
141.86
133.90
129.49
119.35
118.72
117.73
113.85
112.62
105.97
105.95
77.37
77.16
76.95
68.93
58.97
45.94
45.93
41.65
34.67
33.58
29.21
25.93
25.90
23.00
22.27
22.18
18.10
14.98
-4.41
-4.58

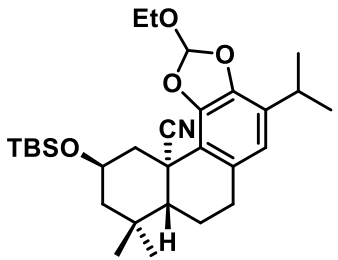

3.71

^{1}H NMR

500 MHz, $CDCl_3$

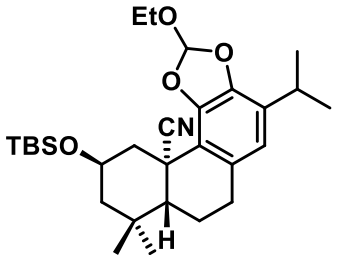

3.71

^{13}C NMR

126 MHz, $CDCl_3$

143.40
142.20
129.83
129.77
122.18
120.32
118.49
116.96
77.41
77.16
76.91
65.89
58.36
50.90
50.49
43.27
39.30
34.88
32.51
31.01
28.97
26.10
22.16
22.13
21.63
21.27
18.42
15.13
-4.39
-4.45

220 210 200 190 180 170 160 150 140 130 120 110 100 90 80 70 60 50 40 30 20 10 0

f1 (ppm)

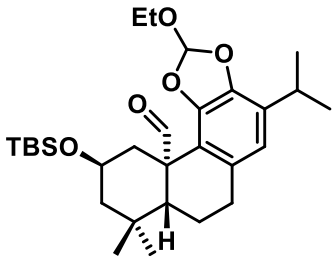

S3.33
^{1}H NMR
500 MHz, $CDCl_3$

f1 (ppm)

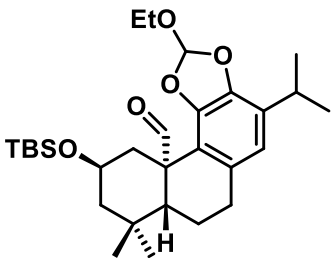

S3.33
^{13}C DEPTQ
151 MHz, $CDCl_3$

197.94
144.58
142.18
131.51
129.38
120.25
118.36
114.56
77.37
77.16
76.95
65.04
58.88
52.18
50.86
39.24
34.76
32.06
31.20
28.81
26.08
26.01
22.23
22.09
21.85
18.54
15.02
-4.39
-4.49

220 210 200 190 180 170 160 150 140 130 120 110 100 90 80 70 60 50 40 30 20 10 0
f1 (ppm)

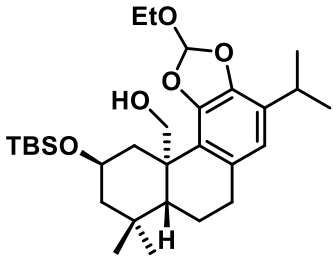

3.72

^{1}H NMR

500 MHz, $CDCl_3$

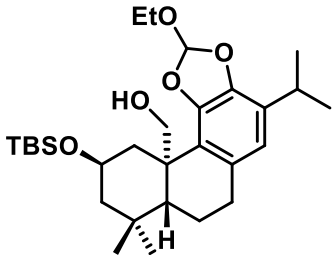

3.72

^{13}C NMR

151 MHz, $CDCl_3$

143.04
141.38
130.80
128.13
123.37
120.33
117.72
77.37
77.16
76.95
66.80
65.43
58.64
51.04
50.94
44.94
42.52
34.61
33.96
30.60
28.77
26.04
23.21
22.33
22.16
18.67
18.37
15.02
-4.38
-4.41

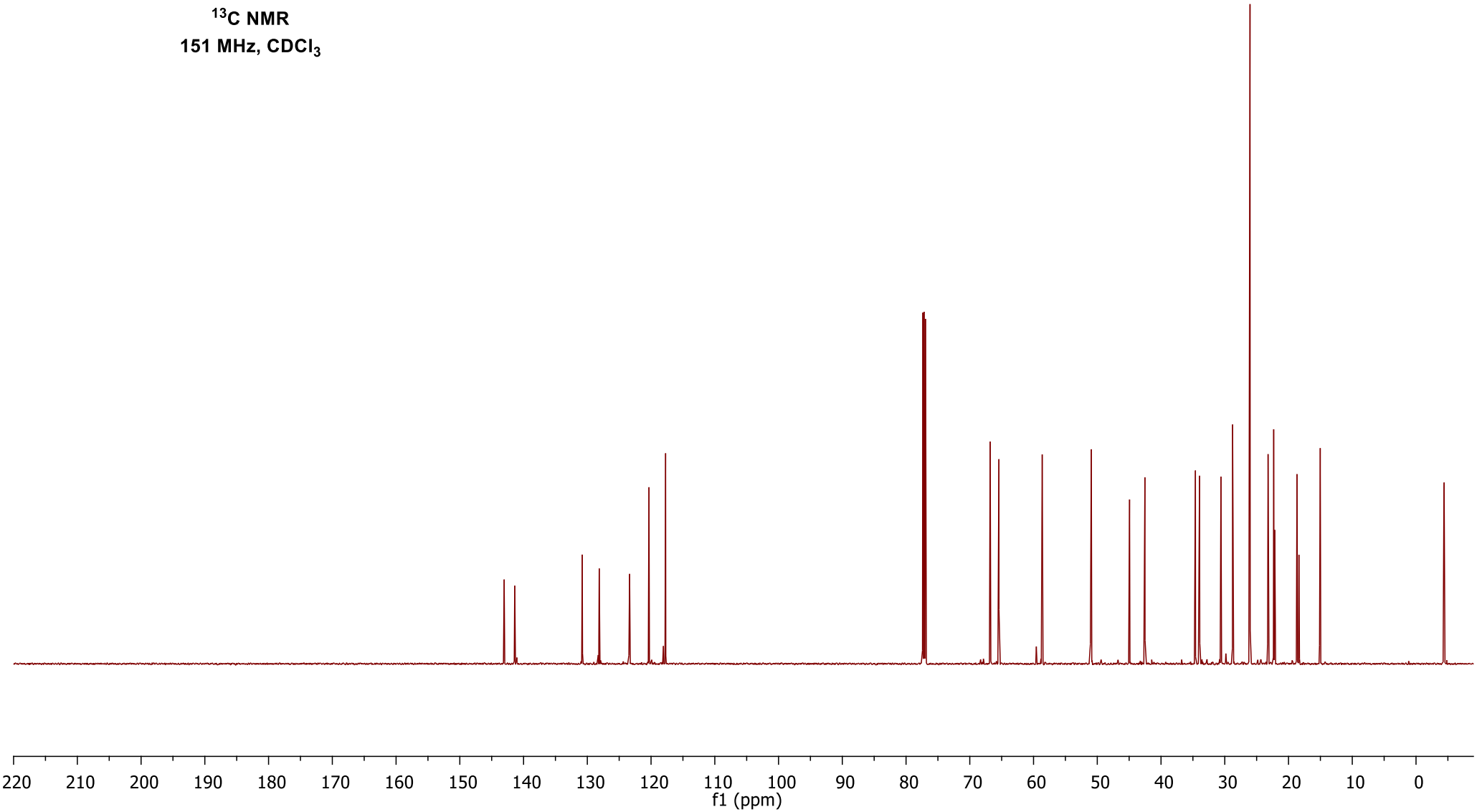

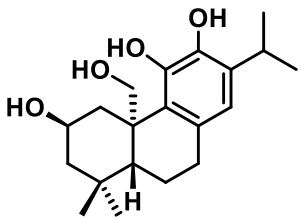

3.73

^{1}H NMR

500 MHz, $CDCl_3$

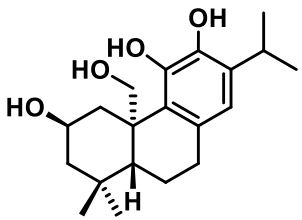

3.73

^{13}C NMR

151 MHz, $CDCl_3$

142.30
142.04
132.94
129.67
127.25
119.14
77.37
77.16
76.95
67.72
65.18
52.50
50.19
45.45
40.47
34.69
34.30
31.99
27.25
23.67
22.70
22.40
18.67

220 210 200 190 180 170 160 150 140 130 120 110 100 90 80 70 60 50 40 30 20 10 0

f1 (ppm)

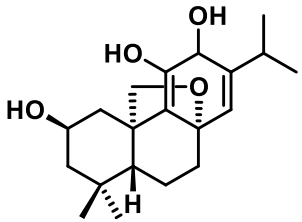

3.14

(+)-2-O-deacetyl plebedipene A

^{1}H NMR

500 MHz, $CDCl_3$

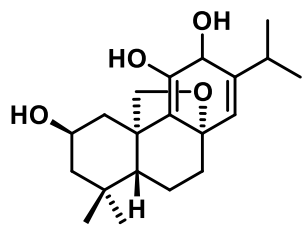

3.14

(+)-2-O-deacetyl plebedipene A

^{13}C NMR

151 MHz, $CDCl_3$

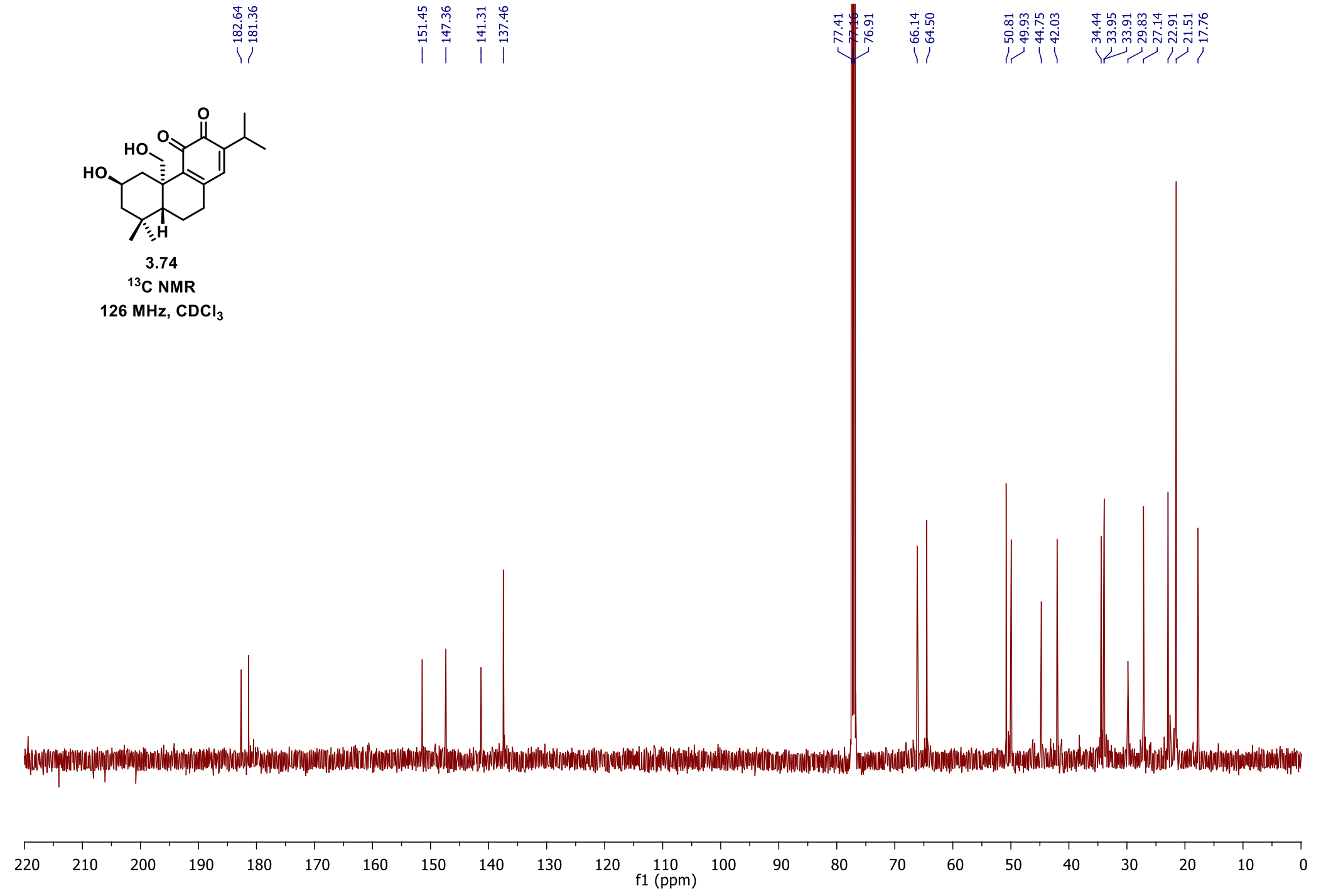
182.64
181.36
151.45
147.36
141.31
137.46
77.41
77.16
76.91
66.14
64.50
50.81
49.93
44.75
42.03
34.44
33.95
33.91
29.83
27.14
22.91
21.51
17.76
O
O
HO
HO
H
3.74
13C NMR
126 MHz, CDCl3
220
210
200
190
180
170
160
150
140
130
120
110
100
90
80
70
60
50
40
30
20
10
0
f1 (ppm)

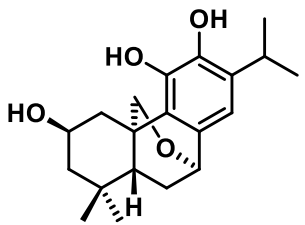

3.17

(+)-2-O-deacetyl plebedipene C

^{1}H NMR

500 MHz, DMSO-d_6

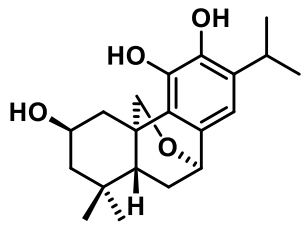

3.17

(+)-2-O-deacetyl plebedipene C

^{13}C NMR

151 MHz, DMSO-d_6

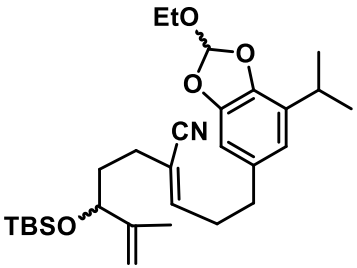

3.76

^{1}H NMR

600 MHz, $CDCl_3$

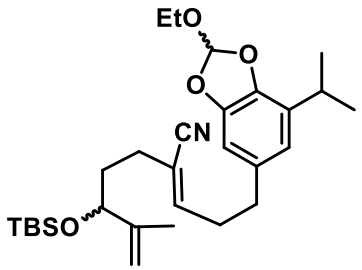

3.76

^{13}C DEPTQ

151 MHz, $CDCl_3$

146.93
146.44
145.95
141.88
133.98
129.55
119.44
118.78
117.67
115.39
111.47
106.06
77.37
77.16
76.95
75.57
59.12
34.87
34.62
33.49
30.33
29.22
25.95
22.35
22.27
18.33
17.42
15.06
-4.62
-4.96

220 210 200 190 180 170 160 150 140 130 120 110 100 90 80 70 60 50 40 30 20 10 0

f1 (ppm)

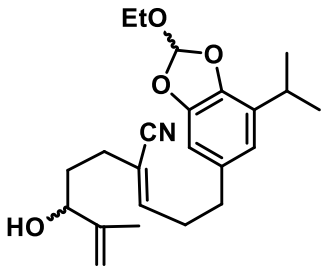

3.77

^{1}H NMR

600 MHz, $CDCl_3$

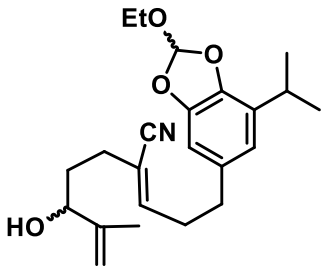

3.77

^{13}C DEPTQ

151 MHz, $CDCl_3$

147.11
147.01
146.97
146.95
145.82
145.72
141.77
133.81
129.59
129.51
119.39
119.36
118.69
117.50
117.47
114.86
114.84
111.38
111.29
106.07
105.99
77.29
77.07
76.86
74.38
74.23
59.14
59.13
34.69
33.39
33.30
33.12
33.01
30.36
29.14
29.12
22.25
22.23
22.18
22.15
17.71
14.95

220 210 200 190 180 170 160 150 140 130 120 110 100 90 80 70 60 50 40 30 20 10 0

f1 (ppm)

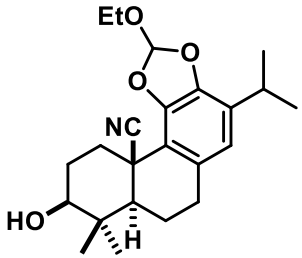

3.78

^{1}H NMR

500 MHz, $CDCl_3$

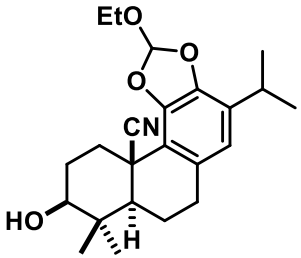

3.78

^{13}C NMR

126 MHz, $CDCl_3$

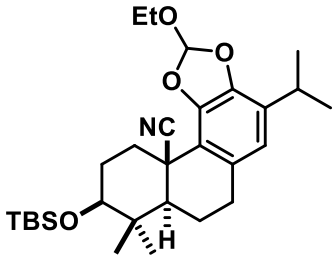

S3.35
^{1}H NMR
500 MHz, $CDCl_3$

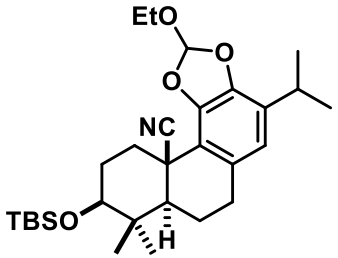

S3.35

^{13}C NMR

126 MHz, $CDCl_3$

143.52
142.13
129.94
129.67
122.23
120.26
118.36
117.29
77.41
77.16
76.91
57.99
50.91
40.16
38.94
32.92
31.08
29.85
28.98
27.68
25.99
22.17
22.13
21.92
18.24
15.03
14.39
-3.69
-4.79

220 210 200 190 180 170 160 150 140 130 120 110 100 90 80 70 60 50 40 30 20 10 0

f1 (ppm)

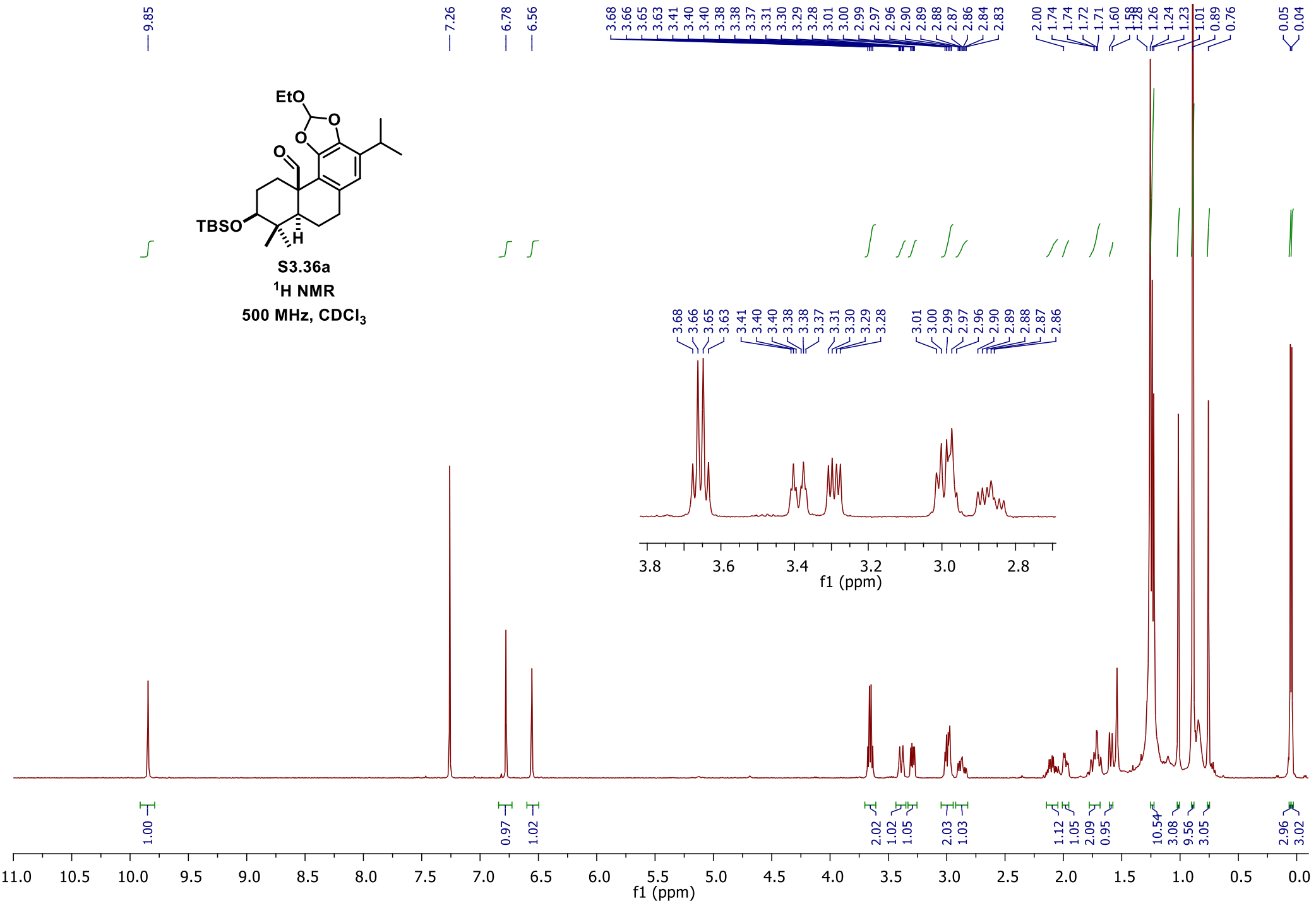
EtO
O
O
O
TBSO
H
S3.36a
^{1}H NMR
500 MHz, $CDCl_3$
f1 (ppm)

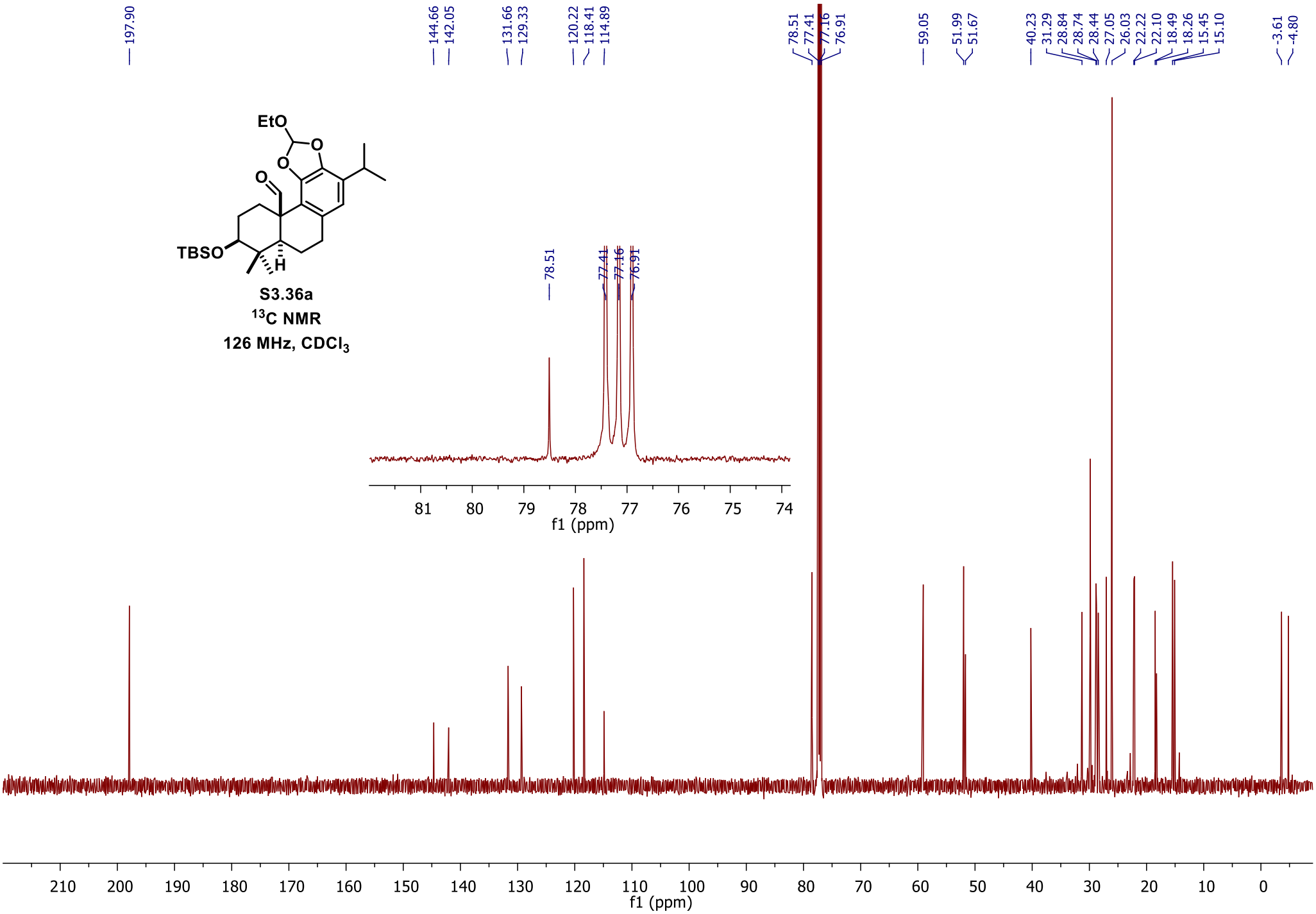
197.90
144.66
142.05
131.66
129.33
120.22
118.41
114.89
78.51
77.41
77.16
76.91
59.05
51.99
51.67
40.23
31.29
28.84
28.74
28.44
27.05
26.03
22.22
22.10
18.49
18.26
15.45
15.10
-3.61
-4.80
EtO
O
O
O
TBSO
H
S3.36a
13C NMR
126 MHz, CDCl3
f1 (ppm)
f1 (ppm)

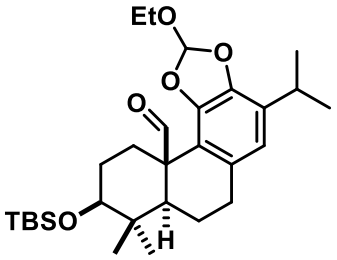

S3.36b
(*minor orthoformate diastereomer, not assigned*)
^{1}H NMR
500 MHz, $CDCl_3$

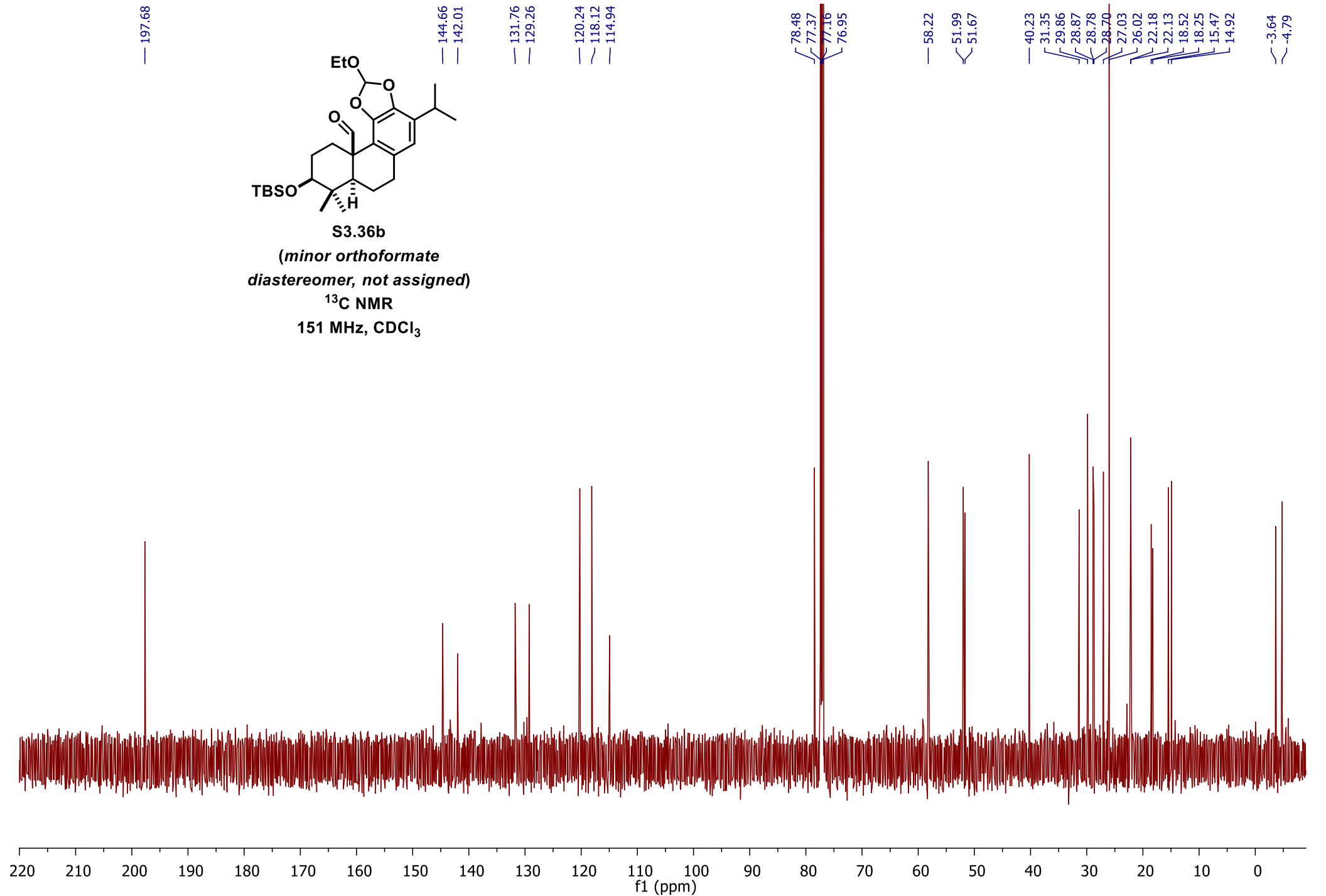
197.68
144.66
142.01
131.76
129.26
120.24
118.12
114.94
78.48
77.37
77.16
76.95
58.22
51.99
51.67
40.23
31.35
29.86
28.87
28.78
28.70
27.03
26.02
22.18
22.13
18.52
18.25
15.47
14.92
-3.64
-4.79
EtO
O
O
O
TBSO
H
S3.36b
(minor orthoformate
diastereomer, not assigned)
13C NMR
151 MHz, CDCl3
220
210
200
190
180
170
160
150
140
130
120
110
100
90
80
70
60
50
40
30
20
10
0
f1 (ppm)

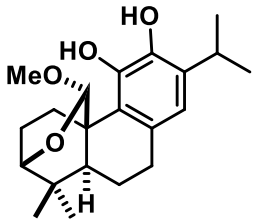

3.16

(+/-)-plebedipene B

^{1}H NMR

600 MHz, $CDCl_3$

f1 (ppm)

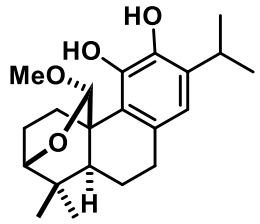

3.16

(+/-)-plebedipene B

^{13}C DEPTQ

151 MHz, $CDCl_3$

142.78
142.35
133.06
128.63
122.34
118.41
103.59
77.37
77.16
76.95
76.91
55.19
51.40
40.33
36.79
31.81
29.60
27.31
24.38
23.39
22.88
22.62
22.34
21.10

220 210 200 190 180 170 160 150 140 130 120 110 100 90 80 70 60 50 40 30 20 10 0

f1 (ppm)

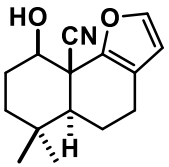

3.88

^{1}H NMR

600 MHz, $CDCl_3$

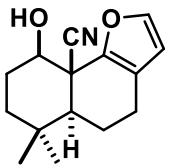

3.88

^{13}C DEPTQ

151 MHz, $CDCl_3$

148.15
142.84
119.78
119.07
110.88
77.37
77.16
76.95
74.76
50.56
46.16
39.39
32.86
31.79
27.53
22.20
21.73
19.98

230 220 210 200 190 180 170 160 150 140 130 120 110 100 90 80 70 60 50 40 30 20 10 0

f1 (ppm)

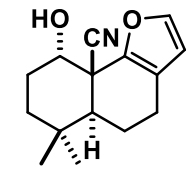

3.89

^{1}H NMR

600 MHz, $CDCl_3$

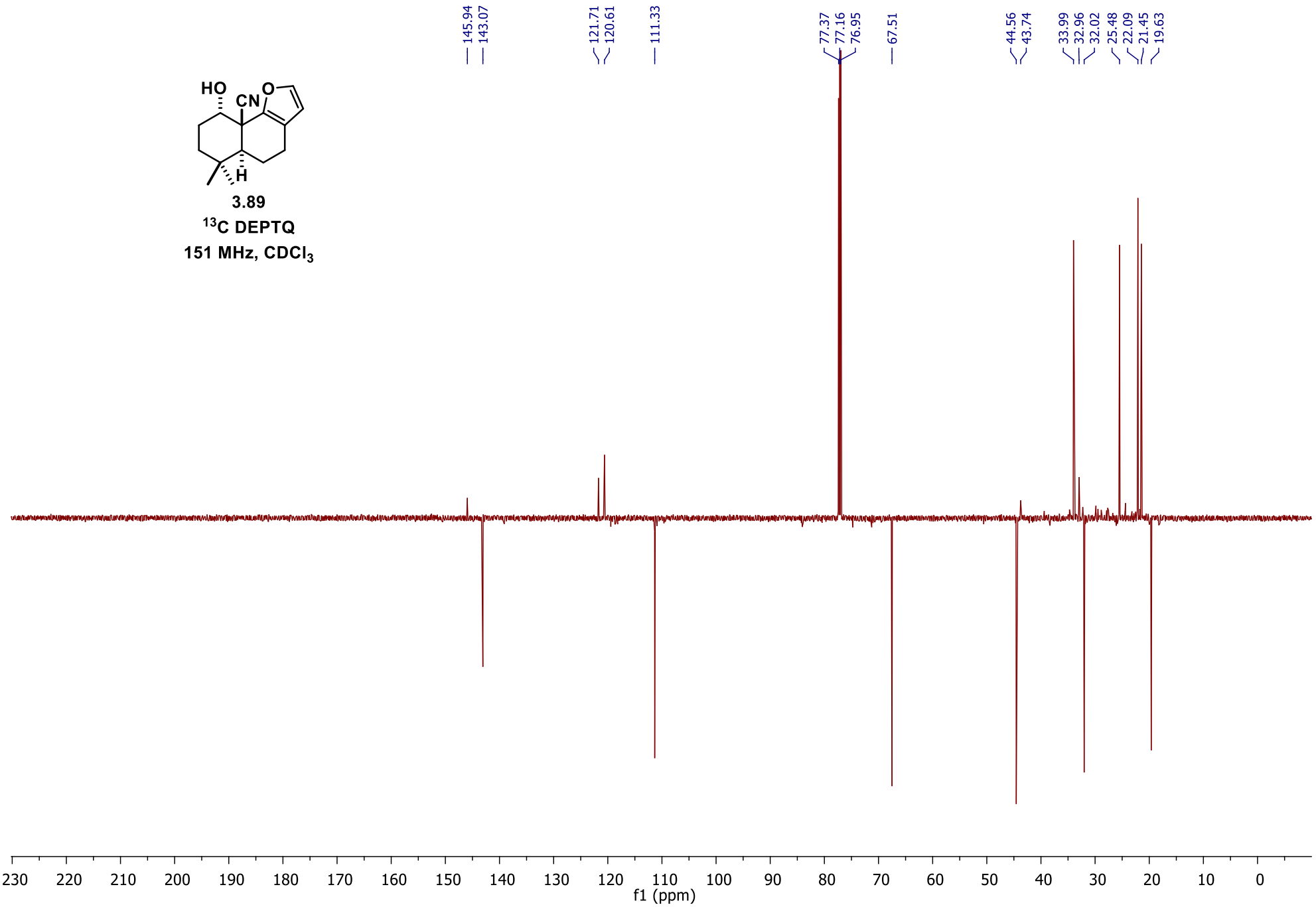
145.94
143.07
121.71
120.61
111.33
77.37
77.16
76.95
67.51
44.56
43.74
33.99
32.96
32.02
25.48
22.09
21.45
19.63
HO
CN
O
H
3.89
13C DEPTQ
151 MHz, CDCl3
230 220 210 200 190 180 170 160 150 140 130 120 110 100 90 80 70 60 50 40 30 20 10 0
f1 (ppm)

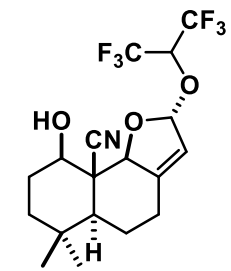

3.90
^{1}H NMR
600 MHz, $CDCl_3$

f1 (ppm)

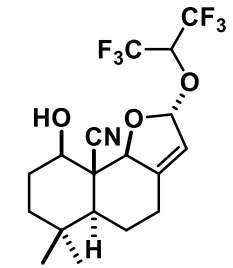

3.90

^{13}C DEPTQ

151 MHz, $CDCl_3$

APPENDIX B: X-RAY CRYSTALLOGRAPHIC DATA

X-ray Data Collection, Structure Solution and Refinement for cdv56 (**2.6e**)

A colorless crystal of approximate dimensions 0.198 x 0.243 x 0.417 mm was mounted in a cryoloop and transferred to a Bruker SMART APEX II diffractometer. The APEX2[1] program package was used to determine the unit-cell parameters and for data collection (30 sec/frame scan time for a sphere of diffraction data). The raw frame data was processed using SAINT[2] and SADABS[3] to yield the reflection data file. Subsequent calculations were carried out using the SHELXTL[4] program. There were no systematic absences nor any diffraction symmetry other than the Friedel condition. The centrosymmetric triclinic space group $P\bar{1}$ was assigned and later determined to be correct.

The structure was solved by dual space methods and refined on F^2 by full-matrix least-squares techniques. The analytical scattering factors[5] for neutral atoms were used throughout the analysis. Hydrogen atoms were located from a difference-Fourier map and refined (x,y,z and U_{iso}).

Least-squares analysis yielded wR2 = 0.1161 and Goof = 1.047 for 291 variables refined against 3705 data (0.74 Å), R1 = 0.0393 for those 3247 data with $I > 2.0\sigma(I)$.

References.

1. APEX2 Version 2014.11-0, Bruker AXS, Inc.; Madison, WI 2014.

2. SAINT Version 8.34a, Bruker AXS, Inc.; Madison, WI 2013.

3. Sheldrick, G. M. SADABS, Version 2014/5, Bruker AXS, Inc.; Madison, WI 2014.

4. Sheldrick, G. M. SHELXTL, Version 2014/7, Bruker AXS, Inc.; Madison, WI 2014.

5. International Tables for Crystallography 1992, Vol. C., Dordrecht: Kluwer Academic Publishers.

Definitions:

$wR2 = [\Sigma[w(F_o^2-F_c^2)^2] / \Sigma[w(F_o^2)^2]]^{1/2}$

$R1 = \Sigma||F_o|-|F_c|| / \Sigma|F_o|$

$Goof = S = [\Sigma[w(F_o^2-F_c^2)^2] / (n-p)]^{1/2}$ where n is the number of reflections and p is the total number of parameters refined.

The thermal ellipsoid plot is shown at the 50% probability level.

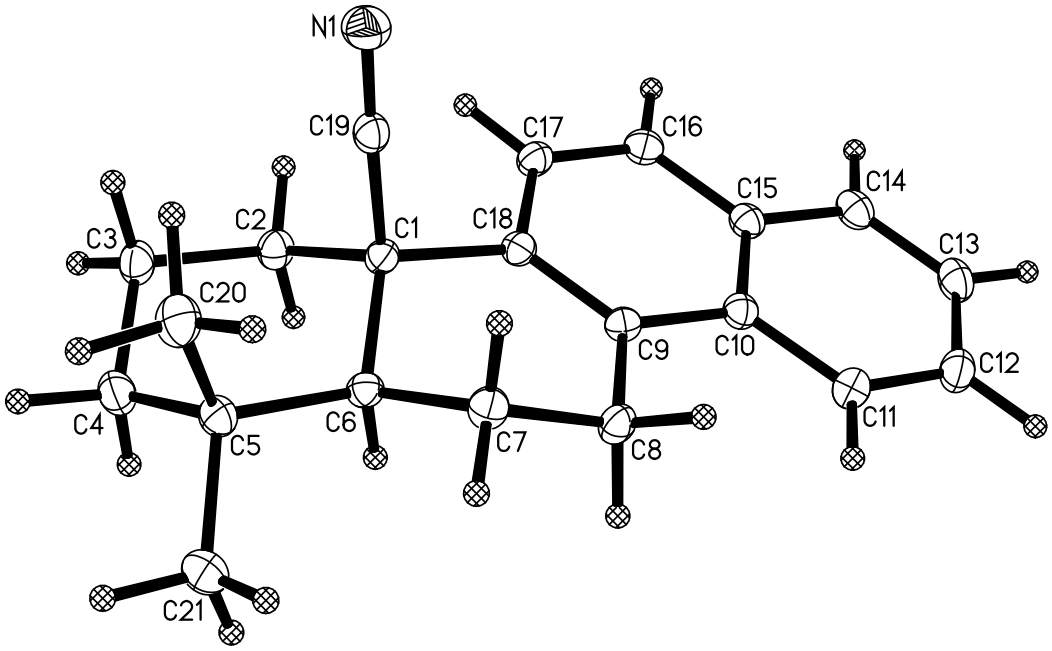

Table 1. Crystal data and structure refinement for cdv56.

Identification code	cdv56 (Darius Vrubliauskas)	
Empirical formula	C_{21} H_{23} N	
Formula weight	289.40	
Temperature	133(2) K	
Wavelength	0.71073 Å	
Crystal system	Triclinic	
Space group	$P\bar{1}$	
Unit cell dimensions	a = 8.0668(10) Å	α = 108.7911(14)°.
	b = 8.2309(10) Å	β = 96.3755(15)°.
	c = 12.7071(15) Å	γ = 97.8034(14)°.
Volume	780.50(16) $Å^3$	
Z	2	
Density (calculated)	1.231 Mg/m^3	
Absorption coefficient	0.071 mm^{-1}	
F(000)	312	
Crystal color	colorless	
Crystal size	0.417 x 0.243 x 0.198 mm^3	
Theta range for data collection	1.716 to 28.741°	
Index ranges	$-10 \le h \le 10$, $-10 \le k \le 11$, $-16 \le l \le 16$	
Reflections collected	9432	
Independent reflections	3705 [R(int) = 0.0275]	
Completeness to theta = 25.242°	99.9 %	
Absorption correction	Semi-empirical from equivalents	
Max. and min. transmission	0.7458 and 0.6770	
Refinement method	Full-matrix least-squares on F^2	
Data / restraints / parameters	3705 / 0 / 291	
Goodness-of-fit on F^2	1.047	
Final R indices [I>2sigma(I) = 3247 data]	R1 = 0.0393, wR2 = 0.1111	
R indices (all data, 0.74 Å)	R1 = 0.0443, wR2 = 0.1161	
Largest diff. peak and hole	0.364 and -0.222 $e.Å^{-3}$	

Table 2. Atomic coordinates (x 10^4) and equivalent isotropic displacement parameters ($Å^2$ x 10^3)
for cdv56. U(eq) is defined as one third of the trace of the orthogonalized U^{ij} tensor.

	x	y	z	U(eq)
N(1)	6114(1)	6143(1)	8157(1)	24(1)
C(1)	6249(1)	2836(1)	7150(1)	14(1)
C(2)	4434(1)	1777(1)	6952(1)	17(1)
C(3)	3882(1)	1745(1)	8057(1)	19(1)
C(4)	5119(1)	1014(1)	8703(1)	20(1)
C(5)	6968(1)	1983(1)	8947(1)	16(1)
C(6)	7481(1)	2091(1)	7825(1)	14(1)
C(7)	9289(1)	3027(1)	7918(1)	16(1)
C(8)	9826(1)	2568(1)	6761(1)	16(1)
C(9)	8494(1)	2670(1)	5860(1)	14(1)
C(10)	8968(1)	2658(1)	4800(1)	15(1)
C(11)	10616(1)	2450(1)	4548(1)	18(1)
C(12)	11052(1)	2482(1)	3540(1)	20(1)
C(13)	9864(1)	2705(1)	2720(1)	20(1)
C(14)	8260(1)	2898(1)	2930(1)	19(1)
C(15)	7778(1)	2882(1)	3969(1)	15(1)
C(16)	6128(1)	3103(1)	4201(1)	17(1)
C(17)	5685(1)	3061(1)	5197(1)	16(1)
C(18)	6852(1)	2821(1)	6034(1)	14(1)
C(19)	6202(1)	4702(1)	7756(1)	16(1)
C(20)	7176(1)	3774(1)	9872(1)	21(1)
C(21)	8088(1)	893(2)	9386(1)	23(1)

—

Table 3. Bond lengths [Å] and angles [°] for cdv56.

N(1)-C(19)	1.1464(13)
C(1)-C(19)	1.4877(13)
C(1)-C(18)	1.5459(12)
C(1)-C(2)	1.5484(13)
C(1)-C(6)	1.5544(12)
C(2)-C(3)	1.5268(13)
C(3)-C(4)	1.5263(14)
C(4)-C(5)	1.5399(14)
C(5)-C(20)	1.5342(14)
C(5)-C(21)	1.5369(13)
C(5)-C(6)	1.5543(12)
C(6)-C(7)	1.5271(13)
C(7)-C(8)	1.5232(13)
C(8)-C(9)	1.5120(12)
C(9)-C(18)	1.3828(13)
C(9)-C(10)	1.4374(13)
C(10)-C(11)	1.4208(13)
C(10)-C(15)	1.4210(13)
C(11)-C(12)	1.3732(14)
C(12)-C(13)	1.4090(15)
C(13)-C(14)	1.3694(14)
C(14)-C(15)	1.4200(13)
C(15)-C(16)	1.4180(13)
C(16)-C(17)	1.3625(13)
C(17)-C(18)	1.4219(13)

C(19)-C(1)-C(18)	104.44(7)
C(19)-C(1)-C(2)	107.95(7)
C(18)-C(1)-C(2)	112.23(7)
C(19)-C(1)-C(6)	112.47(7)
C(18)-C(1)-C(6)	110.72(7)
C(2)-C(1)-C(6)	108.99(7)
C(3)-C(2)-C(1)	111.63(8)
C(4)-C(3)-C(2)	111.57(8)

C(3)-C(4)-C(5)	113.98(8)
C(20)-C(5)-C(21)	108.02(8)
C(20)-C(5)-C(4)	110.41(8)
C(21)-C(5)-C(4)	107.52(8)
C(20)-C(5)-C(6)	113.33(8)
C(21)-C(5)-C(6)	108.80(8)
C(4)-C(5)-C(6)	108.59(7)
C(7)-C(6)-C(5)	115.41(7)
C(7)-C(6)-C(1)	108.53(7)
C(5)-C(6)-C(1)	115.28(7)
C(8)-C(7)-C(6)	110.29(8)
C(9)-C(8)-C(7)	113.23(8)
C(18)-C(9)-C(10)	119.12(8)
C(18)-C(9)-C(8)	122.07(8)
C(10)-C(9)-C(8)	118.79(8)
C(11)-C(10)-C(15)	117.81(9)
C(11)-C(10)-C(9)	122.20(9)
C(15)-C(10)-C(9)	119.98(8)
C(12)-C(11)-C(10)	121.17(9)
C(11)-C(12)-C(13)	120.62(9)
C(14)-C(13)-C(12)	119.86(9)
C(13)-C(14)-C(15)	120.70(9)
C(16)-C(15)-C(14)	121.18(9)
C(16)-C(15)-C(10)	118.99(9)
C(14)-C(15)-C(10)	119.82(9)
C(17)-C(16)-C(15)	120.26(9)
C(16)-C(17)-C(18)	121.56(9)
C(9)-C(18)-C(17)	120.00(8)
C(9)-C(18)-C(1)	122.01(8)
C(17)-C(18)-C(1)	117.91(8)
N(1)-C(19)-C(1)	175.50(10)

Table 4. Anisotropic displacement parameters ($Å^2$ x 10^3) for cdv56. The anisotropic displacement factor exponent takes the form: $-2\pi^2[h^2 a^{*2} U^{11} + ... + 2 h k a^* b^* U^{12}]$

	U^{11}	U^{22}	U^{33}	U^{23}	U^{13}	U^{12}
N(1)	31(1)	20(1)	22(1)	8(1)	8(1)	9(1)
C(1)	13(1)	15(1)	13(1)	4(1)	3(1)	4(1)
C(2)	13(1)	20(1)	18(1)	7(1)	2(1)	2(1)
C(3)	16(1)	23(1)	20(1)	9(1)	6(1)	2(1)
C(4)	20(1)	21(1)	20(1)	10(1)	5(1)	2(1)
C(5)	18(1)	19(1)	14(1)	7(1)	3(1)	4(1)
C(6)	14(1)	15(1)	13(1)	5(1)	2(1)	4(1)
C(7)	15(1)	20(1)	14(1)	6(1)	1(1)	3(1)
C(8)	12(1)	21(1)	16(1)	7(1)	3(1)	5(1)
C(9)	14(1)	13(1)	14(1)	4(1)	2(1)	3(1)
C(10)	16(1)	13(1)	15(1)	4(1)	3(1)	2(1)
C(11)	16(1)	20(1)	19(1)	6(1)	4(1)	4(1)
C(12)	19(1)	20(1)	22(1)	6(1)	9(1)	3(1)
C(13)	26(1)	19(1)	17(1)	6(1)	8(1)	2(1)
C(14)	23(1)	17(1)	15(1)	6(1)	3(1)	2(1)
C(15)	18(1)	13(1)	15(1)	4(1)	3(1)	2(1)
C(16)	17(1)	18(1)	16(1)	7(1)	0(1)	4(1)
C(17)	14(1)	17(1)	17(1)	6(1)	3(1)	4(1)
C(18)	15(1)	13(1)	13(1)	4(1)	2(1)	3(1)
C(19)	16(1)	20(1)	15(1)	8(1)	4(1)	4(1)
C(20)	25(1)	23(1)	14(1)	5(1)	4(1)	4(1)
C(21)	24(1)	28(1)	21(1)	14(1)	4(1)	9(1)

Table 5. Hydrogen coordinates ($x\ 10^4$) and isotropic displacement parameters ($Å^2\ x\ 10^3$) for cdv56.

	x	y	z	U(eq)
H(2A)	3611(17)	2300(17)	6554(11)	27(3)
H(2B)	4431(15)	584(16)	6445(10)	18(3)
H(3A)	3780(16)	2977(17)	8537(11)	22(3)
H(3B)	2727(16)	975(16)	7872(10)	19(3)
H(4A)	5053(16)	-240(17)	8252(11)	23(3)
H(4B)	4733(17)	1026(18)	9438(12)	30(3)
H(6)	7365(15)	835(16)	7305(10)	16(3)
H(7A)	9364(16)	4313(17)	8239(10)	22(3)
H(7B)	10104(17)	2710(17)	8440(11)	26(3)
H(8A)	10911(17)	3370(17)	6808(11)	25(3)
H(8B)	10080(16)	1358(17)	6532(11)	23(3)
H(11)	11459(18)	2273(18)	5090(12)	29(3)
H(12)	12228(17)	2335(17)	3380(11)	26(3)
H(13)	10200(17)	2714(18)	2002(11)	28(3)
H(14)	7394(18)	3057(18)	2358(12)	33(4)
H(16)	5311(18)	3281(18)	3625(11)	30(3)
H(17)	4523(17)	3234(16)	5337(11)	24(3)
H(20A)	8343(18)	4440(18)	10006(11)	31(3)
H(20B)	6942(17)	3585(18)	10574(12)	32(3)
H(20C)	6359(18)	4520(19)	9691(12)	32(3)
H(21A)	8029(18)	-290(19)	8806(12)	33(4)
H(21B)	7696(17)	683(18)	10058(12)	32(4)
H(21C)	9278(19)	1454(18)	9612(12)	31(3)

X-ray Data Collection, Structure Solution and Refinement for cdv64 (**2.6g**)

A colorless crystal of approximate dimensions 0.128 x 0.159 x 0.298 mm was mounted in a cryoloop and transferred to a Bruker SMART APEX II diffractometer. The APEX2[1] program package was used to determine the unit-cell parameters and for data collection (60 sec/frame scan time for a sphere of diffraction data). The raw frame data was processed using SAINT[2] and SADABS[3] to yield the reflection data file. Subsequent calculations were carried out using the SHELXTL[4] program. The diffraction symmetry was 2/*m* and the systematic absences were consistent with the monoclinic space group $P2_1/c$ that was later determined to be correct.

The structure was solved by dual space methods and refined on F^2 by full-matrix least-squares techniques. The analytical scattering factors[5] for neutral atoms were used throughout the analysis. Hydrogen atoms were included using a riding model. There were three molecules of the formula-unit present and one-half molecule of dichloromethane solvent (1/6 molecule of solvent per formula-unit). The solvent atoms were included with site-occupancy-factors = 0.50.

Least-squares analysis yielded wR2 = 0.1143 and Goof = 1.019 for 873 variables refined against 17282 data (0.75 Å), R1 = 0.0467 for those 13089 data with $I > 2.0\sigma(I)$.

References.

6. APEX2 Version 2014.11-0, Bruker AXS, Inc.; Madison, WI 2014.

7. SAINT Version 8.34a, Bruker AXS, Inc.; Madison, WI 2013.

8. Sheldrick, G. M. SADABS, Version 2014/5, Bruker AXS, Inc.; Madison, WI 2014.

9. Sheldrick, G. M. SHELXTL, Version 2014/7, Bruker AXS, Inc.; Madison, WI 2014

10. International Tables for Crystallography 1992, Vol. C., Dordrecht: Kluwer Academic Publishers.

Definitions:

$wR2 = [\Sigma[w(F_o^2-F_c^2)^2] / \Sigma[w(F_o^2)^2]]^{1/2}$

$R1 = \Sigma||F_o|-|F_c|| / \Sigma|F_o|$

$Goof = S = [\Sigma[w(F_o^2-F_c^2)^2] / (n-p)]^{1/2}$ where n is the number of reflections and p is the total number of parameters refined.

The thermal ellipsoid plot is shown at the 50% probability level.

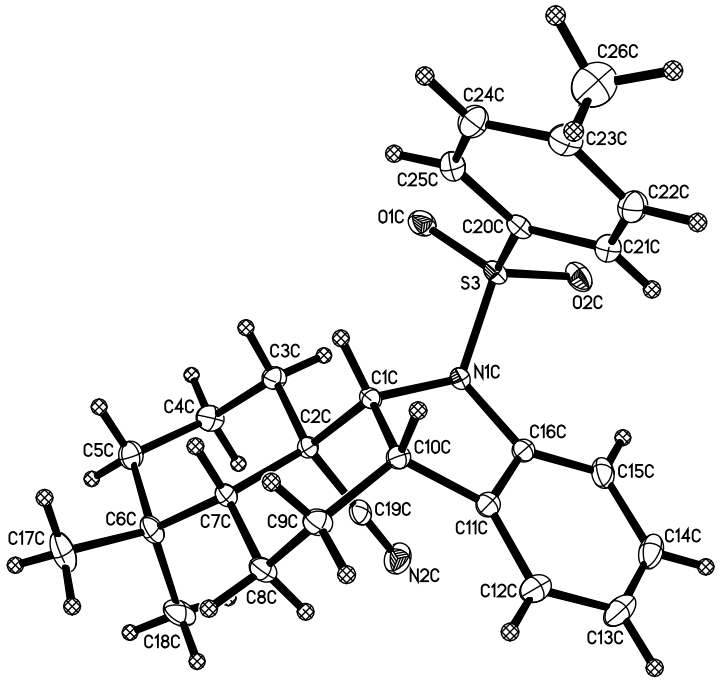

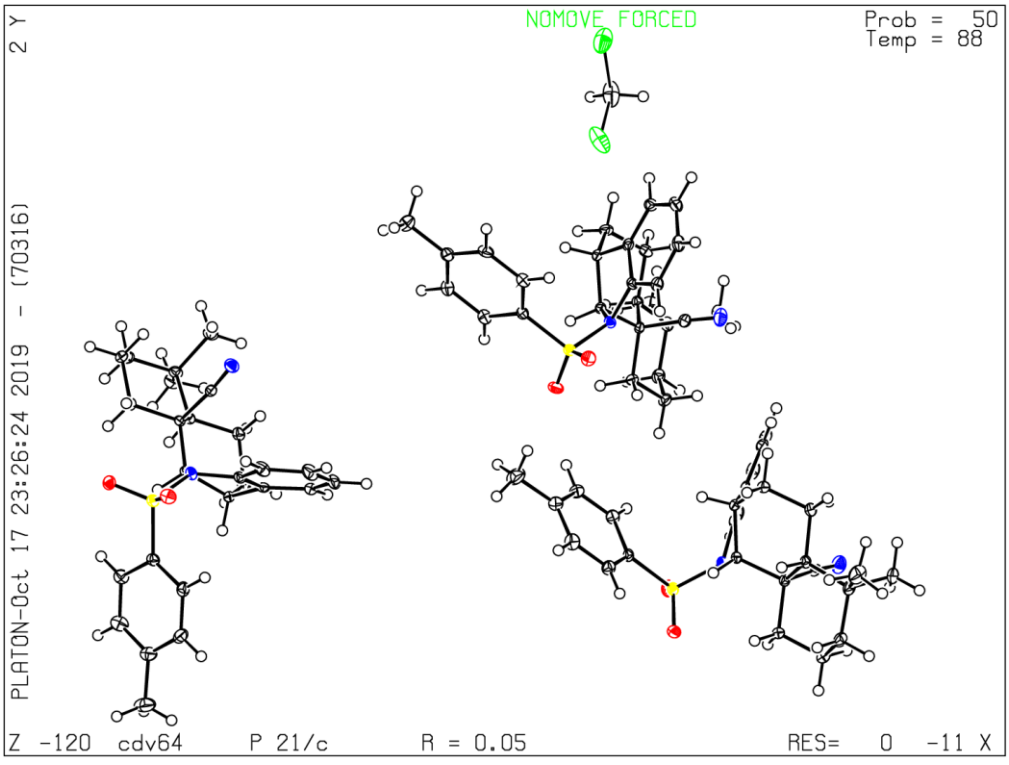

Three molecules and one-half dichloromethane solvent

Table 1. Crystal data and structure refinement for cdv64.

Identification code	cdv64 (Darius Vrubliauskas)	
Empirical formula	$C_{26}\ H_{30}\ N_2\ O_2\ S \bullet 1/6(CH_2Cl_2)$	
Formula weight	448.73	
Temperature	88(2) K	
Wavelength	0.71073 Å	
Crystal system	Monoclinic	
Space group	$P2_1/c$	
Unit cell dimensions	a = 25.696(2) Å	α = 90°.
	b = 24.774(2) Å	β = 97.6915(14)°.
	c = 11.0354(9) Å	γ = 90°.
Volume	6961.8(10) $Å^3$	
Z	12	
Density (calculated)	1.284 Mg/m^3	
Absorption coefficient	0.204 mm^{-1}	
F(000)	2868	
Crystal color	colorless	
Crystal size	0.298 x 0.159 x 0.128 mm^3	
Theta range for data collection	1.147 to 28.281°	
Index ranges	$-34 \le h \le 34$, $-33 \le k \le 33$, $-14 \le l \le 14$	
Reflections collected	96678	
Independent reflections	17282 [R(int) = 0.0631]	
Completeness to theta = 25.500°	100.0 %	
Absorption correction	Semi-empirical from equivalents	
Refinement method	Full-matrix least-squares on F^2	
Data / restraints / parameters	17282 / 0 / 873	
Goodness-of-fit on F^2	1.019	
Final R indices [I>2sigma(I) = 13089 data]	R1 = 0.0467, wR2 = 0.1035	
R indices (all data, 0.75 Å)	R1 = 0.0700, wR2 = 0.1143	
Largest diff. peak and hole	0.406 and -0.428 $e.Å^{-3}$	

Table 2. Atomic coordinates (x 10^4) and equivalent isotropic displacement parameters ($Å^2$ x 10^3)
for cdv64. U(eq) is defined as one third of the trace of the orthogonalized U^{ij} tensor.

	x	y	z	U(eq)
S(1)	-2066(1)	2379(1)	695(1)	12(1)
O(1)	-2420(1)	2675(1)	-173(1)	18(1)
O(2)	-2162(1)	2338(1)	1943(1)	18(1)
N(1)	-2063(1)	1753(1)	192(1)	12(1)
N(2)	-2691(1)	533(1)	-355(1)	23(1)
C(1)	-1968(1)	1658(1)	-1104(1)	11(1)
C(2)	-2433(1)	1318(1)	-1762(1)	10(1)
C(3)	-2921(1)	1682(1)	-2021(2)	13(1)
C(4)	-3367(1)	1396(1)	-2818(2)	15(1)
C(5)	-3189(1)	1222(1)	-4024(2)	16(1)
C(6)	-2717(1)	833(1)	-3869(2)	15(1)
C(7)	-2264(1)	1085(1)	-2964(1)	12(1)
C(8)	-1784(1)	720(1)	-2635(2)	15(1)
C(9)	-1312(1)	1053(1)	-2078(2)	14(1)
C(10)	-1422(1)	1387(1)	-974(1)	11(1)
C(11)	-1405(1)	1104(1)	246(2)	12(1)
C(12)	-1107(1)	675(1)	754(2)	15(1)
C(13)	-1158(1)	511(1)	1940(2)	18(1)
C(14)	-1504(1)	772(1)	2606(2)	17(1)
C(15)	-1818(1)	1194(1)	2101(2)	14(1)
C(16)	-1757(1)	1352(1)	925(2)	12(1)
C(17)	-2524(1)	782(1)	-5126(2)	22(1)
C(18)	-2887(1)	269(1)	-3491(2)	22(1)
C(19)	-2564(1)	873(1)	-957(2)	14(1)
C(20)	-1432(1)	2647(1)	709(2)	13(1)
C(21)	-1042(1)	2524(1)	1676(2)	15(1)
C(22)	-544(1)	2740(1)	1684(2)	17(1)
C(23)	-425(1)	3078(1)	750(2)	17(1)

C(24)	-823(1)	3197(1)	-206(2)	18(1)
C(25)	-1324(1)	2984(1)	-238(2)	16(1)
C(26)	116(1)	3313(1)	778(2)	26(1)
S(2)	-1394(1)	7325(1)	-2582(1)	12(1)
O(1B)	-1007(1)	7626(1)	-3117(1)	17(1)
O(2B)	-1342(1)	7250(1)	-1281(1)	17(1)
N(1B)	-1392(1)	6715(1)	-3169(1)	12(1)
N(2B)	-578(1)	5643(1)	-3288(1)	18(1)
C(1B)	-1446(1)	6652(1)	-4532(1)	10(1)
C(2B)	-940(1)	6378(1)	-4895(1)	10(1)
C(3B)	-489(1)	6794(1)	-4814(2)	13(1)
C(4B)	-9(1)	6562(1)	-5301(2)	16(1)
C(5B)	-152(1)	6394(1)	-6631(2)	16(1)
C(6B)	-590(1)	5966(1)	-6835(2)	14(1)
C(7B)	-1071(1)	6152(1)	-6220(1)	11(1)
C(8B)	-1510(1)	5733(1)	-6248(2)	14(1)
C(9B)	-2021(1)	6004(1)	-6023(2)	14(1)
C(10B)	-1963(1)	6326(1)	-4830(1)	11(1)
C(11B)	-1979(1)	6014(1)	-3656(2)	12(1)
C(12B)	-2250(1)	5549(1)	-3428(2)	16(1)
C(13B)	-2222(1)	5368(1)	-2227(2)	20(1)
C(14B)	-1920(1)	5636(1)	-1282(2)	22(1)
C(15B)	-1630(1)	6093(1)	-1503(2)	19(1)
C(16B)	-1674(1)	6277(1)	-2698(2)	13(1)
C(17B)	-764(1)	5930(1)	-8222(2)	21(1)
C(18B)	-379(1)	5412(1)	-6384(2)	18(1)
C(19B)	-758(1)	5947(1)	-4002(2)	12(1)
C(20B)	-2006(1)	7640(1)	-3020(2)	14(1)
C(21B)	-2414(1)	7564(1)	-2325(2)	17(1)
C(22B)	-2882(1)	7843(1)	-2635(2)	20(1)
C(23B)	-2946(1)	8199(1)	-3623(2)	19(1)
C(24B)	-2535(1)	8262(1)	-4316(2)	21(1)
C(25B)	-2064(1)	7987(1)	-4022(2)	18(1)
C(26B)	-3447(1)	8518(1)	-3920(2)	30(1)
S(3)	-5374(1)	2321(1)	-4274(1)	13(1)
O(1C)	-5754(1)	2616(1)	-3701(1)	17(1)

O(2C)	-5440(1)	2260(1)	-5579(1)	19(1)
N(1C)	-5363(1)	1704(1)	-3710(1)	12(1)
N(2C)	-6030(1)	523(1)	-3504(1)	23(1)
C(1C)	-5285(1)	1638(1)	-2346(1)	11(1)
C(2C)	-5755(1)	1309(1)	-1955(1)	11(1)
C(3C)	-6239(1)	1683(1)	-2013(2)	14(1)
C(4C)	-6692(1)	1403(1)	-1501(2)	17(1)
C(5C)	-6522(1)	1234(1)	-177(2)	18(1)
C(6C)	-6051(1)	843(1)	-17(2)	17(1)
C(7C)	-5595(1)	1090(1)	-633(1)	12(1)
C(8C)	-5112(1)	726(1)	-613(2)	15(1)
C(9C)	-4638(1)	1058(1)	-870(2)	15(1)
C(10C)	-4740(1)	1364(1)	-2079(2)	12(1)
C(11C)	-4716(1)	1053(1)	-3250(2)	13(1)
C(12C)	-4420(1)	607(1)	-3489(2)	18(1)
C(13C)	-4449(1)	422(1)	-4690(2)	23(1)
C(14C)	-4776(1)	673(1)	-5621(2)	23(1)
C(15C)	-5091(1)	1109(1)	-5387(2)	18(1)
C(16C)	-5050(1)	1292(1)	-4192(2)	13(1)
C(17C)	-5866(1)	795(1)	1363(2)	27(1)
C(18C)	-6222(1)	280(1)	-502(2)	22(1)
C(19C)	-5895(1)	859(1)	-2826(2)	14(1)
C(20C)	-4755(1)	2620(1)	-3838(2)	13(1)
C(21C)	-4339(1)	2499(1)	-4487(2)	16(1)
C(22C)	-3857(1)	2747(1)	-4154(2)	19(1)
C(23C)	-3783(1)	3117(1)	-3197(2)	19(1)
C(24C)	-4203(1)	3228(1)	-2557(2)	19(1)
C(25C)	-4689(1)	2980(1)	-2867(2)	16(1)
C(26C)	-3263(1)	3396(1)	-2864(2)	29(1)
C(27)	-272(2)	-102(2)	-5556(4)	36(1)
Cl(1)	-586(1)	368(1)	-4642(1)	46(1)
Cl(2)	351(1)	-278(1)	-4844(1)	44(1)

—

Table 3. Bond lengths [Å] and angles [°] for cdv64.

S(1)-O(1)	1.4326(12)
S(1)-O(2)	1.4345(12)
S(1)-N(1)	1.6473(14)
S(1)-C(20)	1.7578(17)
N(1)-C(16)	1.445(2)
N(1)-C(1)	1.501(2)
N(2)-C(19)	1.147(2)
C(1)-C(10)	1.545(2)
C(1)-C(2)	1.558(2)
C(2)-C(19)	1.483(2)
C(2)-C(3)	1.541(2)
C(2)-C(7)	1.560(2)
C(3)-C(4)	1.523(2)
C(4)-C(5)	1.526(2)
C(5)-C(6)	1.540(2)
C(6)-C(18)	1.537(2)
C(6)-C(17)	1.539(2)
C(6)-C(7)	1.560(2)
C(7)-C(8)	1.532(2)
C(8)-C(9)	1.526(2)
C(9)-C(10)	1.530(2)
C(10)-C(11)	1.513(2)
C(11)-C(12)	1.385(2)
C(11)-C(16)	1.392(2)
C(12)-C(13)	1.394(2)
C(13)-C(14)	1.386(3)
C(14)-C(15)	1.392(2)
C(15)-C(16)	1.384(2)
C(20)-C(25)	1.394(2)
C(20)-C(21)	1.396(2)
C(21)-C(22)	1.386(2)
C(22)-C(23)	1.395(2)
C(23)-C(24)	1.400(2)
C(23)-C(26)	1.503(2)

C(24)-C(25)	1.385(2)
S(2)-O(1B)	1.4316(12)
S(2)-O(2B)	1.4360(12)
S(2)-N(1B)	1.6438(14)
S(2)-C(20B)	1.7640(17)
N(1B)-C(16B)	1.440(2)
N(1B)-C(1B)	1.500(2)
N(2B)-C(19B)	1.141(2)
C(1B)-C(10B)	1.553(2)
C(1B)-C(2B)	1.563(2)
C(2B)-C(19B)	1.487(2)
C(2B)-C(3B)	1.545(2)
C(2B)-C(7B)	1.560(2)
C(3B)-C(4B)	1.523(2)
C(4B)-C(5B)	1.523(2)
C(5B)-C(6B)	1.540(2)
C(6B)-C(18B)	1.536(2)
C(6B)-C(17B)	1.539(2)
C(6B)-C(7B)	1.555(2)
C(7B)-C(8B)	1.532(2)
C(8B)-C(9B)	1.524(2)
C(9B)-C(10B)	1.530(2)
C(10B)-C(11B)	1.515(2)
C(11B)-C(12B)	1.385(2)
C(11B)-C(16B)	1.392(2)
C(12B)-C(13B)	1.392(2)
C(13B)-C(14B)	1.384(3)
C(14B)-C(15B)	1.394(3)
C(15B)-C(16B)	1.385(2)
C(20B)-C(21B)	1.393(2)
C(20B)-C(25B)	1.393(2)
C(21B)-C(22B)	1.389(2)
C(22B)-C(23B)	1.396(3)
C(23B)-C(24B)	1.393(3)
C(23B)-C(26B)	1.508(3)
C(24B)-C(25B)	1.388(2)

S(3)-O(1C)	1.4316(12)
S(3)-O(2C)	1.4356(12)
S(3)-N(1C)	1.6497(14)
S(3)-C(20C)	1.7623(17)
N(1C)-C(16C)	1.445(2)
N(1C)-C(1C)	1.500(2)
N(2C)-C(19C)	1.142(2)
C(1C)-C(10C)	1.549(2)
C(1C)-C(2C)	1.564(2)
C(2C)-C(19C)	1.484(2)
C(2C)-C(3C)	1.545(2)
C(2C)-C(7C)	1.560(2)
C(3C)-C(4C)	1.528(2)
C(4C)-C(5C)	1.526(2)
C(5C)-C(6C)	1.541(2)
C(6C)-C(18C)	1.537(2)
C(6C)-C(17C)	1.539(2)
C(6C)-C(7C)	1.557(2)
C(7C)-C(8C)	1.531(2)
C(8C)-C(9C)	1.525(2)
C(9C)-C(10C)	1.527(2)
C(10C)-C(11C)	1.513(2)
C(11C)-C(12C)	1.387(2)
C(11C)-C(16C)	1.388(2)
C(12C)-C(13C)	1.395(3)
C(13C)-C(14C)	1.384(3)
C(14C)-C(15C)	1.394(3)
C(15C)-C(16C)	1.384(2)
C(20C)-C(25C)	1.387(2)
C(20C)-C(21C)	1.398(2)
C(21C)-C(22C)	1.387(2)
C(22C)-C(23C)	1.393(2)
C(23C)-C(24C)	1.394(3)
C(23C)-C(26C)	1.506(3)
C(24C)-C(25C)	1.391(2)
C(27)-Cl(2)	1.741(5)

C(27)-Cl(1)	1.801(6)
O(1)-S(1)-O(2)	120.22(7)
O(1)-S(1)-N(1)	106.74(7)
O(2)-S(1)-N(1)	105.47(7)
O(1)-S(1)-C(20)	108.48(8)
O(2)-S(1)-C(20)	107.21(8)
N(1)-S(1)-C(20)	108.22(7)
C(16)-N(1)-C(1)	106.29(12)
C(16)-N(1)-S(1)	119.00(11)
C(1)-N(1)-S(1)	118.53(10)
N(1)-C(1)-C(10)	103.89(12)
N(1)-C(1)-C(2)	108.51(12)
C(10)-C(1)-C(2)	115.99(13)
C(19)-C(2)-C(3)	107.50(13)
C(19)-C(2)-C(1)	110.12(13)
C(3)-C(2)-C(1)	108.92(13)
C(19)-C(2)-C(7)	110.22(13)
C(3)-C(2)-C(7)	111.80(13)
C(1)-C(2)-C(7)	108.27(12)
C(4)-C(3)-C(2)	111.47(13)
C(3)-C(4)-C(5)	110.10(13)
C(4)-C(5)-C(6)	113.85(14)
C(18)-C(6)-C(17)	107.88(14)
C(18)-C(6)-C(5)	110.64(14)
C(17)-C(6)-C(5)	107.14(14)
C(18)-C(6)-C(7)	113.83(14)
C(17)-C(6)-C(7)	107.88(14)
C(5)-C(6)-C(7)	109.20(13)
C(8)-C(7)-C(6)	115.09(13)
C(8)-C(7)-C(2)	108.89(13)
C(6)-C(7)-C(2)	115.08(13)
C(9)-C(8)-C(7)	110.40(13)
C(8)-C(9)-C(10)	113.05(13)
C(11)-C(10)-C(9)	118.21(14)
C(11)-C(10)-C(1)	101.62(12)

C(9)-C(10)-C(1)	115.02(13)
C(12)-C(11)-C(16)	119.05(15)
C(12)-C(11)-C(10)	131.55(15)
C(16)-C(11)-C(10)	109.39(14)
C(11)-C(12)-C(13)	119.10(16)
C(14)-C(13)-C(12)	120.69(16)
C(13)-C(14)-C(15)	121.14(16)
C(16)-C(15)-C(14)	117.06(16)
C(15)-C(16)-C(11)	122.92(15)
C(15)-C(16)-N(1)	126.70(15)
C(11)-C(16)-N(1)	110.21(14)
N(2)-C(19)-C(2)	176.70(18)
C(25)-C(20)-C(21)	120.58(16)
C(25)-C(20)-S(1)	119.87(13)
C(21)-C(20)-S(1)	119.55(13)
C(22)-C(21)-C(20)	119.25(16)
C(21)-C(22)-C(23)	121.41(16)
C(22)-C(23)-C(24)	118.18(16)
C(22)-C(23)-C(26)	120.82(16)
C(24)-C(23)-C(26)	121.00(16)
C(25)-C(24)-C(23)	121.48(16)
C(24)-C(25)-C(20)	119.11(16)
O(1B)-S(2)-O(2B)	120.21(7)
O(1B)-S(2)-N(1B)	106.08(7)
O(2B)-S(2)-N(1B)	105.69(7)
O(1B)-S(2)-C(20B)	107.38(8)
O(2B)-S(2)-C(20B)	106.96(8)
N(1B)-S(2)-C(20B)	110.35(7)
C(16B)-N(1B)-C(1B)	107.40(12)
C(16B)-N(1B)-S(2)	121.45(11)
C(1B)-N(1B)-S(2)	119.18(10)
N(1B)-C(1B)-C(10B)	103.23(12)
N(1B)-C(1B)-C(2B)	109.53(12)
C(10B)-C(1B)-C(2B)	115.98(13)
C(19B)-C(2B)-C(3B)	105.86(13)
C(19B)-C(2B)-C(7B)	111.87(13)

C(3B)-C(2B)-C(7B)	111.01(13)
C(19B)-C(2B)-C(1B)	109.91(13)
C(3B)-C(2B)-C(1B)	109.84(12)
C(7B)-C(2B)-C(1B)	108.32(12)
C(4B)-C(3B)-C(2B)	111.47(13)
C(5B)-C(4B)-C(3B)	109.92(14)
C(4B)-C(5B)-C(6B)	114.00(14)
C(18B)-C(6B)-C(17B)	108.26(14)
C(18B)-C(6B)-C(5B)	110.32(14)
C(17B)-C(6B)-C(5B)	107.15(14)
C(18B)-C(6B)-C(7B)	113.00(13)
C(17B)-C(6B)-C(7B)	108.01(13)
C(5B)-C(6B)-C(7B)	109.90(13)
C(8B)-C(7B)-C(6B)	114.66(13)
C(8B)-C(7B)-C(2B)	109.08(13)
C(6B)-C(7B)-C(2B)	115.58(13)
C(9B)-C(8B)-C(7B)	110.34(13)
C(8B)-C(9B)-C(10B)	112.56(13)
C(11B)-C(10B)-C(9B)	117.30(14)
C(11B)-C(10B)-C(1B)	101.81(12)
C(9B)-C(10B)-C(1B)	115.81(13)
C(12B)-C(11B)-C(16B)	119.87(15)
C(12B)-C(11B)-C(10B)	130.66(15)
C(16B)-C(11B)-C(10B)	109.43(14)
C(11B)-C(12B)-C(13B)	118.53(16)
C(14B)-C(13B)-C(12B)	120.98(16)
C(13B)-C(14B)-C(15B)	121.10(17)
C(16B)-C(15B)-C(14B)	117.23(17)
C(15B)-C(16B)-C(11B)	122.21(16)
C(15B)-C(16B)-N(1B)	127.72(15)
C(11B)-C(16B)-N(1B)	109.84(14)
N(2B)-C(19B)-C(2B)	173.79(17)
C(21B)-C(20B)-C(25B)	120.79(16)
C(21B)-C(20B)-S(2)	119.85(13)
C(25B)-C(20B)-S(2)	119.25(13)
C(22B)-C(21B)-C(20B)	119.14(16)

C(21B)-C(22B)-C(23B)	121.07(17)
C(24B)-C(23B)-C(22B)	118.67(16)
C(24B)-C(23B)-C(26B)	120.62(17)
C(22B)-C(23B)-C(26B)	120.70(17)
C(25B)-C(24B)-C(23B)	121.18(17)
C(24B)-C(25B)-C(20B)	119.13(16)
O(1C)-S(3)-O(2C)	120.13(8)
O(1C)-S(3)-N(1C)	106.48(7)
O(2C)-S(3)-N(1C)	105.93(7)
O(1C)-S(3)-C(20C)	108.02(8)
O(2C)-S(3)-C(20C)	107.41(8)
N(1C)-S(3)-C(20C)	108.42(7)
C(16C)-N(1C)-C(1C)	106.67(12)
C(16C)-N(1C)-S(3)	119.94(11)
C(1C)-N(1C)-S(3)	118.28(10)
N(1C)-C(1C)-C(10C)	103.49(12)
N(1C)-C(1C)-C(2C)	109.28(12)
C(10C)-C(1C)-C(2C)	115.57(13)
C(19C)-C(2C)-C(3C)	107.44(13)
C(19C)-C(2C)-C(7C)	110.80(13)
C(3C)-C(2C)-C(7C)	110.94(13)
C(19C)-C(2C)-C(1C)	109.99(13)
C(3C)-C(2C)-C(1C)	108.86(13)
C(7C)-C(2C)-C(1C)	108.79(13)
C(4C)-C(3C)-C(2C)	111.19(13)
C(5C)-C(4C)-C(3C)	110.04(14)
C(4C)-C(5C)-C(6C)	113.76(14)
C(18C)-C(6C)-C(17C)	108.15(15)
C(18C)-C(6C)-C(5C)	110.31(14)
C(17C)-C(6C)-C(5C)	107.26(15)
C(18C)-C(6C)-C(7C)	113.70(14)
C(17C)-C(6C)-C(7C)	108.07(14)
C(5C)-C(6C)-C(7C)	109.13(13)
C(8C)-C(7C)-C(6C)	114.75(13)
C(8C)-C(7C)-C(2C)	109.27(13)
C(6C)-C(7C)-C(2C)	115.16(13)

C(9C)-C(8C)-C(7C)	110.22(13)
C(8C)-C(9C)-C(10C)	112.50(13)
C(11C)-C(10C)-C(9C)	118.10(14)
C(11C)-C(10C)-C(1C)	101.55(13)
C(9C)-C(10C)-C(1C)	115.37(13)
C(12C)-C(11C)-C(16C)	119.76(16)
C(12C)-C(11C)-C(10C)	130.90(16)
C(16C)-C(11C)-C(10C)	109.32(14)
C(11C)-C(12C)-C(13C)	118.77(17)
C(14C)-C(13C)-C(12C)	120.50(17)
C(13C)-C(14C)-C(15C)	121.35(17)
C(16C)-C(15C)-C(14C)	117.21(17)
C(15C)-C(16C)-C(11C)	122.35(16)
C(15C)-C(16C)-N(1C)	127.35(16)
C(11C)-C(16C)-N(1C)	110.07(14)
N(2C)-C(19C)-C(2C)	176.35(18)
C(25C)-C(20C)-C(21C)	120.69(15)
C(25C)-C(20C)-S(3)	119.63(13)
C(21C)-C(20C)-S(3)	119.67(13)
C(22C)-C(21C)-C(20C)	119.15(16)
C(21C)-C(22C)-C(23C)	121.21(16)
C(22C)-C(23C)-C(24C)	118.53(16)
C(22C)-C(23C)-C(26C)	120.86(17)
C(24C)-C(23C)-C(26C)	120.61(17)
C(25C)-C(24C)-C(23C)	121.28(16)
C(20C)-C(25C)-C(24C)	119.12(16)
Cl(2)-C(27)-Cl(1)	111.2(3)

Table 4. Anisotropic displacement parameters ($Å^2$ x 10^3) for cdv64. The anisotropic displacement factor exponent takes the form: $-2\pi^2[h^2 a^{*2} U^{11} + ... + 2 h k a^* b^* U^{12}]$

	U^{11}	U^{22}	U^{33}	U^{23}	U^{13}	U^{12}
S(1)	13(1)	10(1)	15(1)	-3(1)	2(1)	1(1)
O(1)	15(1)	14(1)	23(1)	-3(1)	-2(1)	4(1)
O(2)	20(1)	17(1)	17(1)	-5(1)	7(1)	-1(1)
N(1)	12(1)	10(1)	12(1)	-2(1)	1(1)	0(1)
N(2)	22(1)	22(1)	23(1)	5(1)	1(1)	-7(1)
C(1)	10(1)	10(1)	12(1)	-1(1)	2(1)	-1(1)
C(2)	10(1)	10(1)	11(1)	0(1)	2(1)	-2(1)
C(3)	10(1)	13(1)	15(1)	-1(1)	3(1)	1(1)
C(4)	11(1)	17(1)	17(1)	0(1)	1(1)	-2(1)
C(5)	15(1)	17(1)	15(1)	0(1)	0(1)	-3(1)
C(6)	17(1)	14(1)	13(1)	-2(1)	-1(1)	-2(1)
C(7)	14(1)	11(1)	11(1)	-1(1)	3(1)	0(1)
C(8)	18(1)	13(1)	14(1)	-1(1)	3(1)	3(1)
C(9)	13(1)	16(1)	15(1)	0(1)	4(1)	3(1)
C(10)	10(1)	11(1)	14(1)	-1(1)	2(1)	-2(1)
C(11)	11(1)	12(1)	13(1)	-1(1)	0(1)	-3(1)
C(12)	13(1)	13(1)	18(1)	-2(1)	1(1)	1(1)
C(13)	20(1)	13(1)	19(1)	2(1)	-2(1)	0(1)
C(14)	21(1)	16(1)	14(1)	2(1)	0(1)	-4(1)
C(15)	15(1)	14(1)	13(1)	-3(1)	1(1)	-3(1)
C(16)	12(1)	9(1)	14(1)	-1(1)	-2(1)	-1(1)
C(17)	25(1)	25(1)	15(1)	-6(1)	1(1)	3(1)
C(18)	25(1)	15(1)	25(1)	-5(1)	-3(1)	-6(1)
C(19)	13(1)	14(1)	14(1)	-1(1)	0(1)	-2(1)
C(20)	14(1)	10(1)	15(1)	-4(1)	3(1)	0(1)
C(21)	18(1)	13(1)	14(1)	0(1)	1(1)	1(1)
C(22)	16(1)	15(1)	18(1)	-2(1)	-3(1)	4(1)
C(23)	16(1)	13(1)	22(1)	-4(1)	2(1)	0(1)
C(24)	21(1)	16(1)	17(1)	2(1)	3(1)	-3(1)
C(25)	19(1)	15(1)	14(1)	0(1)	-1(1)	-1(1)
C(26)	17(1)	26(1)	36(1)	2(1)	1(1)	-3(1)

S(2)	14(1)	10(1)	12(1)	-4(1)	2(1)	0(1)
O(1B)	16(1)	13(1)	21(1)	-4(1)	4(1)	-3(1)
O(2B)	20(1)	18(1)	12(1)	-4(1)	-1(1)	1(1)
N(1B)	16(1)	10(1)	10(1)	-1(1)	3(1)	0(1)
N(2B)	19(1)	16(1)	18(1)	3(1)	2(1)	3(1)
C(1B)	13(1)	9(1)	9(1)	-1(1)	2(1)	1(1)
C(2B)	11(1)	9(1)	11(1)	1(1)	2(1)	1(1)
C(3B)	12(1)	12(1)	15(1)	1(1)	2(1)	-2(1)
C(4B)	10(1)	15(1)	22(1)	4(1)	2(1)	0(1)
C(5B)	14(1)	17(1)	18(1)	5(1)	7(1)	3(1)
C(6B)	16(1)	14(1)	13(1)	1(1)	6(1)	4(1)
C(7B)	13(1)	10(1)	10(1)	0(1)	2(1)	1(1)
C(8B)	17(1)	12(1)	12(1)	-3(1)	3(1)	0(1)
C(9B)	13(1)	15(1)	14(1)	-2(1)	0(1)	-1(1)
C(10B)	10(1)	10(1)	13(1)	0(1)	2(1)	0(1)
C(11B)	11(1)	12(1)	15(1)	1(1)	4(1)	3(1)
C(12B)	13(1)	12(1)	22(1)	0(1)	4(1)	1(1)
C(13B)	22(1)	13(1)	27(1)	6(1)	11(1)	2(1)
C(14B)	31(1)	19(1)	19(1)	7(1)	11(1)	6(1)
C(15B)	25(1)	16(1)	15(1)	1(1)	4(1)	4(1)
C(16B)	15(1)	10(1)	15(1)	0(1)	6(1)	2(1)
C(17B)	25(1)	24(1)	14(1)	-1(1)	8(1)	4(1)
C(18B)	20(1)	16(1)	22(1)	1(1)	7(1)	5(1)
C(19B)	11(1)	12(1)	13(1)	-3(1)	3(1)	-1(1)
C(20B)	14(1)	11(1)	14(1)	-4(1)	1(1)	0(1)
C(21B)	18(1)	15(1)	19(1)	-1(1)	3(1)	-3(1)
C(22B)	15(1)	20(1)	25(1)	-5(1)	6(1)	-3(1)
C(23B)	16(1)	20(1)	21(1)	-8(1)	-3(1)	1(1)
C(24B)	24(1)	22(1)	16(1)	-1(1)	-1(1)	4(1)
C(25B)	20(1)	18(1)	15(1)	-2(1)	4(1)	2(1)
C(26B)	18(1)	34(1)	37(1)	-5(1)	-2(1)	7(1)
S(3)	14(1)	12(1)	13(1)	4(1)	2(1)	-1(1)
O(1C)	16(1)	16(1)	21(1)	5(1)	5(1)	3(1)
O(2C)	22(1)	21(1)	13(1)	4(1)	1(1)	-3(1)
N(1C)	16(1)	11(1)	10(1)	1(1)	4(1)	0(1)
N(2C)	25(1)	21(1)	24(1)	-6(1)	9(1)	-6(1)

C(1C)	12(1)	10(1)	11(1)	2(1)	2(1)	0(1)
C(2C)	12(1)	10(1)	12(1)	0(1)	4(1)	-1(1)
C(3C)	12(1)	13(1)	17(1)	1(1)	3(1)	1(1)
C(4C)	12(1)	18(1)	23(1)	2(1)	4(1)	0(1)
C(5C)	17(1)	19(1)	20(1)	1(1)	9(1)	-2(1)
C(6C)	17(1)	18(1)	16(1)	4(1)	6(1)	-3(1)
C(7C)	14(1)	12(1)	12(1)	2(1)	3(1)	-1(1)
C(8C)	16(1)	14(1)	17(1)	4(1)	3(1)	0(1)
C(9C)	12(1)	15(1)	19(1)	3(1)	2(1)	2(1)
C(10C)	10(1)	11(1)	15(1)	0(1)	4(1)	-1(1)
C(11C)	11(1)	11(1)	17(1)	-2(1)	6(1)	-4(1)
C(12C)	12(1)	14(1)	28(1)	-4(1)	7(1)	-3(1)
C(13C)	17(1)	16(1)	38(1)	-11(1)	14(1)	-6(1)
C(14C)	25(1)	22(1)	24(1)	-10(1)	13(1)	-10(1)
C(15C)	20(1)	20(1)	16(1)	-2(1)	8(1)	-7(1)
C(16C)	13(1)	10(1)	18(1)	-1(1)	8(1)	-3(1)
C(17C)	27(1)	37(1)	18(1)	9(1)	9(1)	-2(1)
C(18C)	20(1)	17(1)	29(1)	7(1)	8(1)	-3(1)
C(19C)	11(1)	15(1)	15(1)	2(1)	5(1)	-1(1)
C(20C)	13(1)	12(1)	13(1)	4(1)	2(1)	-1(1)
C(21C)	19(1)	15(1)	15(1)	-1(1)	5(1)	0(1)
C(22C)	16(1)	18(1)	23(1)	-1(1)	7(1)	1(1)
C(23C)	16(1)	18(1)	21(1)	2(1)	1(1)	1(1)
C(24C)	22(1)	19(1)	14(1)	-4(1)	1(1)	-2(1)
C(25C)	18(1)	18(1)	15(1)	1(1)	5(1)	-1(1)
C(26C)	17(1)	33(1)	36(1)	-7(1)	1(1)	-4(1)
C(27)	48(3)	34(3)	21(2)	8(2)	-10(2)	-17(2)
Cl(1)	70(1)	23(1)	41(1)	4(1)	-6(1)	0(1)
Cl(2)	36(1)	52(1)	42(1)	20(1)	-10(1)	-15(1)

Table 5. Hydrogen coordinates (x 10^4) and isotropic displacement parameters ($Å^2$ x 10^3) for cdv64.

	x	y	z	U(eq)
H(1A)	-1953	2012	-1530	13
H(3A)	-3040	1788	-1237	15
H(3B)	-2827	2015	-2438	15
H(4A)	-3672	1642	-2984	18
H(4B)	-3478	1075	-2383	18
H(5A)	-3093	1548	-4465	19
H(5B)	-3486	1045	-4535	19
H(7A)	-2136	1401	-3403	14
H(8A)	-1864	442	-2045	18
H(8B)	-1700	535	-3380	18
H(9A)	-1207	1299	-2709	17
H(9B)	-1014	807	-1823	17
H(10A)	-1155	1682	-865	14
H(12A)	-871	494	299	18
H(13A)	-954	218	2296	21
H(14A)	-1527	661	3421	21
H(15A)	-2064	1367	2544	17
H(17A)	-2813	655	-5730	33
H(17B)	-2234	523	-5072	33
H(17C)	-2404	1135	-5376	33
H(18A)	-3151	123	-4130	34
H(18B)	-3036	295	-2721	34
H(18C)	-2581	29	-3381	34
H(21A)	-1118	2295	2321	19
H(22A)	-278	2655	2340	20
H(24A)	-749	3428	-848	21
H(25A)	-1589	3066	-896	19
H(26A)	127	3540	54	39

H(26B)	200	3533	1517	39
H(26C)	373	3021	783	39
H(1BA)	-1490	7015	-4925	12
H(3BA)	-610	7119	-5292	16
H(3BB)	-392	6904	-3951	16
H(4BA)	274	6836	-5237	19
H(4BB)	123	6245	-4805	19
H(5BA)	166	6249	-6934	19
H(5BB)	-265	6718	-7122	19
H(7BA)	-1227	6461	-6726	13
H(8BA)	-1561	5550	-7053	16
H(8BB)	-1411	5456	-5611	16
H(9BA)	-2294	5724	-5995	17
H(9BB)	-2139	6248	-6714	17
H(10B)	-2259	6592	-4899	13
H(12B)	-2450	5358	-4077	19
H(13B)	-2414	5055	-2054	24
H(14B)	-1910	5507	-469	27
H(15B)	-1413	6271	-862	22
H(17D)	-922	6274	-8519	31
H(17E)	-1023	5641	-8393	31
H(17F)	-459	5853	-8639	31
H(18D)	-256	5430	-5505	28
H(18E)	-86	5309	-6822	28
H(18F)	-659	5142	-6538	28
H(21B)	-2373	7324	-1647	21
H(22B)	-3162	7790	-2166	23
H(24B)	-2577	8498	-5001	25
H(25B)	-1786	8035	-4498	21
H(26D)	-3716	8372	-3461	46
H(26E)	-3569	8494	-4798	46
H(26F)	-3381	8897	-3693	46
H(1CA)	-5271	2002	-1949	13
H(3CA)	-6142	2015	-1537	16
H(3CB)	-6353	1789	-2872	16
H(4CA)	-6996	1651	-1540	21

H(4CB)	-6803	1081	-2001	21
H(5CA)	-6822	1060	143	22
H(5CB)	-6428	1561	319	22
H(7CA)	-5473	1412	-127	15
H(8CA)	-5035	551	197	18
H(8CB)	-5184	440	-1239	18
H(9CA)	-4335	814	-891	18
H(9CB)	-4547	1319	-197	18
H(10C)	-4471	1657	-2047	14
H(12C)	-4201	431	-2847	21
H(13C)	-4243	121	-4871	27
H(14C)	-4786	546	-6436	27
H(15C)	-5324	1274	-6021	22
H(17G)	-5732	1145	1681	40
H(17H)	-5585	525	1504	40
H(17I)	-6161	685	1784	40
H(18G)	-5916	41	-439	32
H(18H)	-6379	308	-1359	32
H(18I)	-6481	132	-16	32
H(21C)	-4385	2251	-5149	19
H(22C)	-3571	2662	-4586	23
H(24C)	-4157	3477	-1897	23
H(25C)	-4971	3057	-2420	20
H(26G)	-3318	3745	-2486	43
H(26H)	-3097	3452	-3603	43
H(26I)	-3034	3171	-2286	43
H(27A)	-490	-431	-5696	43
H(27B)	-242	63	-6362	43

—

Table 6. Torsion angles [°] for cdv64.

O(1)-S(1)-N(1)-C(16)	-176.85(12)
O(2)-S(1)-N(1)-C(16)	-47.90(13)
C(20)-S(1)-N(1)-C(16)	66.57(13)
O(1)-S(1)-N(1)-C(1)	51.35(13)
O(2)-S(1)-N(1)-C(1)	-179.71(11)
C(20)-S(1)-N(1)-C(1)	-65.23(13)
C(16)-N(1)-C(1)-C(10)	-26.01(15)
S(1)-N(1)-C(1)-C(10)	111.21(12)
C(16)-N(1)-C(1)-C(2)	97.97(14)
S(1)-N(1)-C(1)-C(2)	-124.82(12)
N(1)-C(1)-C(2)-C(19)	-43.81(17)
C(10)-C(1)-C(2)-C(19)	72.61(17)
N(1)-C(1)-C(2)-C(3)	73.84(15)
C(10)-C(1)-C(2)-C(3)	-169.74(13)
N(1)-C(1)-C(2)-C(7)	-164.39(12)
C(10)-C(1)-C(2)-C(7)	-47.97(17)
C(19)-C(2)-C(3)-C(4)	-68.57(17)
C(1)-C(2)-C(3)-C(4)	172.13(13)
C(7)-C(2)-C(3)-C(4)	52.52(17)
C(2)-C(3)-C(4)-C(5)	-58.08(18)
C(3)-C(4)-C(5)-C(6)	59.87(18)
C(4)-C(5)-C(6)-C(18)	72.91(18)
C(4)-C(5)-C(6)-C(17)	-169.73(14)
C(4)-C(5)-C(6)-C(7)	-53.14(18)
C(18)-C(6)-C(7)-C(8)	50.9(2)
C(17)-C(6)-C(7)-C(8)	-68.83(18)
C(5)-C(6)-C(7)-C(8)	175.05(14)
C(18)-C(6)-C(7)-C(2)	-77.02(18)
C(17)-C(6)-C(7)-C(2)	163.30(14)
C(5)-C(6)-C(7)-C(2)	47.18(18)
C(19)-C(2)-C(7)-C(8)	-59.50(17)
C(3)-C(2)-C(7)-C(8)	-179.00(13)
C(1)-C(2)-C(7)-C(8)	61.01(16)
C(19)-C(2)-C(7)-C(6)	71.42(17)

C(3)-C(2)-C(7)-C(6)	-48.08(18)
C(1)-C(2)-C(7)-C(6)	-168.07(13)
C(6)-C(7)-C(8)-C(9)	162.98(14)
C(2)-C(7)-C(8)-C(9)	-66.11(17)
C(7)-C(8)-C(9)-C(10)	54.96(18)
C(8)-C(9)-C(10)-C(11)	79.42(18)
C(8)-C(9)-C(10)-C(1)	-40.75(19)
N(1)-C(1)-C(10)-C(11)	28.59(15)
C(2)-C(1)-C(10)-C(11)	-90.39(15)
N(1)-C(1)-C(10)-C(9)	157.53(13)
C(2)-C(1)-C(10)-C(9)	38.56(19)
C(9)-C(10)-C(11)-C(12)	32.2(2)
C(1)-C(10)-C(11)-C(12)	159.04(17)
C(9)-C(10)-C(11)-C(16)	-149.03(14)
C(1)-C(10)-C(11)-C(16)	-22.14(16)
C(16)-C(11)-C(12)-C(13)	-1.5(2)
C(10)-C(11)-C(12)-C(13)	177.18(16)
C(11)-C(12)-C(13)-C(14)	0.2(3)
C(12)-C(13)-C(14)-C(15)	1.6(3)
C(13)-C(14)-C(15)-C(16)	-2.0(2)
C(14)-C(15)-C(16)-C(11)	0.7(2)
C(14)-C(15)-C(16)-N(1)	175.48(15)
C(12)-C(11)-C(16)-C(15)	1.1(2)
C(10)-C(11)-C(16)-C(15)	-177.90(15)
C(12)-C(11)-C(16)-N(1)	-174.46(14)
C(10)-C(11)-C(16)-N(1)	6.56(18)
C(1)-N(1)-C(16)-C(15)	-162.62(15)
S(1)-N(1)-C(16)-C(15)	60.4(2)
C(1)-N(1)-C(16)-C(11)	12.71(17)
S(1)-N(1)-C(16)-C(11)	-124.26(13)
O(1)-S(1)-C(20)-C(25)	-15.38(15)
O(2)-S(1)-C(20)-C(25)	-146.61(13)
N(1)-S(1)-C(20)-C(25)	100.07(14)
O(1)-S(1)-C(20)-C(21)	164.15(13)
O(2)-S(1)-C(20)-C(21)	32.92(15)
N(1)-S(1)-C(20)-C(21)	-80.39(14)

C(25)-C(20)-C(21)-C(22)	-0.1(2)
S(1)-C(20)-C(21)-C(22)	-179.67(13)
C(20)-C(21)-C(22)-C(23)	0.3(3)
C(21)-C(22)-C(23)-C(24)	-0.1(3)
C(21)-C(22)-C(23)-C(26)	179.36(17)
C(22)-C(23)-C(24)-C(25)	-0.3(3)
C(26)-C(23)-C(24)-C(25)	-179.69(17)
C(23)-C(24)-C(25)-C(20)	0.4(3)
C(21)-C(20)-C(25)-C(24)	-0.2(2)
S(1)-C(20)-C(25)-C(24)	179.35(13)
O(1B)-S(2)-N(1B)-C(16B)	170.11(12)
O(2B)-S(2)-N(1B)-C(16B)	41.42(14)
C(20B)-S(2)-N(1B)-C(16B)	-73.88(14)
O(1B)-S(2)-N(1B)-C(1B)	-51.89(13)
O(2B)-S(2)-N(1B)-C(1B)	179.43(11)
C(20B)-S(2)-N(1B)-C(1B)	64.12(13)
C(16B)-N(1B)-C(1B)-C(10B)	25.09(15)
S(2)-N(1B)-C(1B)-C(10B)	-118.17(12)
C(16B)-N(1B)-C(1B)-C(2B)	-99.03(14)
S(2)-N(1B)-C(1B)-C(2B)	117.71(12)
N(1B)-C(1B)-C(2B)-C(19B)	39.76(16)
C(10B)-C(1B)-C(2B)-C(19B)	-76.54(16)
N(1B)-C(1B)-C(2B)-C(3B)	-76.33(15)
C(10B)-C(1B)-C(2B)-C(3B)	167.37(13)
N(1B)-C(1B)-C(2B)-C(7B)	162.27(12)
C(10B)-C(1B)-C(2B)-C(7B)	45.97(17)
C(19B)-C(2B)-C(3B)-C(4B)	67.97(16)
C(7B)-C(2B)-C(3B)-C(4B)	-53.64(17)
C(1B)-C(2B)-C(3B)-C(4B)	-173.41(13)
C(2B)-C(3B)-C(4B)-C(5B)	59.40(17)
C(3B)-C(4B)-C(5B)-C(6B)	-59.26(18)
C(4B)-C(5B)-C(6B)-C(18B)	-73.88(18)
C(4B)-C(5B)-C(6B)-C(17B)	168.48(14)
C(4B)-C(5B)-C(6B)-C(7B)	51.37(18)
C(18B)-C(6B)-C(7B)-C(8B)	-50.25(19)
C(17B)-C(6B)-C(7B)-C(8B)	69.47(17)

C(5B)-C(6B)-C(7B)-C(8B)	-173.95(13)
C(18B)-C(6B)-C(7B)-C(2B)	77.94(18)
C(17B)-C(6B)-C(7B)-C(2B)	-162.33(14)
C(5B)-C(6B)-C(7B)-C(2B)	-45.75(18)
C(19B)-C(2B)-C(7B)-C(8B)	60.65(17)
C(3B)-C(2B)-C(7B)-C(8B)	178.66(13)
C(1B)-C(2B)-C(7B)-C(8B)	-60.66(16)
C(19B)-C(2B)-C(7B)-C(6B)	-70.26(17)
C(3B)-C(2B)-C(7B)-C(6B)	47.75(18)
C(1B)-C(2B)-C(7B)-C(6B)	168.43(13)
C(6B)-C(7B)-C(8B)-C(9B)	-161.37(13)
C(2B)-C(7B)-C(8B)-C(9B)	67.23(16)
C(7B)-C(8B)-C(9B)-C(10B)	-55.48(18)
C(8B)-C(9B)-C(10B)-C(11B)	-80.28(18)
C(8B)-C(9B)-C(10B)-C(1B)	40.07(19)
N(1B)-C(1B)-C(10B)-C(11B)	-28.01(15)
C(2B)-C(1B)-C(10B)-C(11B)	91.76(15)
N(1B)-C(1B)-C(10B)-C(9B)	-156.44(13)
C(2B)-C(1B)-C(10B)-C(9B)	-36.67(19)
C(9B)-C(10B)-C(11B)-C(12B)	-32.2(2)
C(1B)-C(10B)-C(11B)-C(12B)	-159.71(17)
C(9B)-C(10B)-C(11B)-C(16B)	149.95(14)
C(1B)-C(10B)-C(11B)-C(16B)	22.48(16)
C(16B)-C(11B)-C(12B)-C(13B)	2.2(2)
C(10B)-C(11B)-C(12B)-C(13B)	-175.40(16)
C(11B)-C(12B)-C(13B)-C(14B)	-1.7(3)
C(12B)-C(13B)-C(14B)-C(15B)	-0.6(3)
C(13B)-C(14B)-C(15B)-C(16B)	2.3(3)
C(14B)-C(15B)-C(16B)-C(11B)	-1.8(3)
C(14B)-C(15B)-C(16B)-N(1B)	-175.71(16)
C(12B)-C(11B)-C(16B)-C(15B)	-0.5(2)
C(10B)-C(11B)-C(16B)-C(15B)	177.64(15)
C(12B)-C(11B)-C(16B)-N(1B)	174.42(14)
C(10B)-C(11B)-C(16B)-N(1B)	-7.50(18)
C(1B)-N(1B)-C(16B)-C(15B)	162.83(16)
S(2)-N(1B)-C(16B)-C(15B)	-54.9(2)

C(1B)-N(1B)-C(16B)-C(11B)	-11.68(17)
S(2)-N(1B)-C(16B)-C(11B)	130.57(13)
O(1B)-S(2)-C(20B)-C(21B)	-157.48(13)
O(2B)-S(2)-C(20B)-C(21B)	-27.19(16)
N(1B)-S(2)-C(20B)-C(21B)	87.32(14)
O(1B)-S(2)-C(20B)-C(25B)	18.84(15)
O(2B)-S(2)-C(20B)-C(25B)	149.14(13)
N(1B)-S(2)-C(20B)-C(25B)	-96.35(14)
C(25B)-C(20B)-C(21B)-C(22B)	-0.5(3)
S(2)-C(20B)-C(21B)-C(22B)	175.73(13)
C(20B)-C(21B)-C(22B)-C(23B)	-0.4(3)
C(21B)-C(22B)-C(23B)-C(24B)	1.3(3)
C(21B)-C(22B)-C(23B)-C(26B)	-177.33(17)
C(22B)-C(23B)-C(24B)-C(25B)	-1.3(3)
C(26B)-C(23B)-C(24B)-C(25B)	177.35(17)
C(23B)-C(24B)-C(25B)-C(20B)	0.4(3)
C(21B)-C(20B)-C(25B)-C(24B)	0.6(3)
S(2)-C(20B)-C(25B)-C(24B)	-175.73(13)
O(1C)-S(3)-N(1C)-C(16C)	174.33(12)
O(2C)-S(3)-N(1C)-C(16C)	45.36(14)
C(20C)-S(3)-N(1C)-C(16C)	-69.66(14)
O(1C)-S(3)-N(1C)-C(1C)	-52.38(13)
O(2C)-S(3)-N(1C)-C(1C)	178.65(11)
C(20C)-S(3)-N(1C)-C(1C)	63.63(13)
C(16C)-N(1C)-C(1C)-C(10C)	25.64(15)
S(3)-N(1C)-C(1C)-C(10C)	-113.18(12)
C(16C)-N(1C)-C(1C)-C(2C)	-98.02(14)
S(3)-N(1C)-C(1C)-C(2C)	123.16(12)
N(1C)-C(1C)-C(2C)-C(19C)	41.14(17)
C(10C)-C(1C)-C(2C)-C(19C)	-75.04(17)
N(1C)-C(1C)-C(2C)-C(3C)	-76.32(15)
C(10C)-C(1C)-C(2C)-C(3C)	167.49(13)
N(1C)-C(1C)-C(2C)-C(7C)	162.67(12)
C(10C)-C(1C)-C(2C)-C(7C)	46.48(17)
C(19C)-C(2C)-C(3C)-C(4C)	67.46(17)
C(7C)-C(2C)-C(3C)-C(4C)	-53.79(18)

C(1C)-C(2C)-C(3C)-C(4C)	-173.47(13)
C(2C)-C(3C)-C(4C)-C(5C)	58.75(18)
C(3C)-C(4C)-C(5C)-C(6C)	-59.60(19)
C(4C)-C(5C)-C(6C)-C(18C)	-72.60(18)
C(4C)-C(5C)-C(6C)-C(17C)	169.83(15)
C(4C)-C(5C)-C(6C)-C(7C)	52.99(19)
C(18C)-C(6C)-C(7C)-C(8C)	-52.71(19)
C(17C)-C(6C)-C(7C)-C(8C)	67.35(19)
C(5C)-C(6C)-C(7C)-C(8C)	-176.32(14)
C(18C)-C(6C)-C(7C)-C(2C)	75.45(18)
C(17C)-C(6C)-C(7C)-C(2C)	-164.49(14)
C(5C)-C(6C)-C(7C)-C(2C)	-48.16(19)
C(19C)-C(2C)-C(7C)-C(8C)	61.26(17)
C(3C)-C(2C)-C(7C)-C(8C)	-179.49(13)
C(1C)-C(2C)-C(7C)-C(8C)	-59.77(16)
C(19C)-C(2C)-C(7C)-C(6C)	-69.59(17)
C(3C)-C(2C)-C(7C)-C(6C)	49.66(18)
C(1C)-C(2C)-C(7C)-C(6C)	169.38(13)
C(6C)-C(7C)-C(8C)-C(9C)	-162.77(14)
C(2C)-C(7C)-C(8C)-C(9C)	66.16(17)
C(7C)-C(8C)-C(9C)-C(10C)	-56.31(18)
C(8C)-C(9C)-C(10C)-C(11C)	-77.92(18)
C(8C)-C(9C)-C(10C)-C(1C)	42.38(19)
N(1C)-C(1C)-C(10C)-C(11C)	-29.10(15)
C(2C)-C(1C)-C(10C)-C(11C)	90.32(15)
N(1C)-C(1C)-C(10C)-C(9C)	-158.07(13)
C(2C)-C(1C)-C(10C)-C(9C)	-38.65(19)
C(9C)-C(10C)-C(11C)-C(12C)	-30.9(2)
C(1C)-C(10C)-C(11C)-C(12C)	-158.09(17)
C(9C)-C(10C)-C(11C)-C(16C)	150.79(14)
C(1C)-C(10C)-C(11C)-C(16C)	23.57(16)
C(16C)-C(11C)-C(12C)-C(13C)	2.6(2)
C(10C)-C(11C)-C(12C)-C(13C)	-175.57(16)
C(11C)-C(12C)-C(13C)-C(14C)	-1.2(3)
C(12C)-C(13C)-C(14C)-C(15C)	-1.2(3)
C(13C)-C(14C)-C(15C)-C(16C)	2.1(3)

C(14C)-C(15C)-C(16C)-C(11C)	-0.6(2)
C(14C)-C(15C)-C(16C)-N(1C)	-174.61(15)
C(12C)-C(11C)-C(16C)-C(15C)	-1.7(2)
C(10C)-C(11C)-C(16C)-C(15C)	176.82(15)
C(12C)-C(11C)-C(16C)-N(1C)	173.17(14)
C(10C)-C(11C)-C(16C)-N(1C)	-8.27(18)
C(1C)-N(1C)-C(16C)-C(15C)	163.09(16)
S(3)-N(1C)-C(16C)-C(15C)	-58.9(2)
C(1C)-N(1C)-C(16C)-C(11C)	-11.50(17)
S(3)-N(1C)-C(16C)-C(11C)	126.50(13)
O(1C)-S(3)-C(20C)-C(25C)	14.21(16)
O(2C)-S(3)-C(20C)-C(25C)	145.15(13)
N(1C)-S(3)-C(20C)-C(25C)	-100.80(14)
O(1C)-S(3)-C(20C)-C(21C)	-164.59(13)
O(2C)-S(3)-C(20C)-C(21C)	-33.65(16)
N(1C)-S(3)-C(20C)-C(21C)	80.40(15)
C(25C)-C(20C)-C(21C)-C(22C)	-0.3(3)
S(3)-C(20C)-C(21C)-C(22C)	178.47(13)
C(20C)-C(21C)-C(22C)-C(23C)	-0.8(3)
C(21C)-C(22C)-C(23C)-C(24C)	1.3(3)
C(21C)-C(22C)-C(23C)-C(26C)	-178.26(17)
C(22C)-C(23C)-C(24C)-C(25C)	-0.7(3)
C(26C)-C(23C)-C(24C)-C(25C)	178.91(17)
C(21C)-C(20C)-C(25C)-C(24C)	1.0(3)
S(3)-C(20C)-C(25C)-C(24C)	-177.83(13)
C(23C)-C(24C)-C(25C)-C(20C)	-0.5(3)

X-ray Data Collection, Structure Solution and Refinement for cdv73 (**3.29a**)

A colorless crystal of approximate dimensions 0.294 x 0.348 x 0.354 mm was mounted in a cryoloop and transferred to a Bruker SMART APEX II diffractometer. The APEX2[1] program package was used to determine the unit-cell parameters and for data collection (20 sec/frame scan time for a sphere of diffraction data). The raw frame data was processed using SAINT[2] and SADABS[3] to yield the reflection data file. Subsequent calculations were carried out using the SHELXTL[4] program. There were no systematic absences nor any diffraction symmetry other than the Friedel condition. The centrosymmetric triclinic space group $P\bar{1}$ was assigned and later determined to be correct.

The structure was solved by dual space methods and refined on F^2 by full-matrix least-squares techniques. The analytical scattering factors[5] for neutral atoms were used throughout the analysis. Hydrogen atoms were located from a difference-Fourier map and refined (x,y,z and U_{iso}).

Least-squares analysis yielded wR2 = 0.1120 and Goof = 1.023 for 429 variables refined against 9704 data (0.74 Å), R1 = 0.0403 for those 8079 data with $I > 2.0\sigma(I)$.

References.

11. APEX2 Version 2014.11-0, Bruker AXS, Inc.; Madison, WI 2014.

12. SAINT Version 8.34a, Bruker AXS, Inc.; Madison, WI 2013.

13. Sheldrick, G. M. SADABS, Version 2014/5, Bruker AXS, Inc.; Madison, WI 2014.

14. Sheldrick, G. M. SHELXTL, Version 2014/7, Bruker AXS, Inc.; Madison, WI 2014.

15. International Tables for Crystallography 1992, Vol. C., Dordrecht: Kluwer Academic Publishers.

Definitions:

$wR2 = [\Sigma[w(F_o^2-F_c^2)^2] / \Sigma[w(F_o^2)^2]]^{1/2}$

$R1 = \Sigma||F_o|-|F_c|| / \Sigma|F_o|$

$Goof = S = [\Sigma[w(F_o^2-F_c^2)^2] / (n-p)]^{1/2}$ where n is the number of reflections and p is the total number of parameters refined.

The thermal ellipsoid plot is shown at the 50% probability level.

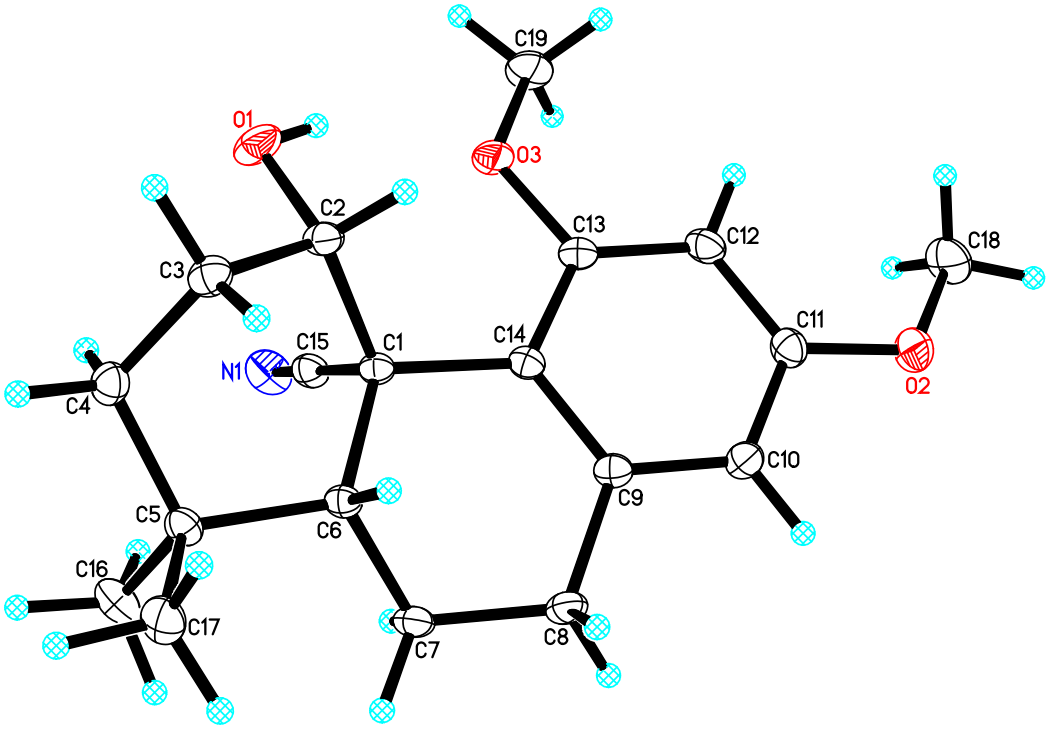
C19
O1
O3
C2
C13
C12
C18
C3
C11
C15
C1
C14
N1
O2
C4
C10
C9
C5
C6
C16
C17
C7
C8

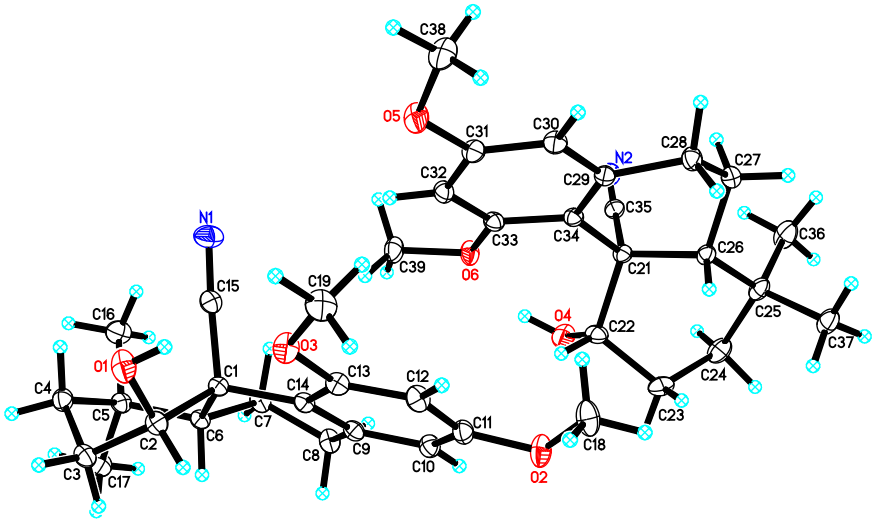
C38
O5
C31
C30
N2
C28
C27
C32
C29
C35
N1
C33
C34
C36
C39
O6
C21
C26
C19
C15
C25
C16
O4
C22
O1
O3
C1
C13
C12
C24
C4
C14
C37
C5
C7
C11
C23
C6
C2
C9
C18
C8
C10
O2
C3
C17

Table 1. Crystal data and structure refinement for cdv73.

Identification code	cdv73 (Darius Vrubliauskas)	
Empirical formula	C_{19} H_{25} N O_3	
Formula weight	315.40	
Temperature	133(2) K	
Wavelength	0.71073 Å	
Crystal system	Triclinic	
Space group	$P\bar{1}$	
Unit cell dimensions	a = 10.7114(5) Å	a = 77.2958(7)°.
	b = 10.9007(5) Å	b = 82.5663(8)°.
	c = 15.0024(7) Å	g = 74.4969(7)°.
Volume	1642.00(13) $Å^3$	
Z	4	
Density (calculated)	1.276 Mg/m^3	
Absorption coefficient	0.086 mm^{-1}	
F(000)	680	
Crystal color	colorless	
Crystal size	0.354 x 0.348 x 0.294 mm^3	
Theta range for data collection	1.395 to 31.054°	
Index ranges	$-15 \le h \le 15$, $-15 \le k \le 15$, $-21 \le l \le 21$	
Reflections collected	40968	
Independent reflections	9704 [R(int) = 0.0303]	
Completeness to theta = 25.242°	100.0 %	
Absorption correction	Semi-empirical from equivalents	
Max. and min. transmission	0.8622 and 0.8259	
Refinement method	Full-matrix least-squares on F^2	
Data / restraints / parameters	9704 / 0 / 429	

Goodness-of-fit on F^2	1.023
Final R indices [I>2sigma(I) = 8079 data]	R1 = 0.0403, wR2 = 0.1049
R indices (all data, 0.69 Å)	R1 = 0.0509, wR2 = 0.1120
Largest diff. peak and hole	0.463 and -0.229 e.$Å^{-3}$

Table 2. Atomic coordinates (x 10^4) and equivalent isotropic displacement parameters ($Å^2$ x 10^3)

for cdv73. U(eq) is defined as one third of the trace of the orthogonalized U^{ij} tensor.

	x	y	z	U(eq)
O(1)	10524(1)	9261(1)	779(1)	22(1)
O(2)	8653(1)	3204(1)	1816(1)	23(1)
O(3)	9183(1)	7551(1)	574(1)	19(1)
N(1)	7736(1)	9640(1)	2046(1)	22(1)
C(1)	9918(1)	7824(1)	2243(1)	12(1)
C(2)	11018(1)	8231(1)	1500(1)	15(1)
C(3)	11967(1)	8728(1)	1916(1)	16(1)
C(4)	11218(1)	9623(1)	2557(1)	16(1)
C(5)	10722(1)	8821(1)	3442(1)	14(1)
C(6)	10416(1)	7611(1)	3213(1)	12(1)
C(7)	9548(1)	6973(1)	3952(1)	15(1)
C(8)	9679(1)	5598(1)	3828(1)	16(1)
C(9)	9500(1)	5547(1)	2855(1)	14(1)
C(10)	9202(1)	4436(1)	2721(1)	16(1)
C(11)	8914(1)	4345(1)	1866(1)	16(1)
C(12)	8891(1)	5388(1)	1133(1)	17(1)
C(13)	9208(1)	6488(1)	1269(1)	14(1)
C(14)	9563(1)	6587(1)	2120(1)	13(1)
C(15)	8702(1)	8874(1)	2135(1)	15(1)
C(16)	9545(1)	9690(1)	3884(1)	21(1)
C(17)	11798(1)	8331(1)	4113(1)	19(1)
C(18)	8017(1)	3176(1)	1045(1)	27(1)
C(19)	8526(1)	7654(1)	-224(1)	23(1)
O(4)	6001(1)	3591(1)	4404(1)	21(1)

O(5)	5039(1)	8453(1)	294(1)	22(1)
O(6)	5694(1)	6013(1)	3298(1)	16(1)
N(2)	2916(1)	4908(1)	4375(1)	19(1)
C(21)	4614(1)	4042(1)	3088(1)	12(1)
C(22)	5981(1)	3370(1)	3509(1)	15(1)
C(23)	6299(1)	1902(1)	3619(1)	19(1)
C(24)	5125(1)	1405(1)	4064(1)	20(1)
C(25)	4037(1)	1776(1)	3402(1)	16(1)
C(26)	4147(1)	3037(1)	2705(1)	13(1)
C(27)	2938(1)	3705(1)	2182(1)	16(1)
C(28)	3317(1)	4579(1)	1310(1)	16(1)
C(29)	4124(1)	5436(1)	1486(1)	13(1)
C(30)	4249(1)	6498(1)	787(1)	15(1)
C(31)	4899(1)	7372(1)	922(1)	15(1)
C(32)	5429(1)	7216(1)	1754(1)	15(1)
C(33)	5289(1)	6174(1)	2445(1)	13(1)
C(34)	4677(1)	5229(1)	2317(1)	12(1)
C(35)	3667(1)	4518(1)	3824(1)	14(1)
C(36)	2712(1)	1891(1)	3952(1)	24(1)
C(37)	4250(1)	694(1)	2852(1)	20(1)
C(38)	4238(1)	8844(1)	-464(1)	23(1)
C(39)	6161(1)	7023(1)	3499(1)	20(1)

Table 3. Bond lengths [Å] and angles [°] for cdv73.

O(1)-C(2)	1.4164(11)
O(1)-H(1)	0.847(17)
O(2)-C(11)	1.3654(12)
O(2)-C(18)	1.4259(13)
O(3)-C(13)	1.3747(11)
O(3)-C(19)	1.4344(11)
N(1)-C(15)	1.1446(13)
C(1)-C(15)	1.4858(13)
C(1)-C(14)	1.5494(13)
C(1)-C(6)	1.5628(12)
C(1)-C(2)	1.5966(13)
C(2)-C(3)	1.5249(13)
C(2)-H(2A)	1.0000
C(3)-C(4)	1.5215(14)
C(3)-H(3A)	0.9900
C(3)-H(3B)	0.9900
C(4)-C(5)	1.5375(14)
C(4)-H(4A)	0.9900
C(4)-H(4B)	0.9900
C(5)-C(16)	1.5318(14)
C(5)-C(17)	1.5364(13)
C(5)-C(6)	1.5575(13)
C(6)-C(7)	1.5224(13)
C(6)-H(6A)	1.0000
C(7)-C(8)	1.5173(14)
C(7)-H(7A)	0.9900
C(7)-H(7B)	0.9900
C(8)-C(9)	1.5110(12)

C(8)-H(8A)	0.9900
C(8)-H(8B)	0.9900
C(9)-C(10)	1.3923(13)
C(9)-C(14)	1.4057(12)
C(10)-C(11)	1.3868(13)
C(10)-H(10A)	0.9500
C(11)-C(12)	1.3947(14)
C(12)-C(13)	1.3928(14)
C(12)-H(12A)	0.9500
C(13)-C(14)	1.4119(12)
C(16)-H(16A)	0.9800
C(16)-H(16B)	0.9800
C(16)-H(16C)	0.9800
C(17)-H(17A)	0.9800
C(17)-H(17B)	0.9800
C(17)-H(17C)	0.9800
C(18)-H(18A)	0.9800
C(18)-H(18B)	0.9800
C(18)-H(18C)	0.9800
C(19)-H(19A)	0.9800
C(19)-H(19B)	0.9800
C(19)-H(19C)	0.9800
O(4)-C(22)	1.4203(12)
O(4)-H(4)	0.829(17)
O(5)-C(31)	1.3666(11)
O(5)-C(38)	1.4327(12)
O(6)-C(33)	1.3649(11)
O(6)-C(39)	1.4267(12)
N(2)-C(35)	1.1448(13)
C(21)-C(35)	1.4825(13)

C(21)-C(34)	1.5445(12)
C(21)-C(26)	1.5576(13)
C(21)-C(22)	1.5937(13)
C(22)-C(23)	1.5193(14)
C(22)-H(22A)	1.0000
C(23)-C(24)	1.5192(15)
C(23)-H(23A)	0.9900
C(23)-H(23B)	0.9900
C(24)-C(25)	1.5427(15)
C(24)-H(24A)	0.9900
C(24)-H(24B)	0.9900
C(25)-C(36)	1.5350(14)
C(25)-C(37)	1.5366(14)
C(25)-C(26)	1.5558(13)
C(26)-C(27)	1.5263(13)
C(26)-H(26A)	1.0000
C(27)-C(28)	1.5186(14)
C(27)-H(27A)	0.9900
C(27)-H(27B)	0.9900
C(28)-C(29)	1.5133(13)
C(28)-H(28A)	0.9900
C(28)-H(28B)	0.9900
C(29)-C(34)	1.3973(12)
C(29)-C(30)	1.4036(13)
C(30)-C(31)	1.3813(14)
C(30)-H(30A)	0.9500
C(31)-C(32)	1.3957(13)
C(32)-C(33)	1.3858(13)
C(32)-H(32A)	0.9500
C(33)-C(34)	1.4164(13)

C(36)-H(36A)	0.9800
C(36)-H(36B)	0.9800
C(36)-H(36C)	0.9800
C(37)-H(37A)	0.9800
C(37)-H(37B)	0.9800
C(37)-H(37C)	0.9800
C(38)-H(38A)	0.9800
C(38)-H(38B)	0.9800
C(38)-H(38C)	0.9800
C(39)-H(39A)	0.9800
C(39)-H(39B)	0.9800
C(39)-H(39C)	0.9800

C(2)-O(1)-H(1)	105.5(11)
C(11)-O(2)-C(18)	117.87(8)
C(13)-O(3)-C(19)	118.70(8)
C(15)-C(1)-C(14)	105.78(7)
C(15)-C(1)-C(6)	111.03(7)
C(14)-C(1)-C(6)	110.09(7)
C(15)-C(1)-C(2)	109.04(7)
C(14)-C(1)-C(2)	113.12(7)
C(6)-C(1)-C(2)	107.80(7)
O(1)-C(2)-C(3)	104.36(8)
O(1)-C(2)-C(1)	113.49(8)
C(3)-C(2)-C(1)	111.94(7)
O(1)-C(2)-H(2A)	109.0
C(3)-C(2)-H(2A)	109.0
C(1)-C(2)-H(2A)	109.0
C(4)-C(3)-C(2)	109.47(8)
C(4)-C(3)-H(3A)	109.8

C(2)-C(3)-H(3A)	109.8
C(4)-C(3)-H(3B)	109.8
C(2)-C(3)-H(3B)	109.8
H(3A)-C(3)-H(3B)	108.2
C(3)-C(4)-C(5)	109.90(8)
C(3)-C(4)-H(4A)	109.7
C(5)-C(4)-H(4A)	109.7
C(3)-C(4)-H(4B)	109.7
C(5)-C(4)-H(4B)	109.7
H(4A)-C(4)-H(4B)	108.2
C(16)-C(5)-C(17)	108.66(8)
C(16)-C(5)-C(4)	109.09(8)
C(17)-C(5)-C(4)	109.15(8)
C(16)-C(5)-C(6)	113.18(8)
C(17)-C(5)-C(6)	107.60(8)
C(4)-C(5)-C(6)	109.08(7)
C(7)-C(6)-C(5)	113.75(7)
C(7)-C(6)-C(1)	111.19(7)
C(5)-C(6)-C(1)	114.93(7)
C(7)-C(6)-H(6A)	105.3
C(5)-C(6)-H(6A)	105.3
C(1)-C(6)-H(6A)	105.3
C(8)-C(7)-C(6)	109.14(8)
C(8)-C(7)-H(7A)	109.9
C(6)-C(7)-H(7A)	109.9
C(8)-C(7)-H(7B)	109.9
C(6)-C(7)-H(7B)	109.9
H(7A)-C(7)-H(7B)	108.3
C(9)-C(8)-C(7)	112.14(8)
C(9)-C(8)-H(8A)	109.2

C(7)-C(8)-H(8A)	109.2
C(9)-C(8)-H(8B)	109.2
C(7)-C(8)-H(8B)	109.2
H(8A)-C(8)-H(8B)	107.9
C(10)-C(9)-C(14)	120.81(8)
C(10)-C(9)-C(8)	116.72(8)
C(14)-C(9)-C(8)	122.40(8)
C(11)-C(10)-C(9)	120.92(9)
C(11)-C(10)-H(10A)	119.5
C(9)-C(10)-H(10A)	119.5
O(2)-C(11)-C(10)	115.63(9)
O(2)-C(11)-C(12)	124.48(9)
C(10)-C(11)-C(12)	119.88(9)
C(13)-C(12)-C(11)	118.85(9)
C(13)-C(12)-H(12A)	120.6
C(11)-C(12)-H(12A)	120.6
O(3)-C(13)-C(12)	121.29(8)
O(3)-C(13)-C(14)	116.17(8)
C(12)-C(13)-C(14)	122.54(9)
C(9)-C(14)-C(13)	116.79(8)
C(9)-C(14)-C(1)	122.10(8)
C(13)-C(14)-C(1)	121.00(8)
N(1)-C(15)-C(1)	176.68(10)
C(5)-C(16)-H(16A)	109.5
C(5)-C(16)-H(16B)	109.5
H(16A)-C(16)-H(16B)	109.5
C(5)-C(16)-H(16C)	109.5
H(16A)-C(16)-H(16C)	109.5
H(16B)-C(16)-H(16C)	109.5
C(5)-C(17)-H(17A)	109.5

C(5)-C(17)-H(17B)	109.5
H(17A)-C(17)-H(17B)	109.5
C(5)-C(17)-H(17C)	109.5
H(17A)-C(17)-H(17C)	109.5
H(17B)-C(17)-H(17C)	109.5
O(2)-C(18)-H(18A)	109.5
O(2)-C(18)-H(18B)	109.5
H(18A)-C(18)-H(18B)	109.5
O(2)-C(18)-H(18C)	109.5
H(18A)-C(18)-H(18C)	109.5
H(18B)-C(18)-H(18C)	109.5
O(3)-C(19)-H(19A)	109.5
O(3)-C(19)-H(19B)	109.5
H(19A)-C(19)-H(19B)	109.5
O(3)-C(19)-H(19C)	109.5
H(19A)-C(19)-H(19C)	109.5
H(19B)-C(19)-H(19C)	109.5
C(22)-O(4)-H(4)	105.7(11)
C(31)-O(5)-C(38)	117.05(8)
C(33)-O(6)-C(39)	117.94(7)
C(35)-C(21)-C(34)	107.01(7)
C(35)-C(21)-C(26)	110.17(8)
C(34)-C(21)-C(26)	109.25(7)
C(35)-C(21)-C(22)	108.45(7)
C(34)-C(21)-C(22)	112.29(7)
C(26)-C(21)-C(22)	109.63(7)
O(4)-C(22)-C(23)	104.72(8)
O(4)-C(22)-C(21)	112.47(8)
C(23)-C(22)-C(21)	111.62(8)
O(4)-C(22)-H(22A)	109.3

C(23)-C(22)-H(22A)	109.3
C(21)-C(22)-H(22A)	109.3
C(24)-C(23)-C(22)	109.89(8)
C(24)-C(23)-H(23A)	109.7
C(22)-C(23)-H(23A)	109.7
C(24)-C(23)-H(23B)	109.7
C(22)-C(23)-H(23B)	109.7
H(23A)-C(23)-H(23B)	108.2
C(23)-C(24)-C(25)	111.39(8)
C(23)-C(24)-H(24A)	109.4
C(25)-C(24)-H(24A)	109.4
C(23)-C(24)-H(24B)	109.4
C(25)-C(24)-H(24B)	109.4
H(24A)-C(24)-H(24B)	108.0
C(36)-C(25)-C(37)	108.75(8)
C(36)-C(25)-C(24)	109.67(9)
C(37)-C(25)-C(24)	108.43(8)
C(36)-C(25)-C(26)	113.42(8)
C(37)-C(25)-C(26)	107.20(8)
C(24)-C(25)-C(26)	109.25(8)
C(27)-C(26)-C(25)	114.25(8)
C(27)-C(26)-C(21)	110.40(7)
C(25)-C(26)-C(21)	115.51(7)
C(27)-C(26)-H(26A)	105.2
C(25)-C(26)-H(26A)	105.2
C(21)-C(26)-H(26A)	105.2
C(28)-C(27)-C(26)	108.83(8)
C(28)-C(27)-H(27A)	109.9
C(26)-C(27)-H(27A)	109.9
C(28)-C(27)-H(27B)	109.9

C(26)-C(27)-H(27B)	109.9
H(27A)-C(27)-H(27B)	108.3
C(29)-C(28)-C(27)	112.24(8)
C(29)-C(28)-H(28A)	109.2
C(27)-C(28)-H(28A)	109.2
C(29)-C(28)-H(28B)	109.2
C(27)-C(28)-H(28B)	109.2
H(28A)-C(28)-H(28B)	107.9
C(34)-C(29)-C(30)	120.78(9)
C(34)-C(29)-C(28)	122.31(8)
C(30)-C(29)-C(28)	116.85(8)
C(31)-C(30)-C(29)	120.19(8)
C(31)-C(30)-H(30A)	119.9
C(29)-C(30)-H(30A)	119.9
O(5)-C(31)-C(30)	124.46(8)
O(5)-C(31)-C(32)	114.98(8)
C(30)-C(31)-C(32)	120.51(8)
C(33)-C(32)-C(31)	119.00(9)
C(33)-C(32)-H(32A)	120.5
C(31)-C(32)-H(32A)	120.5
O(6)-C(33)-C(32)	122.29(8)
O(6)-C(33)-C(34)	115.70(8)
C(32)-C(33)-C(34)	121.97(8)
C(29)-C(34)-C(33)	117.39(8)
C(29)-C(34)-C(21)	122.50(8)
C(33)-C(34)-C(21)	120.10(8)
N(2)-C(35)-C(21)	178.19(10)
C(25)-C(36)-H(36A)	109.5
C(25)-C(36)-H(36B)	109.5
H(36A)-C(36)-H(36B)	109.5

C(25)-C(36)-H(36C)	109.5
H(36A)-C(36)-H(36C)	109.5
H(36B)-C(36)-H(36C)	109.5
C(25)-C(37)-H(37A)	109.5
C(25)-C(37)-H(37B)	109.5
H(37A)-C(37)-H(37B)	109.5
C(25)-C(37)-H(37C)	109.5
H(37A)-C(37)-H(37C)	109.5
H(37B)-C(37)-H(37C)	109.5
O(5)-C(38)-H(38A)	109.5
O(5)-C(38)-H(38B)	109.5
H(38A)-C(38)-H(38B)	109.5
O(5)-C(38)-H(38C)	109.5
H(38A)-C(38)-H(38C)	109.5
H(38B)-C(38)-H(38C)	109.5
O(6)-C(39)-H(39A)	109.5
O(6)-C(39)-H(39B)	109.5
H(39A)-C(39)-H(39B)	109.5
O(6)-C(39)-H(39C)	109.5
H(39A)-C(39)-H(39C)	109.5
H(39B)-C(39)-H(39C)	109.5

Table 4. Anisotropic displacement parameters ($Å^2$ x 10^3) for cdv73. The anisotropic displacement factor exponent takes the form: $-2p^2[h^2 a^{*2} U^{11} + ... + 2 h k a^* b^* U^{12}]$

	U^{11}	U^{22}	U^{33}	U^{23}	U^{13}	U^{12}
O(1)	28(1)	26(1)	14(1)	5(1)	-7(1)	-15(1)
O(2)	32(1)	21(1)	21(1)	-5(1)	-5(1)	-13(1)
O(3)	28(1)	21(1)	10(1)	0(1)	-6(1)	-9(1)
N(1)	19(1)	24(1)	23(1)	-6(1)	-7(1)	0(1)
C(1)	12(1)	13(1)	10(1)	-2(1)	-2(1)	-3(1)
C(2)	15(1)	17(1)	11(1)	-2(1)	1(1)	-5(1)
C(3)	14(1)	19(1)	16(1)	-2(1)	-1(1)	-6(1)
C(4)	17(1)	16(1)	17(1)	-2(1)	-3(1)	-6(1)
C(5)	14(1)	15(1)	13(1)	-4(1)	-3(1)	-4(1)
C(6)	12(1)	14(1)	10(1)	-2(1)	-3(1)	-3(1)
C(7)	16(1)	20(1)	10(1)	-3(1)	-1(1)	-7(1)
C(8)	19(1)	19(1)	11(1)	0(1)	-3(1)	-8(1)
C(9)	12(1)	16(1)	12(1)	-2(1)	-2(1)	-4(1)
C(10)	16(1)	16(1)	15(1)	-1(1)	-2(1)	-6(1)
C(11)	16(1)	17(1)	18(1)	-5(1)	-1(1)	-6(1)
C(12)	19(1)	21(1)	13(1)	-6(1)	-2(1)	-6(1)
C(13)	15(1)	17(1)	11(1)	-2(1)	-1(1)	-4(1)
C(14)	12(1)	15(1)	12(1)	-3(1)	-1(1)	-3(1)
C(15)	16(1)	18(1)	12(1)	-3(1)	-3(1)	-5(1)
C(16)	20(1)	23(1)	21(1)	-11(1)	-2(1)	-3(1)
C(17)	20(1)	20(1)	19(1)	-3(1)	-9(1)	-6(1)
C(18)	32(1)	31(1)	24(1)	-11(1)	-5(1)	-16(1)
C(19)	28(1)	27(1)	13(1)	-1(1)	-9(1)	-7(1)
O(4)	27(1)	16(1)	18(1)	0(1)	-11(1)	-4(1)

O(5)	29(1)	20(1)	16(1)	7(1)	-7(1)	-12(1)
O(6)	22(1)	16(1)	14(1)	0(1)	-7(1)	-9(1)
N(2)	21(1)	19(1)	18(1)	-4(1)	1(1)	-5(1)
C(21)	12(1)	11(1)	11(1)	0(1)	-1(1)	-3(1)
C(22)	13(1)	16(1)	15(1)	1(1)	-4(1)	-2(1)
C(23)	18(1)	16(1)	19(1)	-1(1)	-4(1)	1(1)
C(24)	28(1)	13(1)	17(1)	2(1)	-2(1)	-4(1)
C(25)	19(1)	11(1)	18(1)	-1(1)	3(1)	-5(1)
C(26)	14(1)	11(1)	14(1)	-2(1)	0(1)	-4(1)
C(27)	15(1)	15(1)	19(1)	-3(1)	-2(1)	-5(1)
C(28)	19(1)	15(1)	16(1)	-2(1)	-6(1)	-6(1)
C(29)	13(1)	13(1)	14(1)	-2(1)	-2(1)	-3(1)
C(30)	17(1)	15(1)	12(1)	-1(1)	-3(1)	-4(1)
C(31)	16(1)	14(1)	13(1)	2(1)	-1(1)	-5(1)
C(32)	15(1)	14(1)	16(1)	0(1)	-3(1)	-6(1)
C(33)	12(1)	14(1)	13(1)	-1(1)	-3(1)	-3(1)
C(34)	12(1)	12(1)	12(1)	0(1)	-1(1)	-3(1)
C(35)	15(1)	12(1)	14(1)	1(1)	-3(1)	-4(1)
C(36)	25(1)	18(1)	27(1)	-5(1)	11(1)	-10(1)
C(37)	22(1)	13(1)	24(1)	-4(1)	3(1)	-6(1)
C(38)	36(1)	19(1)	13(1)	3(1)	-8(1)	-9(1)
C(39)	27(1)	17(1)	20(1)	-3(1)	-9(1)	-9(1)

Table 5. Hydrogen coordinates ($x\ 10^4$) and isotropic displacement parameters ($Å^2\ x\ 10^3$) for cdv73.

	x	y	z	U(eq)
H(1)	10006(16)	8993(16)	532(11)	33
H(2A)	11509	7459	1234	18
H(3A)	12589	7987	2260	20
H(3B)	12465	9206	1423	20
H(4A)	10475	10252	2252	19
H(4B)	11792	10115	2708	19
H(6A)	11269	6954	3201	15
H(7A)	9807	6956	4565	18
H(7B)	8633	7475	3906	18
H(8A)	10549	5059	3994	19
H(8B)	9023	5227	4248	19
H(10A)	9197	3731	3221	19
H(12A)	8663	5348	550	20
H(16A)	8822	9940	3490	31
H(16B)	9774	10470	3962	31
H(16C)	9287	9215	4484	31
H(17A)	12591	7859	3811	28
H(17B)	11518	7750	4653	28
H(17C)	11971	9071	4302	28
H(18A)	7815	2332	1122	40
H(18B)	8588	3313	486	40
H(18C)	7210	3865	996	40
H(19A)	8518	8493	-631	34

H(19B)	7631	7588	-39	34
H(19C)	8980	6952	-547	34
H(4)	5993(15)	4368(16)	4338(10)	31
H(22A)	6678	3707	3098	19
H(23A)	6548	1657	3011	23
H(23B)	7043	1503	4003	23
H(24A)	4791	1776	4620	24
H(24B)	5390	449	4254	24
H(26A)	4844	2747	2230	16
H(27A)	2563	3047	2029	19
H(27B)	2276	4226	2566	19
H(28A)	3817	4036	871	20
H(28B)	2520	5132	1025	20
H(30A)	3885	6616	220	18
H(32A)	5879	7815	1845	18
H(36A)	2534	2625	4266	35
H(36B)	2725	1090	4405	35
H(36C)	2033	2032	3535	35
H(37A)	5154	491	2597	30
H(37B)	3670	983	2352	30
H(37C)	4062	-84	3256	30
H(38A)	4343	9683	-820	34
H(38B)	3326	8922	-234	34
H(38C)	4496	8193	-855	34
H(39A)	6406	6790	4133	30
H(39B)	5477	7833	3421	30
H(39C)	6921	7142	3082	30

Table 6. Torsion angles [°] for cdv73.

C(15)-C(1)-C(2)-O(1)	-16.38(11)
C(14)-C(1)-C(2)-O(1)	101.01(9)
C(6)-C(1)-C(2)-O(1)	-137.02(8)
C(15)-C(1)-C(2)-C(3)	101.44(9)
C(14)-C(1)-C(2)-C(3)	-141.17(8)
C(6)-C(1)-C(2)-C(3)	-19.20(10)
O(1)-C(2)-C(3)-C(4)	80.34(9)
C(1)-C(2)-C(3)-C(4)	-42.80(10)
C(2)-C(3)-C(4)-C(5)	73.32(10)
C(3)-C(4)-C(5)-C(16)	-156.42(8)
C(3)-C(4)-C(5)-C(17)	84.99(9)
C(3)-C(4)-C(5)-C(6)	-32.32(10)
C(16)-C(5)-C(6)-C(7)	-40.77(11)
C(17)-C(5)-C(6)-C(7)	79.30(10)
C(4)-C(5)-C(6)-C(7)	-162.41(8)
C(16)-C(5)-C(6)-C(1)	89.02(10)
C(17)-C(5)-C(6)-C(1)	-150.91(8)
C(4)-C(5)-C(6)-C(1)	-32.62(10)
C(15)-C(1)-C(6)-C(7)	71.55(10)
C(14)-C(1)-C(6)-C(7)	-45.24(10)
C(2)-C(1)-C(6)-C(7)	-169.07(8)
C(15)-C(1)-C(6)-C(5)	-59.48(10)
C(14)-C(1)-C(6)-C(5)	-176.28(7)
C(2)-C(1)-C(6)-C(5)	59.90(10)
C(5)-C(6)-C(7)-C(8)	-161.09(7)
C(1)-C(6)-C(7)-C(8)	67.27(10)
C(6)-C(7)-C(8)-C(9)	-50.60(10)
C(7)-C(8)-C(9)-C(10)	-160.84(9)

C(7)-C(8)-C(9)-C(14)	16.09(13)
C(14)-C(9)-C(10)-C(11)	-2.38(15)
C(8)-C(9)-C(10)-C(11)	174.60(9)
C(18)-O(2)-C(11)-C(10)	163.32(10)
C(18)-O(2)-C(11)-C(12)	-15.96(15)
C(9)-C(10)-C(11)-O(2)	179.24(9)
C(9)-C(10)-C(11)-C(12)	-1.45(15)
O(2)-C(11)-C(12)-C(13)	-178.40(9)
C(10)-C(11)-C(12)-C(13)	2.35(15)
C(19)-O(3)-C(13)-C(12)	15.20(14)
C(19)-O(3)-C(13)-C(14)	-164.36(9)
C(11)-C(12)-C(13)-O(3)	-179.02(9)
C(11)-C(12)-C(13)-C(14)	0.51(15)
C(10)-C(9)-C(14)-C(13)	5.02(13)
C(8)-C(9)-C(14)-C(13)	-171.79(9)
C(10)-C(9)-C(14)-C(1)	-178.76(9)
C(8)-C(9)-C(14)-C(1)	4.43(14)
O(3)-C(13)-C(14)-C(9)	175.42(8)
C(12)-C(13)-C(14)-C(9)	-4.14(14)
O(3)-C(13)-C(14)-C(1)	-0.84(13)
C(12)-C(13)-C(14)-C(1)	179.60(9)
C(15)-C(1)-C(14)-C(9)	-109.83(9)
C(6)-C(1)-C(14)-C(9)	10.20(12)
C(2)-C(1)-C(14)-C(9)	130.87(9)
C(15)-C(1)-C(14)-C(13)	66.22(11)
C(6)-C(1)-C(14)-C(13)	-173.75(8)
C(2)-C(1)-C(14)-C(13)	-53.07(11)
C(35)-C(21)-C(22)-O(4)	-10.00(11)
C(34)-C(21)-C(22)-O(4)	108.04(9)
C(26)-C(21)-C(22)-O(4)	-130.32(8)

C(35)-C(21)-C(22)-C(23)	107.36(9)
C(34)-C(21)-C(22)-C(23)	-134.59(8)
C(26)-C(21)-C(22)-C(23)	-12.96(10)
O(4)-C(22)-C(23)-C(24)	75.21(10)
C(21)-C(22)-C(23)-C(24)	-46.74(11)
C(22)-C(23)-C(24)-C(25)	71.03(11)
C(23)-C(24)-C(25)-C(36)	-152.10(9)
C(23)-C(24)-C(25)-C(37)	89.29(10)
C(23)-C(24)-C(25)-C(26)	-27.22(11)
C(36)-C(25)-C(26)-C(27)	-41.84(12)
C(37)-C(25)-C(26)-C(27)	78.21(10)
C(24)-C(25)-C(26)-C(27)	-164.50(8)
C(36)-C(25)-C(26)-C(21)	87.85(10)
C(37)-C(25)-C(26)-C(21)	-152.10(8)
C(24)-C(25)-C(26)-C(21)	-34.81(11)
C(35)-C(21)-C(26)-C(27)	68.62(9)
C(34)-C(21)-C(26)-C(27)	-48.67(10)
C(22)-C(21)-C(26)-C(27)	-172.11(7)
C(35)-C(21)-C(26)-C(25)	-62.91(10)
C(34)-C(21)-C(26)-C(25)	179.80(7)
C(22)-C(21)-C(26)-C(25)	56.36(10)
C(25)-C(26)-C(27)-C(28)	-158.97(8)
C(21)-C(26)-C(27)-C(28)	68.85(10)
C(26)-C(27)-C(28)-C(29)	-48.72(11)
C(27)-C(28)-C(29)-C(34)	12.96(13)
C(27)-C(28)-C(29)-C(30)	-164.28(9)
C(34)-C(29)-C(30)-C(31)	-1.48(15)
C(28)-C(29)-C(30)-C(31)	175.80(9)
C(38)-O(5)-C(31)-C(30)	13.54(15)
C(38)-O(5)-C(31)-C(32)	-164.14(9)

C(29)-C(30)-C(31)-O(5)	-178.06(9)
C(29)-C(30)-C(31)-C(32)	-0.49(15)
O(5)-C(31)-C(32)-C(33)	177.54(9)
C(30)-C(31)-C(32)-C(33)	-0.25(15)
C(39)-O(6)-C(33)-C(32)	6.01(14)
C(39)-O(6)-C(33)-C(34)	-171.99(9)
C(31)-C(32)-C(33)-O(6)	-174.89(9)
C(31)-C(32)-C(33)-C(34)	2.98(15)
C(30)-C(29)-C(34)-C(33)	4.00(14)
C(28)-C(29)-C(34)-C(33)	-173.13(9)
C(30)-C(29)-C(34)-C(21)	-177.28(8)
C(28)-C(29)-C(34)-C(21)	5.60(14)
O(6)-C(33)-C(34)-C(29)	173.19(8)
C(32)-C(33)-C(34)-C(29)	-4.82(14)
O(6)-C(33)-C(34)-C(21)	-5.56(13)
C(32)-C(33)-C(34)-C(21)	176.43(8)
C(35)-C(21)-C(34)-C(29)	-106.83(10)
C(26)-C(21)-C(34)-C(29)	12.43(12)
C(22)-C(21)-C(34)-C(29)	134.29(9)
C(35)-C(21)-C(34)-C(33)	71.86(10)
C(26)-C(21)-C(34)-C(33)	-168.88(8)
C(22)-C(21)-C(34)-C(33)	-47.03(11)

Table 7. Hydrogen bonds for cdv73 [Å and °].

D-H...A	d(D-H)	d(H...A)	d(D...A)	<(DHA)
O(1)-H(1)...O(3)	0.847(17)	1.983(17)	2.7254(11)	145.7(15)
O(4)-H(4)...O(6)	0.829(17)	2.083(16)	2.7528(10)	137.6(14)

X-ray Data Collection, Structure Solution and Refinement for cdv75 (**3.90**)

A colorless crystal of approximate dimensions 0.068 x 0.444 x 0.551 mm was mounted in a cryoloop and transferred to a Bruker SMART APEX II diffractometer system. The APEX2[1] program package was used to determine the unit-cell parameters and for data collection (20 sec/frame scan time). The raw frame data was processed using SAINT[2] and SADABS[3] to yield the reflection data file. Subsequent calculations were carried out using the SHELXTL[4] program package. The diffraction symmetry was 2/*m* and the systematic absences were consistent with the monoclinic space groups *Cc* and *C*2/*c*. It was later determined that space group *C*2/*c* was correct.

The structure was solved by direct methods and refined on F^2 by full-matrix least-squares techniques. The analytical scattering factors[5] for neutral atoms were used throughout the analysis. Hydrogen atoms were located from a difference-Fourier map and refined (x,y,z and U_{iso}).

Least-squares analysis yielded wR2 = 0.1096 and Goof = 1.009 for 337 variables refined against 4043 data (0.80 Å), R1 = 0.0414 for those 2938 data with $I > 2.0\sigma(I)$. It was necessary to collect data at 208 K due to crystal cracking at lower temperatures.

References.

16. APEX2 Version 2014.11-0, Bruker AXS, Inc.; Madison, WI 2014.

17. SAINT Version 8.34a, Bruker AXS, Inc.; Madison, WI 2013.

18. Sheldrick, G. M. SADABS, Version 2014/5, Bruker AXS, Inc.; Madison, WI 2014.

19. Sheldrick, G. M. SHELXTL, Version 2014/7, Bruker AXS, Inc.; Madison, WI 2014.

20. International Tables for Crystallography 1992, Vol. C., Dordrecht: Kluwer Academic Publishers.

Definitions:

$wR2 = [\Sigma[w(F_o^2-F_c^2)^2] / \Sigma[w(F_o^2)^2]]^{1/2}$

$R1 = \Sigma||F_o|-|F_c|| / \Sigma|F_o|$

$Goof = S = [\Sigma[w(F_o^2-F_c^2)^2] / (n-p)]^{1/2}$ where n is the number of reflections and p is the total number of parameters refined.

The thermal ellipsoid plot is shown at the 30% probability level.

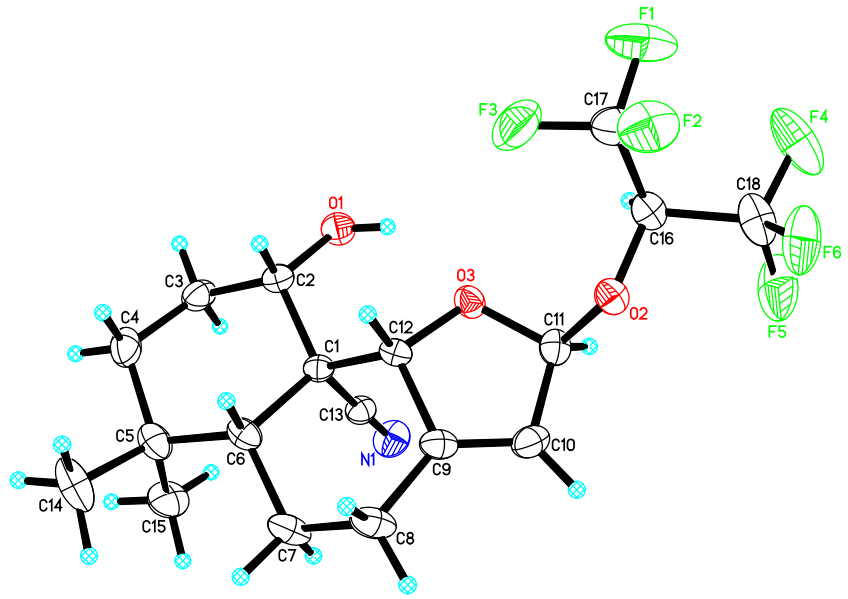

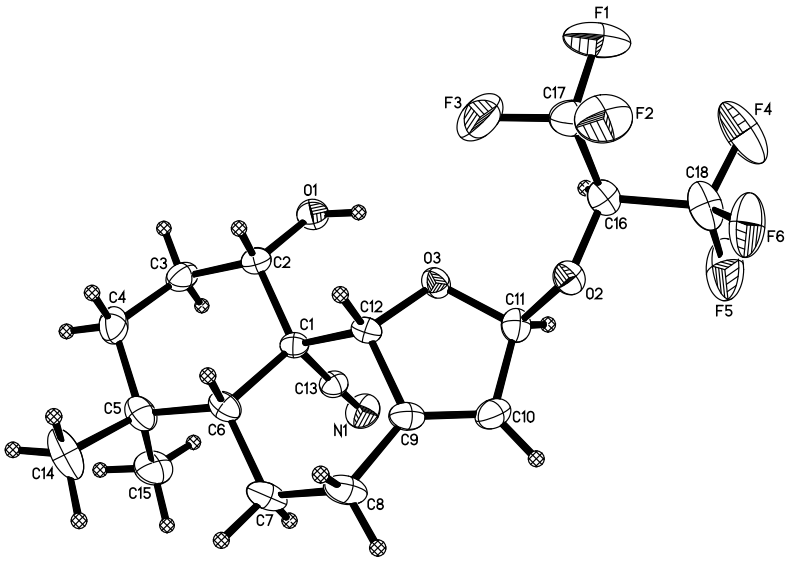

Table 1. Crystal data and structure refinement for cdv75.

Identification code	cdv75 (Darius Vrubliauskas)	
Empirical formula	C_{18} H_{21} F_6 N O_3	
Formula weight	413.36	
Temperature	208(2) K	
Wavelength	0.71073 Å	
Crystal system	Monoclinic	
Space group	*C*2/*c*	
Unit cell dimensions	a = 32.175(5) Å	□ = 90°.
	b = 7.4047(10) Å	□ = 125.2267(19)°.
	c = 20.212(3) Å	□ = 90°.
Volume	3933.6(10) Å^3	
Z	8	
Density (calculated)	1.396 Mg/m^3	
Absorption coefficient	0.131 mm^{-1}	
F(000)	1712	
Crystal color	colorless	
Crystal size	0.551 x 0.444 x 0.068 mm^3	
Theta range for data collection	1.550 to 26.392°	
Index ranges	$-40 \leq h \leq 40$, $-9 \leq k \leq 9$, $-25 \leq l \leq 25$	
Reflections collected	36753	
Independent reflections	4043 [R(int) = 0.0454]	
Completeness to theta = 25.242°	100.0 %	
Absorption correction	Semi-empirical from equivalents	
Max. and min. transmission	0.8620 and 0.7978	
Refinement method	Full-matrix least-squares on F^2	
Data / restraints / parameters	4043 / 0 / 337	
Goodness-of-fit on F^2	1.009	
Final R indices [I>2sigma(I) = 2938 data]	R1 = 0.0414, wR2 = 0.0946	

R indices (all data, 0.80 Å)	R1 = 0.0653, wR2 = 0.1096
Largest diff. peak and hole	0.218 and -0.228 e.Å^{-3}

Table 2. Atomic coordinates (x 10^4) and equivalent isotropic displacement parameters (Å^2 x 10^3)

for cdv75. U(eq) is defined as one third of the trace of the orthogonalized U^{ij} tensor.

	x	y	z	U(eq)
O(1)	3088(1)	2347(2)	3574(1)	46(1)
O(2)	1564(1)	5516(2)	3141(1)	39(1)
O(3)	2360(1)	4760(2)	3432(1)	38(1)
N(1)	3138(1)	6634(2)	2928(1)	53(1)
F(1)	1100(1)	1069(2)	2927(1)	115(1)
F(2)	1143(1)	3154(2)	3695(1)	83(1)
F(3)	1818(1)	2189(2)	3844(1)	97(1)
F(4)	430(1)	3246(3)	1671(1)	121(1)
F(5)	713(1)	5764(3)	1578(1)	104(1)
F(6)	542(1)	5440(2)	2447(1)	92(1)
C(1)	3280(1)	5324(2)	4246(1)	30(1)
C(2)	3422(1)	3304(2)	4306(1)	36(1)
C(3)	3957(1)	3093(3)	4534(1)	47(1)
C(4)	4338(1)	4029(3)	5332(1)	53(1)
C(5)	4250(1)	6069(3)	5332(1)	49(1)
C(6)	3689(1)	6413(2)	5023(1)	39(1)
C(7)	3539(1)	8420(3)	4912(1)	49(1)
C(8)	3022(1)	8725(3)	4774(1)	51(1)
C(9)	2634(1)	7490(2)	4128(1)	38(1)
C(10)	2176(1)	7758(3)	3461(1)	46(1)

C(11)	1954(1)	6016(3)	3033(1)	40(1)
C(12)	2774(1)	5546(2)	4169(1)	31(1)
C(13)	3203(1)	6078(2)	3506(1)	35(1)
C(14)	4599(1)	6744(5)	6212(2)	80(1)
C(15)	4397(1)	7050(3)	4824(2)	62(1)
C(16)	1278(1)	4003(3)	2703(1)	42(1)
C(17)	1331(1)	2599(3)	3291(2)	62(1)
C(18)	735(1)	4615(4)	2099(1)	66(1)

__ Table 3. Bond lengths [Å] and angles [°] for cdv75.

O(1)-C(2)	1.419(2)
O(1)-H(1)	0.83(2)
O(2)-C(16)	1.395(2)
O(2)-C(11)	1.4439(19)
O(3)-C(11)	1.416(2)
O(3)-C(12)	1.4296(19)
N(1)-C(13)	1.139(2)
F(1)-C(17)	1.322(3)
F(2)-C(17)	1.332(2)
F(3)-C(17)	1.332(3)
F(4)-C(18)	1.326(3)
F(5)-C(18)	1.325(3)
F(6)-C(18)	1.324(3)
C(1)-C(13)	1.478(2)
C(1)-C(2)	1.548(2)
C(1)-C(12)	1.550(2)
C(1)-C(6)	1.569(2)
C(2)-C(3)	1.512(2)
C(2)-H(2A)	0.973(17)

C(3)-C(4)	1.518(3)
C(3)-H(3A)	1.020(19)
C(3)-H(3B)	0.91(2)
C(4)-C(5)	1.537(3)
C(4)-H(4A)	0.99(2)
C(4)-H(4B)	0.98(2)
C(5)-C(15)	1.537(3)
C(5)-C(14)	1.540(3)
C(5)-C(6)	1.554(3)
C(6)-C(7)	1.538(3)
C(6)-H(6A)	1.003(18)
C(7)-C(8)	1.537(3)
C(7)-H(7A)	0.99(2)
C(7)-H(7B)	0.99(2)
C(8)-C(9)	1.488(3)
C(8)-H(8A)	0.98(2)
C(8)-H(8B)	0.97(2)
C(9)-C(10)	1.319(3)
C(9)-C(12)	1.497(2)
C(10)-C(11)	1.486(3)
C(10)-H(10A)	0.93(2)
C(11)-H(11A)	1.003(17)
C(12)-H(12A)	0.982(16)
C(14)-H(14A)	0.96(3)
C(14)-H(14B)	0.99(3)
C(14)-H(14C)	1.04(3)
C(15)-H(15A)	0.99(2)
C(15)-H(15B)	0.98(3)
C(15)-H(15C)	1.01(2)
C(16)-C(17)	1.512(3)

C(16)-C(18)	1.513(3)
C(16)-H(16A)	0.92(2)

C(2)-O(1)-H(1)	109.6(17)
C(16)-O(2)-C(11)	114.98(12)
C(11)-O(3)-C(12)	109.01(12)
C(13)-C(1)-C(2)	108.25(13)
C(13)-C(1)-C(12)	107.75(13)
C(2)-C(1)-C(12)	110.86(12)
C(13)-C(1)-C(6)	111.84(13)
C(2)-C(1)-C(6)	112.25(13)
C(12)-C(1)-C(6)	105.80(12)
O(1)-C(2)-C(3)	108.00(15)
O(1)-C(2)-C(1)	112.92(14)
C(3)-C(2)-C(1)	110.92(14)
O(1)-C(2)-H(2A)	109.8(10)
C(3)-C(2)-H(2A)	109.6(10)
C(1)-C(2)-H(2A)	105.6(10)
C(2)-C(3)-C(4)	110.82(16)
C(2)-C(3)-H(3A)	108.8(11)
C(4)-C(3)-H(3A)	112.2(11)
C(2)-C(3)-H(3B)	108.2(13)
C(4)-C(3)-H(3B)	112.1(13)
H(3A)-C(3)-H(3B)	104.5(16)
C(3)-C(4)-C(5)	114.38(17)
C(3)-C(4)-H(4A)	109.1(12)
C(5)-C(4)-H(4A)	109.5(12)
C(3)-C(4)-H(4B)	108.9(12)
C(5)-C(4)-H(4B)	107.5(12)
H(4A)-C(4)-H(4B)	107.3(16)

C(4)-C(5)-C(15)	109.71(18)
C(4)-C(5)-C(14)	107.9(2)
C(15)-C(5)-C(14)	108.5(2)
C(4)-C(5)-C(6)	109.39(15)
C(15)-C(5)-C(6)	112.83(17)
C(14)-C(5)-C(6)	108.38(18)
C(7)-C(6)-C(5)	114.21(15)
C(7)-C(6)-C(1)	109.85(15)
C(5)-C(6)-C(1)	115.32(14)
C(7)-C(6)-H(6A)	107.8(10)
C(5)-C(6)-H(6A)	105.8(10)
C(1)-C(6)-H(6A)	102.8(10)
C(8)-C(7)-C(6)	112.56(15)
C(8)-C(7)-H(7A)	108.9(12)
C(6)-C(7)-H(7A)	111.0(12)
C(8)-C(7)-H(7B)	108.5(12)
C(6)-C(7)-H(7B)	110.0(12)
H(7A)-C(7)-H(7B)	105.7(16)
C(9)-C(8)-C(7)	109.94(15)
C(9)-C(8)-H(8A)	108.4(12)
C(7)-C(8)-H(8A)	108.3(12)
C(9)-C(8)-H(8B)	110.2(12)
C(7)-C(8)-H(8B)	110.3(12)
H(8A)-C(8)-H(8B)	109.7(17)
C(10)-C(9)-C(8)	132.93(18)
C(10)-C(9)-C(12)	108.94(15)
C(8)-C(9)-C(12)	117.99(16)
C(9)-C(10)-C(11)	110.04(16)
C(9)-C(10)-H(10A)	129.1(12)
C(11)-C(10)-H(10A)	120.8(12)

O(3)-C(11)-O(2)	110.03(13)
O(3)-C(11)-C(10)	105.27(14)
O(2)-C(11)-C(10)	107.54(14)
O(3)-C(11)-H(11A)	108.0(10)
O(2)-C(11)-H(11A)	108.3(10)
C(10)-C(11)-H(11A)	117.6(10)
O(3)-C(12)-C(9)	105.30(13)
O(3)-C(12)-C(1)	110.83(12)
C(9)-C(12)-C(1)	111.88(12)
O(3)-C(12)-H(12A)	109.4(9)
C(9)-C(12)-H(12A)	112.6(9)
C(1)-C(12)-H(12A)	106.9(9)
N(1)-C(13)-C(1)	178.7(2)
C(5)-C(14)-H(14A)	108.8(15)
C(5)-C(14)-H(14B)	109.3(17)
H(14A)-C(14)-H(14B)	105(2)
C(5)-C(14)-H(14C)	110.1(18)
H(14A)-C(14)-H(14C)	110(2)
H(14B)-C(14)-H(14C)	114(3)
C(5)-C(15)-H(15A)	107.1(13)
C(5)-C(15)-H(15B)	111.9(15)
H(15A)-C(15)-H(15B)	106.3(19)
C(5)-C(15)-H(15C)	111.7(14)
H(15A)-C(15)-H(15C)	107.2(19)
H(15B)-C(15)-H(15C)	112(2)
O(2)-C(16)-C(17)	108.60(15)
O(2)-C(16)-C(18)	107.63(16)
C(17)-C(16)-C(18)	113.25(17)
O(2)-C(16)-H(16A)	112.5(12)
C(17)-C(16)-H(16A)	108.0(12)

C(18)-C(16)-H(16A)	106.9(12)
F(1)-C(17)-F(2)	107.37(18)
F(1)-C(17)-F(3)	106.4(2)
F(2)-C(17)-F(3)	106.7(2)
F(1)-C(17)-C(16)	112.22(19)
F(2)-C(17)-C(16)	112.54(18)
F(3)-C(17)-C(16)	111.17(17)
F(6)-C(18)-F(5)	107.5(2)
F(6)-C(18)-F(4)	107.75(19)
F(5)-C(18)-F(4)	106.91(19)
F(6)-C(18)-C(16)	112.73(17)
F(5)-C(18)-C(16)	109.89(17)
F(4)-C(18)-C(16)	111.8(2)

Table 4. Anisotropic displacement parameters ($Å^2$ x 10^3) for cdv75. The anisotropic displacement factor exponent takes the form: $-2\pi^2[h^2 a^{*2} U^{11} + ... + 2 h k a^* b^* U^{12}]$

	U^{11}	U^{22}	U^{33}	U^{23}	U^{13}	U^{12}
O(1)	48(1)	38(1)	50(1)	-10(1)	27(1)	1(1)
O(2)	38(1)	45(1)	40(1)	-4(1)	26(1)	-2(1)
O(3)	33(1)	38(1)	40(1)	-10(1)	19(1)	-3(1)
N(1)	62(1)	59(1)	48(1)	14(1)	37(1)	4(1)
F(1)	161(2)	56(1)	158(2)	-23(1)	109(2)	-38(1)
F(2)	113(1)	88(1)	89(1)	12(1)	82(1)	0(1)
F(3)	93(1)	87(1)	111(1)	52(1)	58(1)	30(1)
F(4)	66(1)	180(2)	91(1)	-53(1)	29(1)	-58(1)
F(5)	64(1)	170(2)	59(1)	44(1)	24(1)	21(1)

F(6)	57(1)	140(1)	86(1)	13(1)	46(1)	34(1)
C(1)	35(1)	29(1)	31(1)	1(1)	22(1)	-2(1)
C(2)	41(1)	32(1)	38(1)	2(1)	24(1)	0(1)
C(3)	46(1)	37(1)	63(1)	8(1)	35(1)	8(1)
C(4)	34(1)	67(1)	54(1)	14(1)	22(1)	2(1)
C(5)	38(1)	59(1)	50(1)	-4(1)	24(1)	-11(1)
C(6)	40(1)	43(1)	37(1)	-6(1)	24(1)	-11(1)
C(7)	54(1)	41(1)	63(1)	-19(1)	40(1)	-19(1)
C(8)	61(1)	36(1)	71(1)	-18(1)	47(1)	-13(1)
C(9)	46(1)	31(1)	52(1)	-4(1)	37(1)	-4(1)
C(10)	51(1)	35(1)	64(1)	9(1)	40(1)	6(1)
C(11)	36(1)	49(1)	37(1)	4(1)	23(1)	2(1)
C(12)	36(1)	30(1)	32(1)	-4(1)	22(1)	-6(1)
C(13)	38(1)	34(1)	39(1)	3(1)	25(1)	1(1)
C(14)	42(1)	116(3)	62(2)	-22(2)	18(1)	-22(2)
C(15)	52(1)	59(1)	91(2)	2(1)	51(1)	-8(1)
C(16)	41(1)	49(1)	42(1)	-10(1)	28(1)	-3(1)
C(17)	74(2)	51(1)	77(2)	-1(1)	53(1)	-5(1)
C(18)	43(1)	102(2)	47(1)	-6(1)	24(1)	-8(1)

Table 5. Hydrogen coordinates (x 10^4) and isotropic displacement parameters ($Å^2$ x 10^3) for cdv75.

	x	y	z	U(eq)
H(1)	2789(9)	2610(30)	3387(14)	76(8)
H(2A)	3402(6)	2800(20)	4733(10)	34(4)
H(3A)	3969(7)	3580(30)	4073(11)	48(5)

H(3B)	4023(7)	1900(30)	4552(12)	53(6)
H(4A)	4687(8)	3810(30)	5481(12)	60(6)
H(4B)	4320(8)	3490(30)	5756(12)	59(6)
H(6A)	3654(6)	5900(20)	5449(11)	42(5)
H(7A)	3802(8)	9140(30)	5389(12)	58(6)
H(7B)	3523(7)	8920(30)	4447(12)	53(6)
H(8A)	3058(8)	8440(30)	5279(13)	58(6)
H(8B)	2916(8)	9970(30)	4625(12)	59(6)
H(10A)	1992(7)	8830(30)	3255(11)	48(5)
H(11A)	1805(6)	5970(20)	2439(11)	37(4)
H(12A)	2817(6)	4910(20)	4632(10)	30(4)
H(14A)	4941(11)	6370(30)	6433(15)	85(8)
H(14B)	4510(11)	6110(40)	6548(17)	99(10)
H(14C)	4580(11)	8150(50)	6229(18)	118(12)
H(15A)	4761(9)	6800(30)	5078(14)	72(7)
H(15B)	4366(9)	8360(40)	4839(15)	82(8)
H(15C)	4201(9)	6570(30)	4250(15)	78(8)
H(16A)	1384(7)	3500(30)	2411(11)	50(5)

__ Table 6. Torsion angles [°] for cdv75.

C(13)-C(1)-C(2)-O(1)	-49.03(18)
C(12)-C(1)-C(2)-O(1)	68.96(17)
C(6)-C(1)-C(2)-O(1)	-172.96(13)
C(13)-C(1)-C(2)-C(3)	72.36(18)
C(12)-C(1)-C(2)-C(3)	-169.65(14)
C(6)-C(1)-C(2)-C(3)	-51.57(18)
O(1)-C(2)-C(3)-C(4)	-177.87(15)
C(1)-C(2)-C(3)-C(4)	57.9(2)
C(2)-C(3)-C(4)-C(5)	-60.0(2)

C(3)-C(4)-C(5)-C(15)	-72.2(2)
C(3)-C(4)-C(5)-C(14)	169.79(19)
C(3)-C(4)-C(5)-C(6)	52.1(2)
C(4)-C(5)-C(6)-C(7)	-174.06(17)
C(15)-C(5)-C(6)-C(7)	-51.6(2)
C(14)-C(5)-C(6)-C(7)	68.5(2)
C(4)-C(5)-C(6)-C(1)	-45.4(2)
C(15)-C(5)-C(6)-C(1)	77.0(2)
C(14)-C(5)-C(6)-C(1)	-162.8(2)
C(13)-C(1)-C(6)-C(7)	55.53(18)
C(2)-C(1)-C(6)-C(7)	177.44(14)
C(12)-C(1)-C(6)-C(7)	-61.52(16)
C(13)-C(1)-C(6)-C(5)	-75.24(19)
C(2)-C(1)-C(6)-C(5)	46.67(19)
C(12)-C(1)-C(6)-C(5)	167.70(14)
C(5)-C(6)-C(7)-C(8)	-168.51(17)
C(1)-C(6)-C(7)-C(8)	60.1(2)
C(6)-C(7)-C(8)-C(9)	-49.5(2)
C(7)-C(8)-C(9)-C(10)	-128.7(2)
C(7)-C(8)-C(9)-C(12)	46.5(2)
C(8)-C(9)-C(10)-C(11)	179.89(18)
C(12)-C(9)-C(10)-C(11)	4.35(19)
C(12)-O(3)-C(11)-O(2)	-103.37(15)
C(12)-O(3)-C(11)-C(10)	12.24(17)
C(16)-O(2)-C(11)-O(3)	-72.42(17)
C(16)-O(2)-C(11)-C(10)	173.42(14)
C(9)-C(10)-C(11)-O(3)	-10.37(19)
C(9)-C(10)-C(11)-O(2)	106.94(16)
C(11)-O(3)-C(12)-C(9)	-9.83(16)
C(11)-O(3)-C(12)-C(1)	-131.00(13)

C(10)-C(9)-C(12)-O(3)	3.22(17)
C(8)-C(9)-C(12)-O(3)	-173.07(14)
C(10)-C(9)-C(12)-C(1)	123.70(15)
C(8)-C(9)-C(12)-C(1)	-52.6(2)
C(13)-C(1)-C(12)-O(3)	54.27(16)
C(2)-C(1)-C(12)-O(3)	-64.02(16)
C(6)-C(1)-C(12)-O(3)	174.05(12)
C(13)-C(1)-C(12)-C(9)	-62.93(17)
C(2)-C(1)-C(12)-C(9)	178.78(14)
C(6)-C(1)-C(12)-C(9)	56.85(17)
C(11)-O(2)-C(16)-C(17)	121.30(16)
C(11)-O(2)-C(16)-C(18)	-115.75(16)
O(2)-C(16)-C(17)-F(1)	-175.42(17)
C(18)-C(16)-C(17)-F(1)	65.1(2)
O(2)-C(16)-C(17)-F(2)	63.3(2)
C(18)-C(16)-C(17)-F(2)	-56.2(2)
O(2)-C(16)-C(17)-F(3)	-56.3(2)
C(18)-C(16)-C(17)-F(3)	-175.84(18)
O(2)-C(16)-C(18)-F(6)	-56.4(2)
C(17)-C(16)-C(18)-F(6)	63.6(3)
O(2)-C(16)-C(18)-F(5)	63.4(2)
C(17)-C(16)-C(18)-F(5)	-176.54(19)
O(2)-C(16)-C(18)-F(4)	-178.02(16)
C(17)-C(16)-C(18)-F(4)	-58.0(2)

Table 7. Hydrogen bonds for cdv75 [Å and °].

D-H...A	d(D-H)	d(H...A)	d(D...A)	<(DHA)
O(1)-H(1)...O(3)	0.83(2)	2.14(3)	2.8273(18)	140(2)